NASA CONTRACTOR REPORT

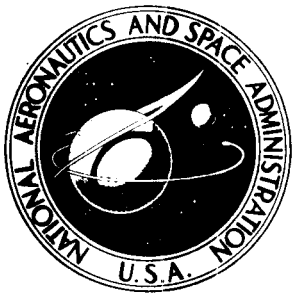

NASA CR-2836

NASA CR-2836

ANALYSIS AND COMPILATION OF MISSILE AERODYNAMIC DATA

Volume II - Performance Analysis

John E. Burkhalter

Prepared by
AUBURN UNIVERSITY
Auburn, Ala. 36830
for Langley Research Center

NATIONAL AERONAUTICS AND SPACE ADMINISTRATION · WASHINGTON, D. C. · MAY 1977

1. Report No.	2. Government Accession No.	3. Recipient's Catalog No.
NASA CR-2836		

4. Title and Subtitle	5. Report Date
ANALYSIS AND COMPILATION OF MISSILE AERODYNAMIC DATA - VOLUME II PERFORMANCE ANALYSIS	May 1977
	6. Performing Organization Code
7. Author(s)	8. Performing Organization Report No.
John E. Burkhalter	
	10. Work Unit No.
9. Performing Organization Name and Address	
Aerospace Engineering Department Auburn University Auburn, Alabama 36830	11. Contract or Grant No.
	NSG 1002
	13. Type of Report and Period Covered
12. Sponsoring Agency Name and Address	Contractor Report
National Aeronautics and Space Administration Langley Research Center Hampton, VA 23365	14. Sponsoring Agency Code

15. Supplementary Notes

Langley Technical Monitor: M. Leroy Spearman

Volume II of Final Report

16. Abstract

This report provides a general analysis of the flight dynamics of several surface-to-air and two air-to-air missile configurations. The analysis involves three phases: vertical climb, straight and level flight, and constant altitude turn. Wind tunnel aerodynamic data and full scale missile characteristics are used where available; unknown data are estimated. For the constant altitude turn phase, a three degree of freedom flight simulation is used. Important parameters considered in this analysis are the vehicle weight, Mach number, heading angle, thrust level, sideslip angle, g loading, and time to make the turn. The actual flight path during the turn is also determined. Results are presented in graphical form.

17. Key Words (Suggested by Author(s))	18. Distribution Statement
Missiles Missile Configurations Missile Performance	UNCLASSIFIED - UNLIMITED Subject Category 02

19. Security Classif. (of this report)	20. Security Classif. (of this page)	21. No. of Pages	22. Price*
UNCLASSIFIED	UNCLASSIFIED	314	$9.75

*For sale by the National Technical Information Service, Springfield, Virginia 22161

TABLE OF CONTENTS

SUMMARY

This report provides a general analysis of the flight dynamics of several surface-to-air and two air-to-air missile configurations. The analysis involves three phases: vertical climb, straight and level flight, and constant altitude turn. Wind tunnel aerodynamic data and full scale missile characteristics are used where available; unknown data are estimated. For the constant altitude turn phase, a three degree of freedom flight simulation is used. Important parameters considered in this analysis are the vehicle weight, Mach number, heading angle, thrust level, sideslip angle, g loading, and time to make the turn. The actual flight path during the turn is also determined. Results are presented in graphical form.

NOMENCLATURE (CONT'D)

Symbol	Definition
W_g	Weight of propellant grain
W_o	Initial weight of missile
$\dot{W}$	Weight flow rate of fuel
X	Coordinate axis
X_w	Summation of forces on missile along X wind axis
Y_w	Summation of forces on missile along Y wind axis
Z	Coordinate axis
α	Angle of attack
β	Sideslip angle
δ_E	Elevator deflection
δ_R	Rudder deflection
ρ	Atmospheric density
ψ	Heading angle

NOMENCLATURE

Symbol	Definition
a	Speed of sound
C_D	Drag coefficient
C_{D_o}	Zero lift drag coefficient
C_L	Lift coefficient
C_m	Pitching moment coefficient
C_n	Yawing moment coefficient
C_y	Side force coefficient
d	Reference length (diameter)
g	Acceleration of gravity
Isp	Specific impulse of grain
I_{zz}	Moment inertia of missile about z axis
m	Mass of missile
M	Mach number
P	Atmospheric pressure
q	Dynamic pressure
R_b	Body axis yaw rate
S	Reference area
t	Time
T	Thrust
t_{bo}	Time at burnout of grain
V	Vehicle speed
W	Weight of missile

I. INTRODUCTION

In Volume I of this report, aerodynamic coefficients for approximately 30 recently declassified missile configurations were compiled and tabulated in a consistent format. The purpose of this report, Volume II, is to provide a general aerodynamic analysis of several missile configurations with maximum utilization of the data in Volume I. In this respect, several similar missiles in the surface-to-air and air-to-air classes are analyzed, and results are presented in a format for performance comparisons.

Classically, analyses in flight dynamics are divided into three major areas. The first is performance, where such items as maximum speed, range, ceiling and endurance are considered. These items have special forms where tactical missiles are concerned. The second area is stability and control. Here maneuverability (control effectiveness) and dynamic stability are especially important when coupled with automatic control systems. Finally, there is aeroelasticity. The high-g maneuvers of missiles impose stringent requirements on the aerostructure; however, the slender, low aspect ratio configurations in use today are relatively insensitive to classical aeroelastic problems.

The aerodynamic behavior and performance characteristics of a missile are highly dependent on the class of mission for which it was designed. In the surface-to-air category five configurations of one missile are considered; a wingless version, two similar winged versions, and a winged design with aft-tail controls and canard controls. In the air-to-air class, two specific designs are examined.

There are two approaches for performance anlayses. One is strictly an aerodynamic comparison of different designs with all variables other than the aerodynamic coefficients remaining fixed. The other is a dynamic comparison incorporating actual variables and initial conditions for each configuration, which is the method used herein. Since most of the configurations investigated are operational, information such as overall dimensions, weight, and grain size is available. Other variables - e.g., specific impulse and moments-of-inertia - could be reliably estimated.

As stated previously, the objective of this analysis is to provide data on several missiles in certain aerodynamic environments. The analysis consists of three phases; two under performance and one under stability and control. The two phases in performance involve straight line horizontal flight and straight line vertical climb. Constant altitude horizontal turns due to constant rudder are examined in the stability and control phase.

In each phase, the applicable rigid body equations of motion, in the form given by Fogarty and Howe in Ref. 1, are solved numerically on the digital computer. The coordinate system used for translational displacements is referenced to the flight path and, as pointed out in Ref. 1, "...makes much lower accuracy and speed demands on the computer than does the body-axis system." For the rotational equations, the body axis system is used since again maximum utilization of computer time is realized. Assumptions, approximations and details of solutions are discussed in subsequent sections.

II. ANALYSIS

Performance - Phase I: Horizontal Flight

The performance phase for horizontal flight consists of two parts. In the first part, the thrust required to produce a given steady state Mach number is determined. Initially the vehicle force and moment equations were written in the vertical and horizontal planes and were solved simultaneously in an iterative manner. These equations were

$$T \cos \alpha = qS\ C_D\ (M,\alpha) \tag{1}$$

$$T \sin \alpha + qS\ C_L(M,\alpha,\delta_E) = W \tag{2}$$

and

$$qSdC_m(M,\alpha,\delta_E) = 0 \tag{3}$$

Various vehicle weights were considered and the thrust required versus Mach number was determined at several altitudes. The results of these initial computations indicate that the vehicle weight had little effect on the thrust required, as shown in Fig. 1. Consequently, Equations (2) and (3) were dropped and the angle of attack was set at zero. Equation (1) then reduced to

$$T = qS\ C_{D_o}\ (M). \tag{4}$$

The second part of the horizontal flight calculations was the solution of the simplified (α=0) horizontal equations of motion. The purpose of these computations was to provide initial condition inputs to Phase III, the constant altitude turn, and to further illustrate the

dependence of the vehicle flight Mach number on the thrust and drag. These equations were written as

$$\ddot{X} = (T - qS\, C_{D_o}(M)/m, \tag{5}$$

$$\dot{X} = \int \ddot{X}\, dt, \tag{6}$$

$$M = \dot{X}/a, \tag{7}$$

$$W = W_o - \int \dot{W}\, dt. \tag{8}$$

For these equations it was assumed that $\alpha=0$, $\dot{W}$ = const = T/Isp and that the altitude was constant (sea level). These equations simulate a horizontal launch in which the missile is allowed to accelerate until the grain is consumed, at which point the flight is terminated. The vehicle flight Mach number is thus determined as a function of the vehicle weight or weight of grain consumed.

In making these computations, the initial vehicle weight and initial grain weight had to be estimated. A total vehicle density of 100 lbs/ft^3 was assumed. As a further check on the weight estimations, the parameter W/S = 750 which was used by Spearman and Fournier in Ref. 2, served as a guide. Data given in Ref. 3 was also used as a guideline. As a general rule, this number falls within the range of the initial weight estimate and the weight of the vehicle after the grain burns out.

Since portions of these flights were subsonic, subsonic aerodynamic data were required. In the majority of the wind tunnel test reports, subsonic data were not available, and subsonic drag coefficients had to be estimated using the methods of Ref. 4.

Performance - Phase II: Vertical Climb

The vertical climb phase of the analysis consists of vertical launch at some constant thrust level. As in the other phases, the initial weight of the vehicle as well as the initial propellant or grain weight was required. For each flight the specific impulse of the grain was assumed constant at 250 seconds. As a further simplification the weight flow rate of propellant was assumed to be

$$\dot{W} = T/Isp \tag{9}$$

Obviously, the drag and thrust are quite important in this analysis. In order to accurately compute the drag, the drag coefficient was written as

$$C_D = C_D(M) \tag{10}$$

Altitude effects were taken into account through equations defining the standard atmospheric density and speed of sound as functions of the height Z. Because of the dependence of total aerodynamic forces on both Mach number and altitude, maximum thrust levels do not necessarily mean maximum altitudes. That is, if the thrust level is high, the missile accelerations are high which lead to high drag at low altitudes. On the other hand, lower thrust levels may produce lower drags at higher altitudes. For some of the missile configurations presented in this analysis, the thrust levels which produced maximum altitudes were determined.

Because of the vertical launch from the ground, subsonic drag coefficient data were also required in this phase. It was also necessary

to extrapolate the data to higher Mach numbers than those run in the wind tunnel tests.

The procedure for each flight was to set the thrust at a given level, then solve the equations of motion for the subsequent trajectory and desired data. The governing equations for vertical flight are

$$(W/g)\ \ddot{Z} = T - qS\ C_{D_o}(M) - W, \tag{11}$$

$$q = .5\ \rho a^2\ M^2 \tag{12}$$

$$W = W_o - \int \dot{W}\ dt\ , \tag{13}$$

$$\dot{Z} = \int \ddot{Z}\ dt \tag{14}$$

$$M = \dot{Z}/a \tag{15}$$

and

$$Z = h = \int \dot{Z}\ dt \tag{16}$$

Flights were made at each of four different thrust levels. The thrust levels chosen were designed to cover the range of thrust that any one particular missile was assumed capable of producing. During each flight the vehicle weight, drag, Mach number and time of flight was recorded at specific altitude intervals and appropriate plots were made.

Stability and Control - Phase III: Constant Altitude Turn

The third phase of the analysis consisted of a constant altitude turn. It is understood that all the missiles considered in this report will, in all likelihood, not be required to make a full 180° turn. However, the ability of the missile to make a turn is indicative of its

ability to maneuver. Consequently the information derived from a turn analysis is very descriptive of the missile aerodynamic efficiency.

Three different altitudes were selected at which the turns were to be made; namely, sea level, 25,000, and 50,000 feet. Thrust levels during the turn were constant until the fuel was consumed or until the 180° turn is completed. Vehicle weight, grain weight, and Mach number at the initiation of the turn maneuver was required. In order to be as realistic as possible and still stay within the constraints of the overall analysis effort, the weight of the vehicle, corresponding grain weight, and Mach number were obtained from the vertical climb phase of the analysis. For example, during the vertical climb phase, the missile total weight, weight of fuel remaining, and Mach number at 25,000 feet were stored for future reference. These three parameters then served as initial conditions for the turn at that altitude. This same procedure was used for the 50,000-foot altitude turn.

For the sea level turn, a slightly different approach was taken. From Phase I, the missile is allowed to boost horizontally until a Mach number of 1.5 is obtained, then the turn procedure is initiated. The input weights, vehicle and grain, are obtained from the Phase I analysis as previously explained.

The turn maneuver was begun with the missile centerline on the X-coordinate axis. The rudder or control surface to initiate the turn is deflected a given amount δ_R and the missile then attempts to negotiate the turn. The vehicle aerodynamics which dictate the flight path and subsequent trajectory were obtained from the wind tunnel data. Because

of the varying weight, thrust cutoff and c.g. shift, the radius during each turn was not a constant. It was assumed that the grain was located in the aft portion of the vehicle and consequently the c.g. shifted forward as the grain was consumed. This forward c.g. travel and its effect on moment of inertia was taken into account in the analysis, since stability of the missile is dependent on the location of the c.g. Other parameters which had to be estimated were the moments of inertia and the damping derivatives $C_{y_{\dot{\psi}}}$ and $C_{n_{\dot{\psi}}}$. The damping derivatives were estimated using Lifting Surface and Slender Body Theory techniques.

In the initial solutions of the governing equations, the angle of attack, α, was included as a variable and was computed along with other parameters. However, it was observed that under the constraints of the constant turn maneuver, α had a negligible effect on the resultant flight path or other pertinent variables. Consequently, α was eliminated in the remainder of the computations. Initial efforts to use linear aerodynamics led to incorrect results; consequently, values of C_Y vs. β and C_n vs. β were input in tabular form to include nonlinear effects.

Double interpolation algorithms were set up in order to determine accurately the side force coefficients and yawing moment coefficients. Drag coefficients, as in Phases I and II, were extrapolated to M = 1.0 and M = 6.0 and were also linearly interpolated from input tables.

As previously mentioned, the thrust level for any one flight was held constant at one of four preselected values. At the beginning of each turn, the burnout time for the grain was determined from

$$t_{bo} = W_g/\dot{W} \quad . \tag{17}$$

It was then assumed that tailoff (final burning of grain) occurred over a two-second period and the thrust linearly decayed to zero during this time.

Since the turn was at a constant altitude, motion was restricted to the x-y plane. The missile was assumed to "slide" through the turn (no roll) with the fins or cruciform wings in the "plus" configuration.

With these restrictions and assumptions, the resultant equations of motion were written:

$$X_w = T \cos \alpha \cos \beta + qS(-C_D \cos \beta + C_Y \sin \beta), \tag{18}$$

$$Y_w = - T \cos \alpha \sin \beta + qS(C_D \sin \beta + C_Y \cos \beta), \tag{19}$$

$$\dot{R}_b = qSd\, C_n/I_{zz} , \tag{20}$$

$$R_b = \int \dot{R}_b \, dt , \tag{21}$$

$$\dot{\psi} = R_b/\cos \alpha , \tag{22}$$

$$\psi = \int \dot{\psi} \, dt , \tag{23}$$

$$\dot{V} = X_w/m , \tag{24}$$

$$V = \int \dot{V} \, dt , \tag{25}$$

$$\dot{\beta} = Y_w/(mV) - \dot{\psi} \tag{26}$$

$$\beta = \int \dot{\beta} \, dt , \tag{27}$$

$$C_Y = C_Y(\beta, M) , \tag{28}$$

$$C_D = C_{D_o} + C_D(\delta_R) \tag{29}$$

$$C_n = C_n(\beta, M) \ . \tag{30}$$

These equations (18) through (30) were solved digitally and the desired parameters plotted. The output from the simultaneous solution of these equations includes (1) X versus Y, (2) g-level during turn, (3) ψ during turn, (4) β during turn, (5) Mach number during turn, (6) weight of vehicle during turn, and (7) time required to make the turn.

III. RESULTS

The table below is a general summary of the missiles which were analyzed as described in the preceding sections.

TABLE

	PHASE I	PHASE II	PHASE III		
			$\delta=10°$	$\delta=20°$	$\delta=40°$
TM X-2774	X	X	X	———	———
TM X-1751	X	X	X	X	X
TM X-1025	X	X	X	X	X
TM X-3070	X	———	X	X	———
TM X-846	X	———	X	X	———
TM X-2780/A	X	X	X	X	X
TM X-2780/C	X	X	X	X	X

For each missile configuration plots are presented which depict the results from each of the three "missions." On each graph is an identification number which is indicative of certain parameters as described below. Example:

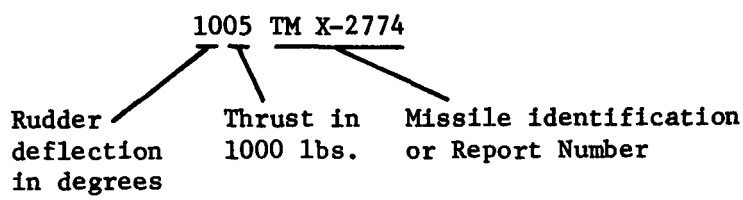

For this example the rudder deflection is 10 degrees, the thrust is 5000 lbs., and the missile is taken from NASA Report Number TM X-2274. Data on each graph is presented for three different altitudes; sea level, 25,000 ft., and 50,000 ft.

In addition to the identification number the figures are numbered relative to the respective "mission." The Roman numeral is respective of the mission as outlined below.

I - Horizontal Flight
II - Vertical Flight
III - Constant Altitude Turn

Other numbers in the figure number designation are in consecutive order.

As a typical example of the data presented for each missile, the missile designated TM X-2774 is discussed in detail. From the horizontal flight phase Fig. 2-I depicts the terminal Mach number versus thrust levels for various altitudes. For example, if the thrust were 10,000 pounds, the maximum Mach number the missile could obtain at sea level would be about M=3.3 but at 20,000 feet altitude the missile could reach a Mach number of M=5.5.

Continuing with Fig. 3-II, the time required to climb vertically to various altitudes is presented. Note that on this particular missile the maximum altitudes are very high - in excess of 100 miles - and consequently the trajectories or data presented for these high altitude regimes may be somewhat in error. In Fig. 4-II, the Mach number - Altitude trace is presented. Note that maximum Mach numbers range from 5.5, at 5000 lbs. thrust, to 6.5 at 20,000 lbs.

The last figure in the Phase II flight set is the vehicle Weight versus Altitude. Fig. 5-II depicts the weight of the vehicle during the vertical boost. From this graph the initial weight of the vehicle may be obtained as well as the final burnout weight.

The third phase flight, constant altitude turn, is presented in the next series of curves. In Fig 6-III through 9-III, the flight time and vehicle weight are presented as functions of the downrange distance, Y. The initial weight of the vehicle at the constant turn altitudes are obtained from Fig. 5-II. The first of the figures, Fig. 6-III, is for a thrust level of 5000 lbs. while the second, third and fourth are for 10,000, 15,000, and 20,000 lbs. thrust, respectively.

In order to get a clear picture of the missile performance, all the figures in this phase should be considered since they are all interrelated. The Mach number during the flight and "heading angle," ψ, are presented in Figs. 10-III through 13-III. Note that the initial Mach number for each altitude is different. The initial values for the vehicle flight Mach number is taken from the vertical flight phase, Fig. 4-III. Note that for this particular missile and thrust = 5000 lbs. at altitude of 50,000 feet, the grain burns out before the 180° turn is completed. However, for the other two altitudes, fuel still remains after the turn is completed. Increasing the thrust level as shown on Figs. 11-III through 13-III produces somewhat different results. The next set of curves, Figs. 14-IV through 17-III, present the g loading and sideslip angle, β, as functions of the downrange distance, y. Note that at the beginning of the turn maneuver, the missile oscillates about some nominal sideslip angle but then damps out and maintains a near constant β.

The final set in the Phase III series is the most descriptive for the constant altitude turn. In Figs. 18-III through 21-III the flight

path, X versus Y, for each thrust level is presented. Small replicas of the missile shape are drawn on the flight path trajectory at discrete locations at its correct heading and sideslip angle. The flight for each of the three different altitudes are shown on these figures.

The same general figures as discussed above are presented for the other missiles as outlined in the Table. There are a few exceptions; for example, there is no Phase I or Phase II flights for TM X-3070 and TM X-846 since these are air launched air-to-air missiles. The interpretation of the results of these computations are left to the reader.

REFERENCES

1. Fogarty, L. E., and R. M. Howe, "Computer Mechanization of Six-Degree of Freedom Flight Equations," Simulation, Vol. II, No. 4, October 1968.

2. Spearman, M. L., and R. H. Fournier, "An Aerodynamic Assessment of Various Missile Configuration Concepts," Paper presentation at the Ninth U.S. Navy Symposium on Aeroballistics, Silver Spring, Maryland, May 1972.

3. Jane's All the World's Aircraft; edited by J. W. R. Taylor,Jane's Yearbooks, Paulton House, London, England; 1966-1975 editions.

4. Moore, F. G., "Aerodynamics of Guided and Unguided Weapons," NWL Technical Report TR-3018, U.S. Naval Weapons Laboratory, Dahlgren, Virginia, December 1973.

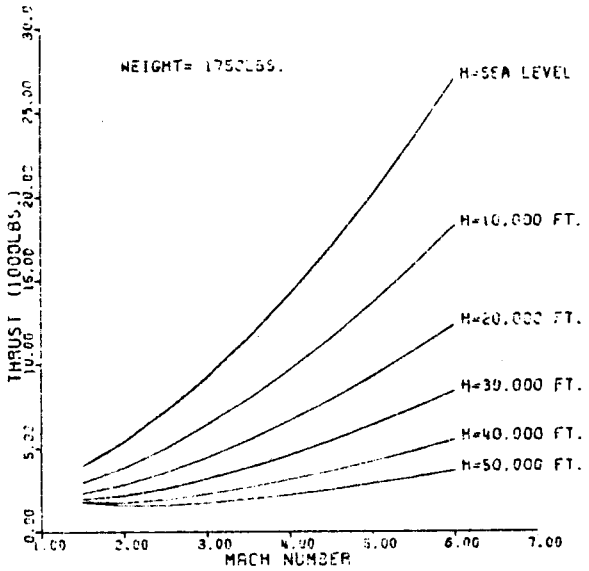

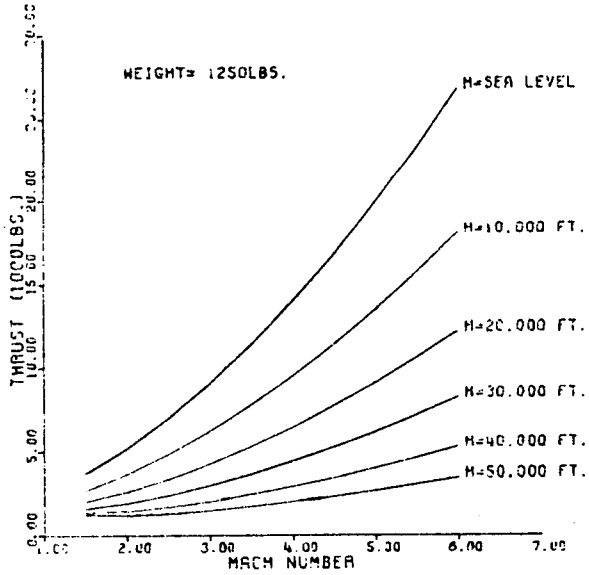

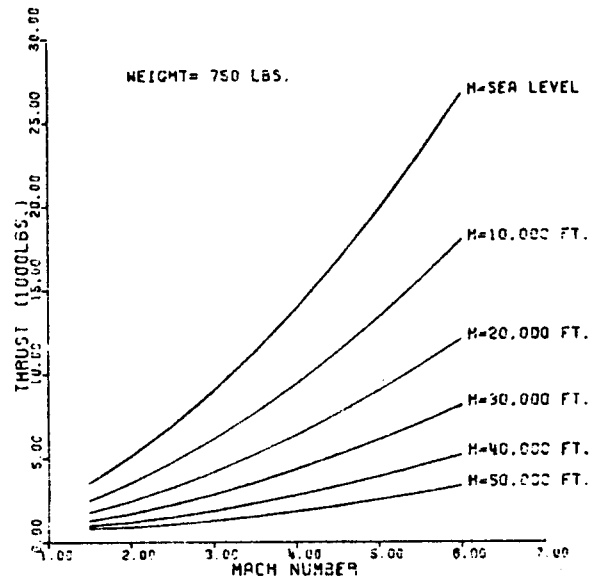

Fig. 1-I. Thrust vs. Terminal Mach No., TM X 2774

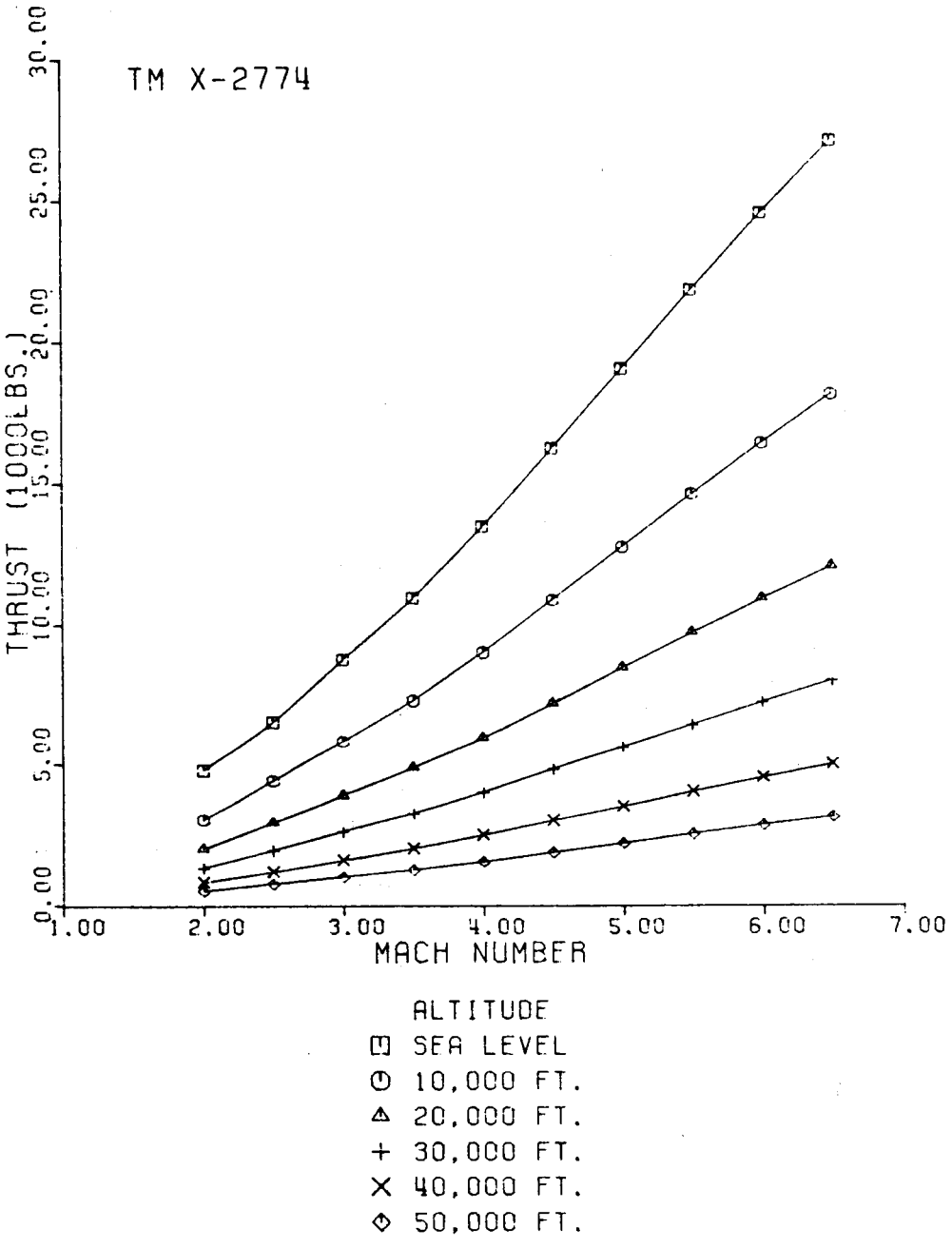

Fig. 2-I. Thrust vs. Terminal Mach No.

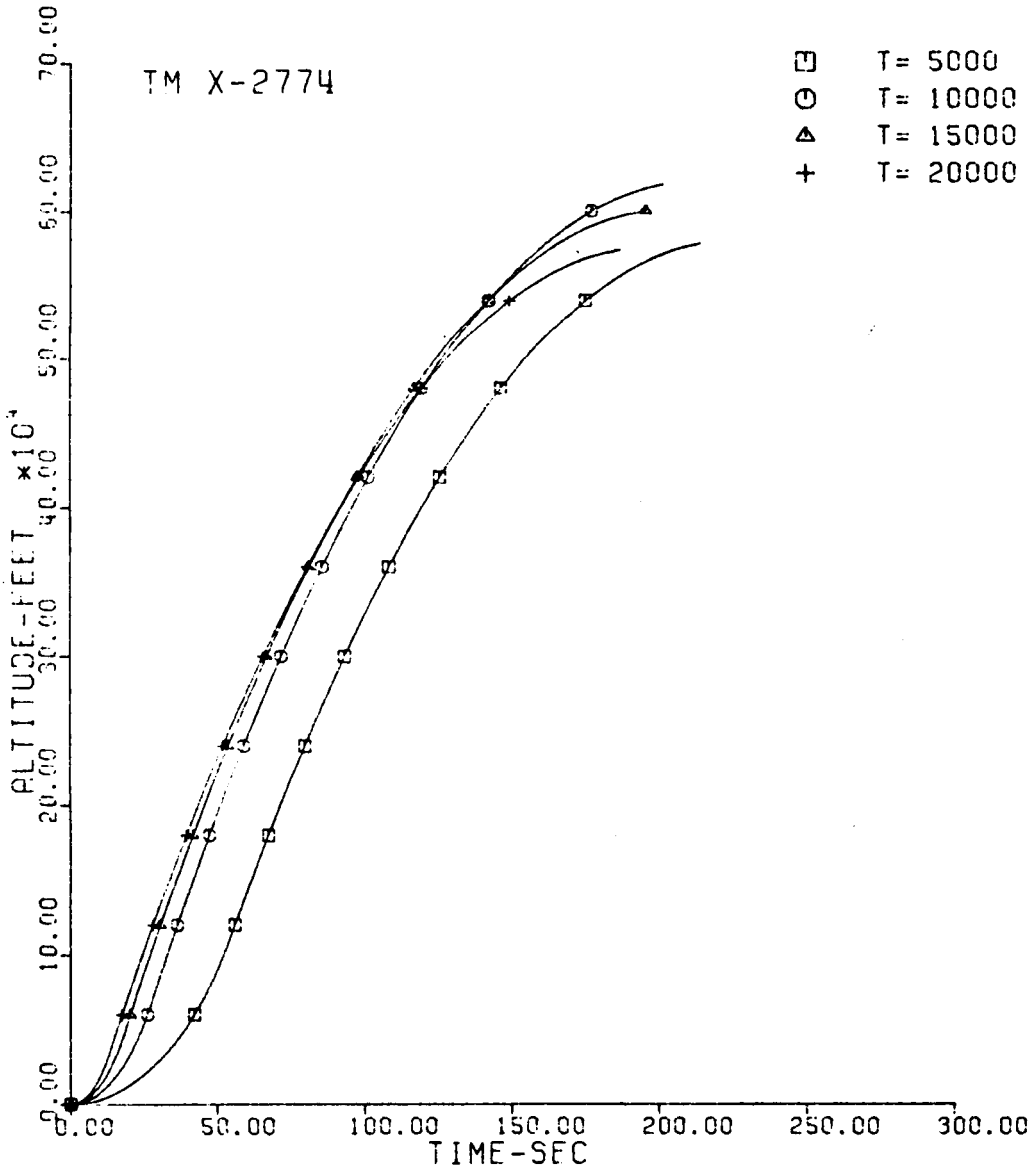

Fig. 3-II. Altitude vs. Flight Time.

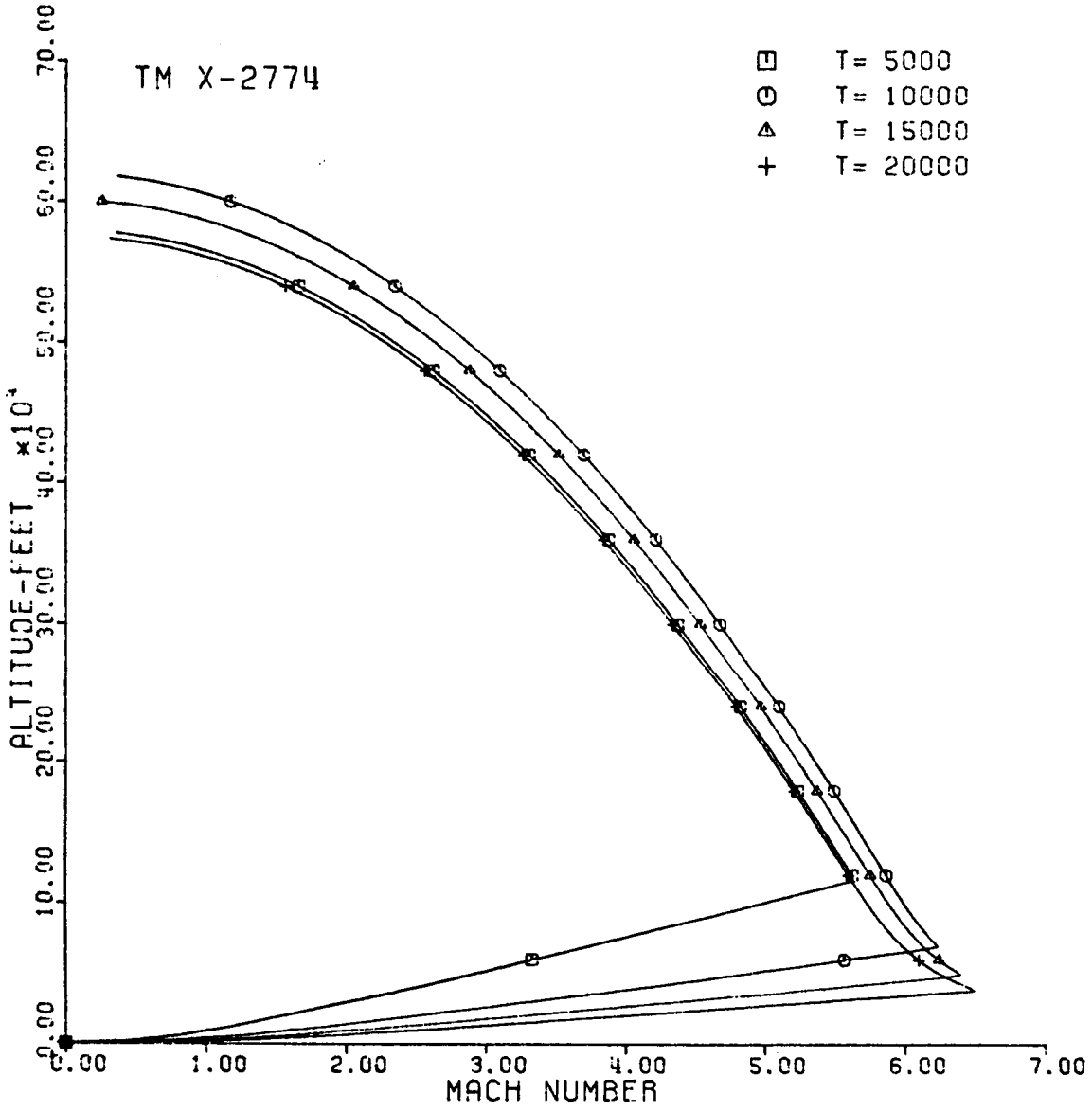

Fig. 4-II. Altitude vs. Mach No.

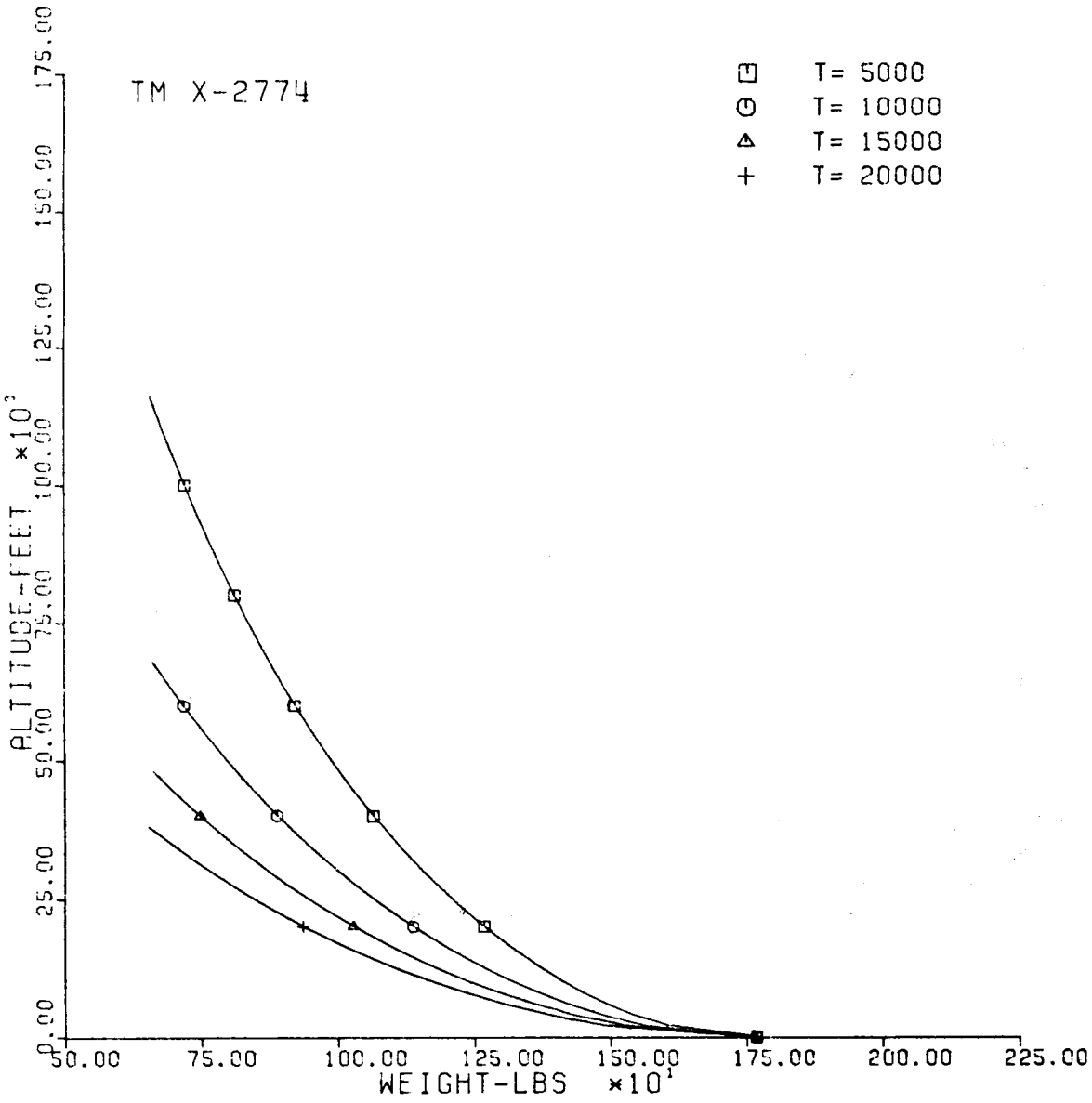

Fig. 5-II. Altitude vs. Vehicle Weight.

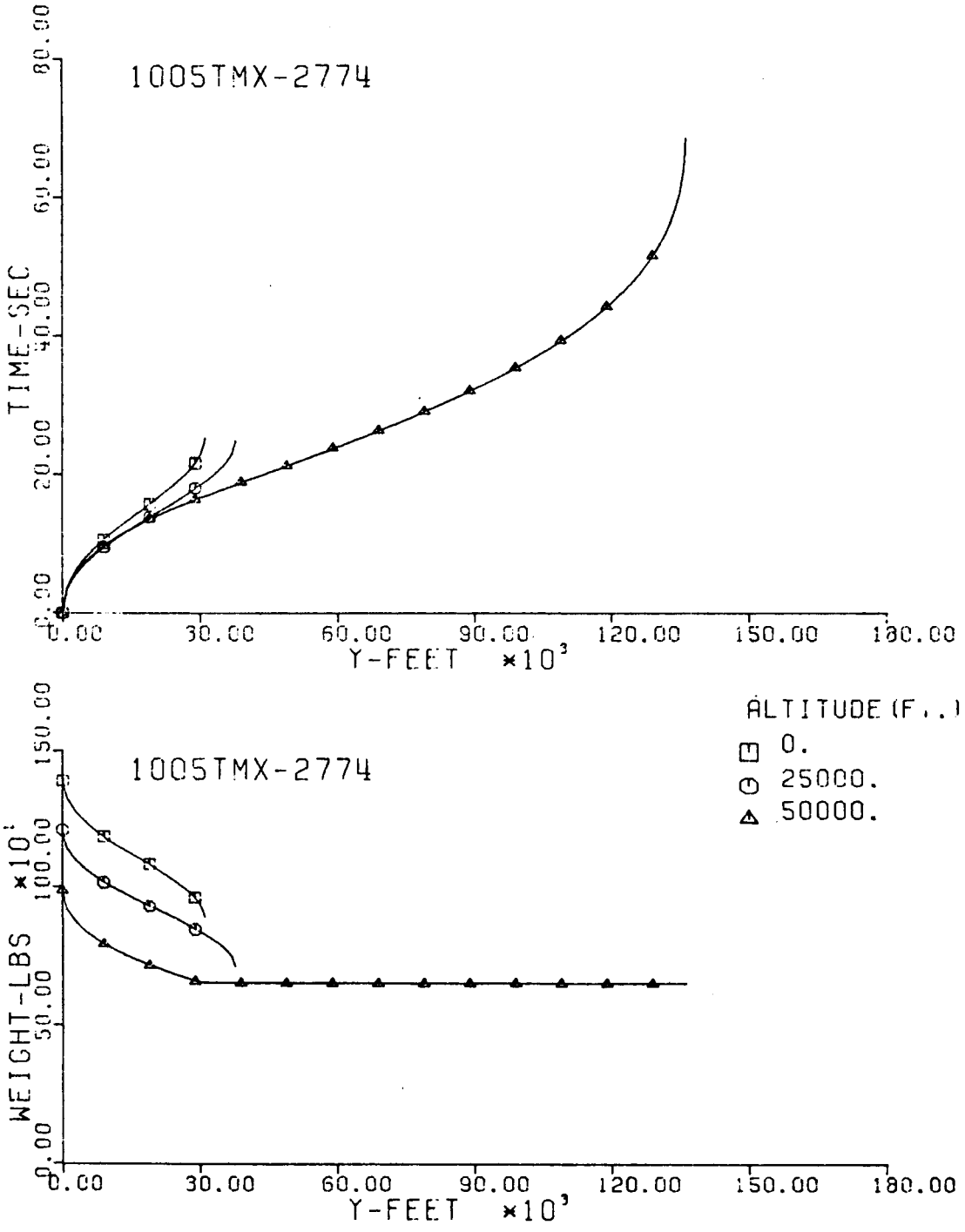

Fig. 6-III. Flight Time and Vehicle Weight vs. Downrange Distance, Y.

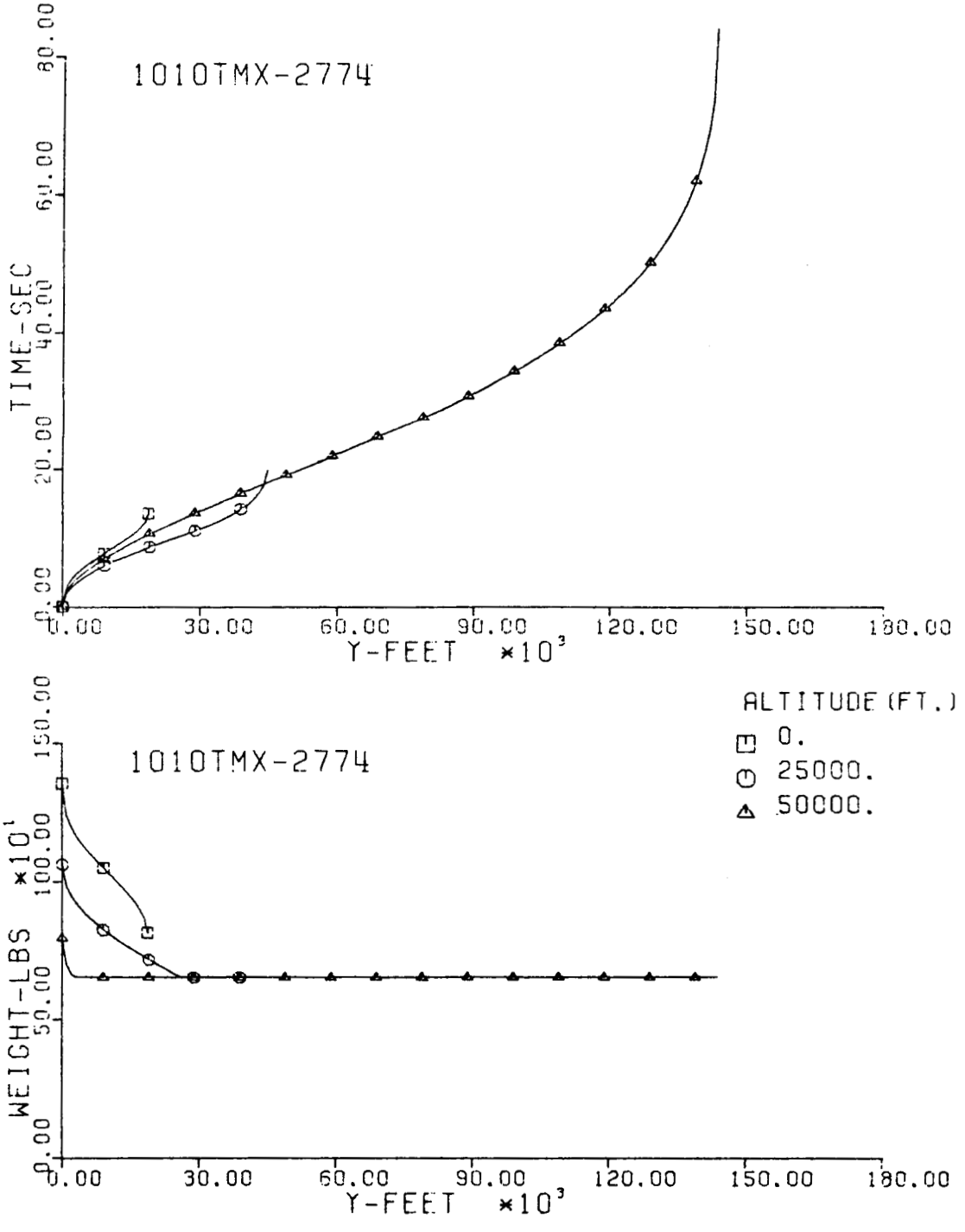

Fig. 7-III. Flight Time and Vehicle Weight vs. Downrange Distance, Y.

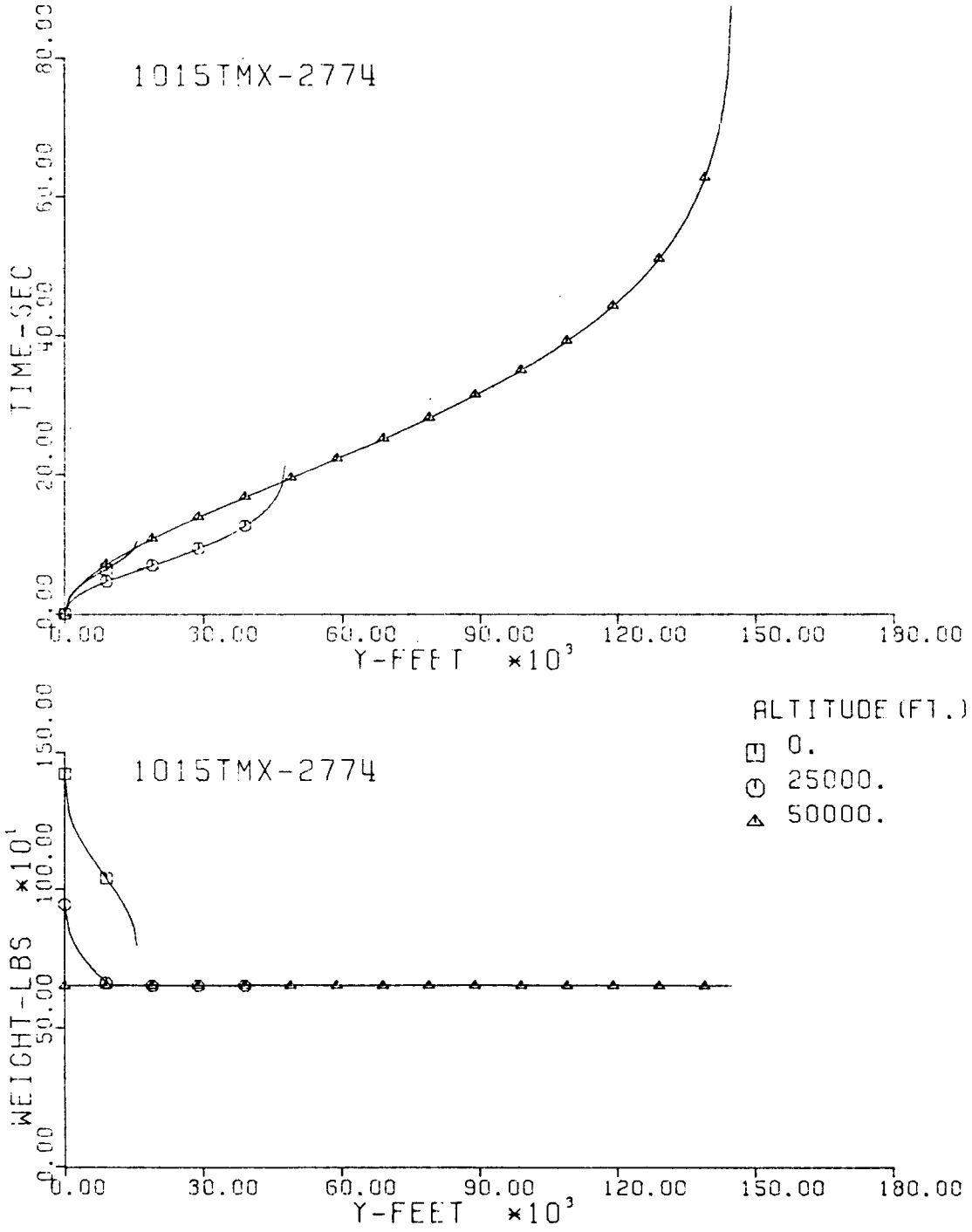

Fig. 8-III. Flight Time and Vehicle Weight vs. Downrange Distance, Y.

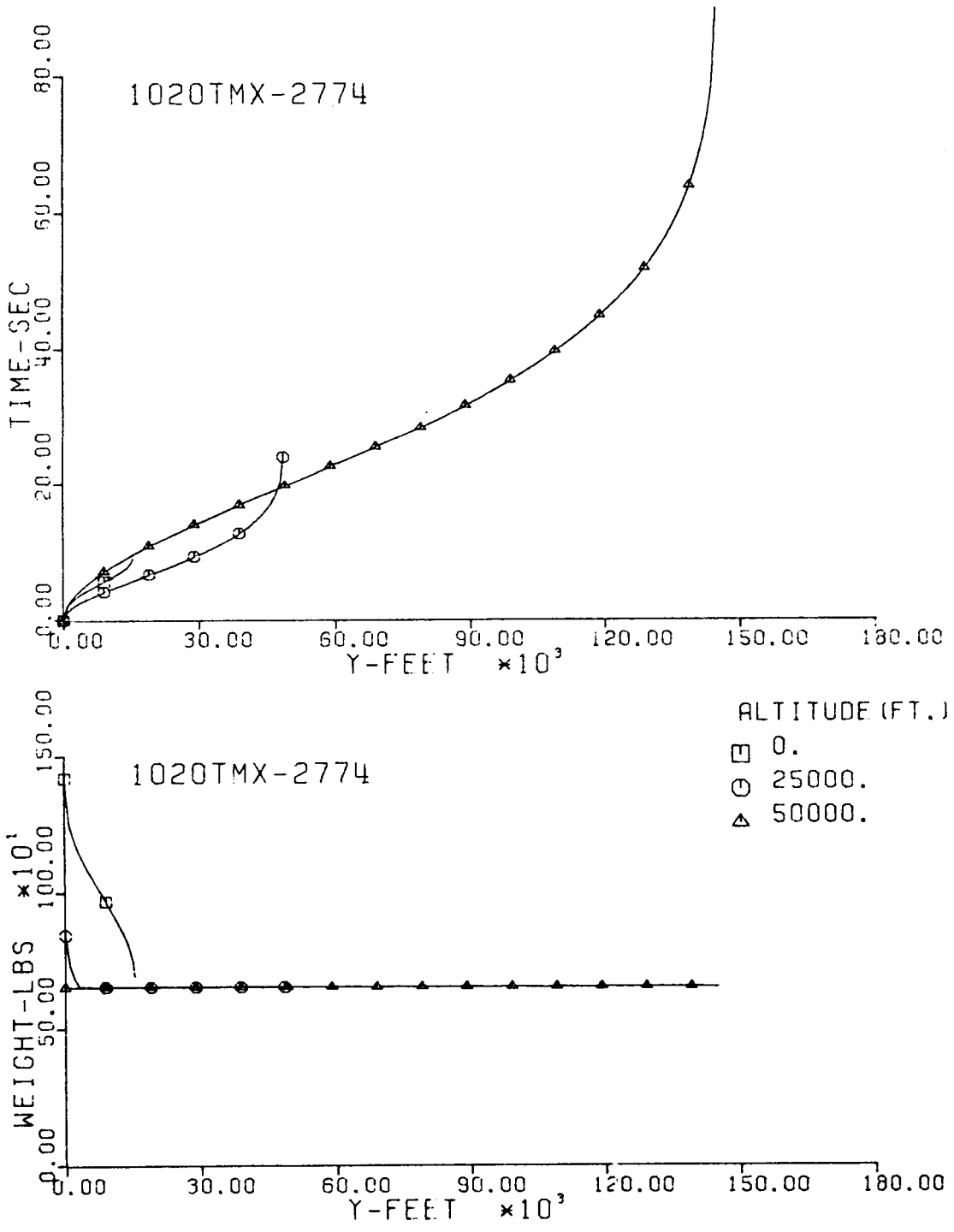

Fig. 9-III. Flight Time and Vehicle Weight vs. Downrange Distance, Y.

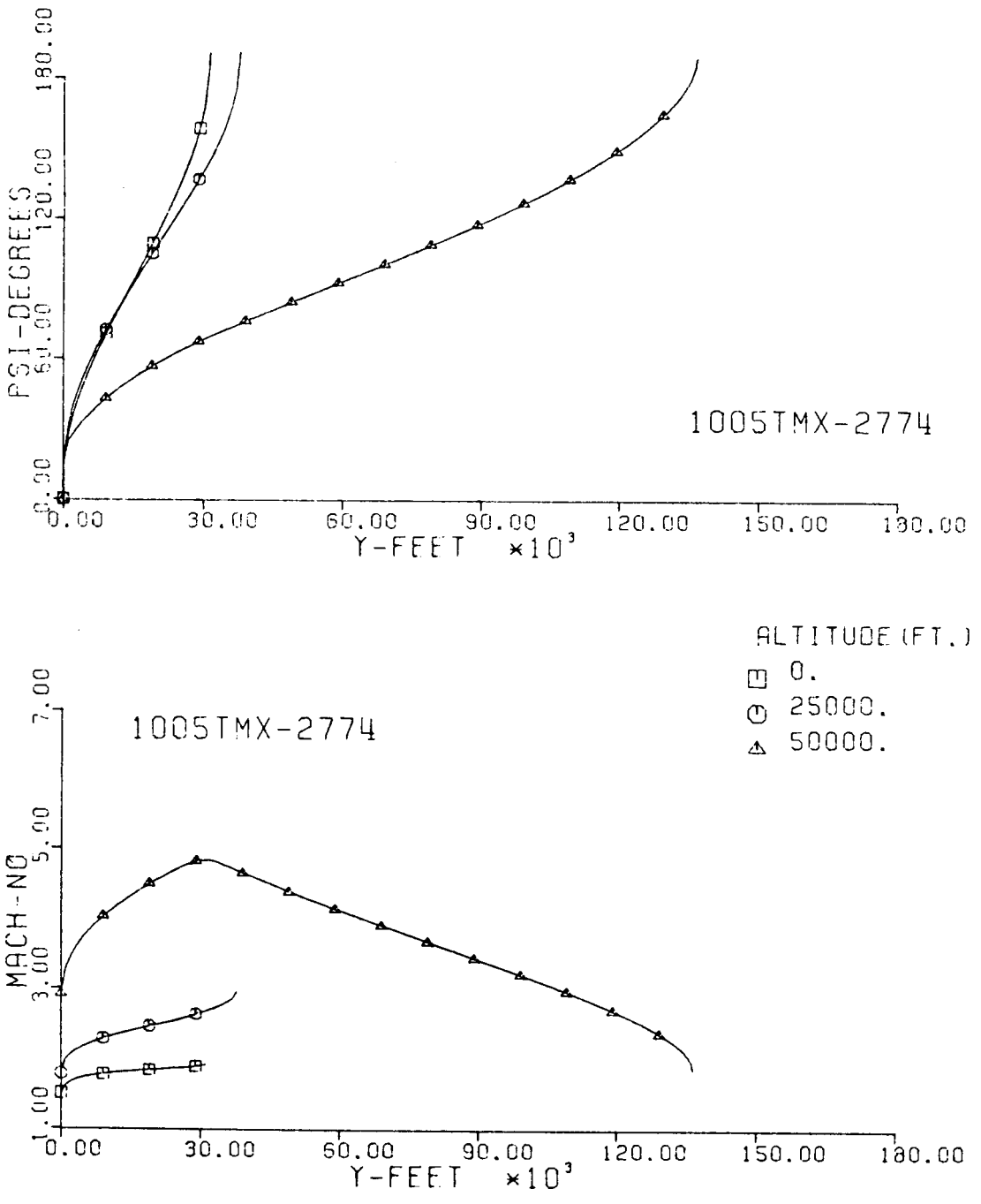

Fig. 10-III. Heading Angle and Mach No. vs. Downrange Distance, Y.

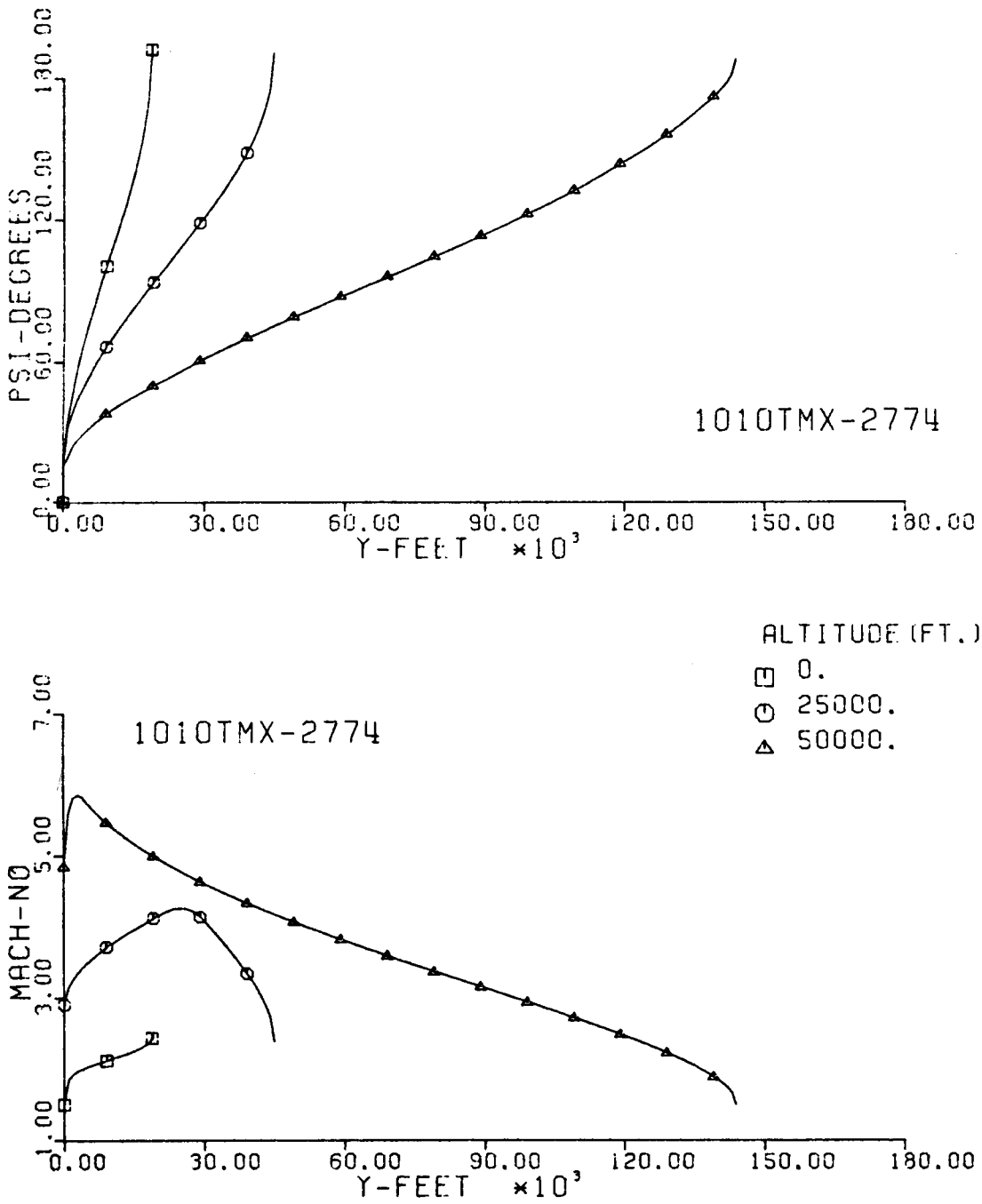

Fig. 11-III. Heading Angle and Mach No. vs. Downrange Distance, Y.

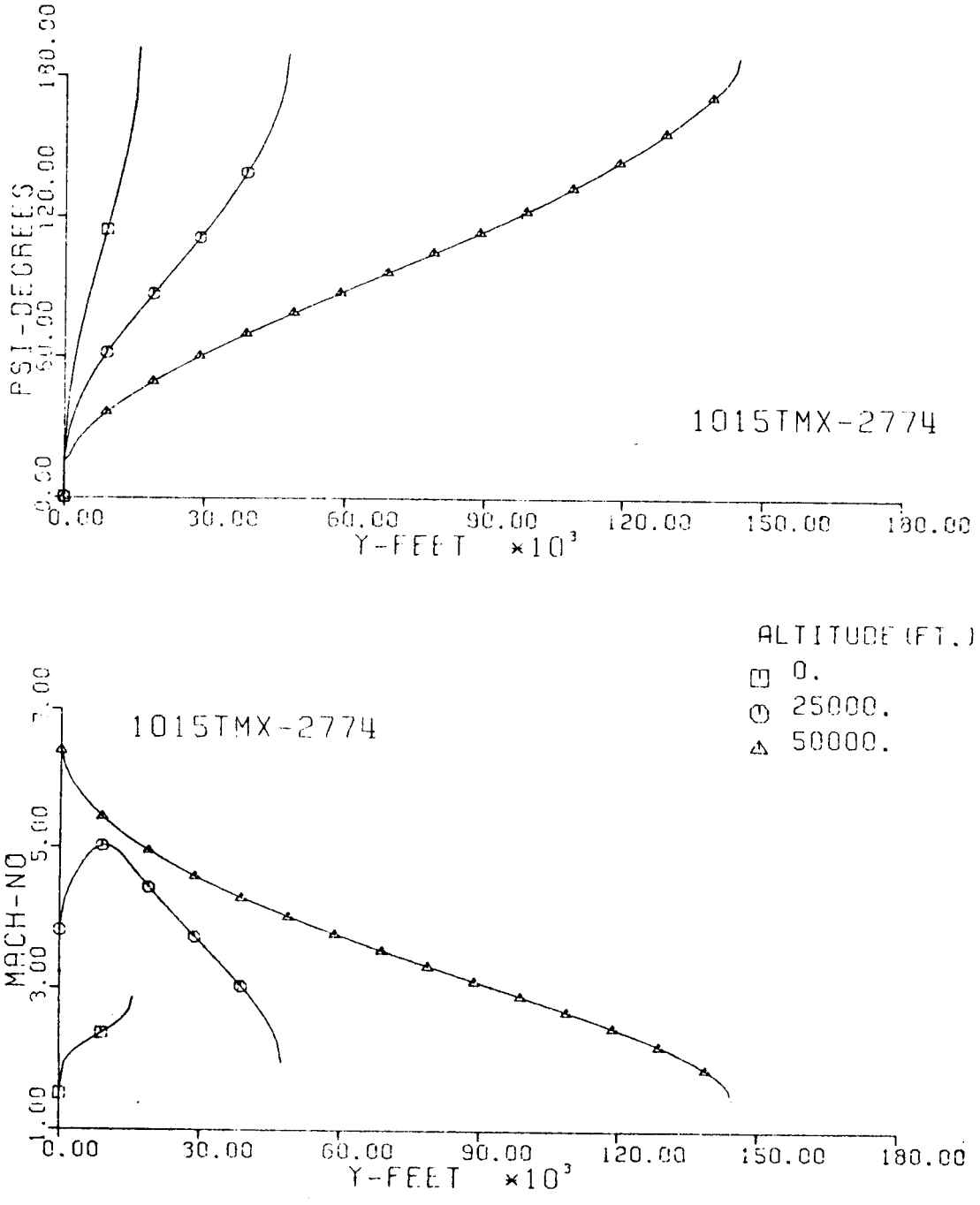

Fig. 12-III. Heading Angle and Mach No. vs. Downrange Distance, Y.

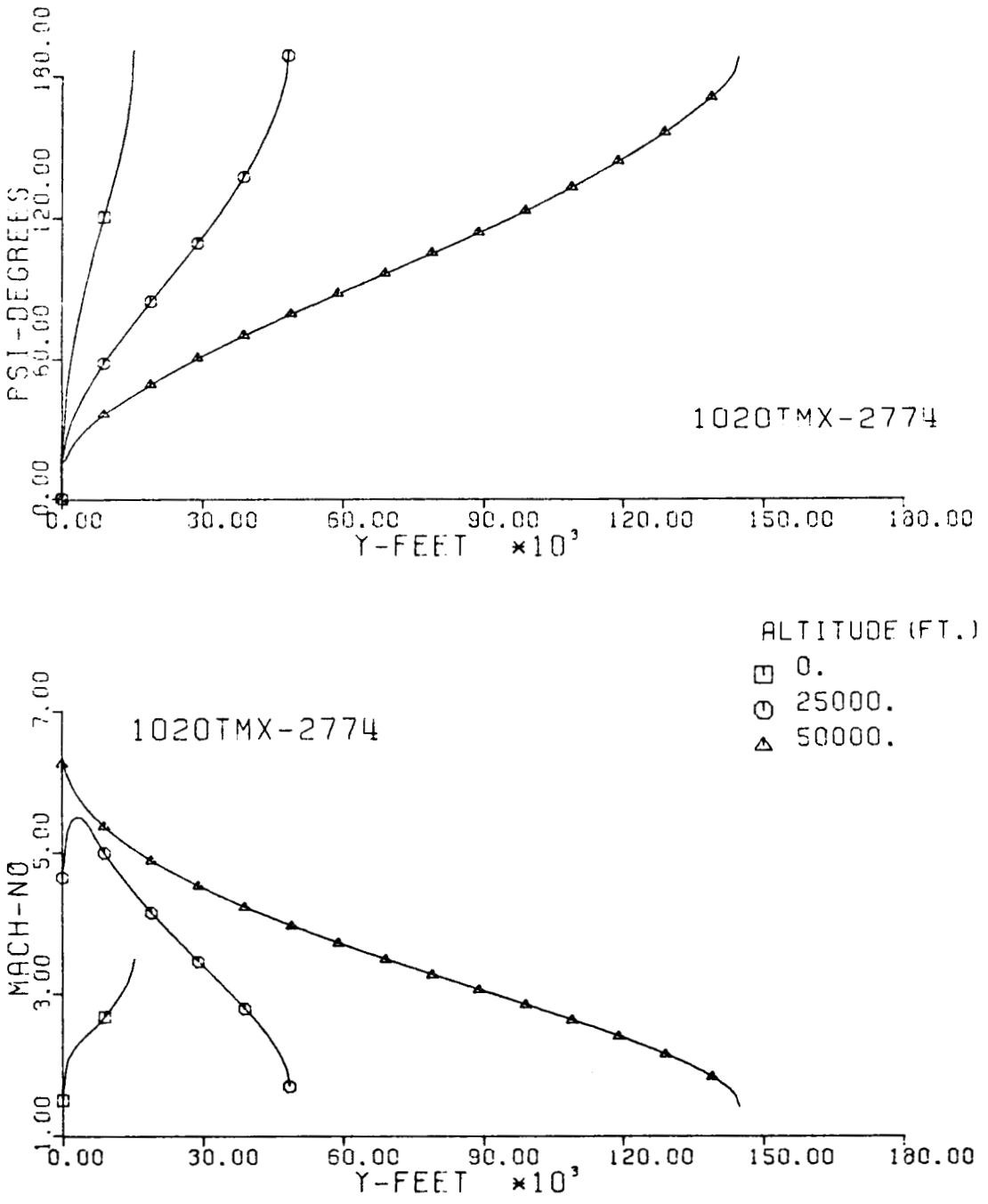

Fig. 13-III. Heading Angle and Mach No. vs. Downrange Distance, Y.

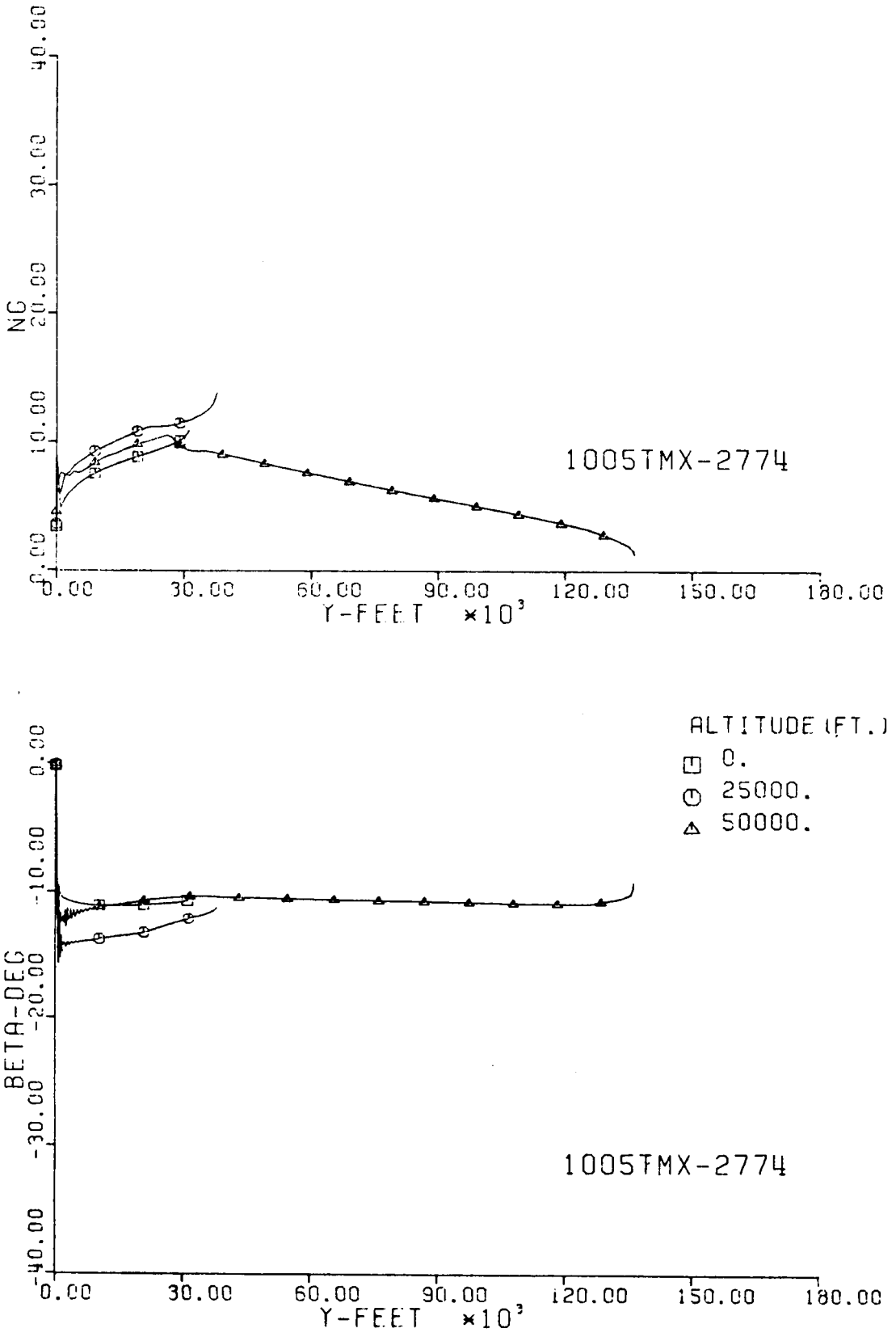

Fig. 14-III. Number of G's and Sideslip Angle vs. Downrange Distance, Y.

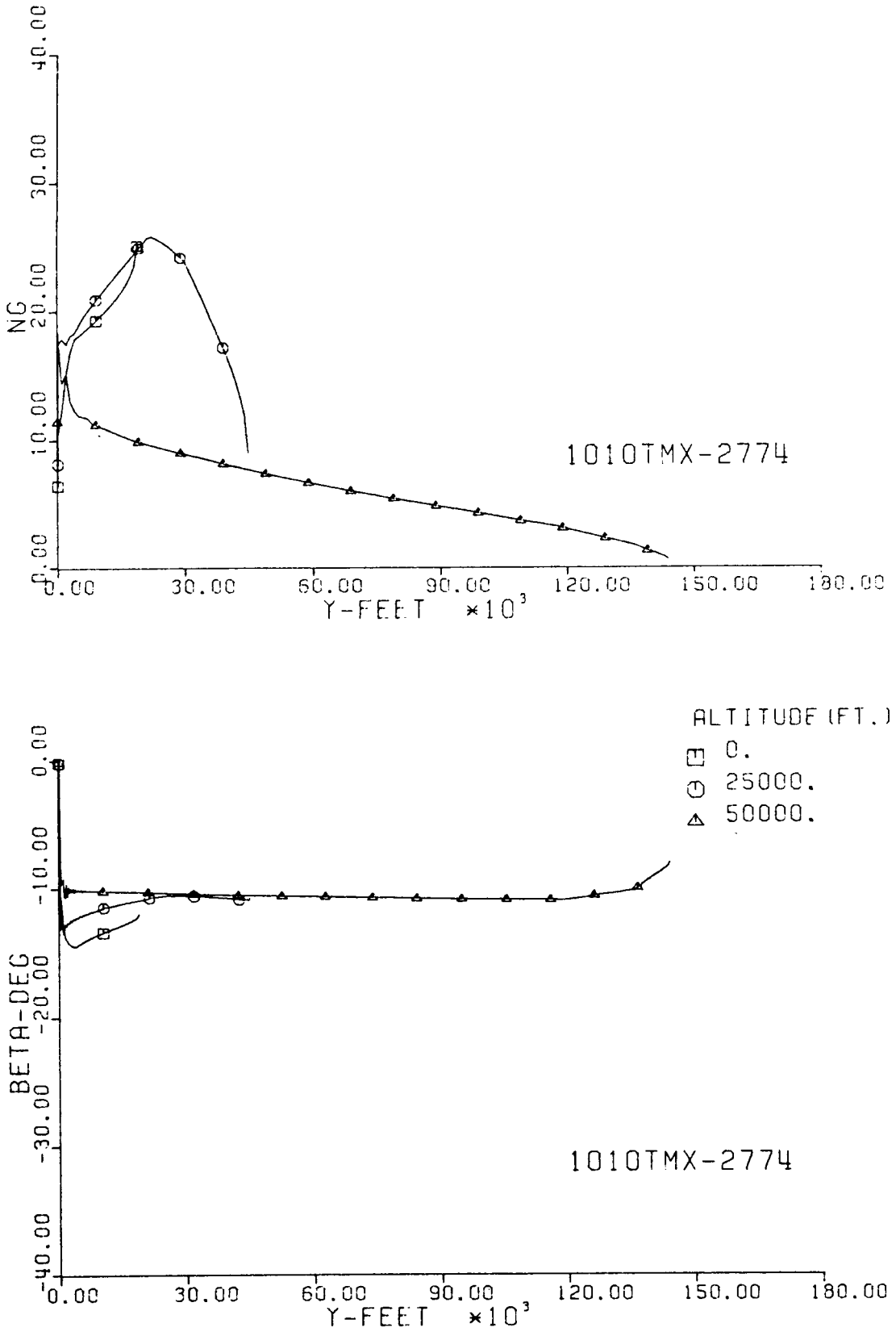

Fig. 15-III. Number of G's and Sideslip Angle vs. Downrange Distance, Y.

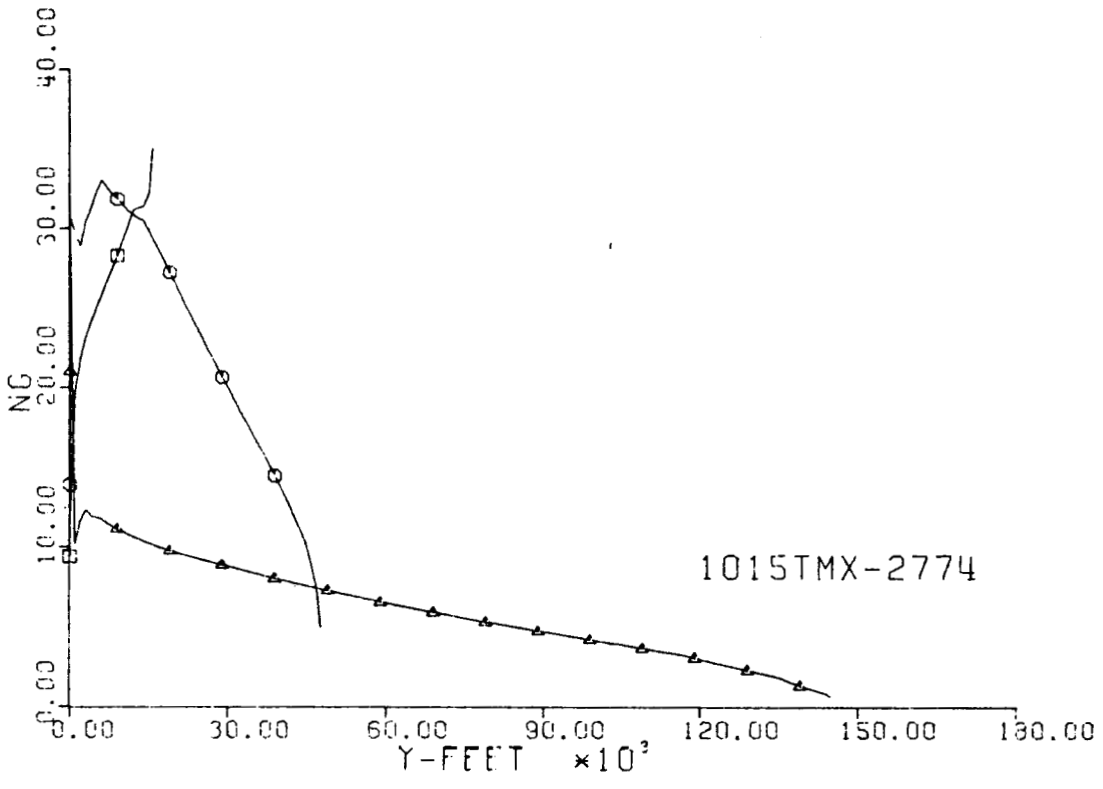

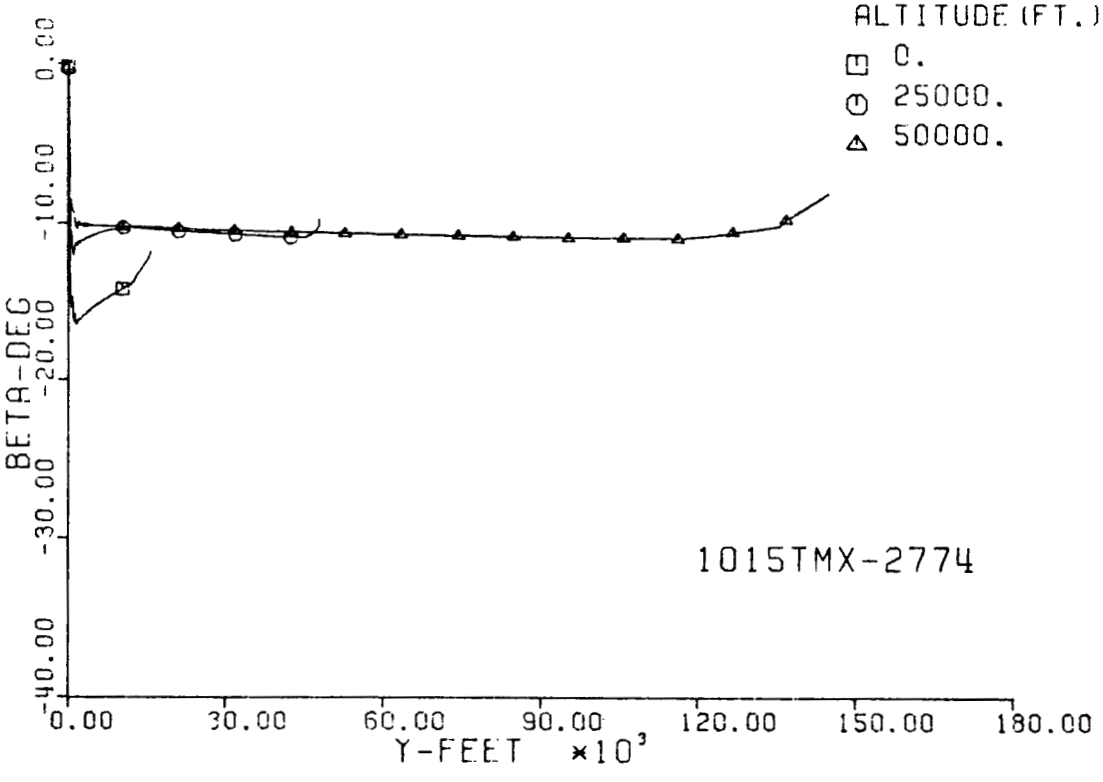

Fig. 16-III. Number of G's and Sideslip Angle vs. Downrange Distance, Y.

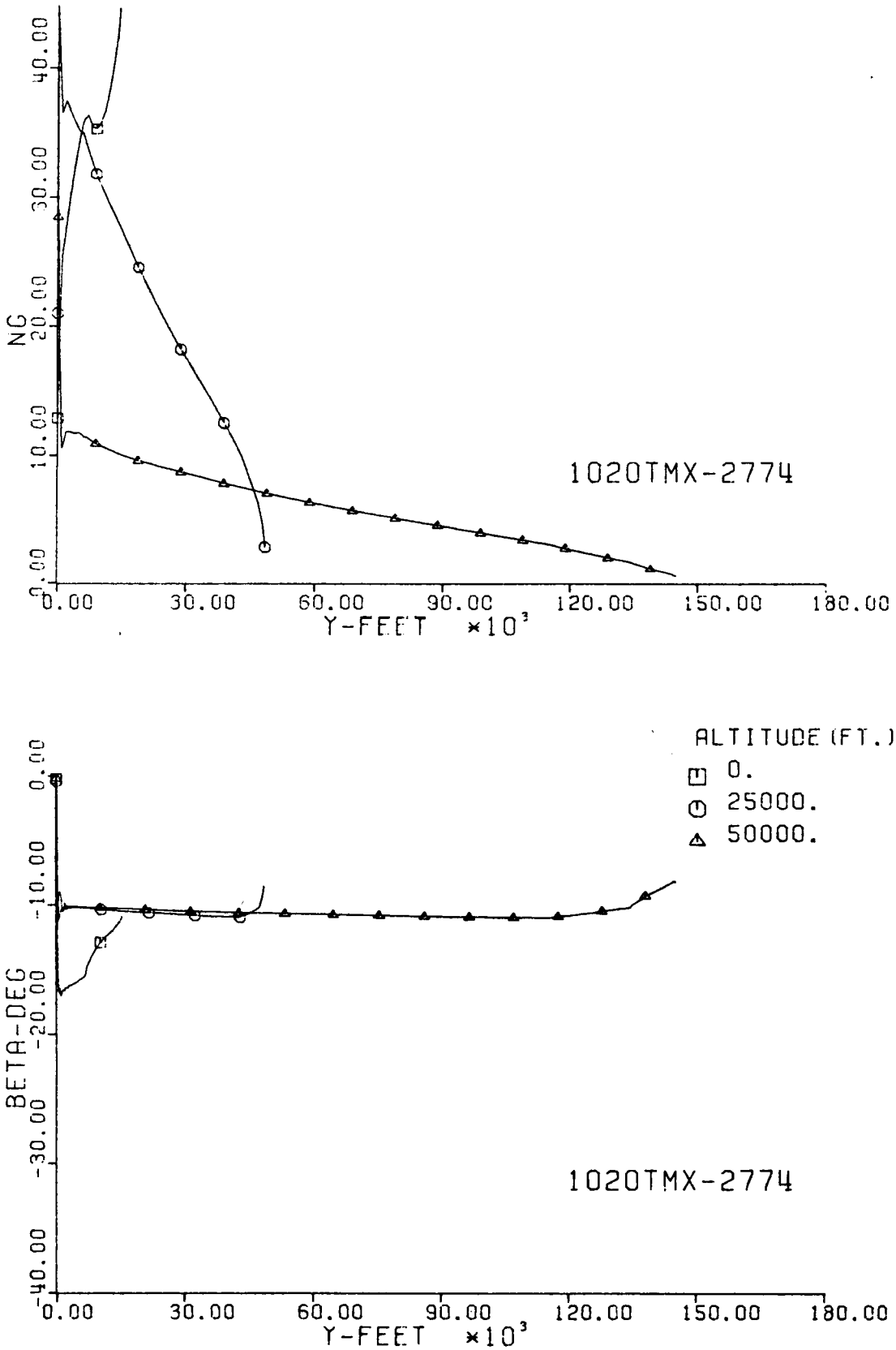

Fig. 17-III. Number of G's and Sideslip Angle vs. Downrange Distance, Y.

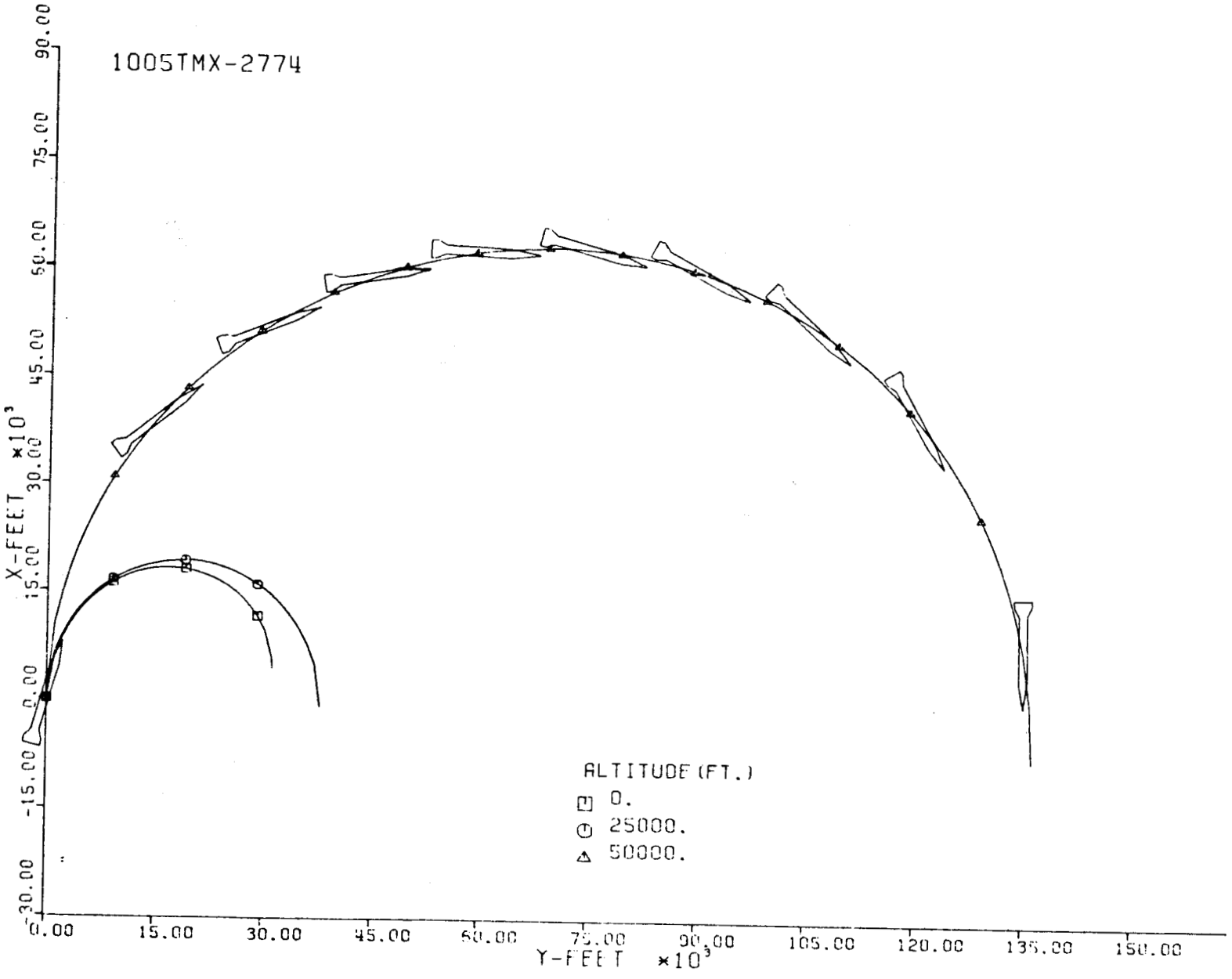

Fig. 18-III Constant Altitude Flight Path, X vs. Y.

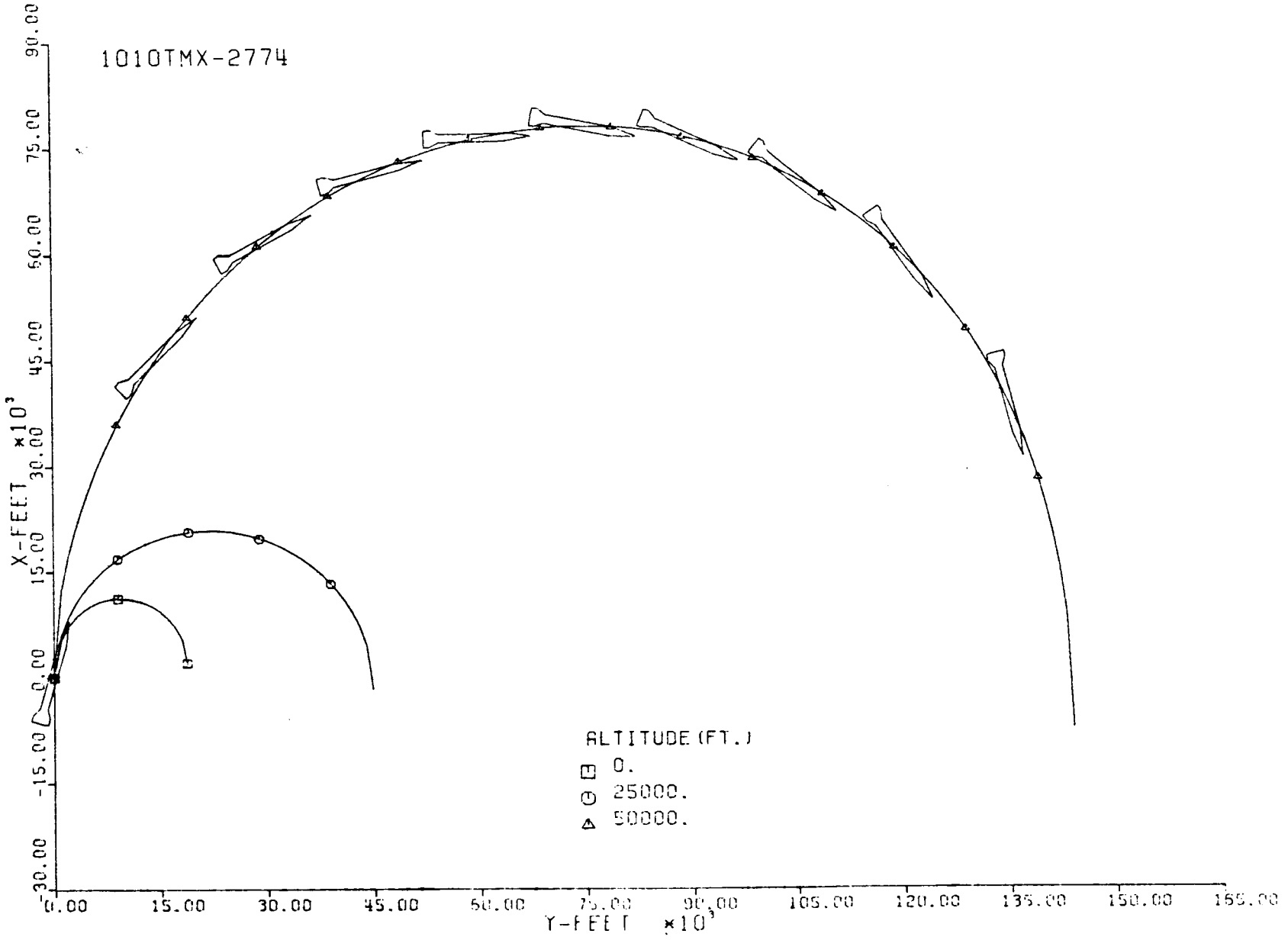

Fig. 19-III. Constant Altitude Flight Path, X vs. Y.

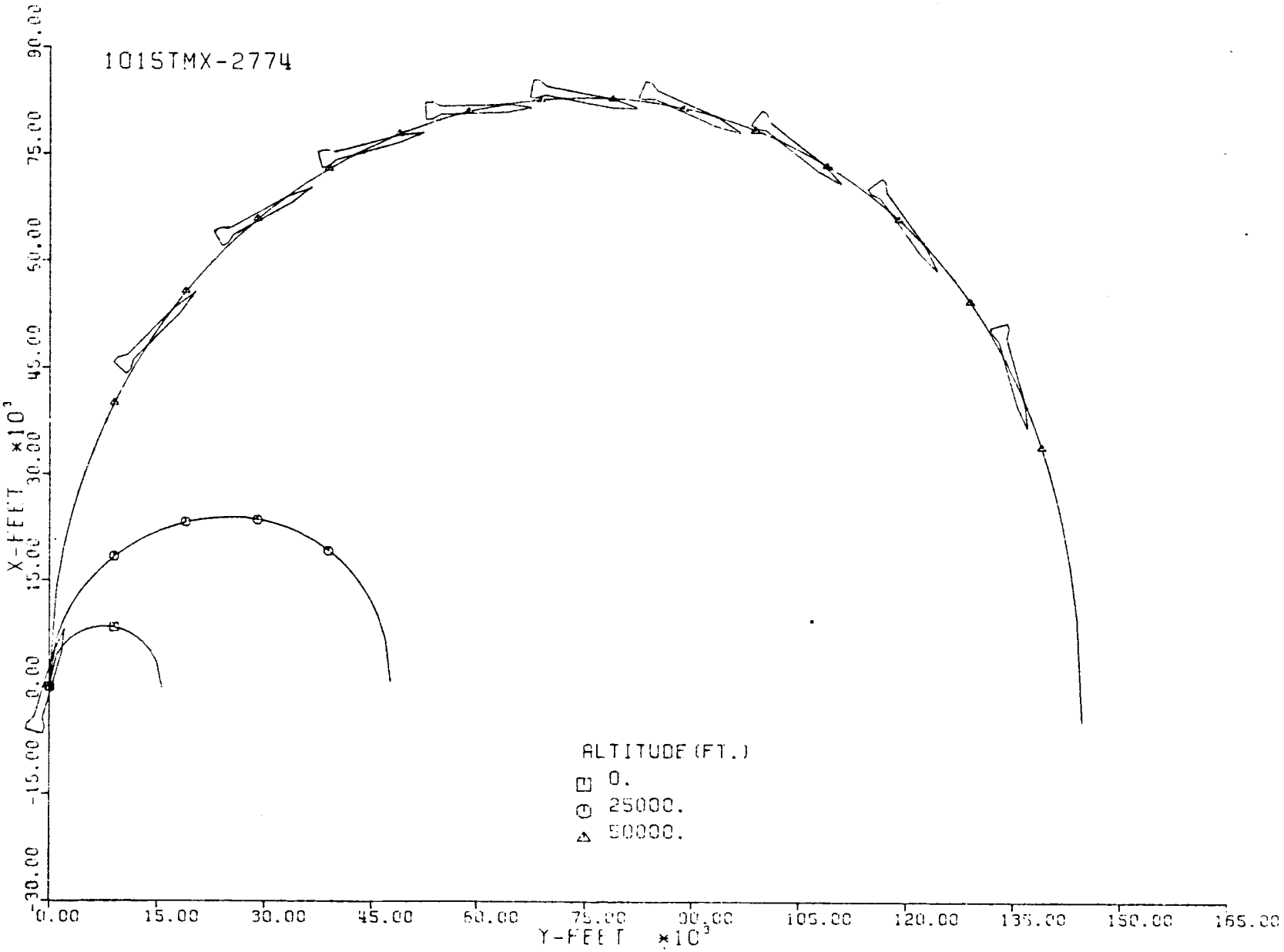

Fig. 20-III. Constant Altitude Flight Path, X vs. Y.

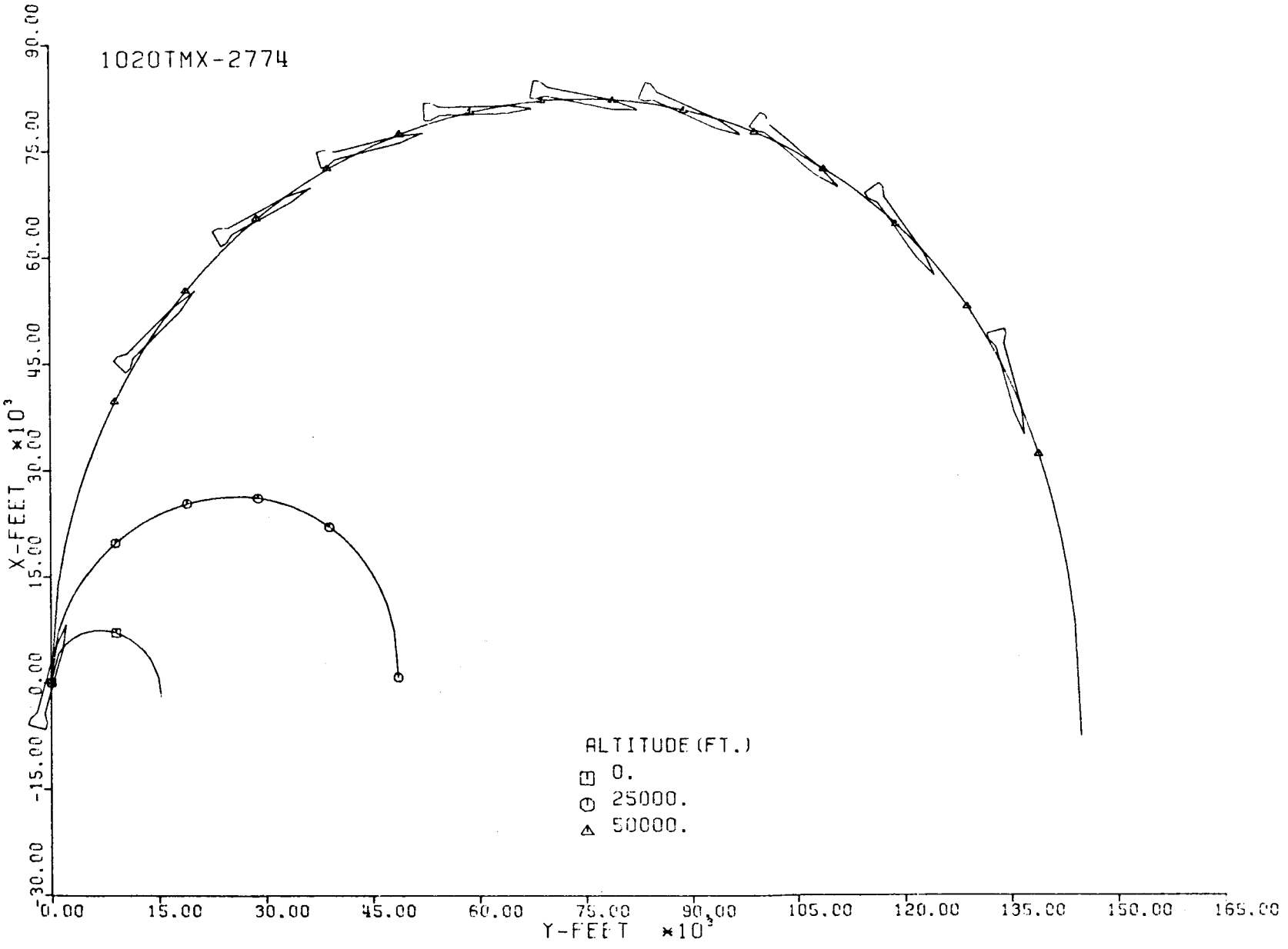

Fig. 21-III. Constant Altitude Flight Path, X vs. Y.

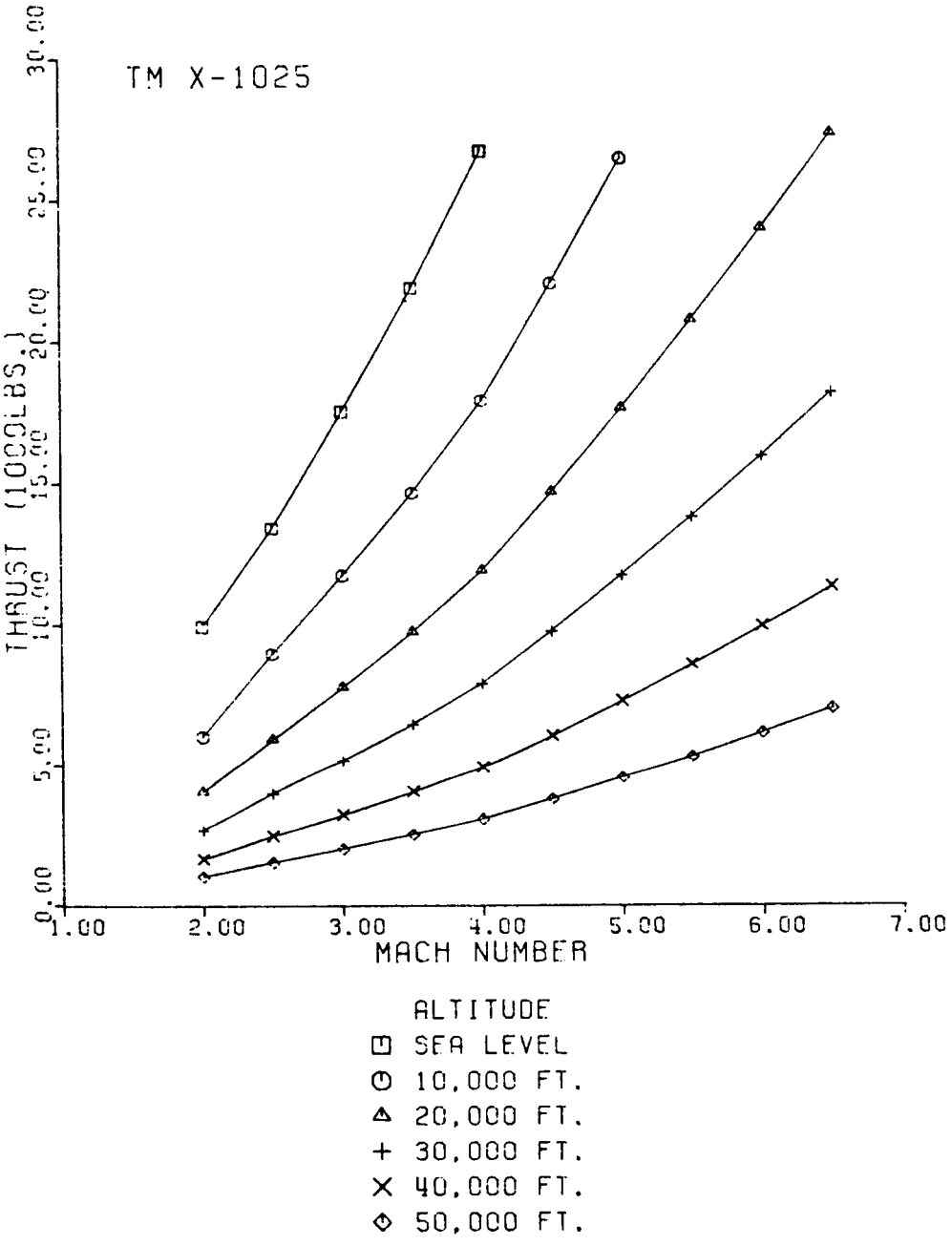

Fig. 22-I. Thrust vs. Terminal Mach No.

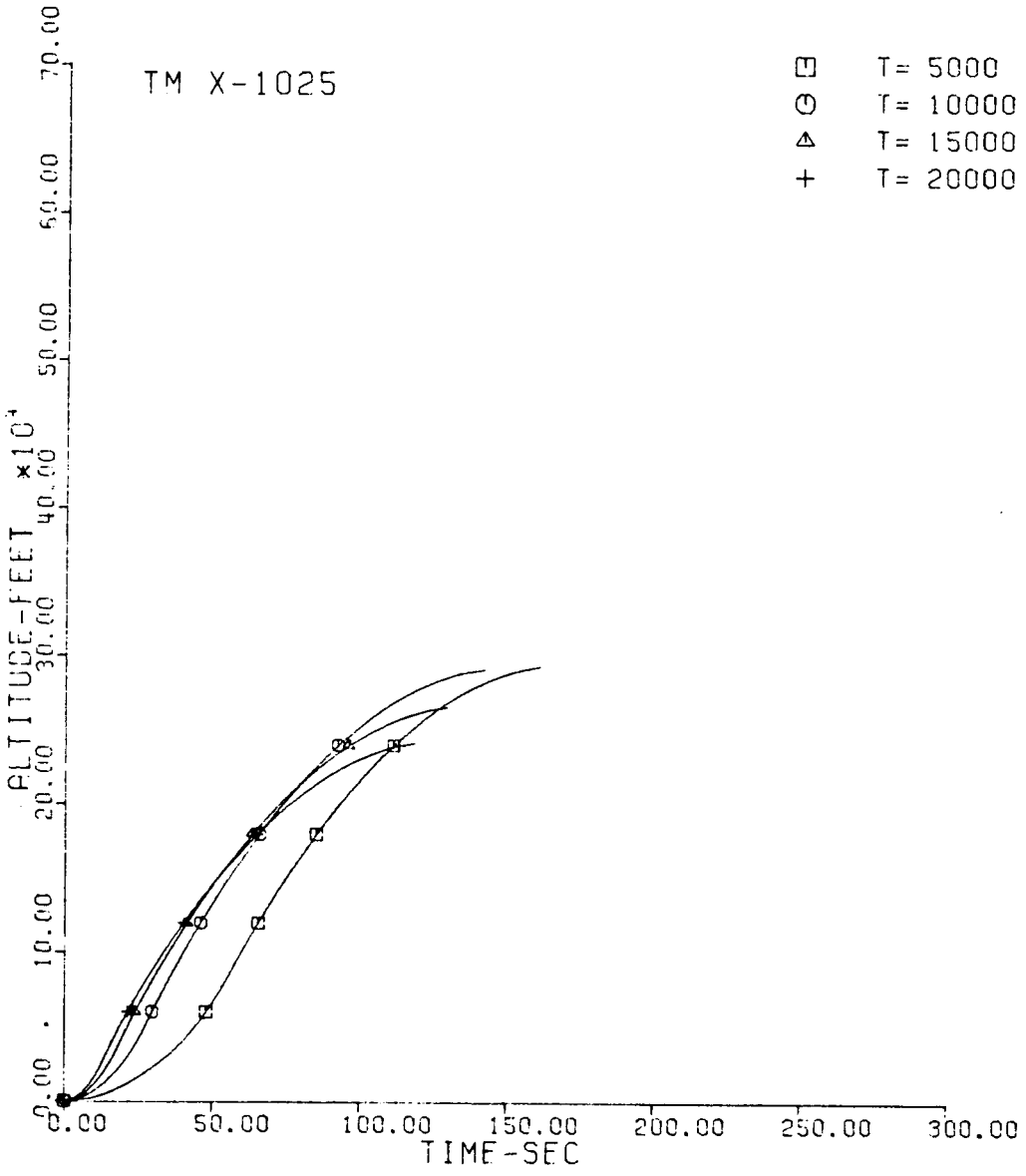

Fig. 23-II. Altitude vs. Flight Time.

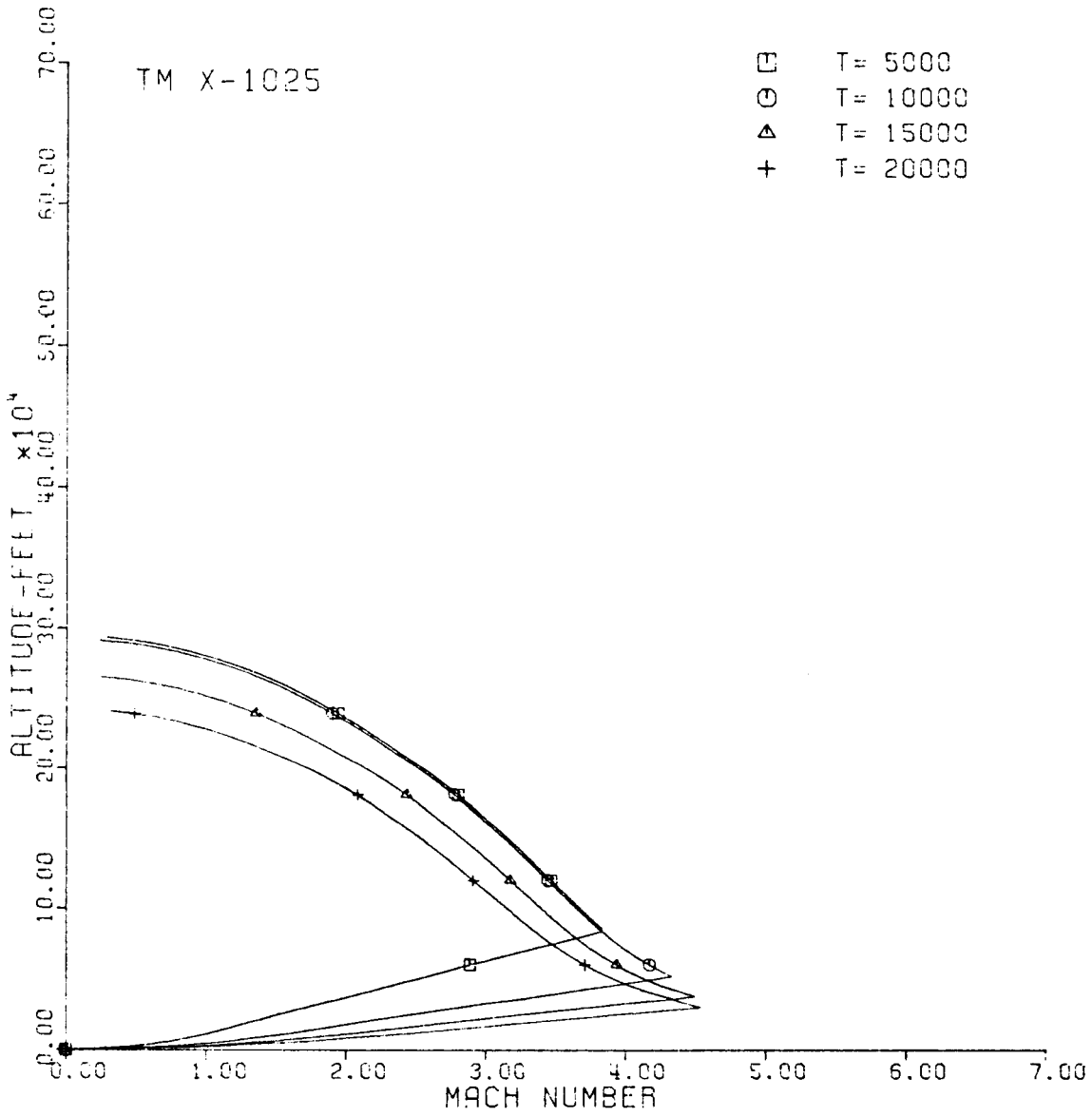

Fig. 24-II. Altitude vs. Mach No.

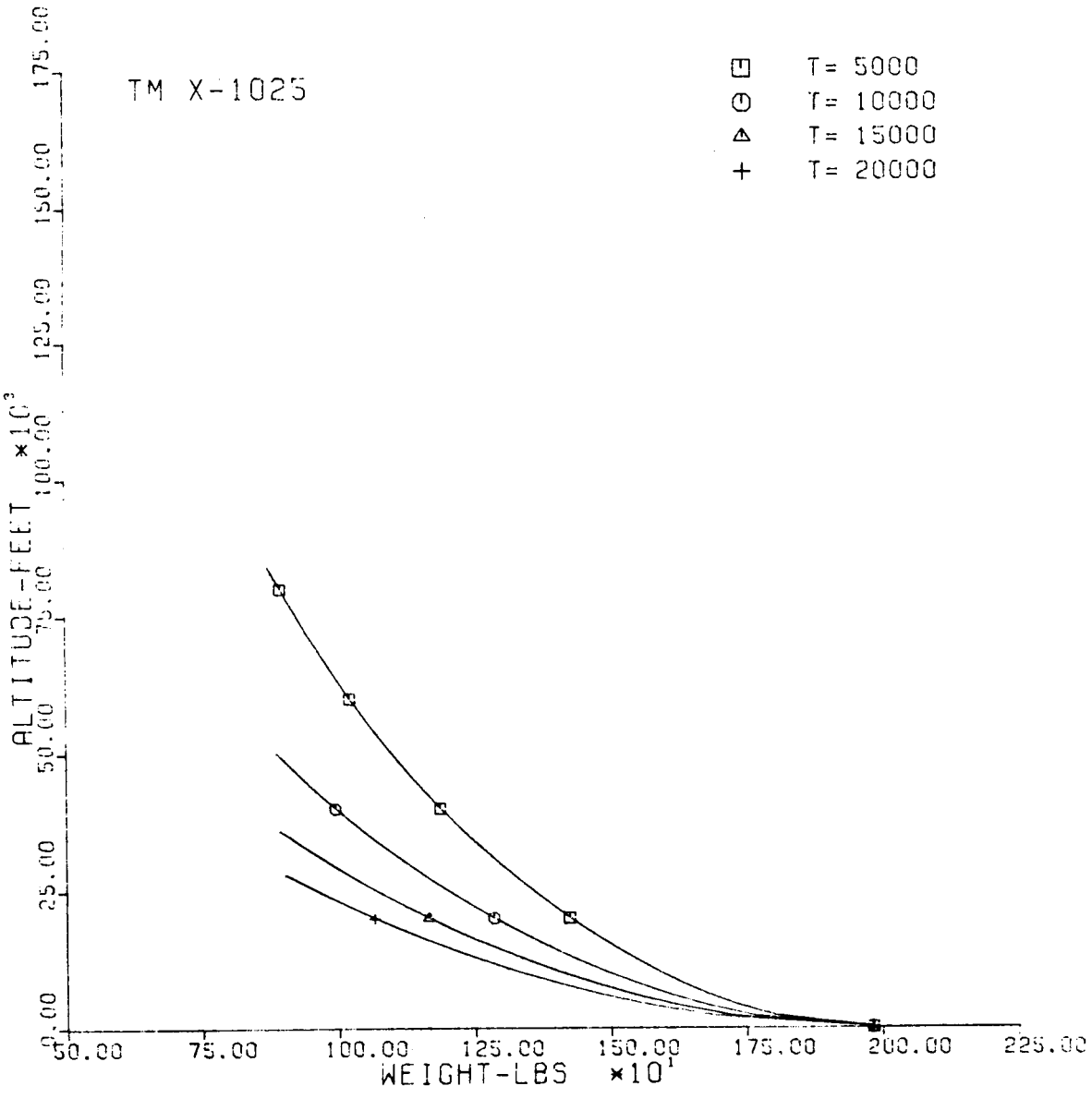

Fig. 25-II. Altitude vs. Vehicle Weight.

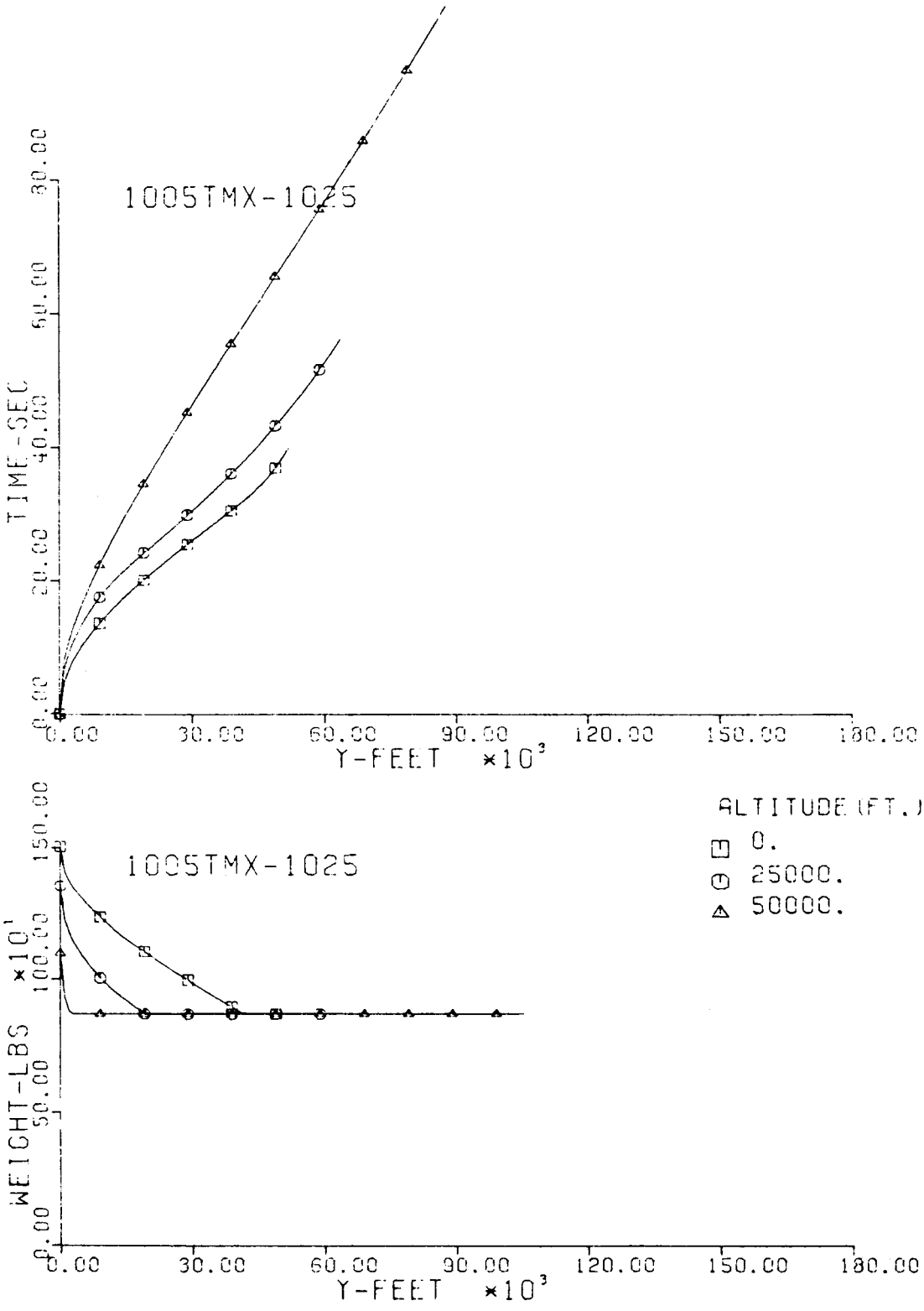

Fig. 26-III. Flight Time and Vehicle Weight vs. Downrange Distance, Y.

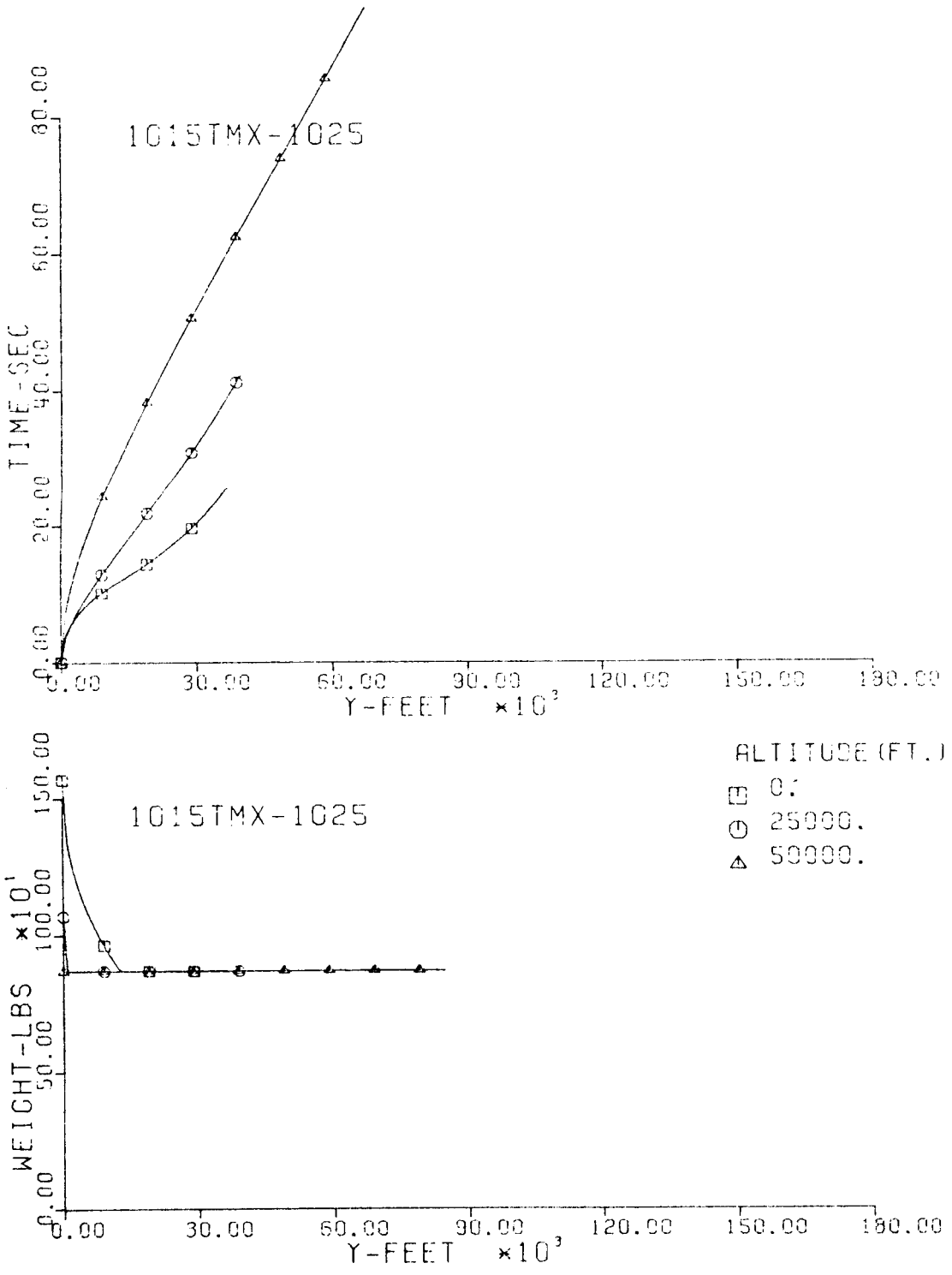

Fig. 27-III. Flight Time and Vehicle Weight vs. Downrange Distance, Y.

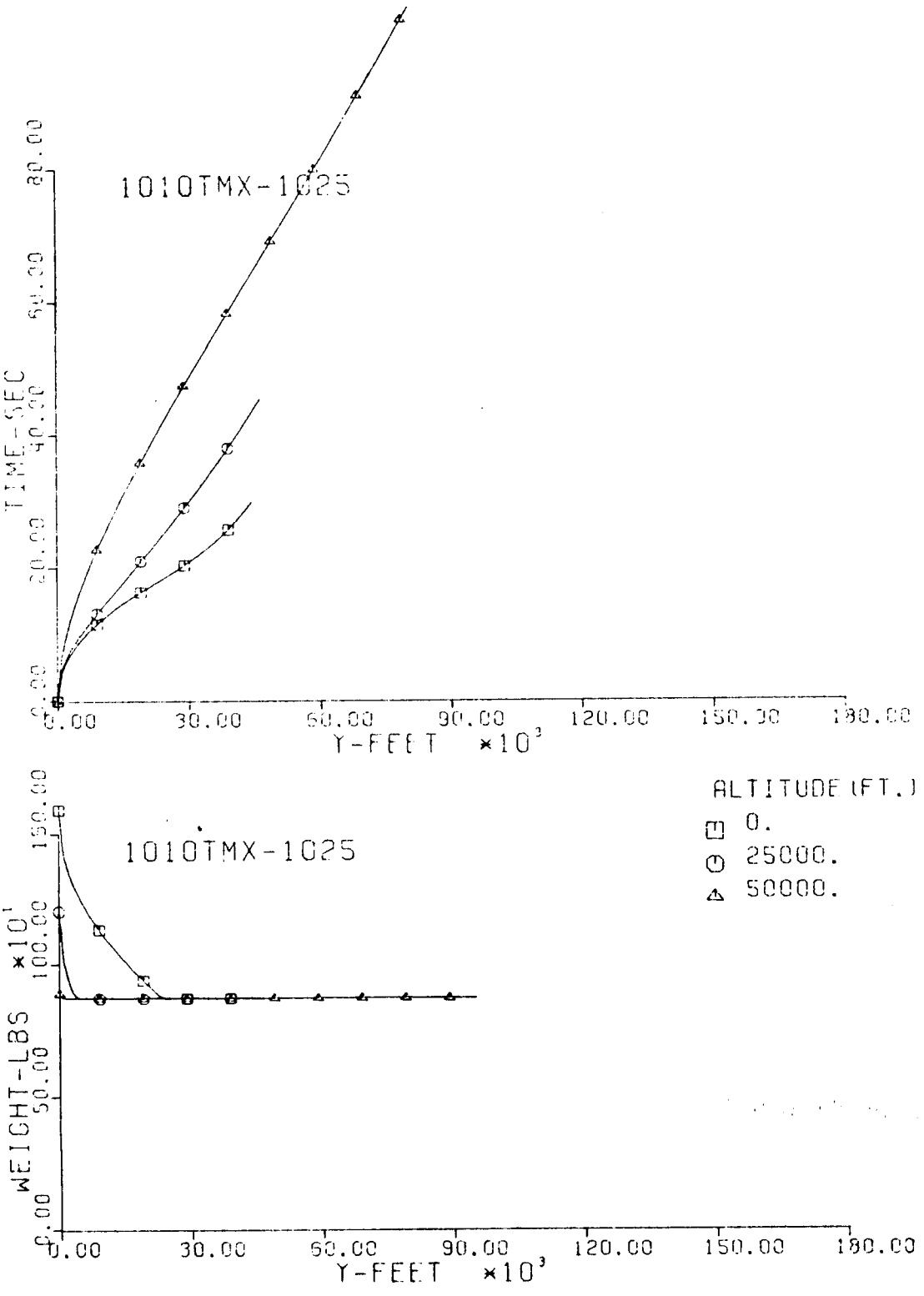

Fig. 28-III. Flight Time and Vehicle Weight vs. Downrange Distance, Y.

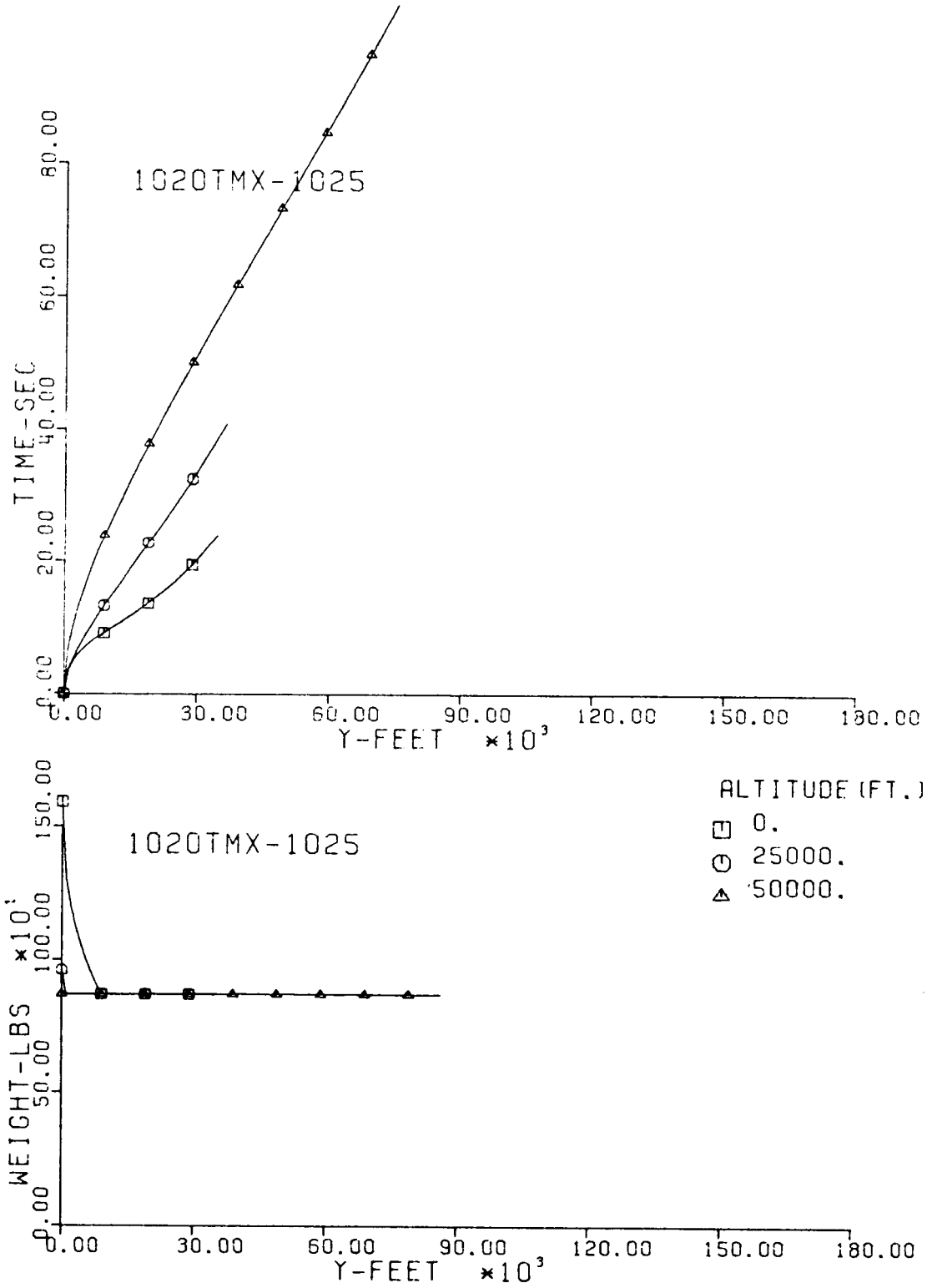

Fig. 29-III. Flight Time and Vehicle Weight vs. Downrange Distance, Y.

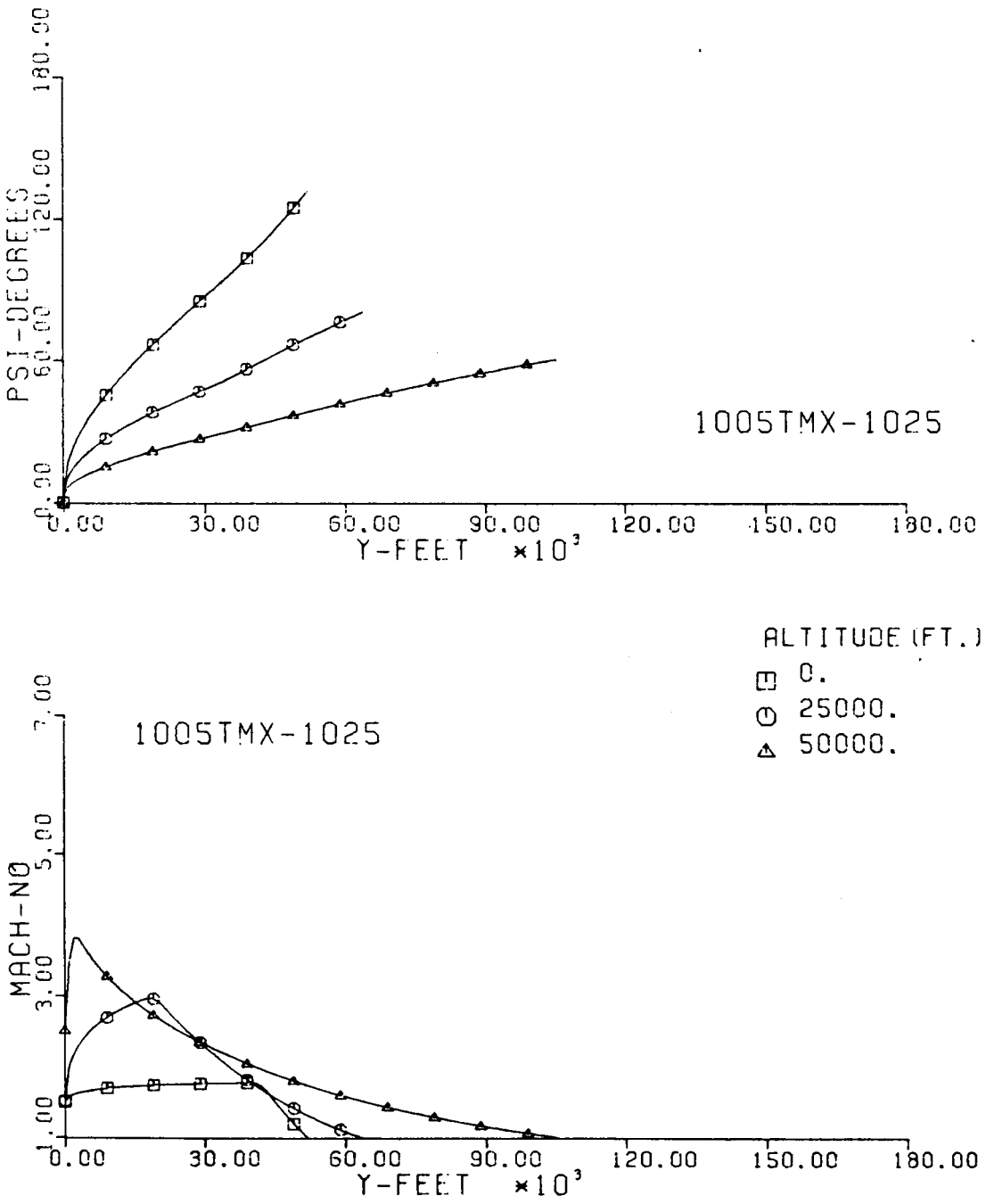

Fig. 30-III. Heading Angle and Mach No. vs. Downrange Distance, Y.

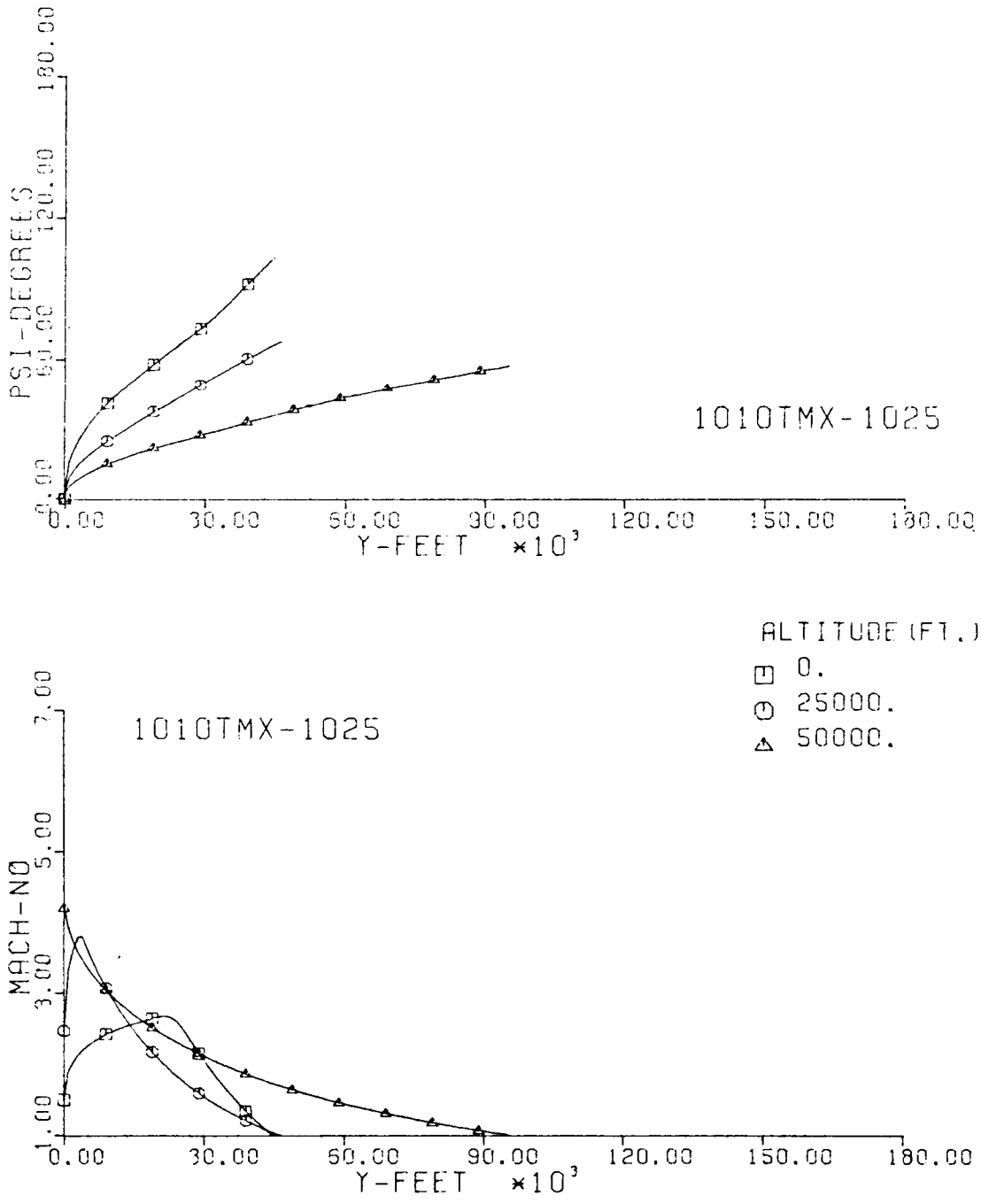

Fig. 31-III. Heading Angle and Mach No. vs. Downrange Distance, Y.

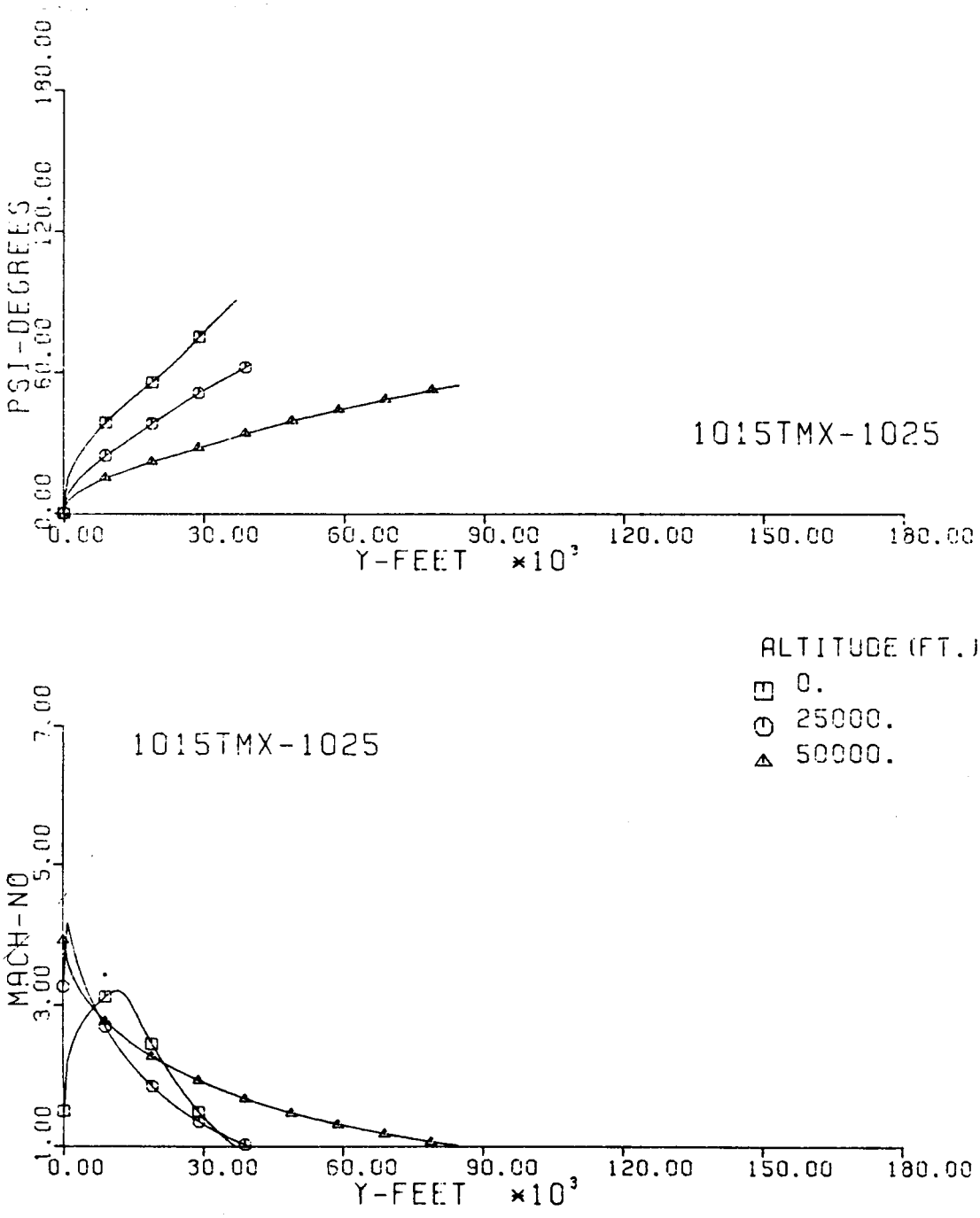

Fig. 32-III. Heading Angle and Mach No. vs. Downrange Distance, Y.

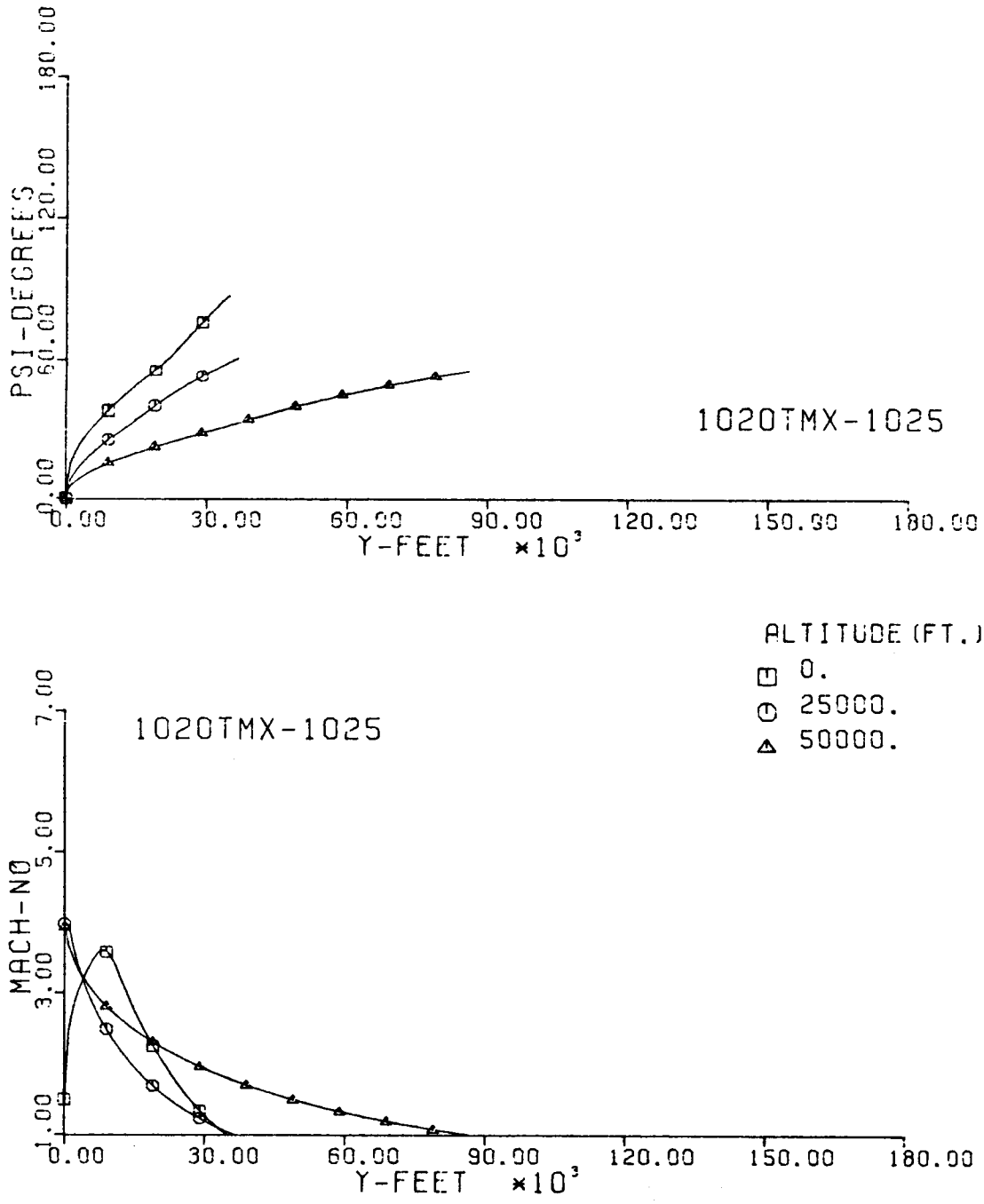

Fig. 33-III. Heading Angle and Mach No. vs. Downrange Distance, Y.

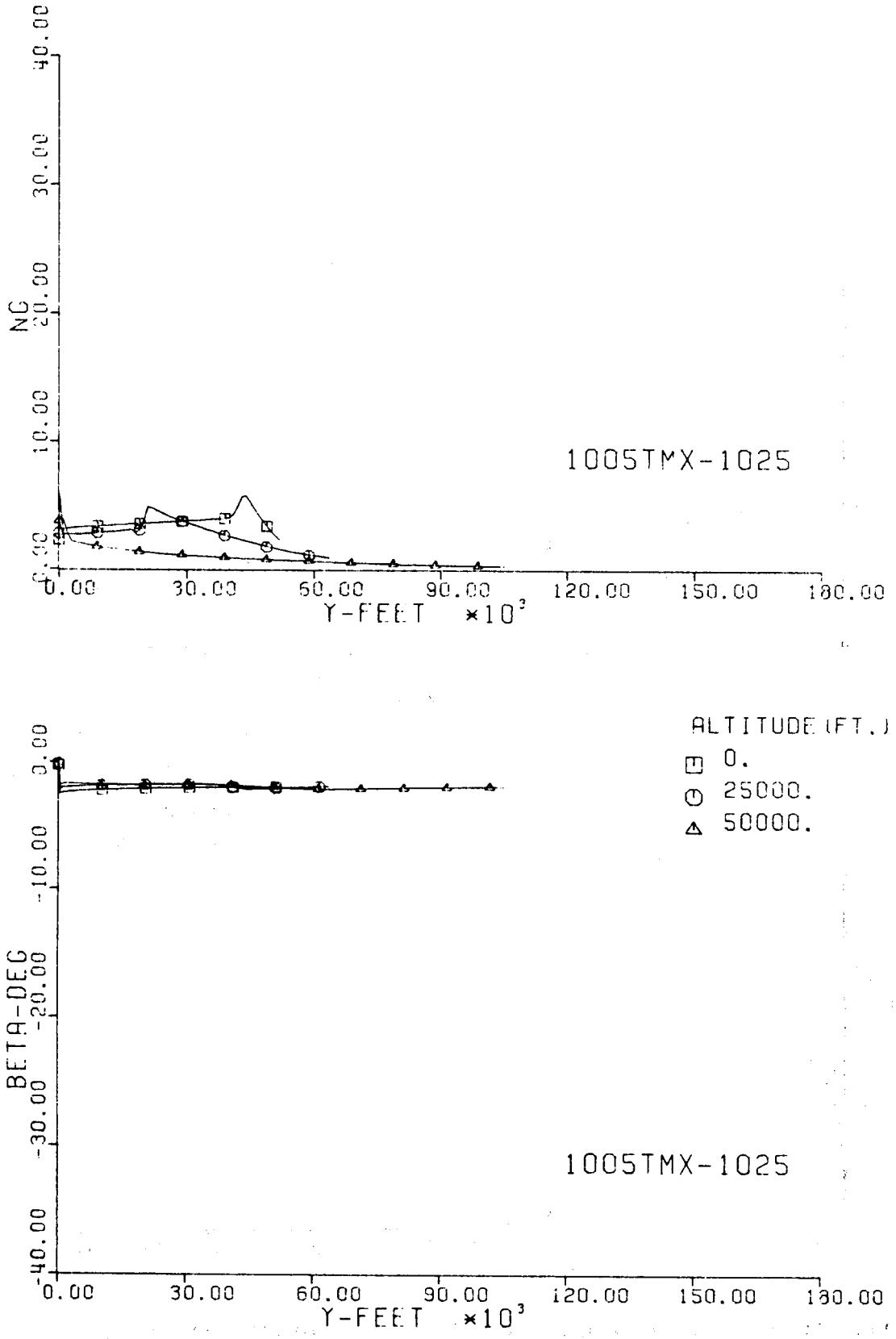

Fig. 34-III. Number of G's and Sideslip Angle vs. Downrange Distance, Y.

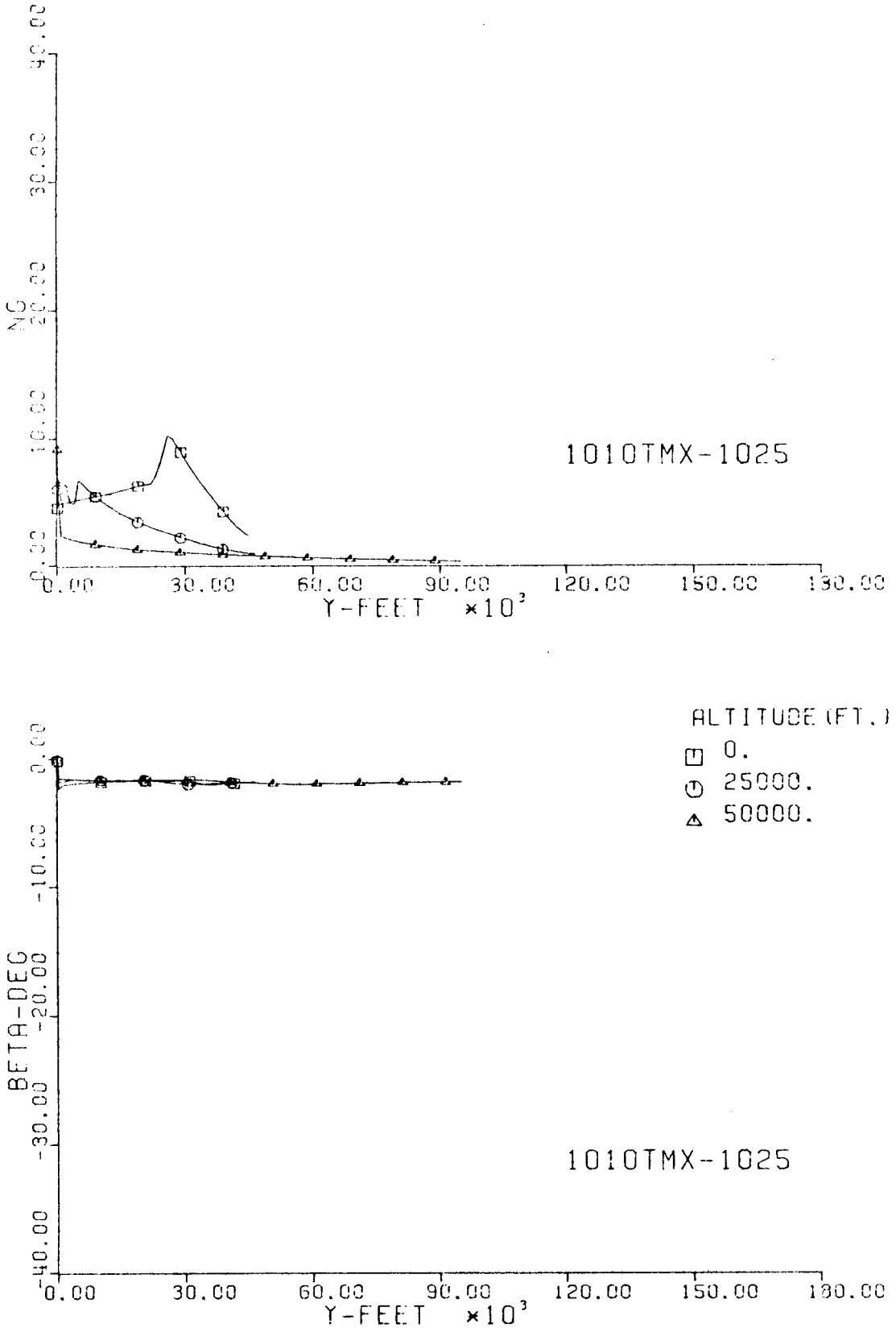

Fig. 35-III. Number of G's and Sideslip Angle vs. Downrange Distance, Y.

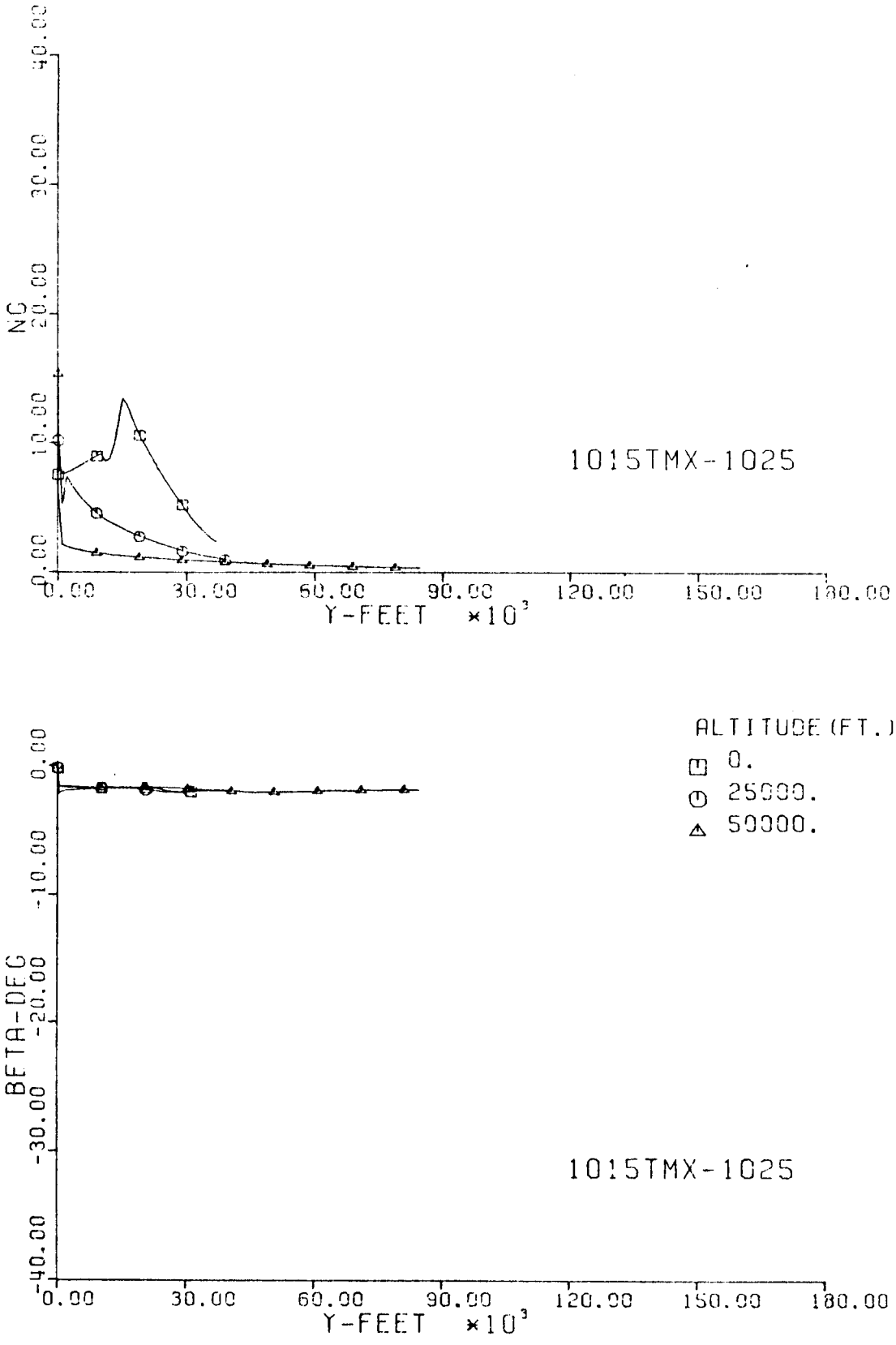

Fig. 36-III. Number of G's and Sideslip Angle vs. Downrange Distance, Y.

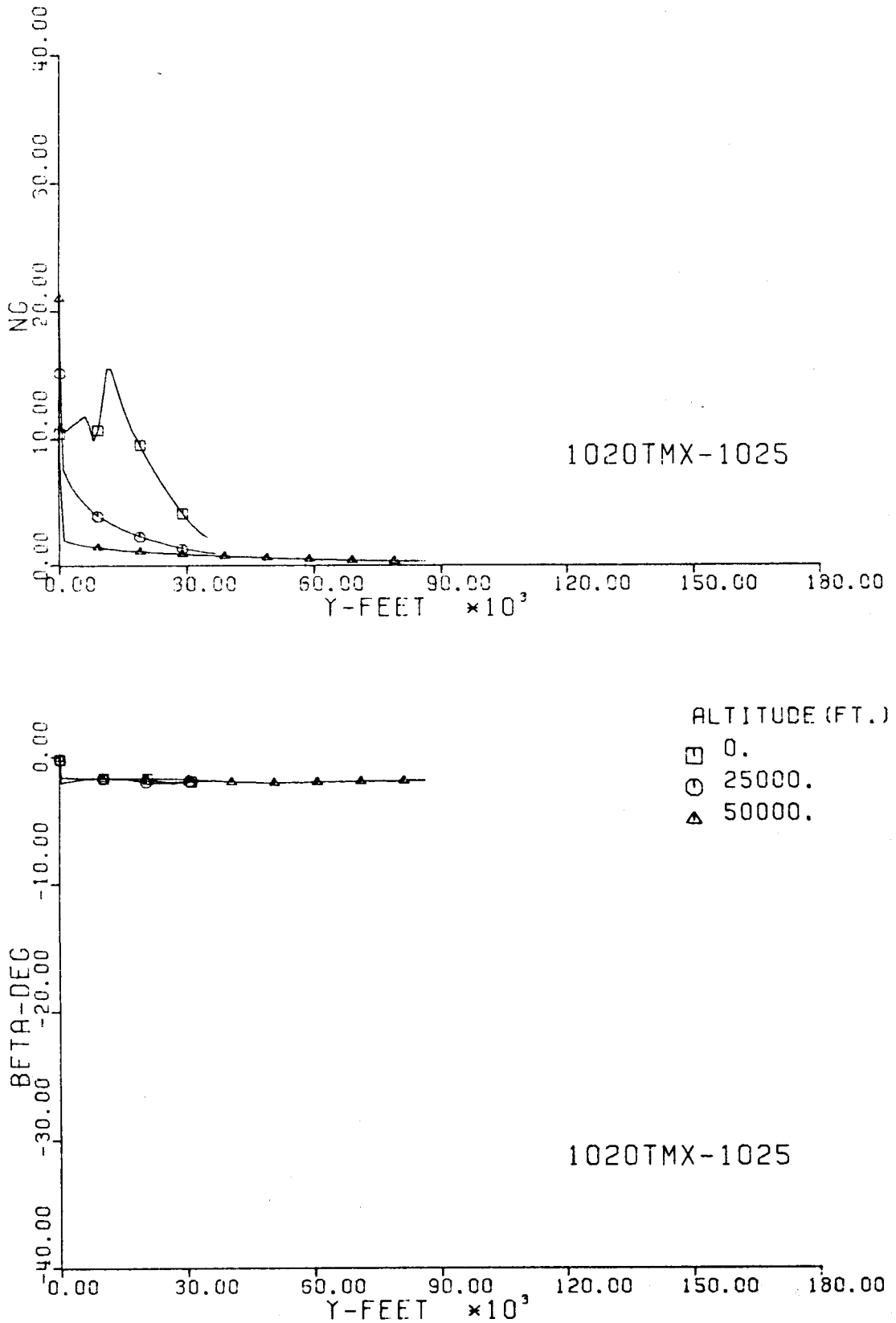

Fig. 37-III. Number of G's and Sideslip Angle vs. Downrange Distance, Y.

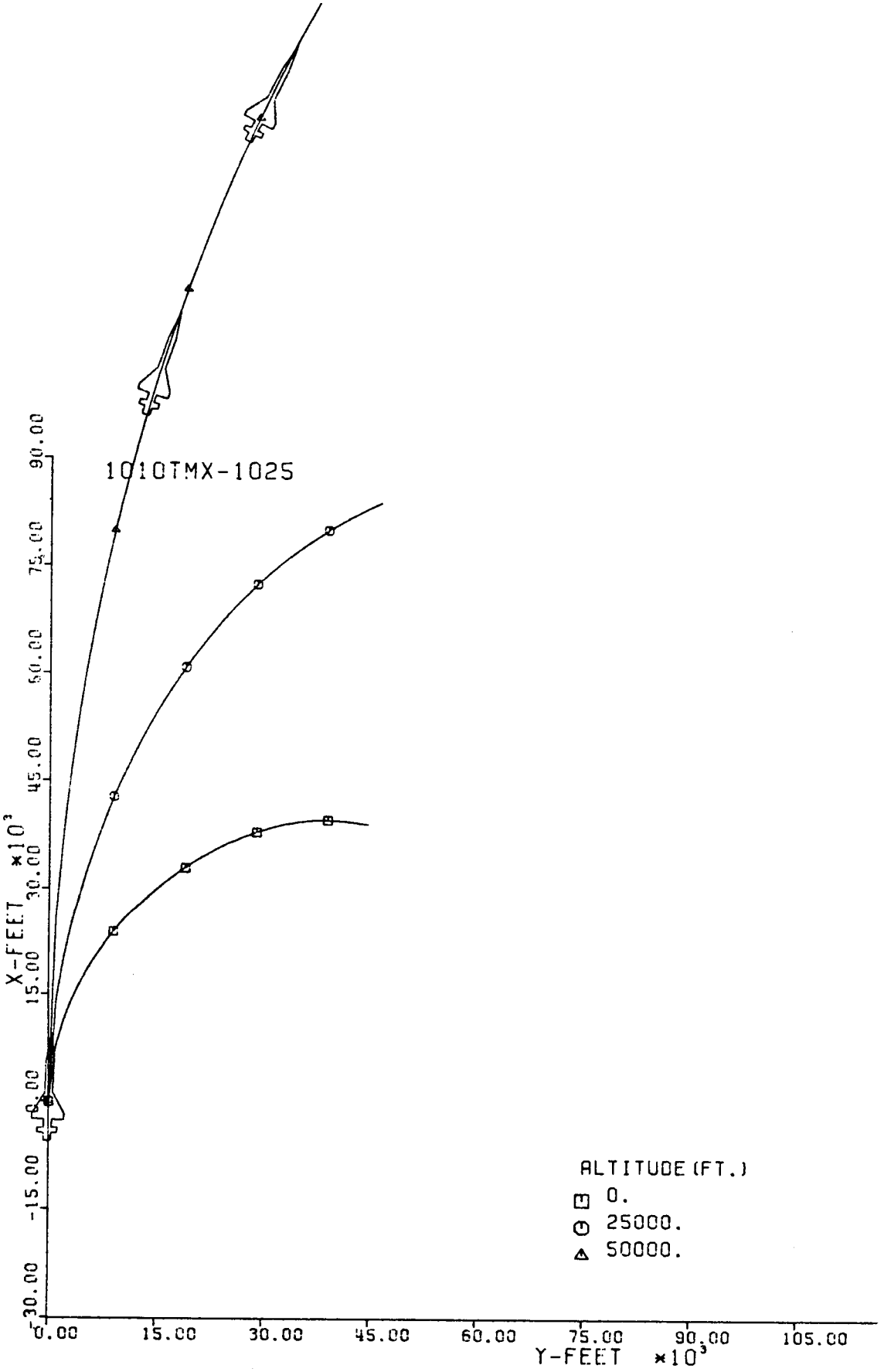

Fig. 39-III. Constant Altitude Flight Path, X vs. Y.

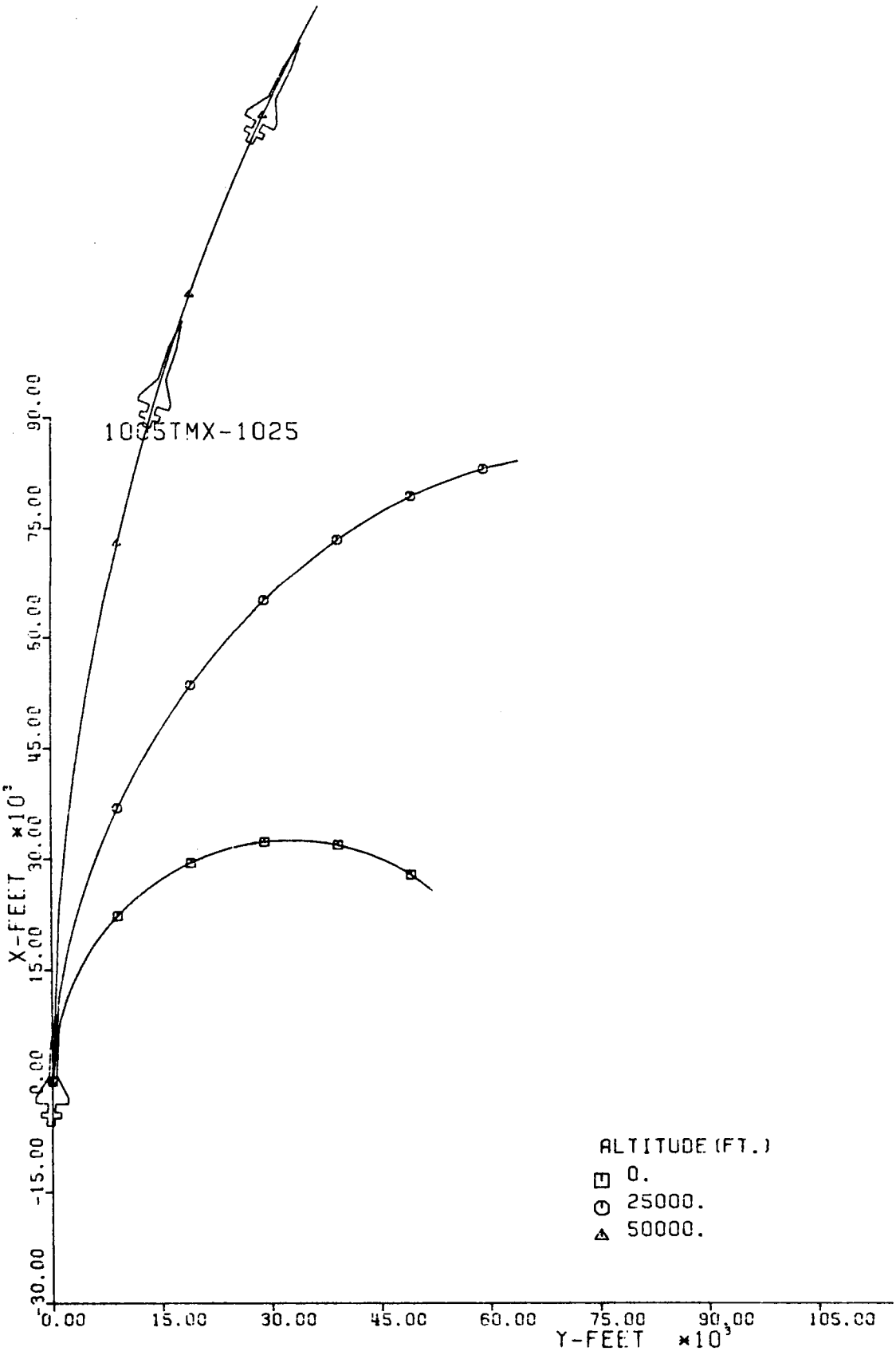

Fig. 38-III. Constant Altitude Flight Path, X vs. Y.

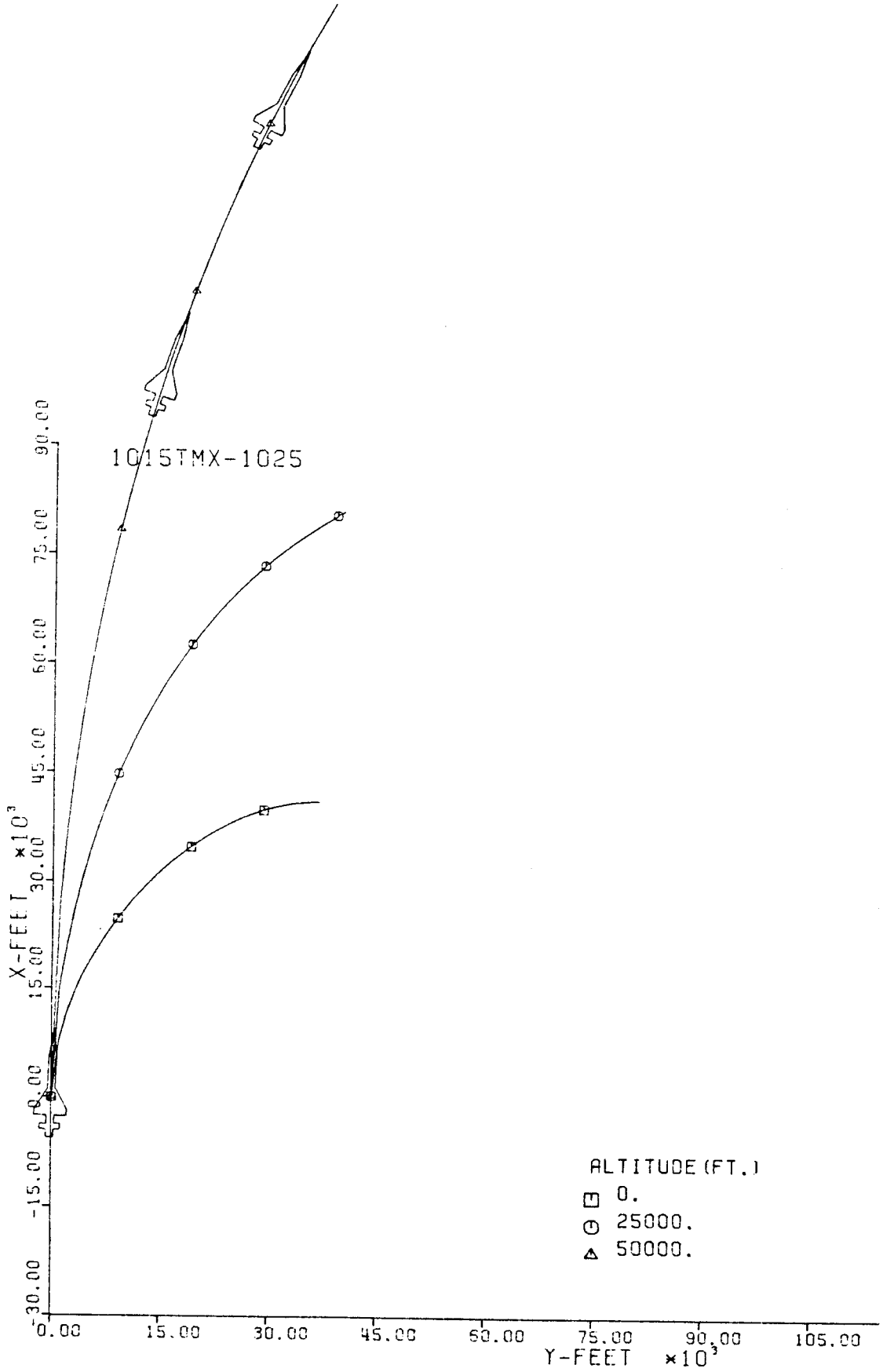

Fig. 40-III. Constant Altitude Flight Path, X vs. Y.

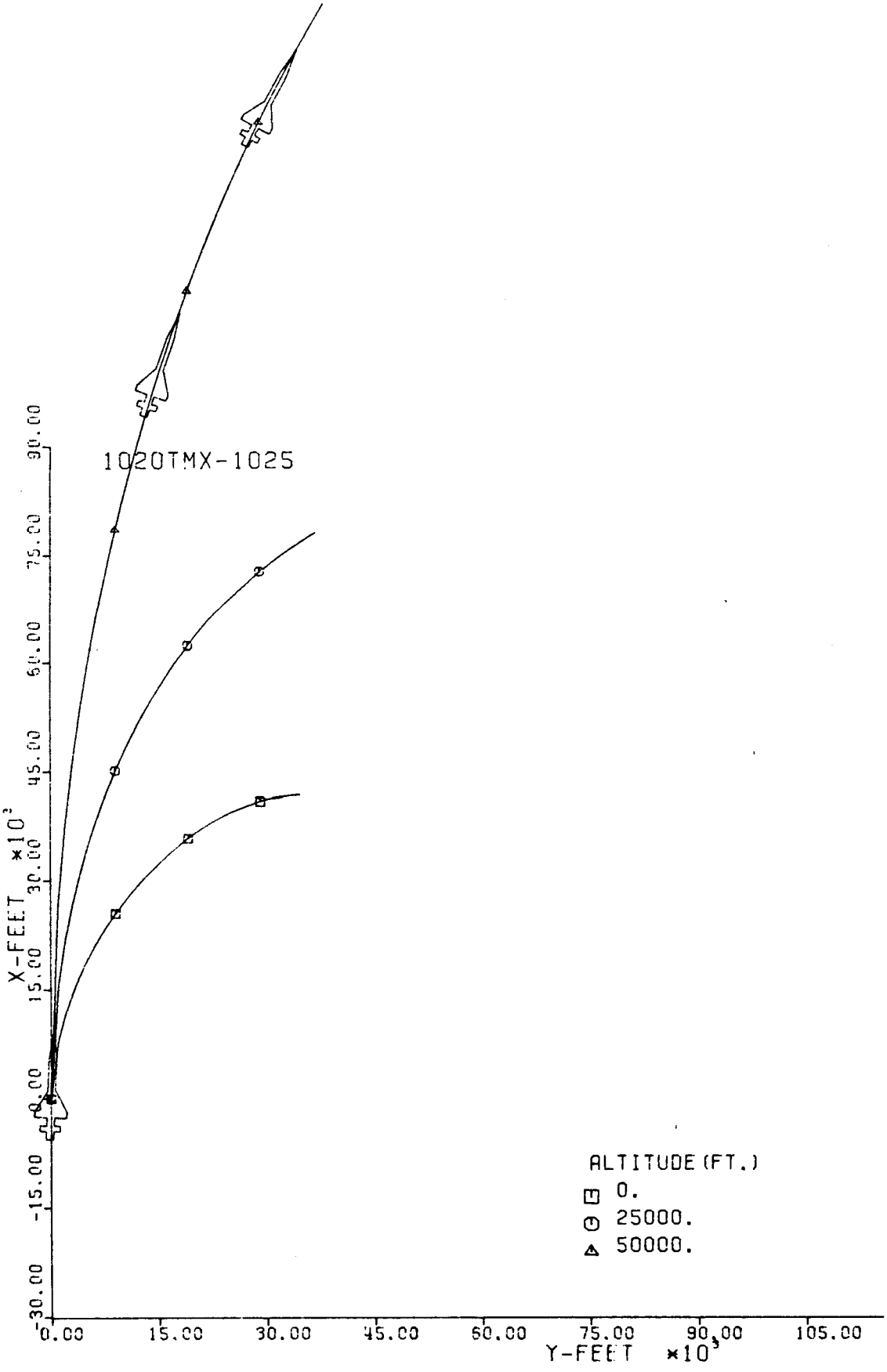

Fig. 41-III. Constant Altitude Flight Path, X vs. Y.

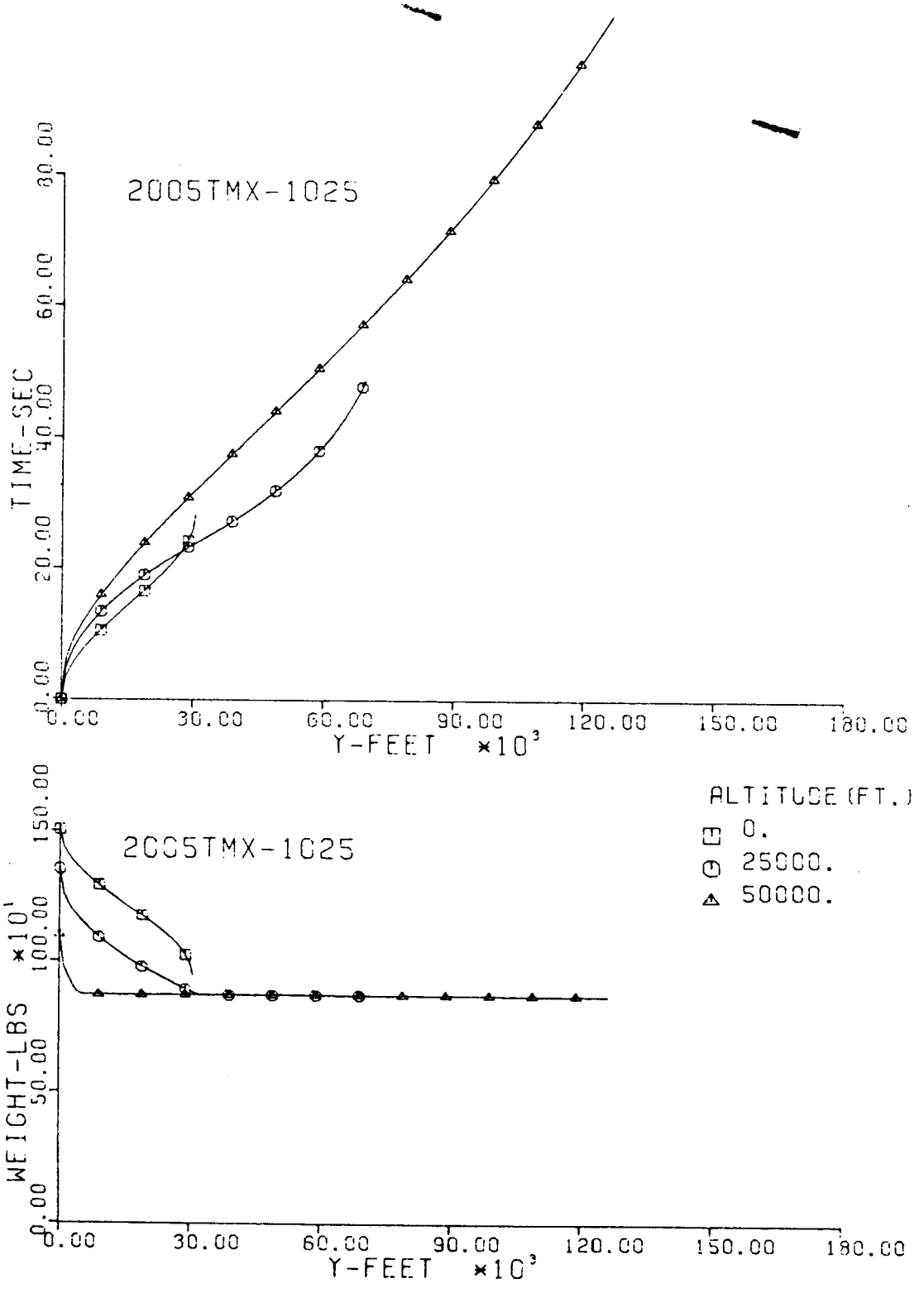

Fig. 42-III. Flight Time and Vehicle Weight vs. Downrange Distance, Y.

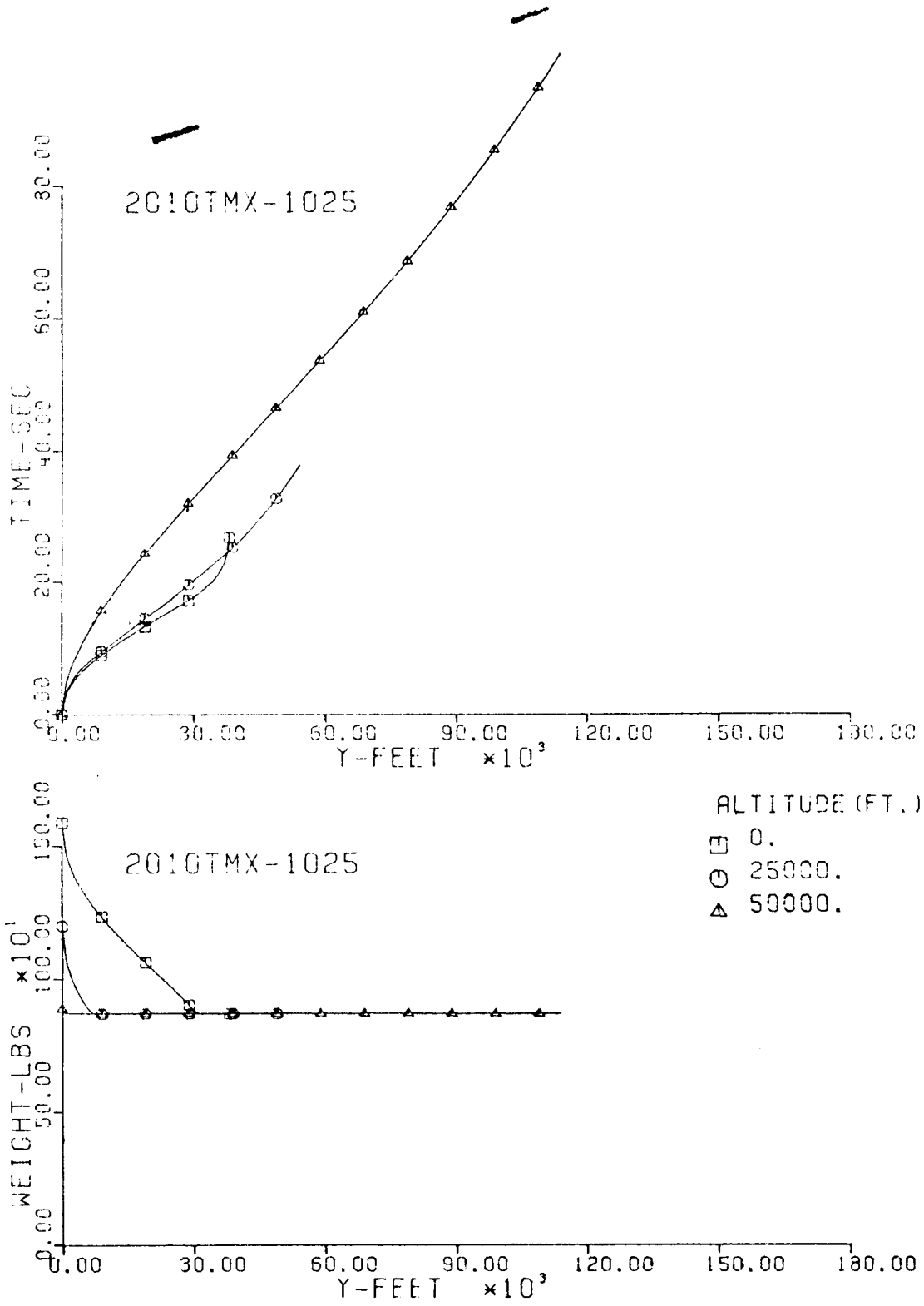

Fig. 43-III. Flight Time and Vehicle Weight vs. Downrange Distance, Y.

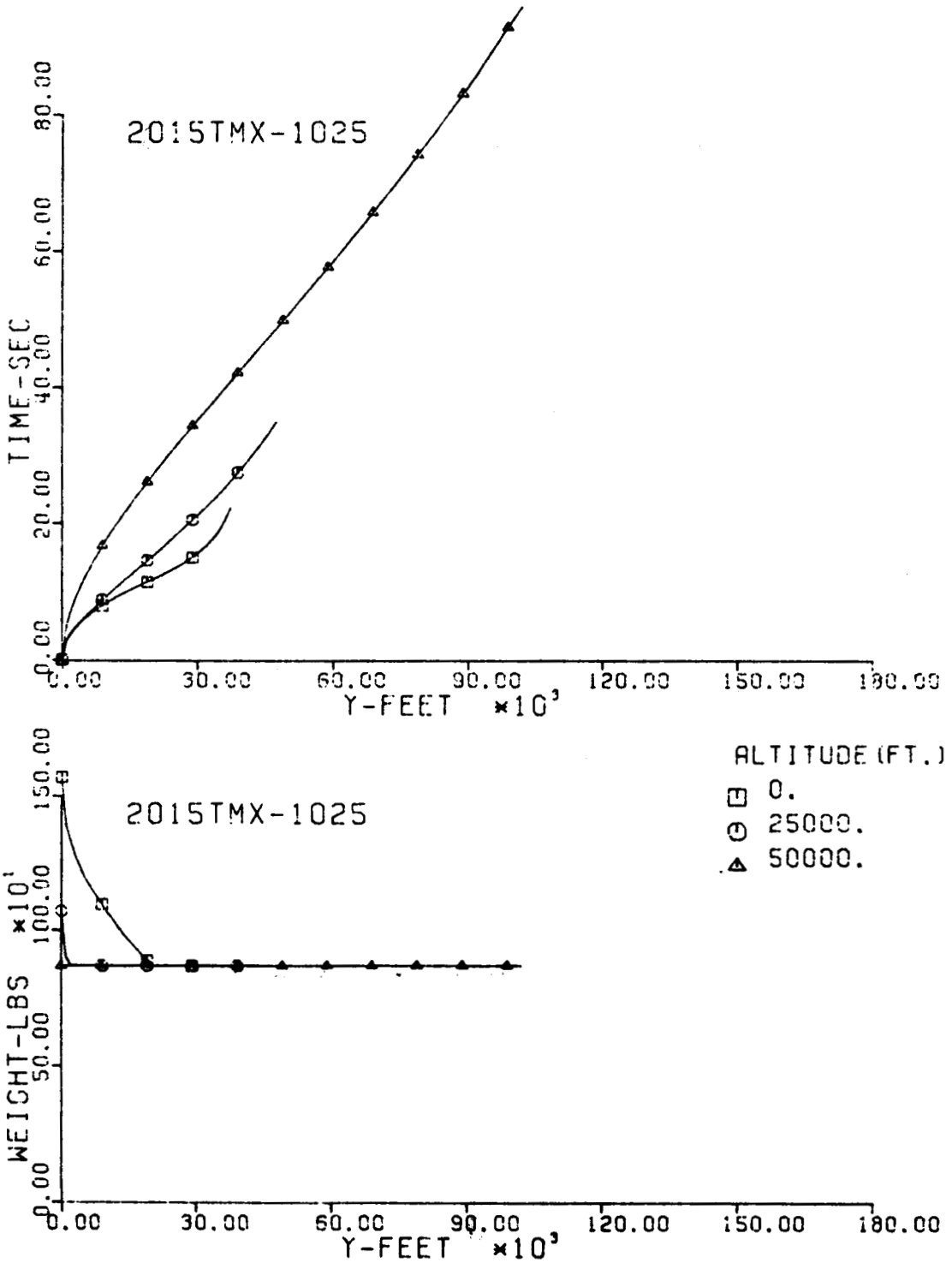

Fig. 44-III. Flight Time and Vehicle Weight vs. Downrange Distance, Y.

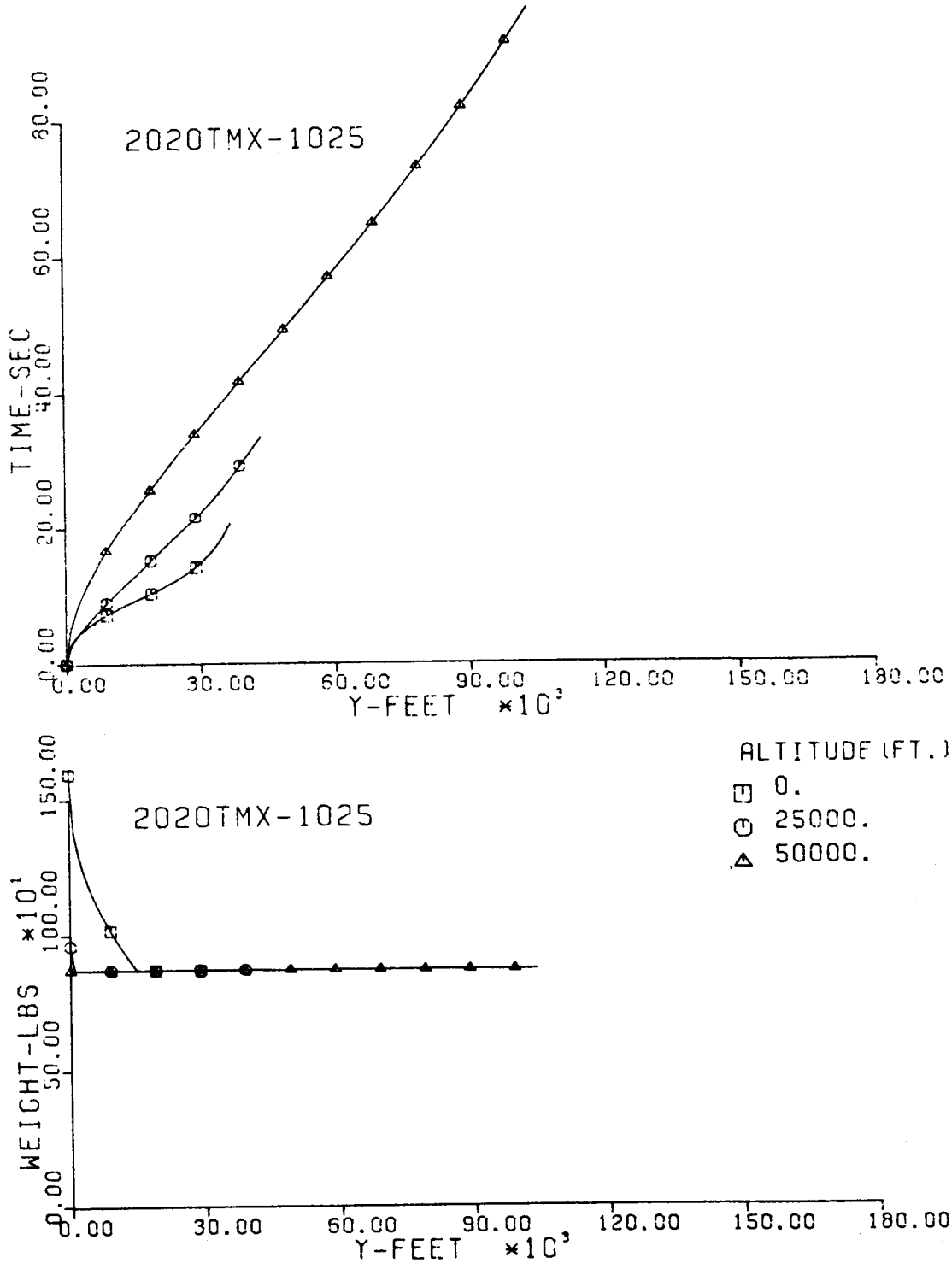

Fig. 45-III. Flight Time and Vehicle Weight vs. Downrange Distance, Y.

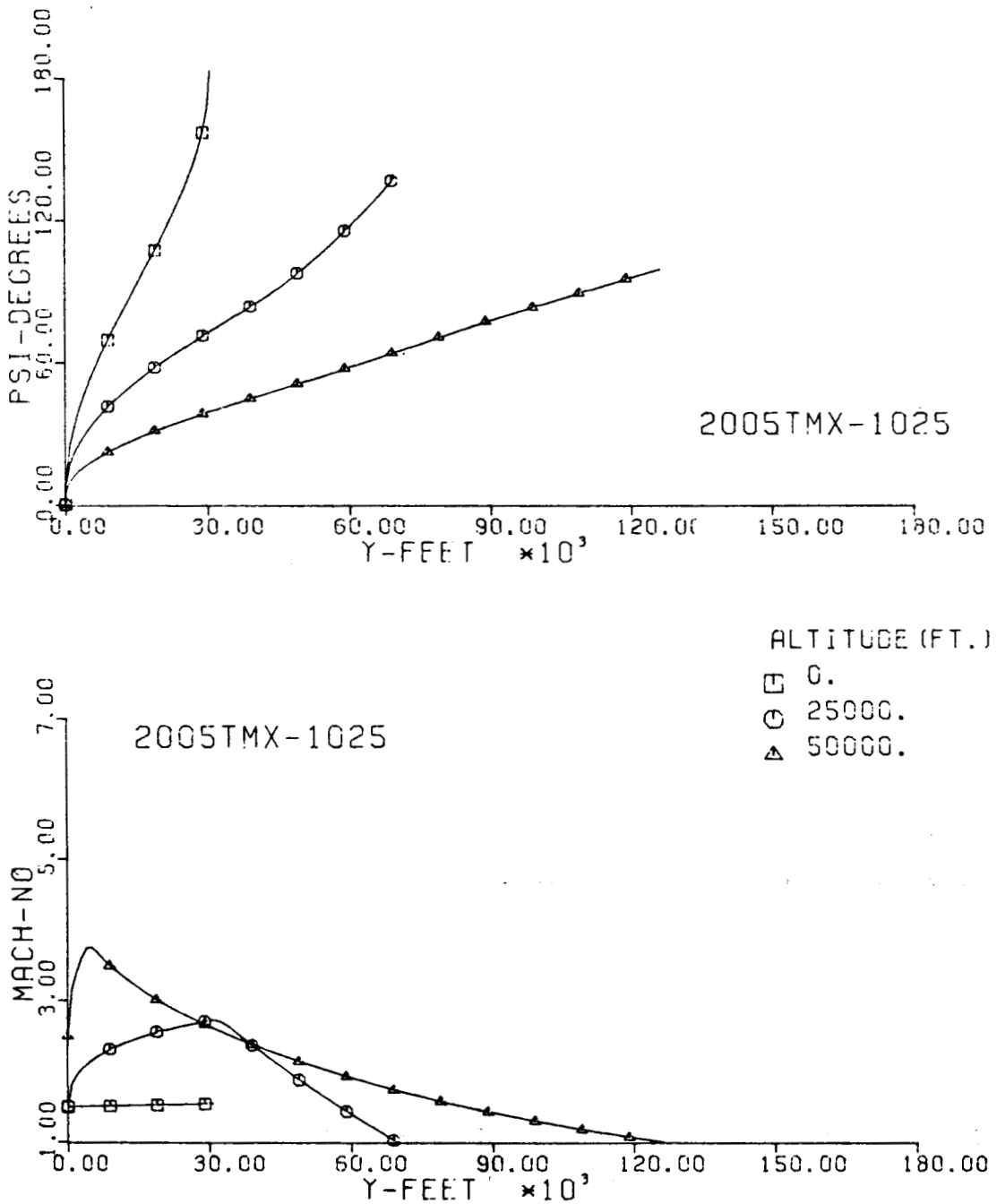

Fig. 46-III. Heading Angle and Mach No. vs. Downrange Distance, Y.

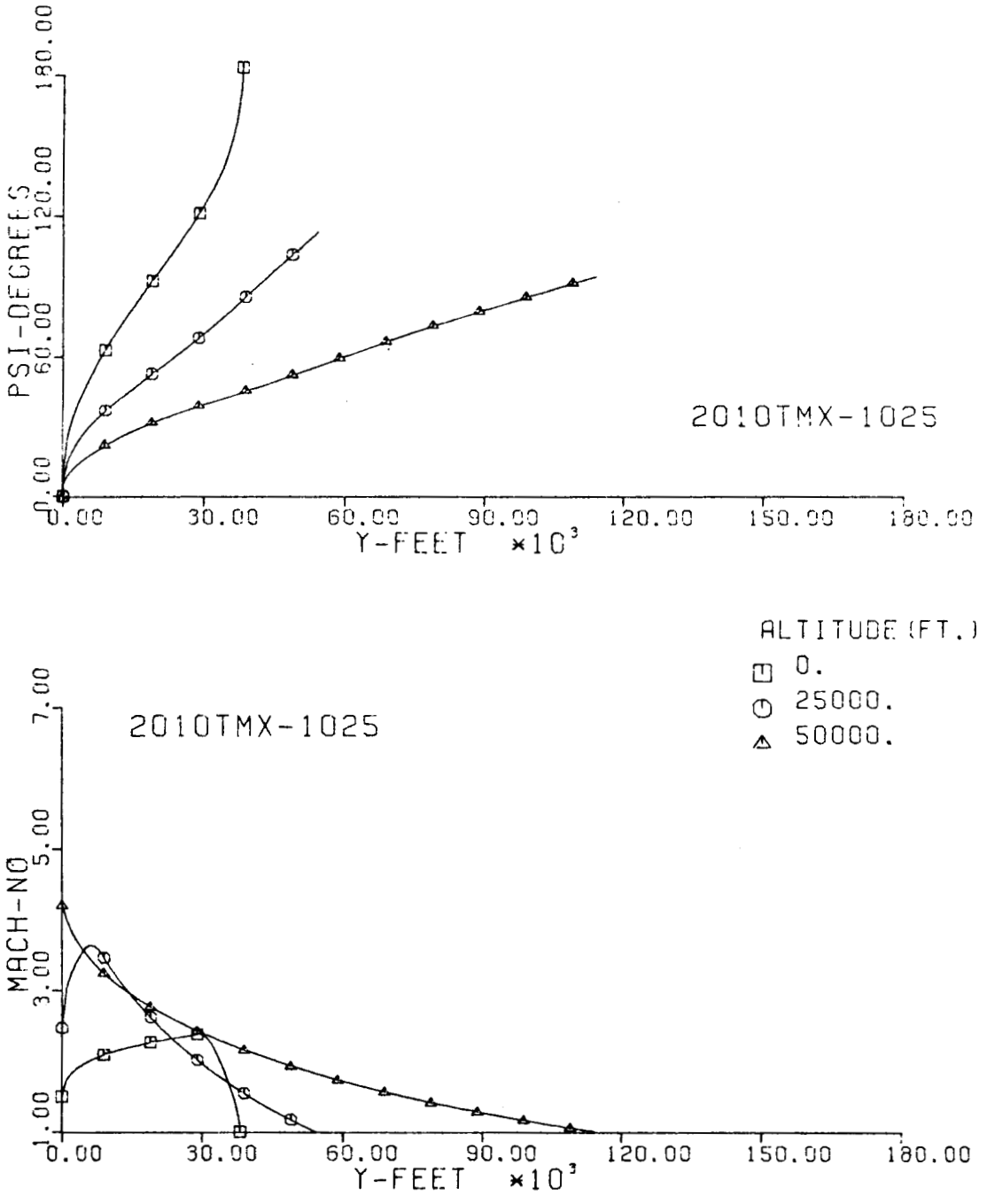

Fig. 47-III. Heading Angle and Mach No. vs. Downrange Distance, Y.

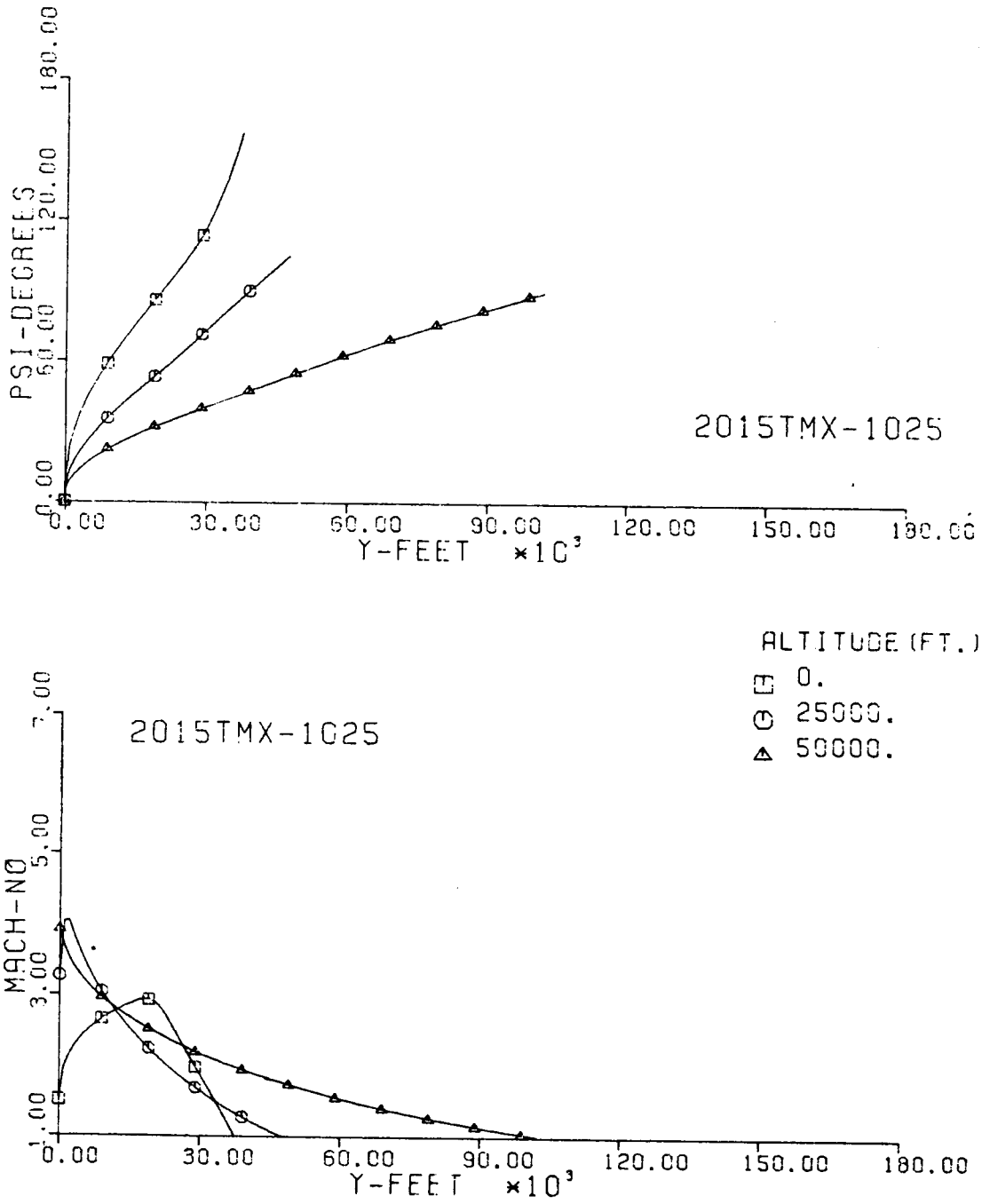

Fig. 48-III. Heading Angle and Mach No. vs. Downrange Distance, Y.

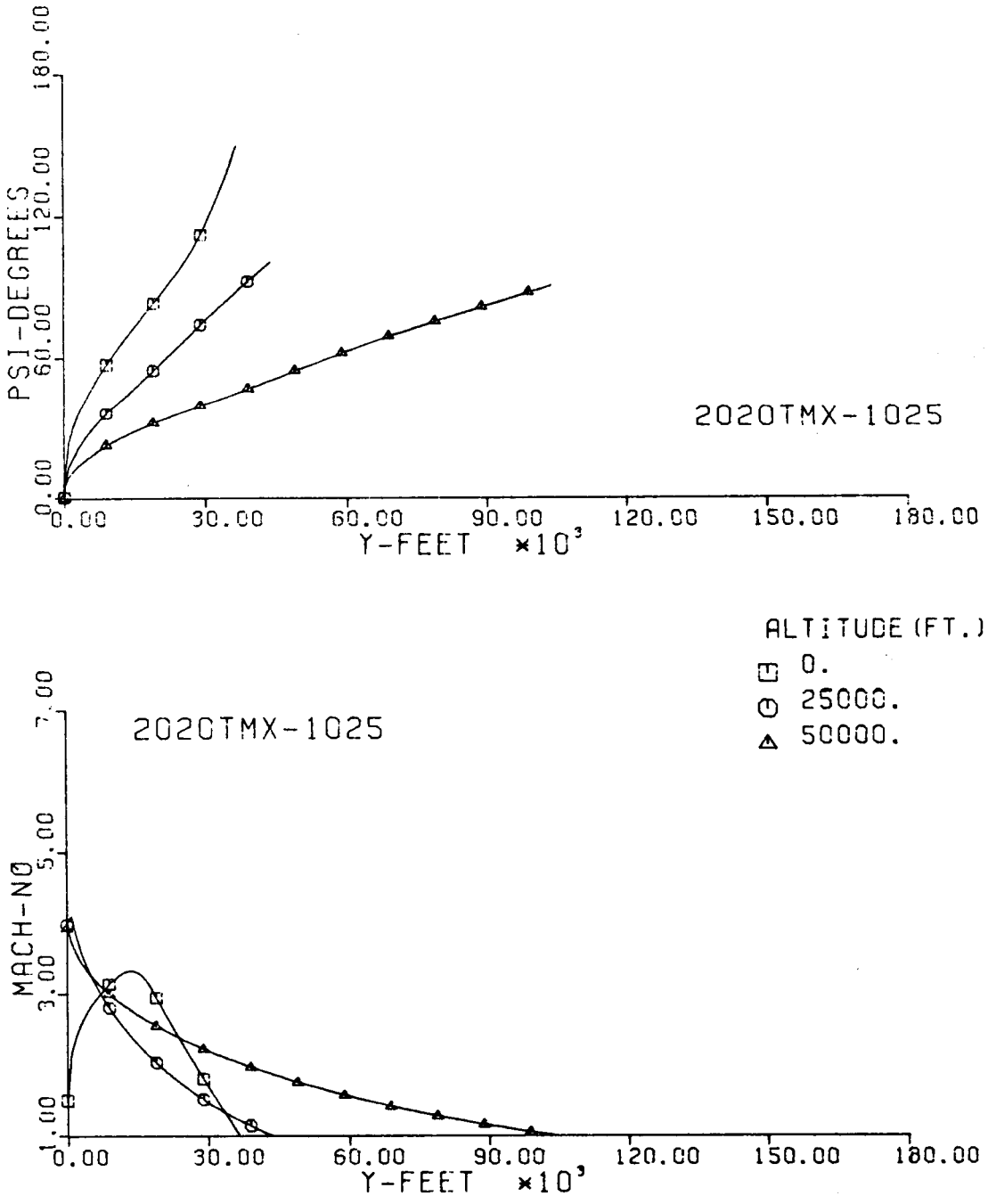

Fig. 49-III. Heading Angle and Mach No. vs. Downrange Distance, Y.

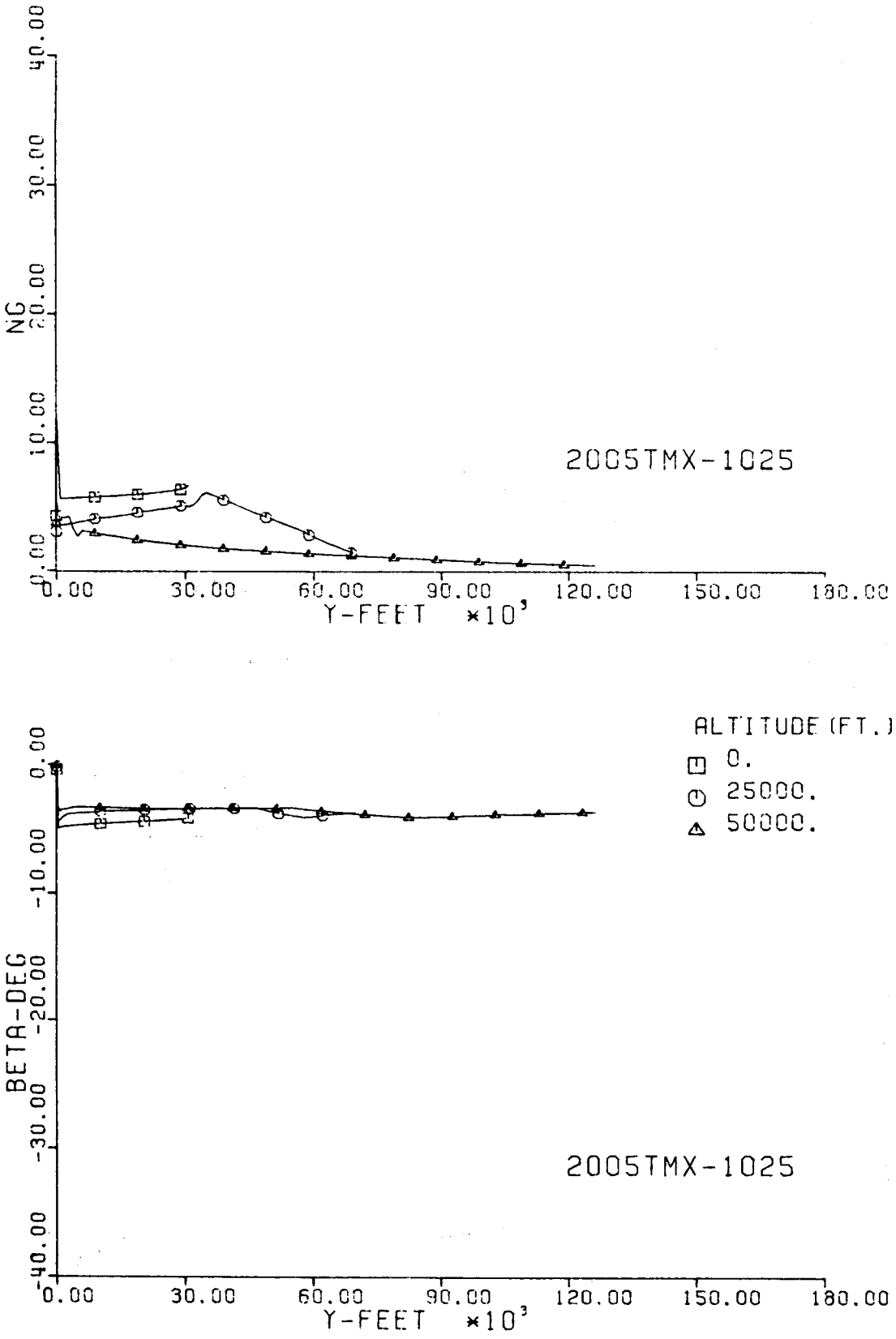

Fig. 50-III. Number of G's and Sideslip Angle vs. Downrange Distance, Y.

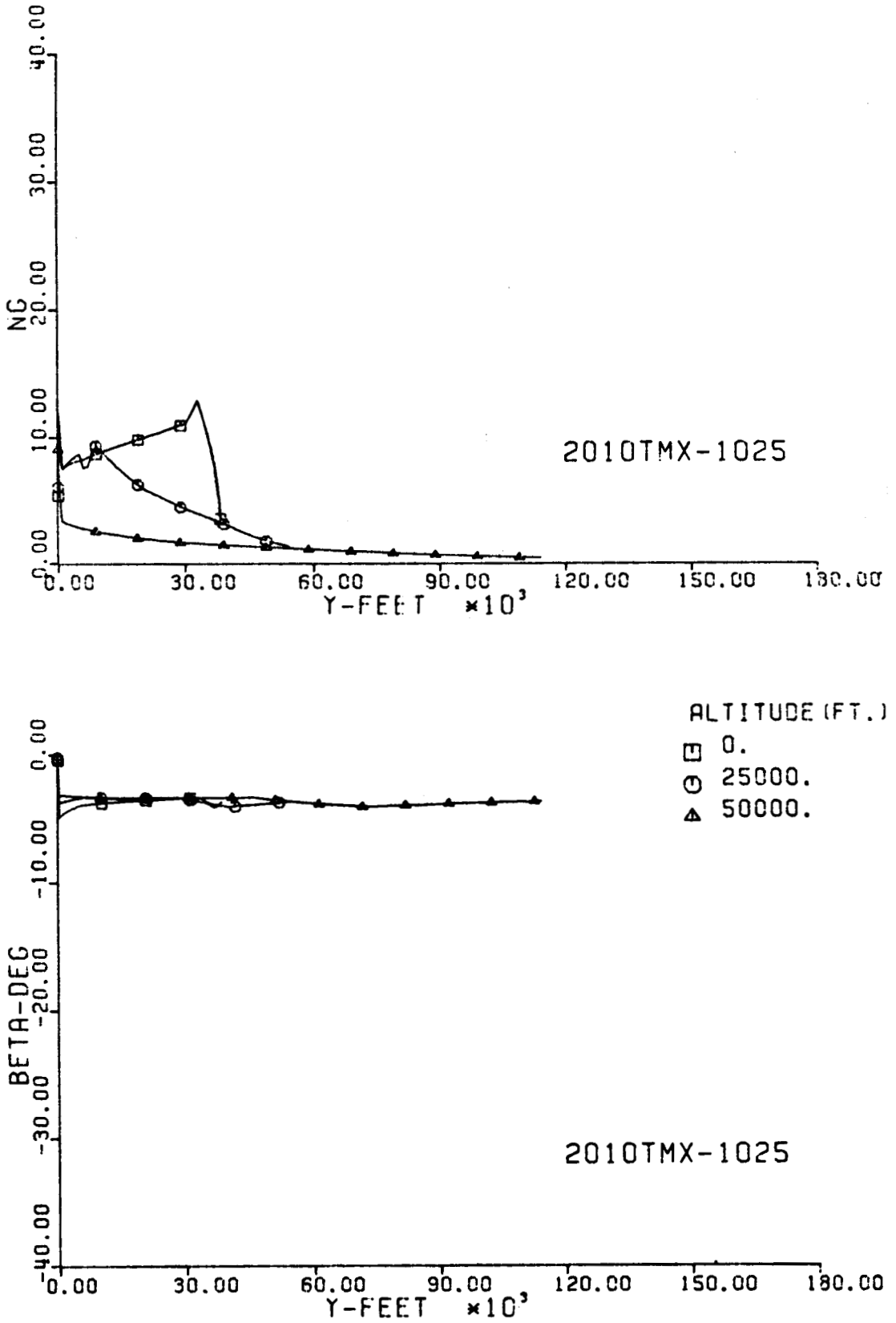

Fig. 51-III. Number of G's and Sideslip Angle vs. Downrange Distance, Y.

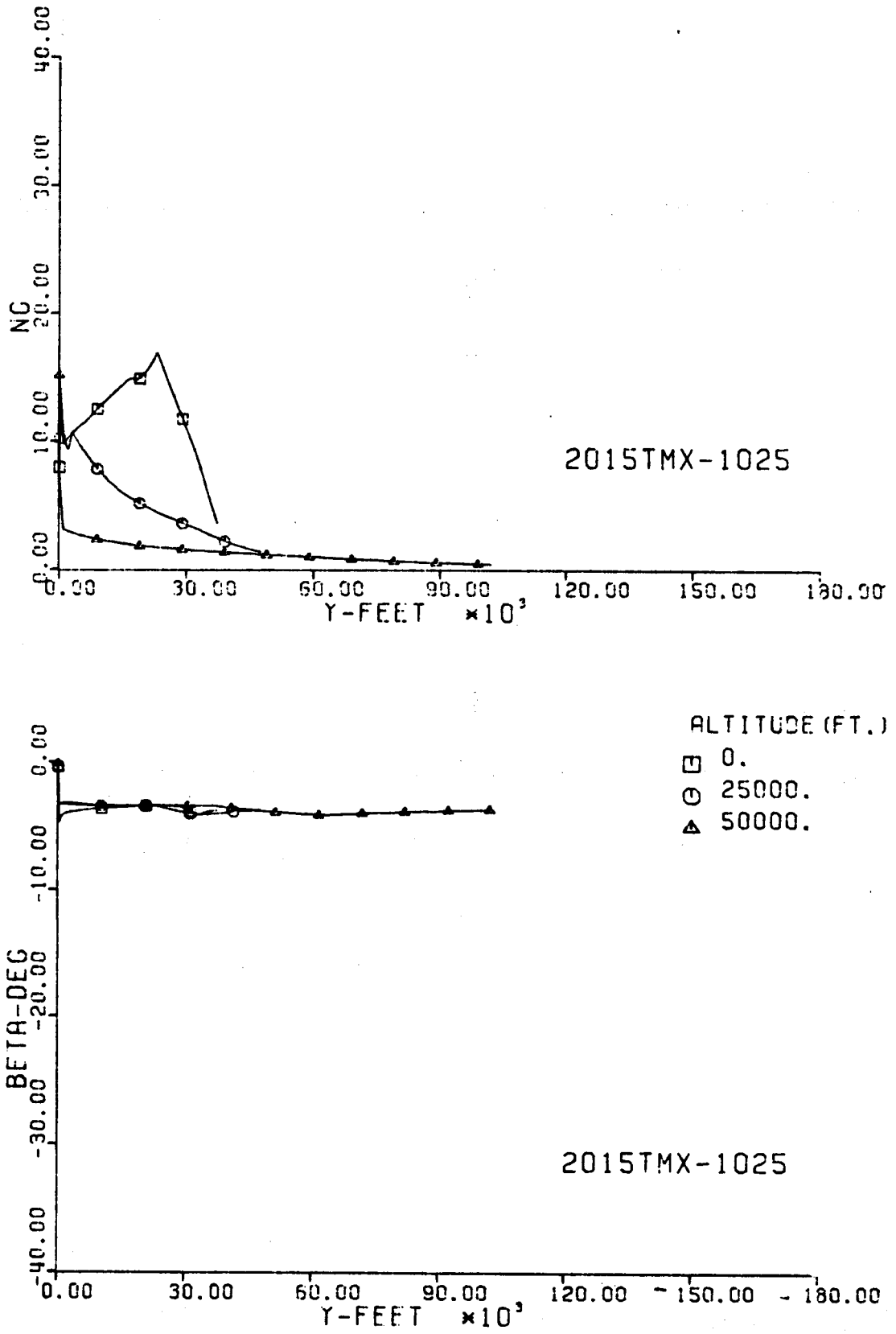

Fig. 52-III. Number of G's and Sideslip Angle vs. Downrange Distance, Y.

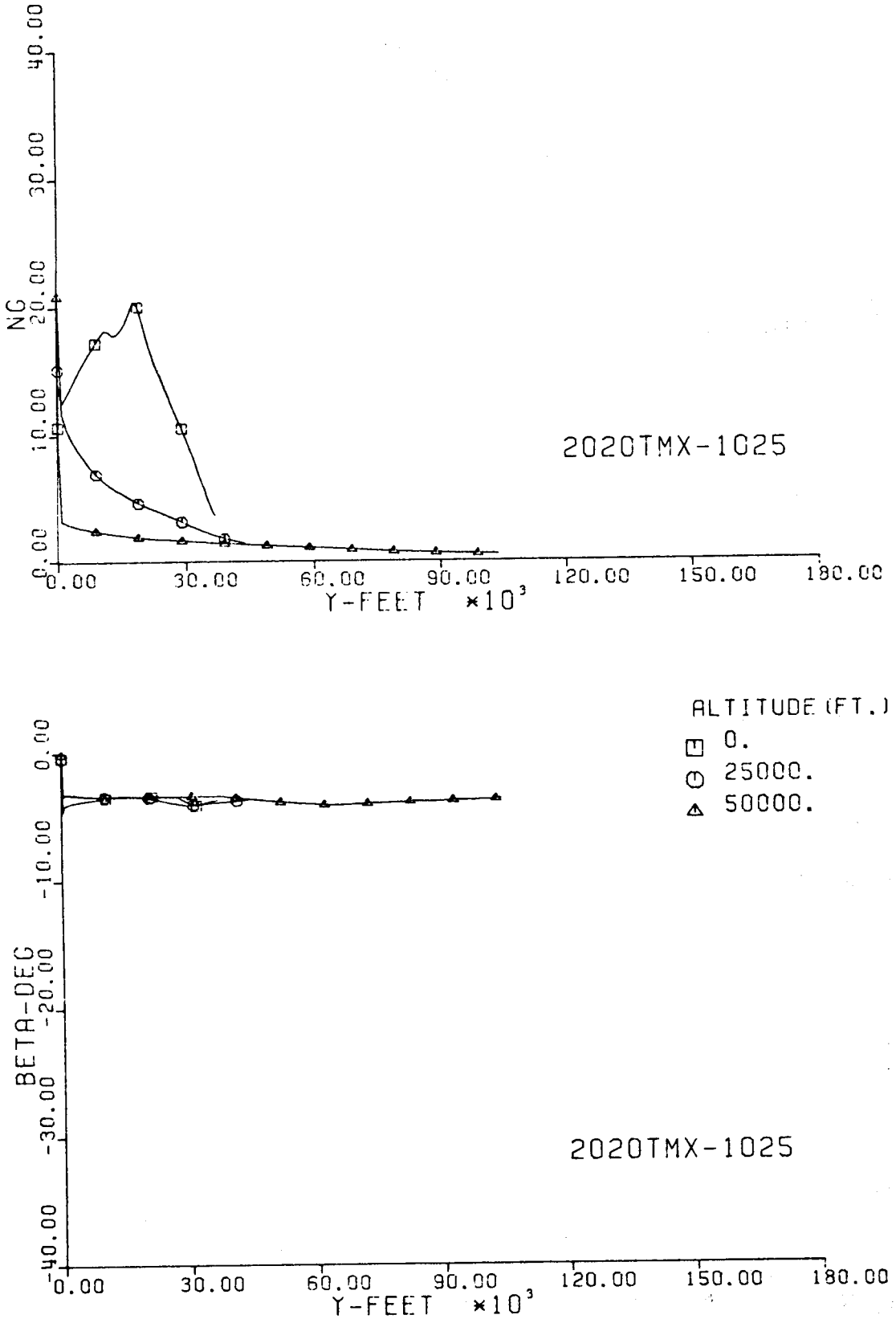

Fig. 53-III. Number of G's and Sideslip Angle vs. Downrange Distance, Y.

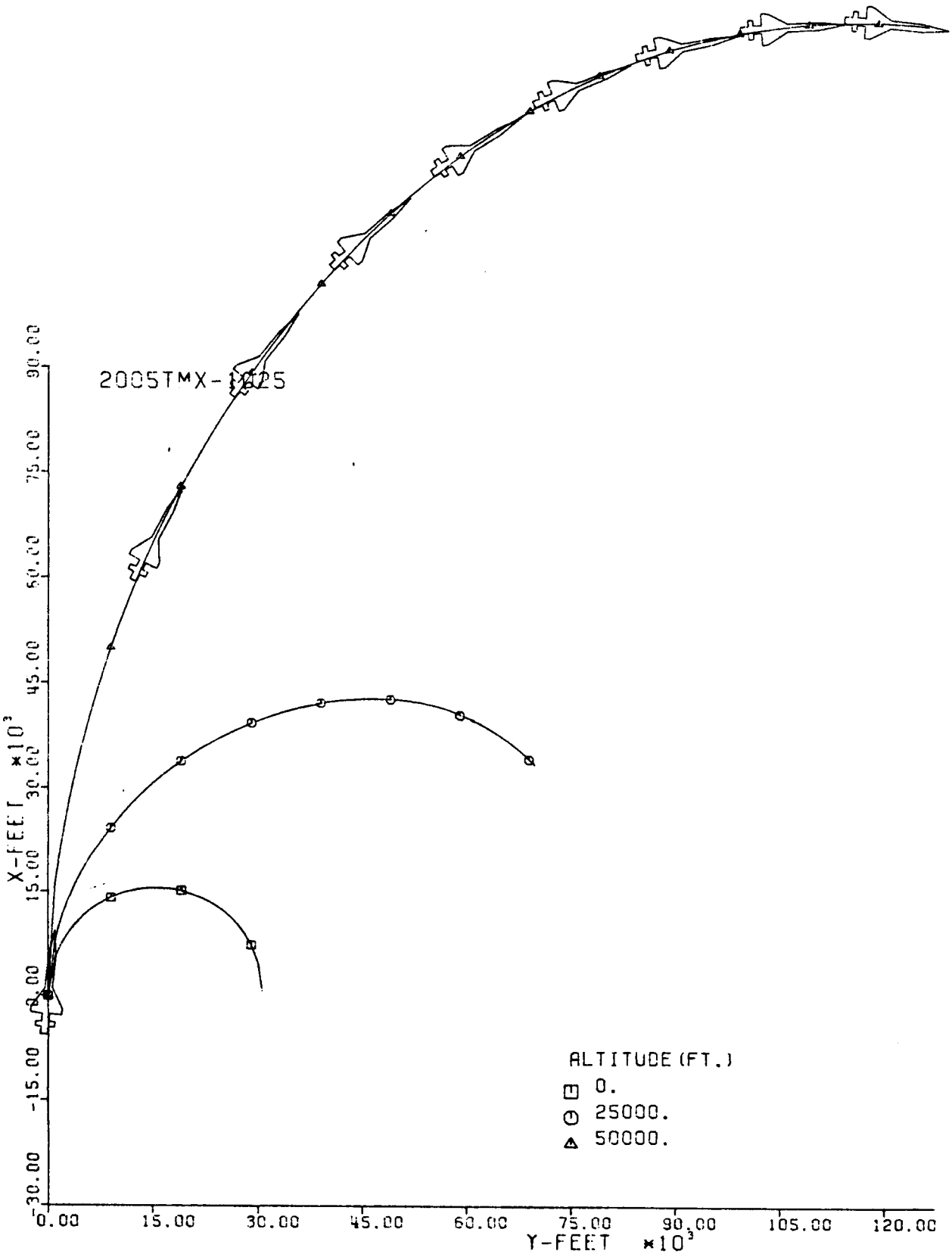

Fig. 54-III. Constant Altitude Flight Path, X vs. Y.

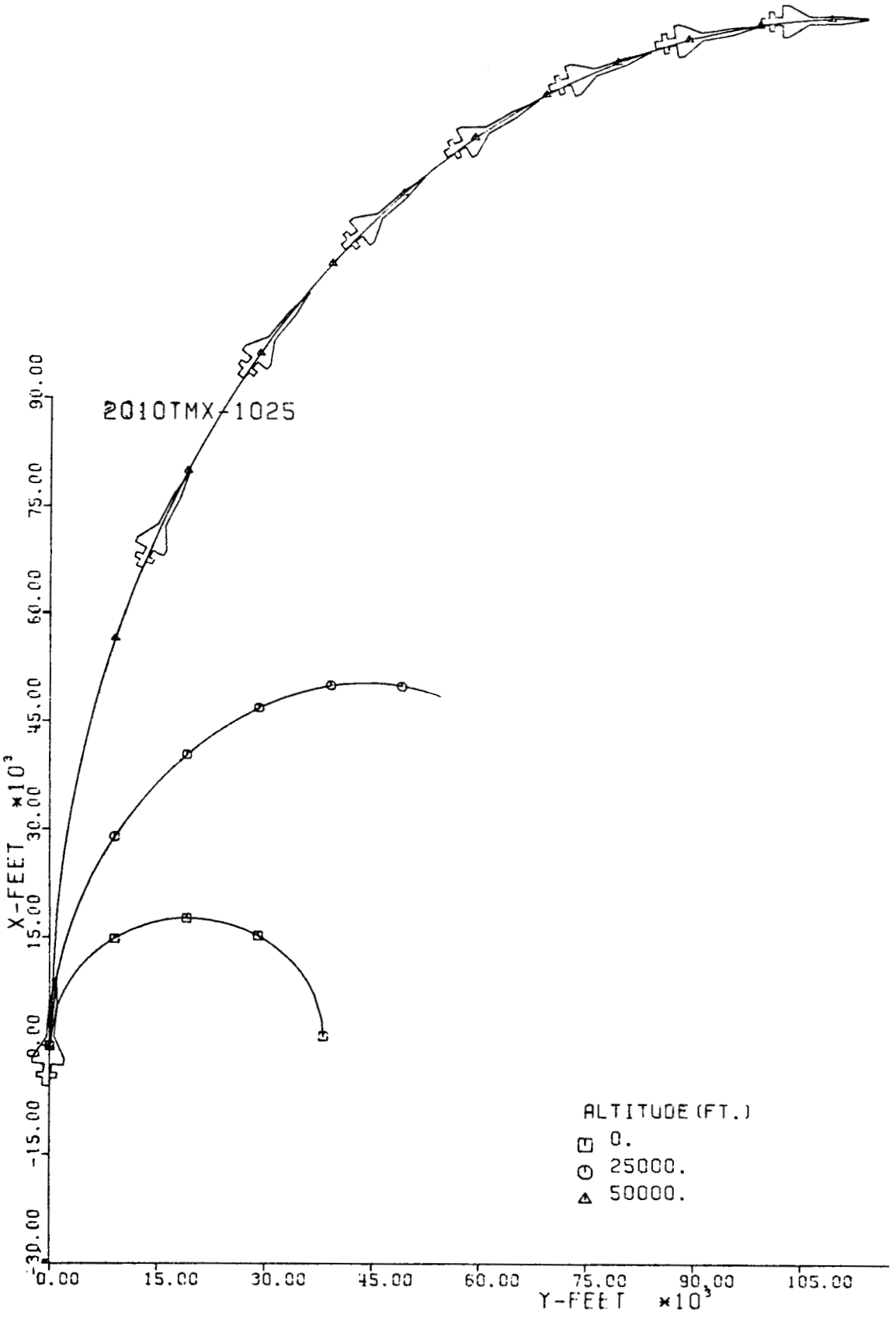

Fig. 55-III. Constant Altitude Flight Path, X vs. Y.

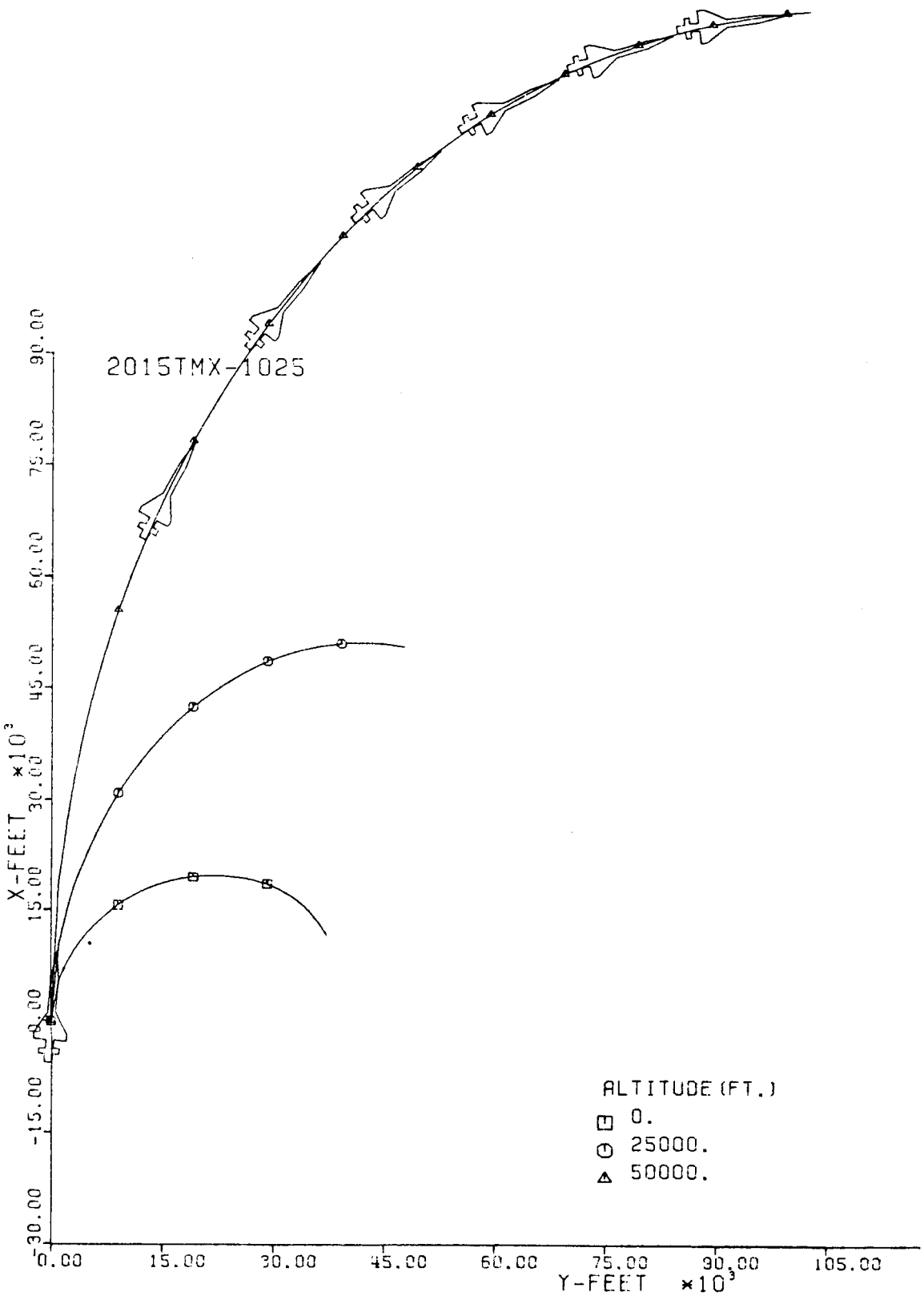

Fig. 56-III. Constant Altitude Flight Path, X vs. Y.

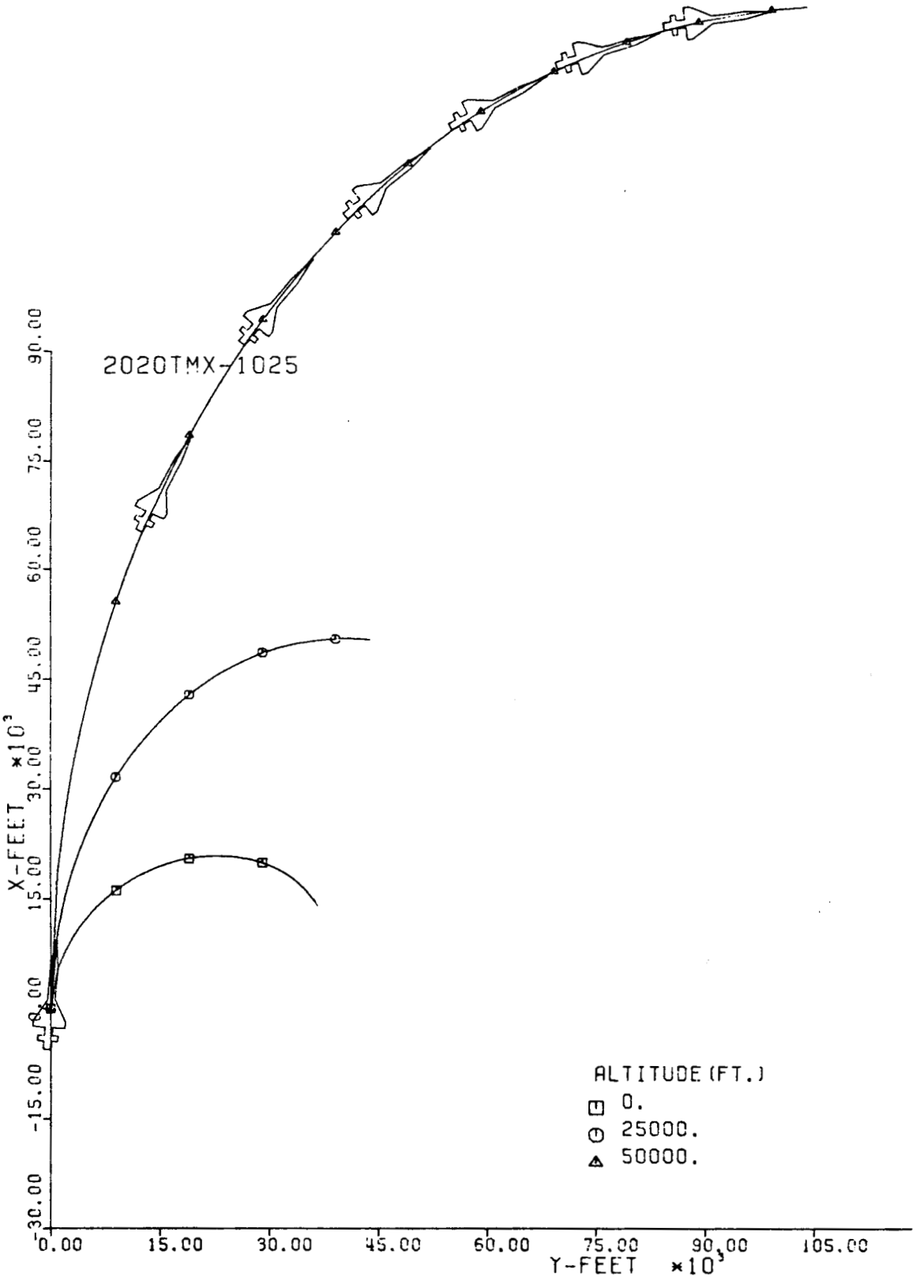

Fig. 57-III. Constant Altitude Flight Path, X vs. Y.

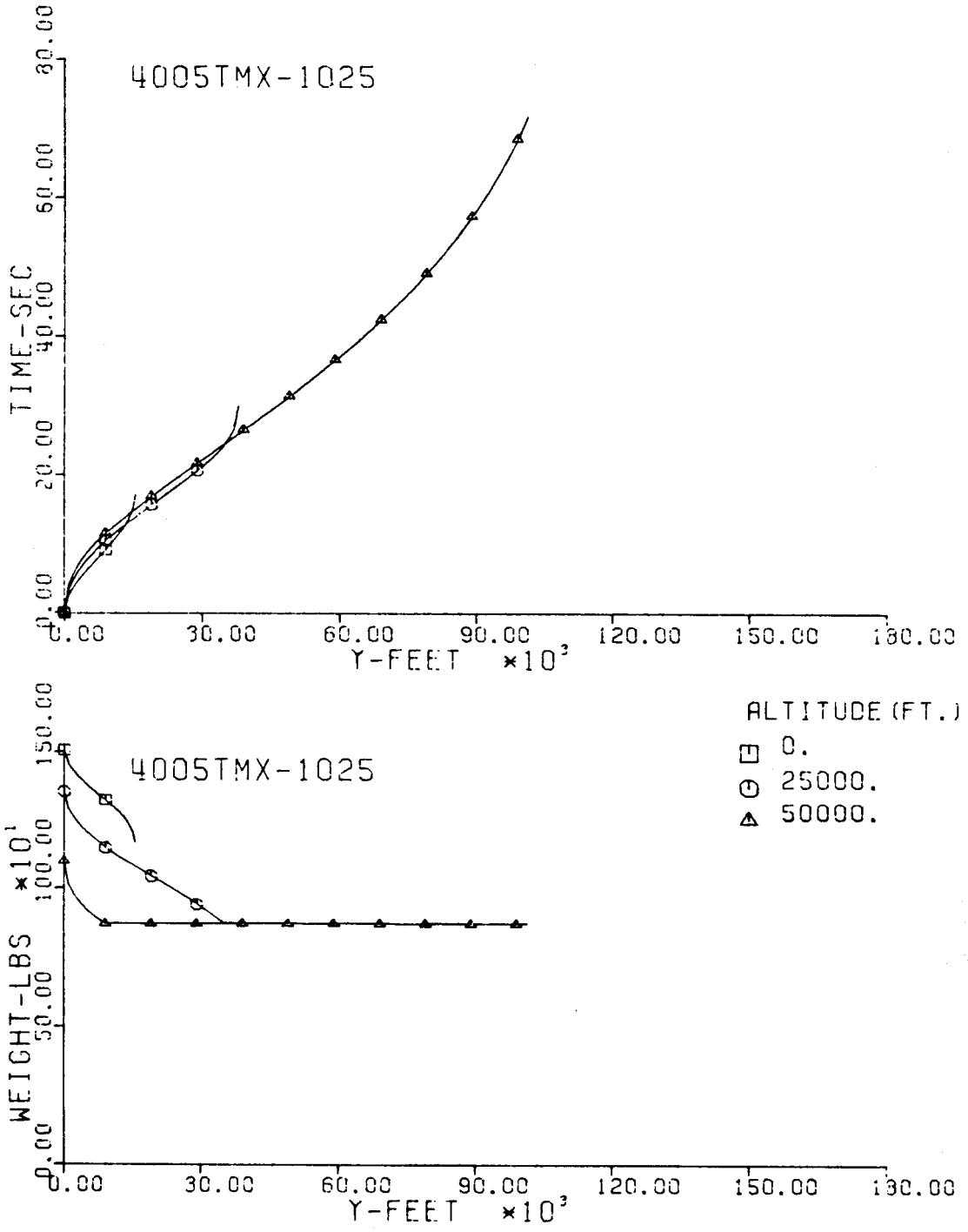

Fig. 58-III. Flight Time and Vehicle Weight vs. Downrange Distance, Y.

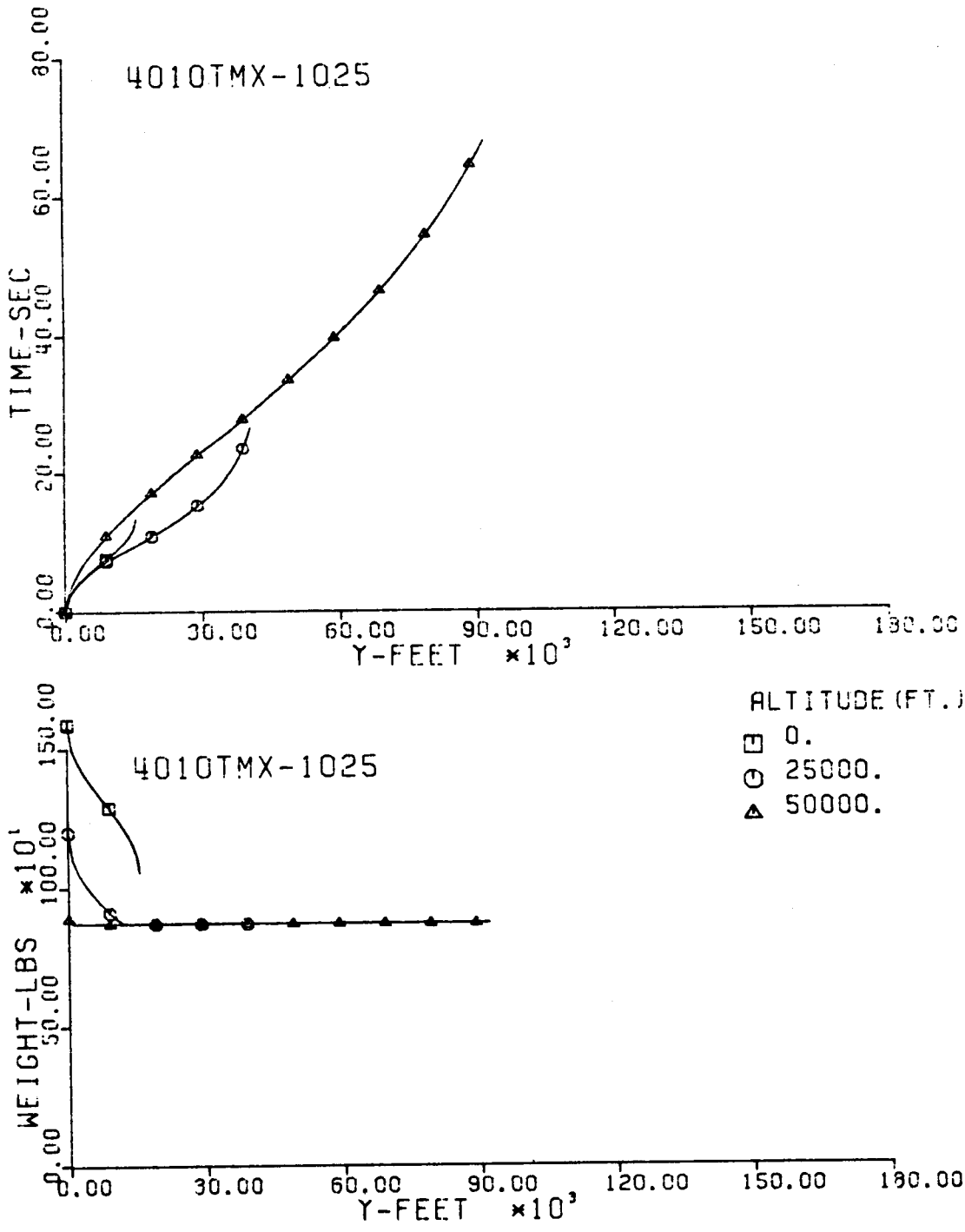

Fig. 59-III. Flight Time and Vehicle Weight vs. Downrange Distance, Y.

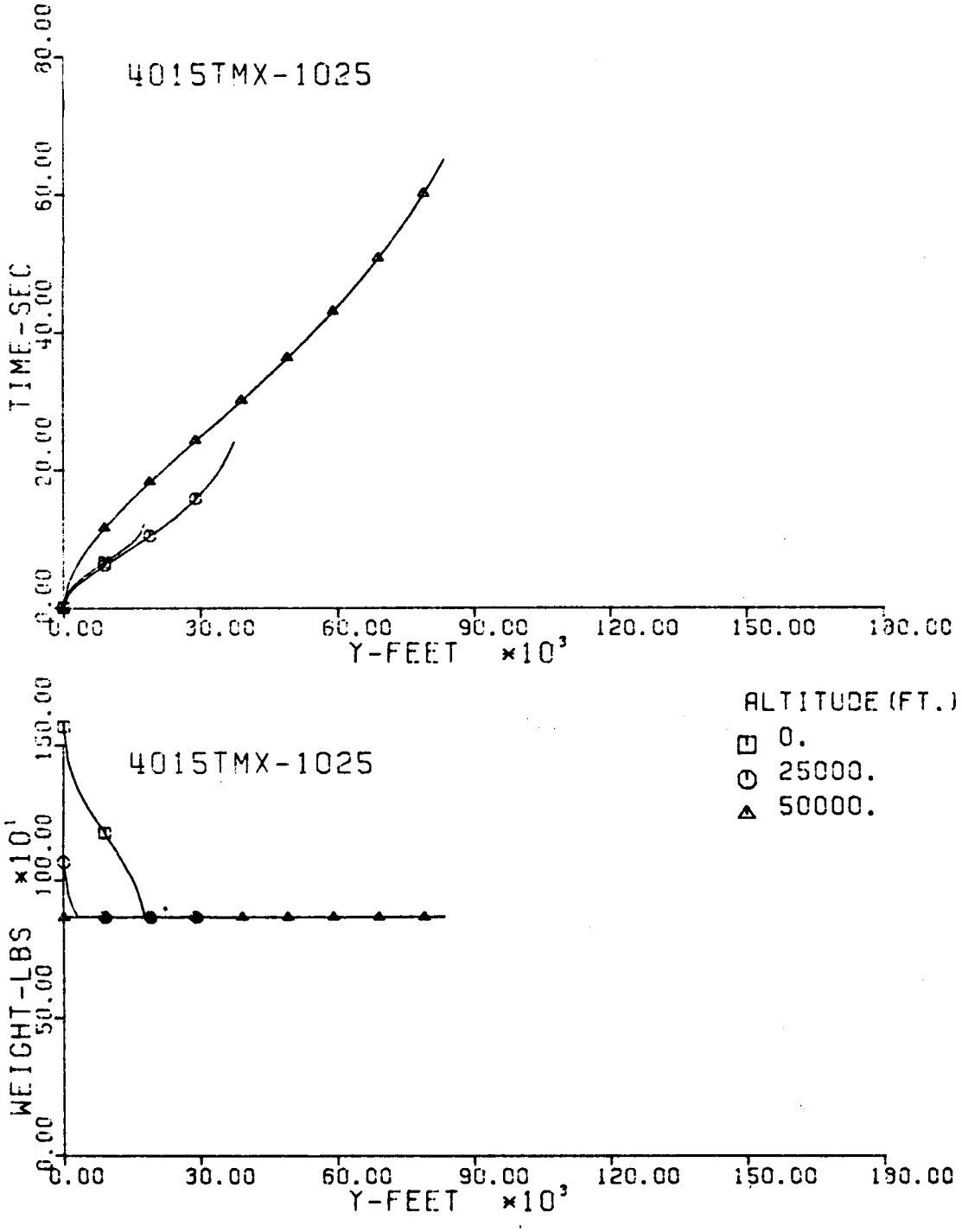

Fig. 60-III. Flight Time and Vehicle Weight vs. Downrange Distance, Y.

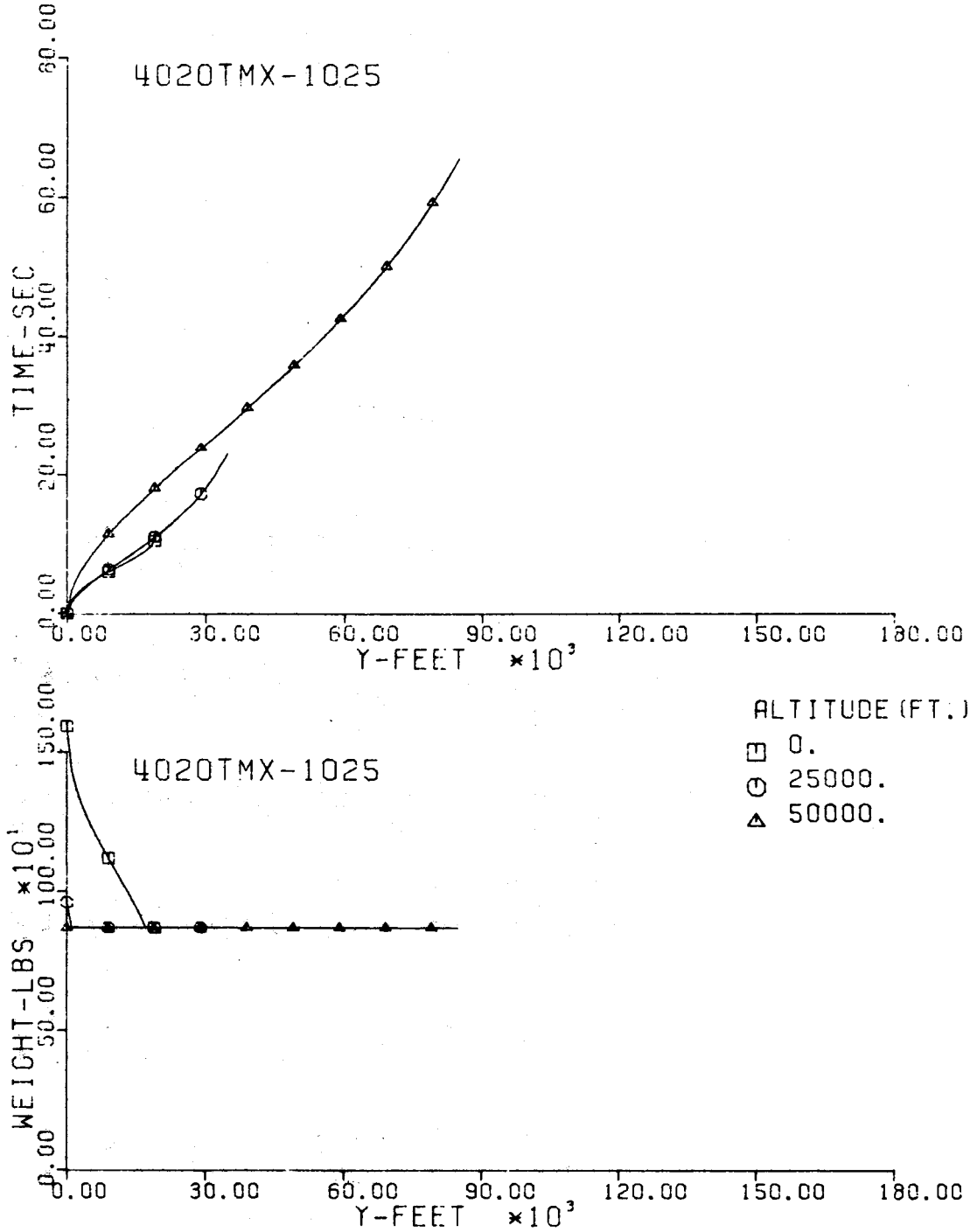

Fig. 61-III. Flight Time and Vehicle Weight vs. Downrange Distance, Y.

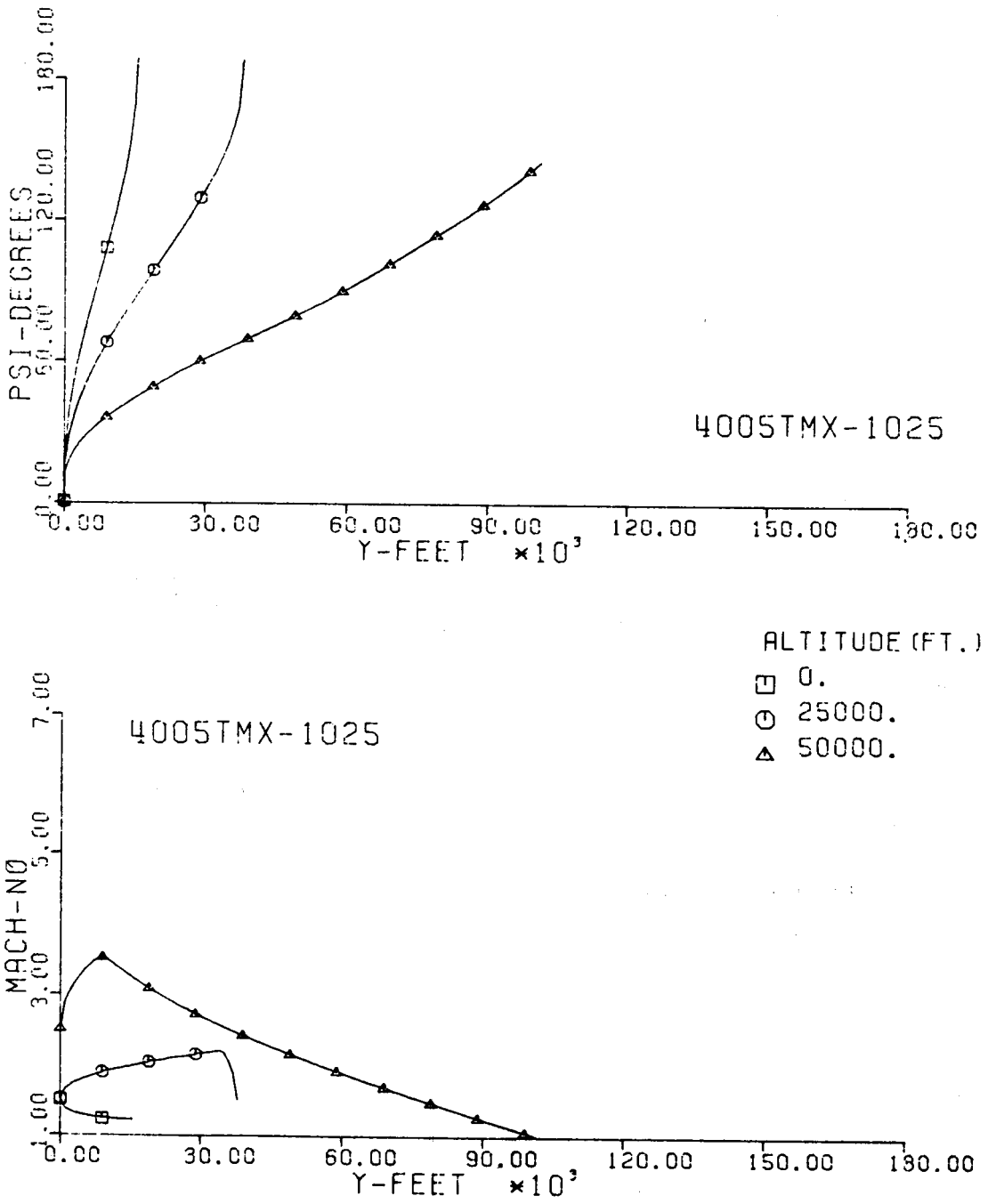

Fig. 62-III. Heading Angle and Mach No. vs. Downrange Distance, Y.

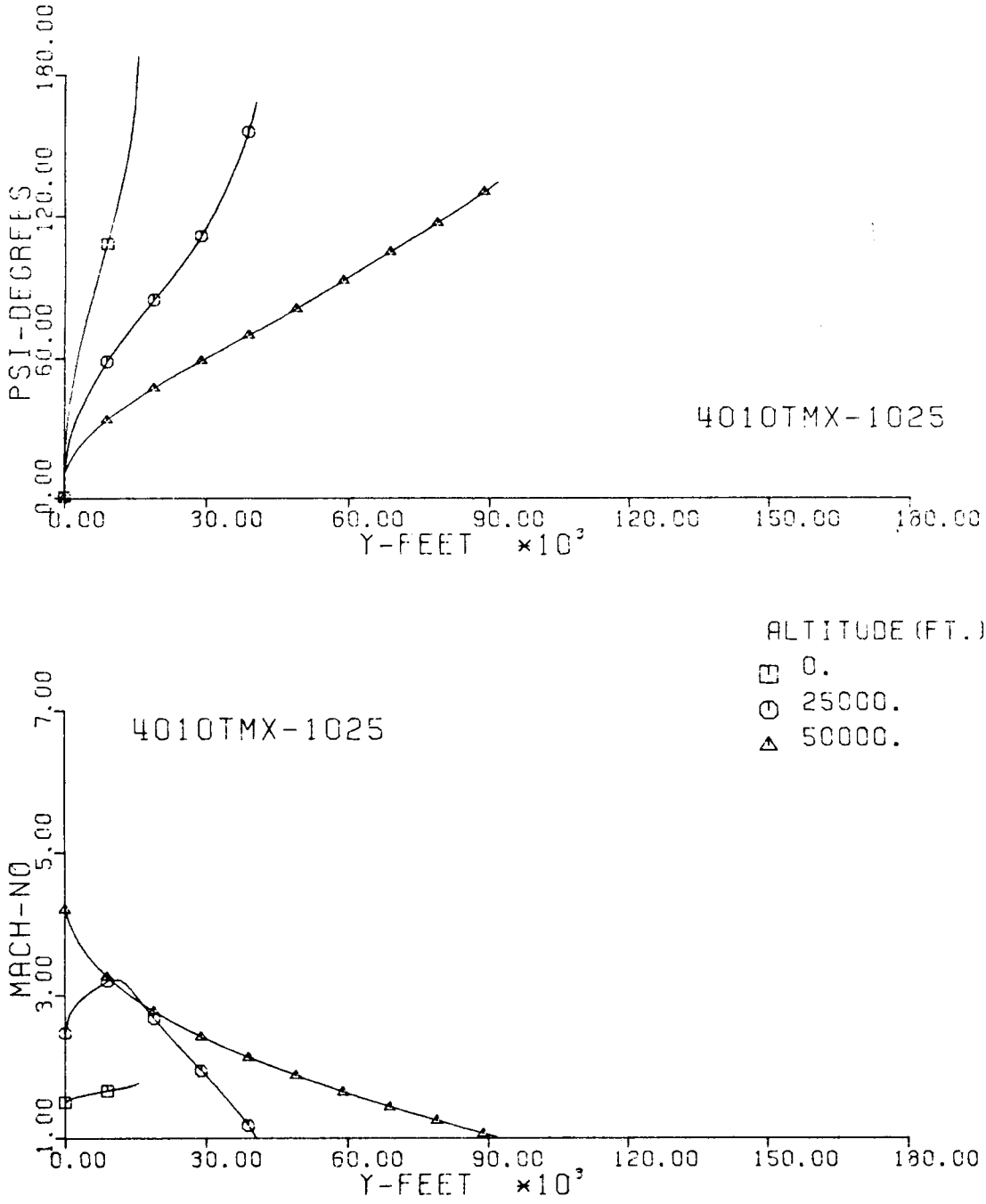

Fig. 63-III. Heading Angle and Mach No. vs. Downrange Distance, Y.

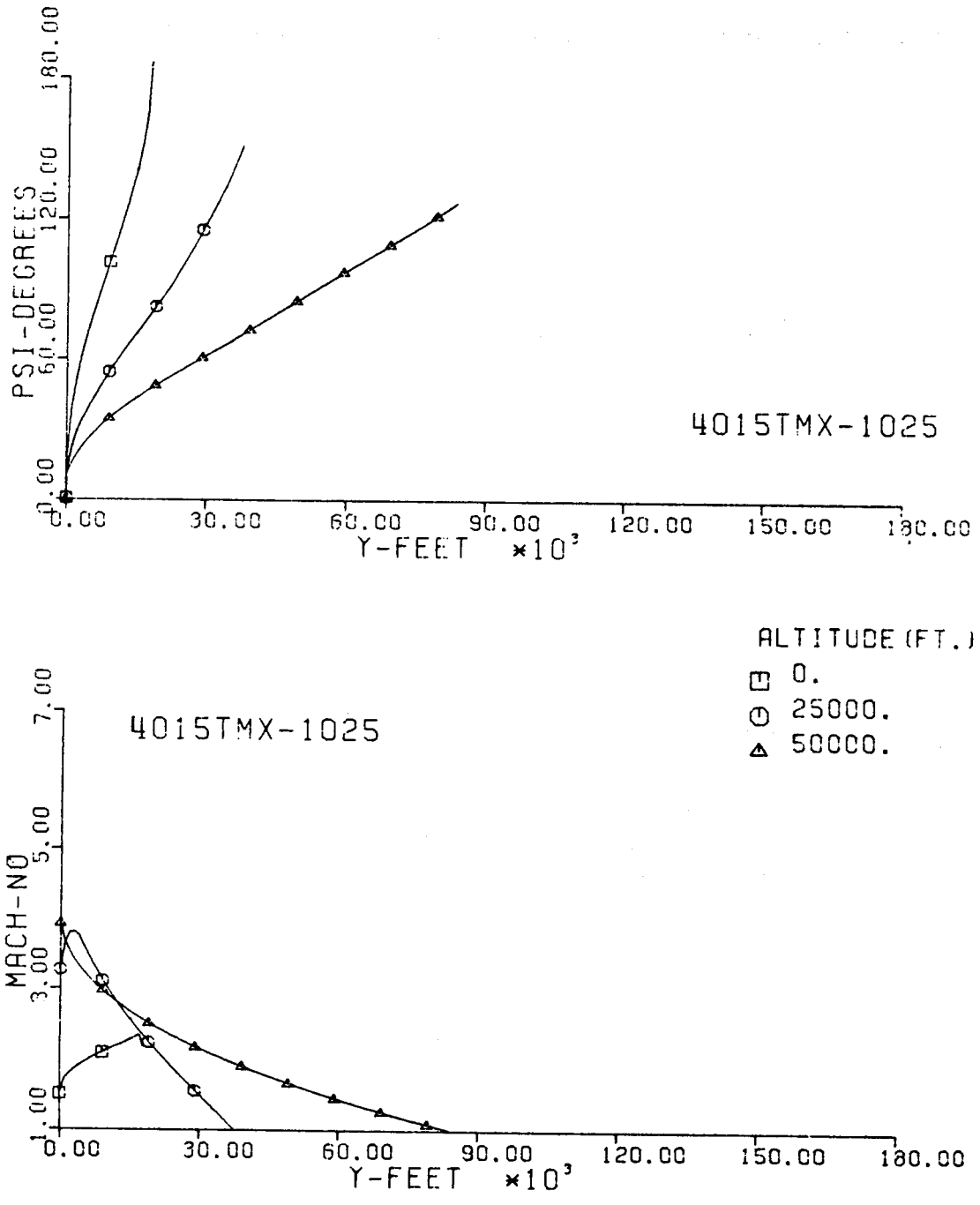

Fig. 64-III. Heading Angle and Mach No. vs. Downrange Distance, Y.

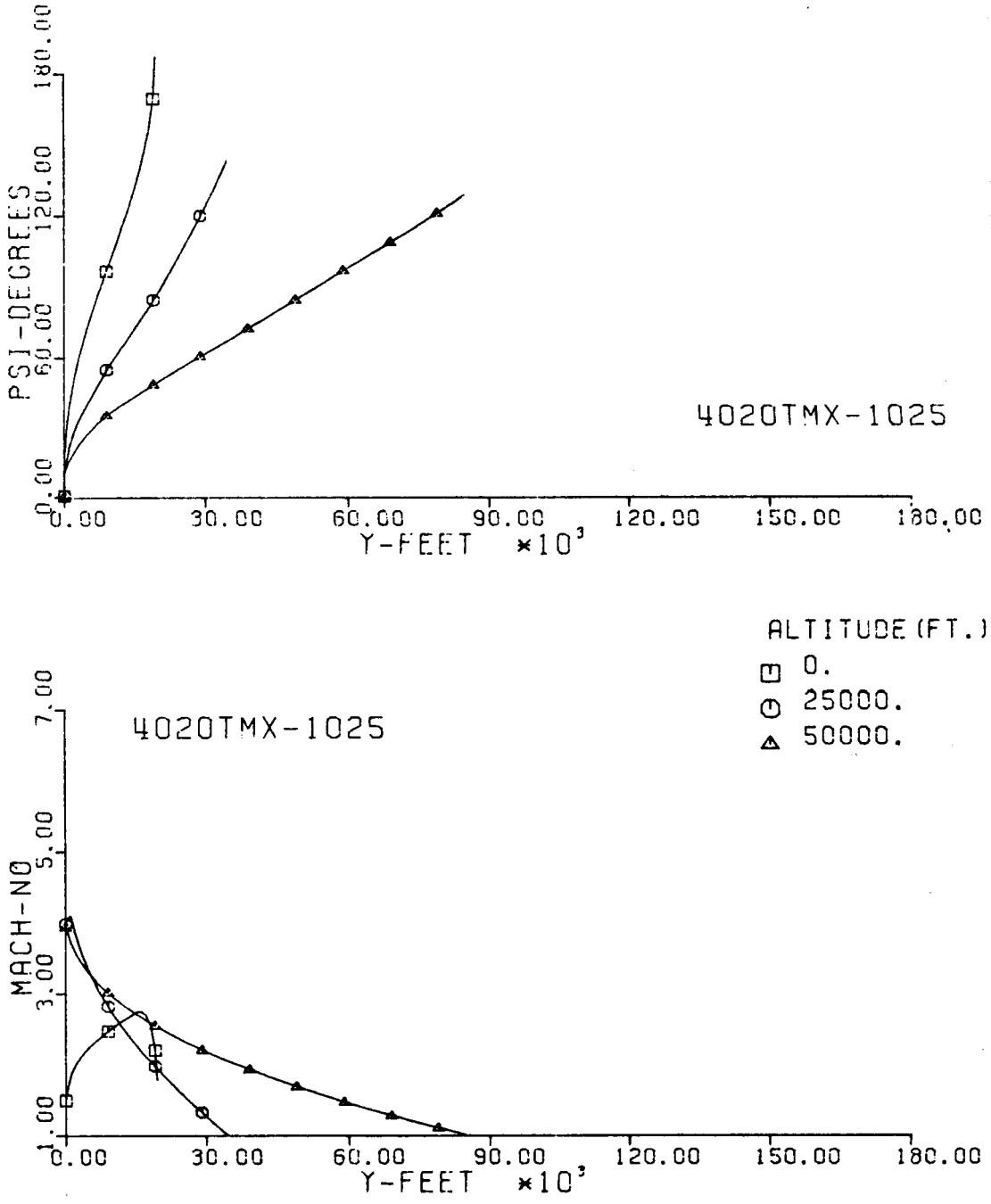

Fig. 65-III. Heading Angle and Mach No. vs. Downrange Distance, Y.

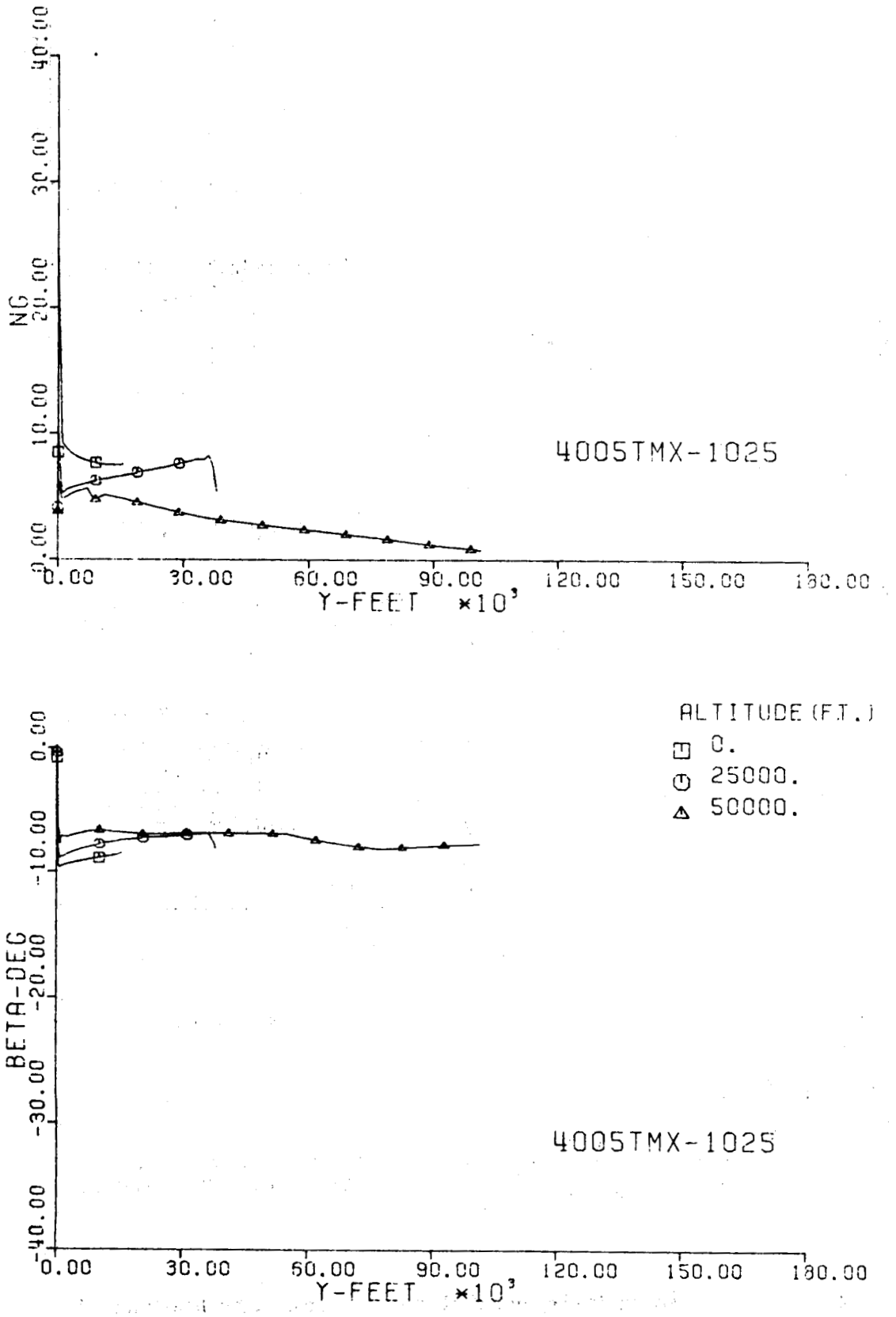

Fig. 66-III. Number of G's and Sideslip Angle vs. Downrange Distance, Y.

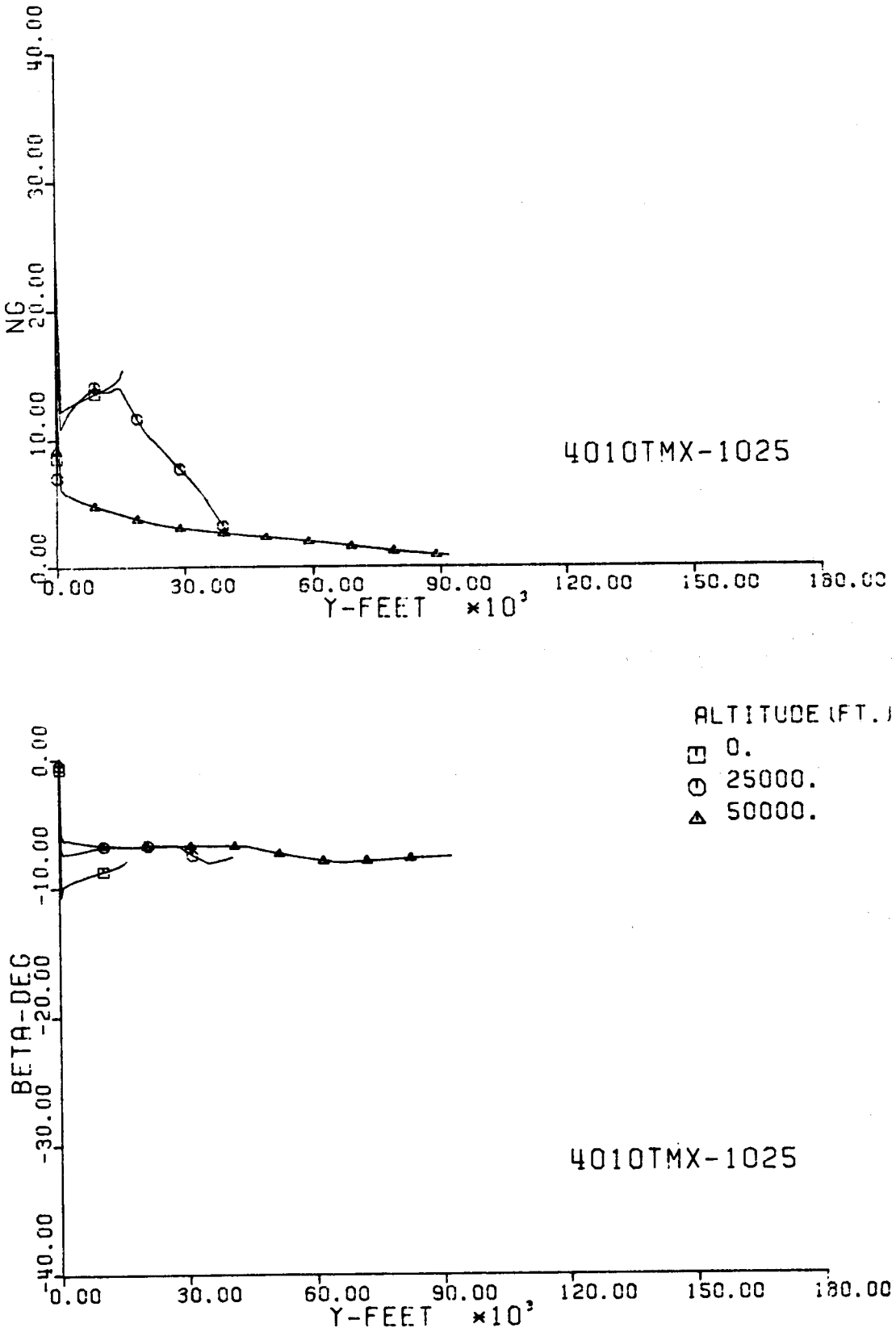

Fig. 67-III. Number of G's and Sideslip Angle vs. Downrange Distance, Y.

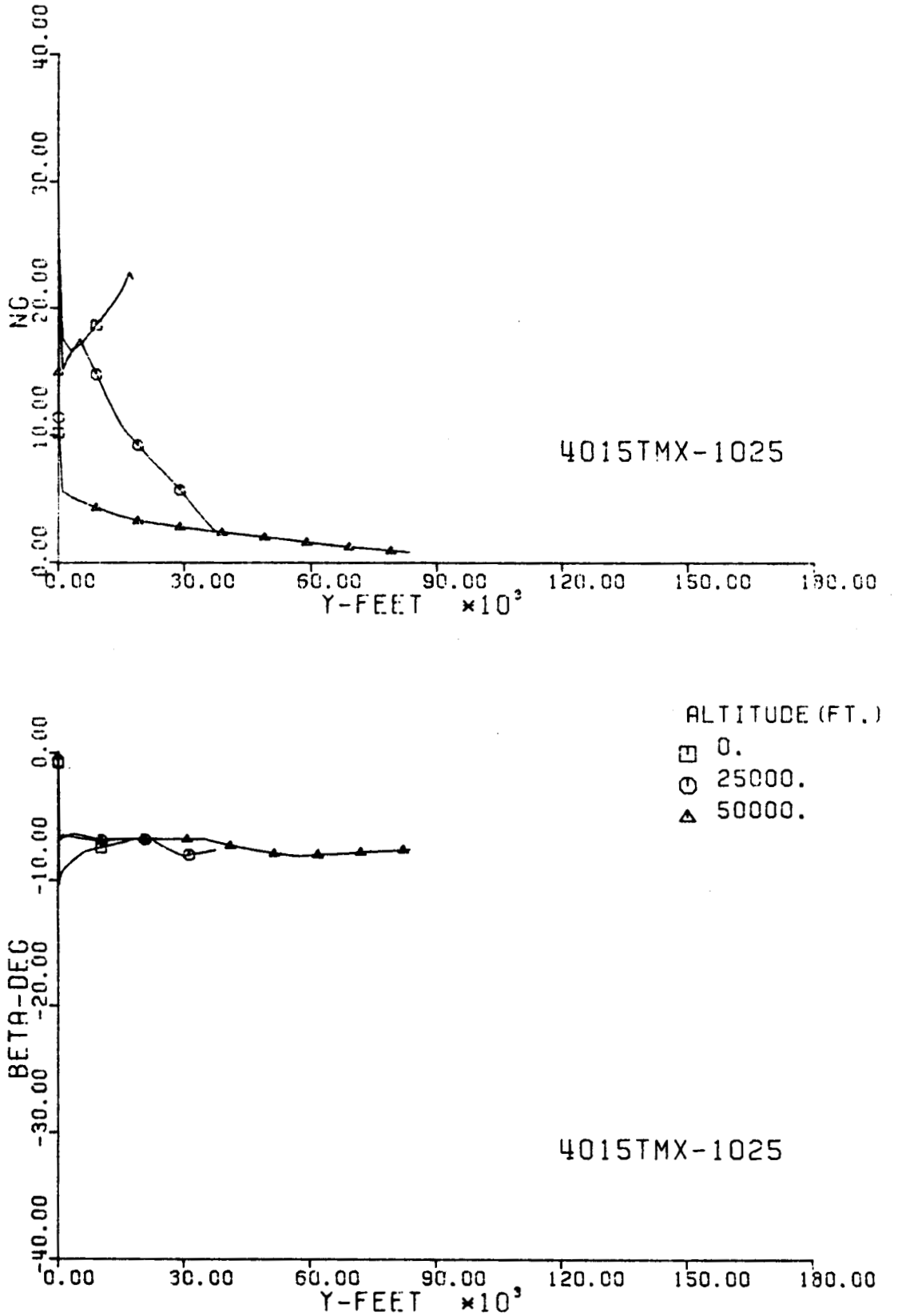

Fig. 68-III. Number of G's and Sideslip Angle vs. Downrange Distance, Y.

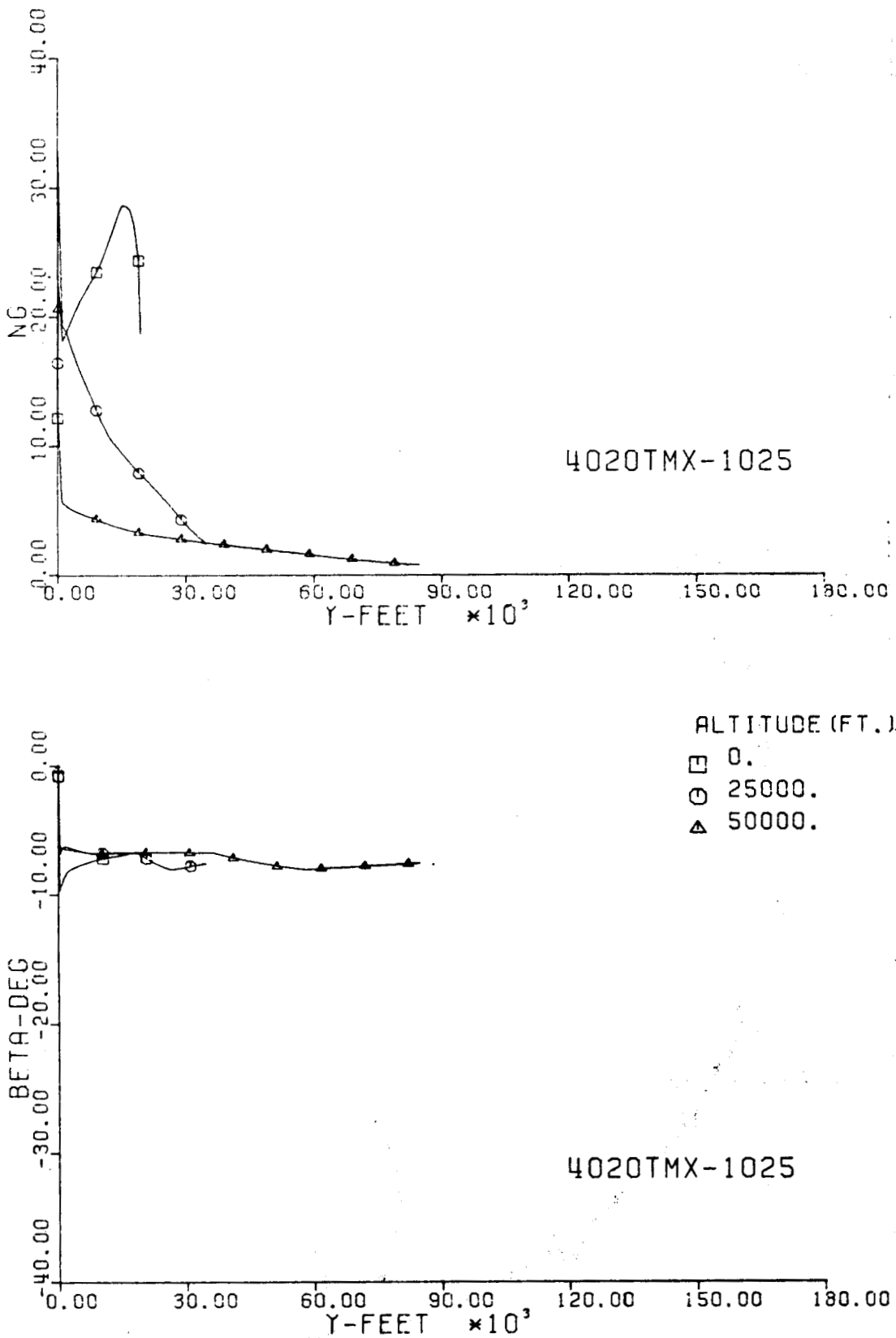

Fig. 69-III. Number of G's and Sideslip Angle vs. Downrange Distance, Y.

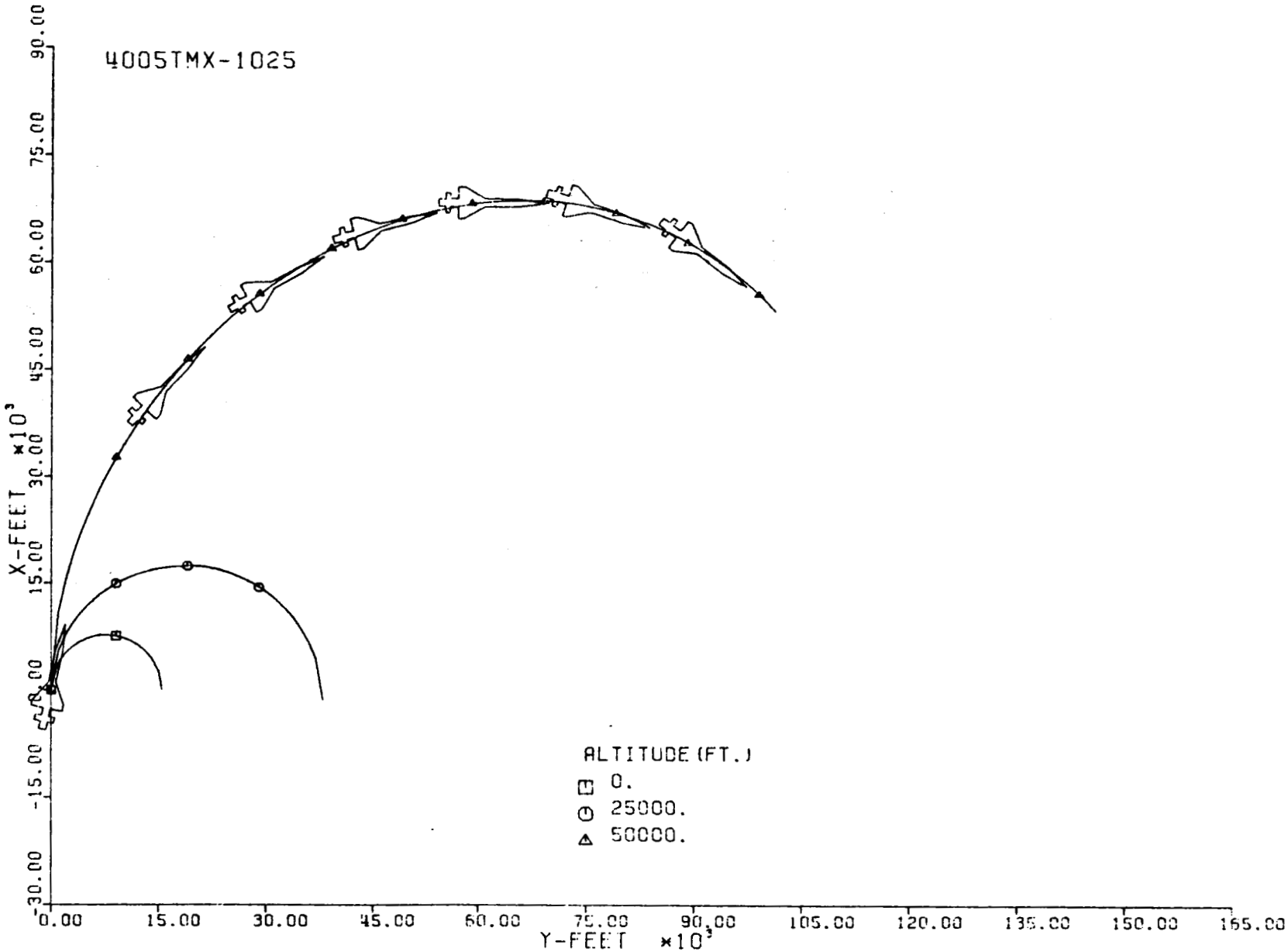

Fig. 70-III. Constant Altitude Flight Path, X vs. Y.

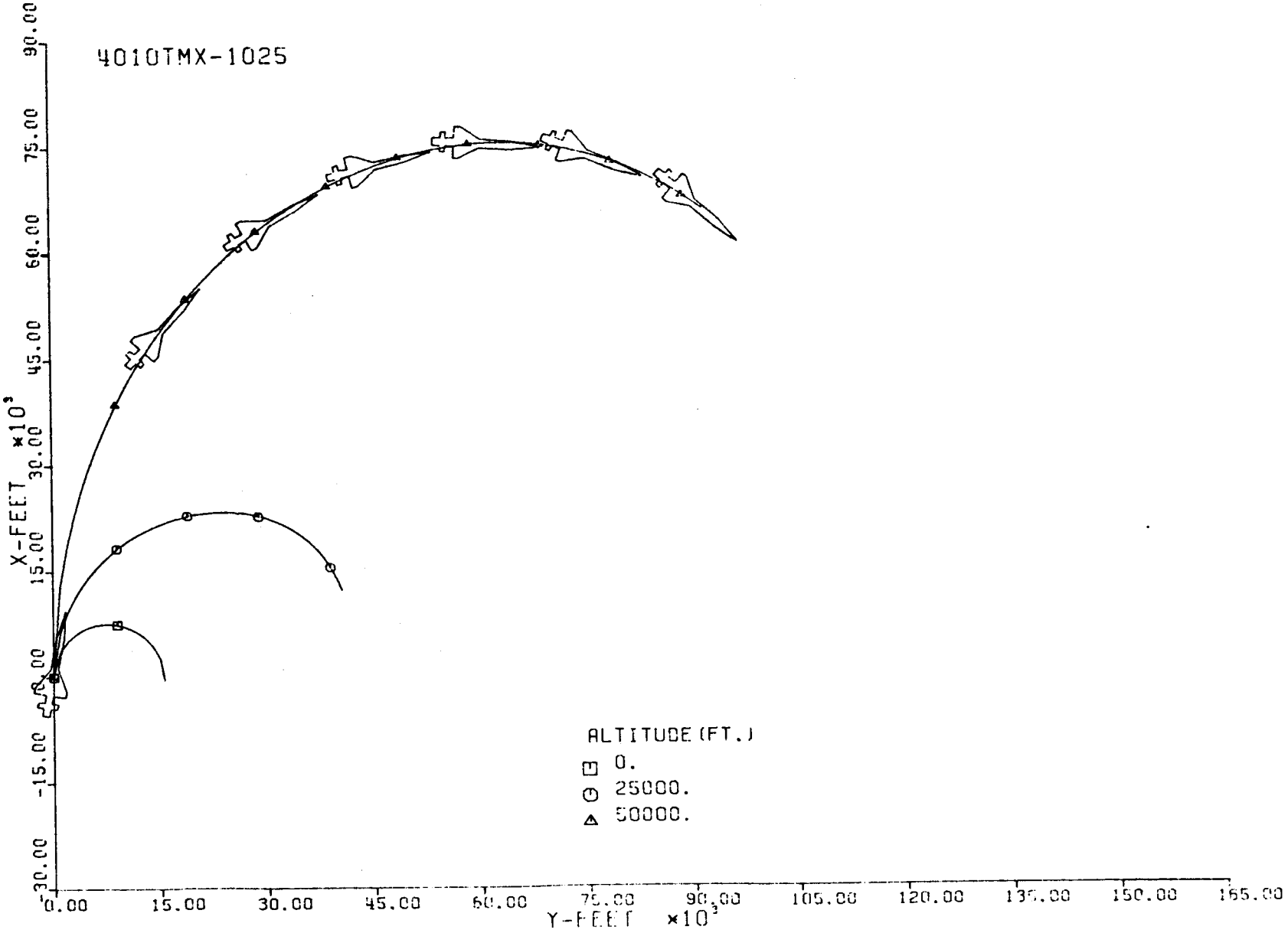

Fig. 71-III. Constant Altitude Flight Path, X vs. Y.

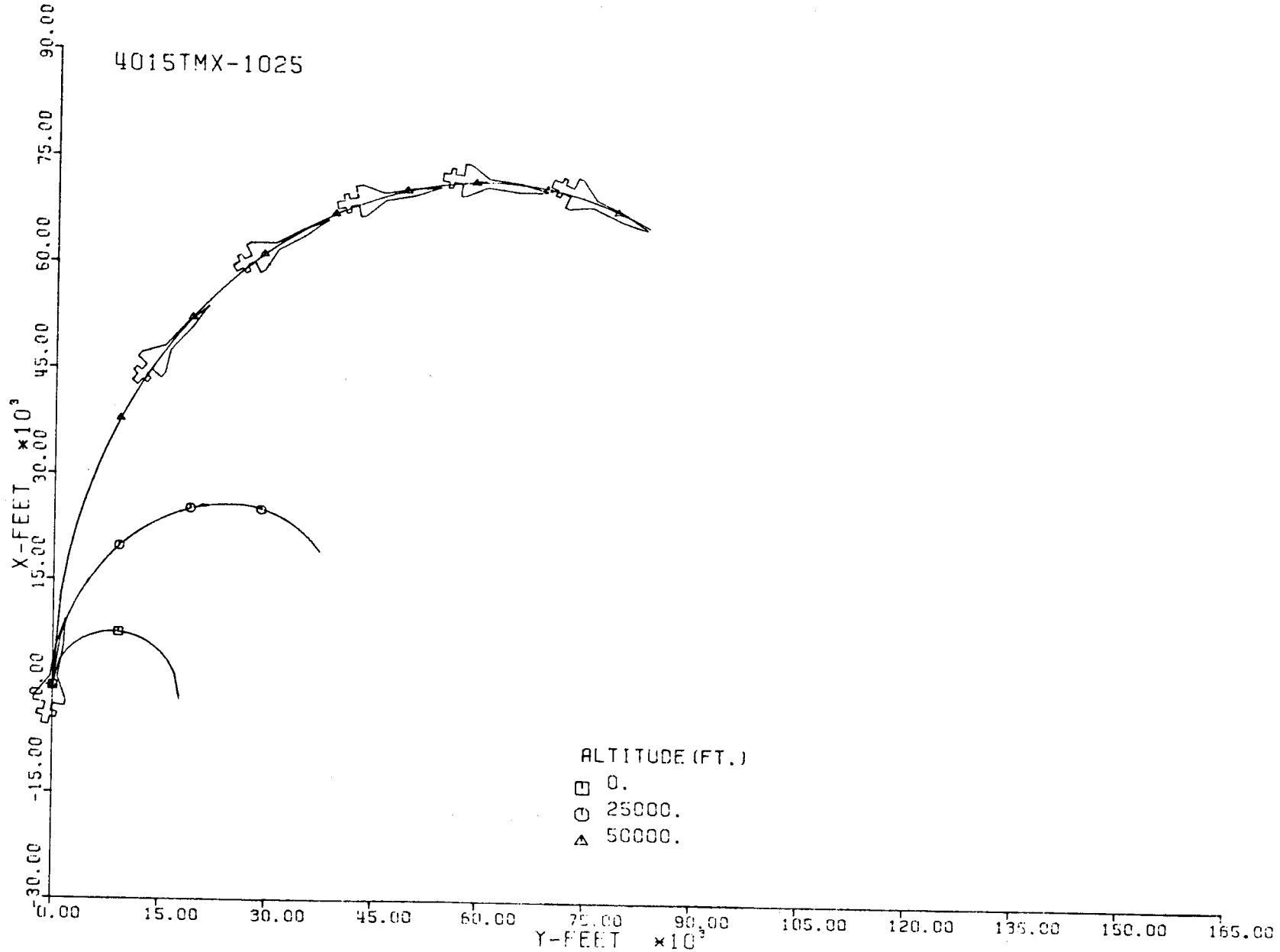

Fig. 72-III. Constant Altitude Flight Path, X vs. Y.

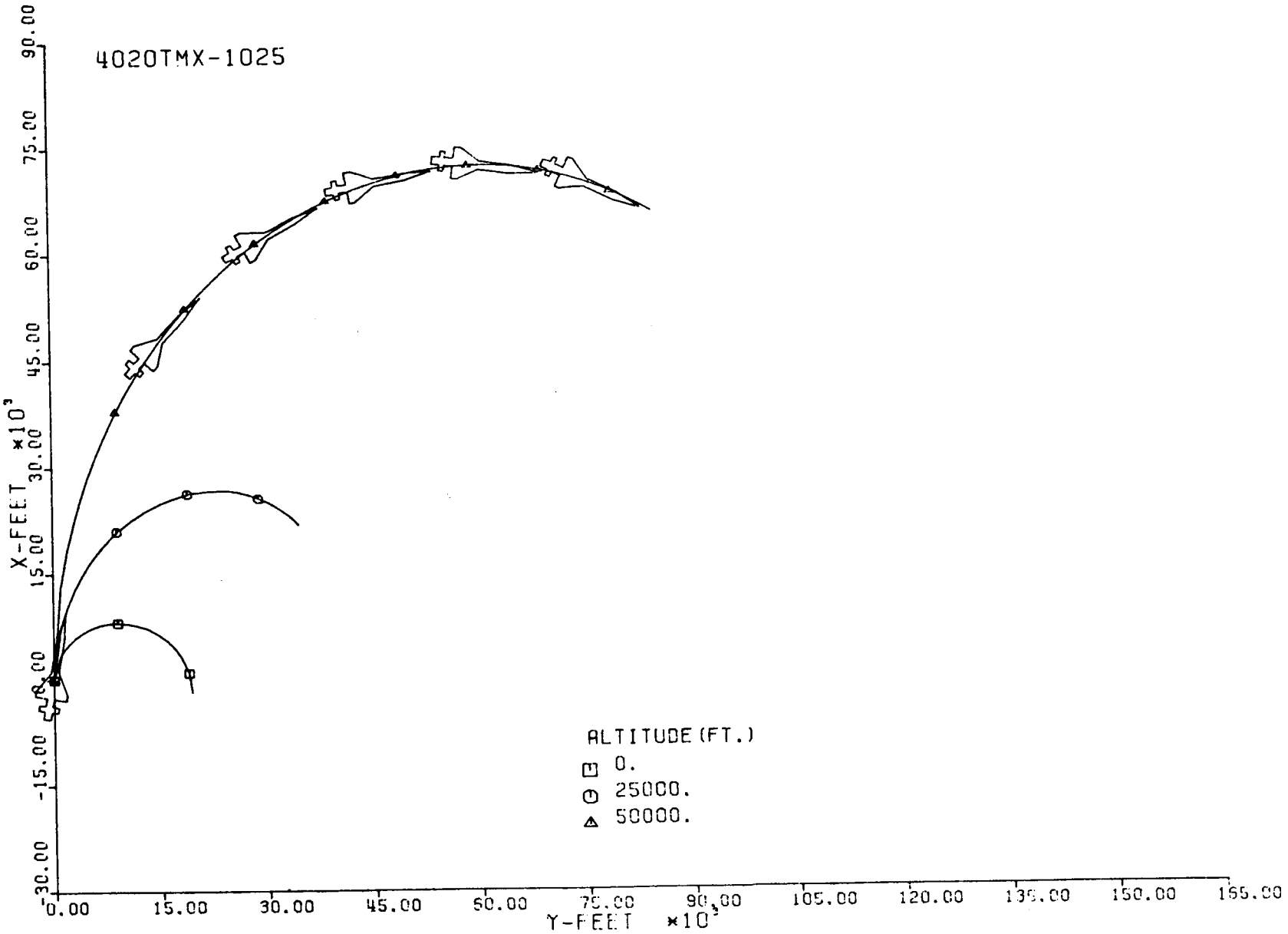

Fig. 73-III. Constant Altitude Flight Path, X vs. Y.

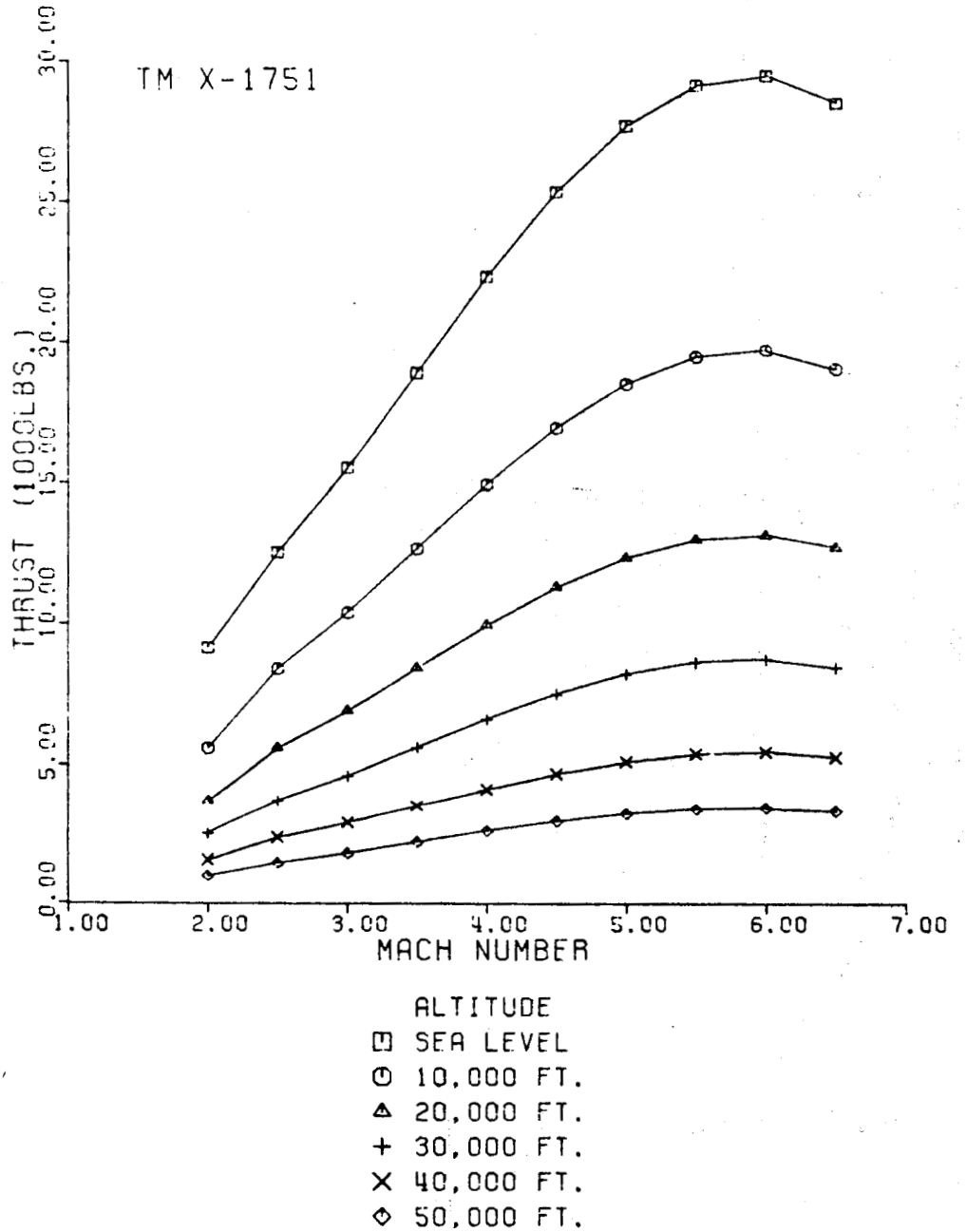

Fig. 74-I. Thrust vs. Terminal Mach No.

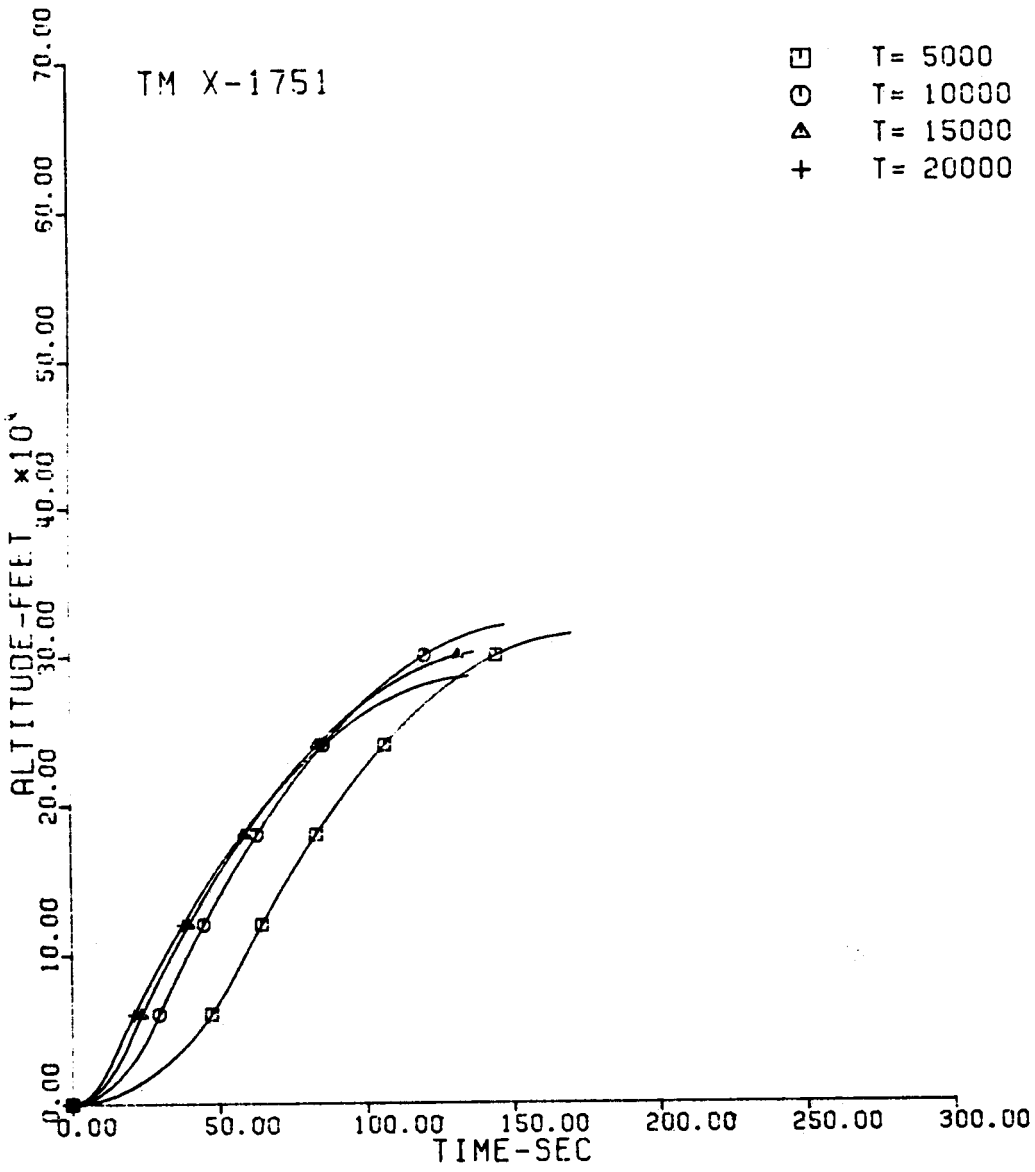

Fig. 75-II. Altitude vs. Flight Time.

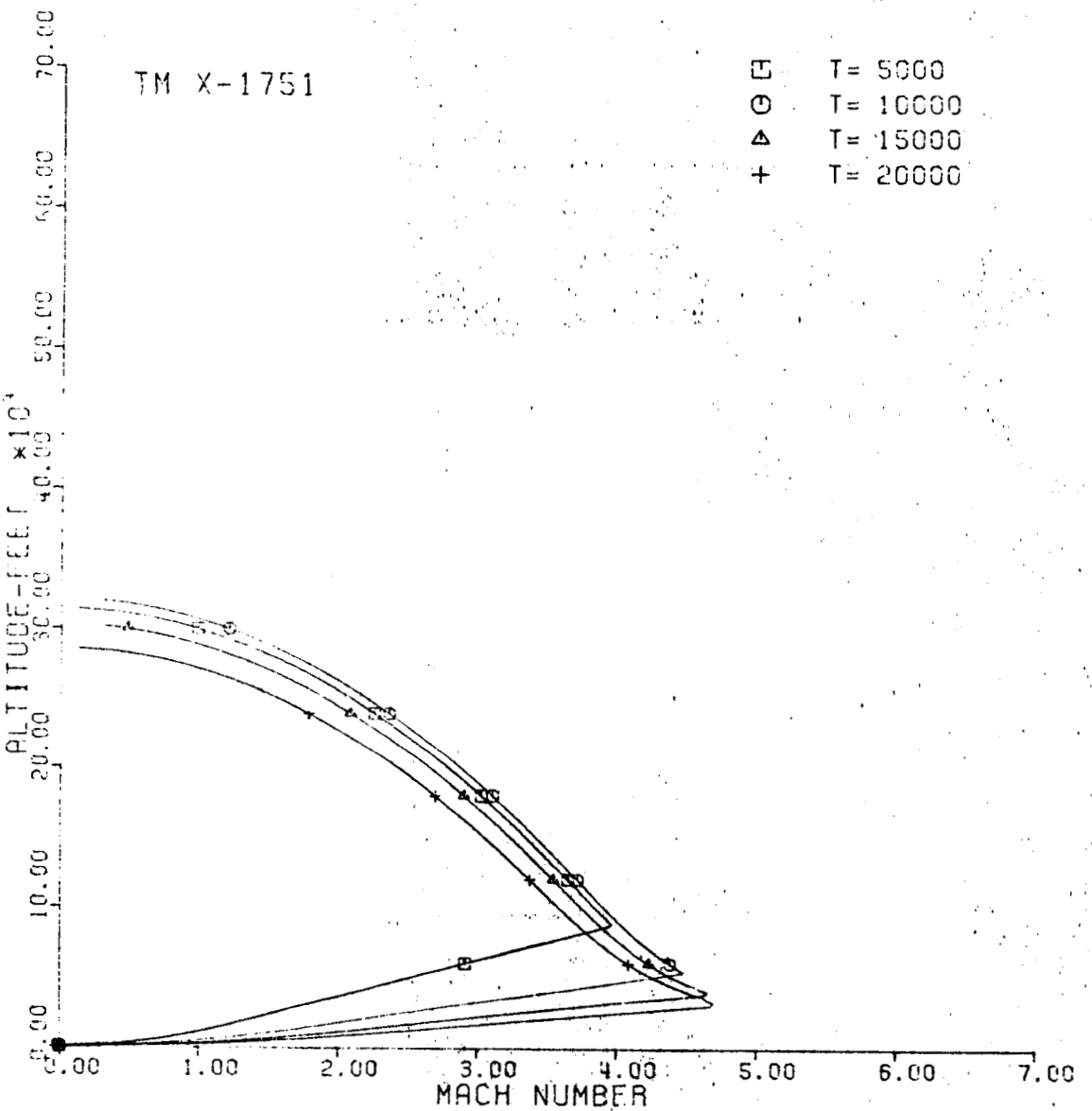

Fig. 76-II. Altitude vs. Mach No.

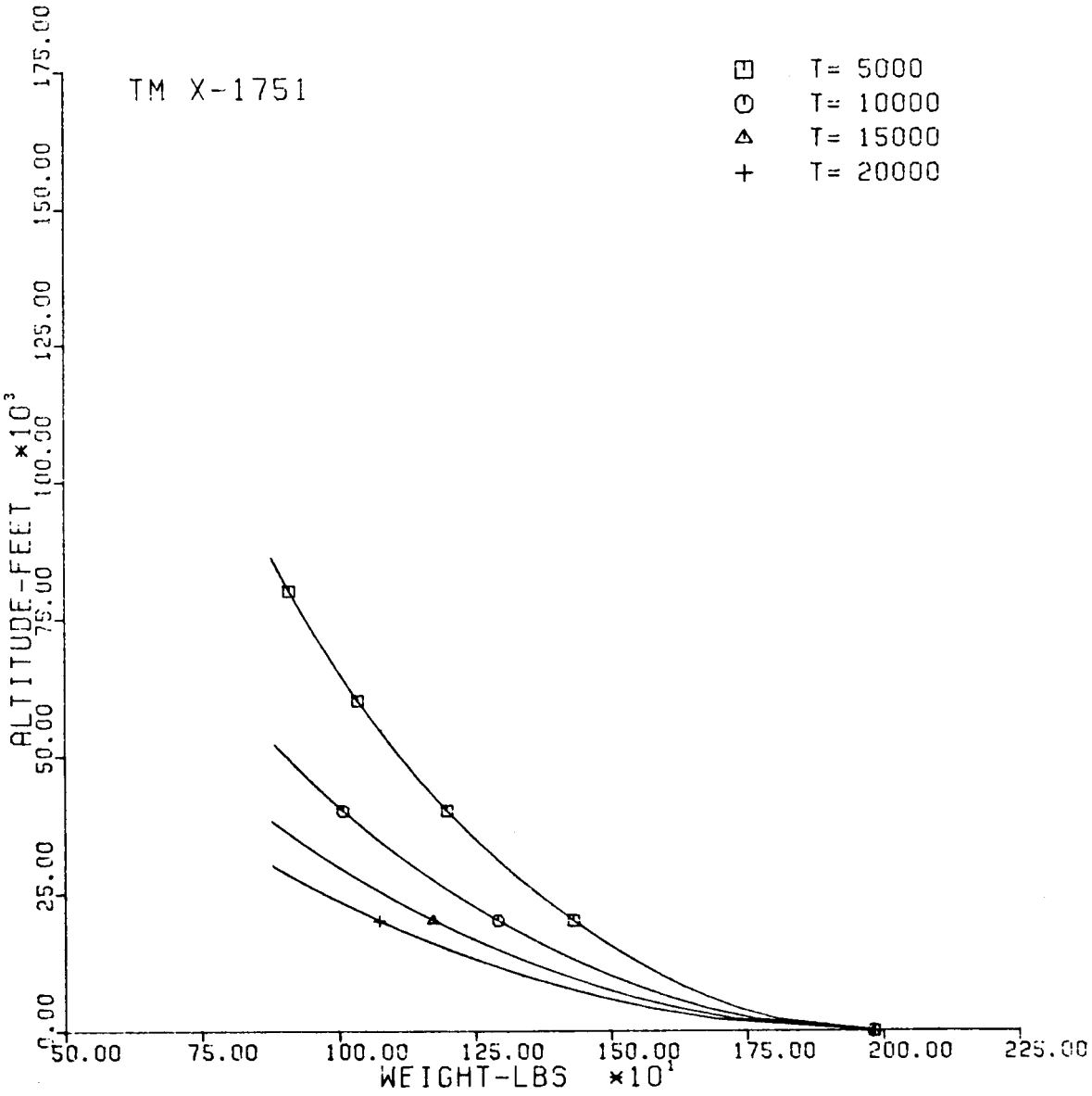

Fig. 77-II. Altitude vs. Vehicle Weight.

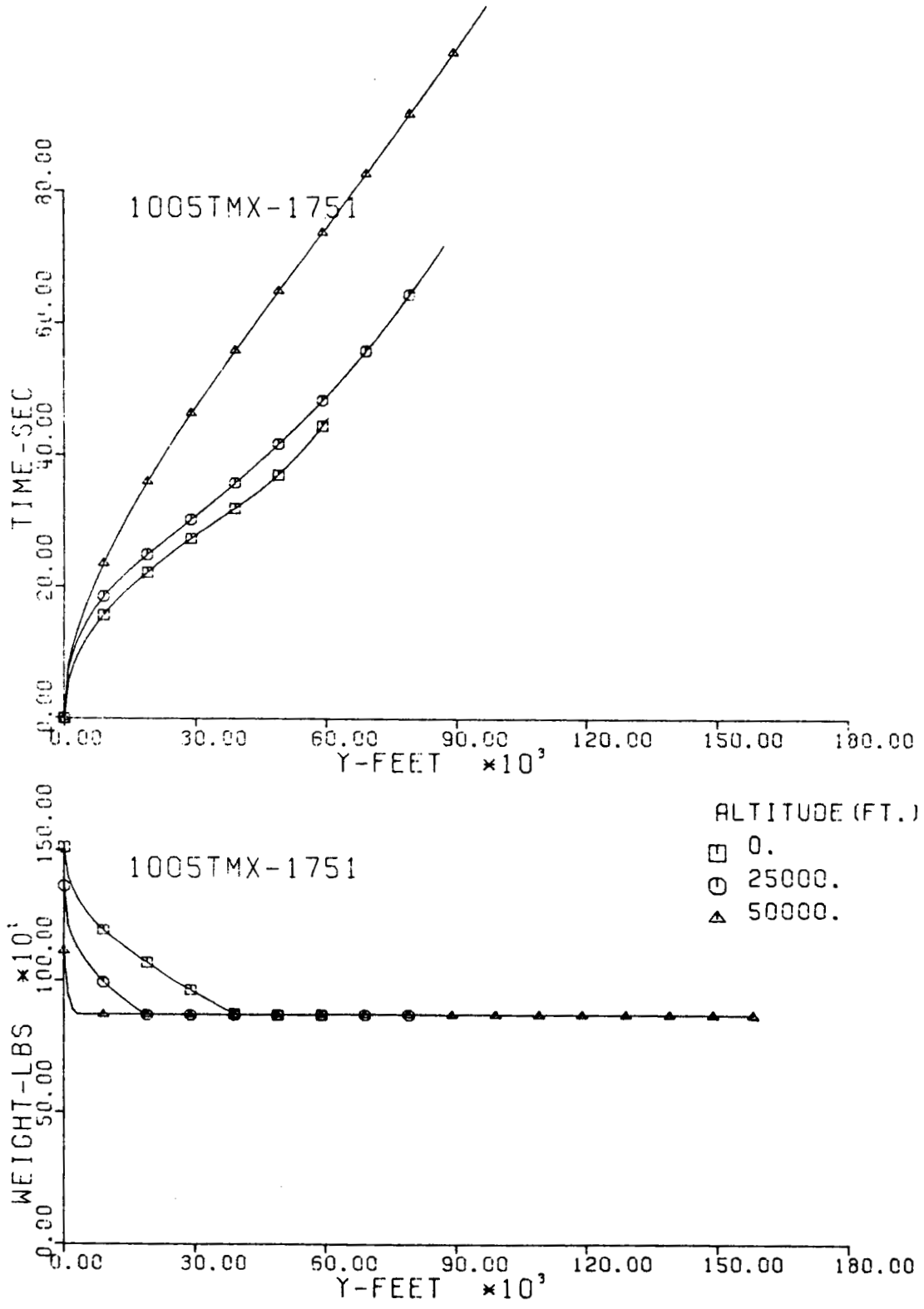

Fig. 78-III. Flight Time and Vehicle Weight vs. Downrange Distance, Y.

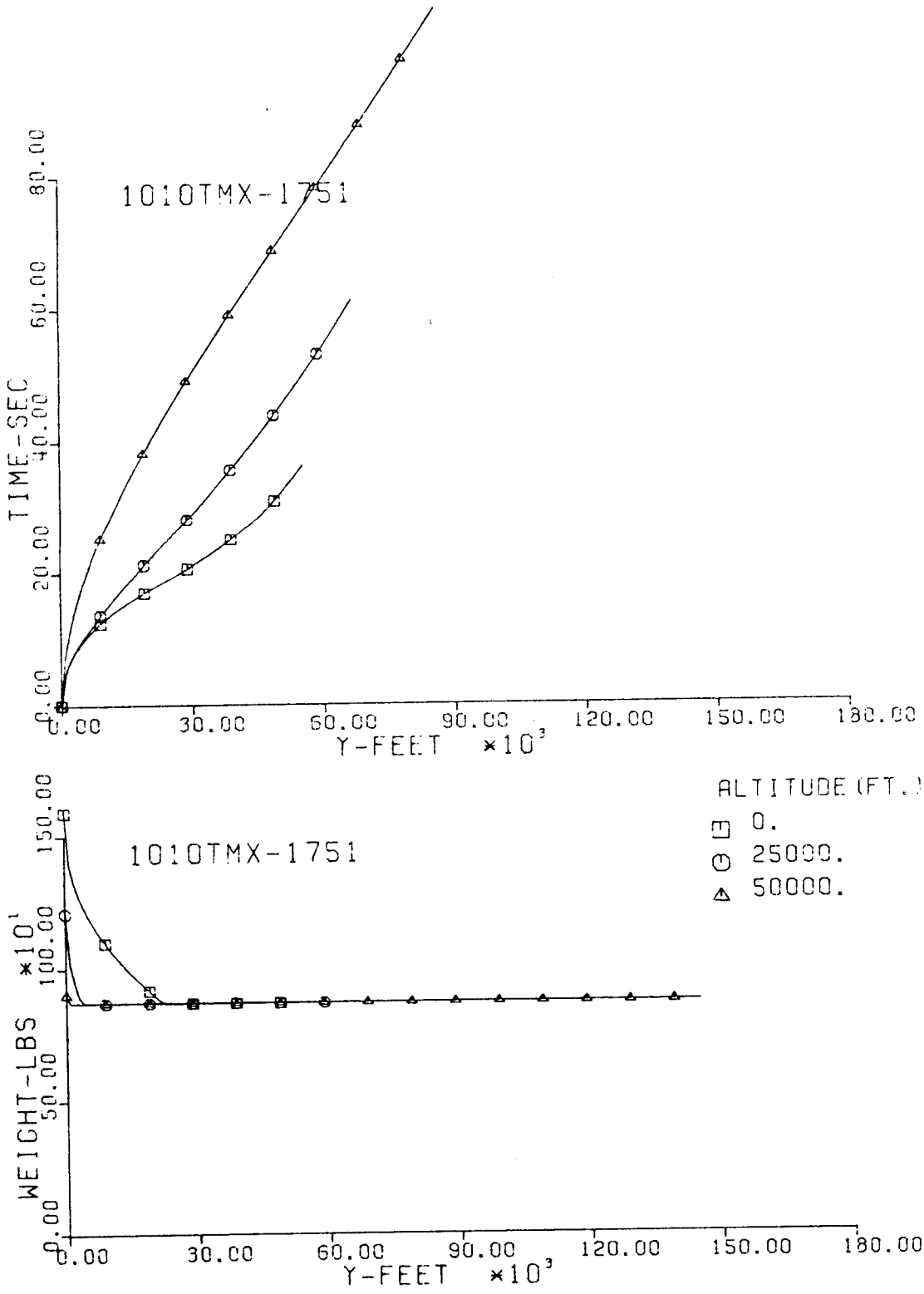

Fig. 79-III. Flight Time and Vehicle Weight vs. Downrange Distance, Y.

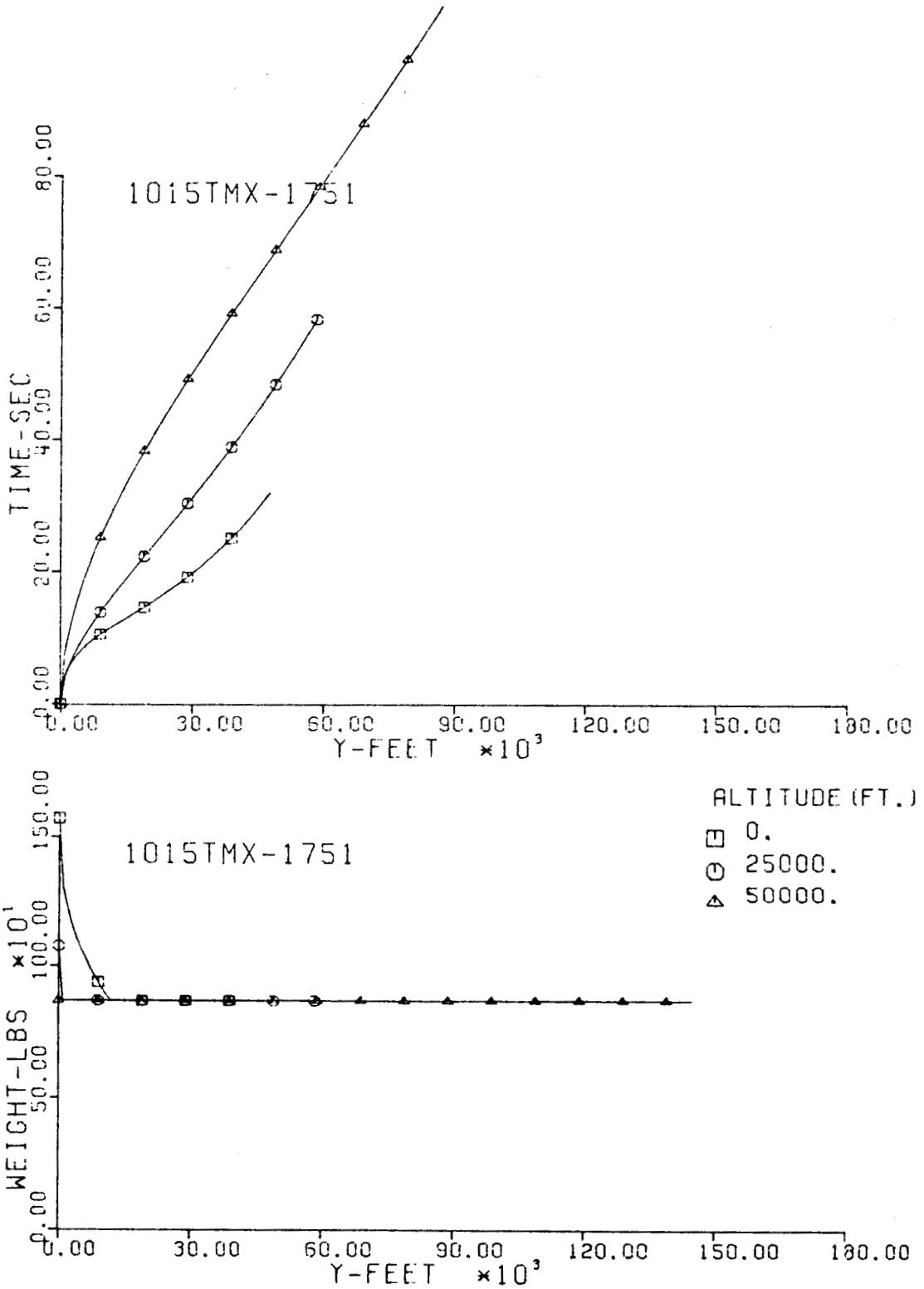

Fig. 80-III. Flight Time and Vehicle Weight vs. Downrange Distance, Y.

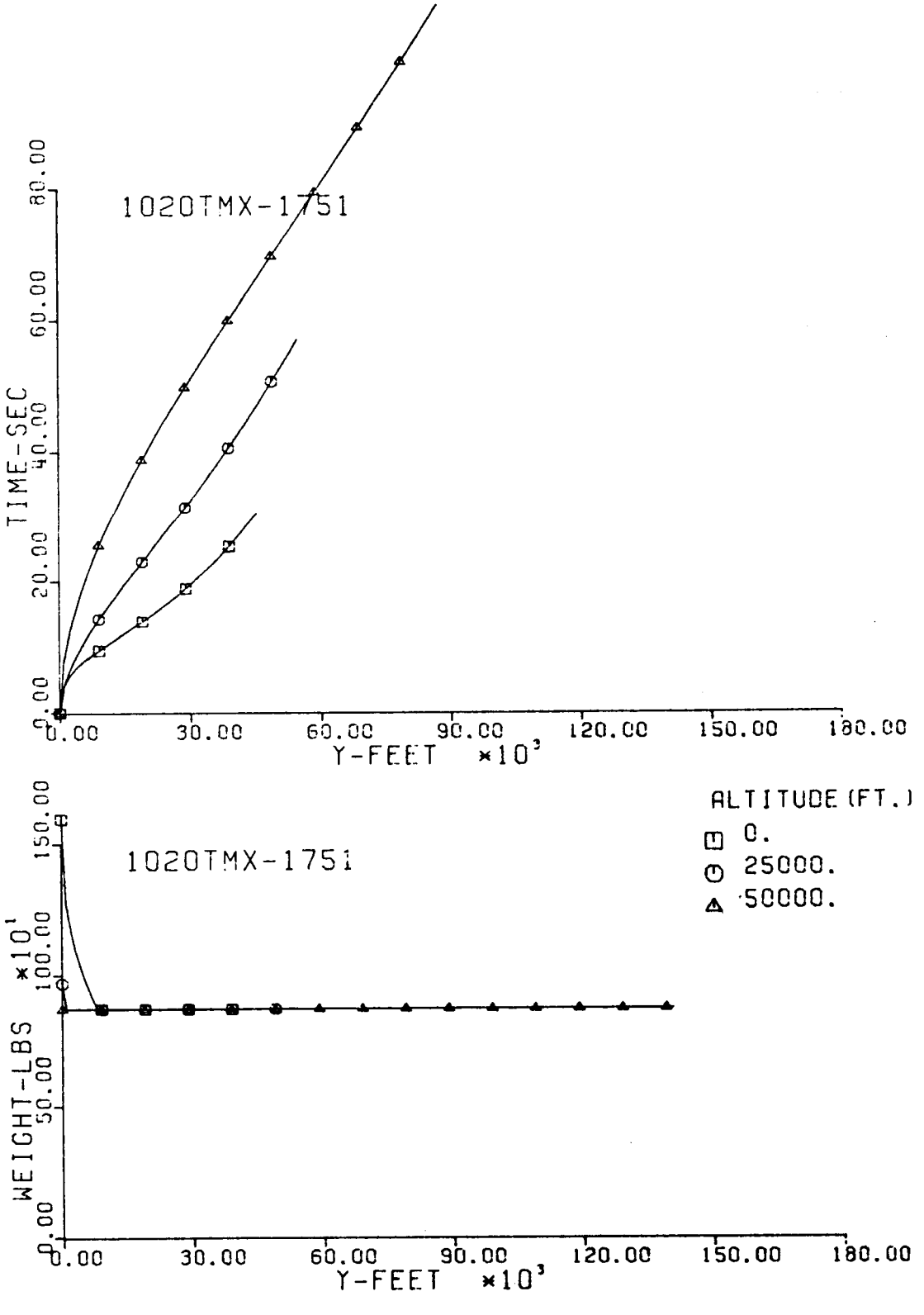

Fig. 81-III. Flight Time and Vehicle Weight vs. Downrange Distance, Y.

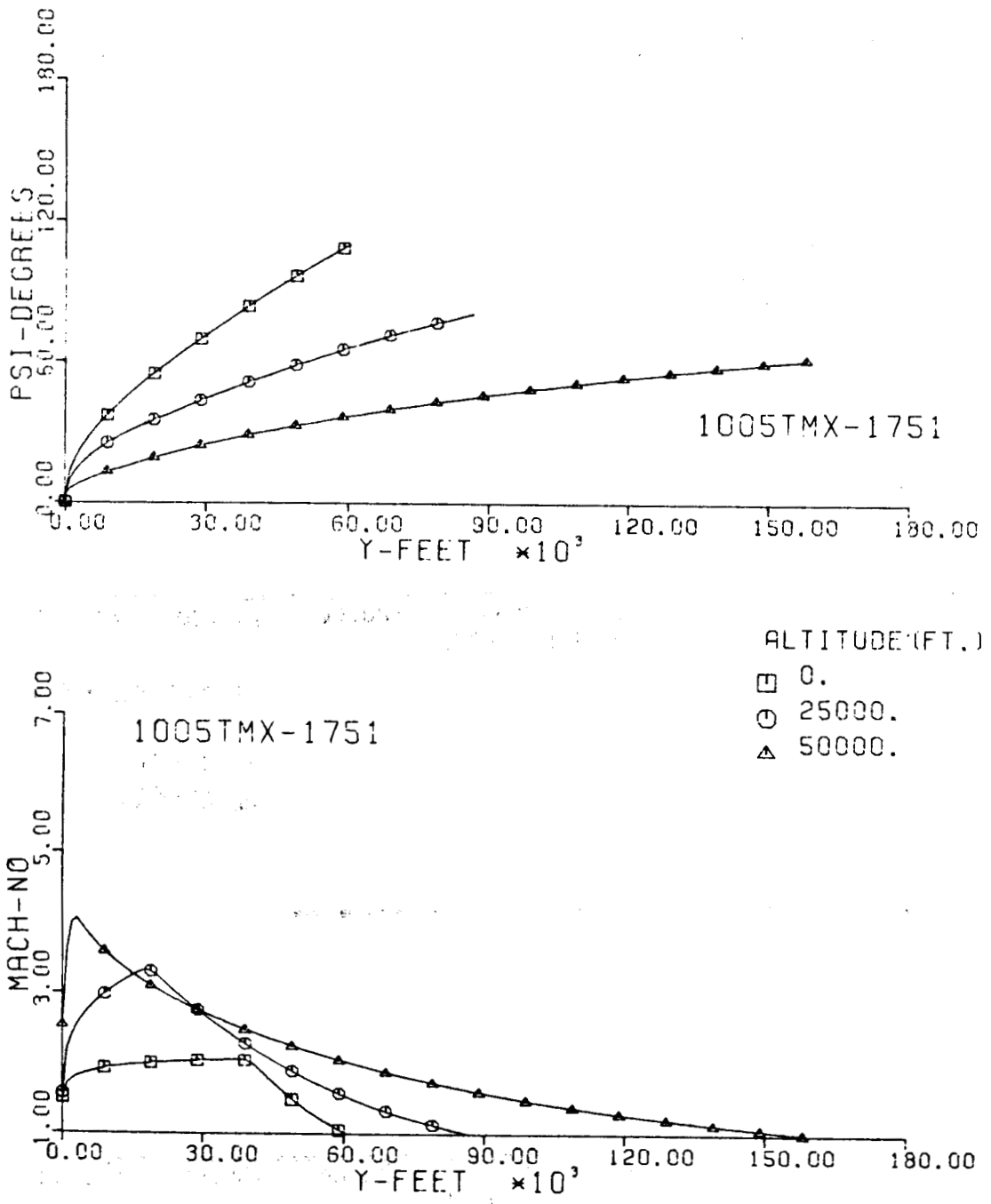

Fig. 82-III. Heading Angle and Mach No. vs. Downrange Distance, Y.

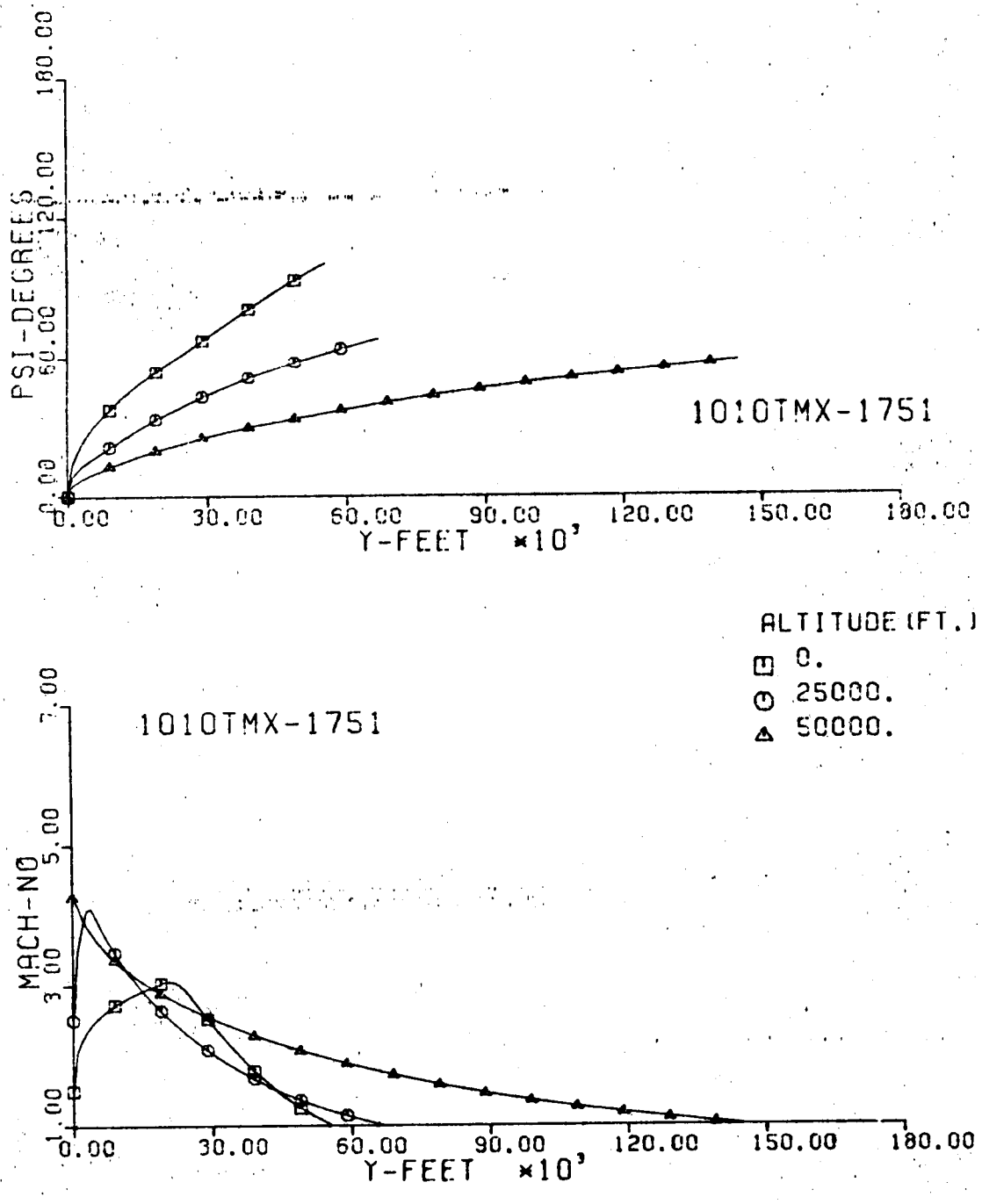

Fig. 83-III. Heading Angle and Mach No. vs. Downrange Distance, Y.

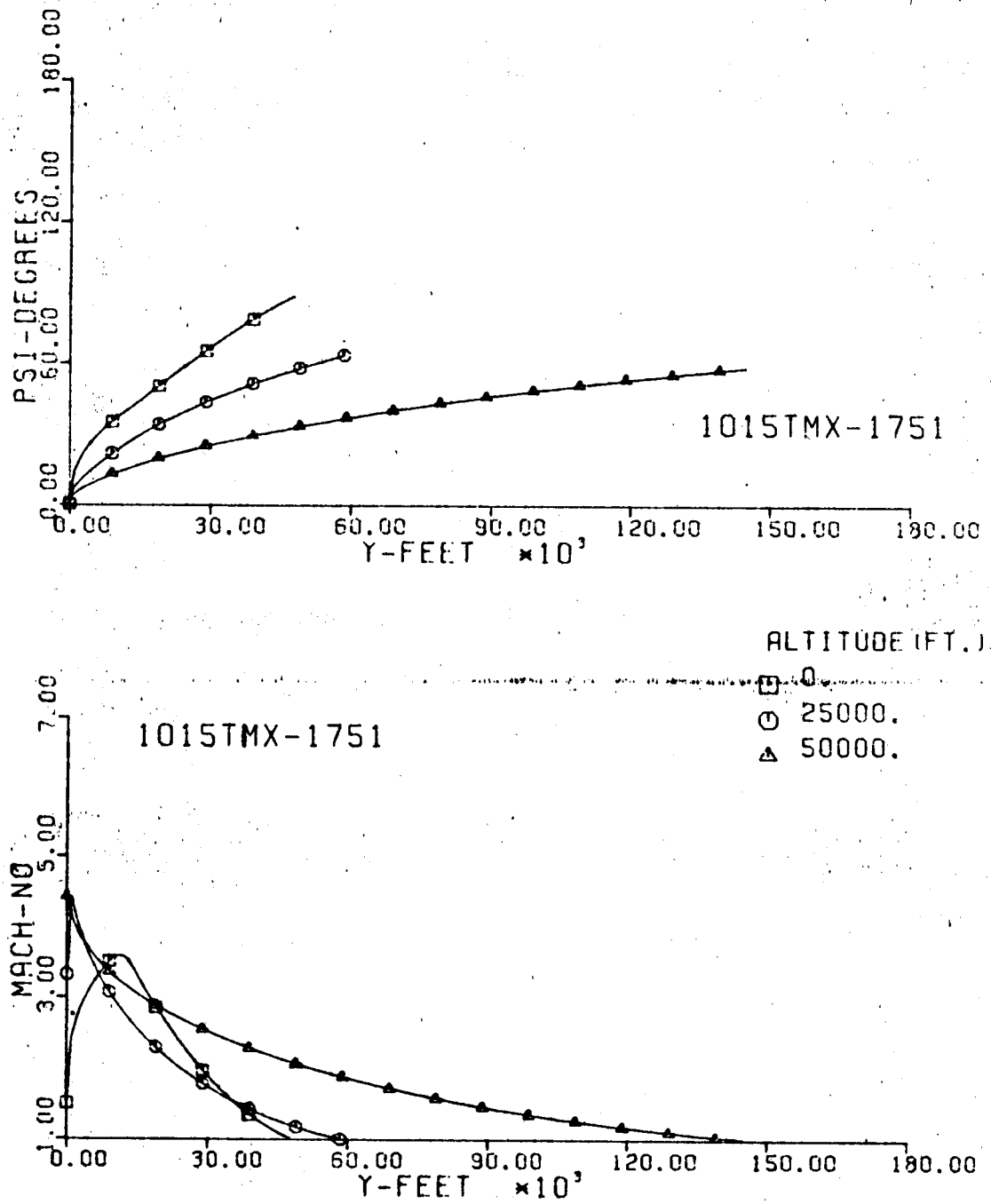

Fig. 84-III. Heading Angle and Mach No. vs. Downrange Distance, Y.

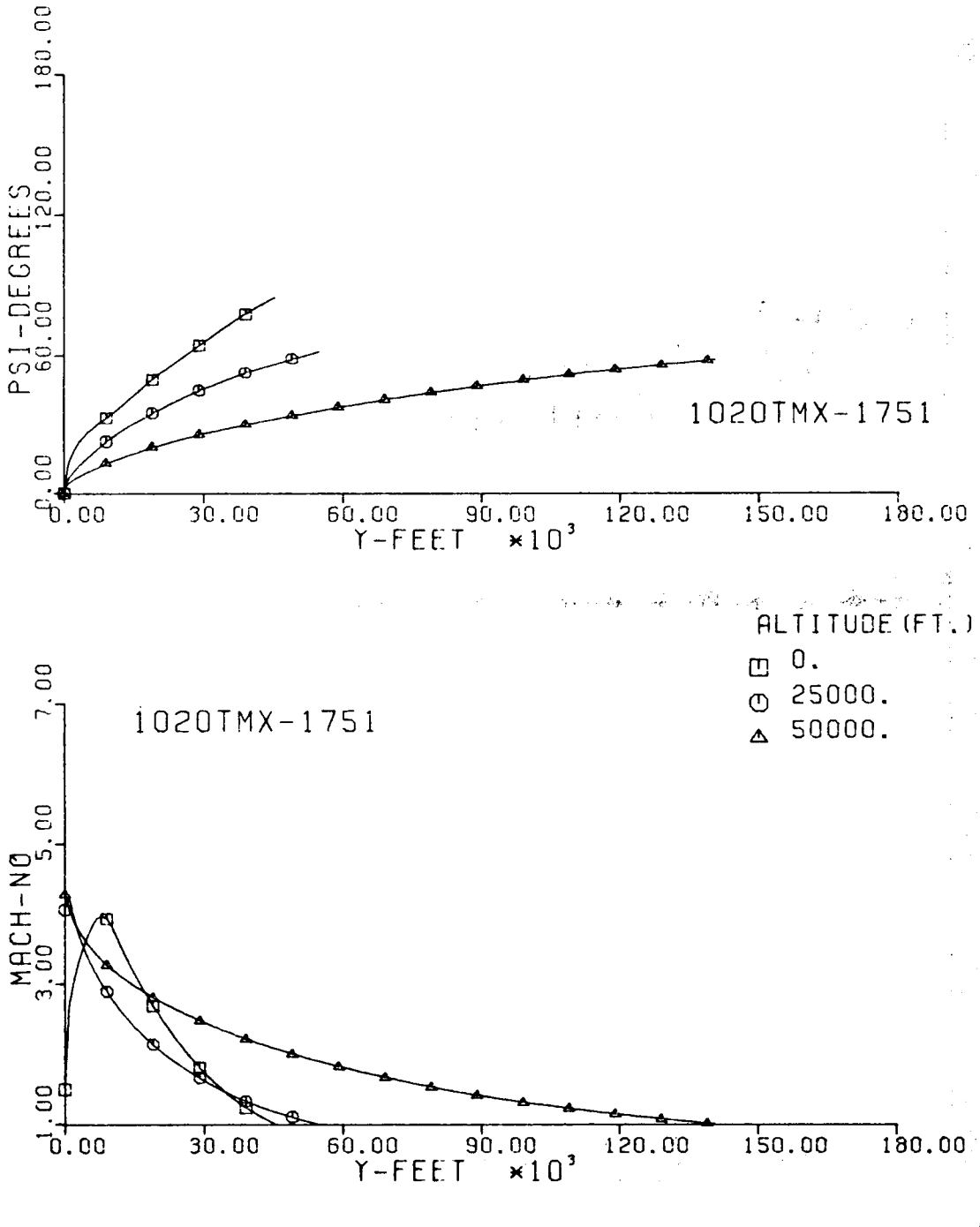

Fig. 85-III. Heading Angle and Mach No. vs. Downrange Distance, Y.

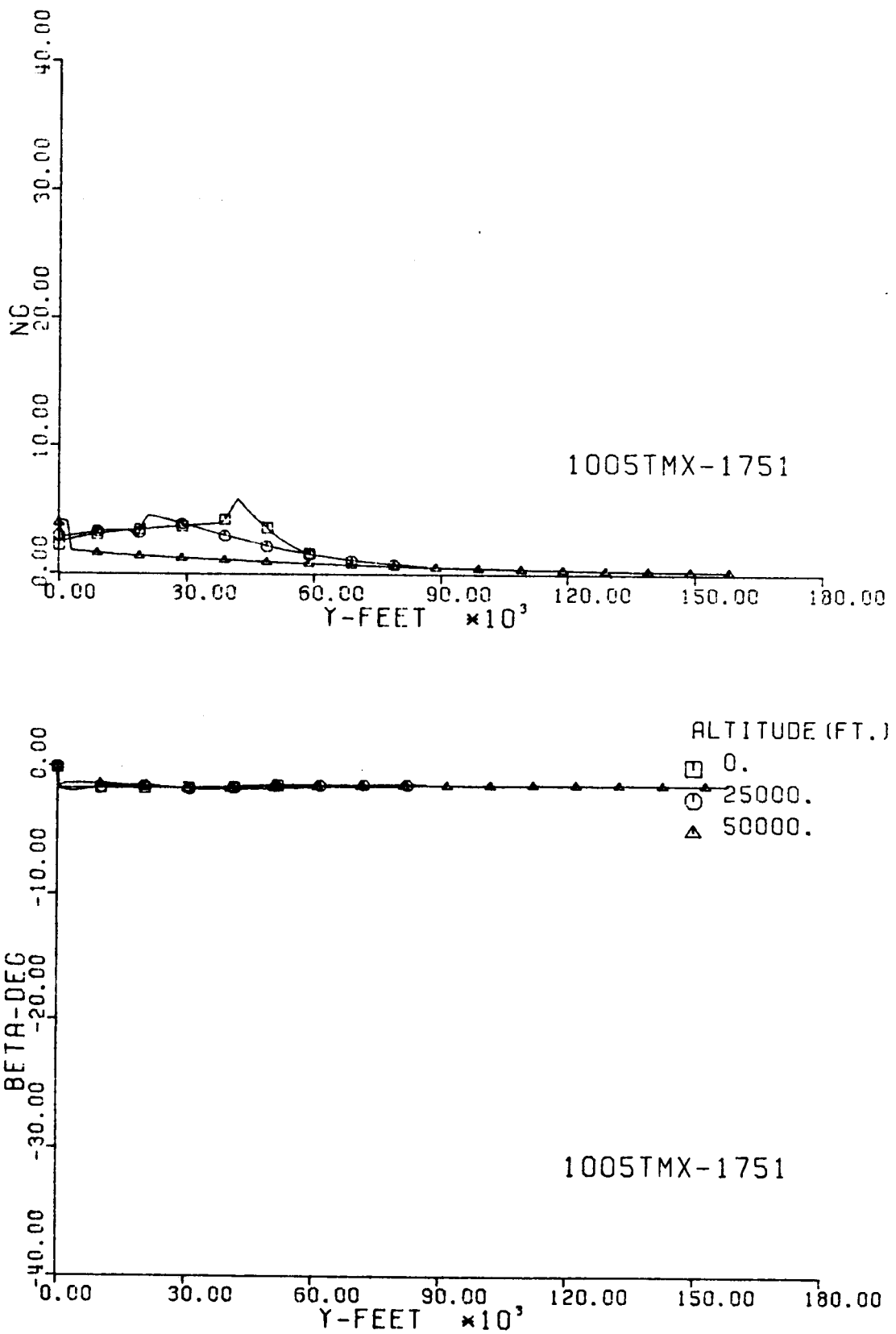

Fig. 86-III. Number of G's and Sideslip Angle vs. Downrange Distance, Y.

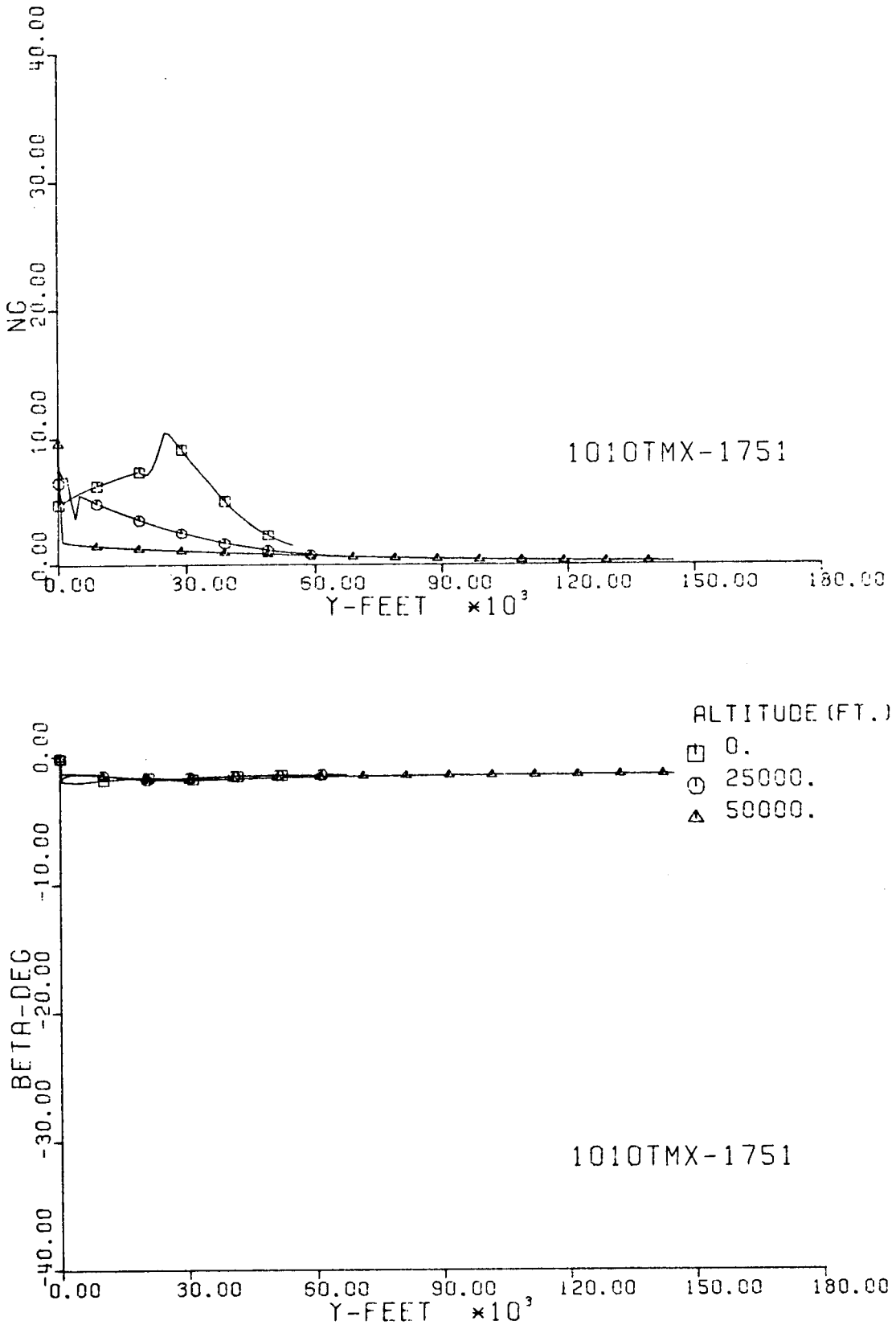

Fig. 87-III. Number of G's and Sideslip Angle vs. Downrange Distance, Y.

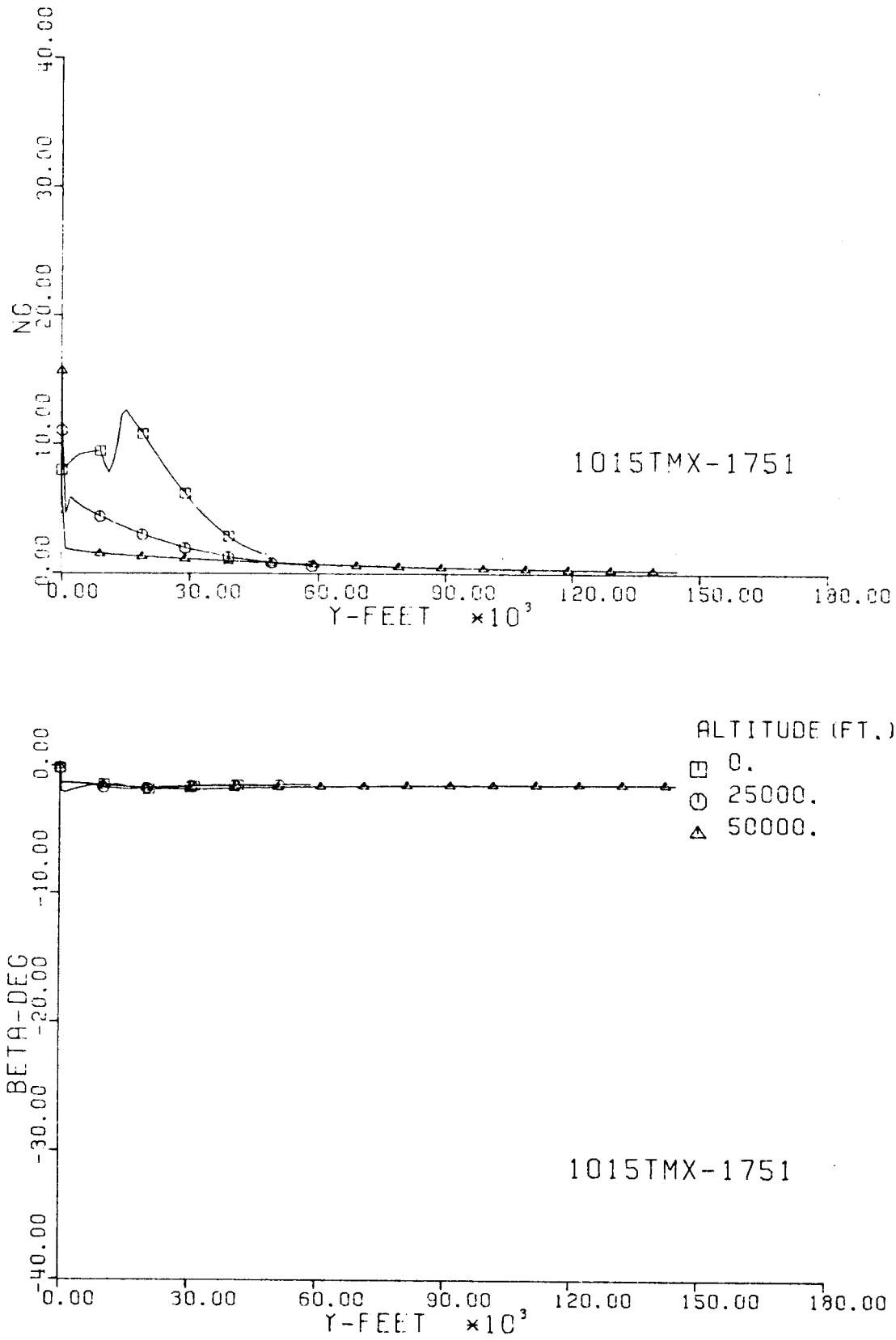

Fig. 88-III. Number of G's and Sideslip Angle vs. Downrange Distance, Y.

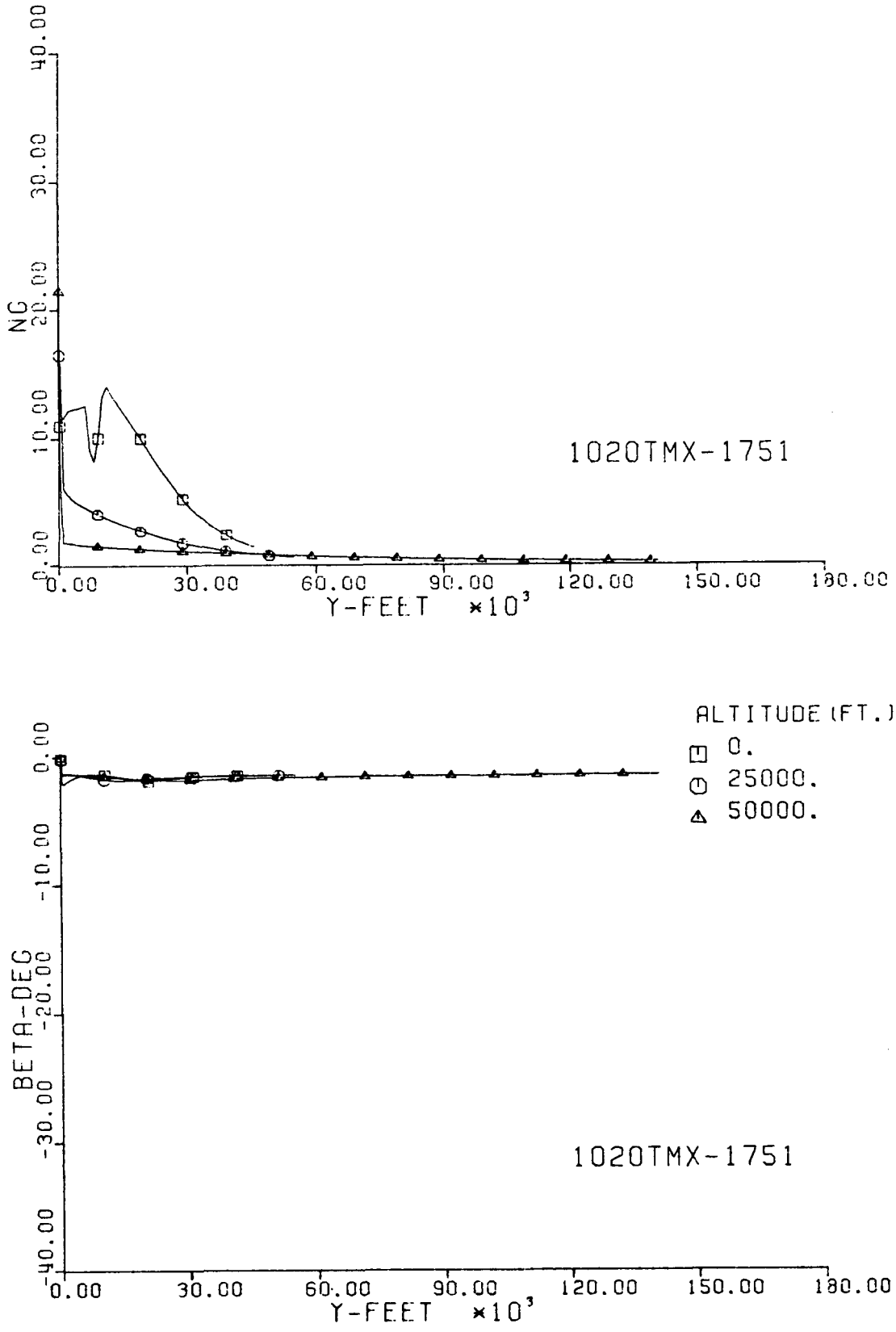

Fig. 89-III. Number of G's and Sideslip Angle vs. Downrange Distance, Y.

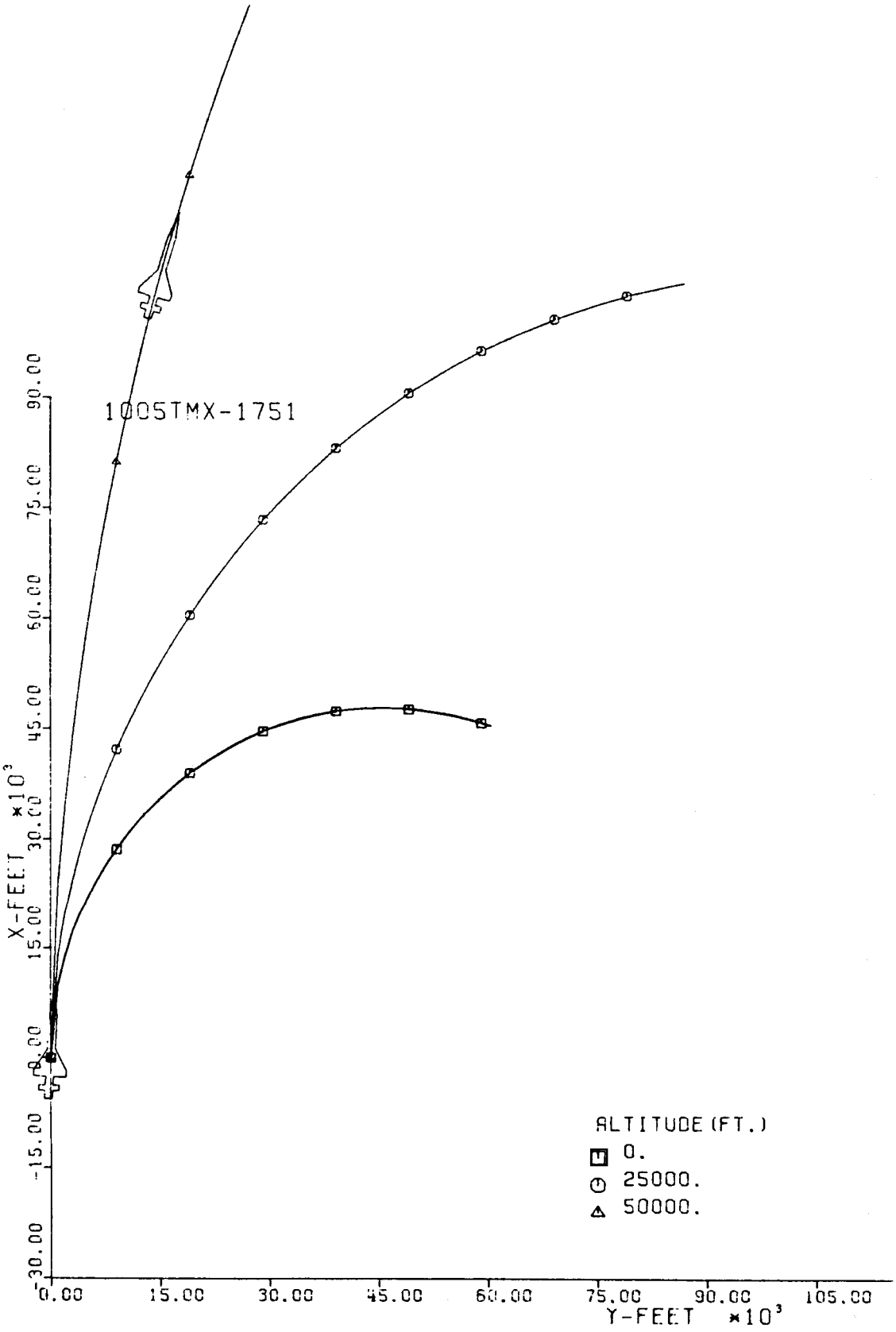

Fig. 90-III. Constant Altitude Flight Path, X vs. Y.

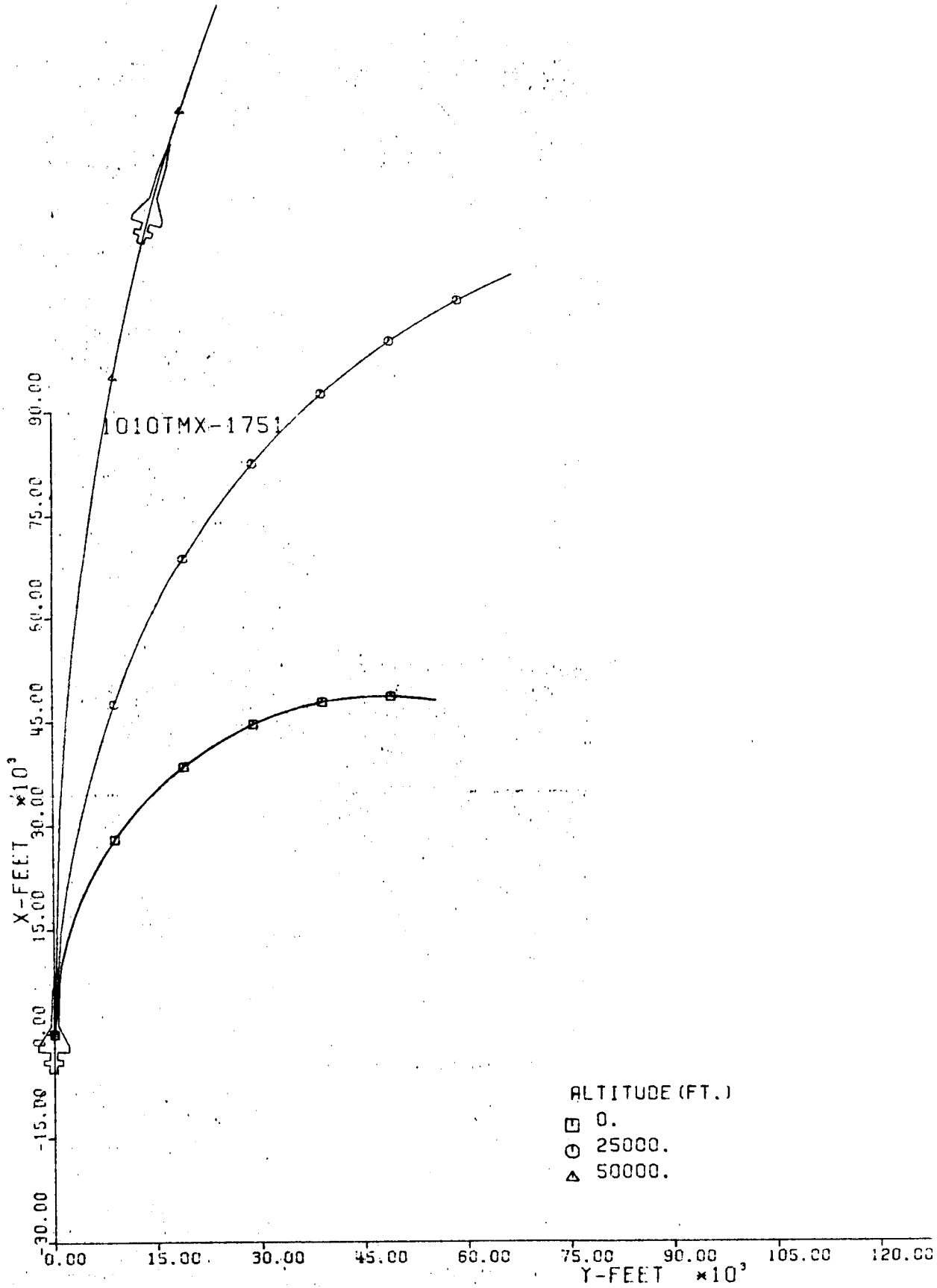

Fig. 91-III. Constant Altitude Flight Path, X vs. Y.

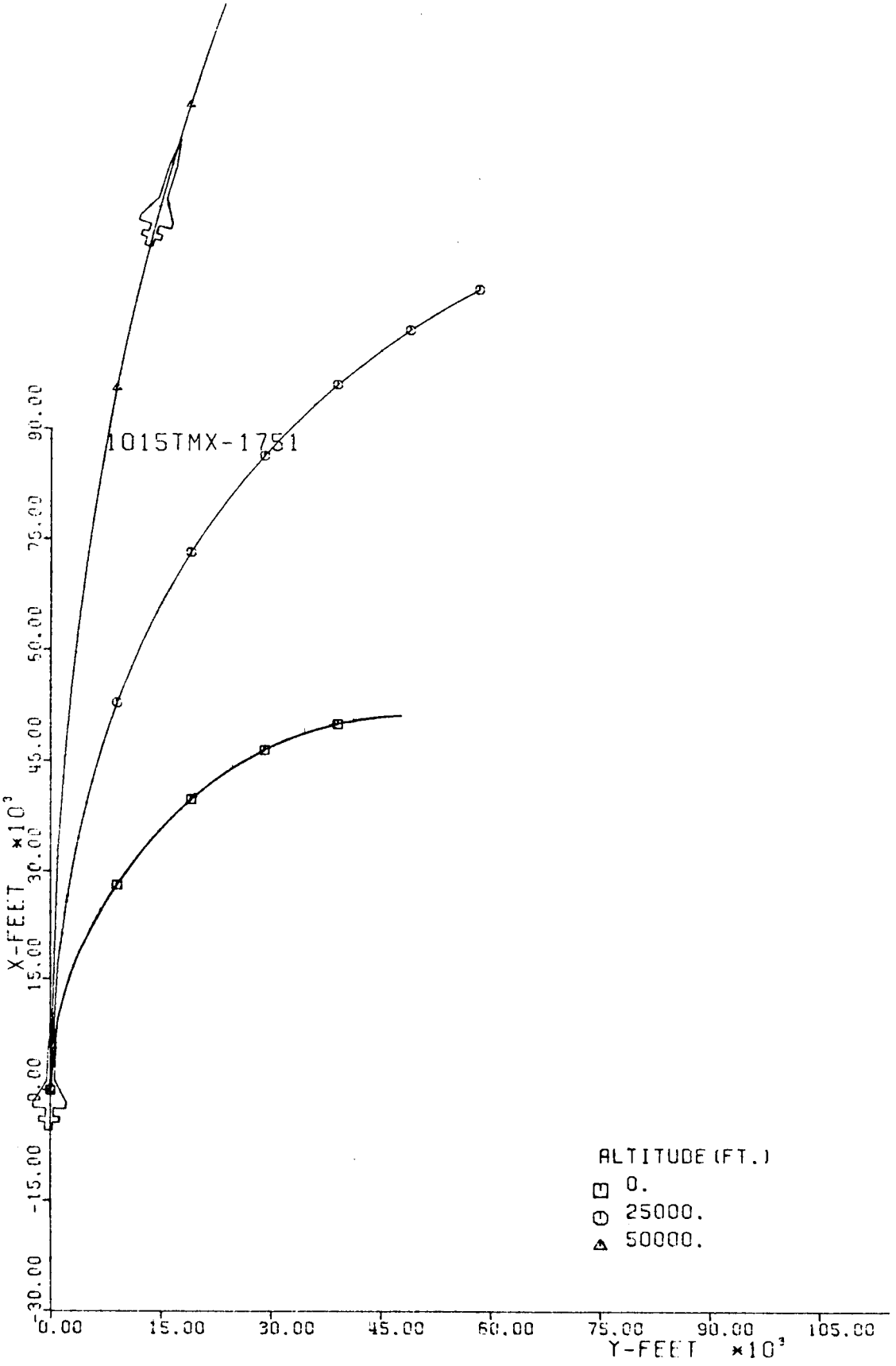

Fig. 92-III. Constant Altitude Flight Path, X vs. Y.

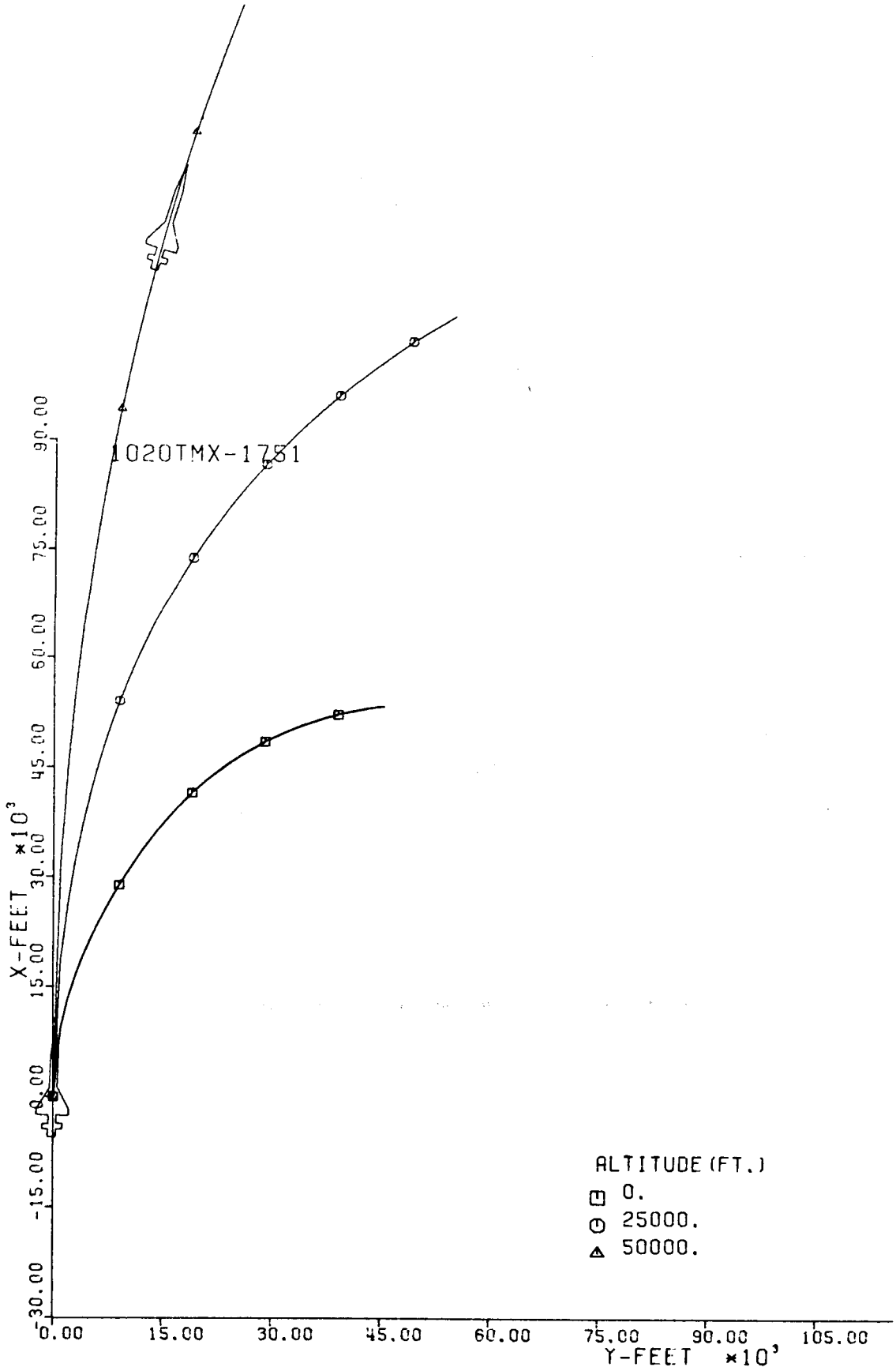

Fig. 93-III. Constant Altitude Flight Path, X vs. Y.

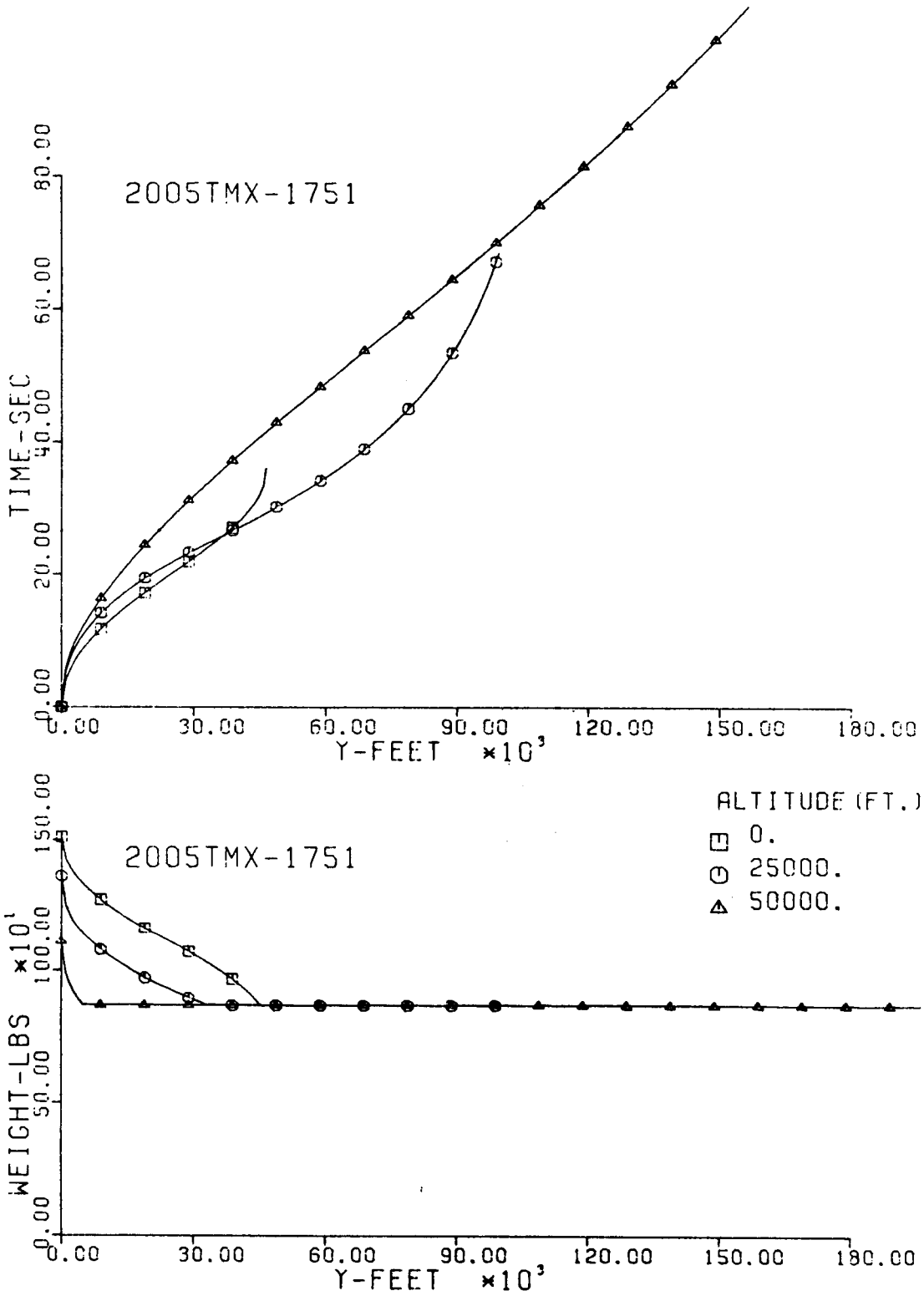

Fig. 94-III. Flight Time and Vehicle Weight vs. Downrange Distance, Y.

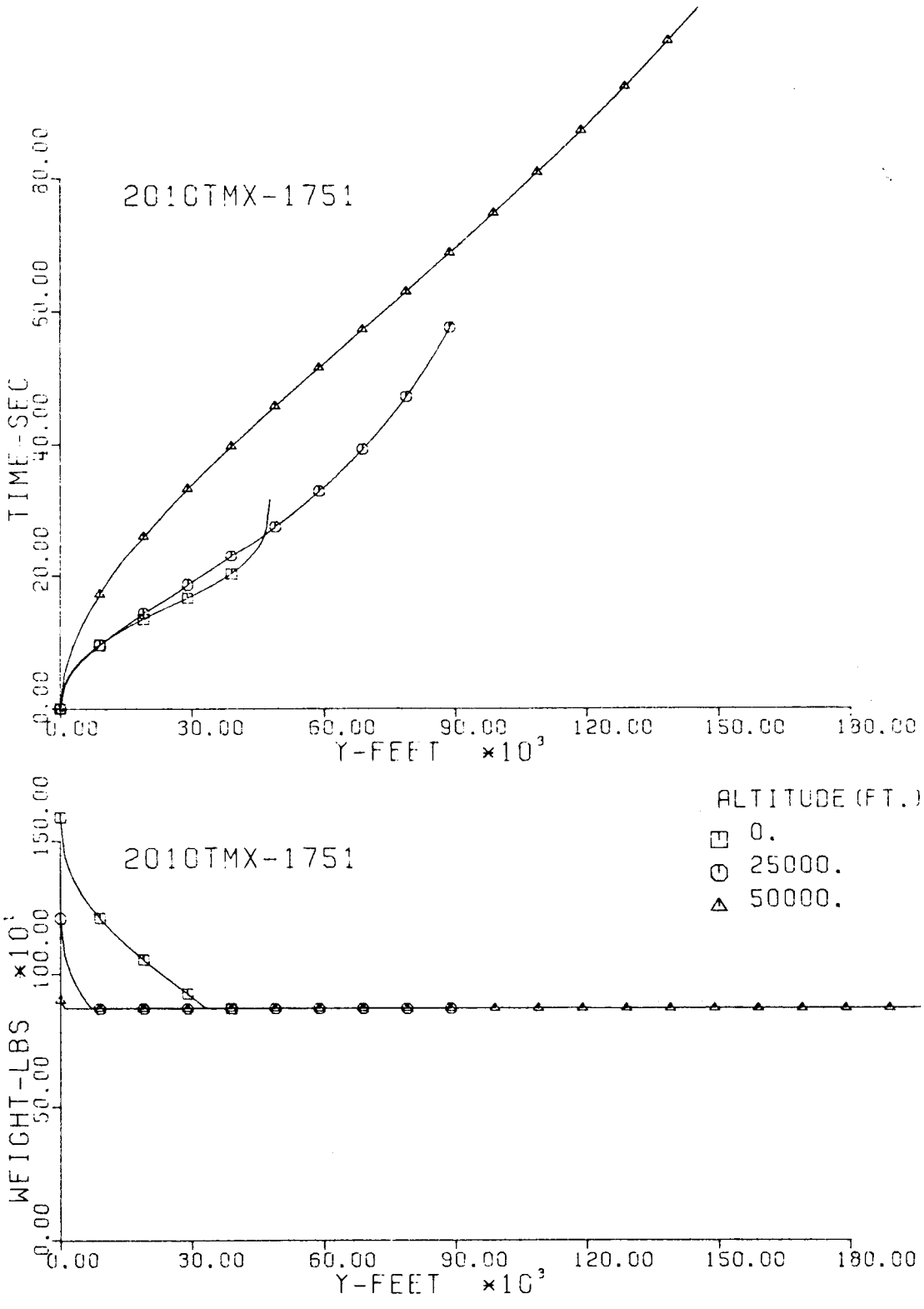

Fig. 95-III. Flight Time and Vehicle Weight vs. Downrange Distance, Y.

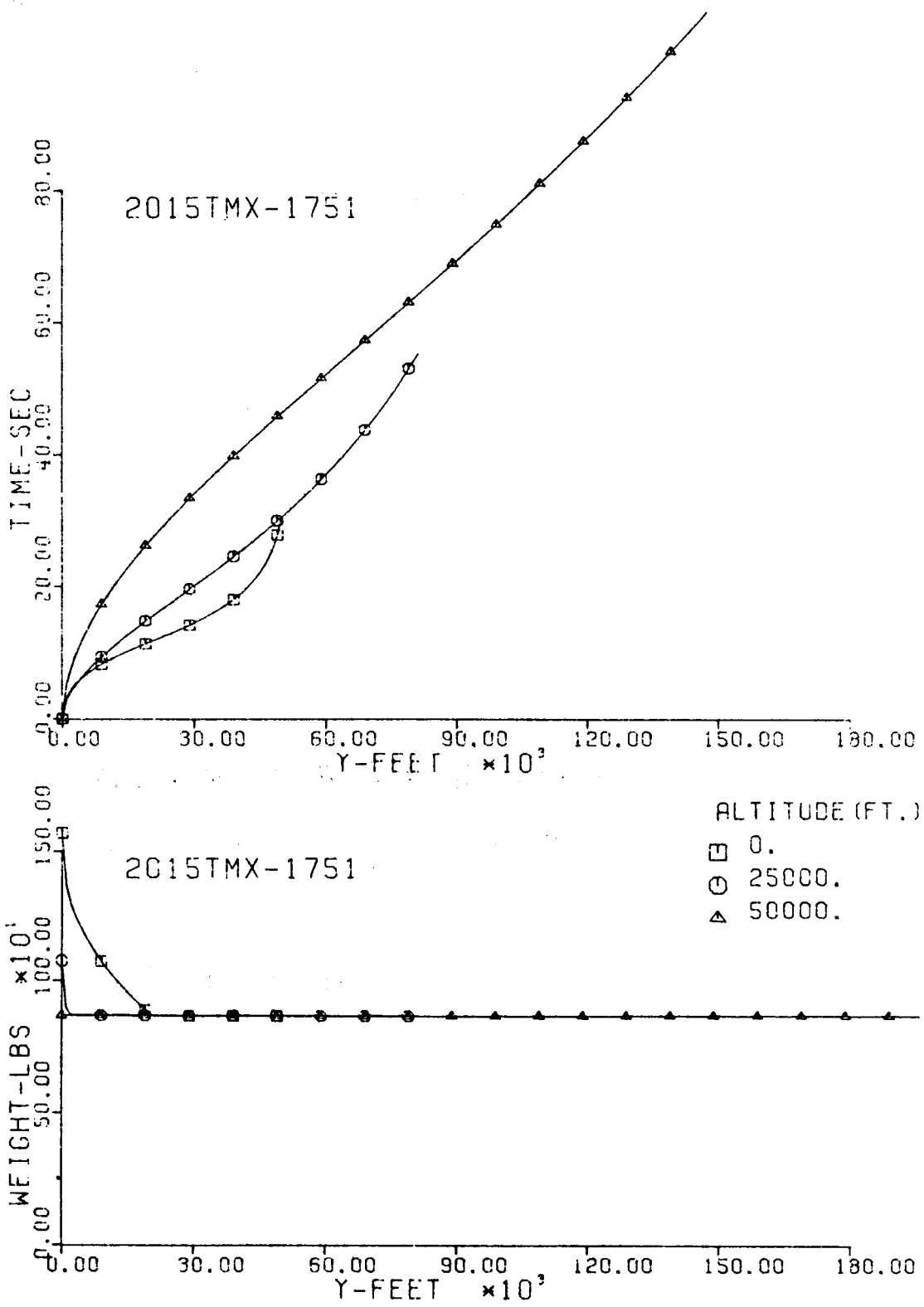

Fig. 96-III. Flight Time and Vehicle Weight vs. Downrange Distance, Y.

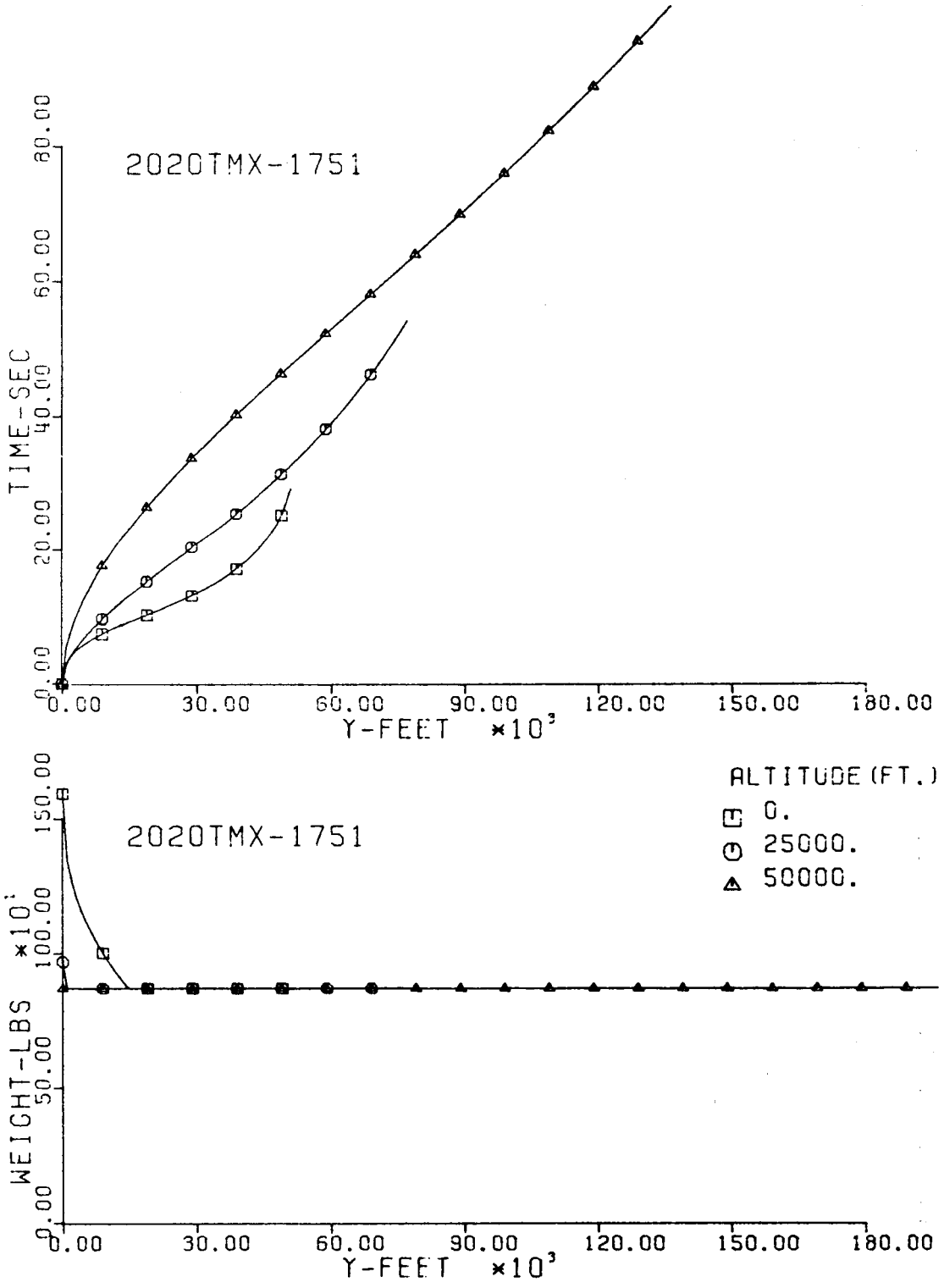

Fig. 97-III. Flight Time and Vehicle Weight vs. Downrange Distance, Y.

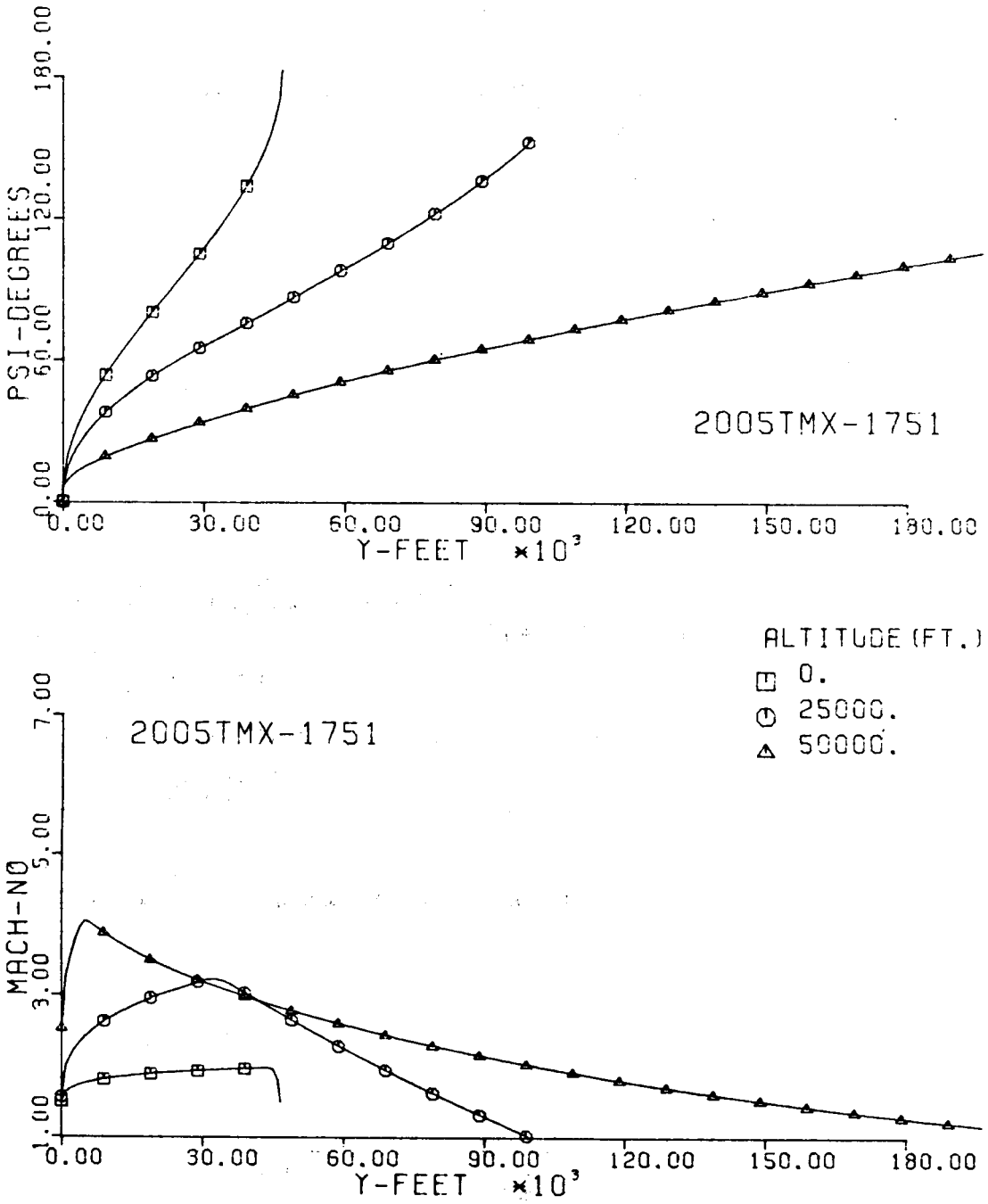

Fig. 98-III. Heading Angle and Mach No. vs. Downrange Distance, Y.

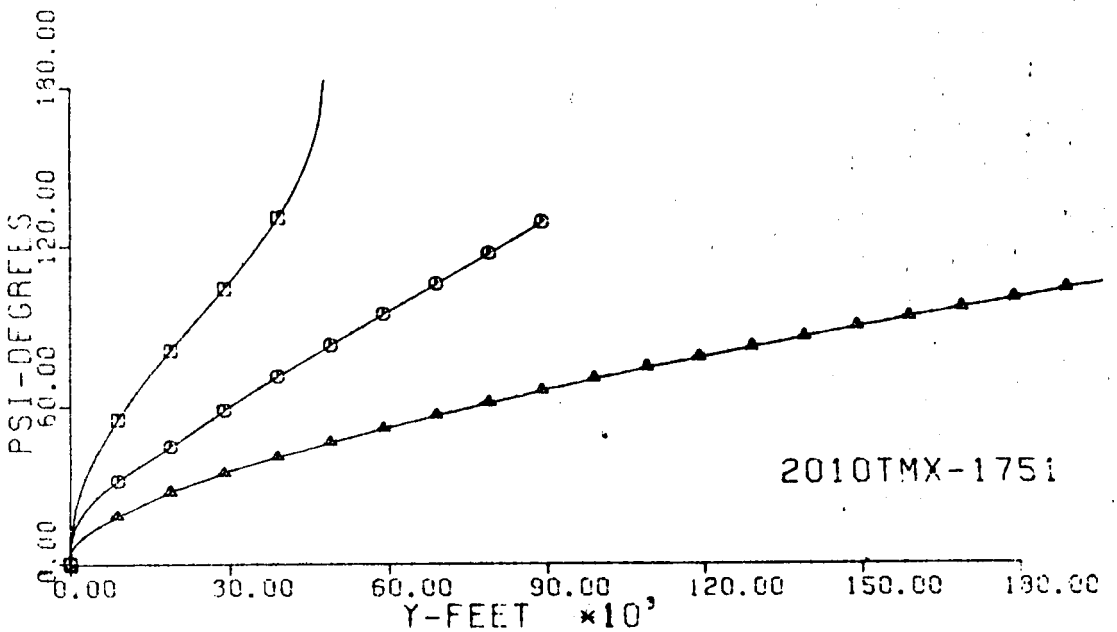

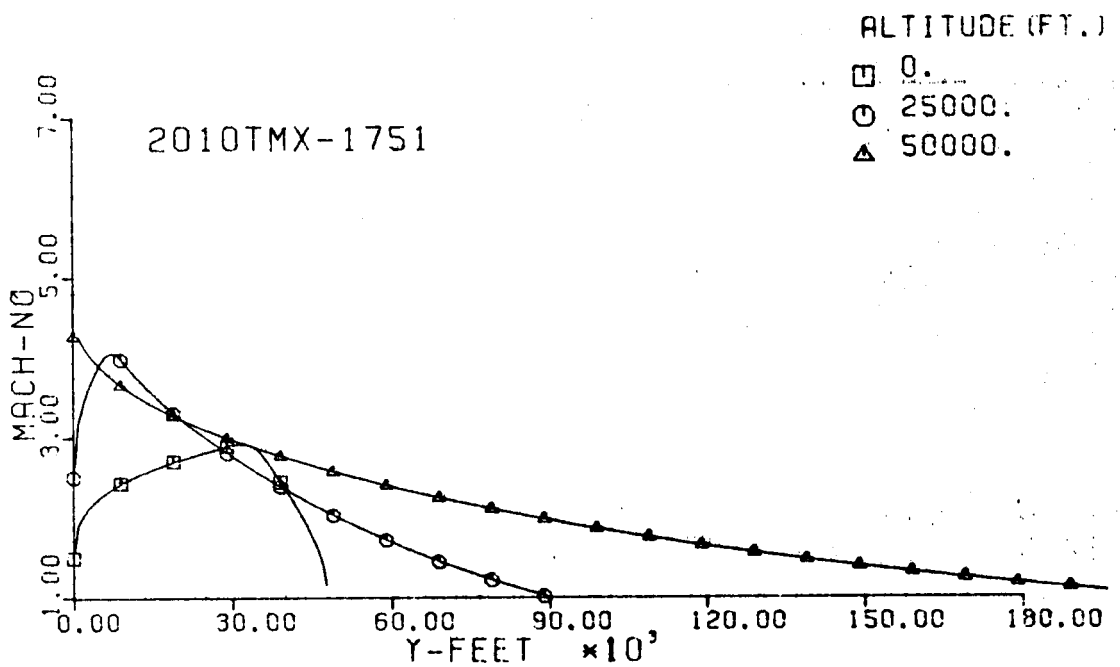

Fig. 99-III. Heading Angle and Mach No. vs. Downrange Distance, Y.

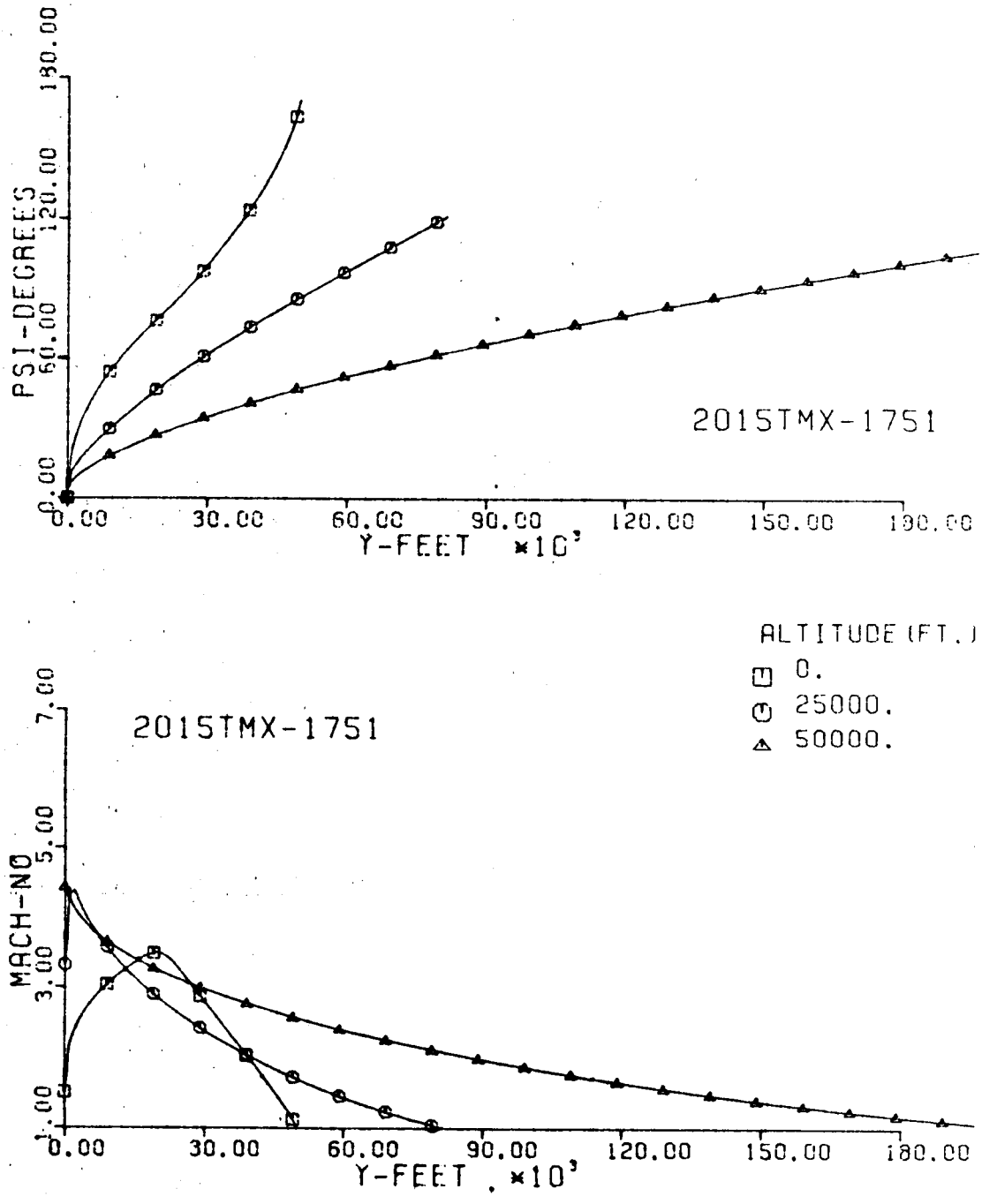

Fig. 100-III. Heading Angle and Mach No. vs. Downrange Distance, Y.

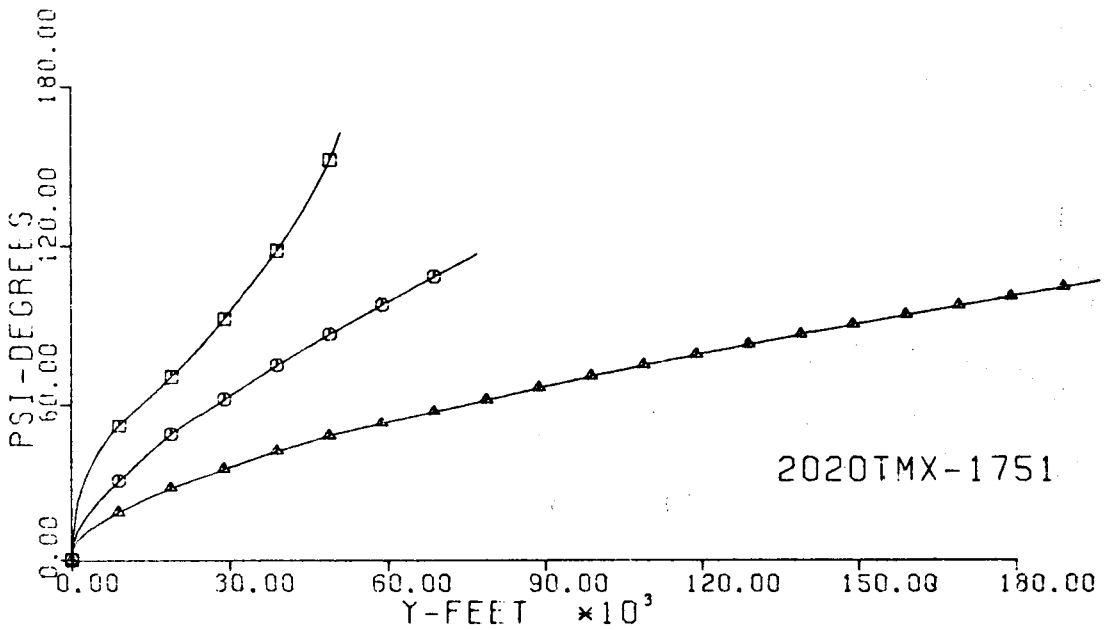

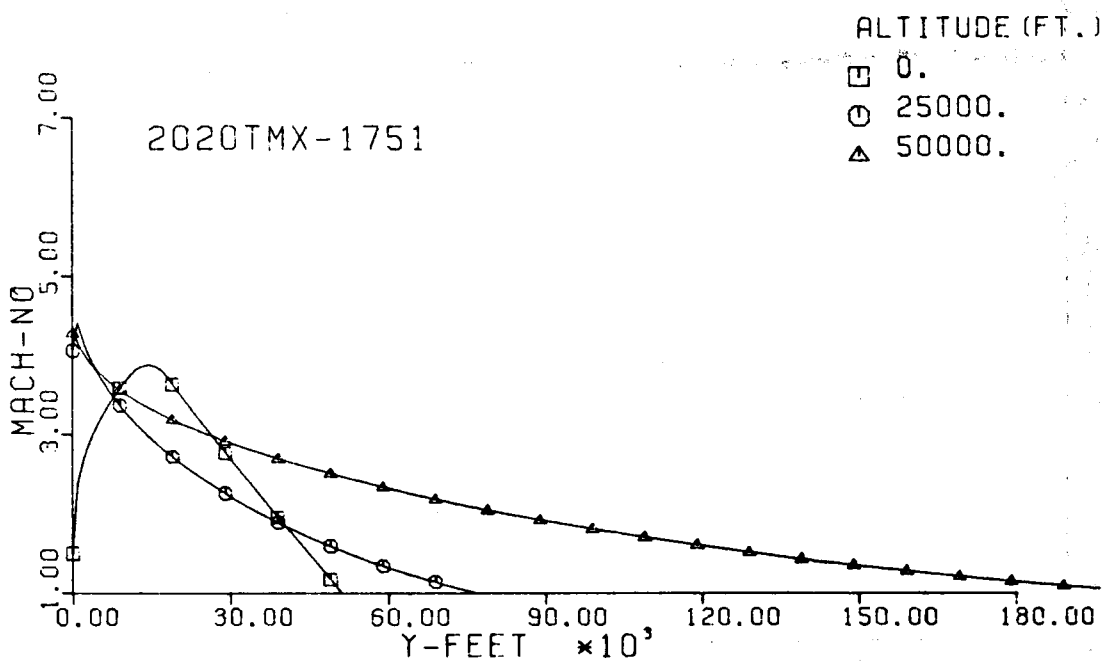

Fig. 101-III. Heading Angle and Mach No. vs. Downrange Distance, Y.

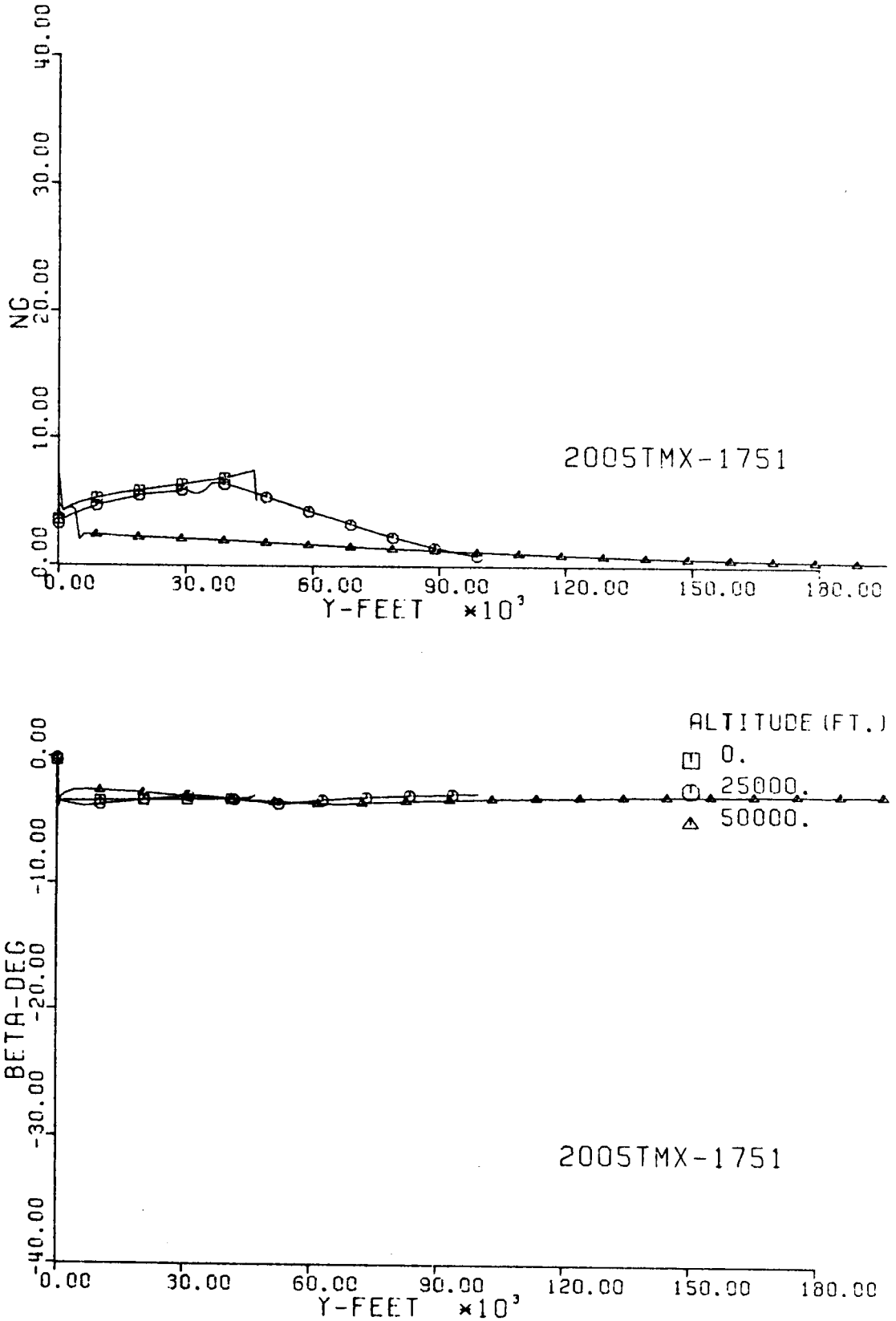

Fig. 102-III. Number of G's and Sideslip Angle vs. Downrange Distance, Y.

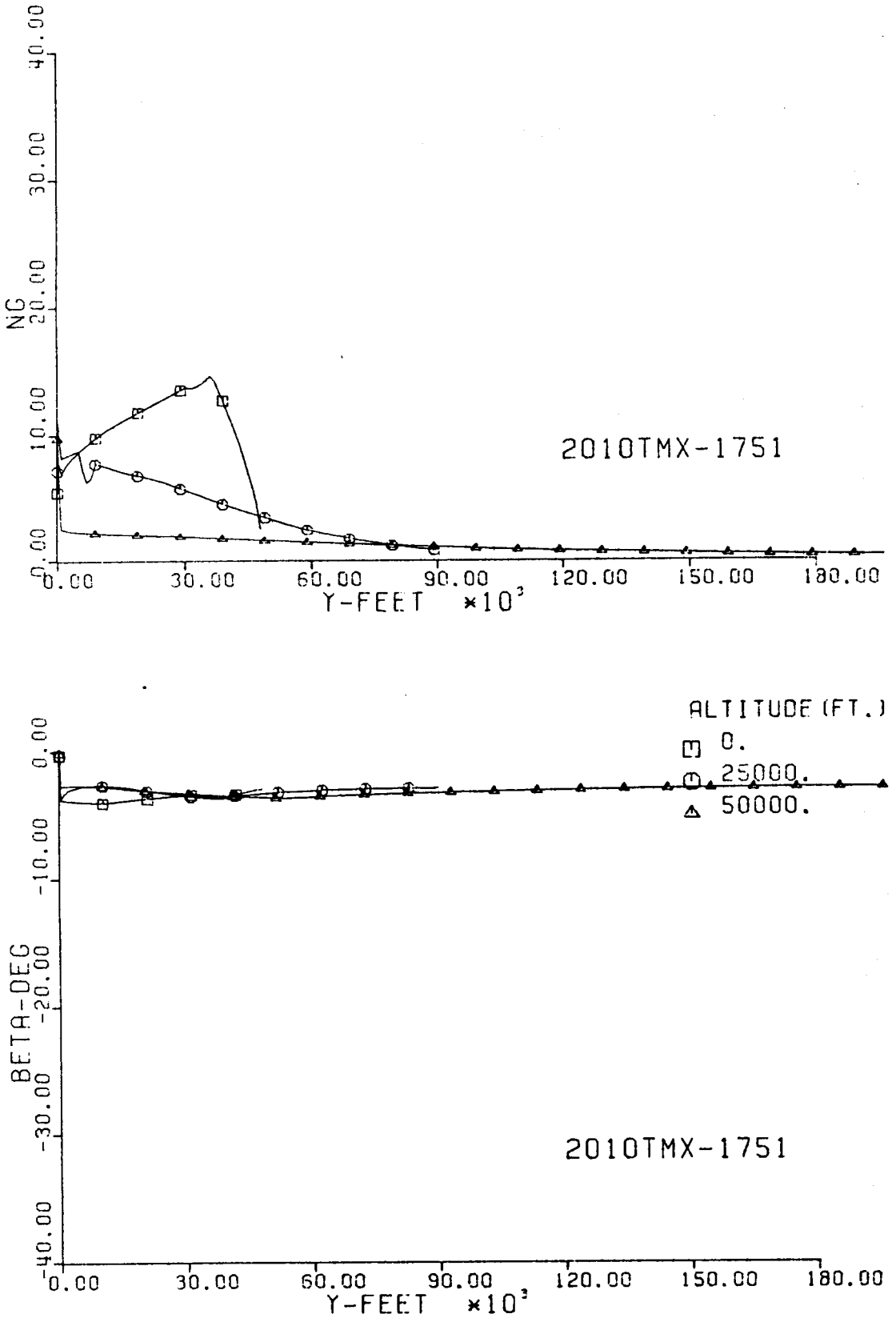

Fig. 103-III. Number of G's and Sideslip Angle vs. Downrange Distance, Y.

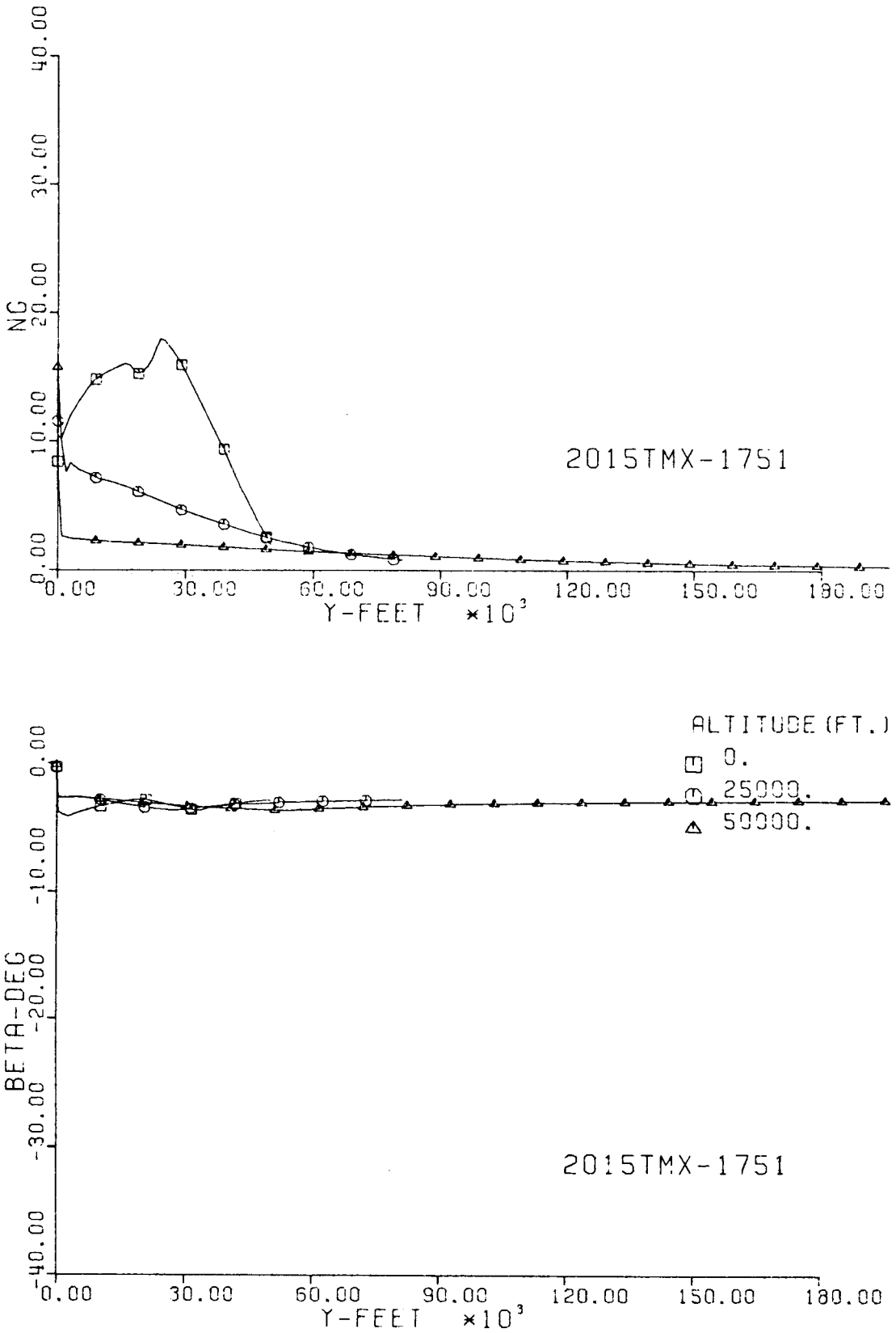

Fig. 104-III. Number of G's and Sideslip Angle vs. Downrange Distance, Y.

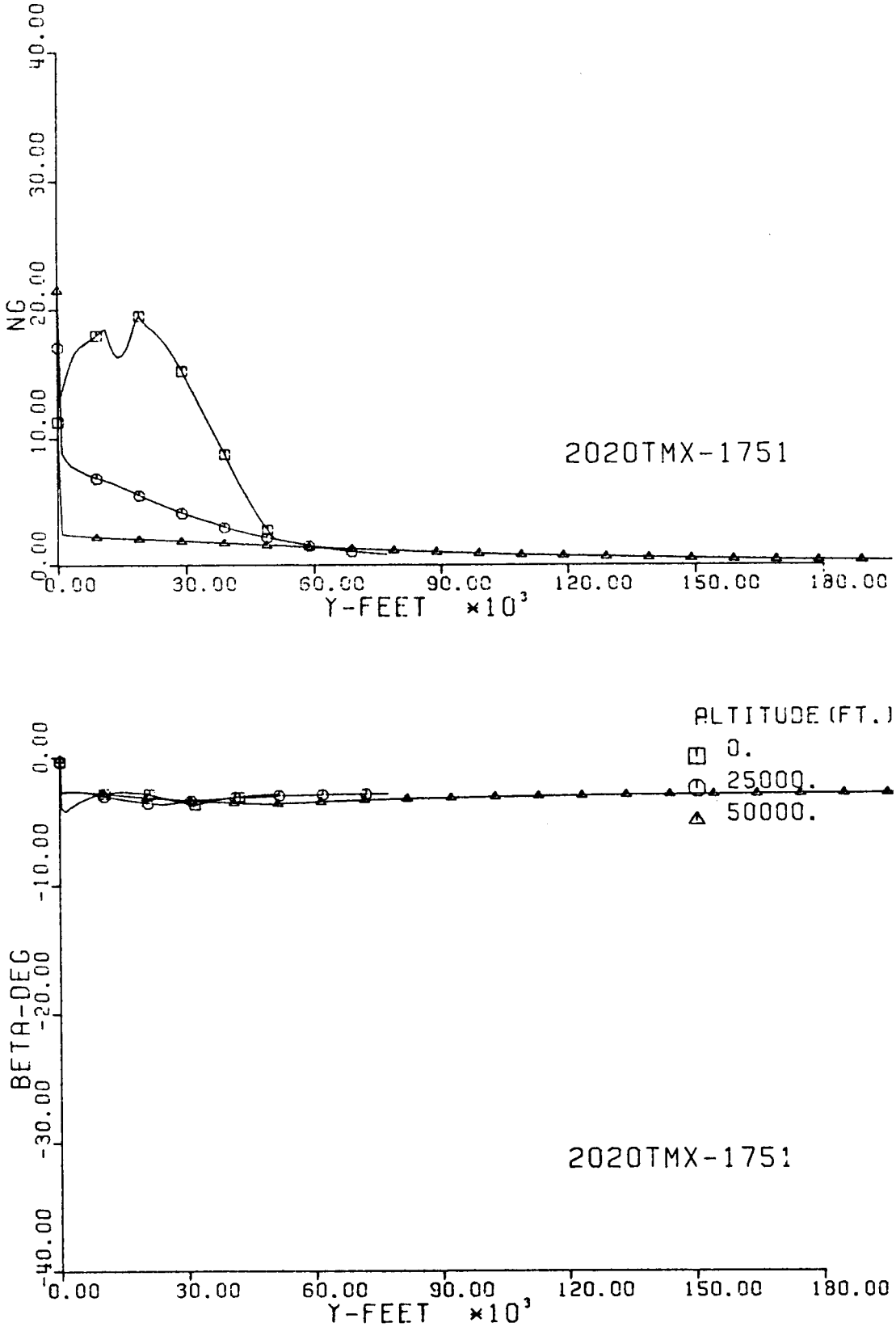

Fig. 105-III. Number of G's and Sideslip Angle vs. Downrange Distance, Y.

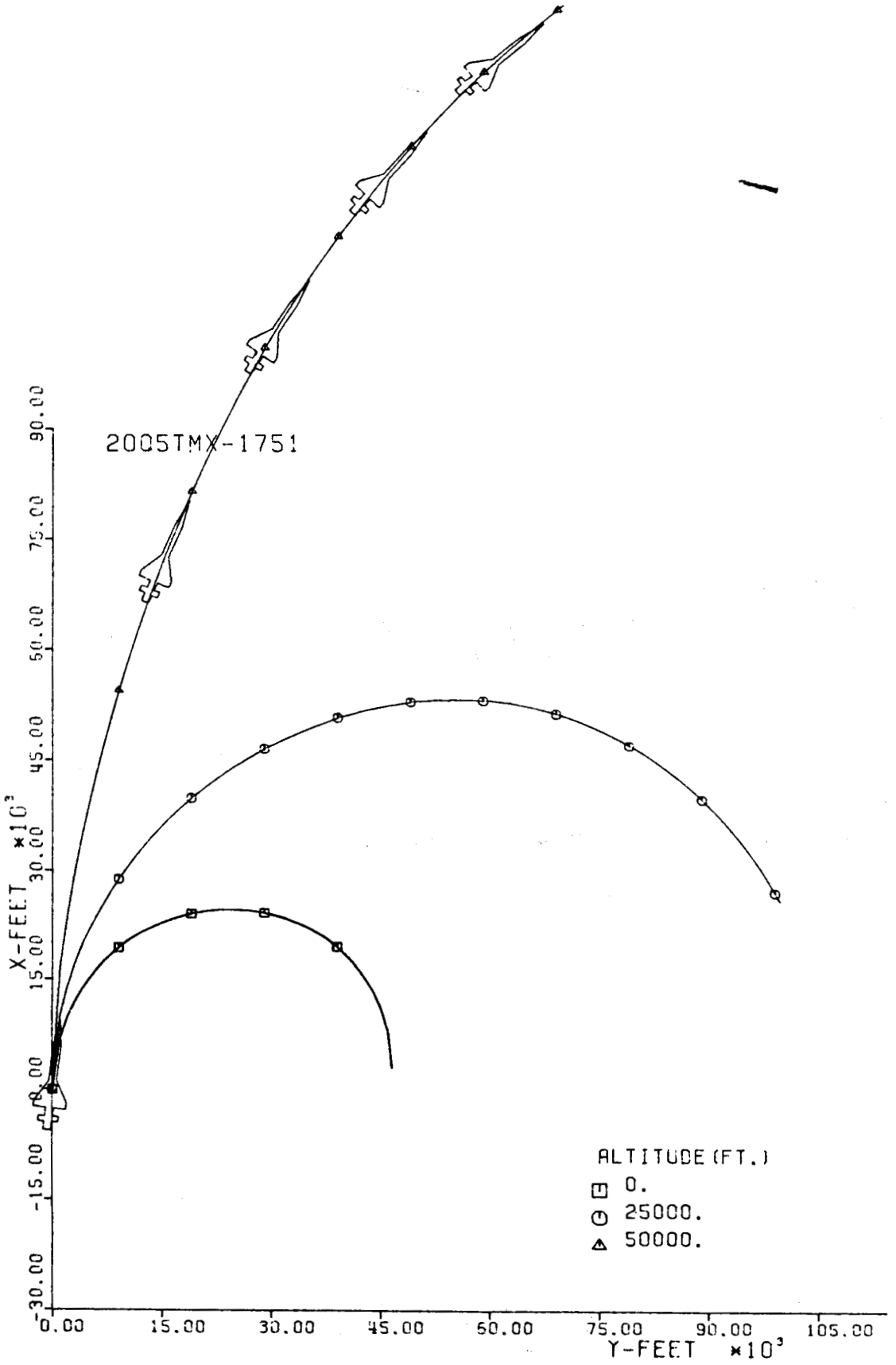

Fig. 106-III. Constant Altitude Flight Path, X vs. Y.

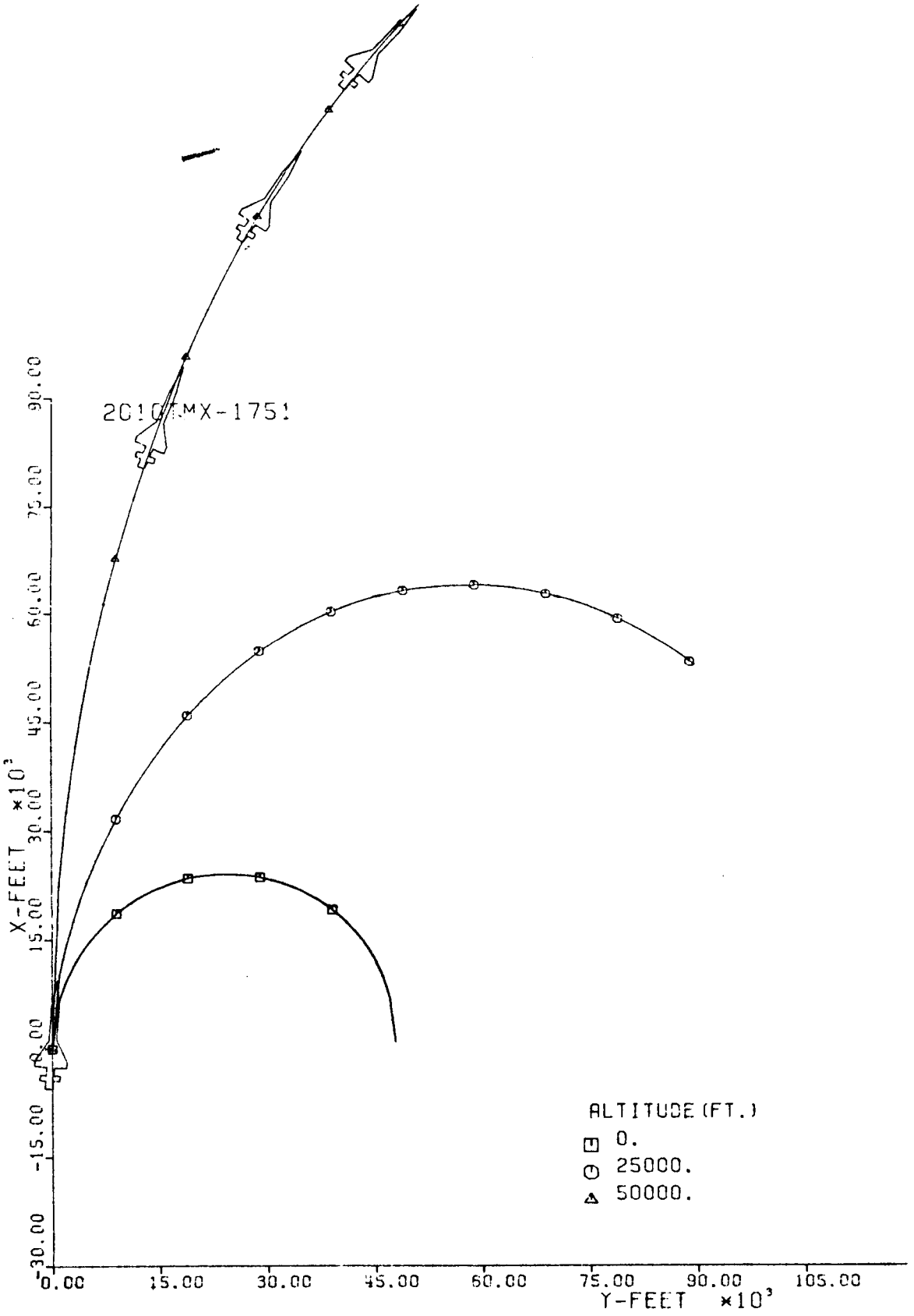

Fig. 107-III. Constant Altitude Flight Path, X vs. Y.

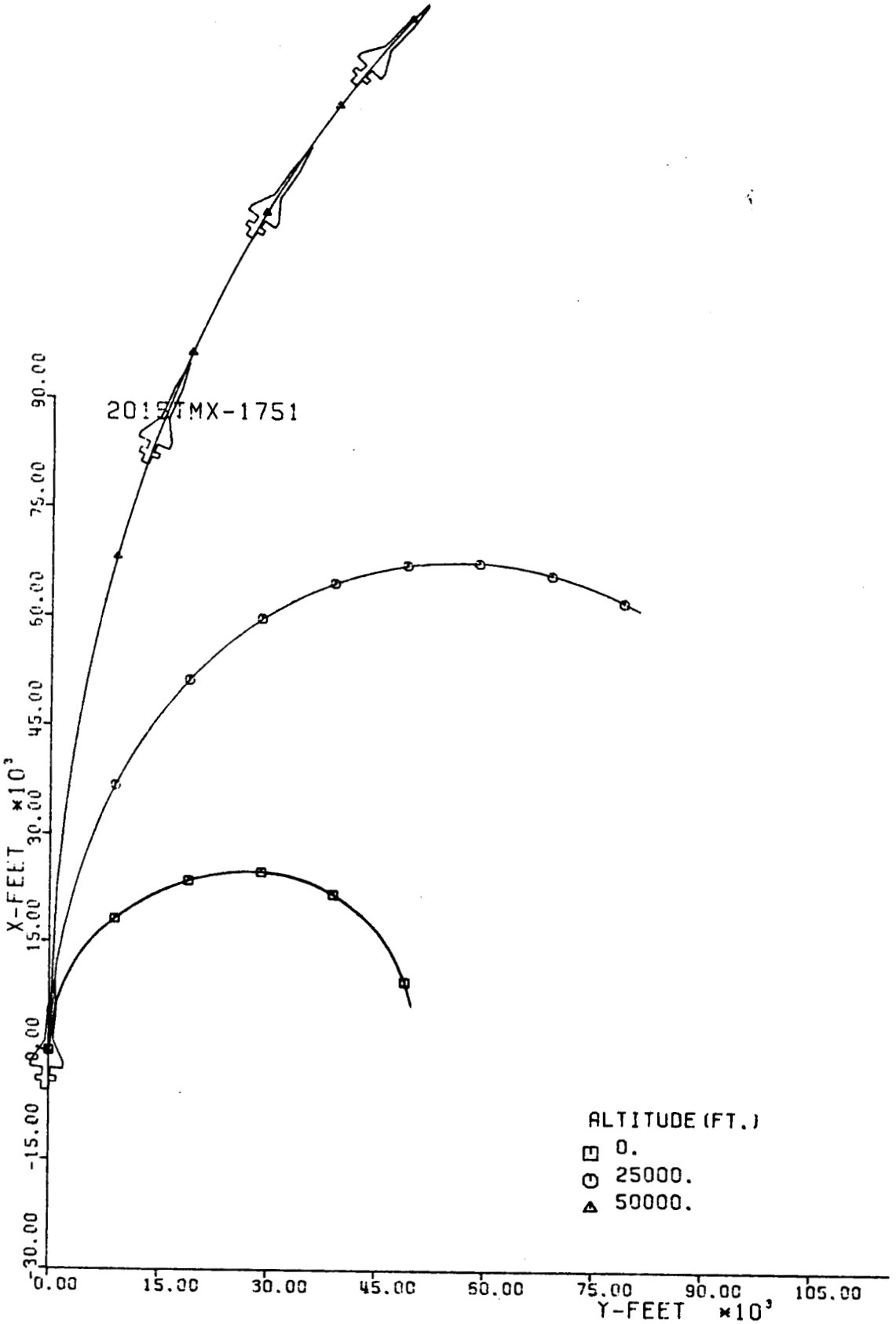

Fig. 108-III. Constant Altitude Flight Path, X vs. Y.

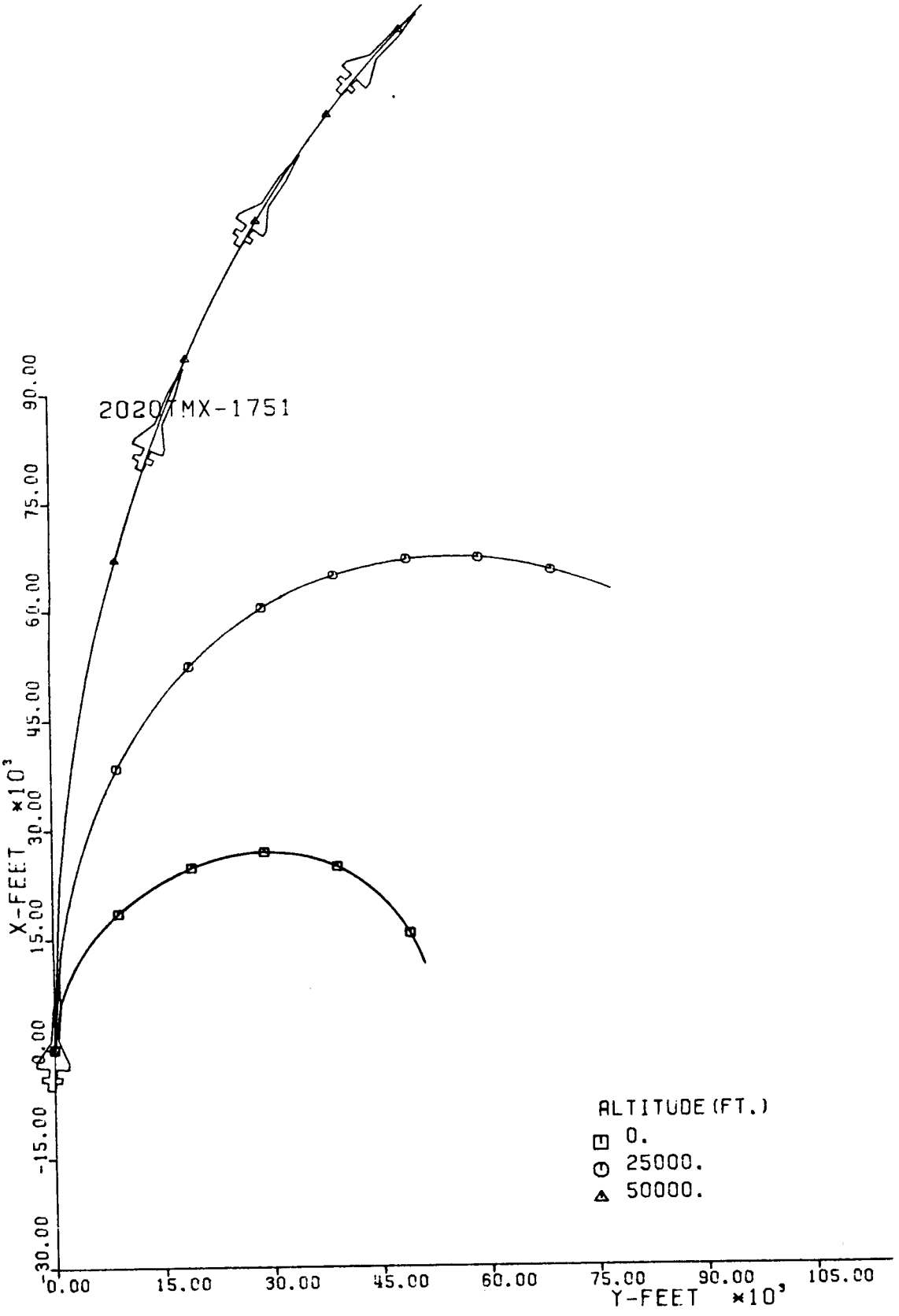

Fig. 109-III. Constant Altitude Flight Path, X vs. Y.

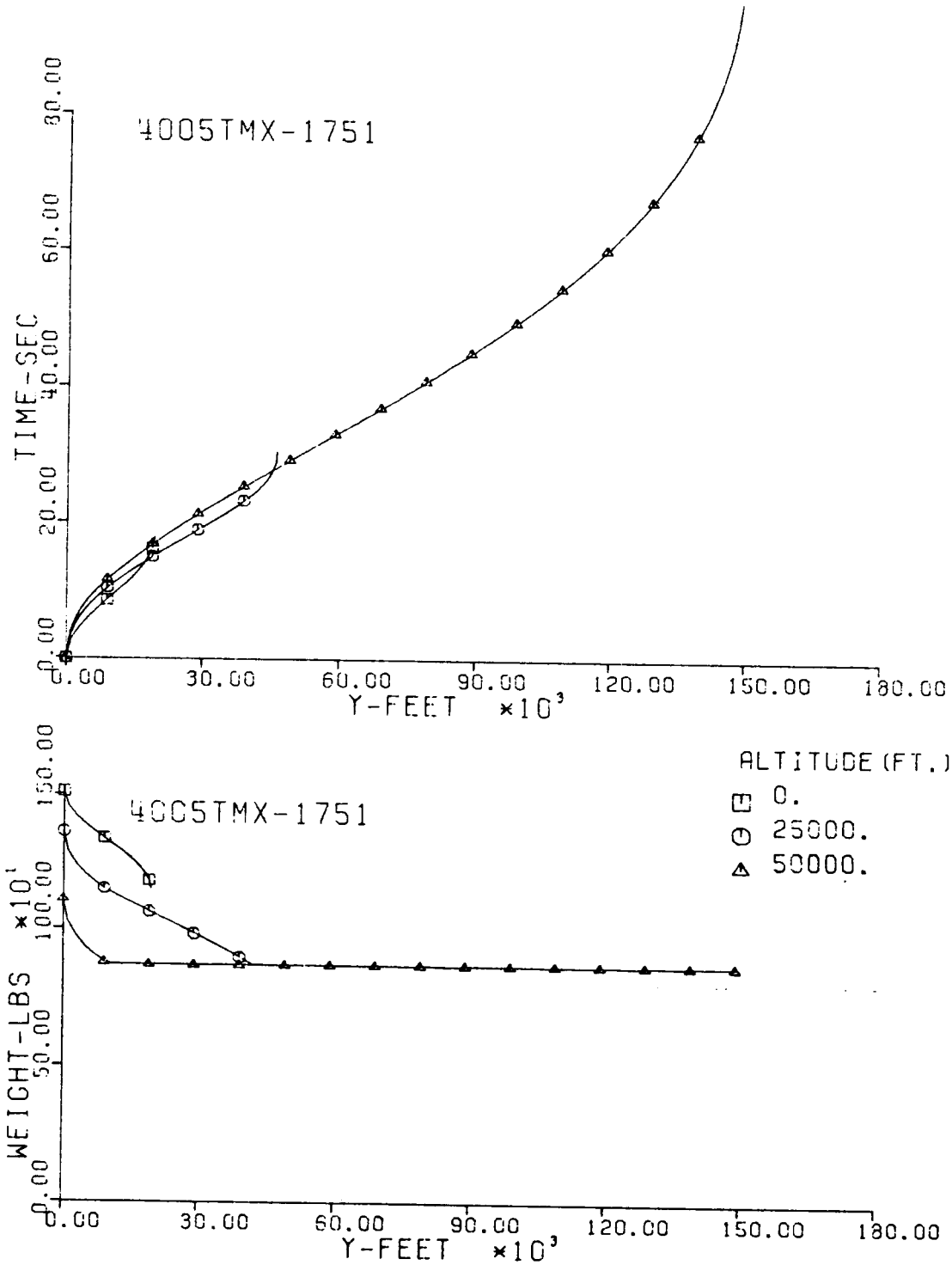

Fig. 110-III. Flight Time and Vehicle Weight vs. Downrange Distance, Y.

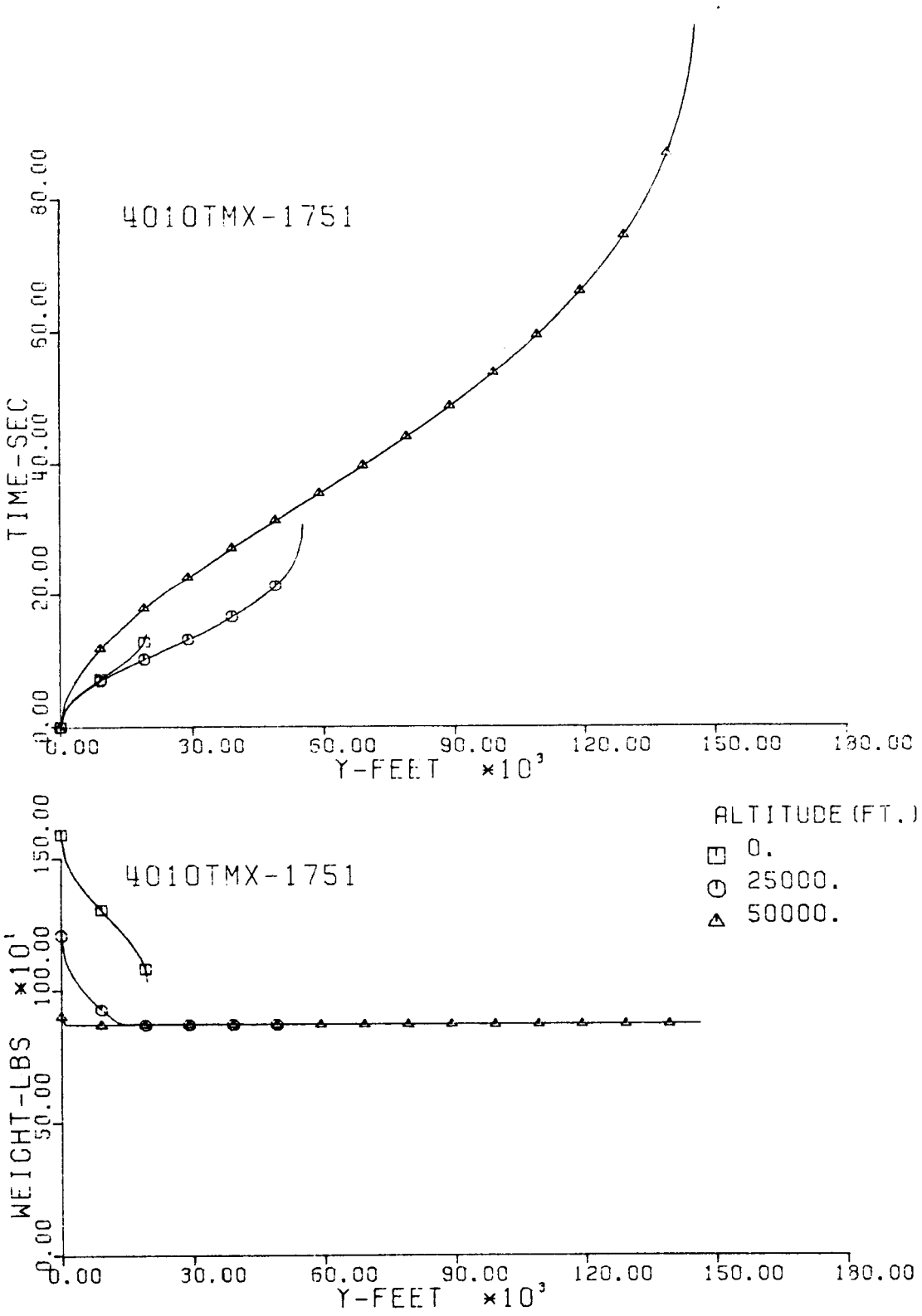

Fig. 111-III. Flight Time and Vehicle Weight vs. Downrange Distance, Y.

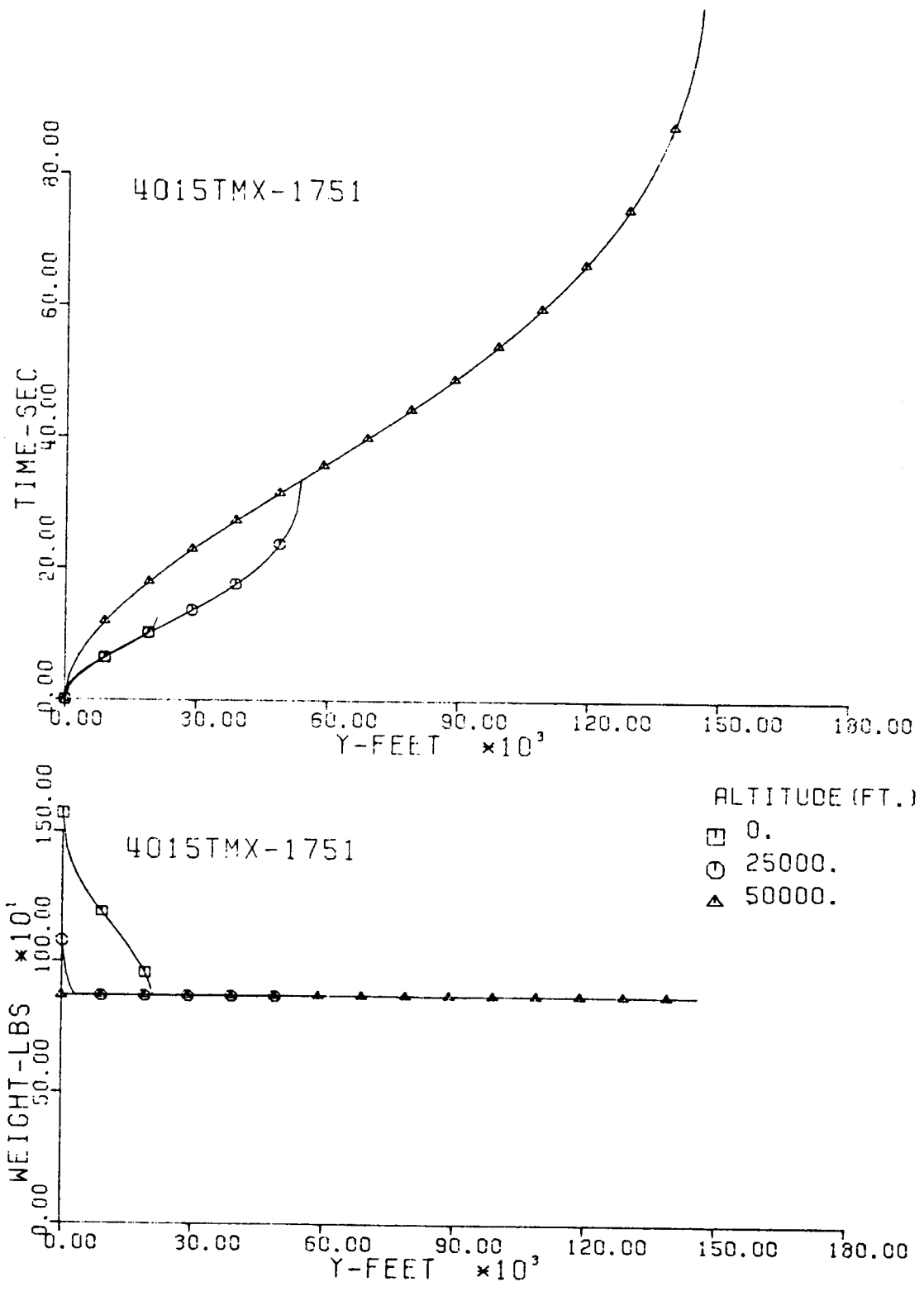

Fig. 112-III. Flight Time and Vehicle Weight vs. Downrange Distance, Y.

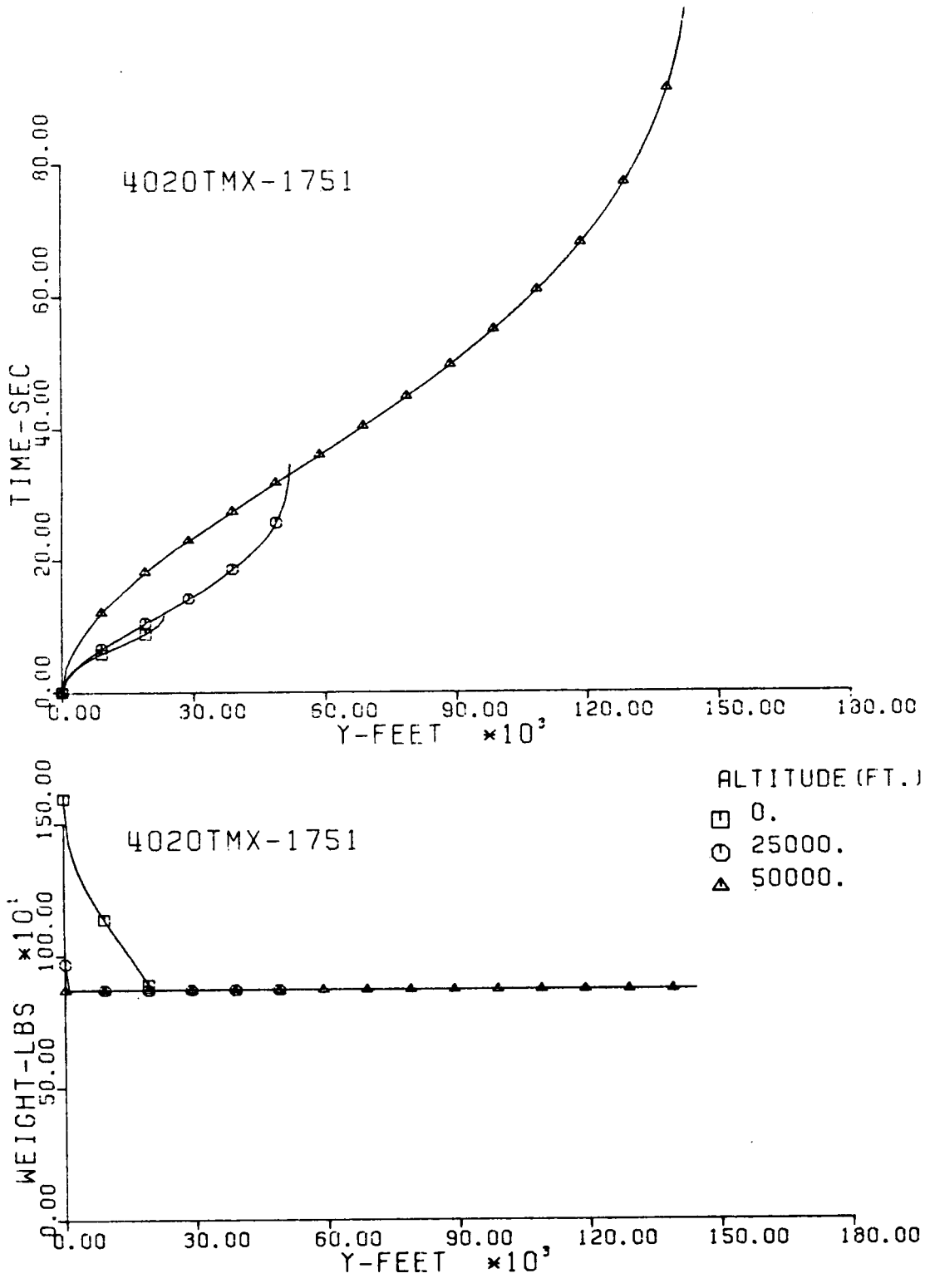

Fig. 113-III. Flight Time and Vehicle Weight vs. Downrange Distance, Y.

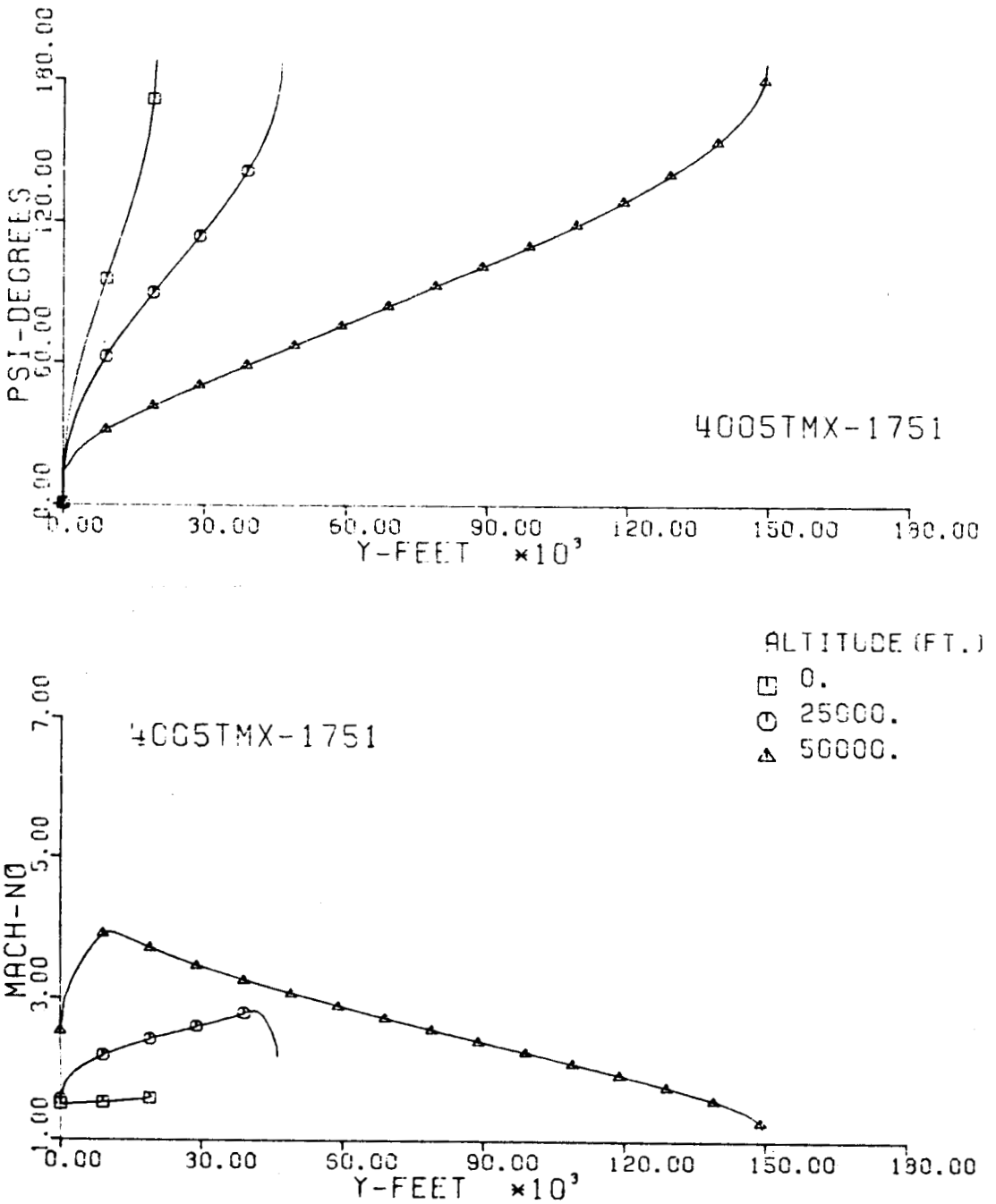

Fig. 114-III. Heading Angle and Mach No. vs. Downrange Distance, Y.

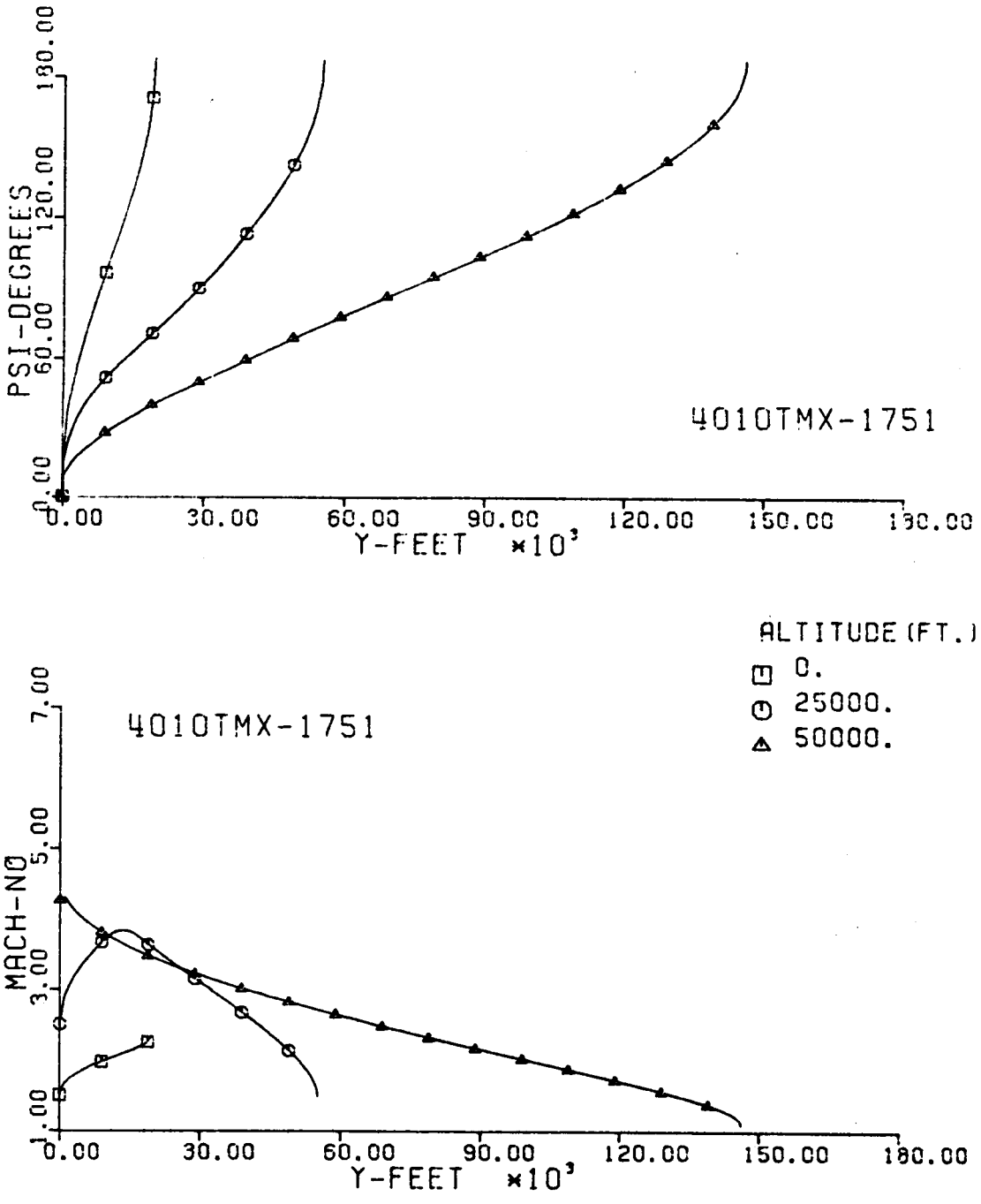

Fig. 115-III. Heading Angle and Mach No. vs. Downrange Distance, Y.

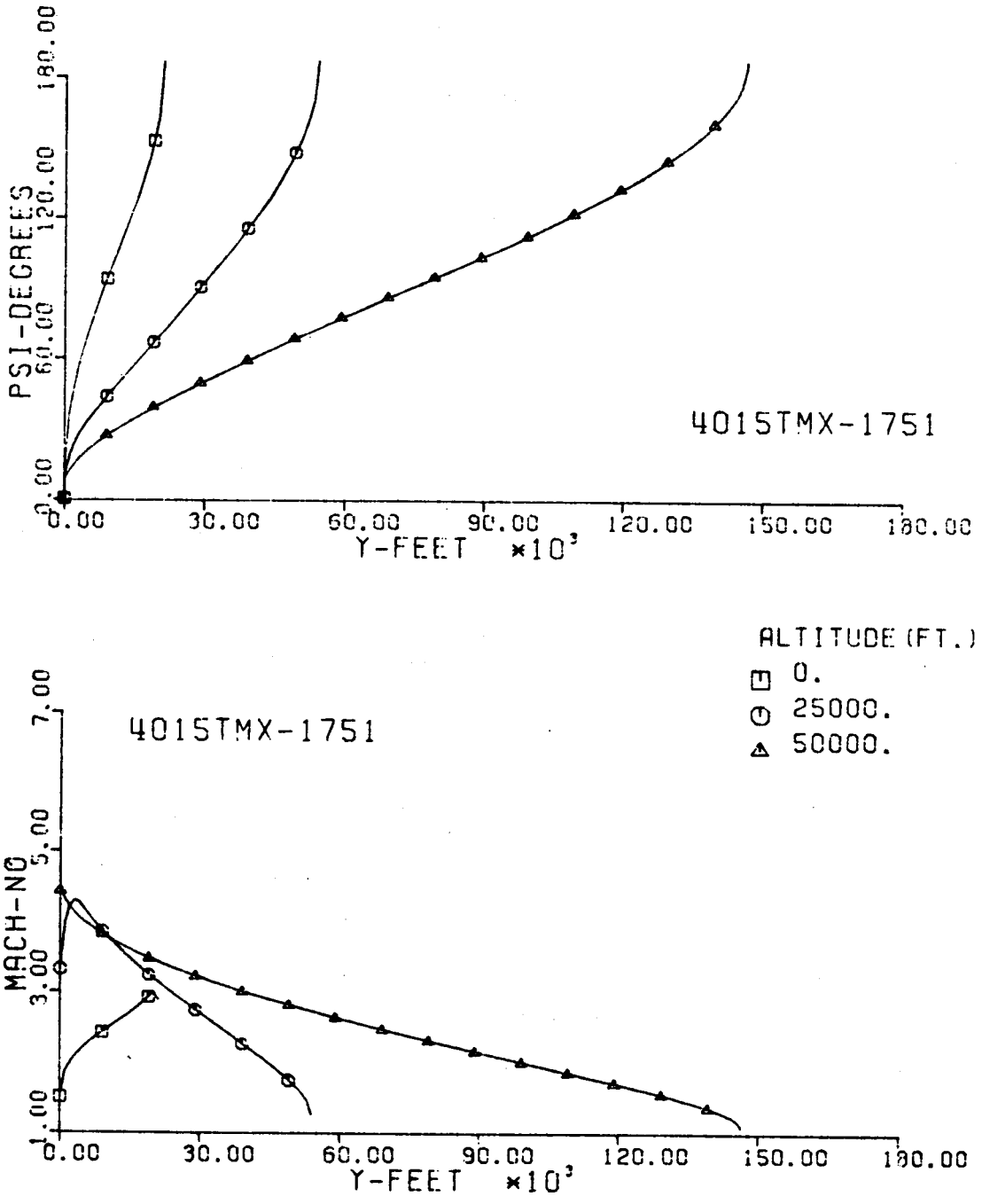

Fig. 116-III. Heading Angle and Mach No. vs. Downrange Distance, Y.

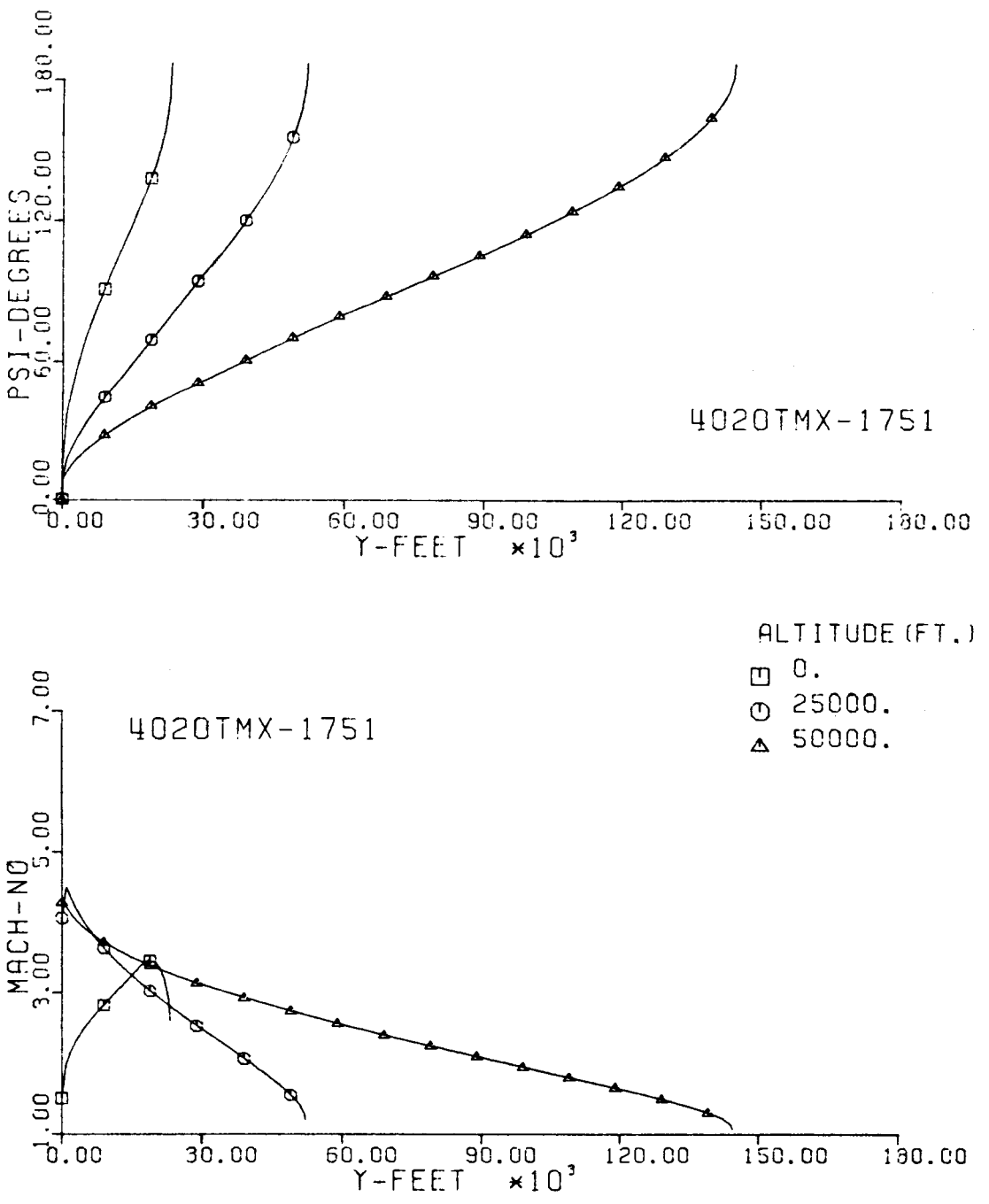

Fig. 117-III. Heading Angle and Mach No. vs. Downrange Distance, Y.

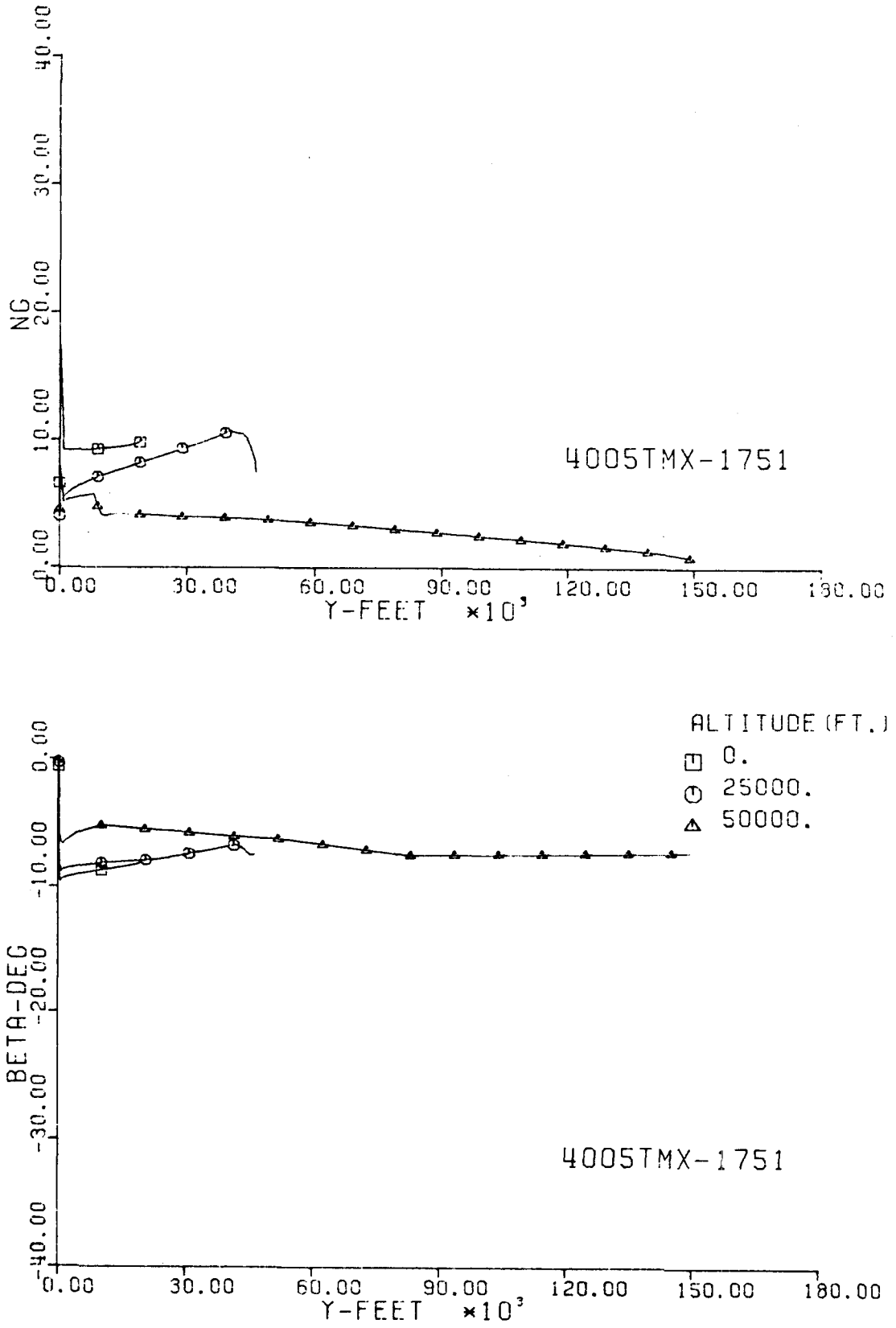

Fig. 118-III. Number of G's and Sideslip Angle vs. Downrange Distance, Y.

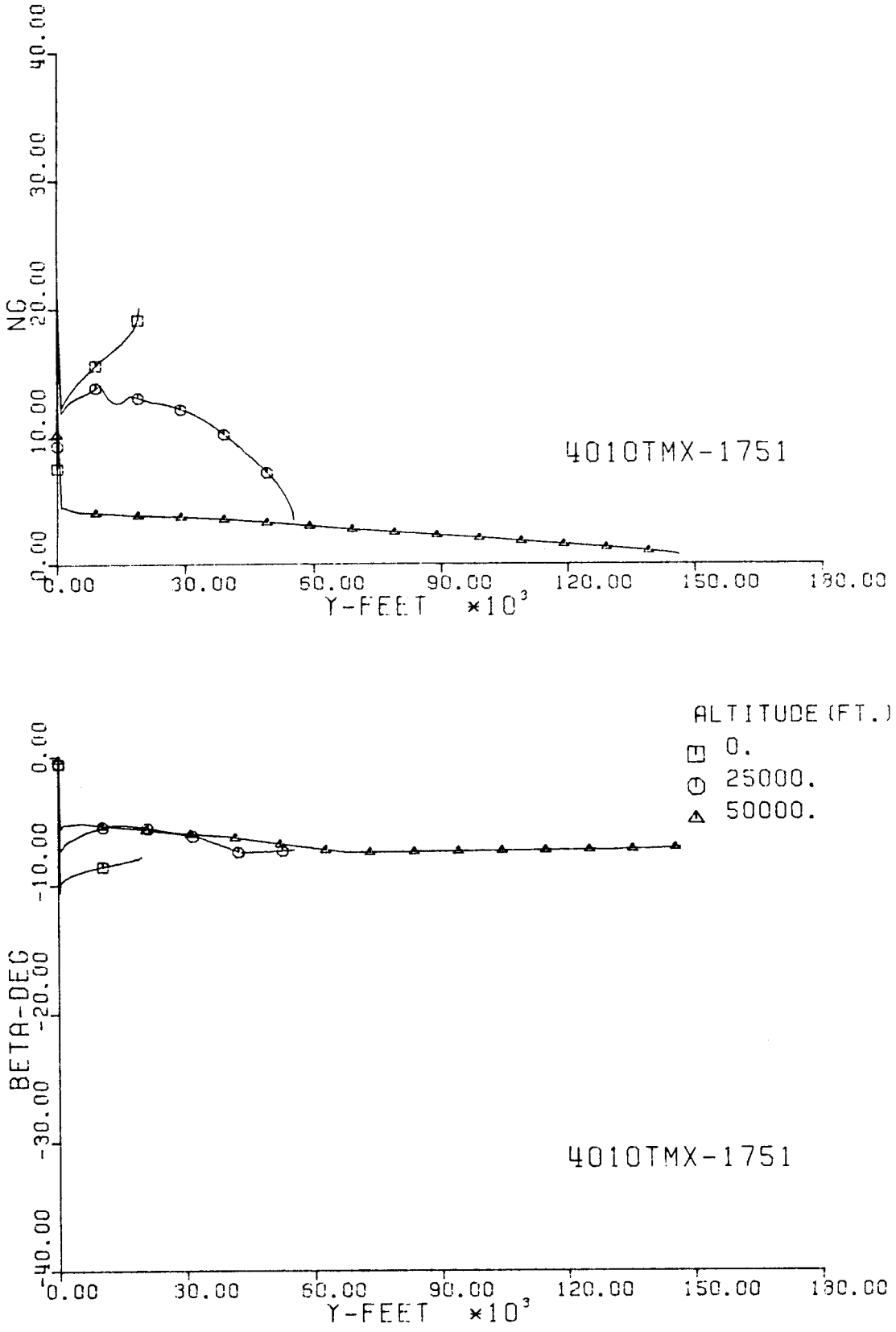

Fig. 119-III. Number of G's and Sideslip Angle vs. Downrange Distance, Y.

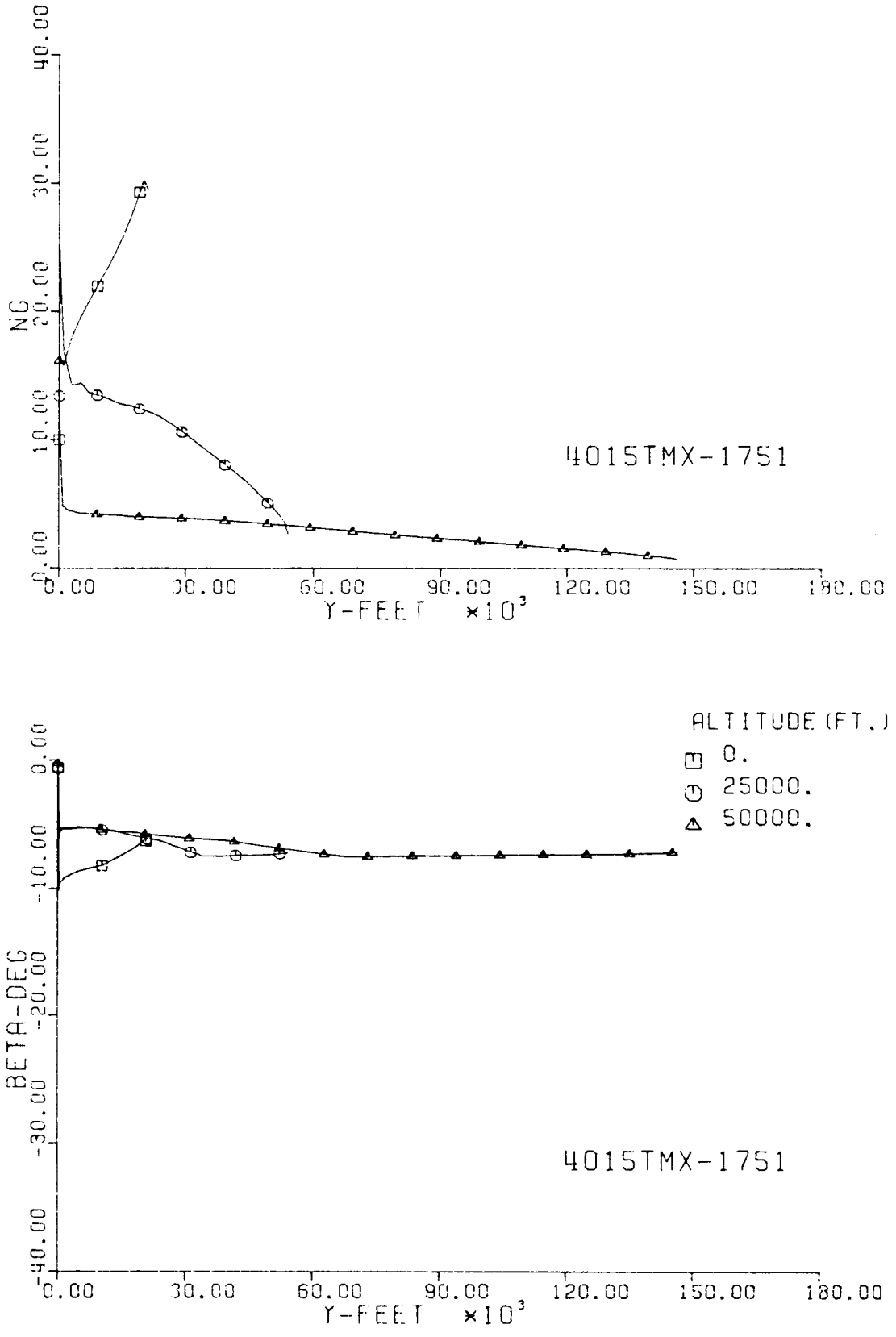

Fig. 120-III. Number of G's and Sideslip Angle vs. Downrange Distance, Y.

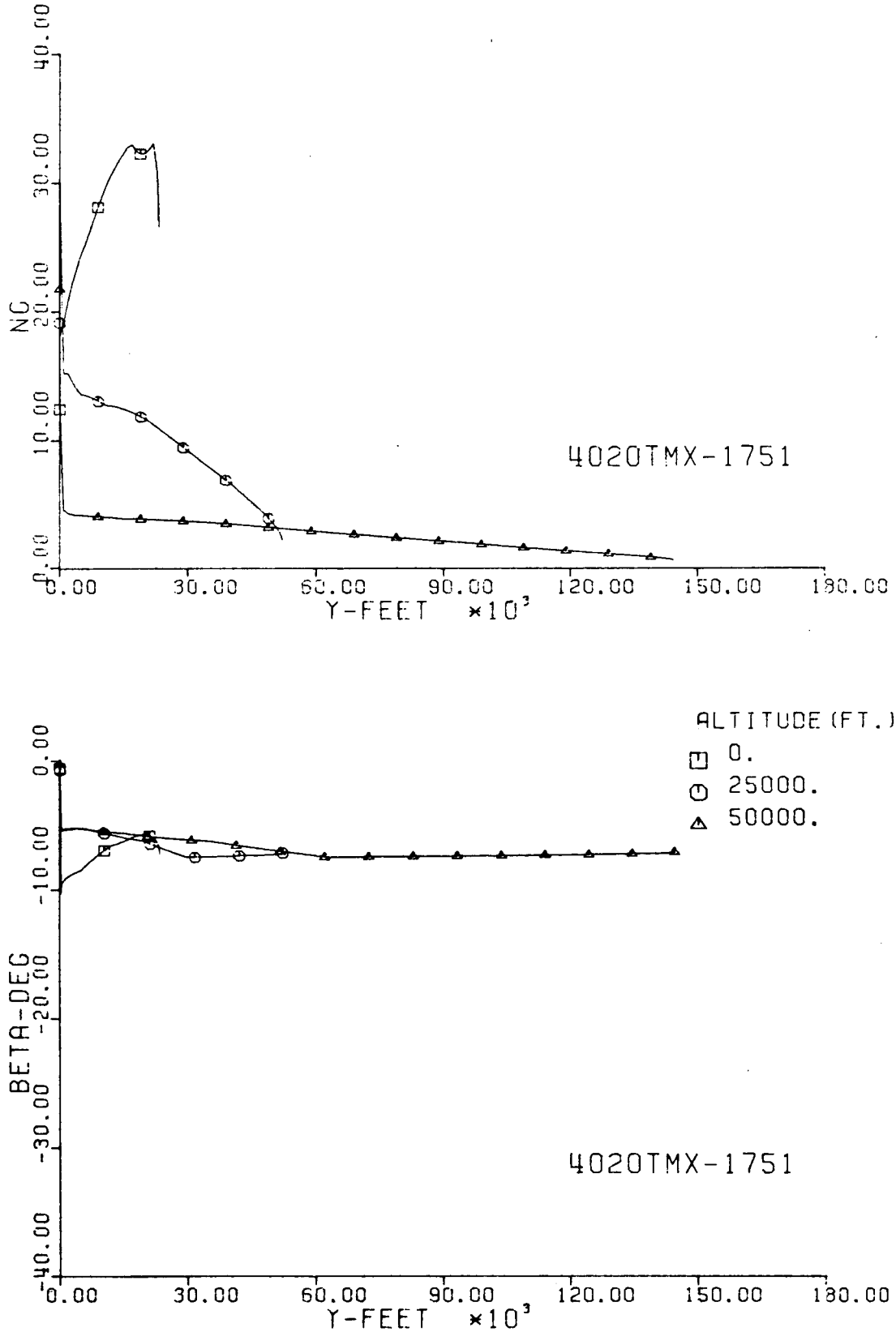

Fig. 121-III. Number of G's and Sideslip Angle vs. Downrange Distance, Y.

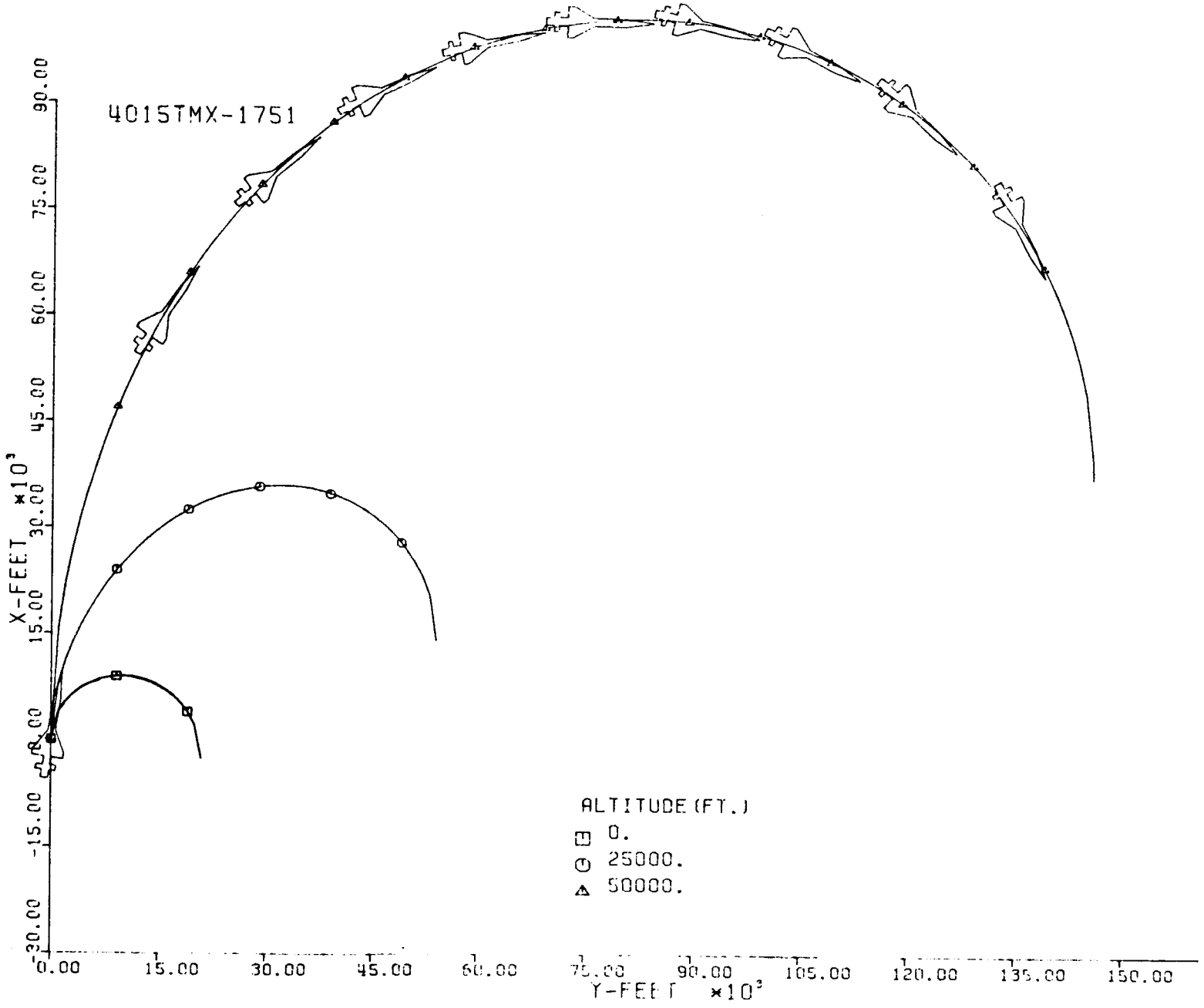

Fig. 122-III. Constant Altitude Flight Path, X vs. Y.

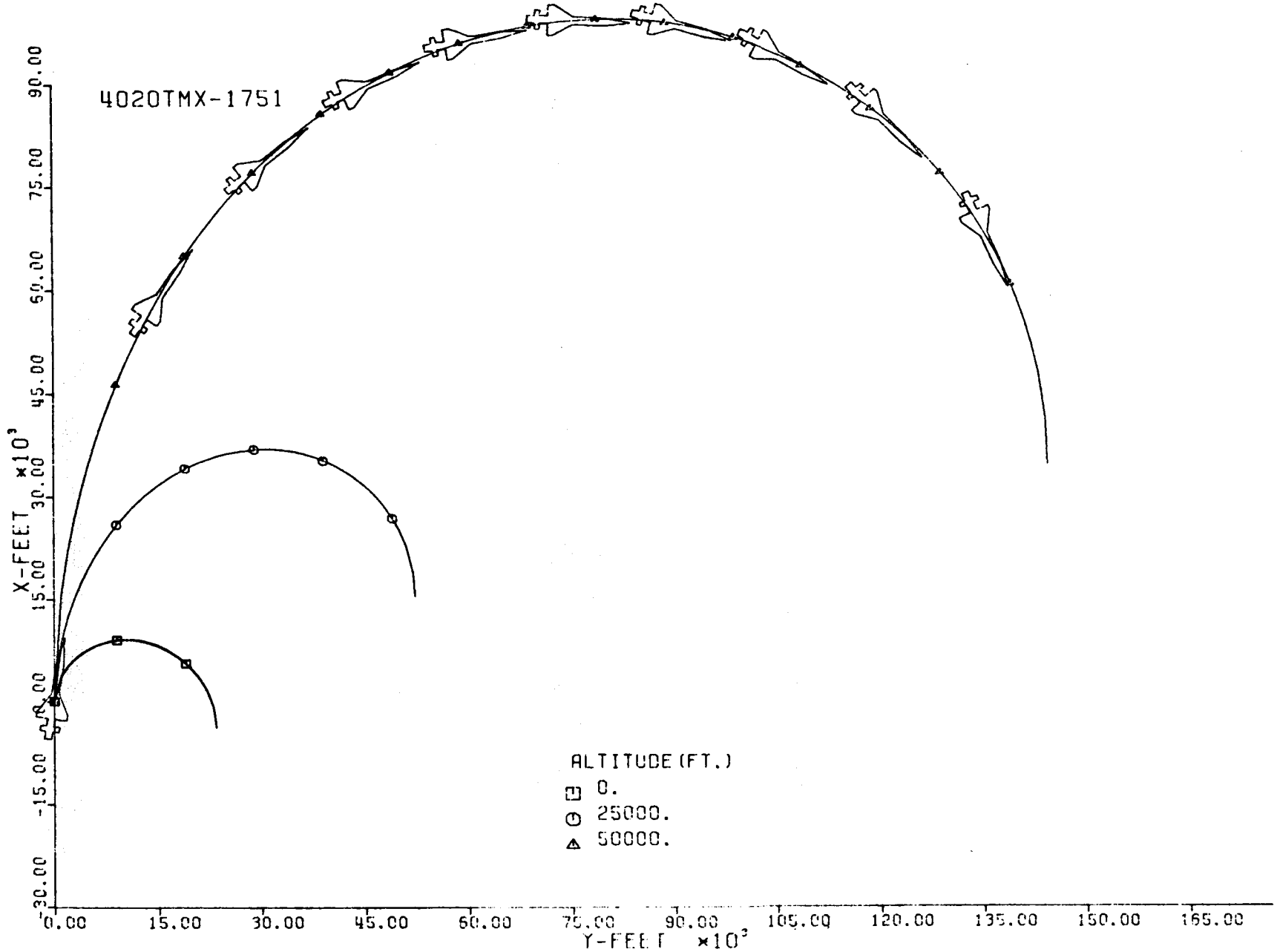

Fig. 123-III. Constant Altitude Flight Path, X vs. Y.

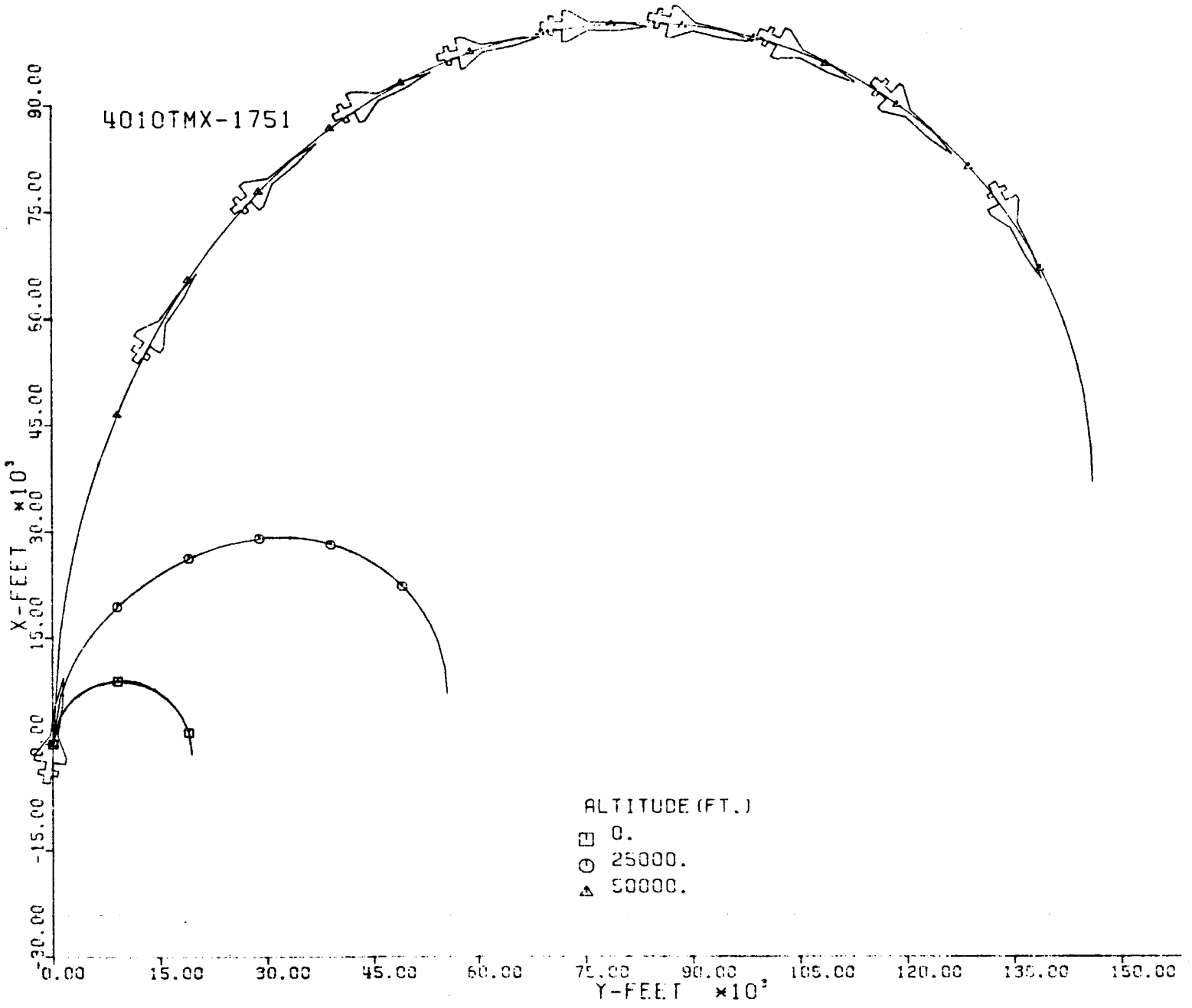

Fig. 124-III. Constant Altitude Flight Path, X vs. Y.

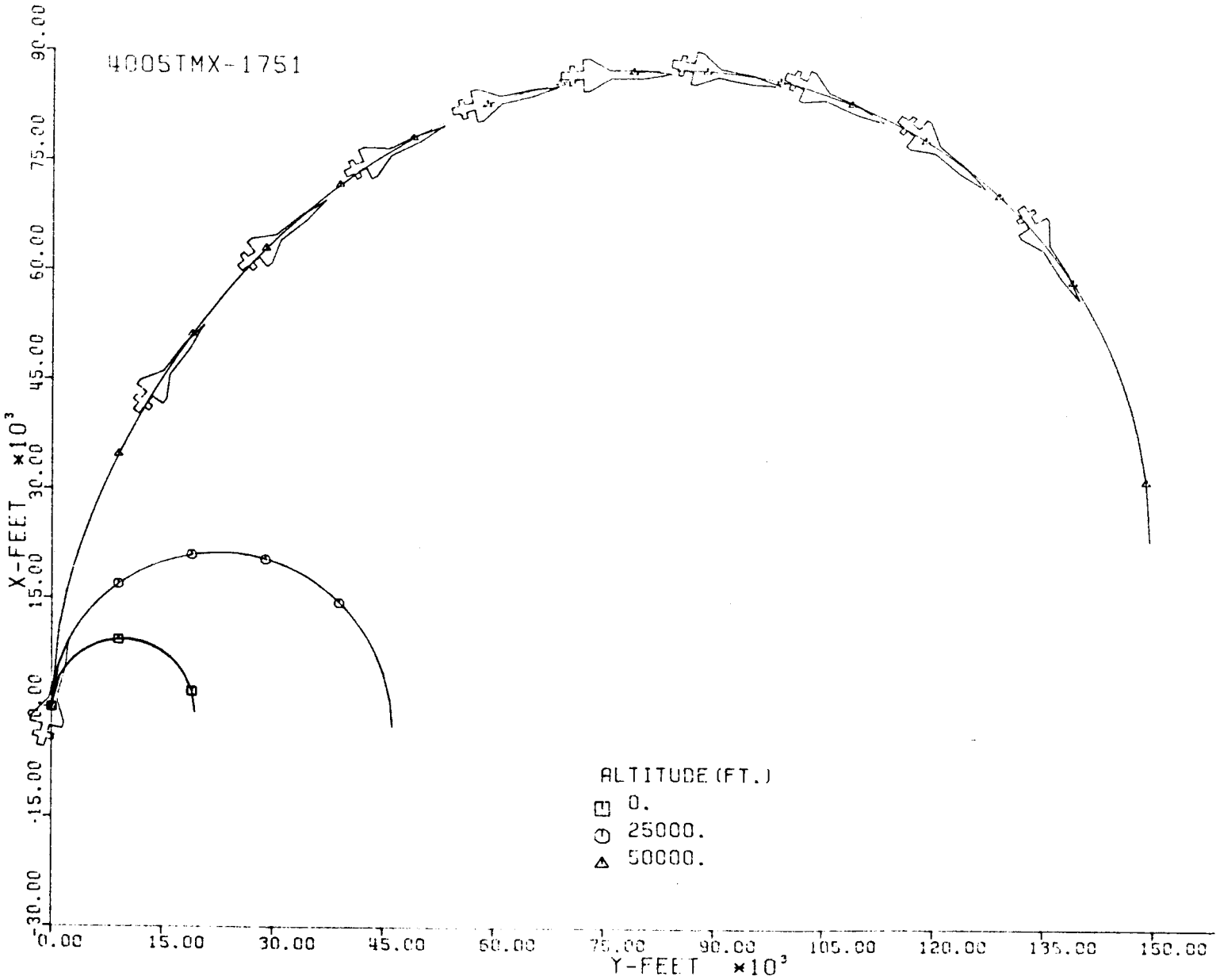

Fig. 125-III. Constant Altitude Flight Path, X vs. Y.

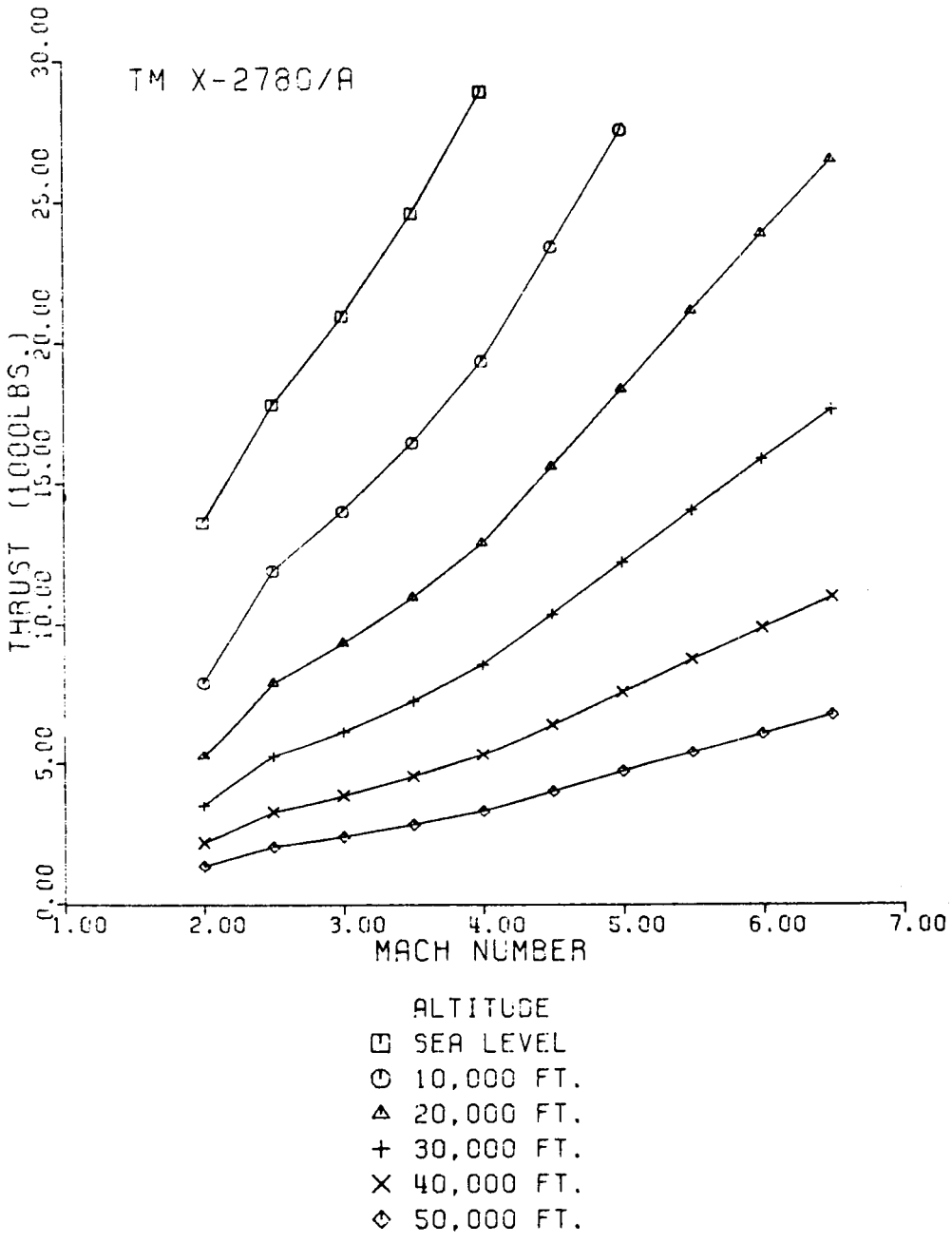

Fig. 126-I. Thrust vs. Terminal Mach No.

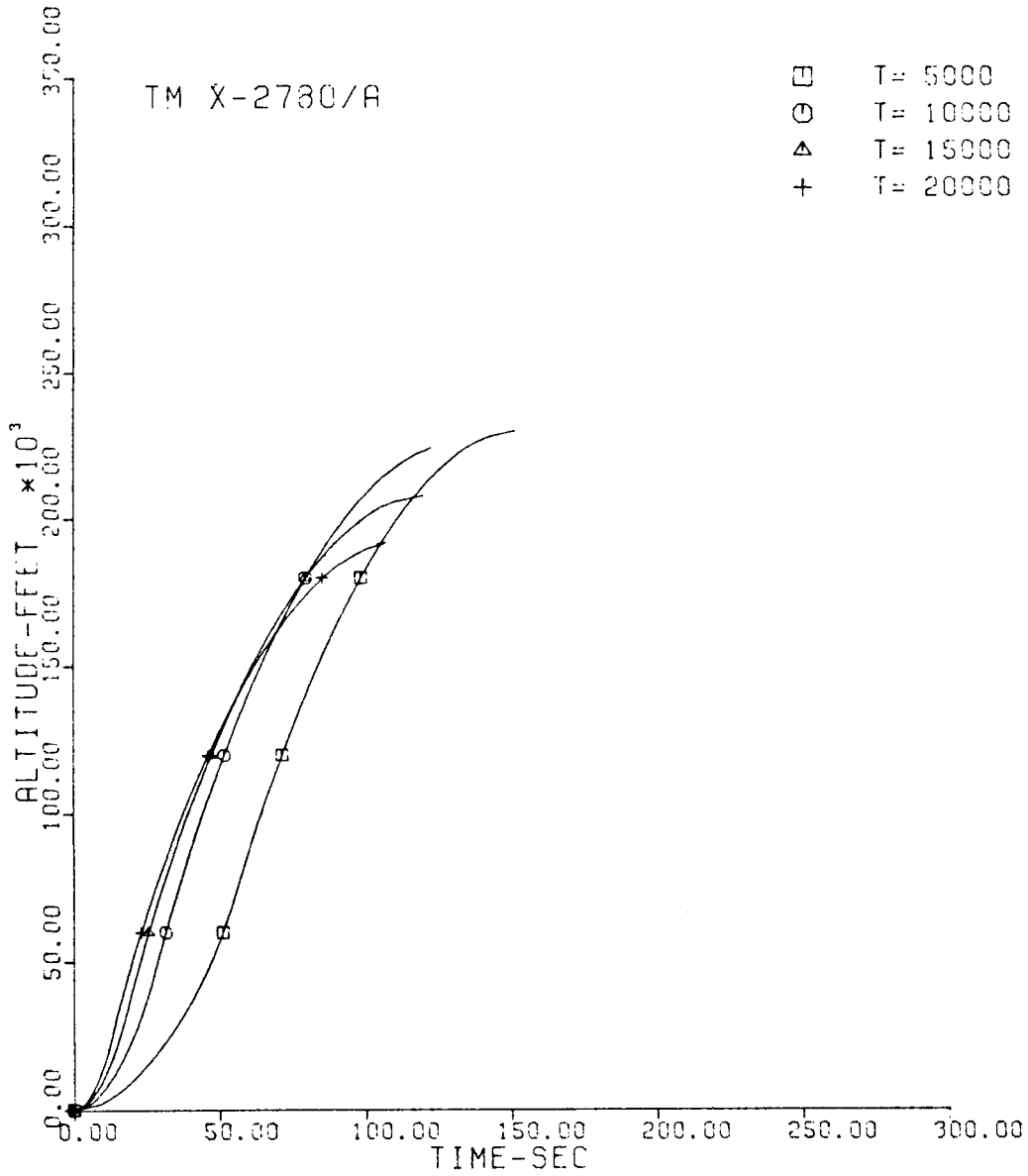

Fig. 127-II. Altitude vs. Flight Time.

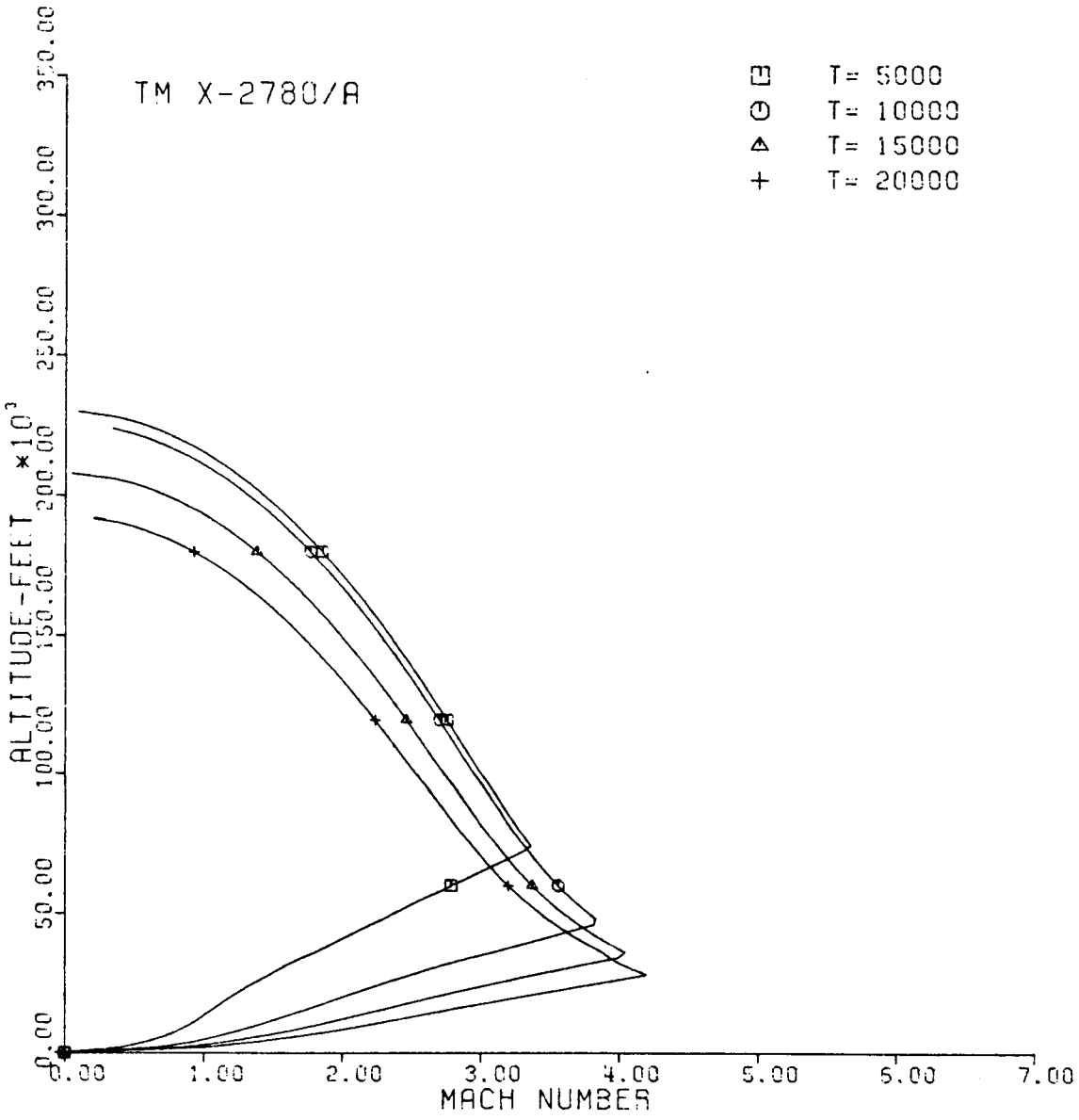

Fig. 128-II. Altitude vs. Mach No.

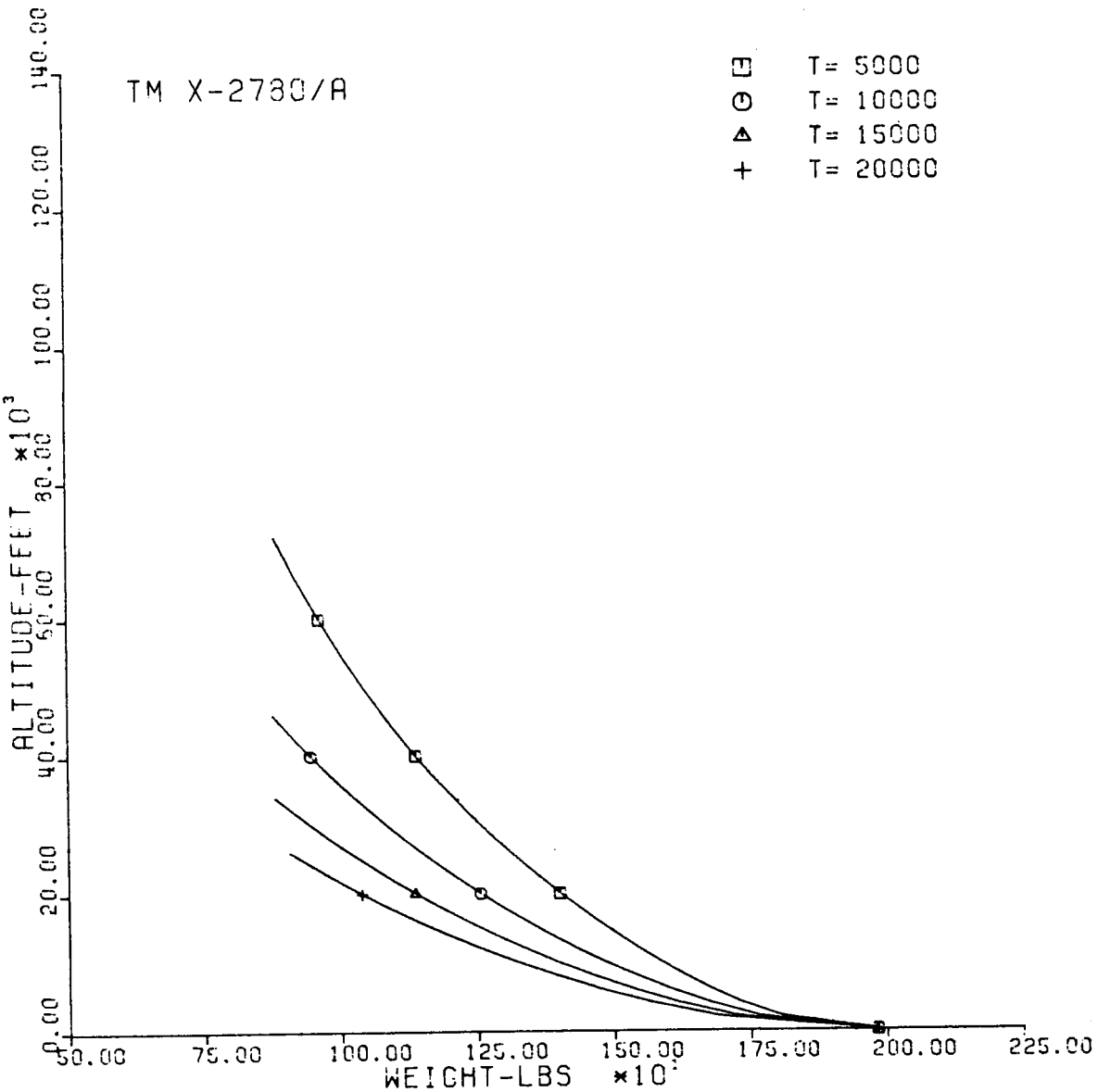

Fig. 129-II. Altitude vs. Vehicle Weight.

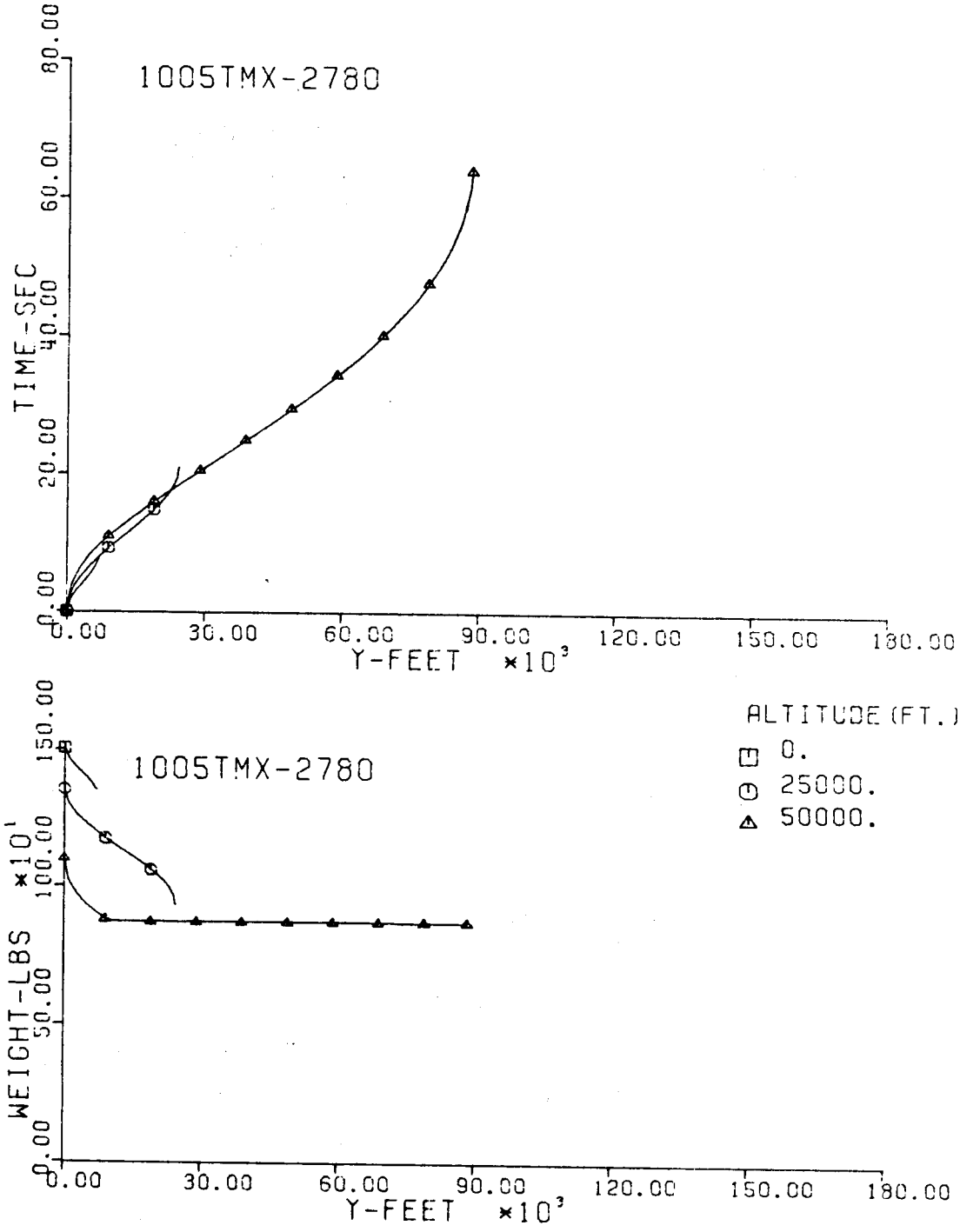

Fig. 130-III. Flight Time and Vehicle Weight vs. Downrange Distance, Y.

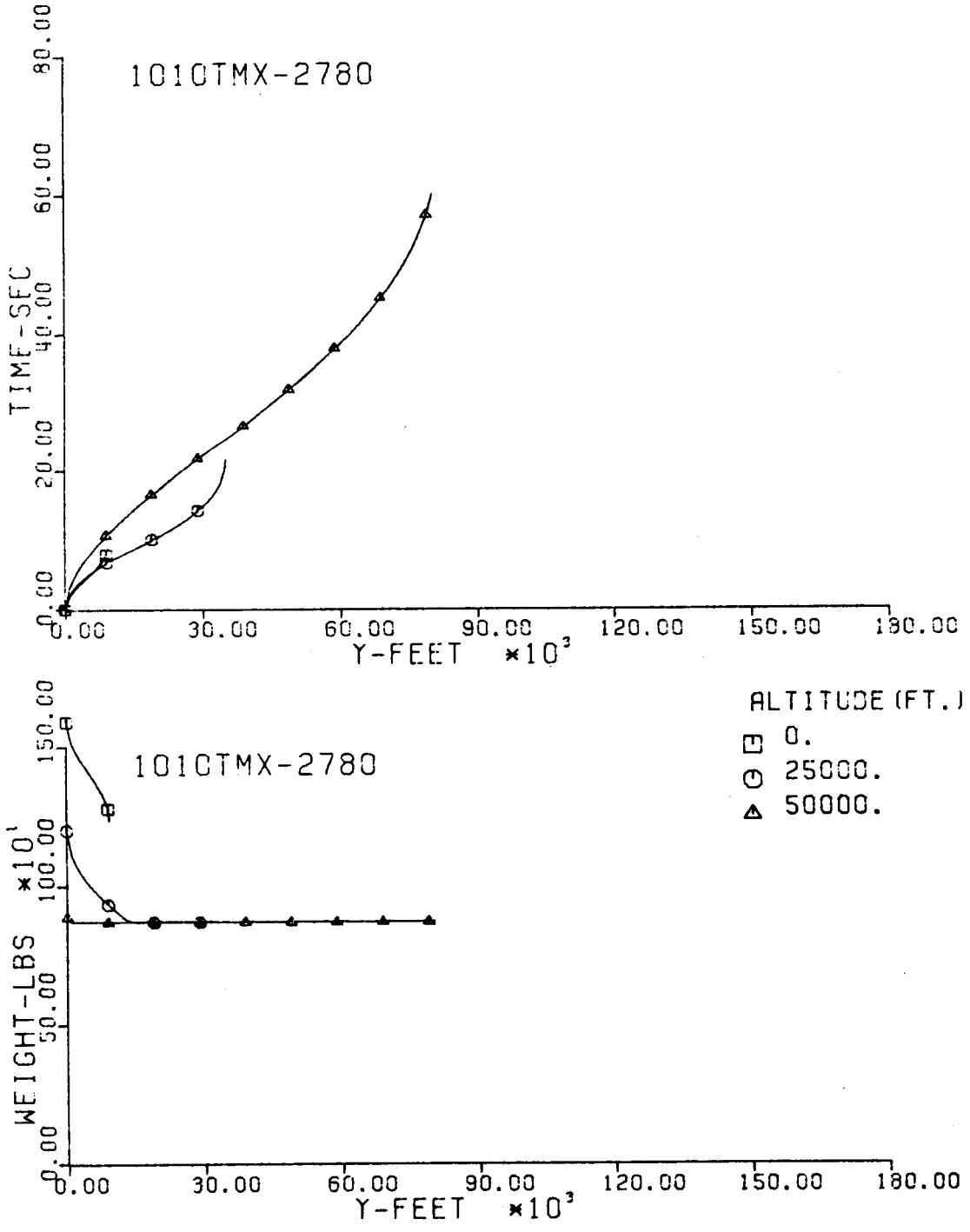

Fig. 131-III. Flight Time and Vehicle Weight vs. Downrange Distance, Y.

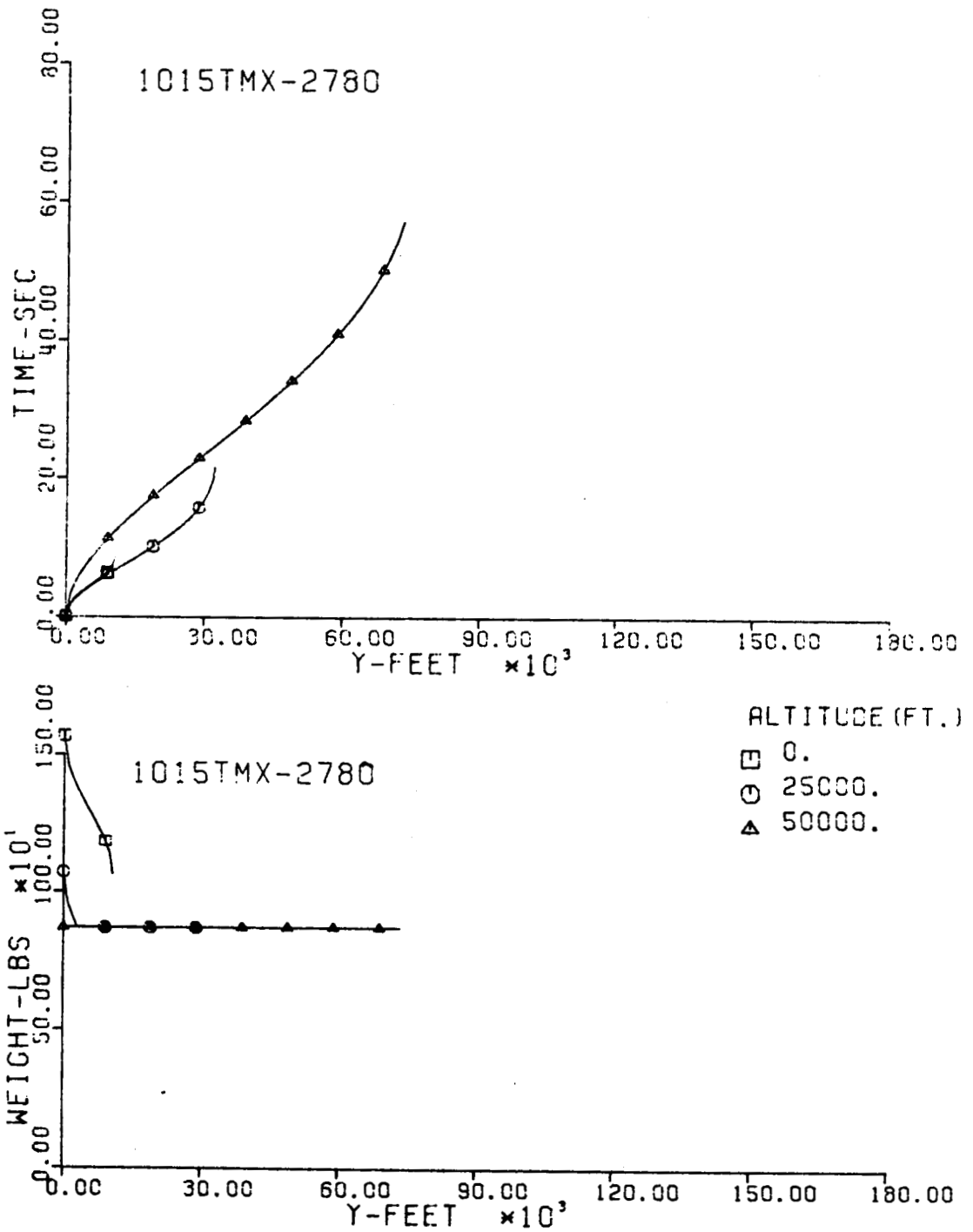

Fig. 132-III. Flight Time and Vehicle Weight vs. Downrange Distance, Y.

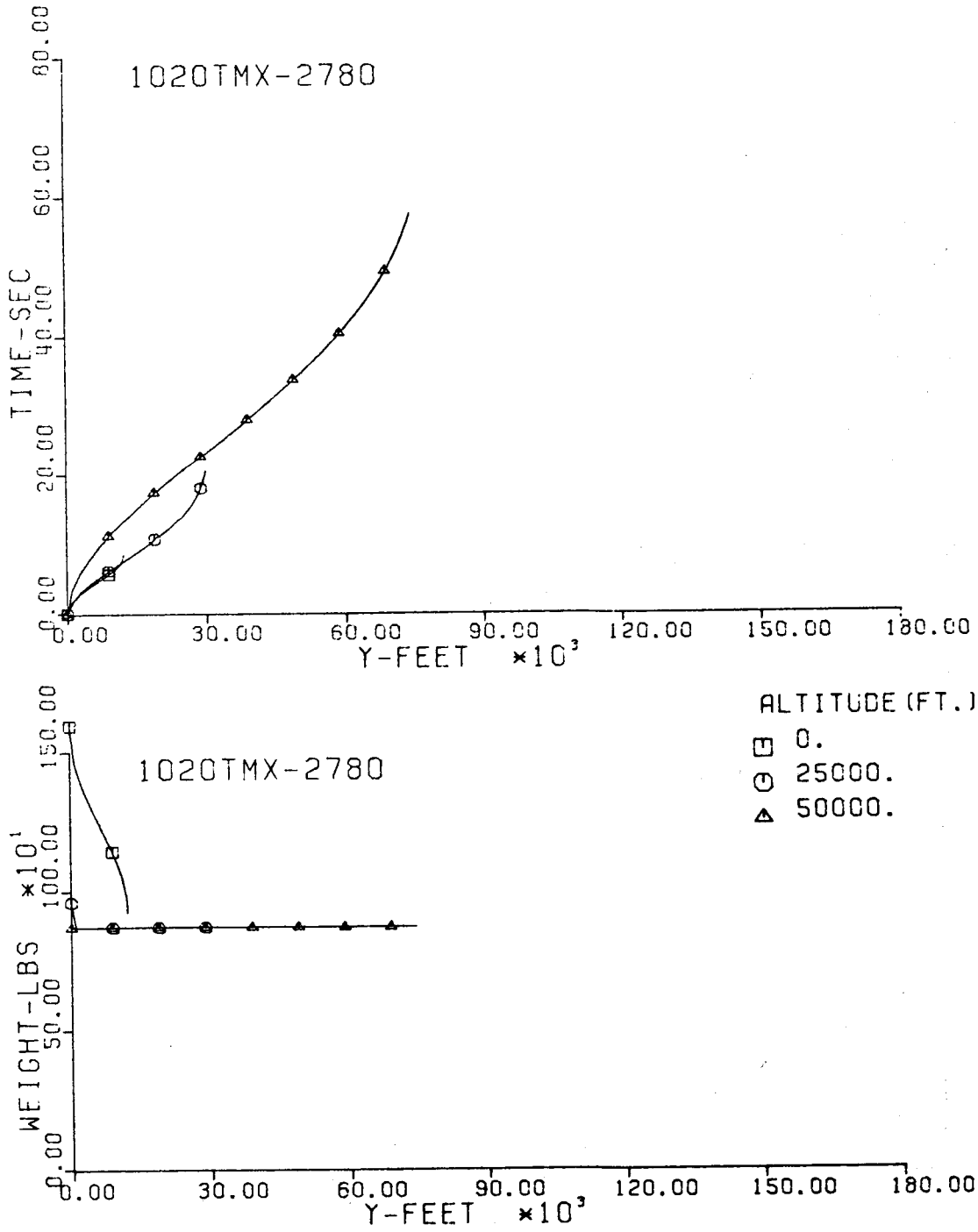

Fig. 133-III. Flight Time and Vehicle Weight vs. Downrange Distance, Y.

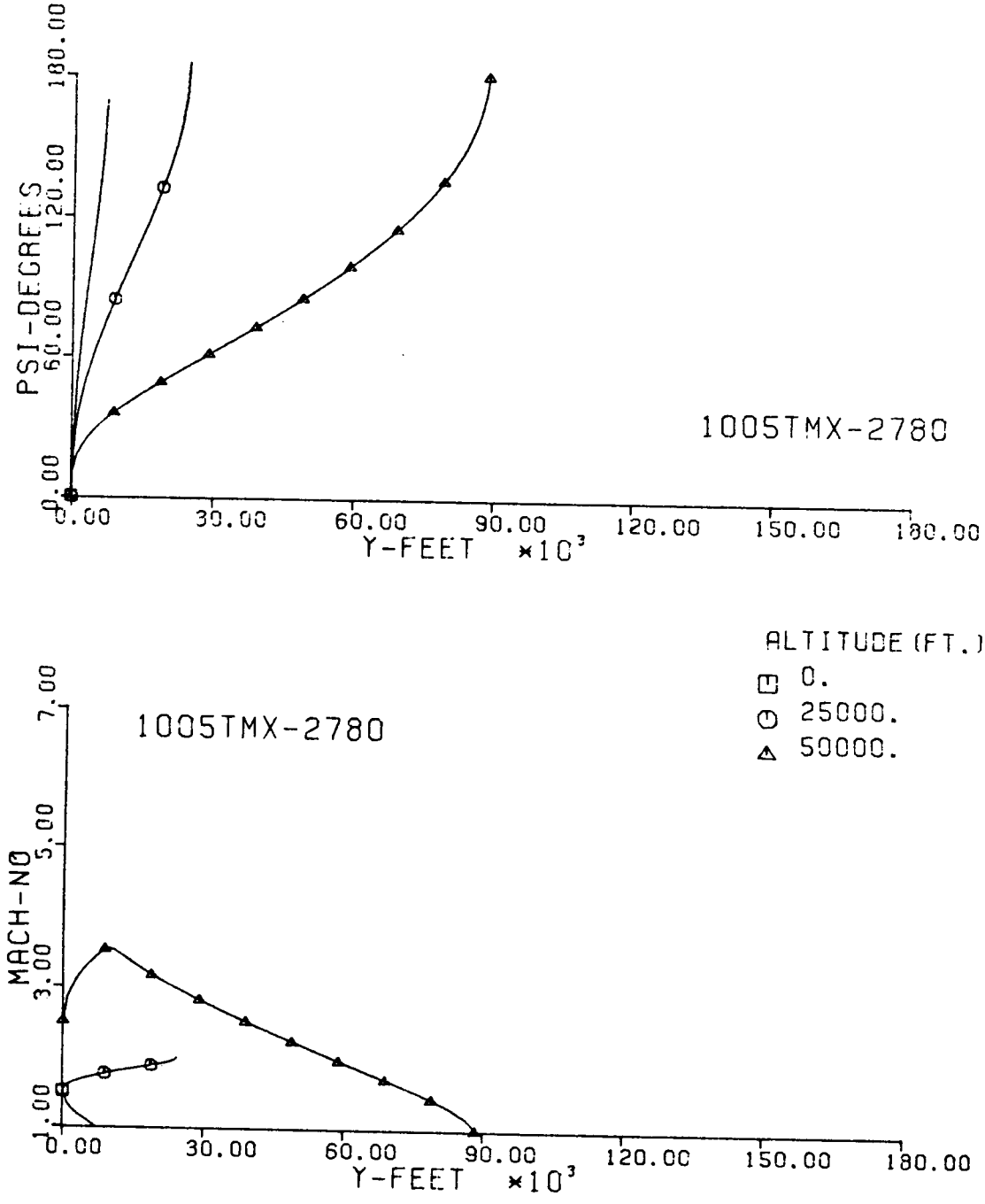

Fig. 134-III. Heading Angle and Mach No. vs. Downrange Distance, Y.

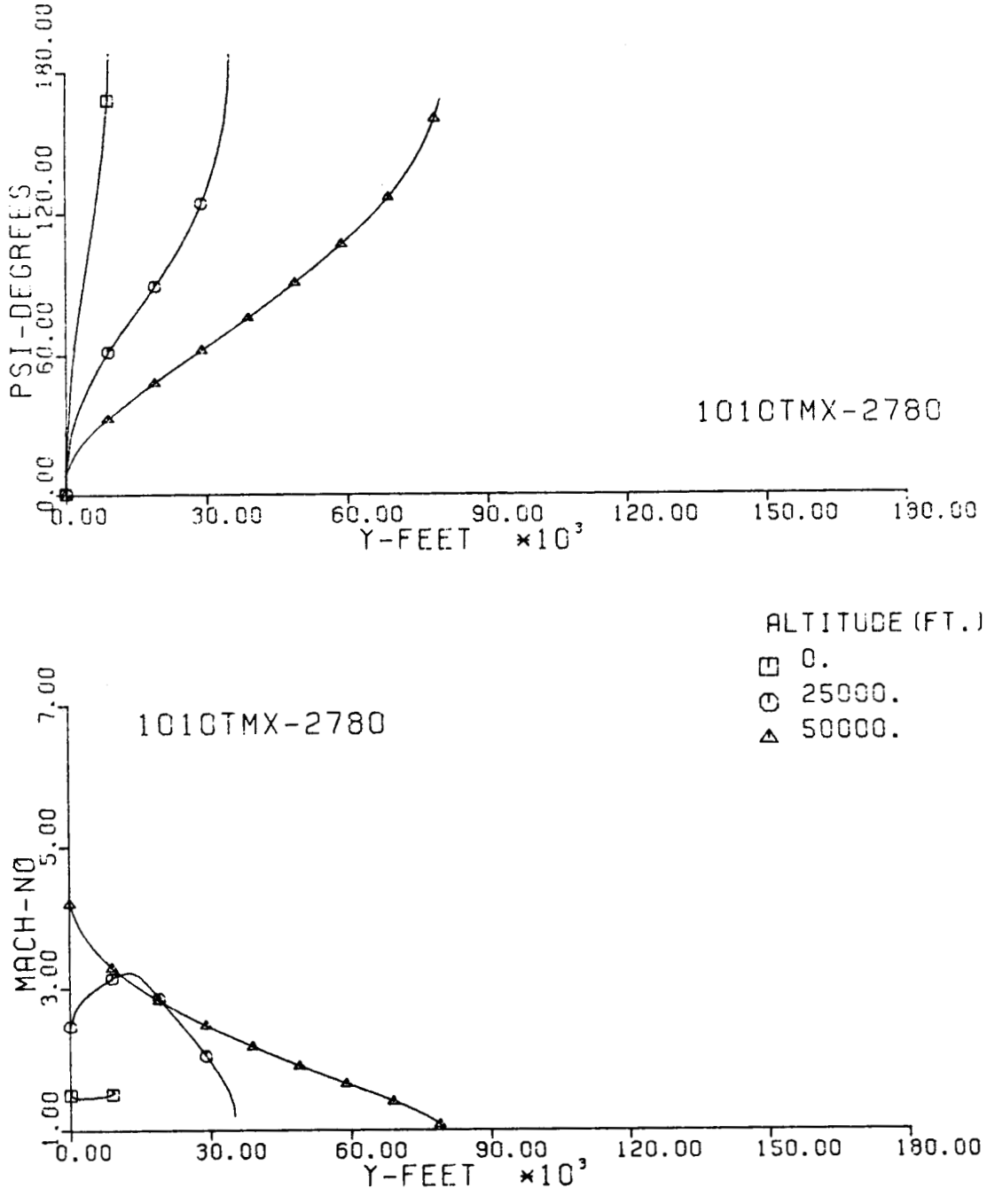

Fig. 135-III. Heading Angle and Mach No. vs. Downrange Distance, Y.

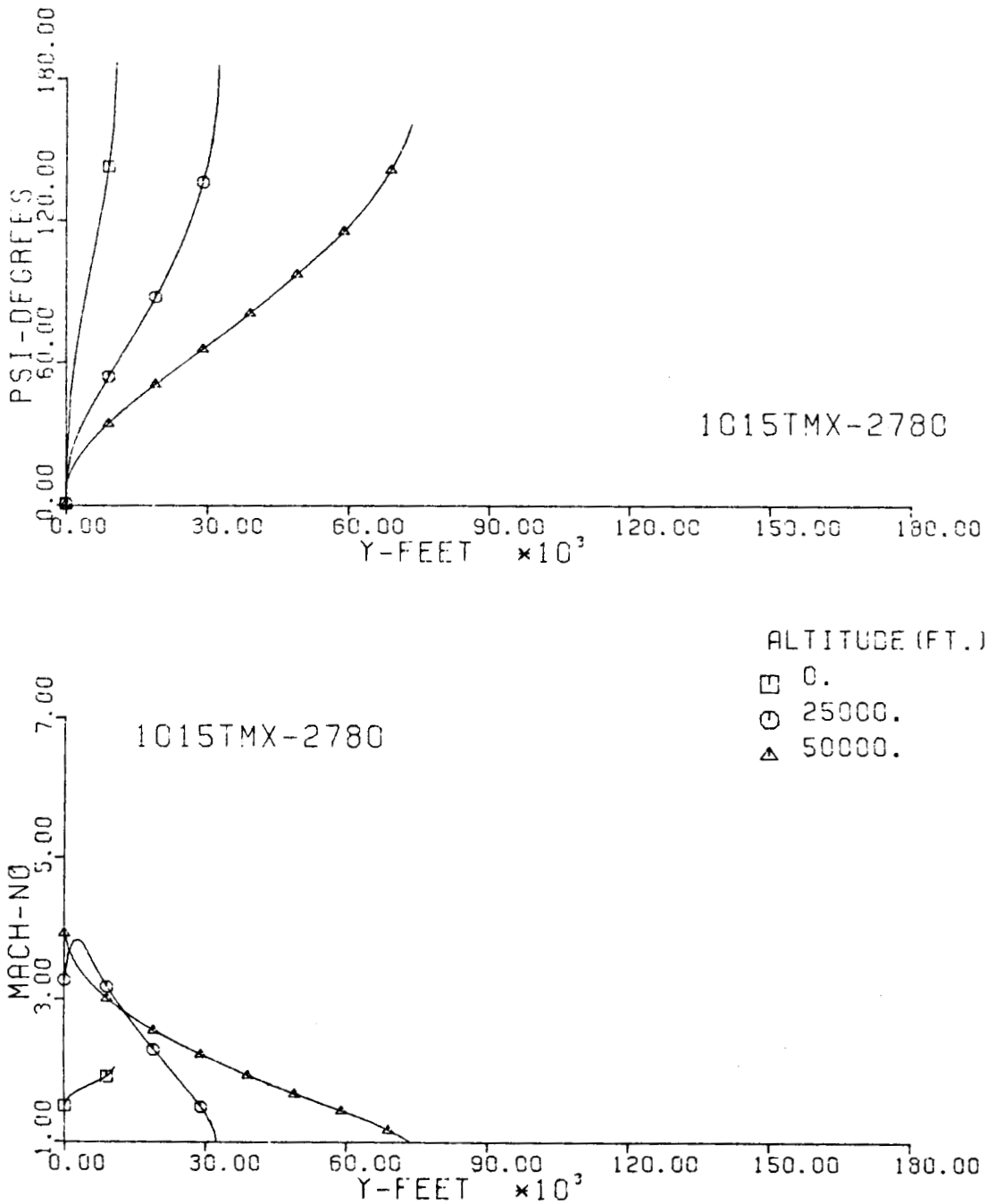

Fig. 136-III. Heading Angle and Mach No. vs. Downrange Distance, Y.

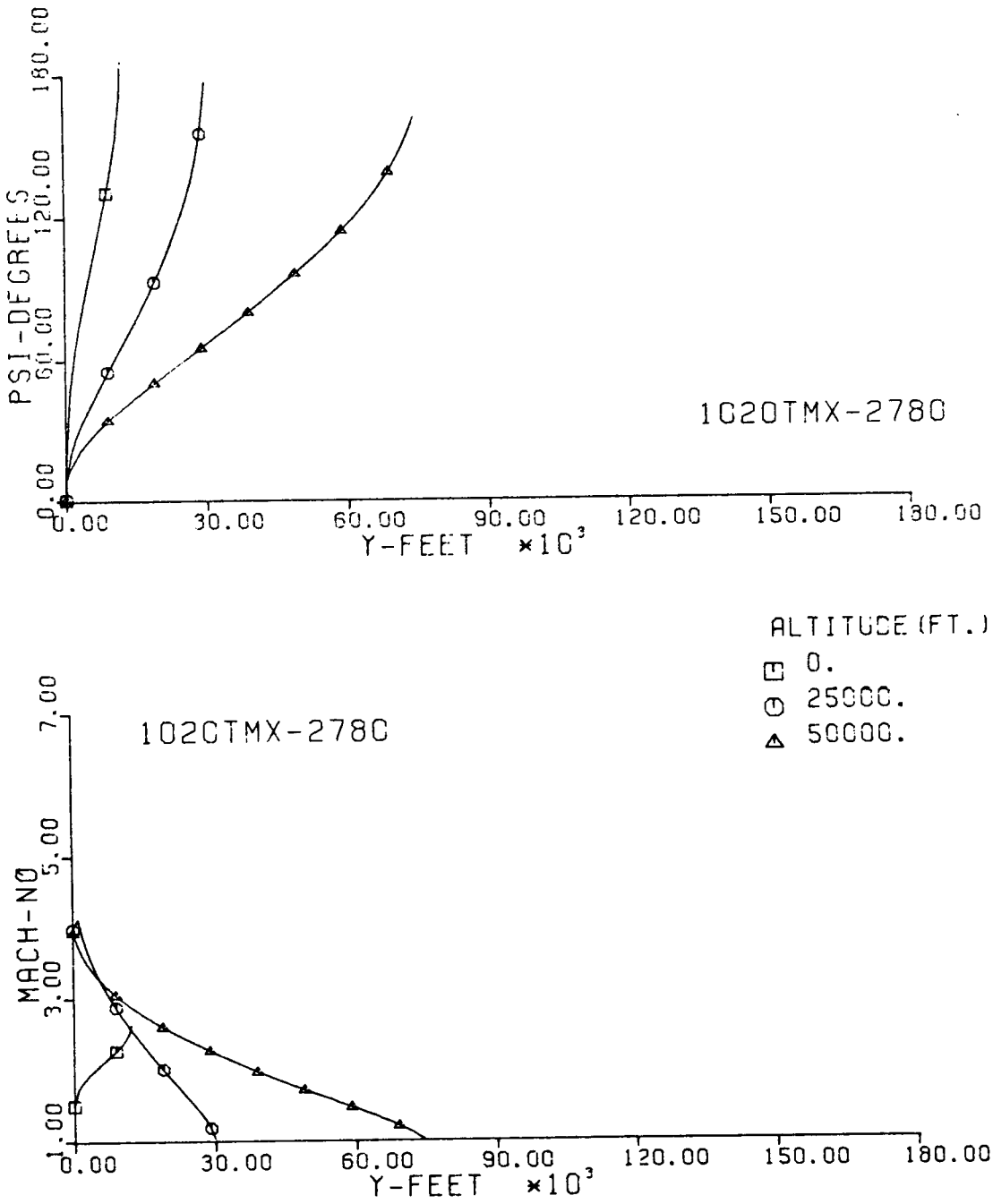

Fig. 137-III. Heading Angle and Mach No. vs. Downrange Distance, Y.

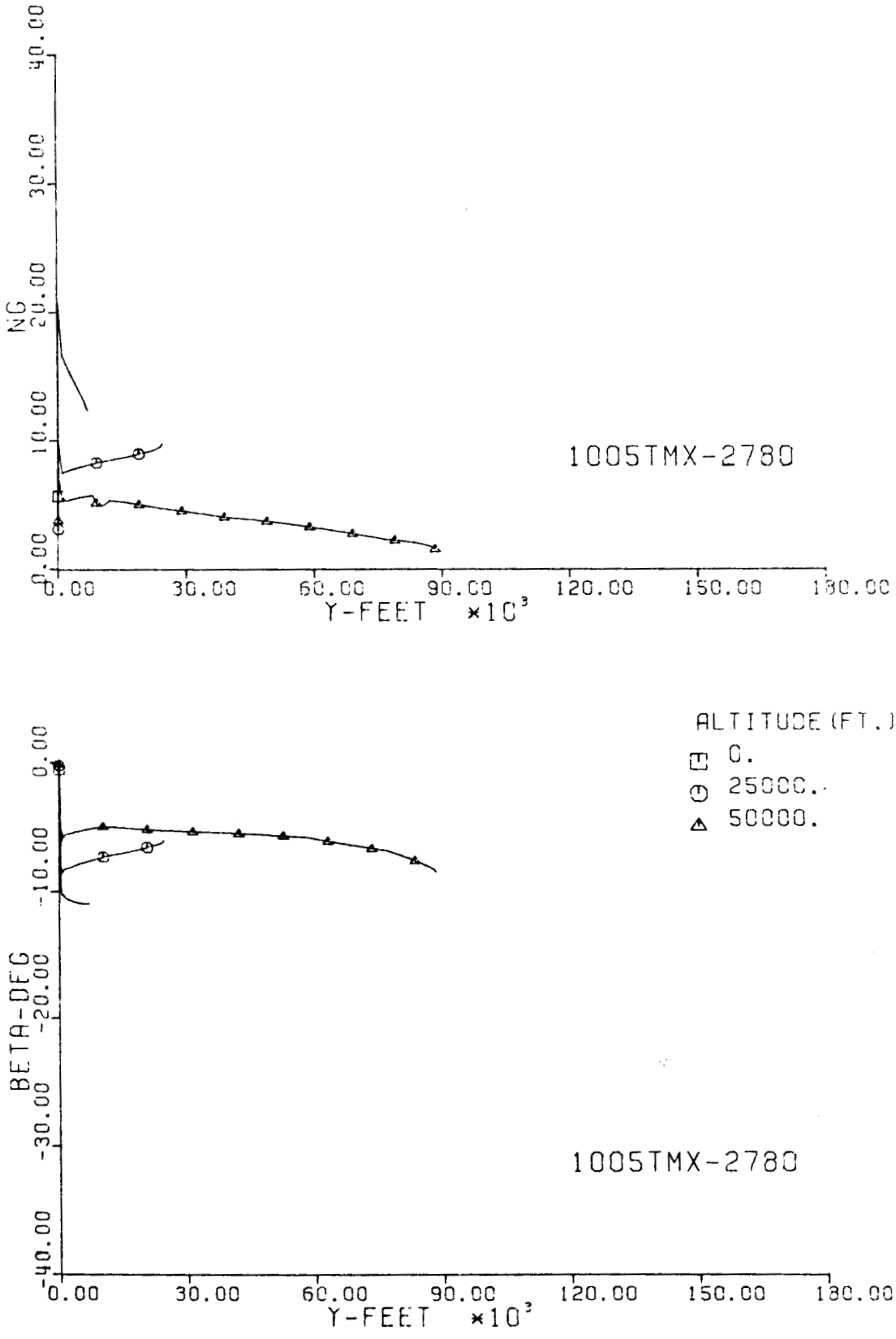

Fig. 138-III. Number of G's and Sideslip Angle vs. Downrange Distance, Y.

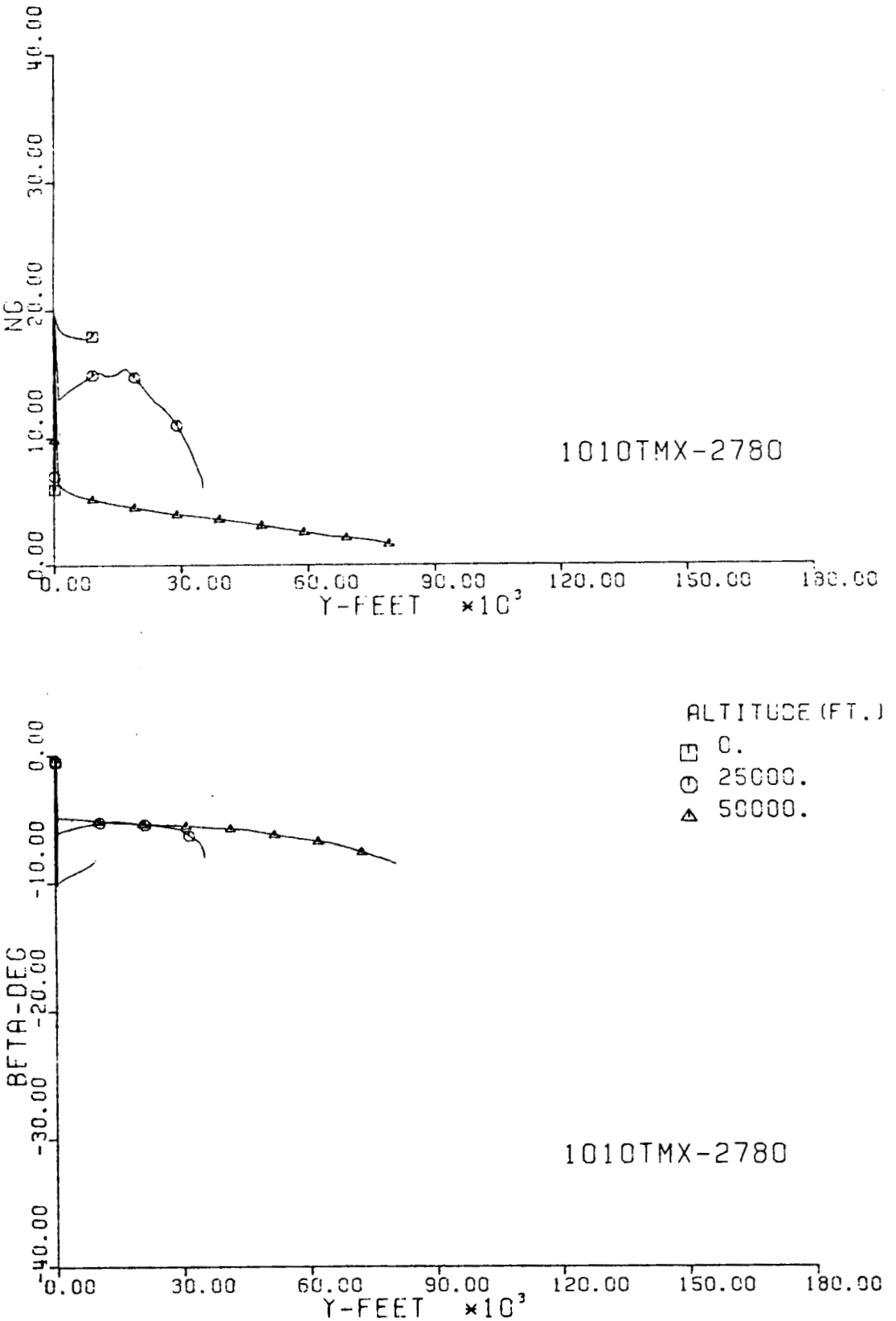

Fig. 139-III. Number of G's and Sideslip Angle vs. Downrange Distance, Y.

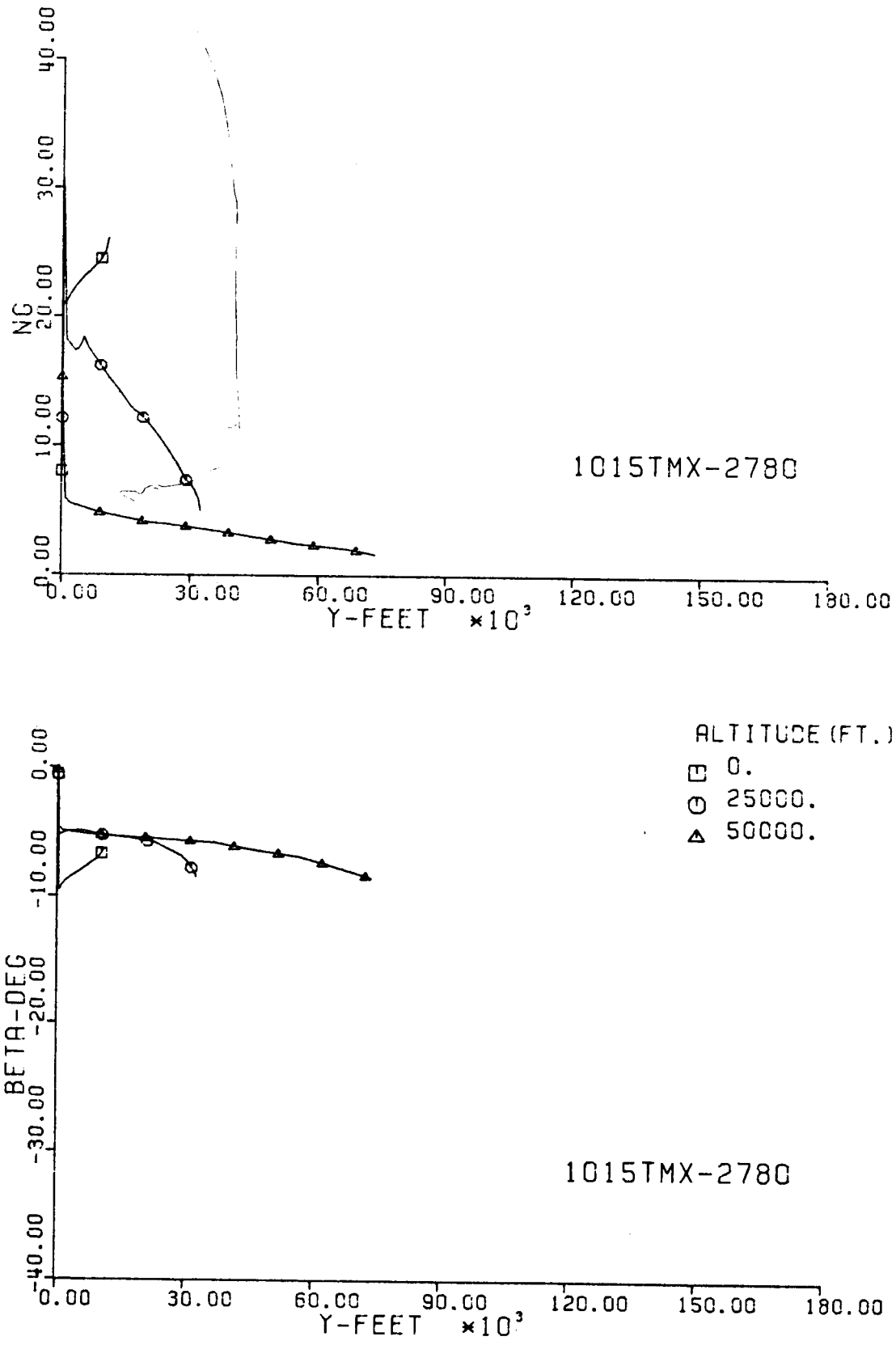

Fig. 140-III. Number of G's and Sideslip Angle vs. Downrange Distance, Y.

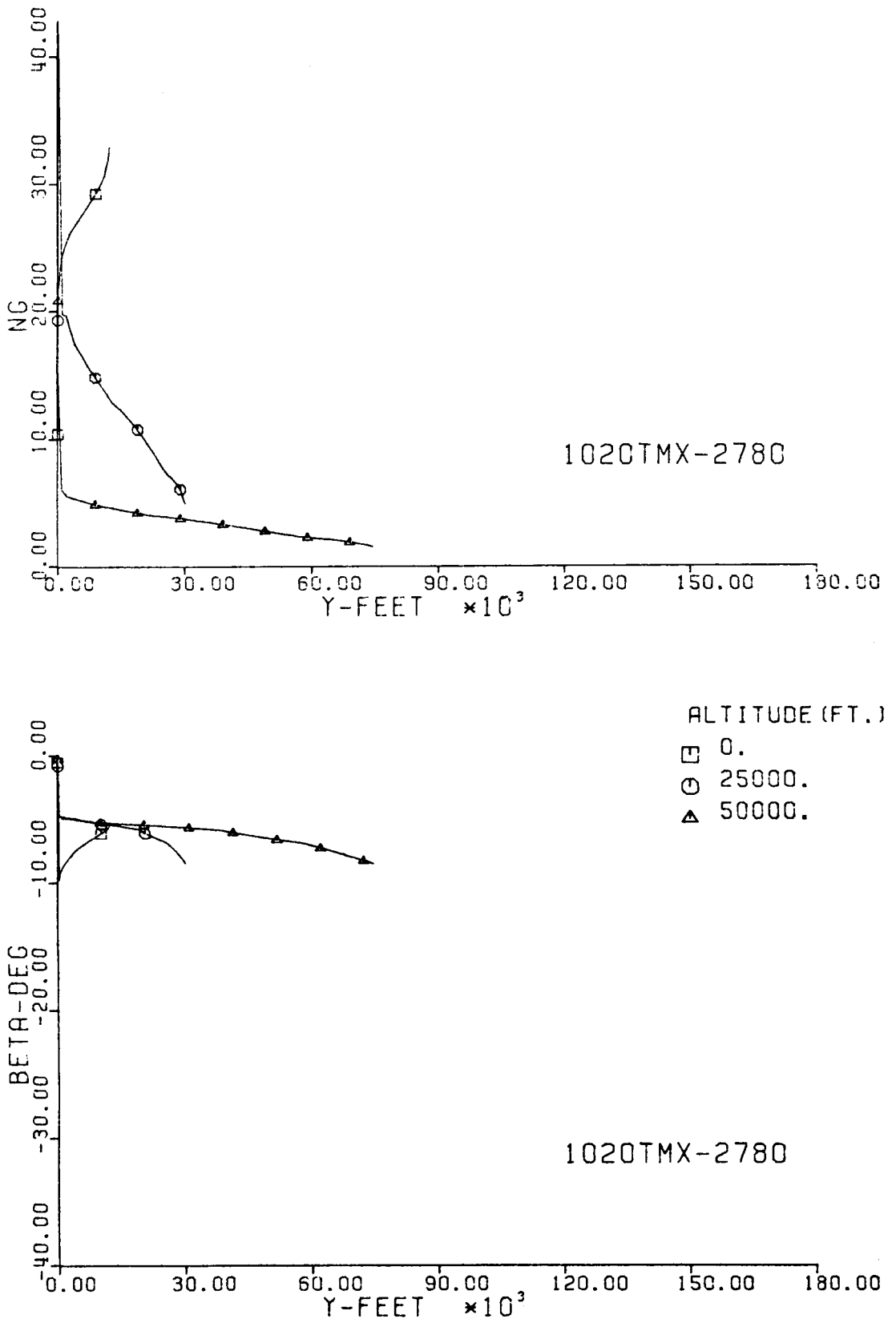

Fig. 141-III. Number of G's and Sideslip Angle vs. Downrange Distance, Y.

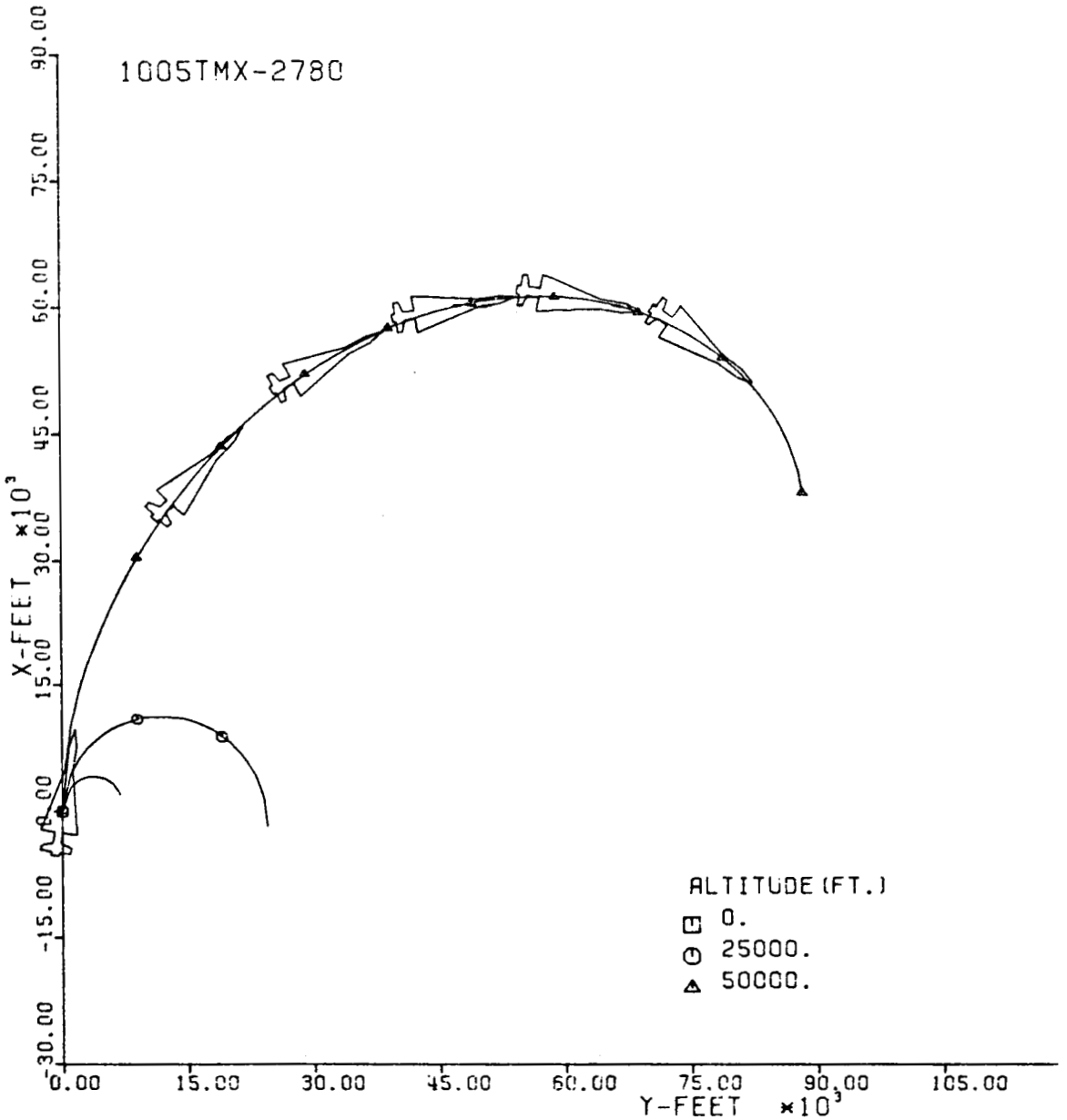

Fig. 142-III. Constant Altitude Flight Path, X vs. Y.

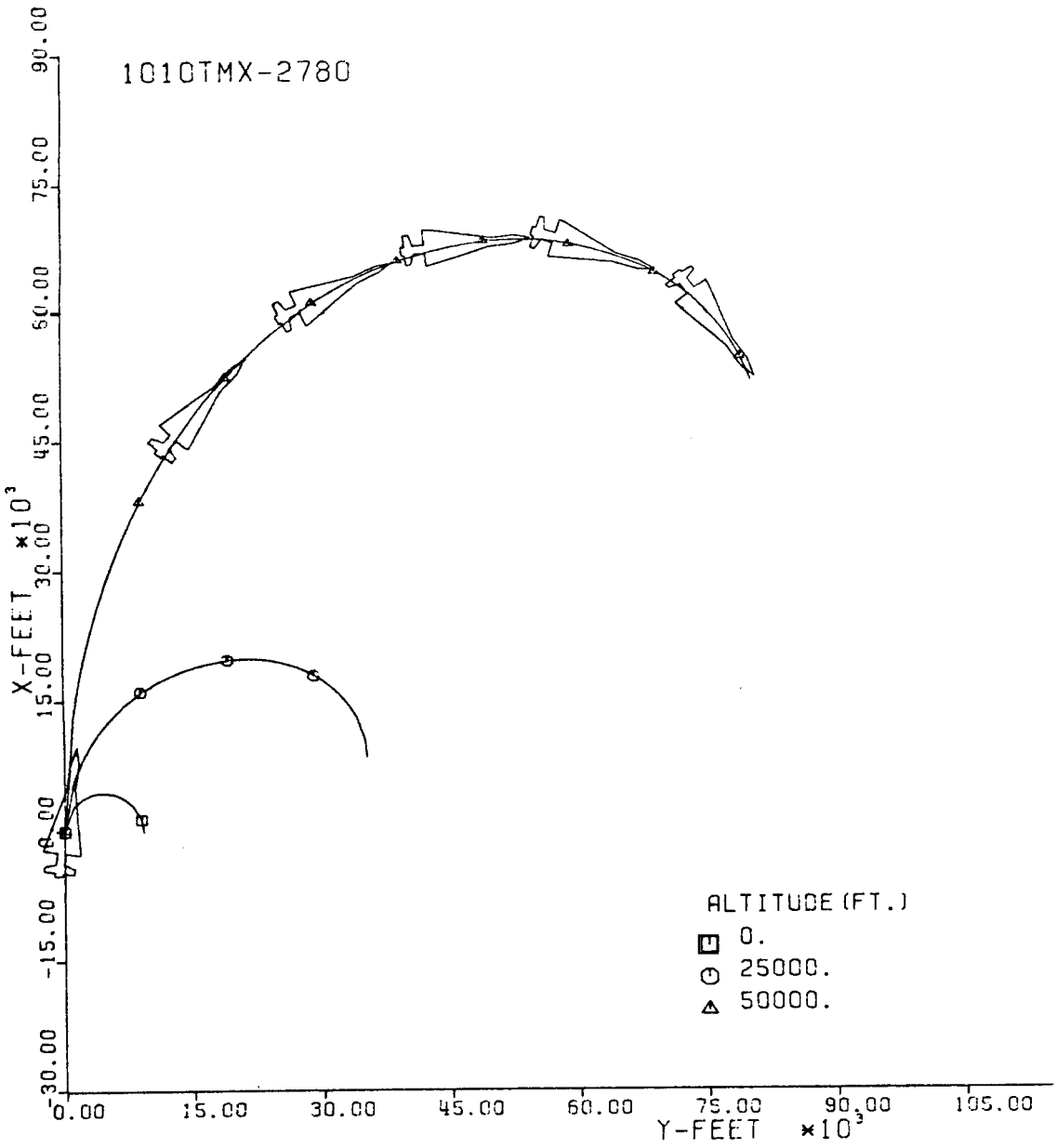

Fig. 143-III. Constant Altitude Flight Path, X vs. Y.

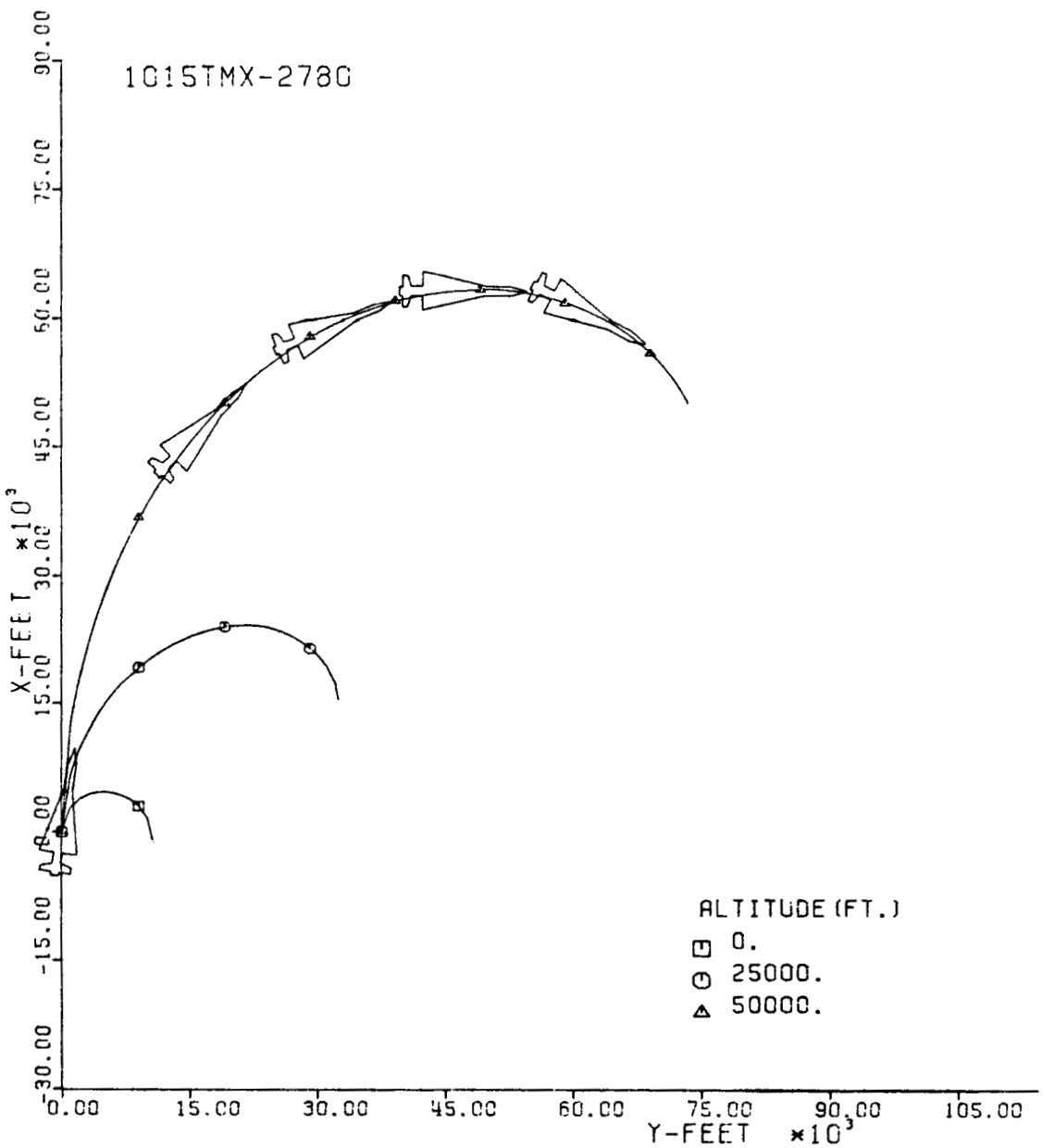

Fig. 144-III. Constant Altitude Flight Path, X vs. Y.

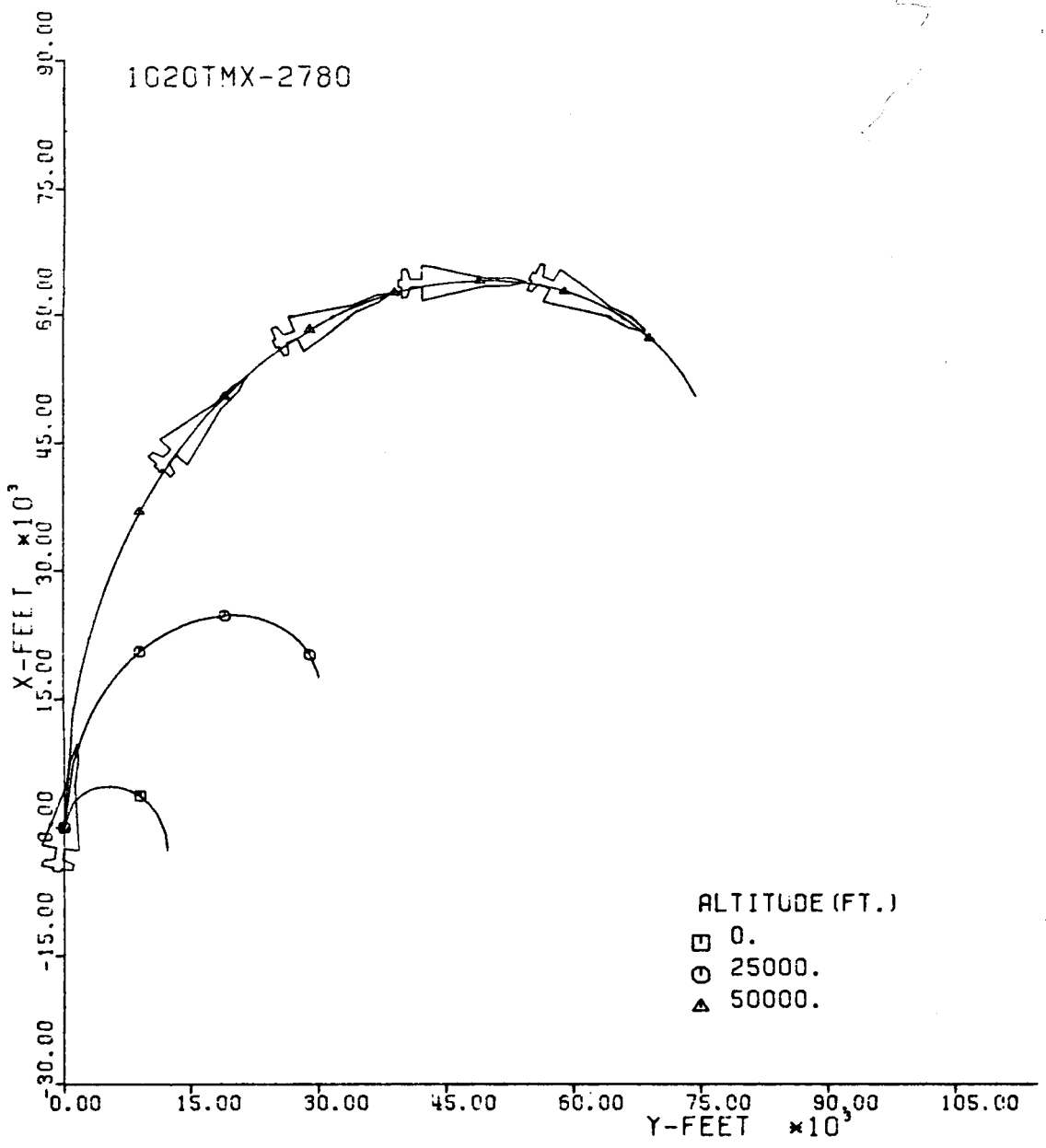

Fig. 145-III. Constant Altitude Flight Path, X vs. Y.

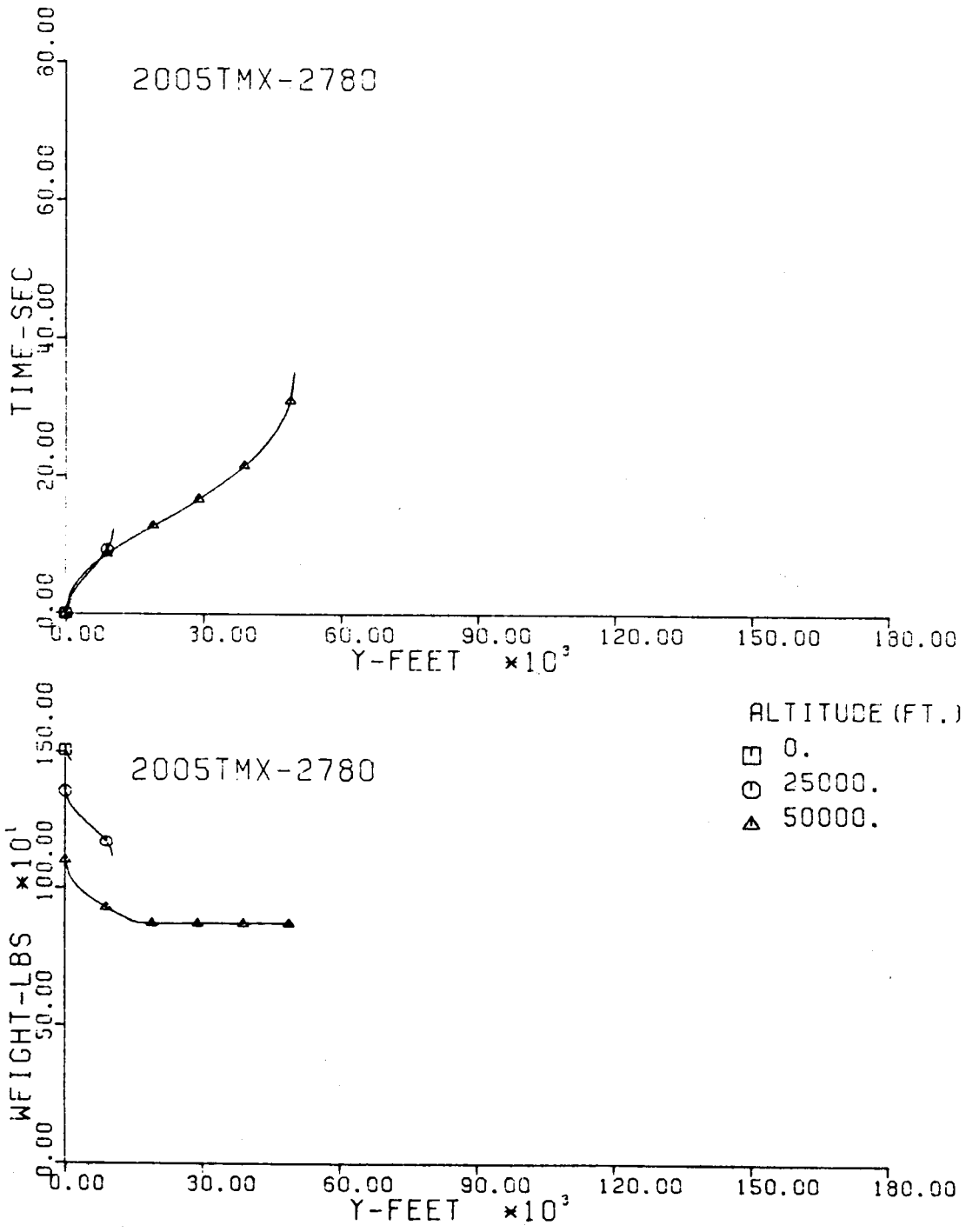

Fig. 146-III. Flight Time and Vehicle Weight vs. Downrange Distance, Y.

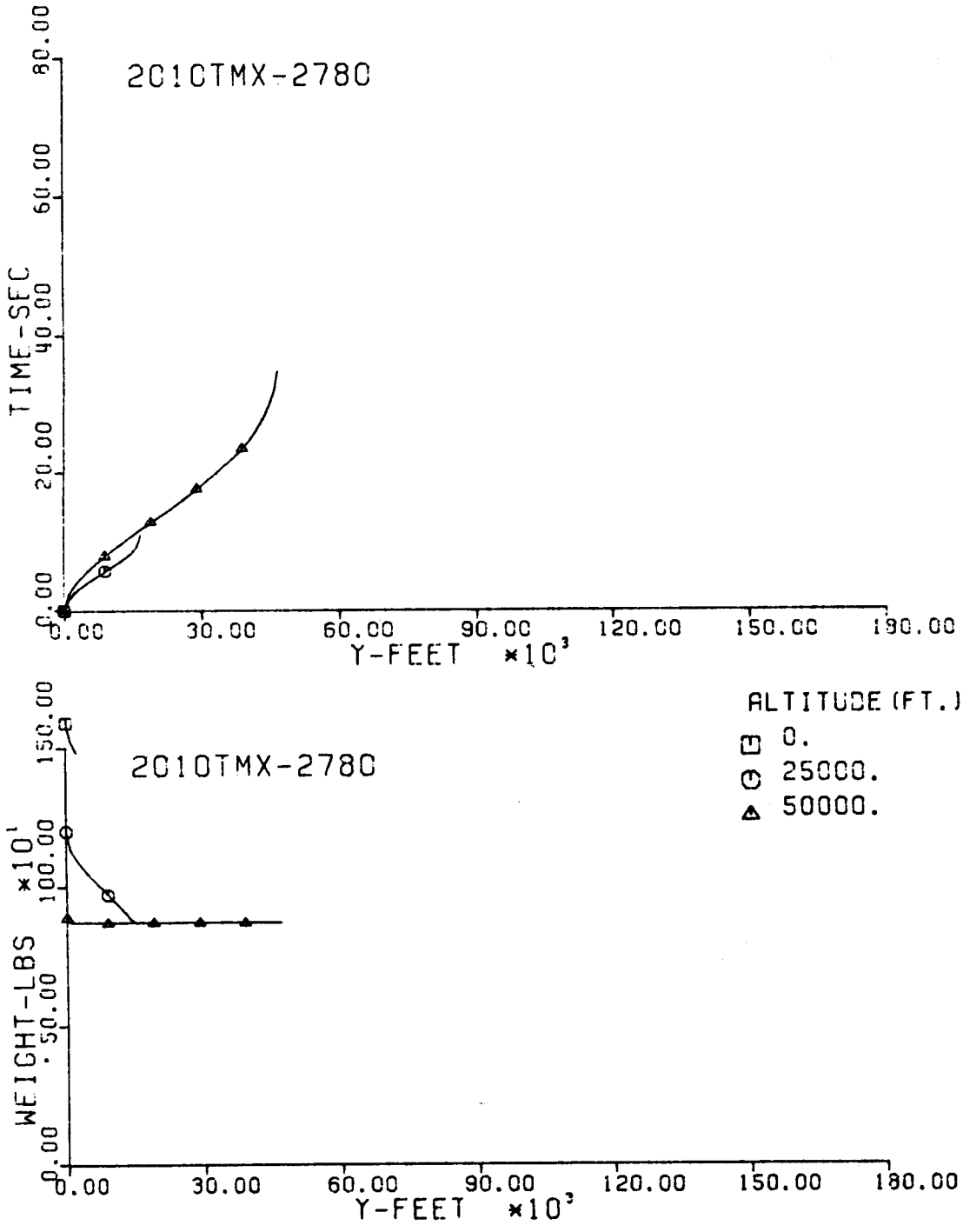

Fig. 147-III. Flight Time and Vehicle Weight vs. Downrange Distance, Y.

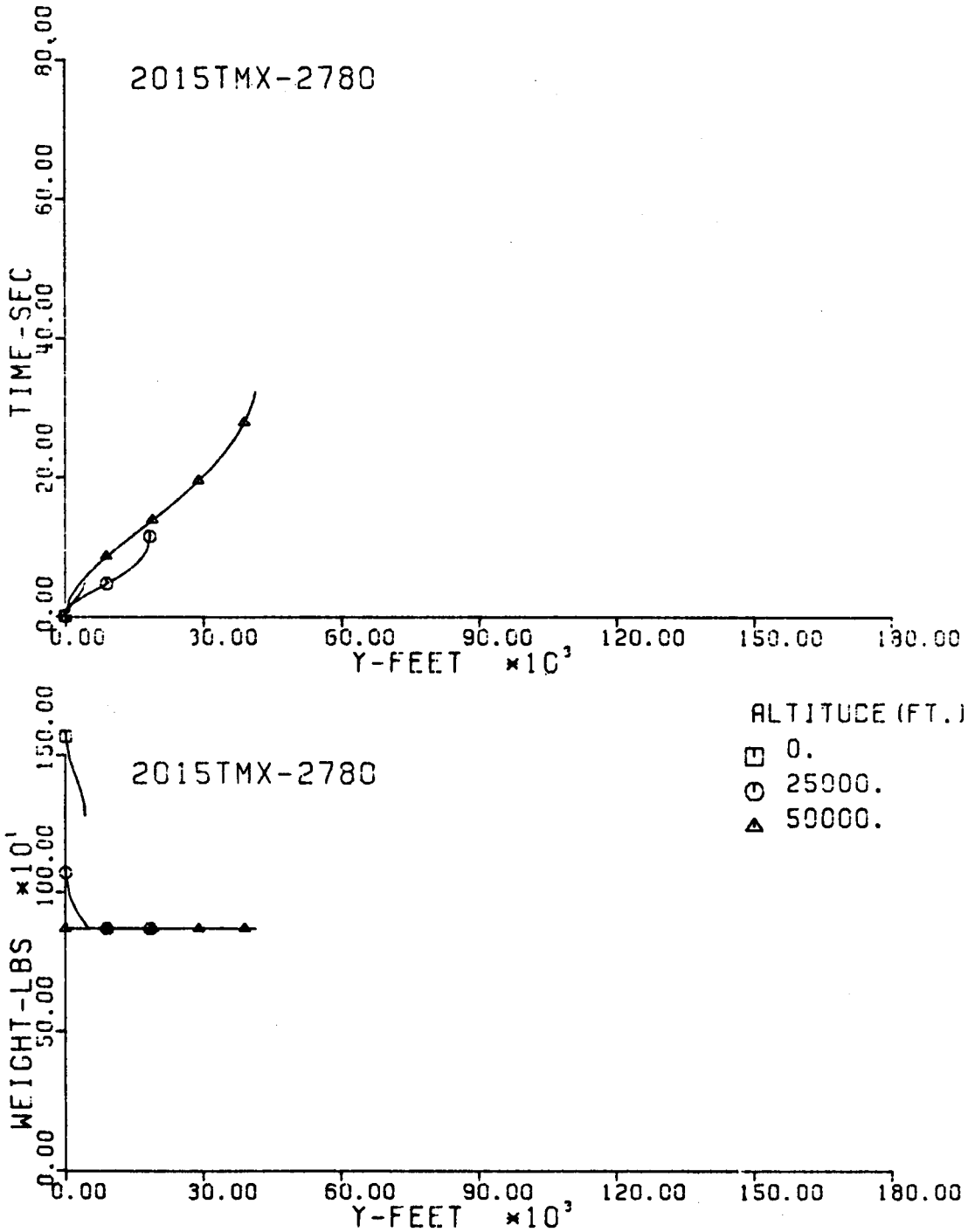

Fig. 148-III. Flight Time and Vehicle Weight vs. Downrange Distance, Y.

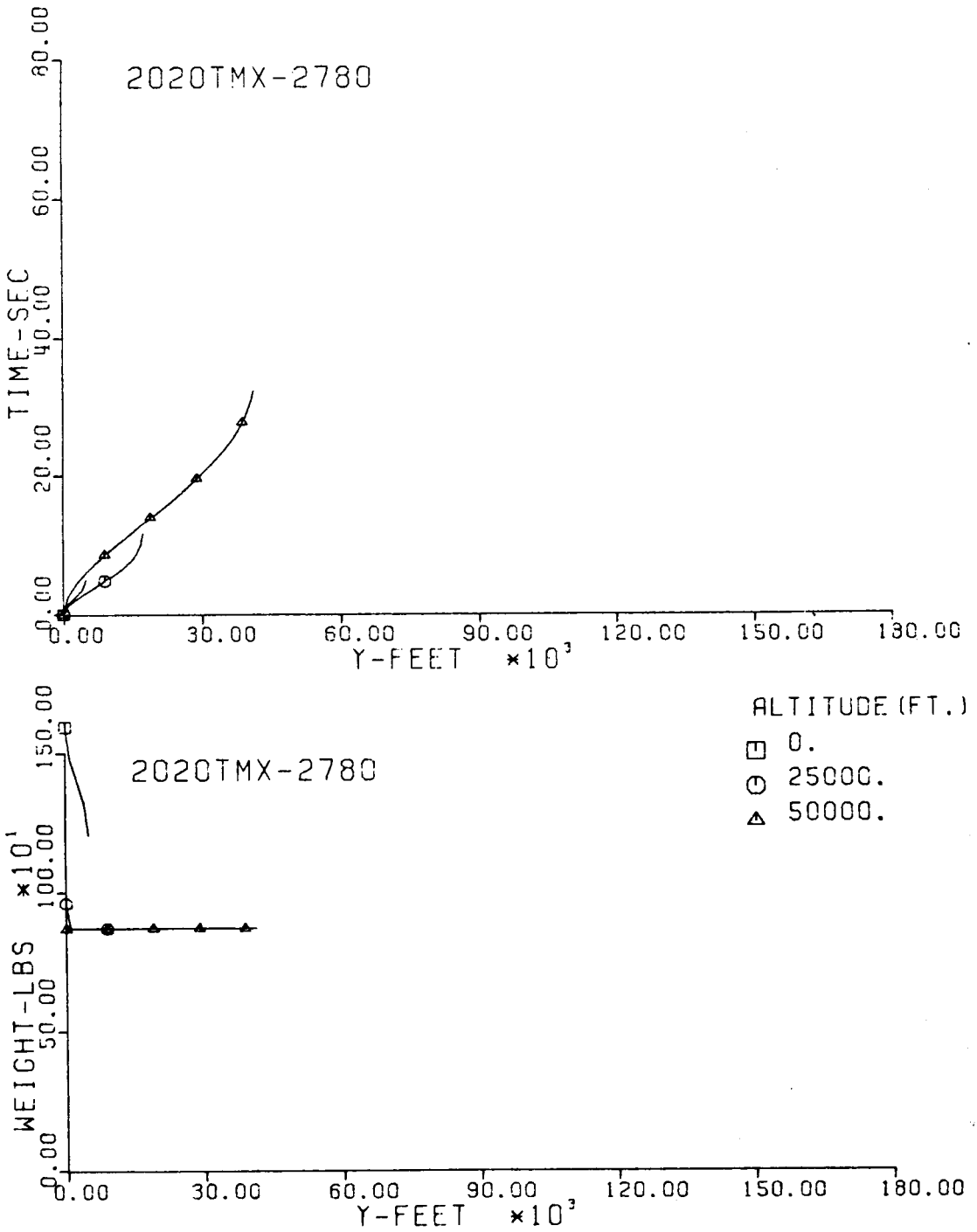

Fig. 149-III. Flight Time and Vehicle Weight vs. Downrange Distance, Y.

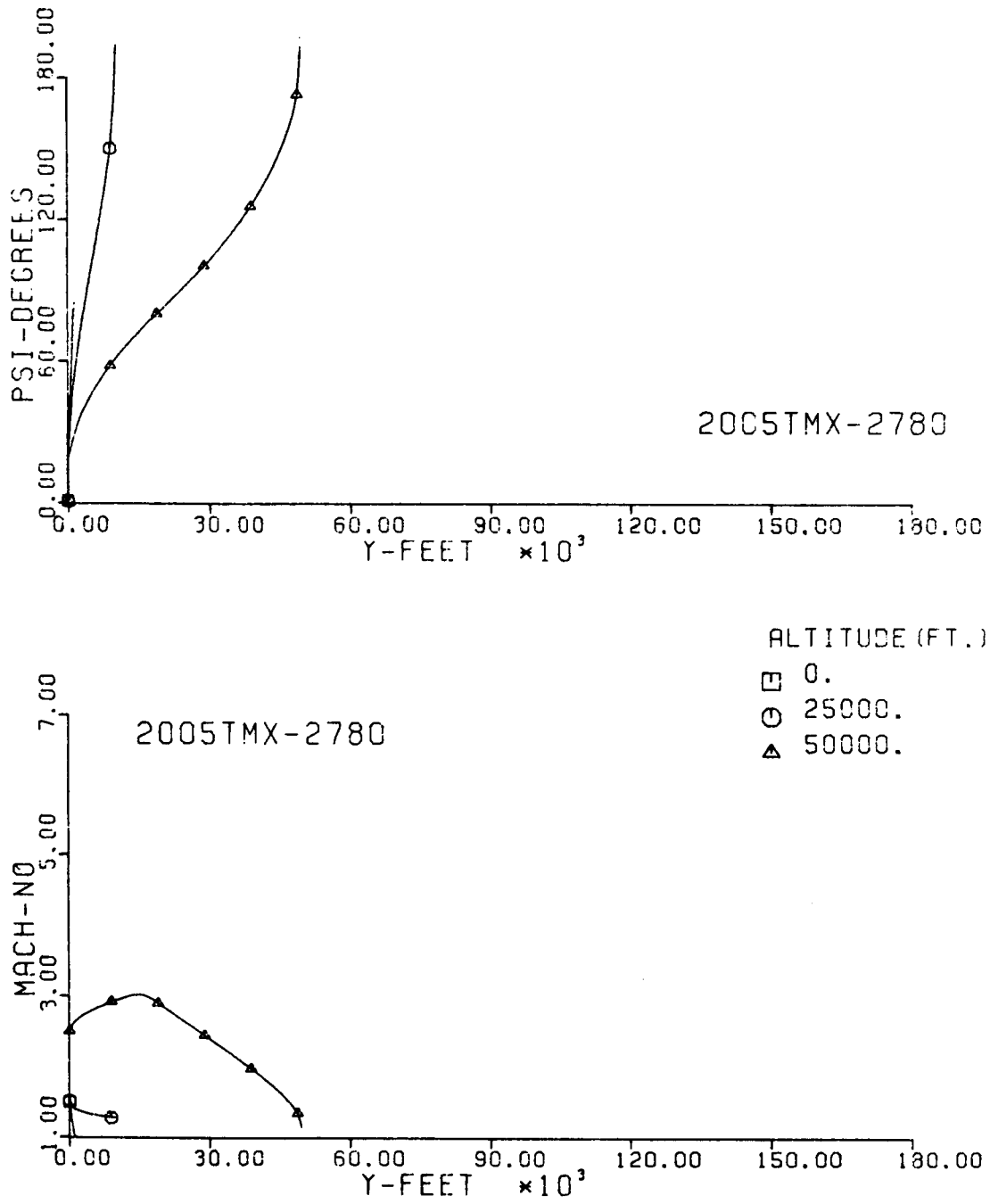

Fig. 150-III. Heading Angle and Mach No. vs. Downrange Distance, Y.

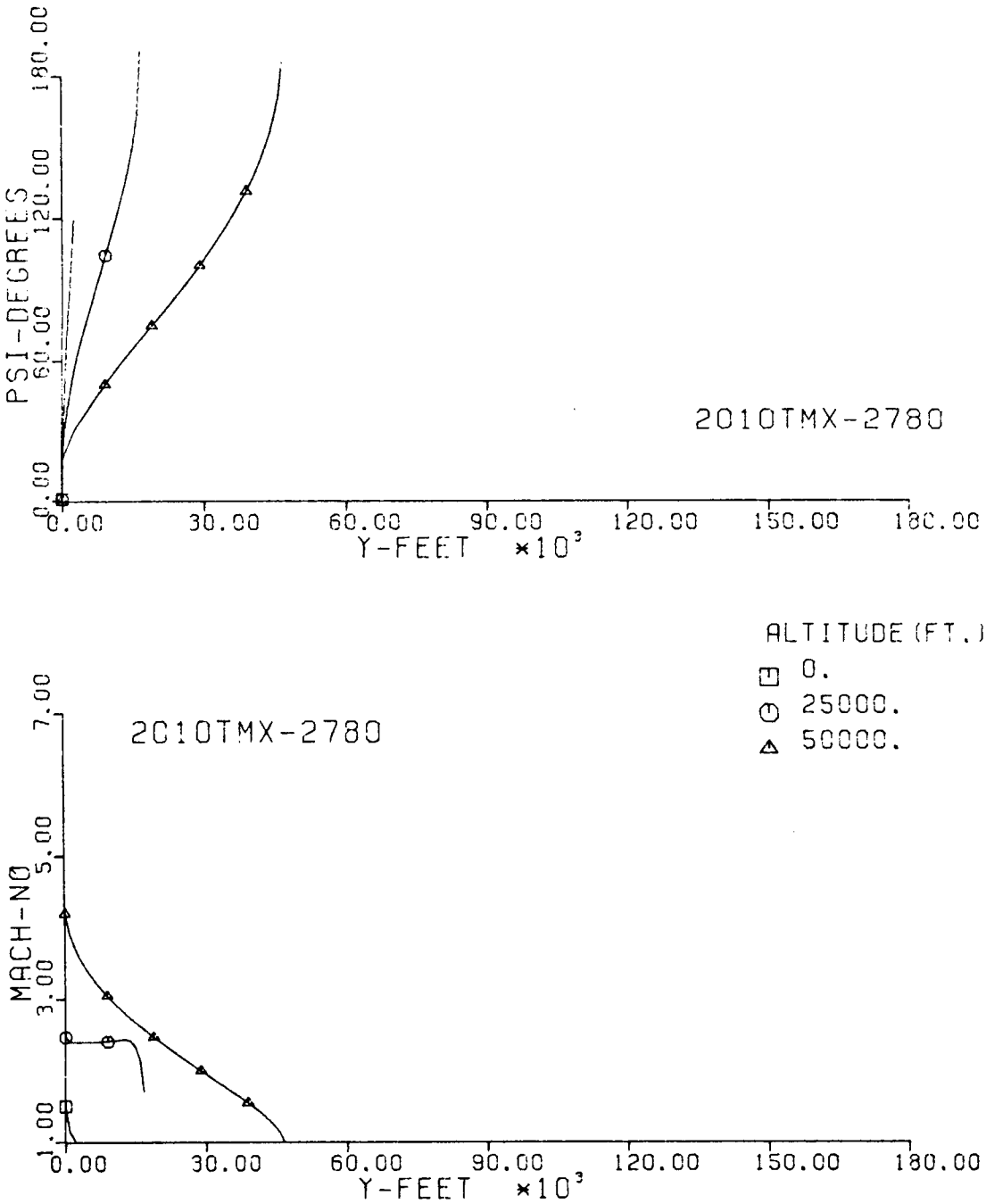

Fig. 151-III. Heading Angle and Mach No. vs. Downrange Distance, Y.

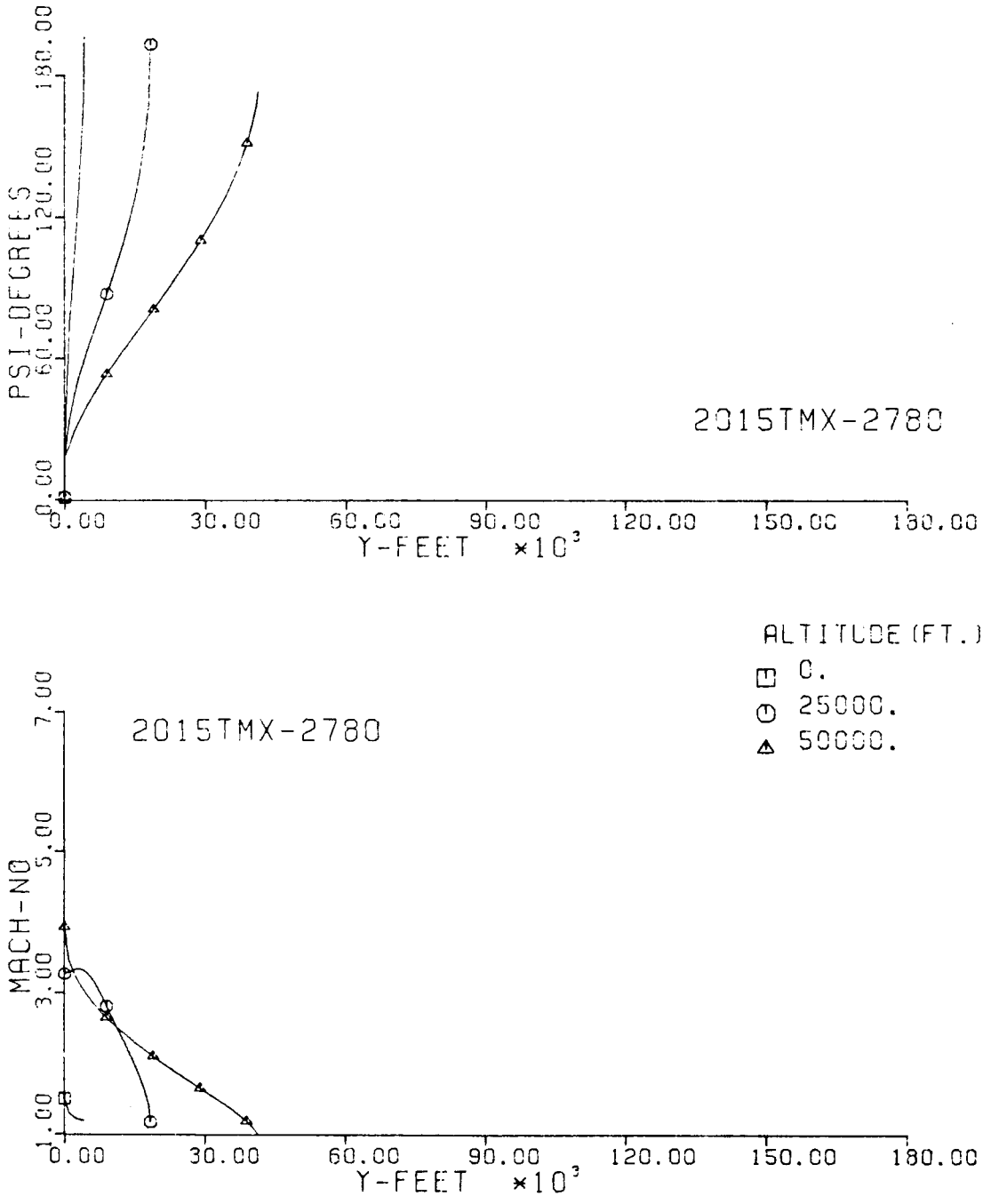

Fig. 152-III. Heading Angle and Mach No. vs. Downrange Distance, Y.

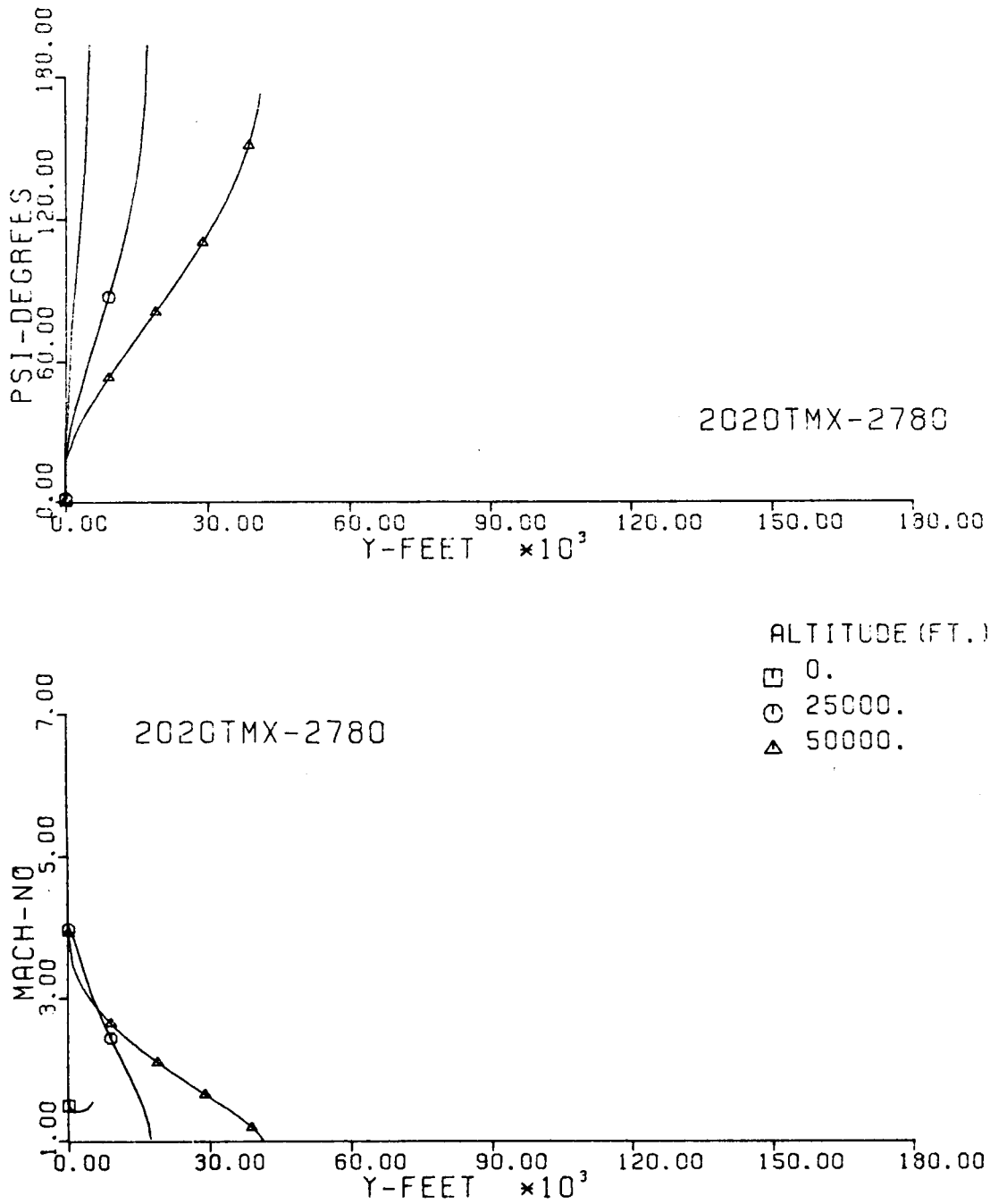

Fig. 153-III. Heading Angle and Mach No. vs. Downrange Distance, Y.

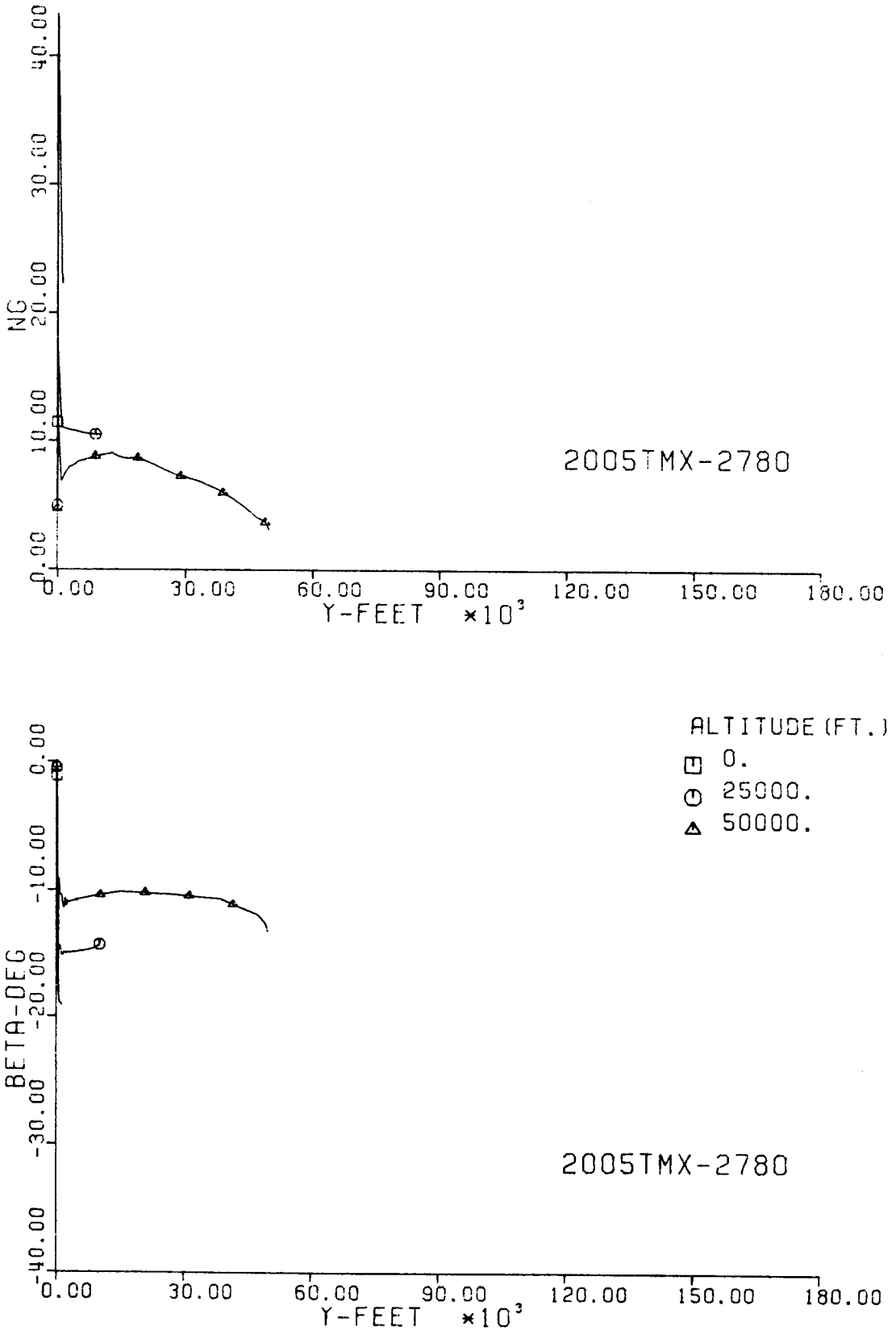

Fig. 154-III. Number of G's and Sideslip Angle vs. Downrange Distance, Y.

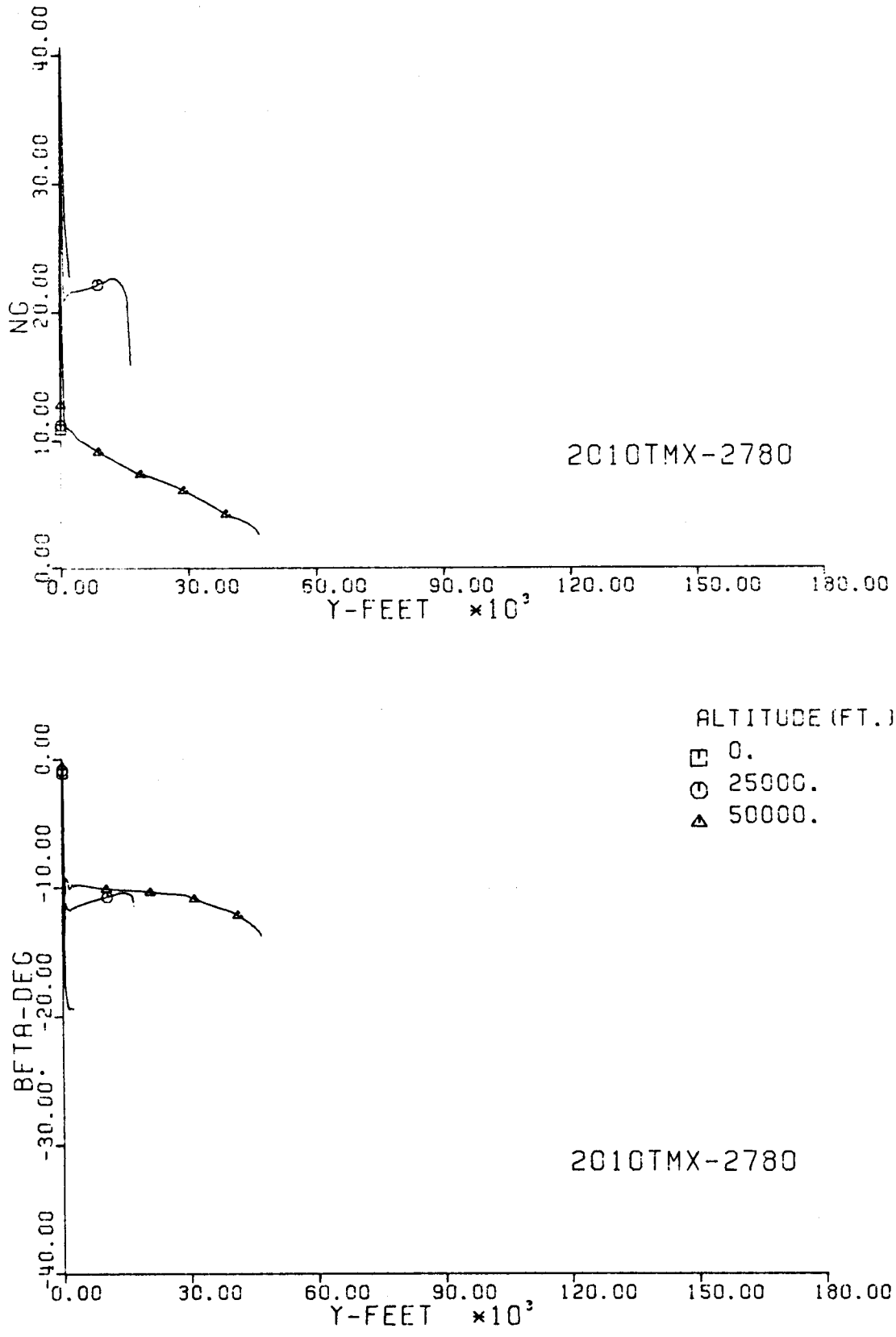

Fig. 155-III. Number of G's and Sideslip Angle vs. Downrange Distance, Y.

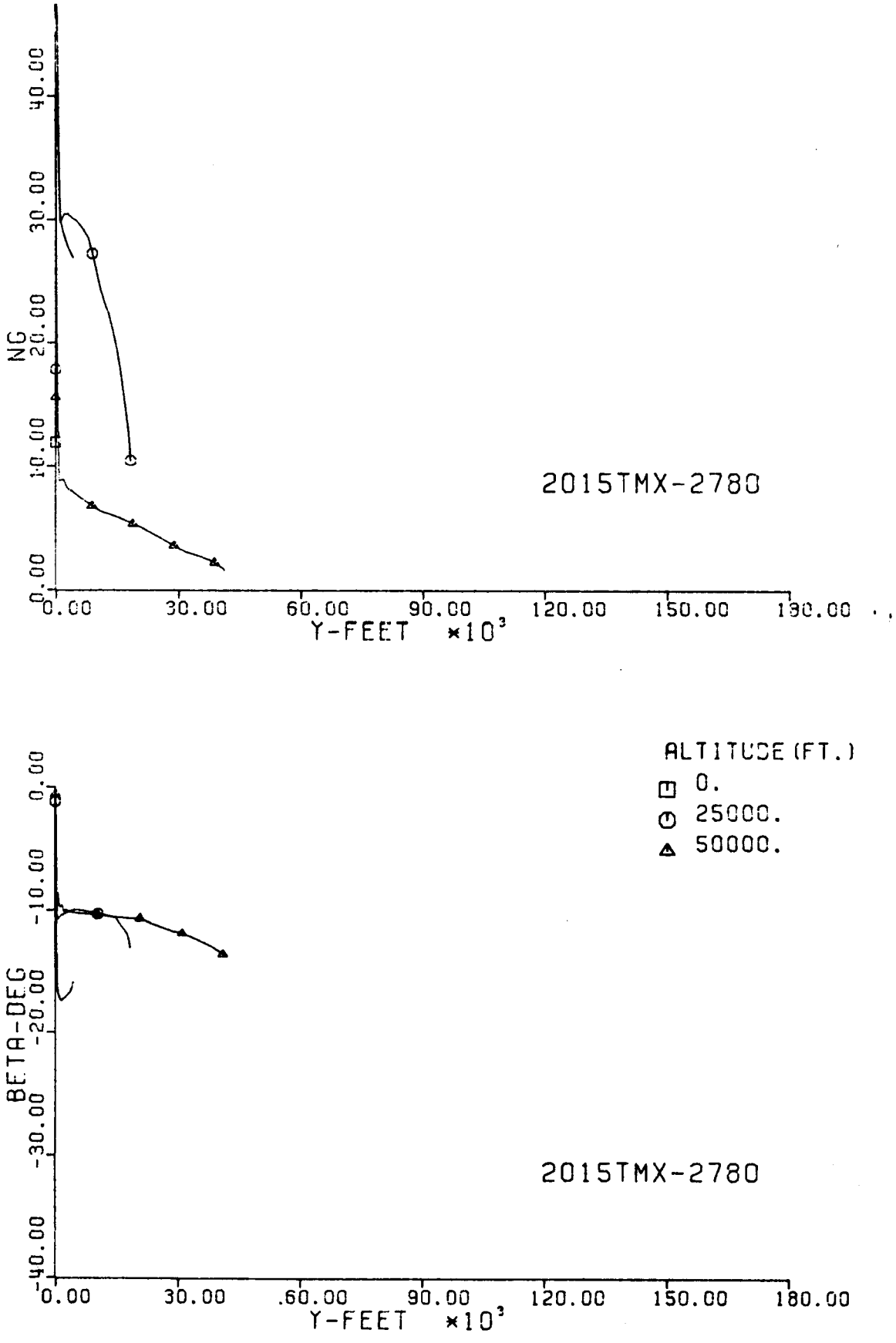

Fig. 156-III. Number of G's and Sideslip Angle vs. Downrange Distance, Y.

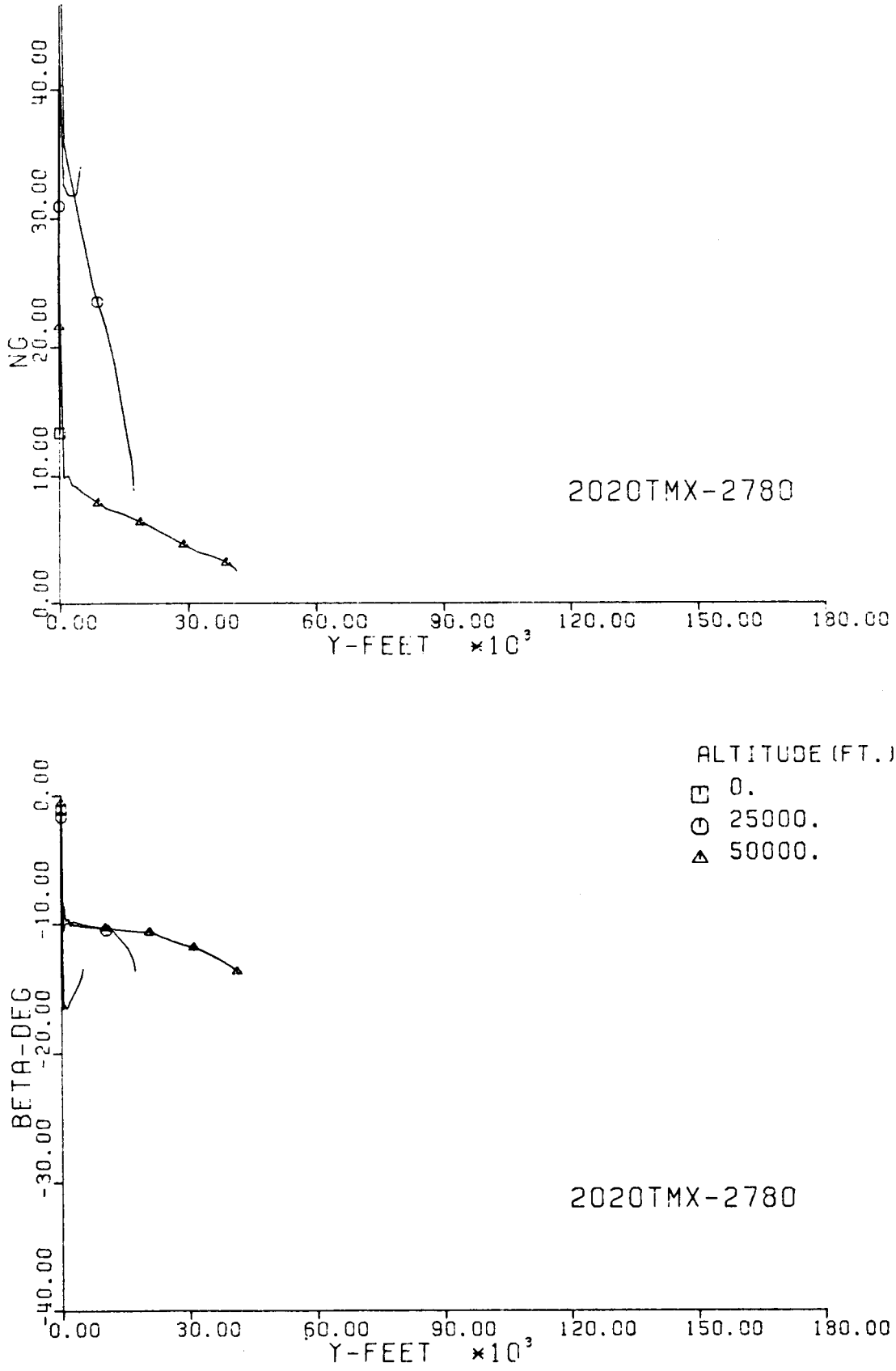

Fig. 157-III. Number of G's and Sideslip Angle vs. Downrange Distance, Y.

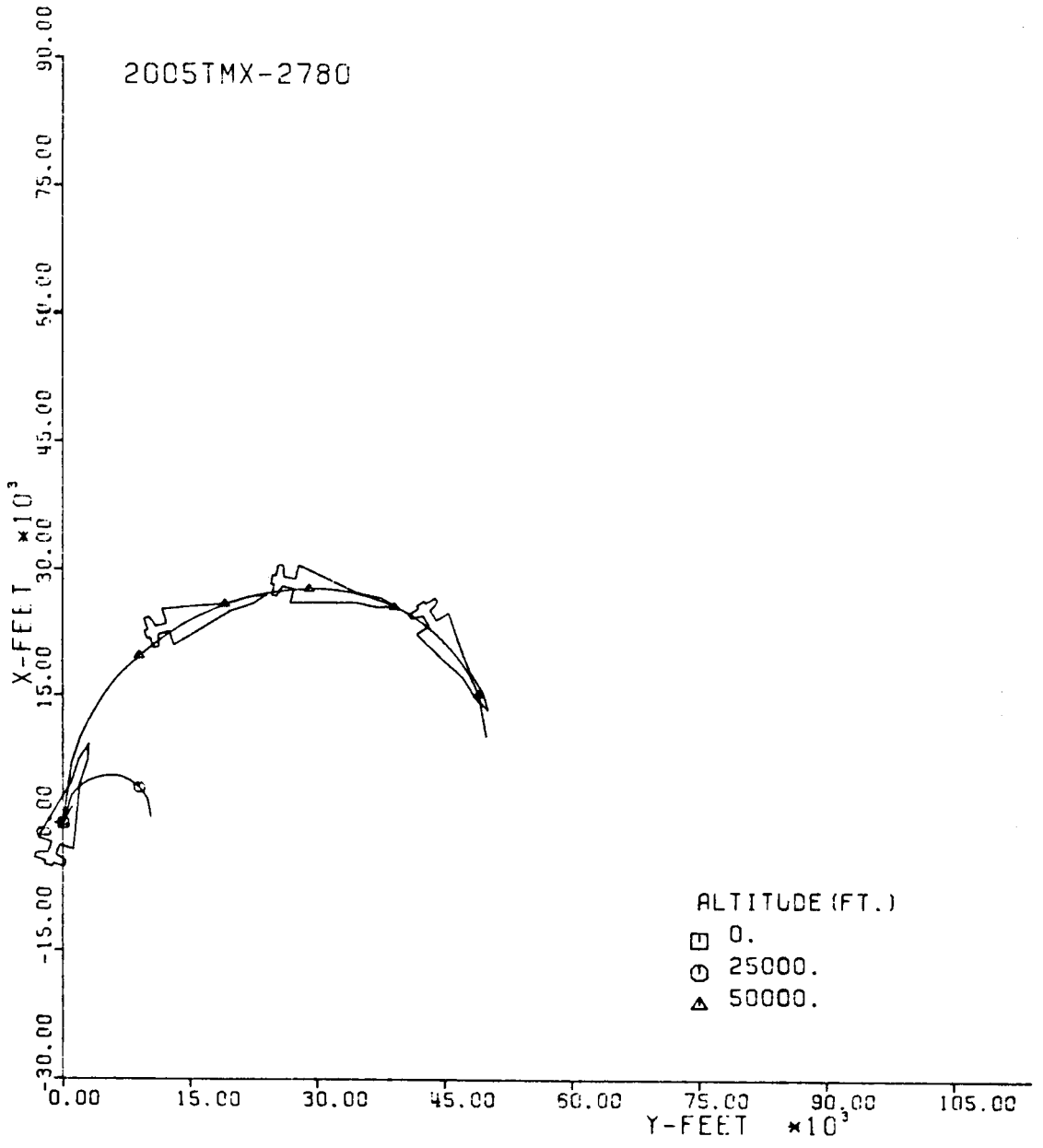

Fig. 158-III. Constant Altitude Flight Path, X vs. Y.

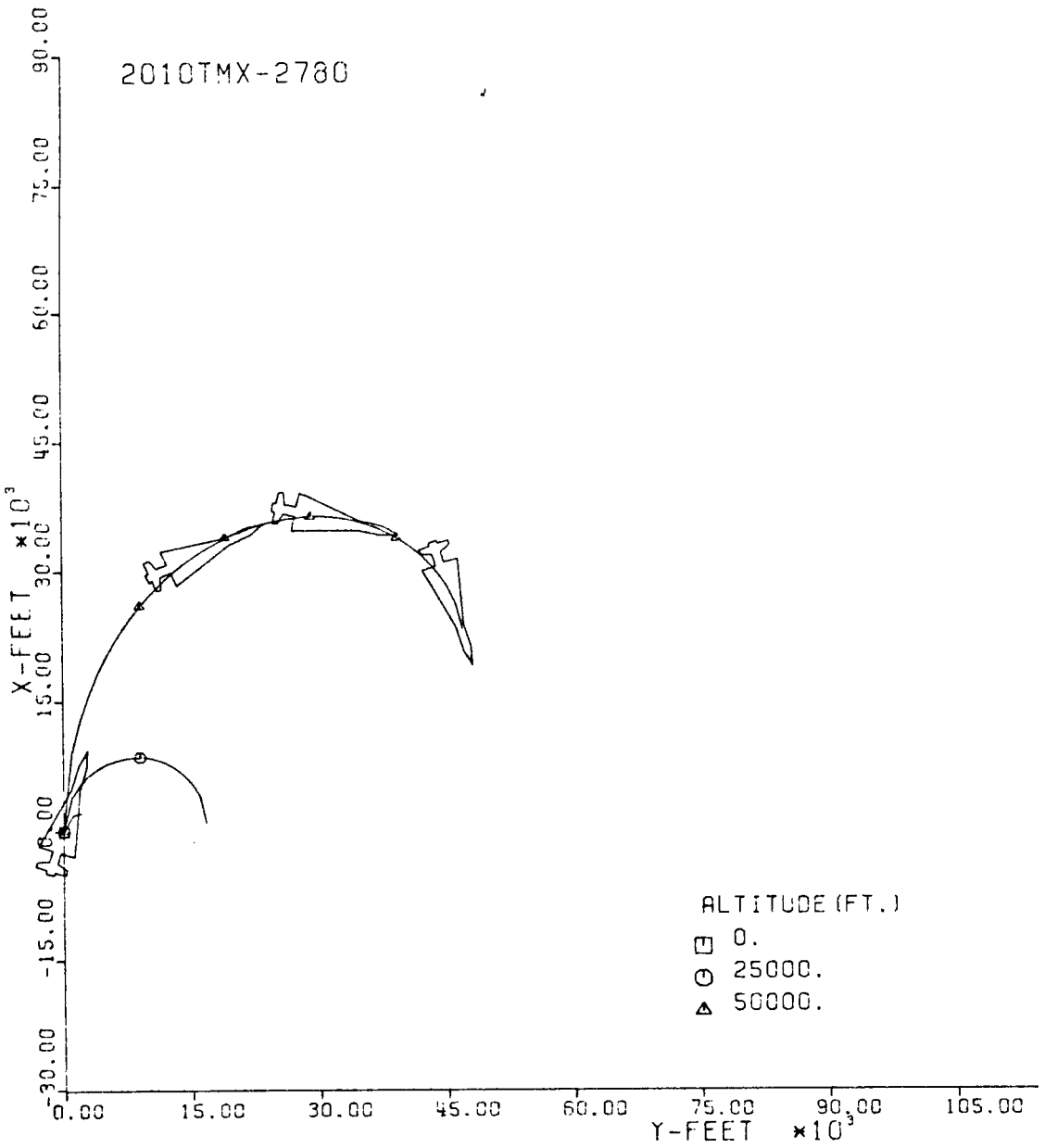

Fig. 159-III. Constant Altitude Flight Path, X vs. Y.

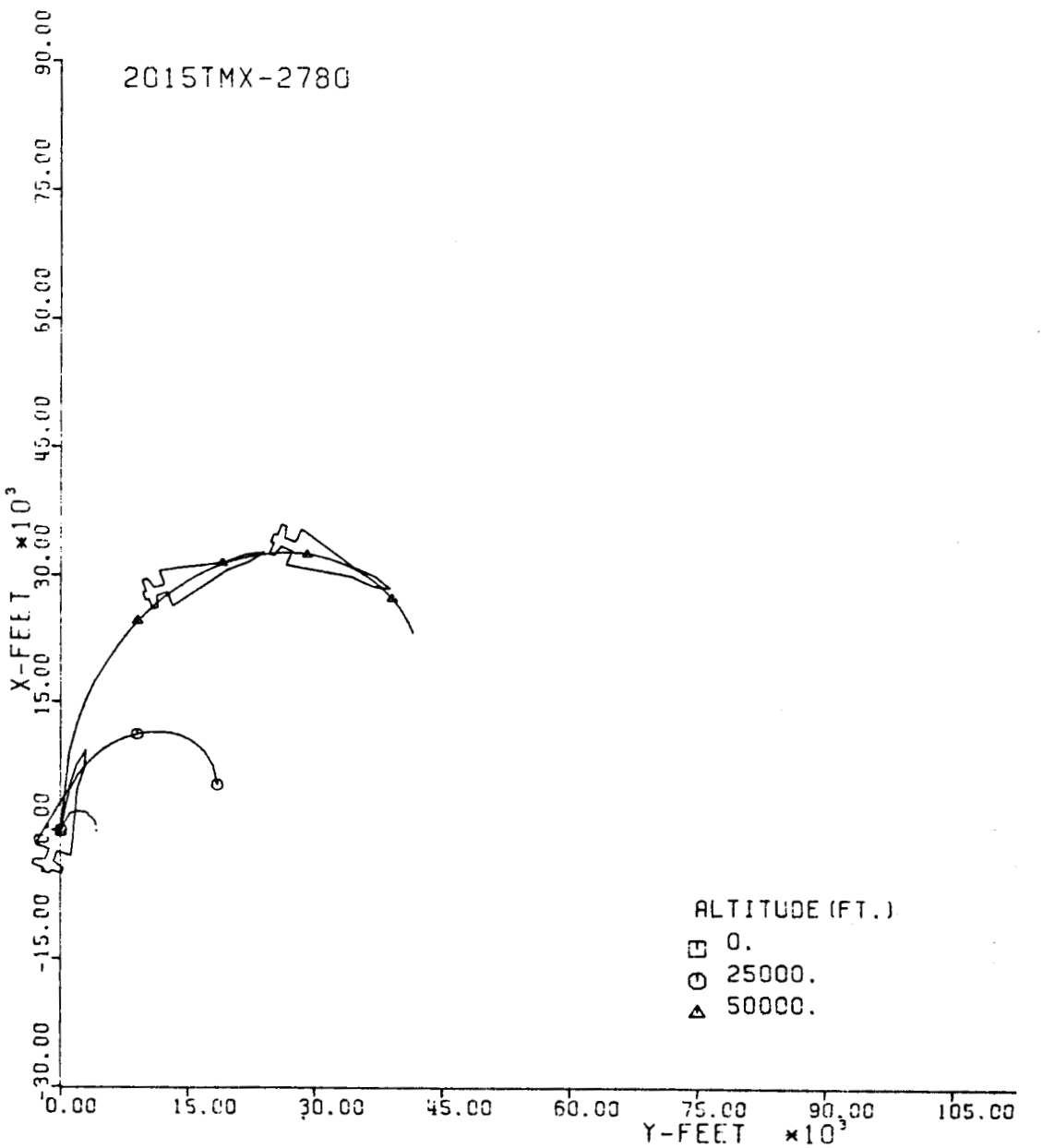

Fig. 160-III. Constant Altitude Flight Path, X vs. Y.

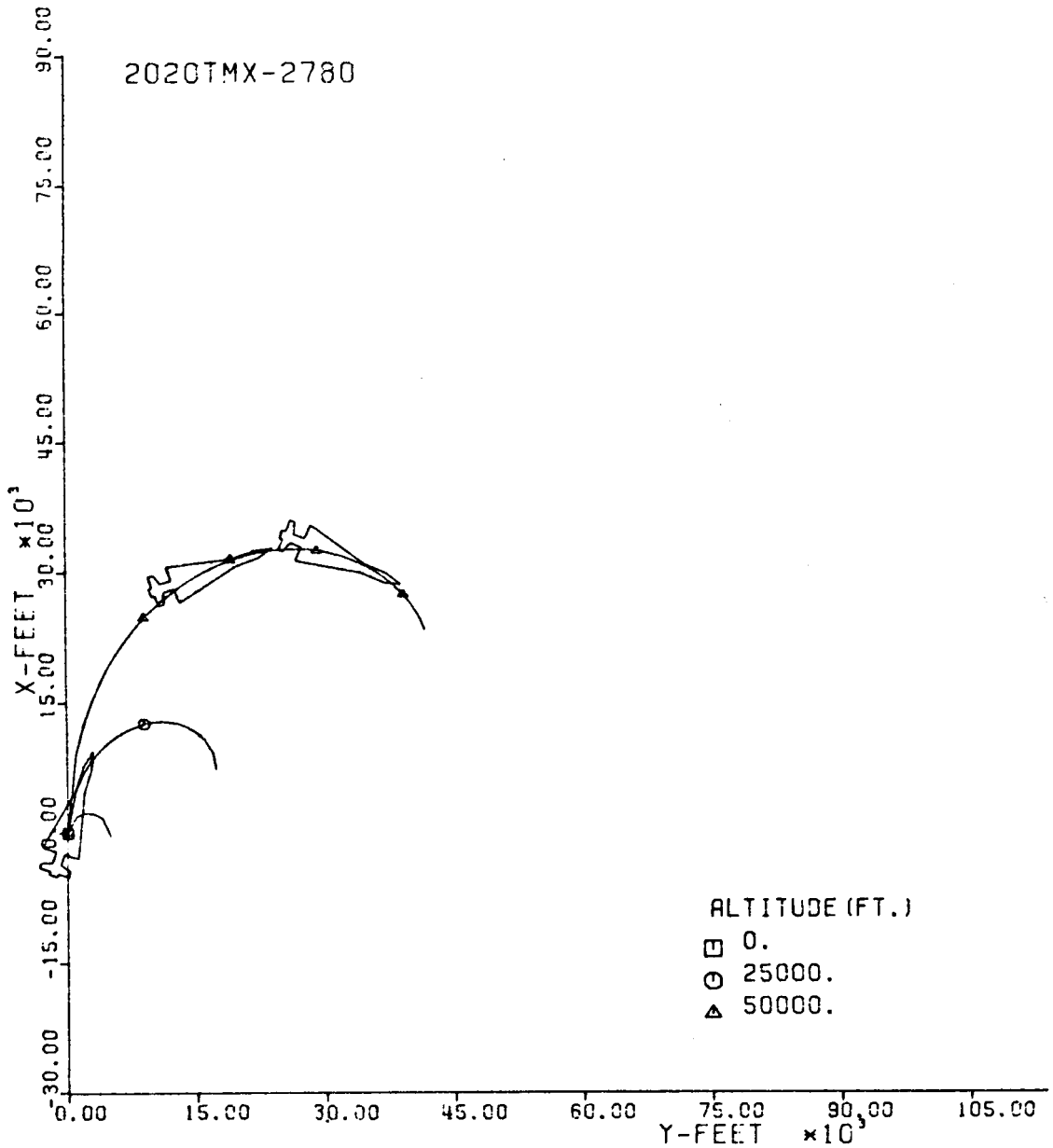

Fig. 161-III. Constant Altitude Flight Path, X vs. Y.

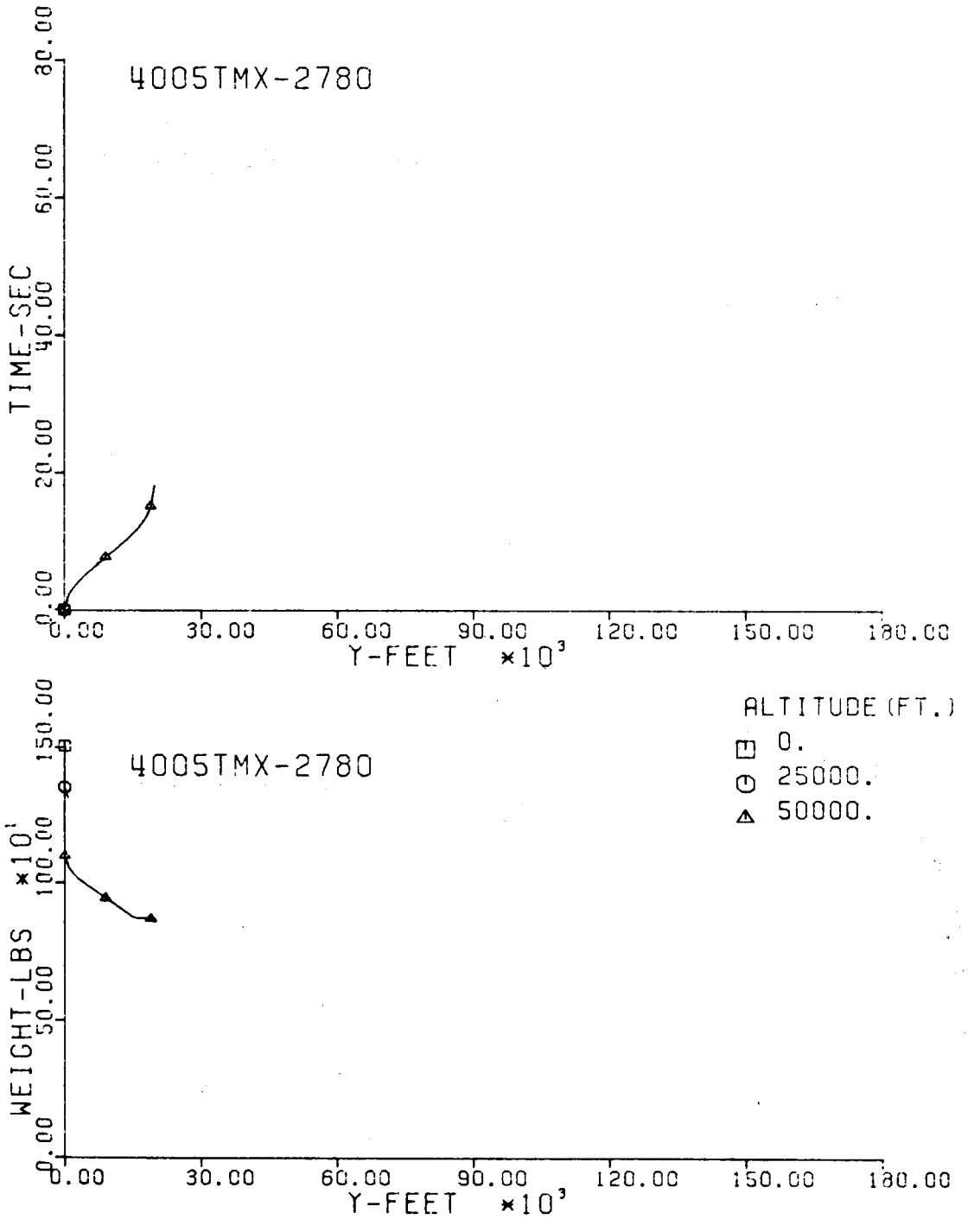

Fig. 162-III. Flight Time and Vehicle Weight vs. Downrange Distance, Y.

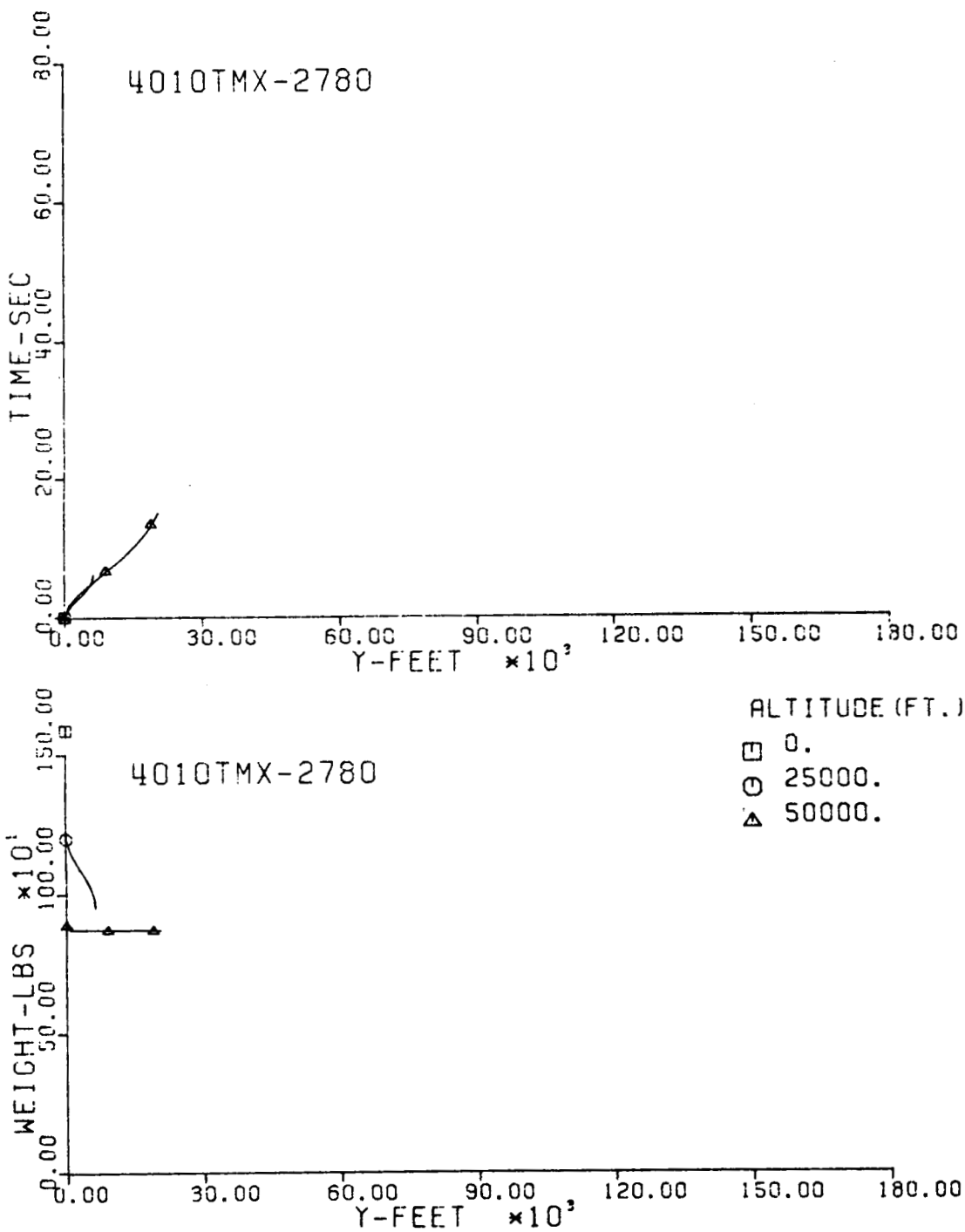

Fig. 163-III. Flight Time and Vehicle Weight vs. Downrange Distance, Y.

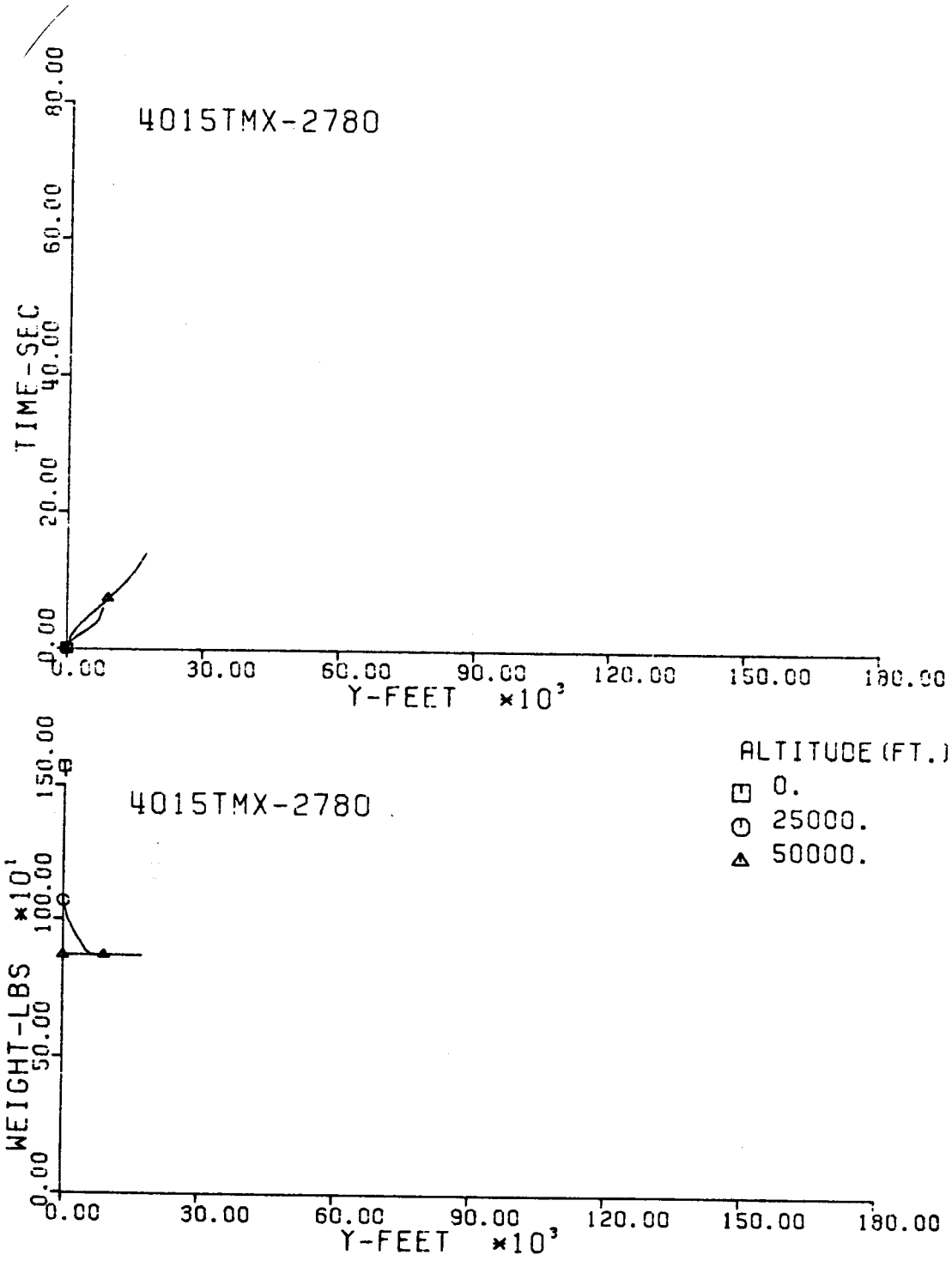

Fig. 164-III. Flight Time and Vehicle Weight vs. Downrange Distance, Y.

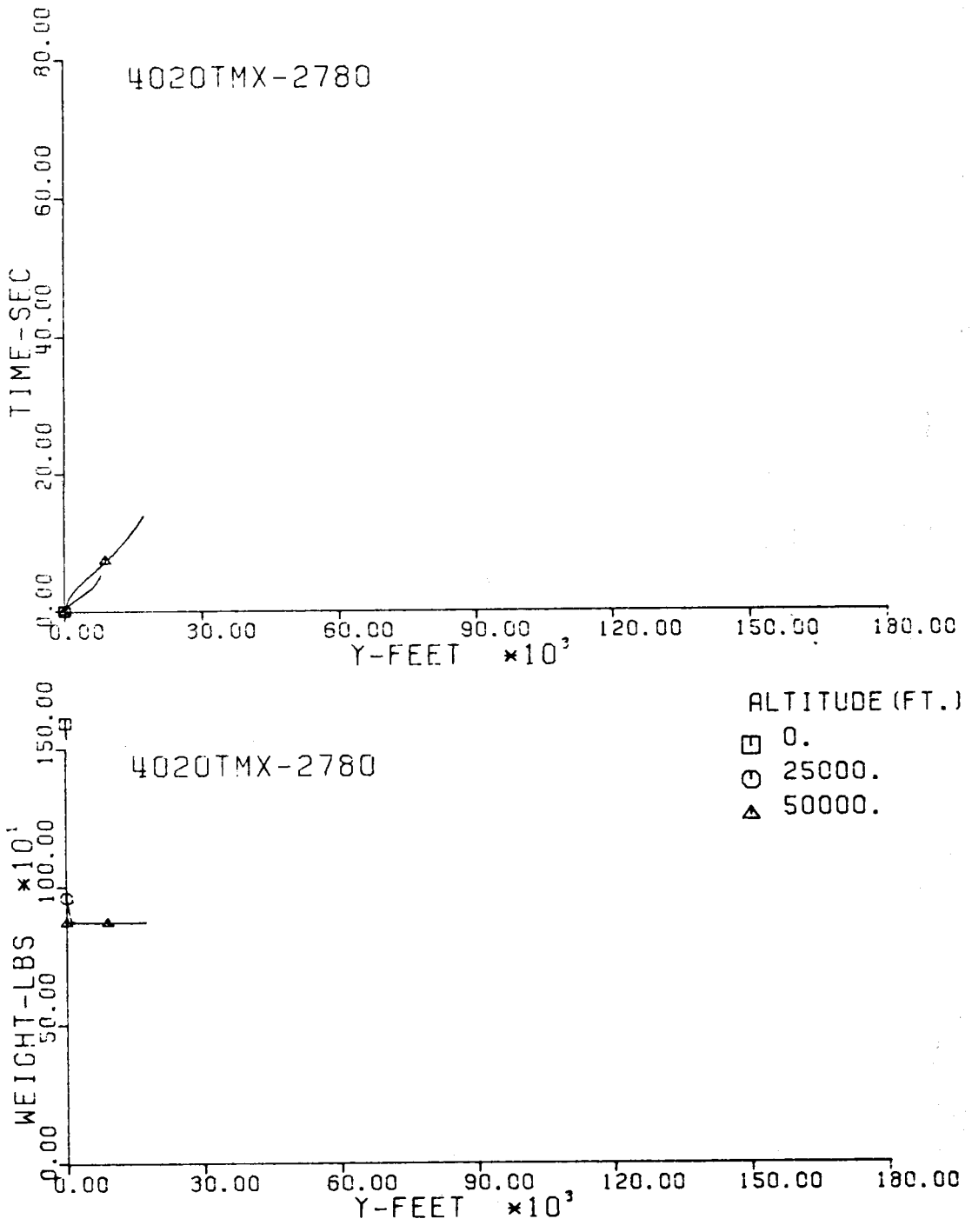

Fig. 165-III. Flight Time and Vehicle Weight vs. Downrange Distance, Y.

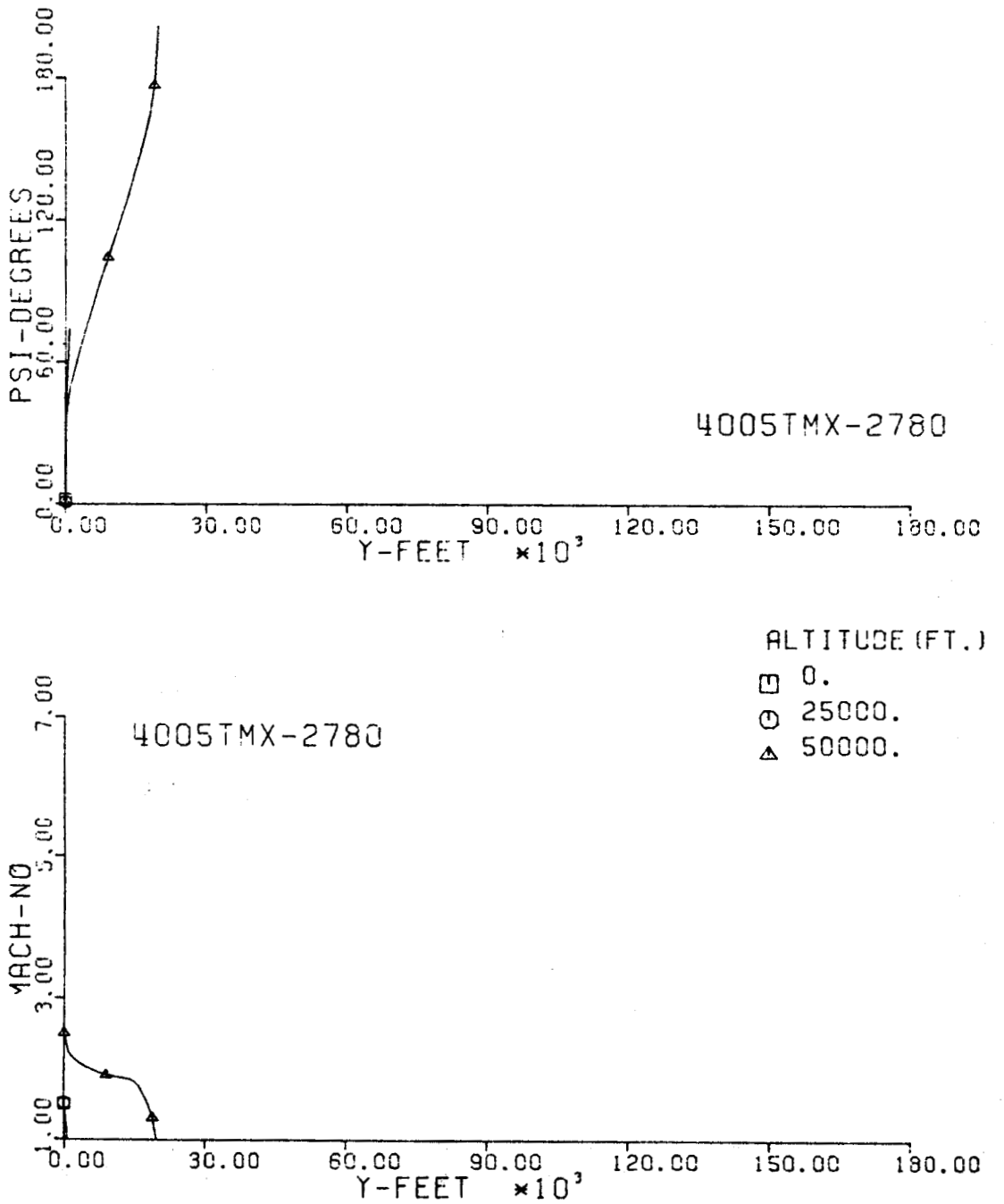

Fig. 166-III. Heading Angle and Mach No. vs. Downrange Distance, Y.

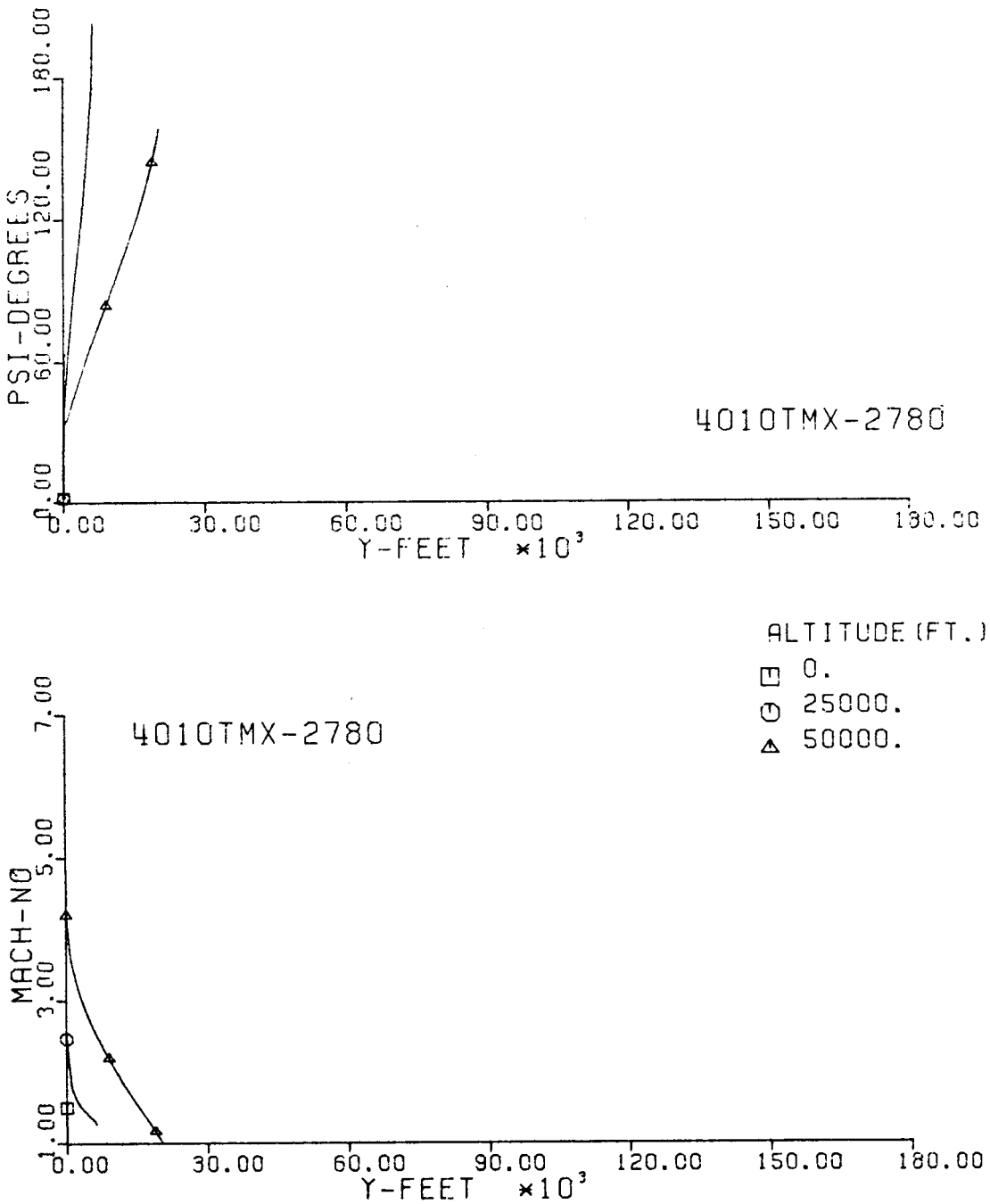

Fig. 167-III. Heading Angle and Mach No. vs. Downrange Distance, Y.

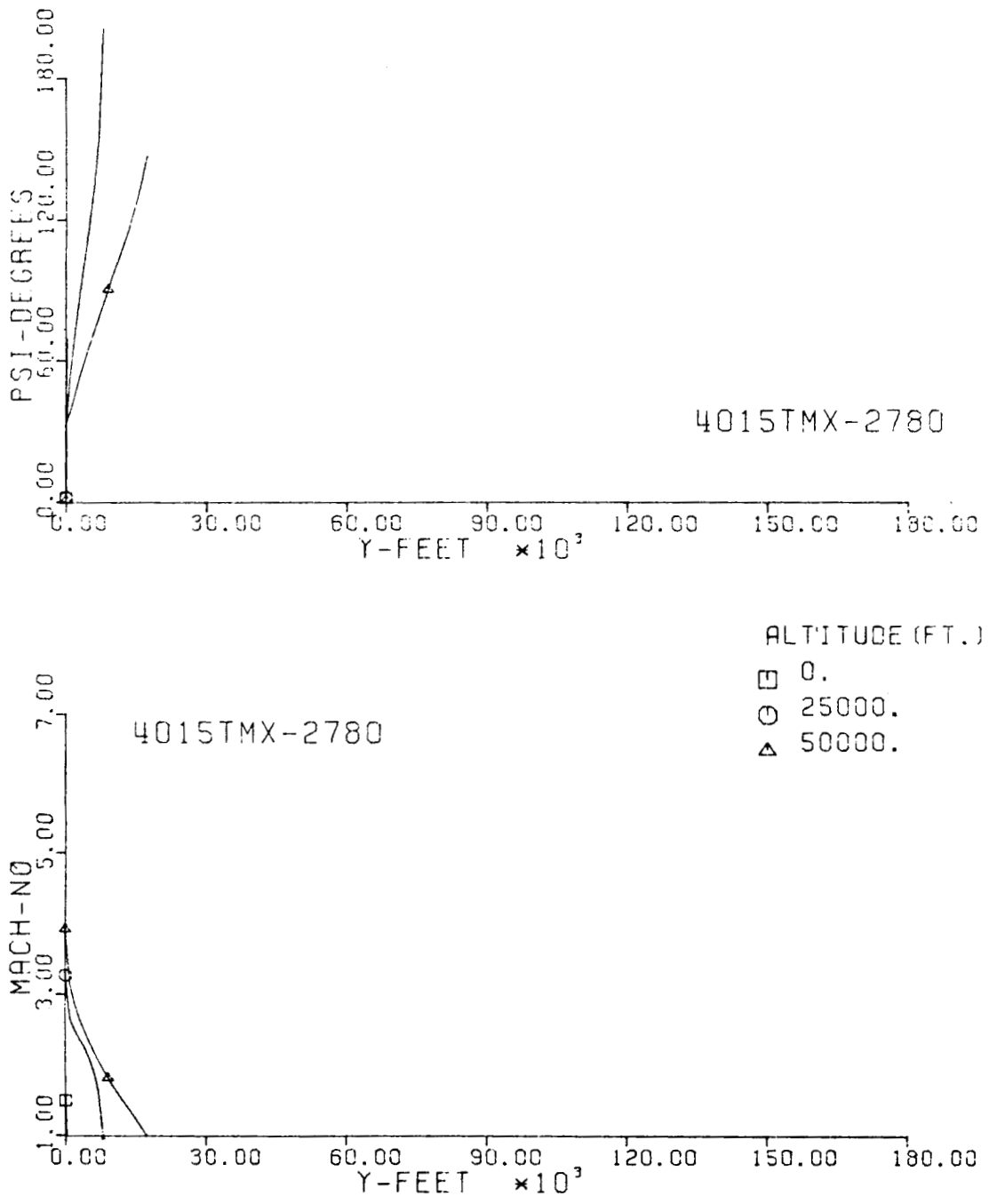

Fig. 168-III. Heading Angle and Mach No. vs. Downrange Distance, Y.

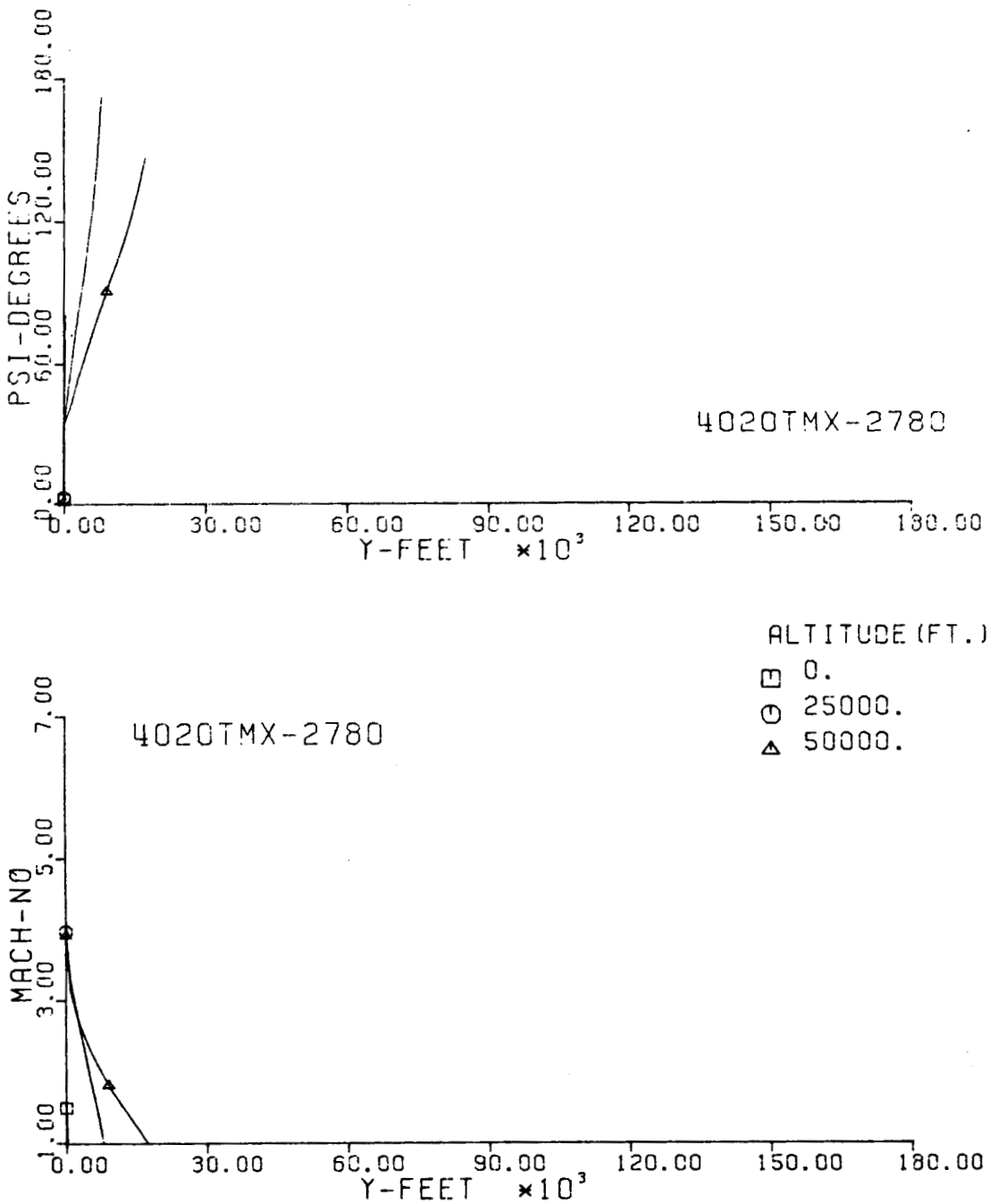

Fig. 169-III. Heading Angle and Mach No. vs. Downrange Distance, Y.

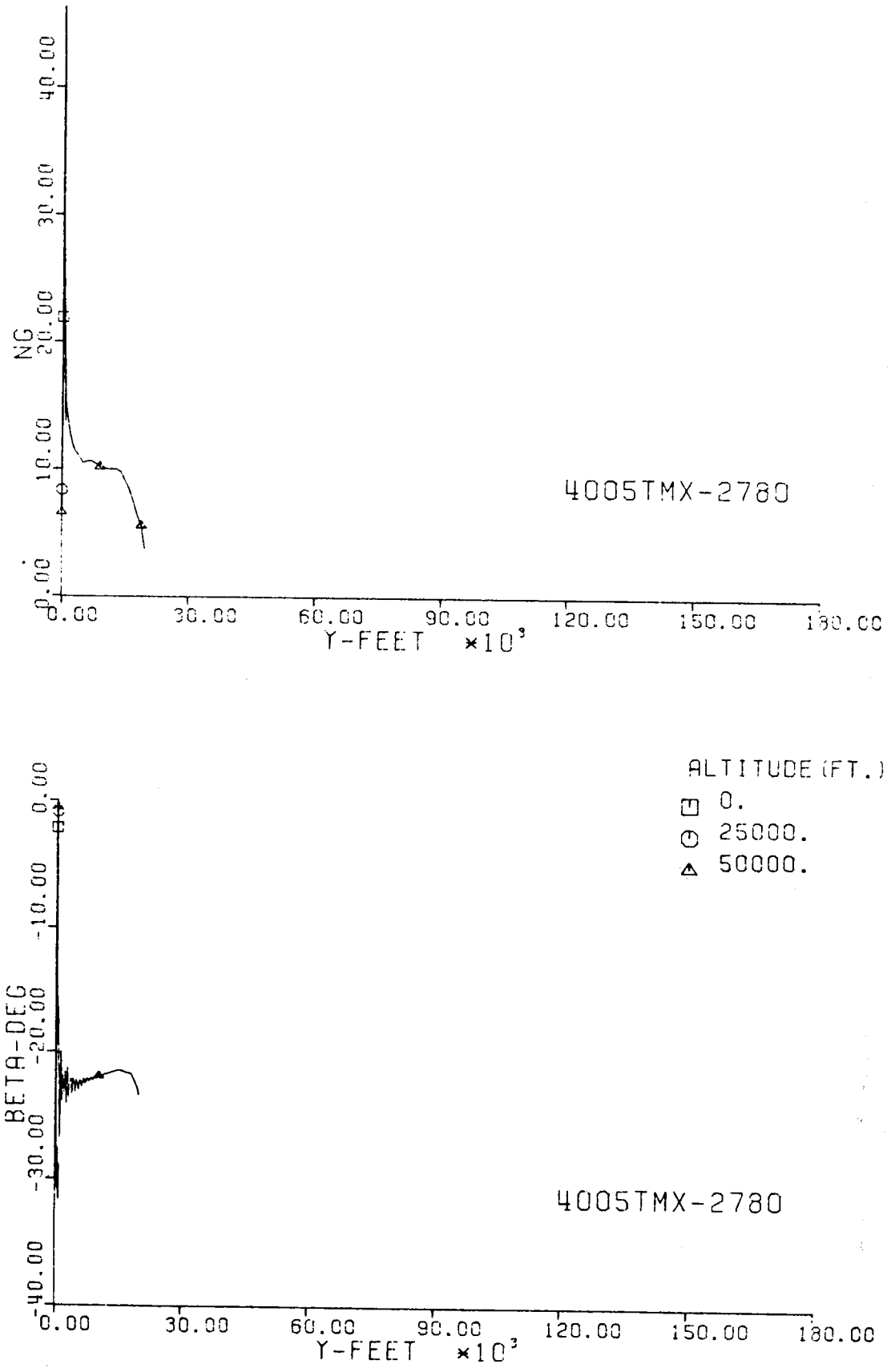

Fig. 170-III. Number of G's and Sideslip Angle vs. Downrange Distance, Y.

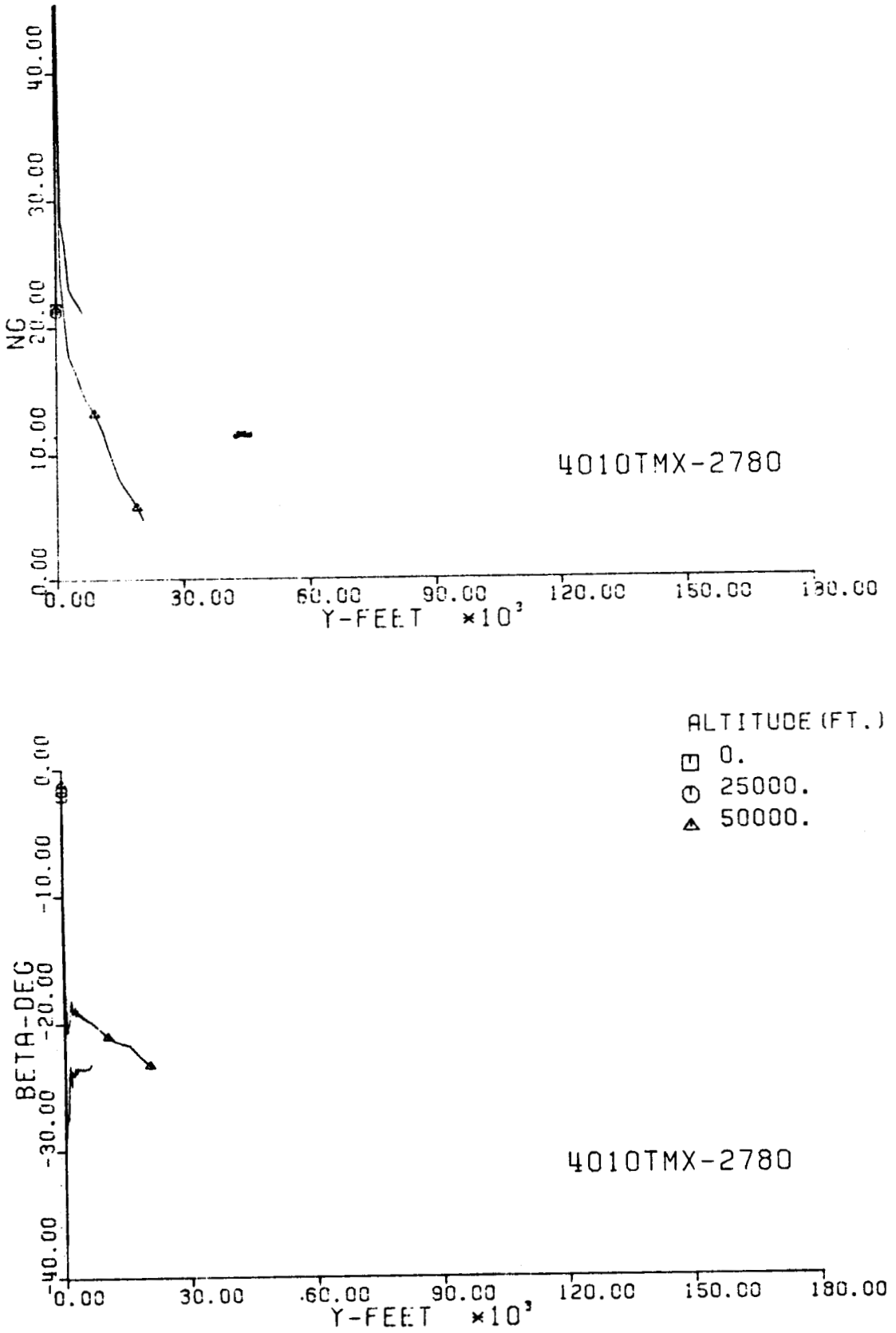

Fig. 171-III. Number of G's and Sideslip Angle vs. Downrange Distance, Y.

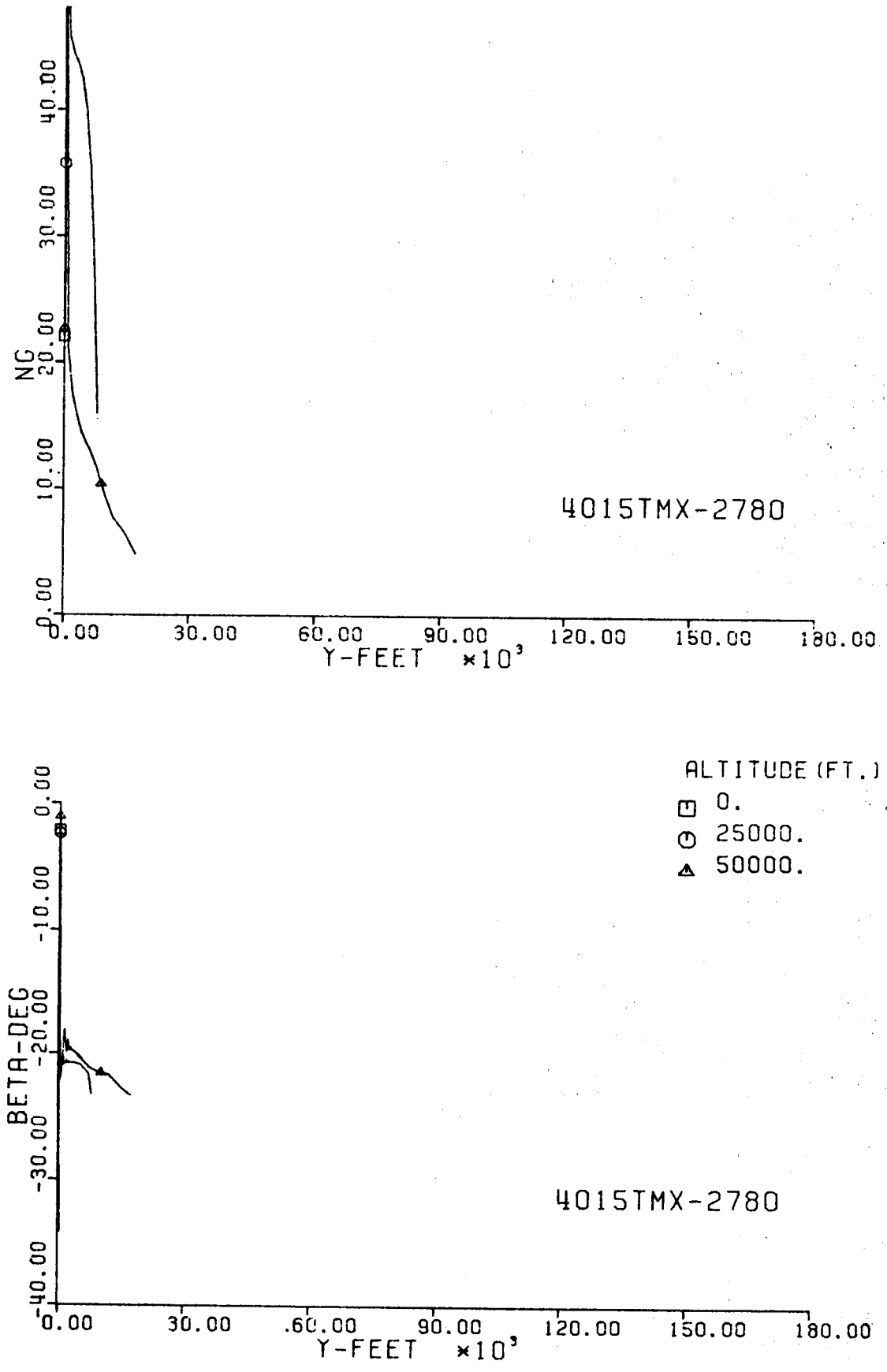

Fig. 172-III. Number of G's and Sideslip Angle vs. Downrange Distance, Y.

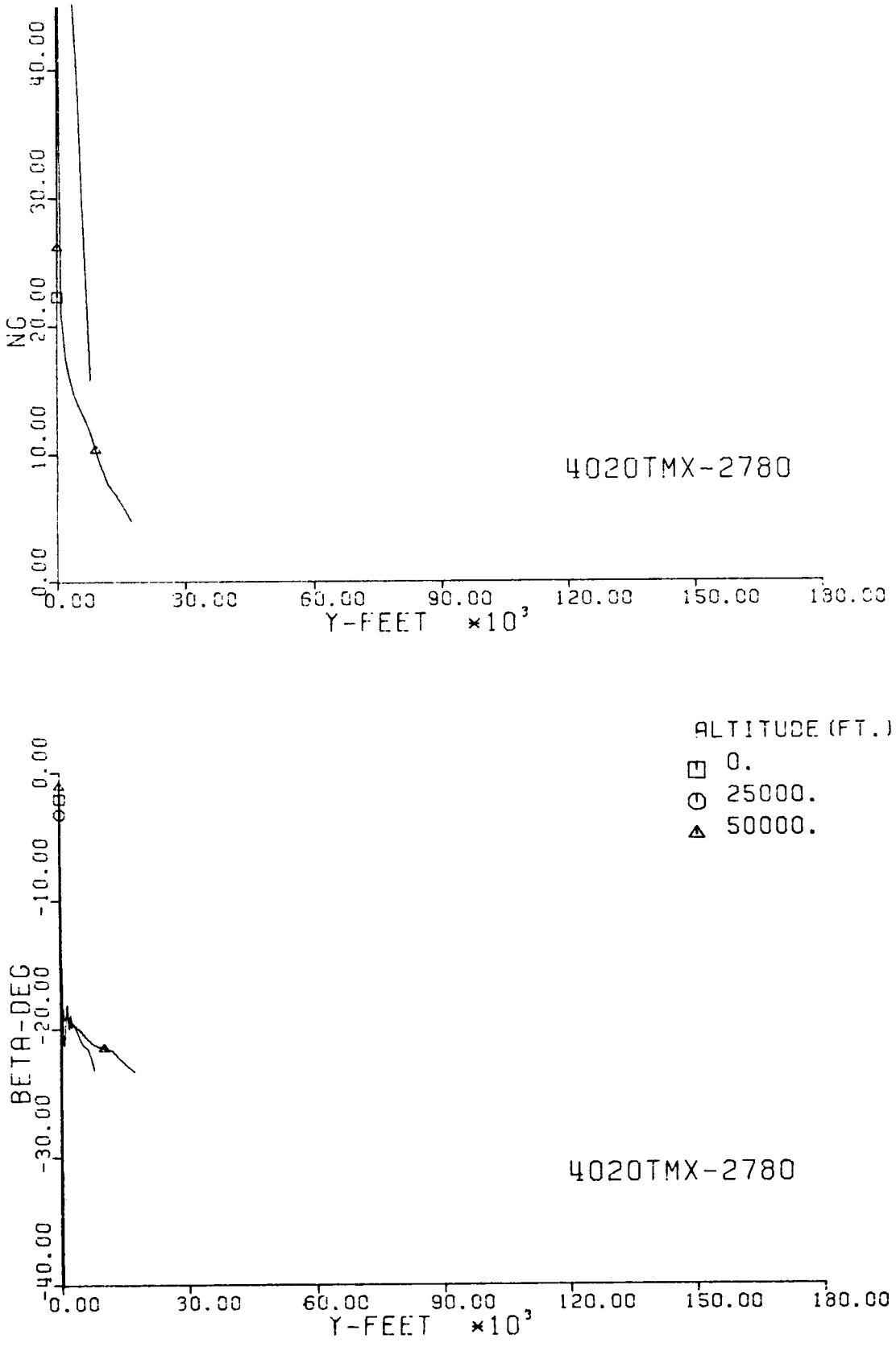

Fig. 173-III. Number of G's and Sideslip Angle vs. Downrange Distance, Y.

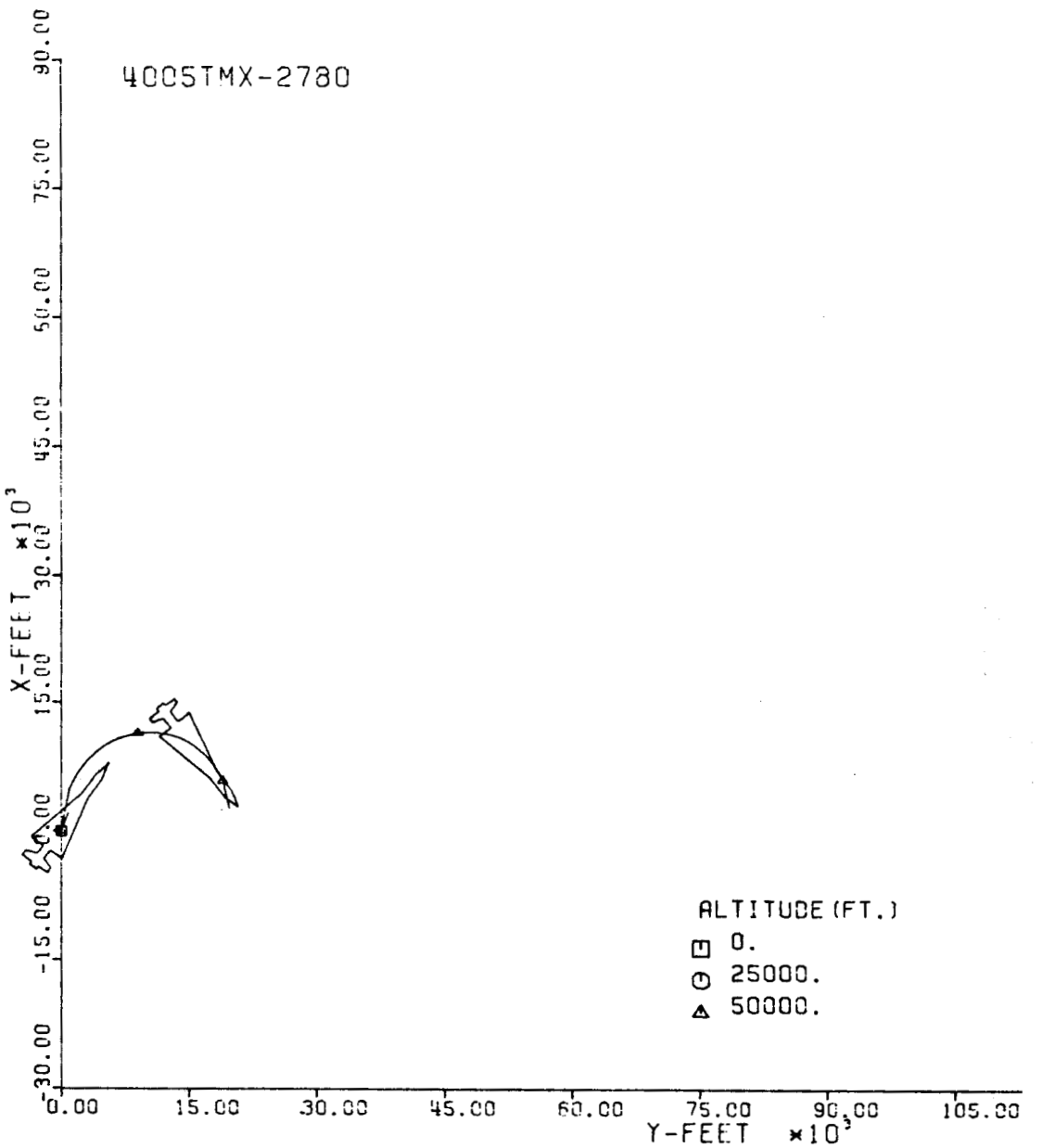

Fig. 174-III. Constant Altitude Flight Path, X vs. Y.

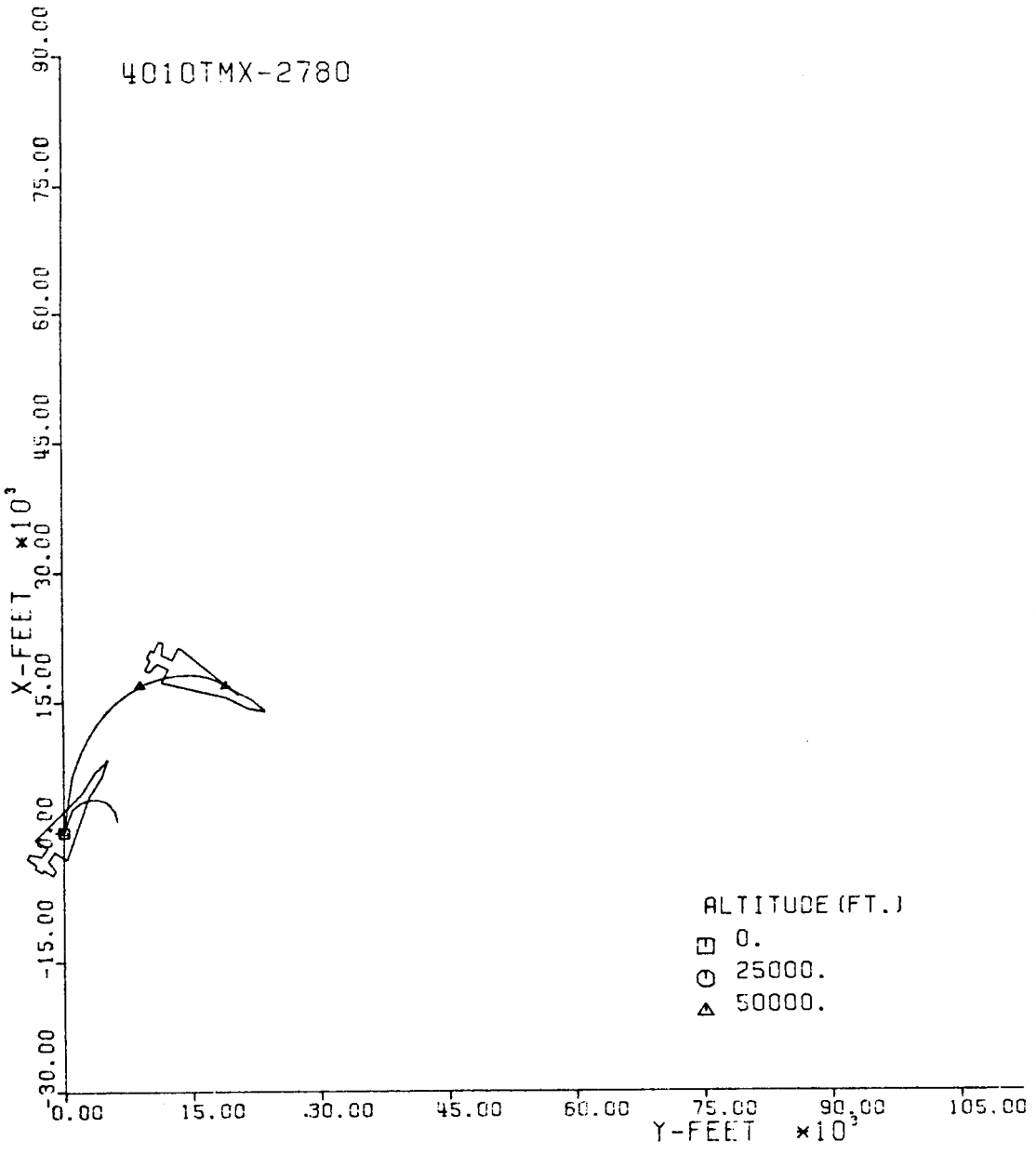

Fig. 175-III. Constant Altitude Flight Path, X vs. Y.

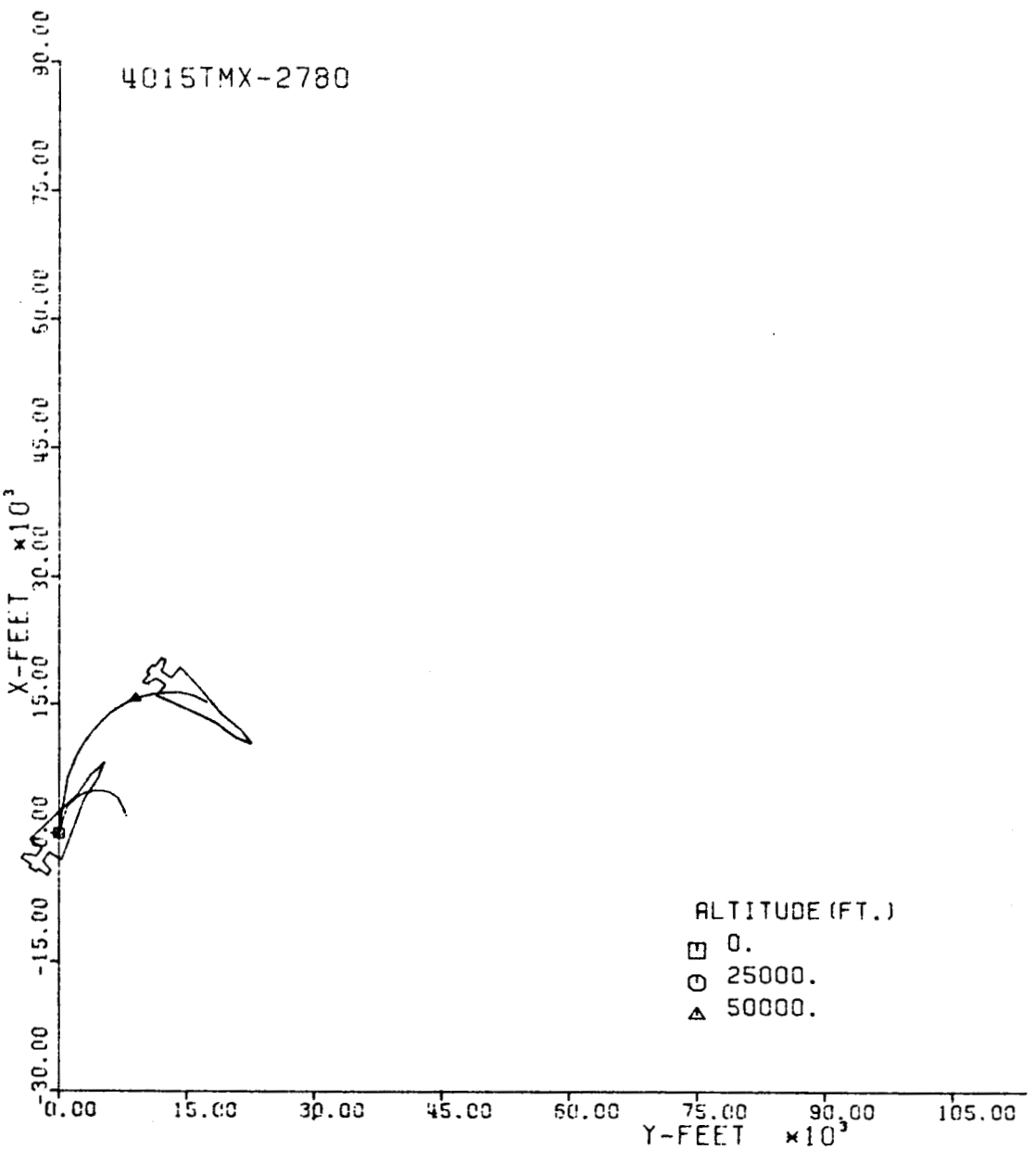

Fig. 176-III. Constant Altitude Flight Path, X vs. Y.

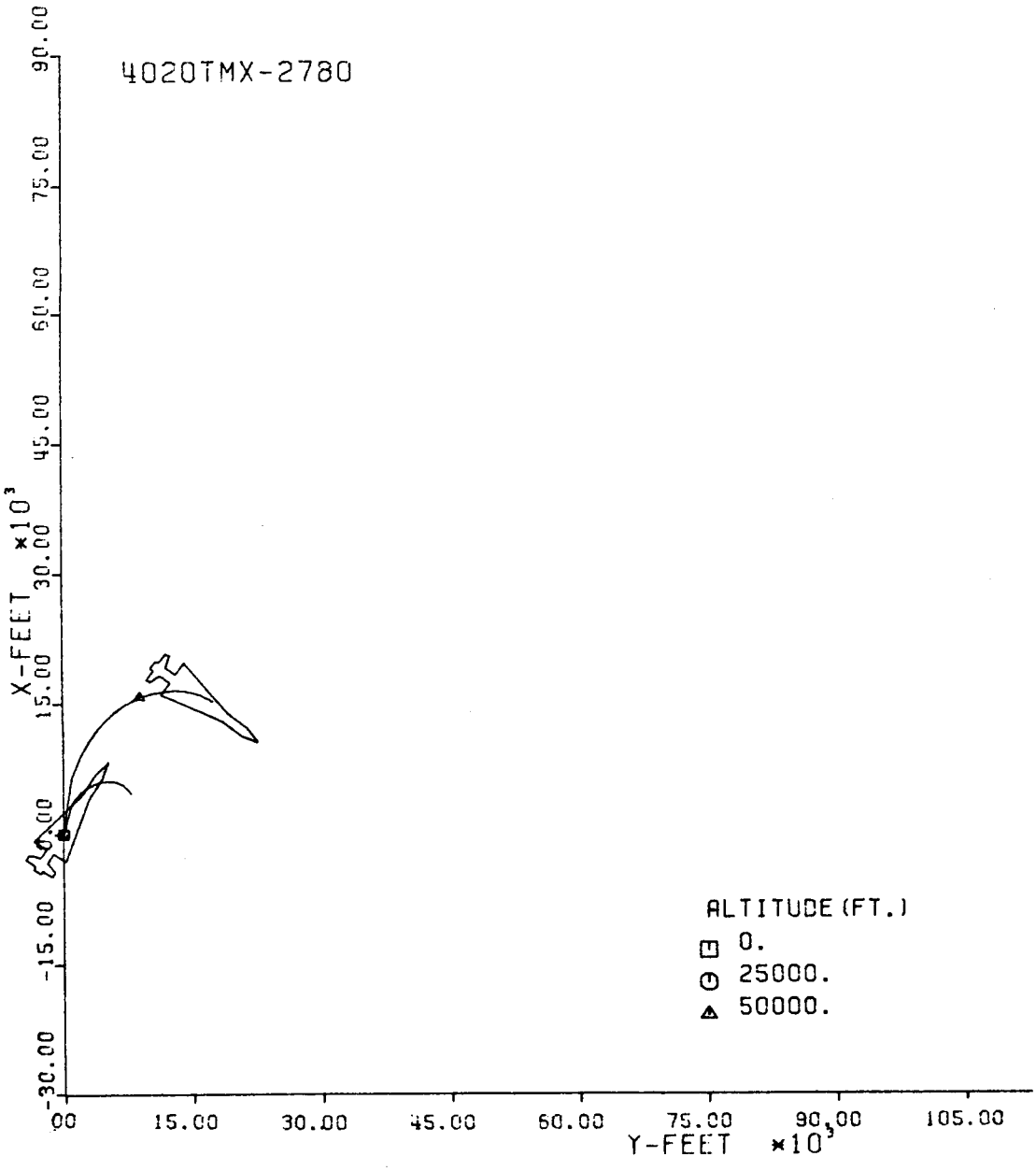

Fig. 177-III. Constant Altitude Flight Path, X vs. Y.

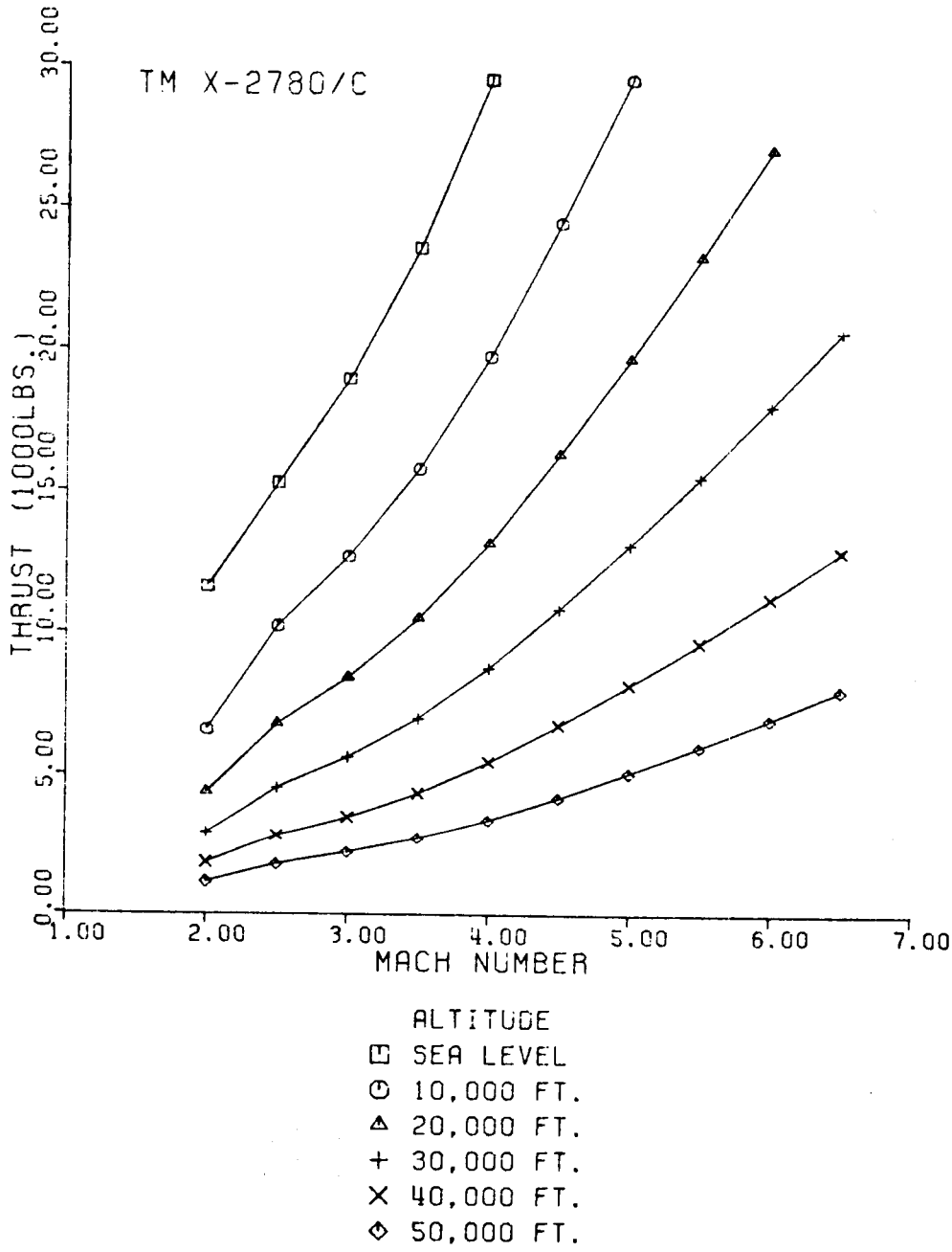

Fig. 178-I. Thrust vs. Terminal Mach No.

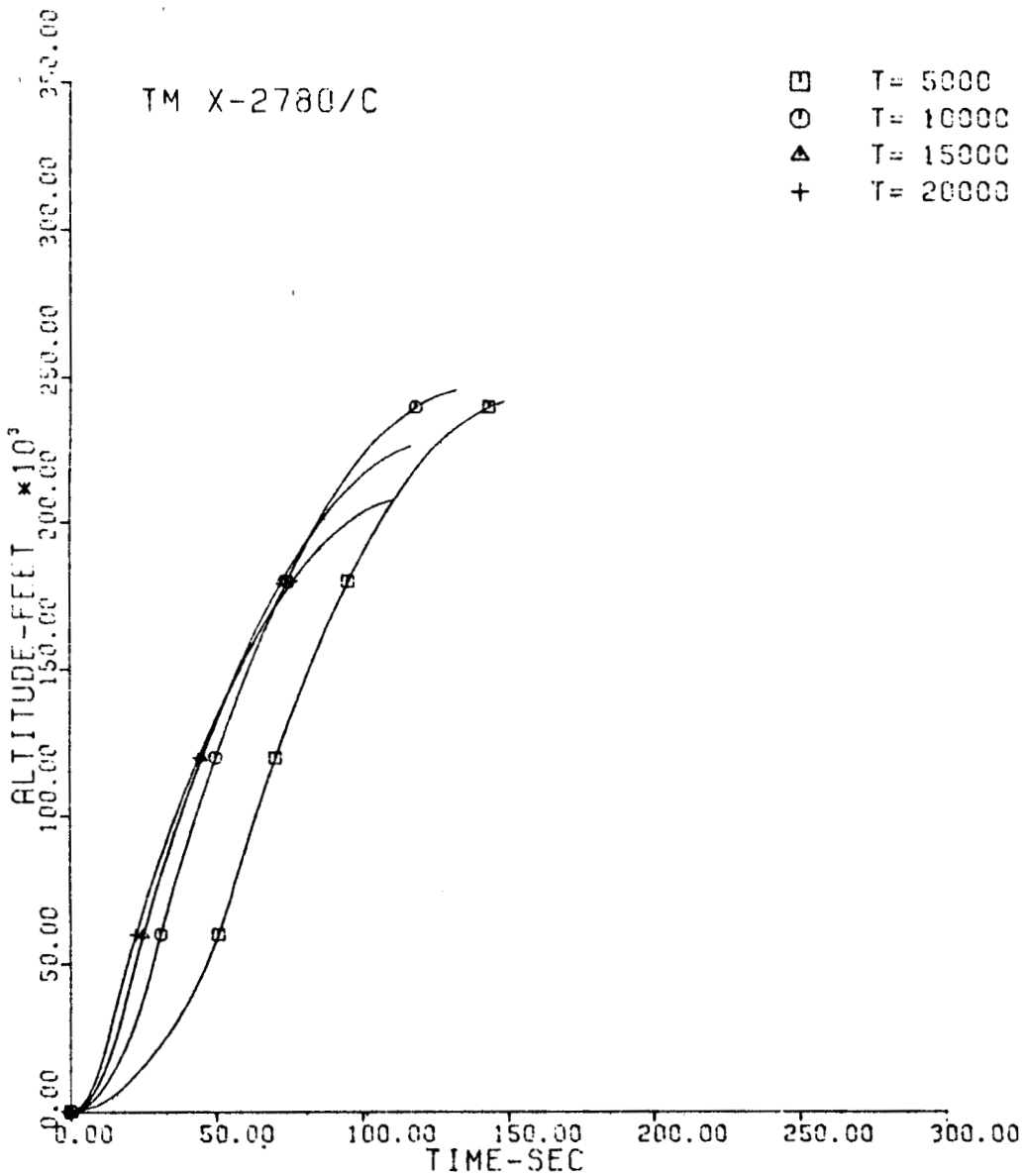

Fig. 179-II. Altitude vs. Flight Time.

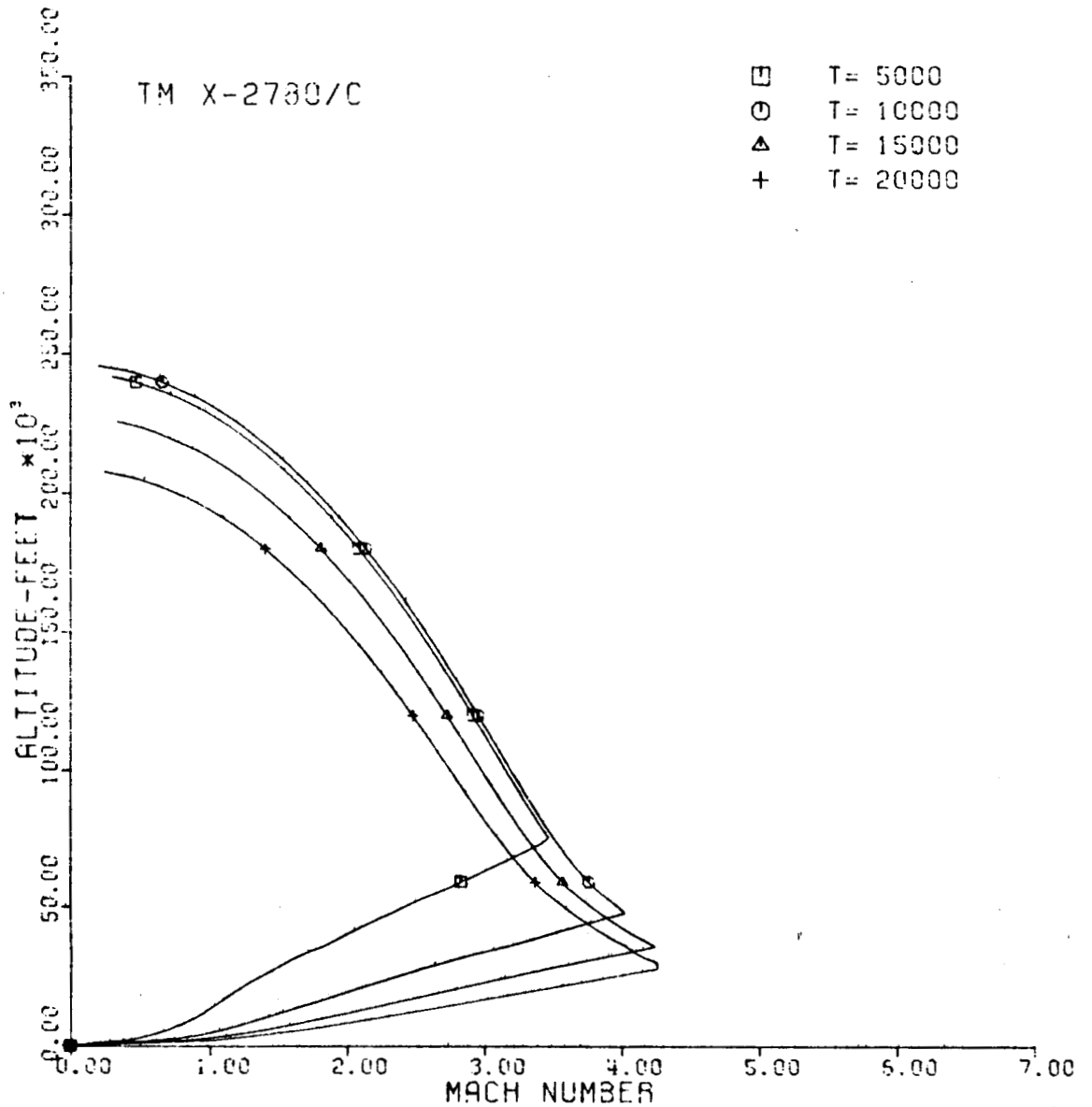

Fig. 180-II. Altitude vs. Mach No.

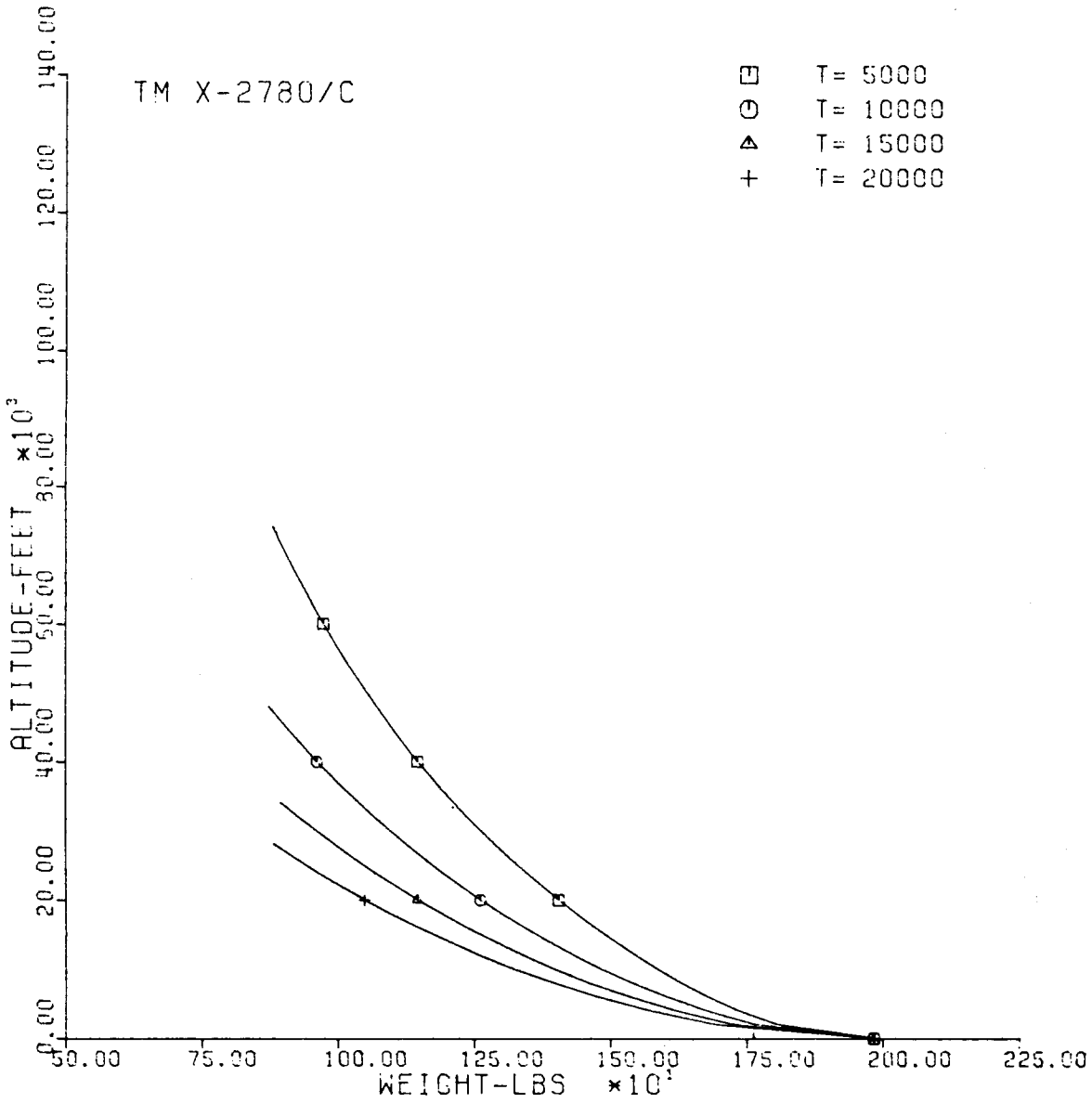

Fig. 181-II. Altitude vs. Vehicle Weight.

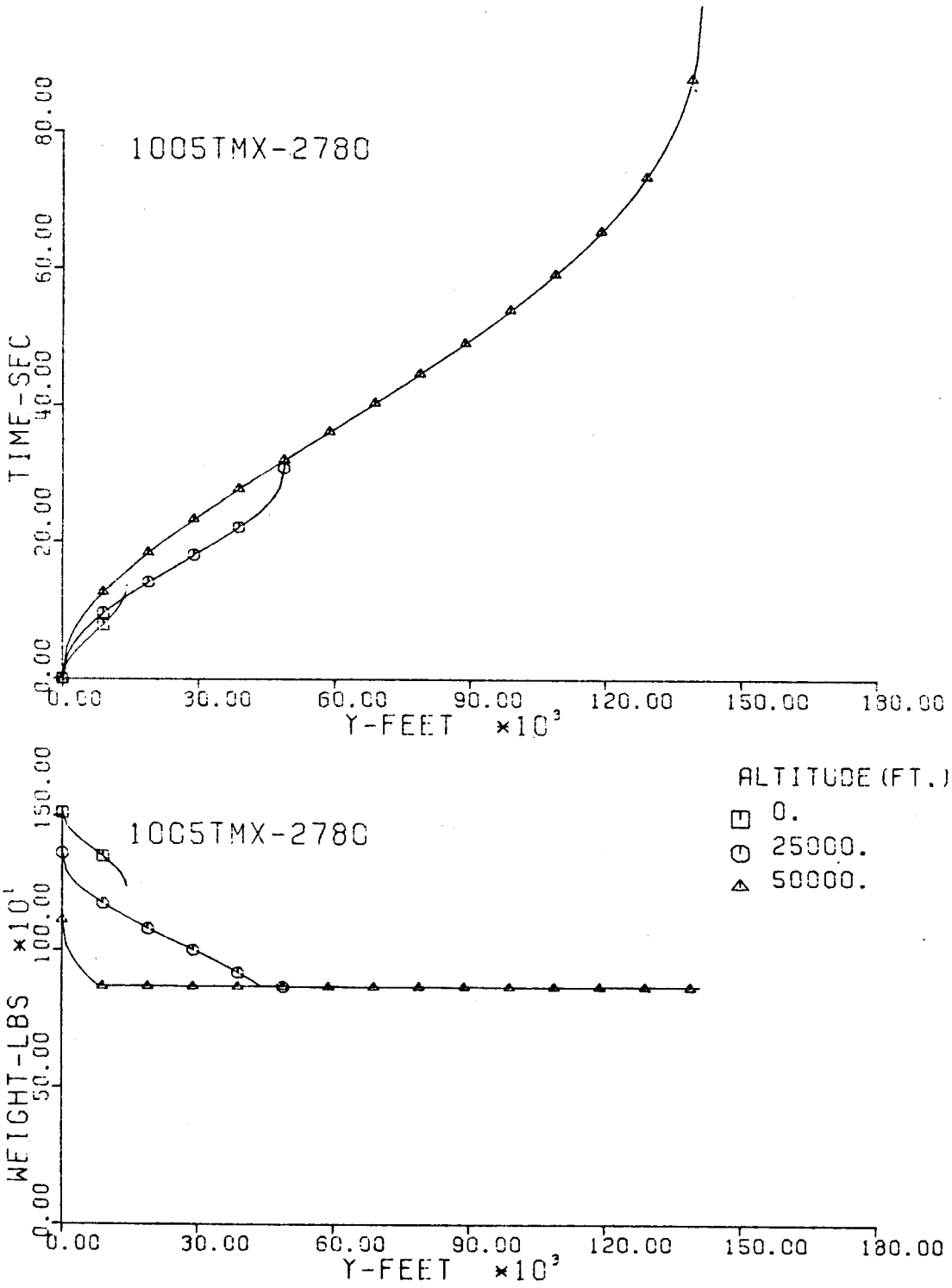

Fig. 182-III. Flight Time and Vehicle Weight vs. Downrange Distance, Y.

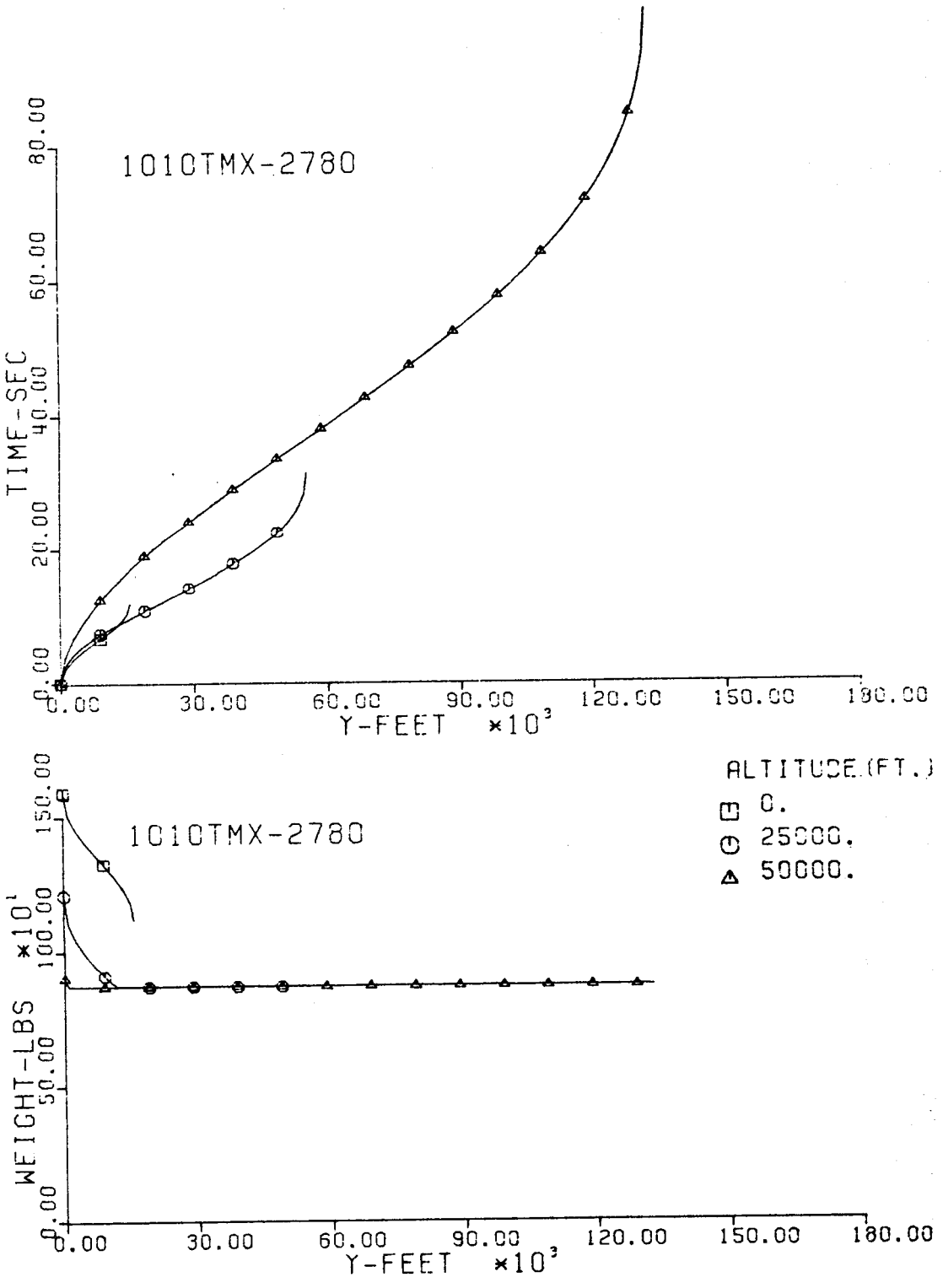

Fig. 183-III. Flight Time and Vehicle Weight vs. Downrange Distance, Y.

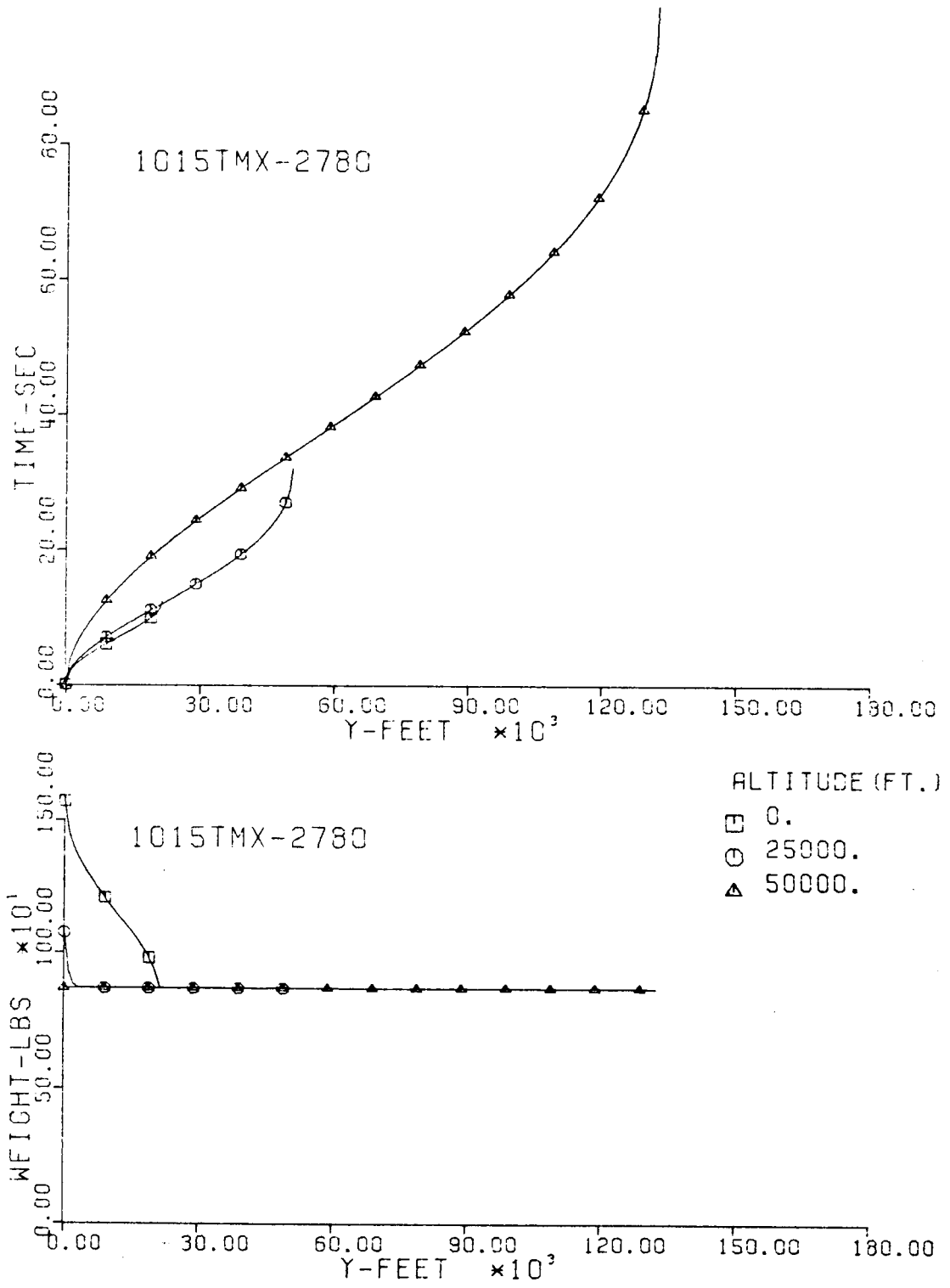

Fig. 184-III. Flight Time and Vehicle Weight vs. Downrange Distance, Y.

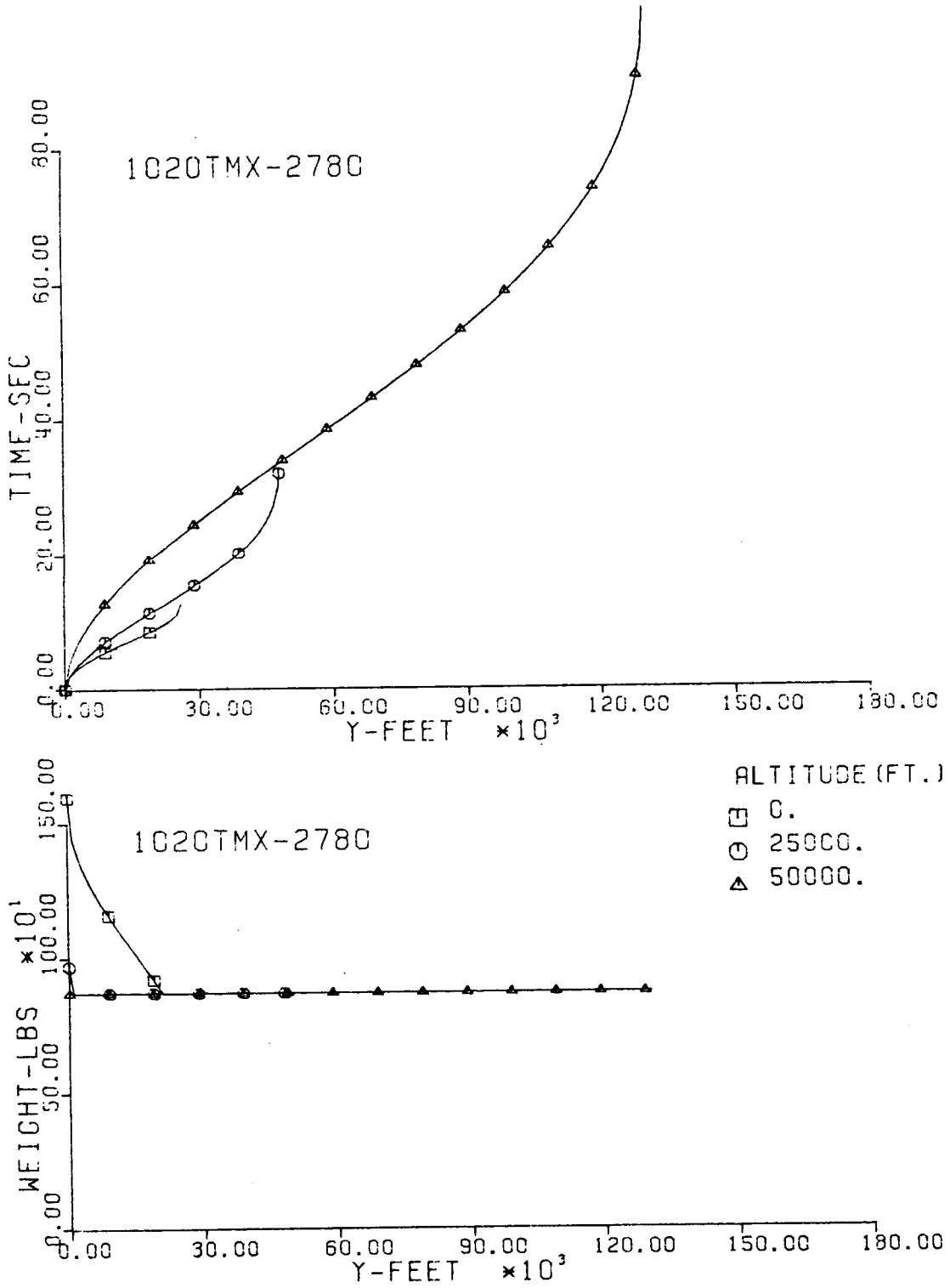

Fig. 185-III. Flight Time and Vehicle Weight vs. Downrange Distance, Y.

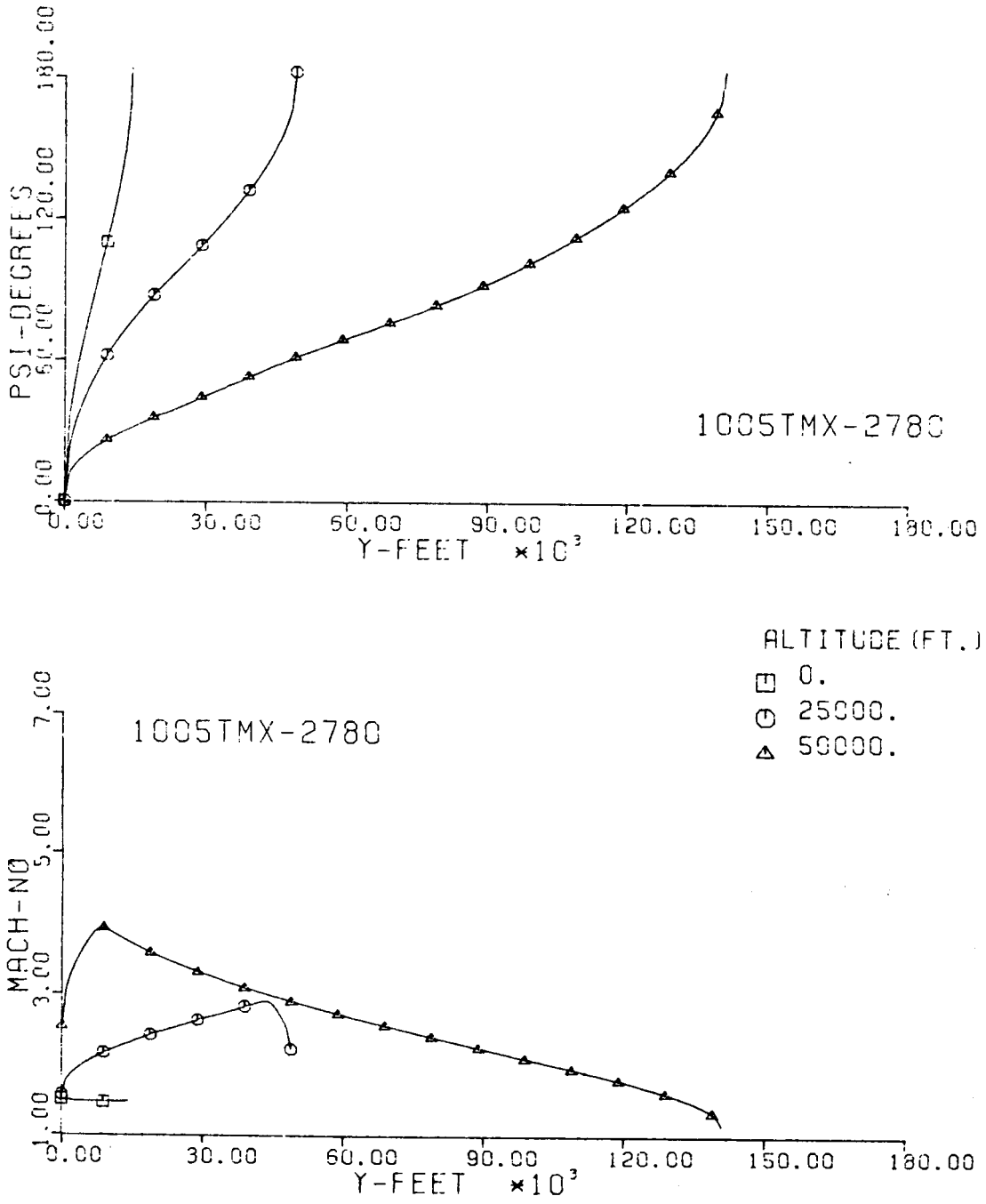

Fig. 186-III. Heading Angle and Mach No. vs. Downrange Distance, Y.

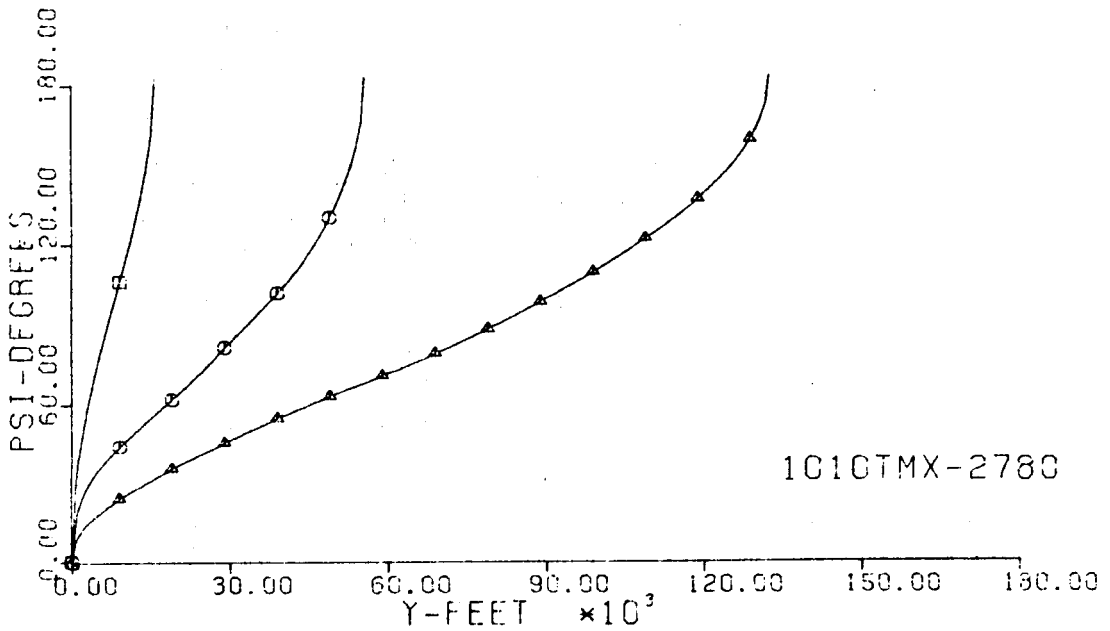

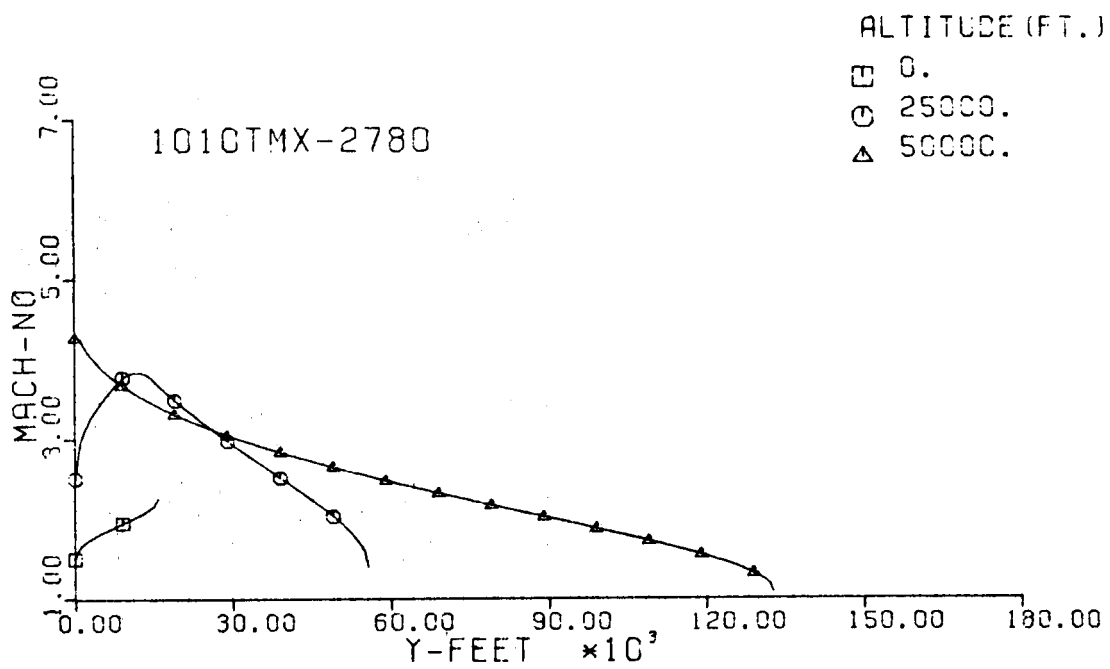

Fig. 187-III. Heading Angle and Mach No. vs. Downrange Distance, Y.

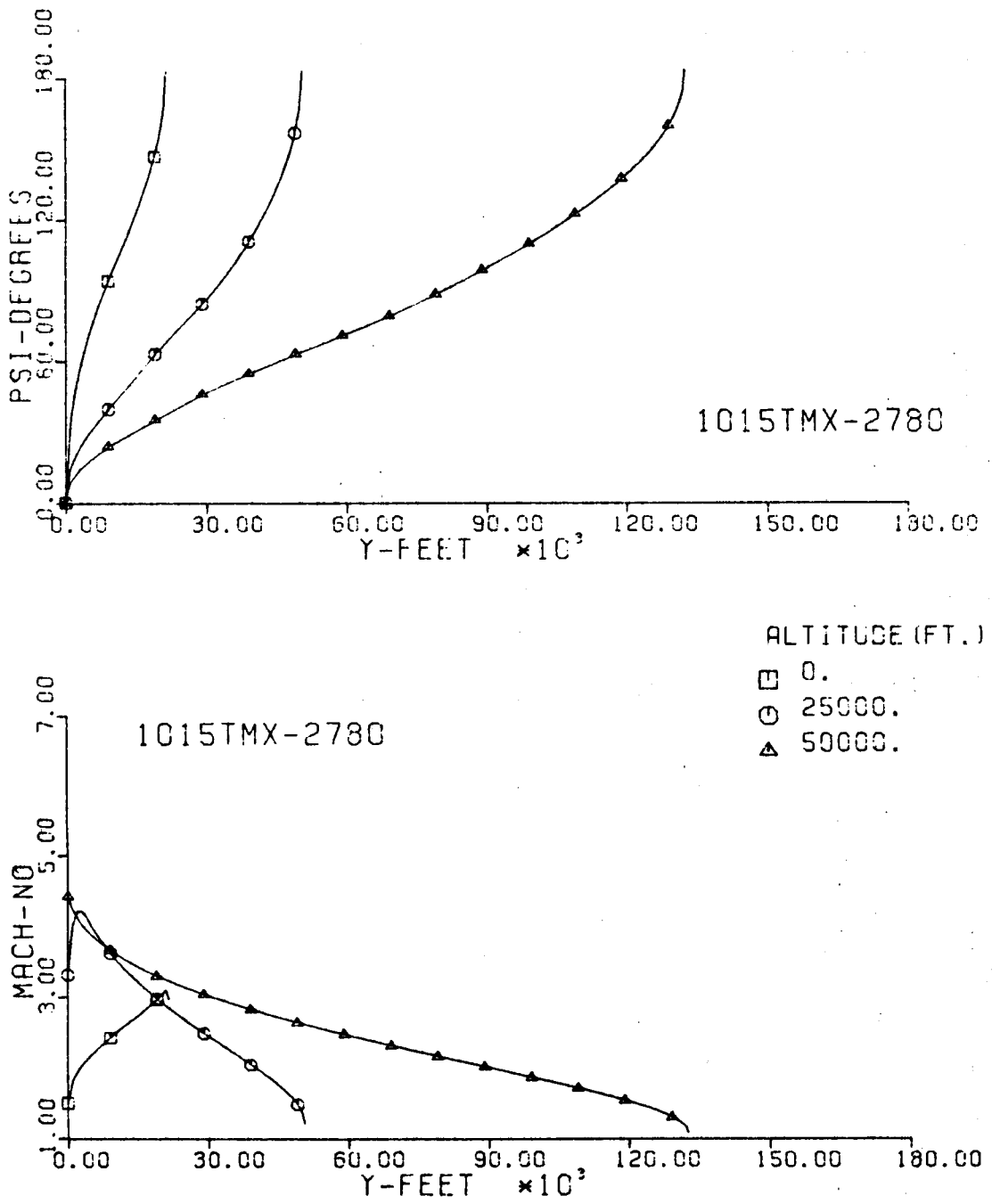

Fig. 188-III. Heading Angle and Mach No. vs. Downrange Distance, Y.

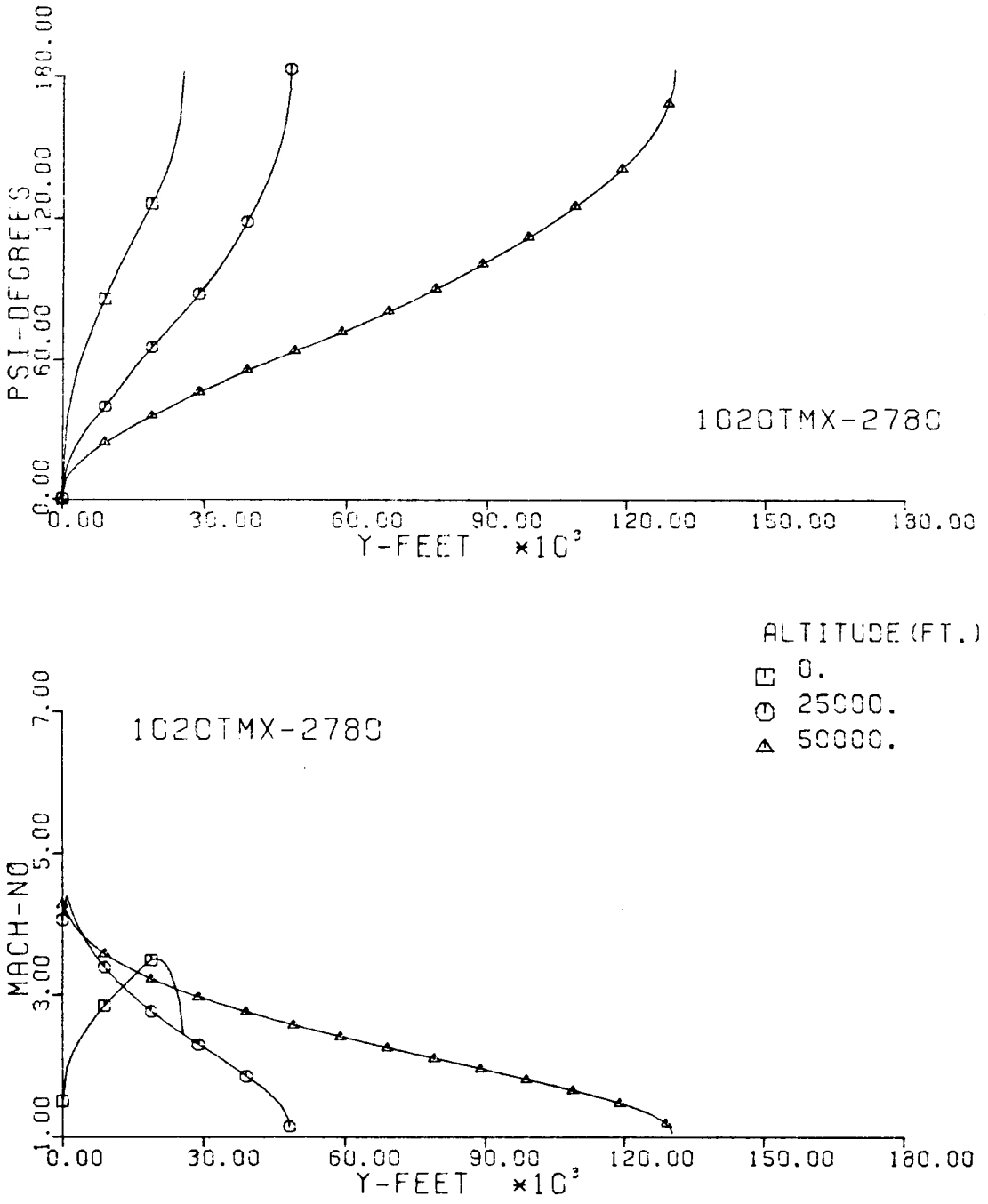

Fig. 189-III. Heading Angle and Mach No. vs. Downrange Distance, Y.

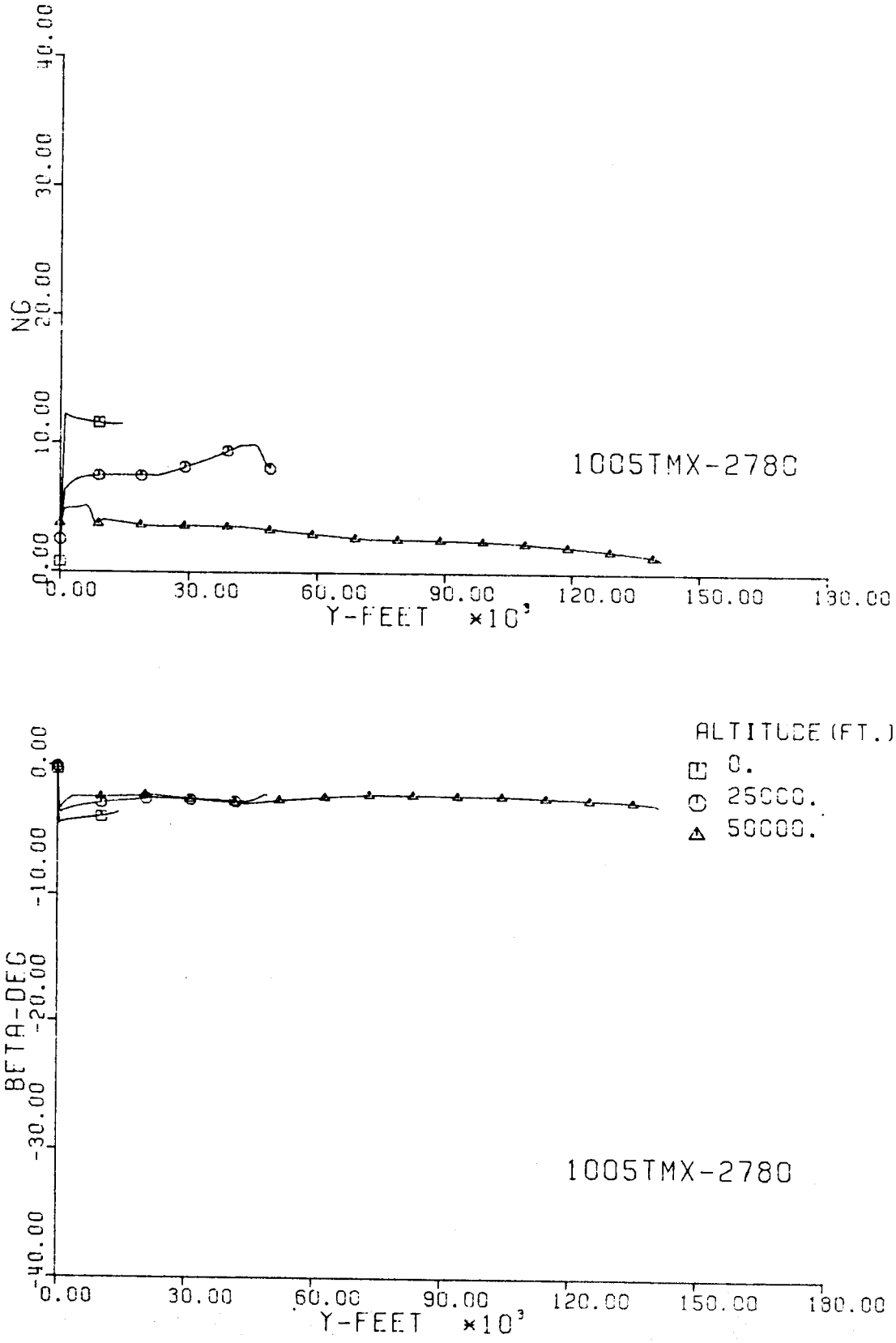

Fig. 190-III. Number of G's and Sideslip Angle vs. Downrange Distance, Y.

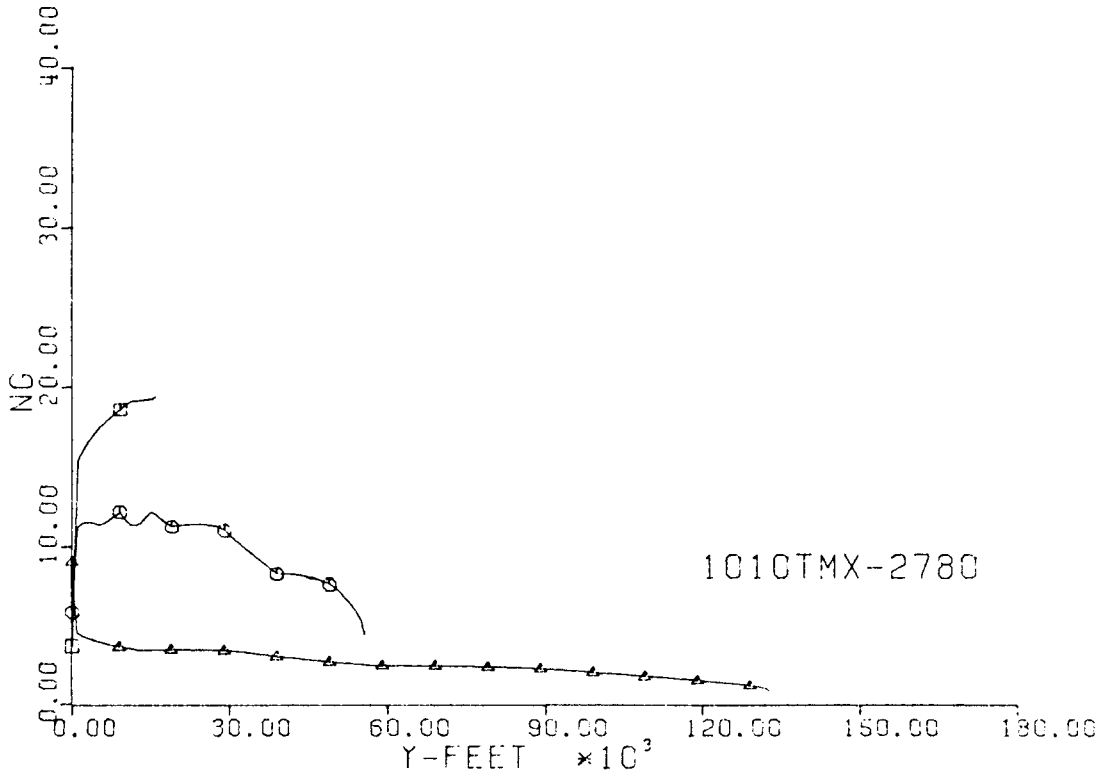

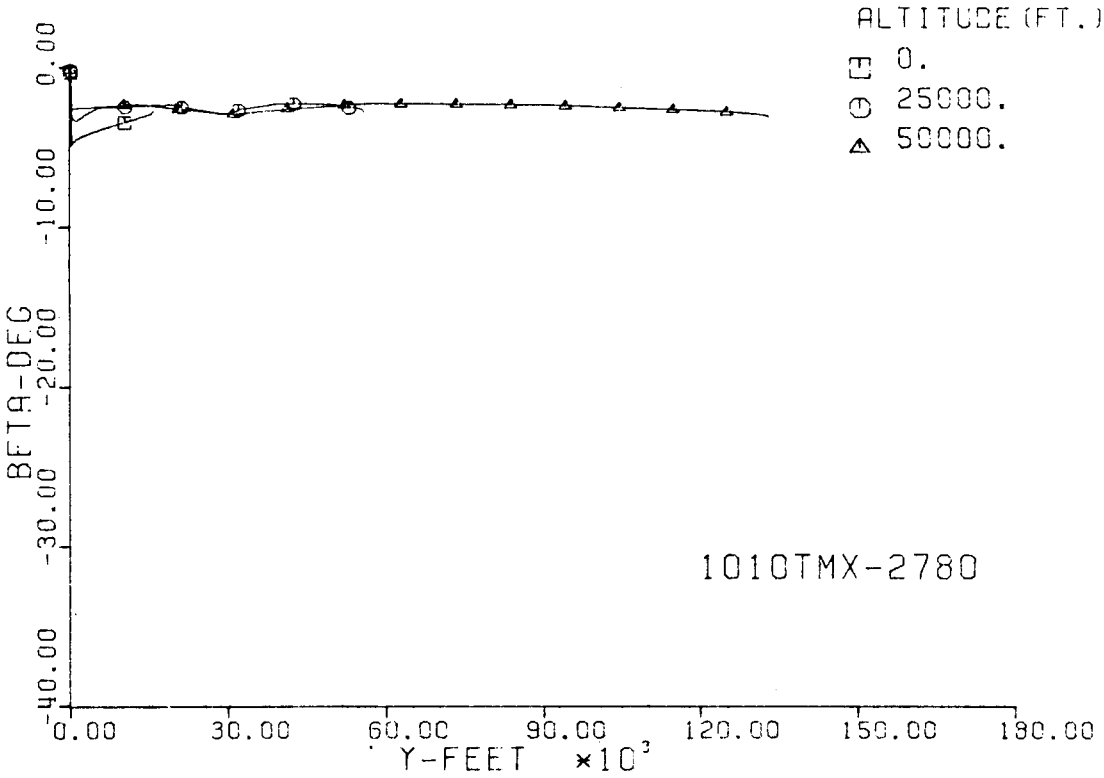

Fig. 191-III. Number of G's and Sideslip Angle vs. Downrange Distance, Y.

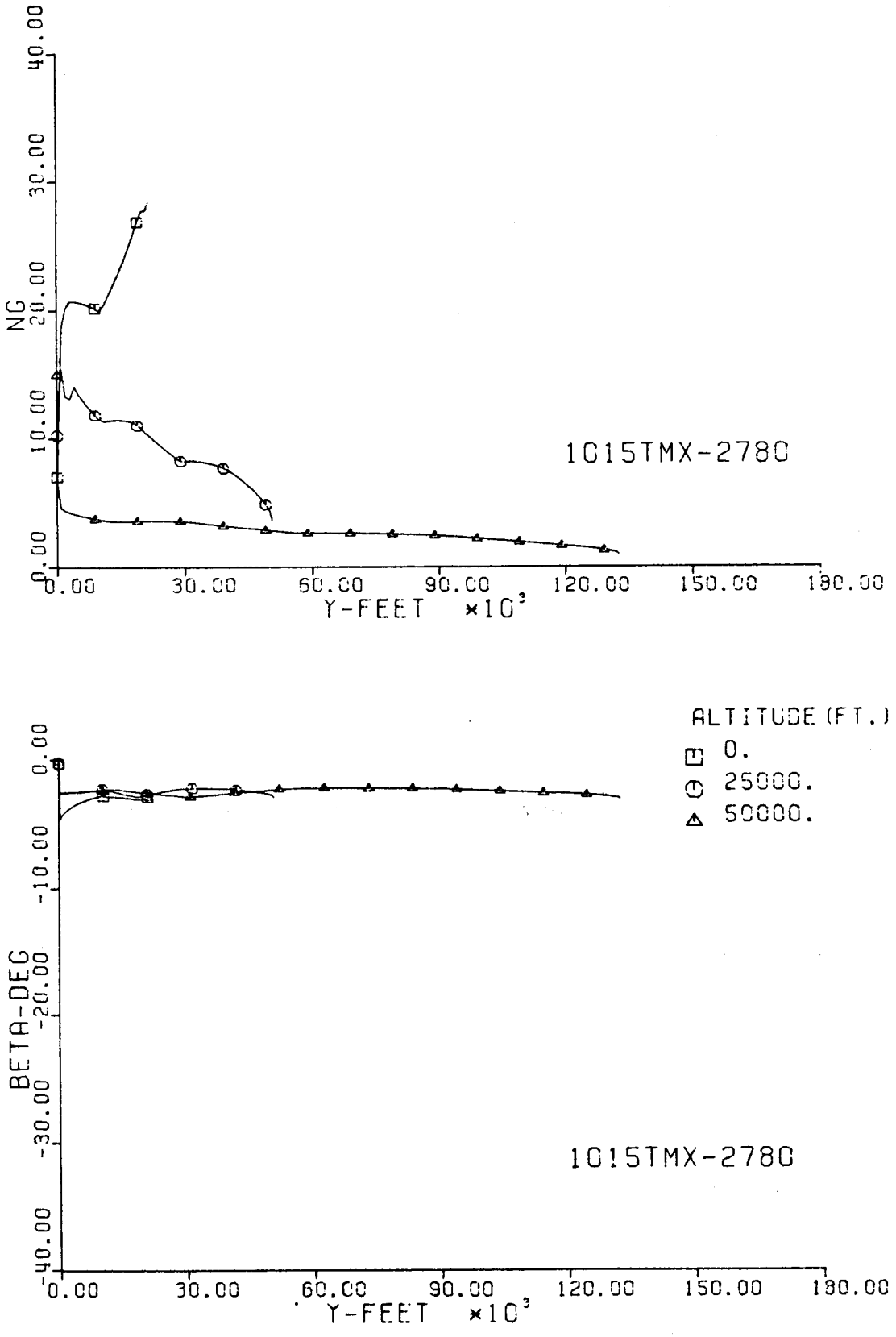

Fig. 192-III. Number of G's and Sideslip Angle vs. Downrange Distance, Y.

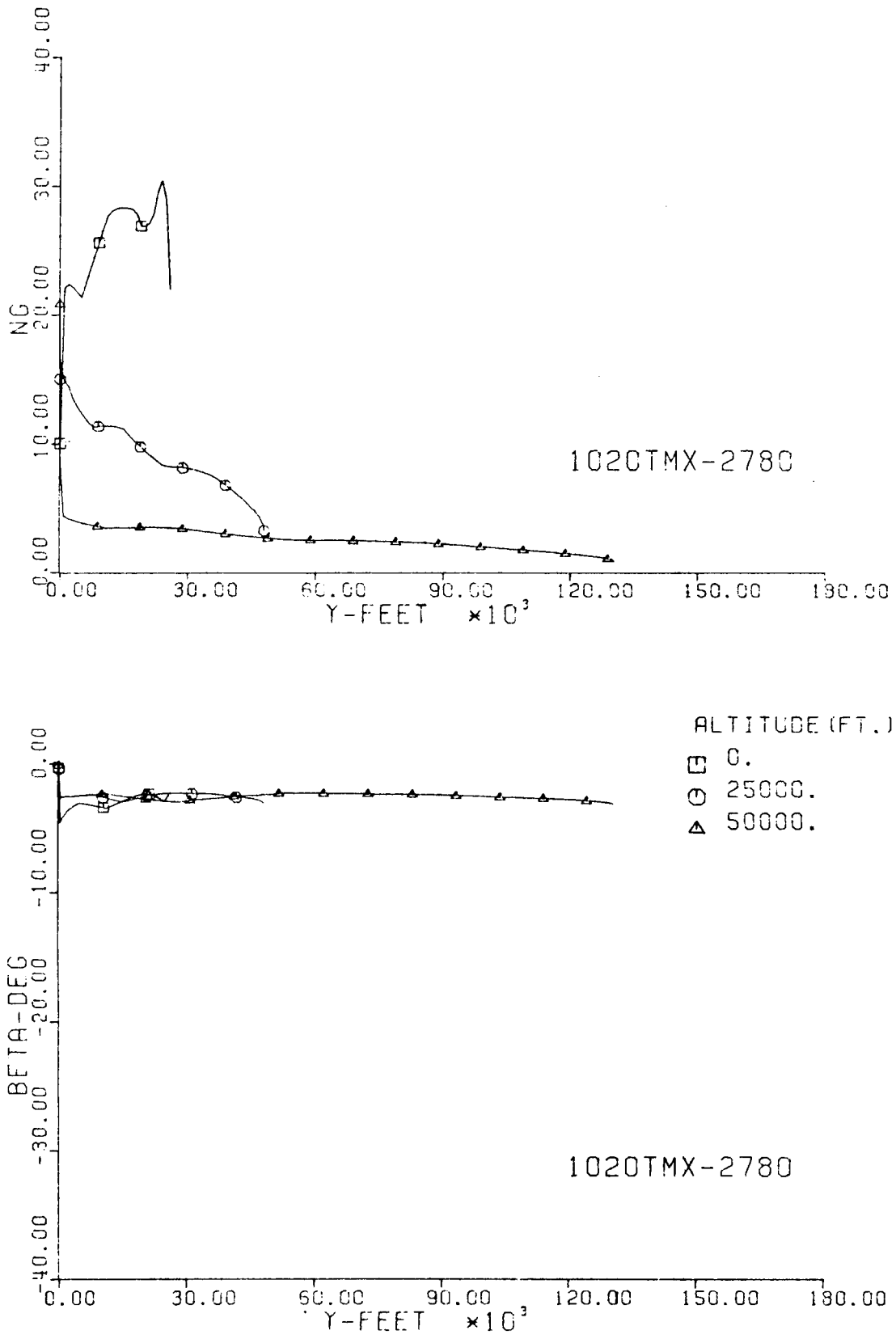

Fig. 193-III. Number of G's and Sideslip Angle vs. Downrange Distance, Y.

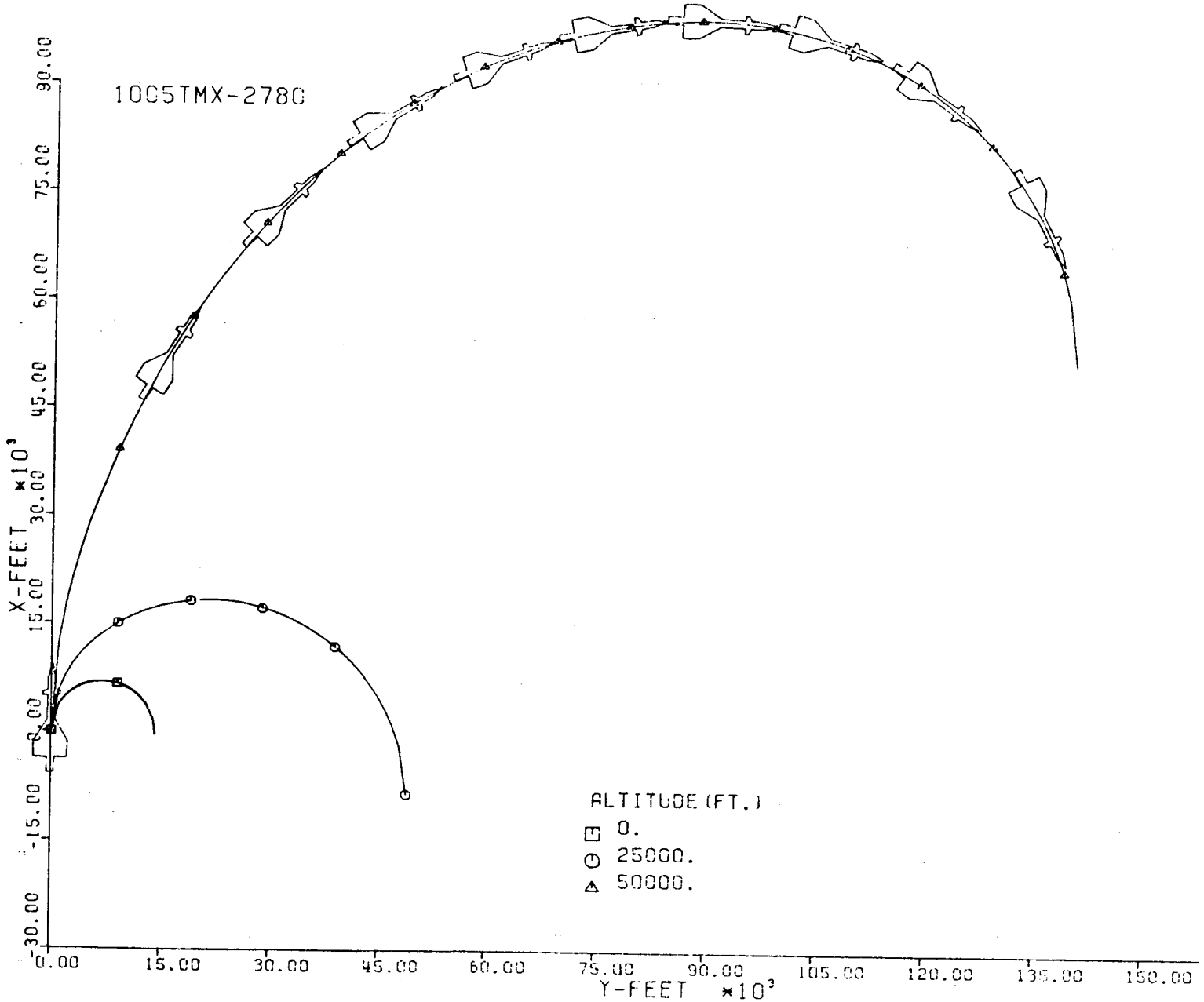

Fig. 194-III. Constant Altitude Flight Path, X vs. Y.

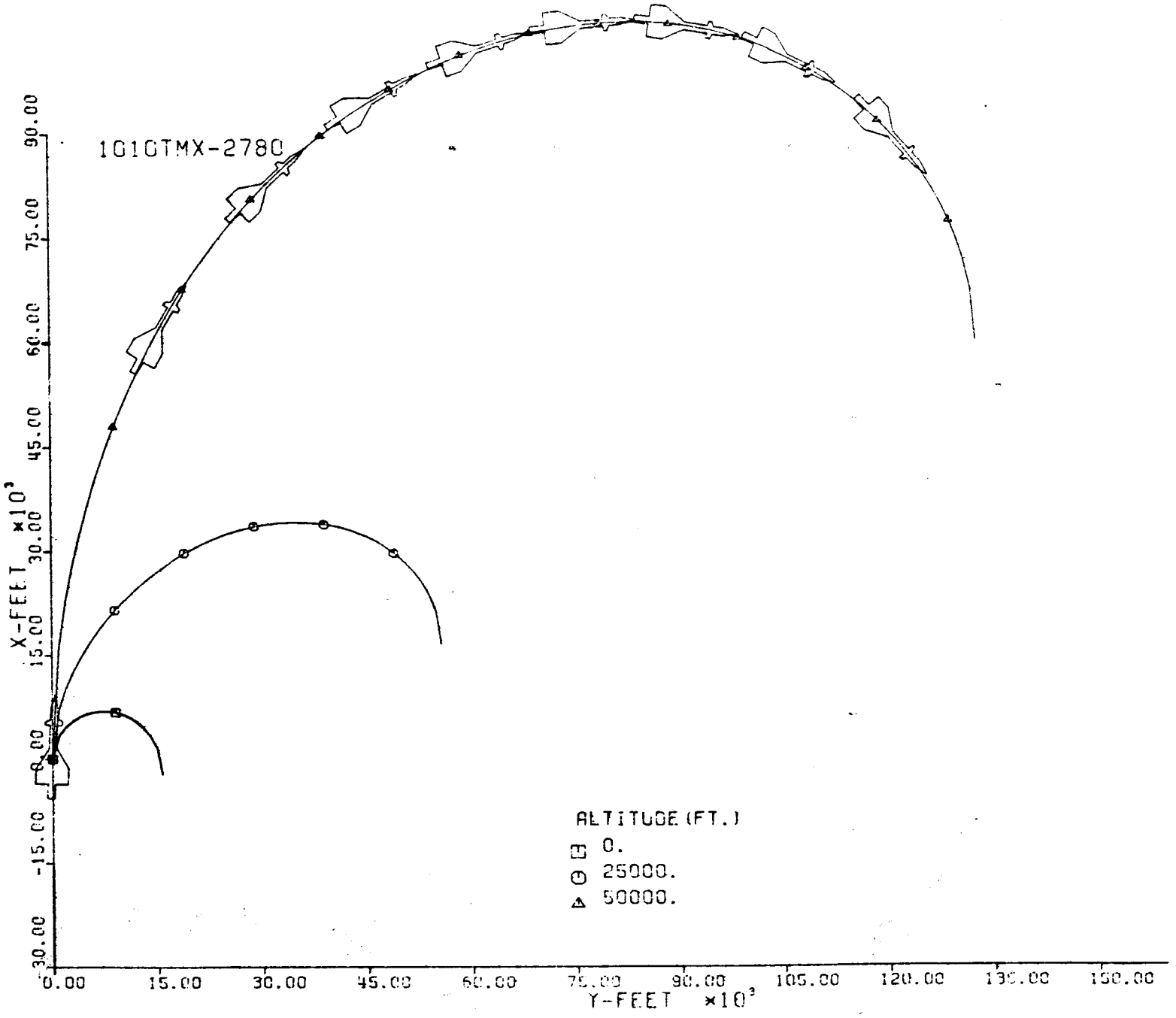
1010TMX-2780
90.00
75.00
60.00
45.00
30.00
15.00
0.00
-15.00
-30.00
X-FEET ×10³
0.00
15.00
30.00
45.00
60.00
75.00
90.00
105.00
120.00
135.00
150.00
Y-FEET ×10³
ALTITUDE (FT.)
□ 0.
○ 25000.
△ 50000.

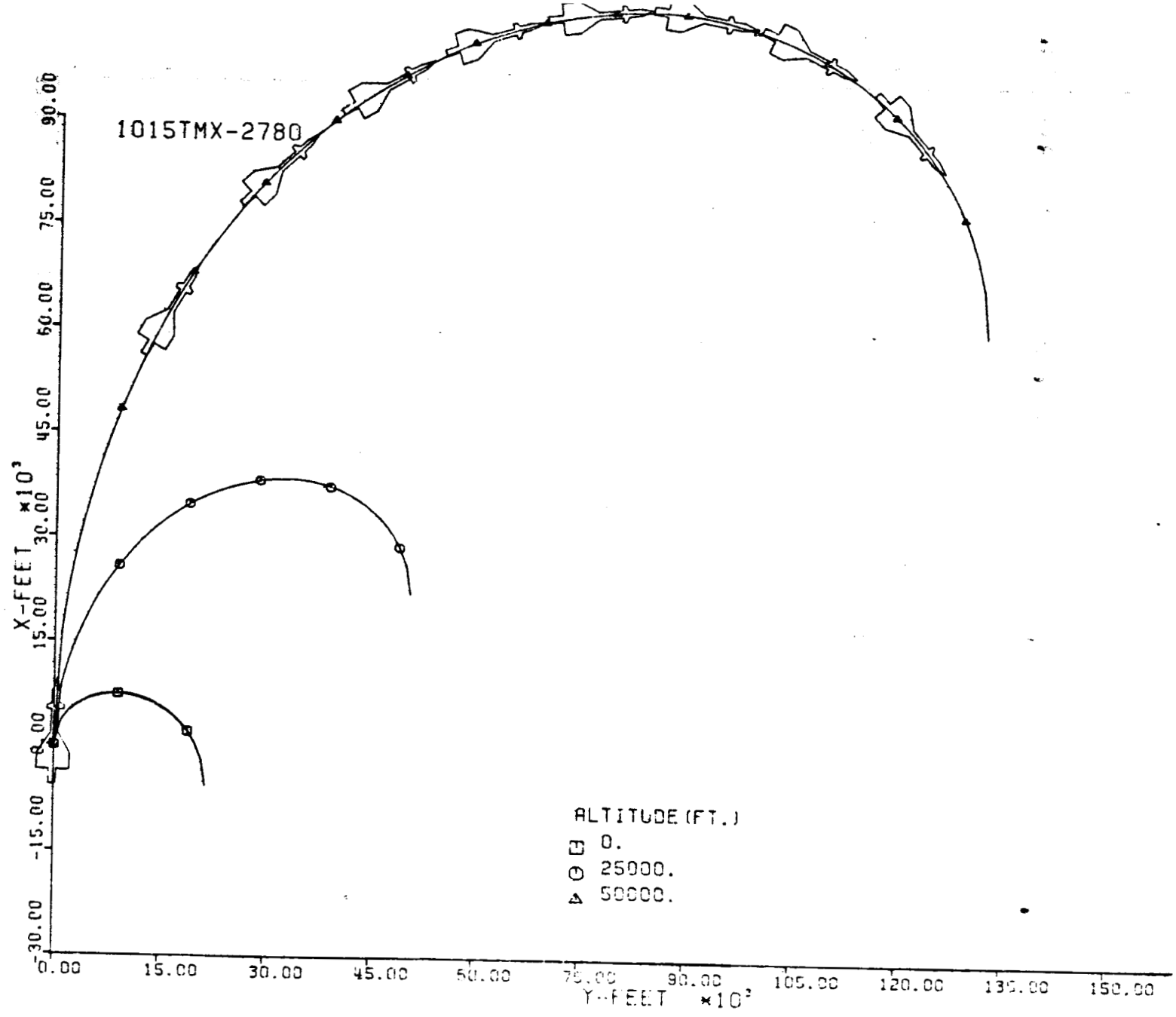

Fig. 196-III. Constant Altitude Flight Path, X vs. Y.

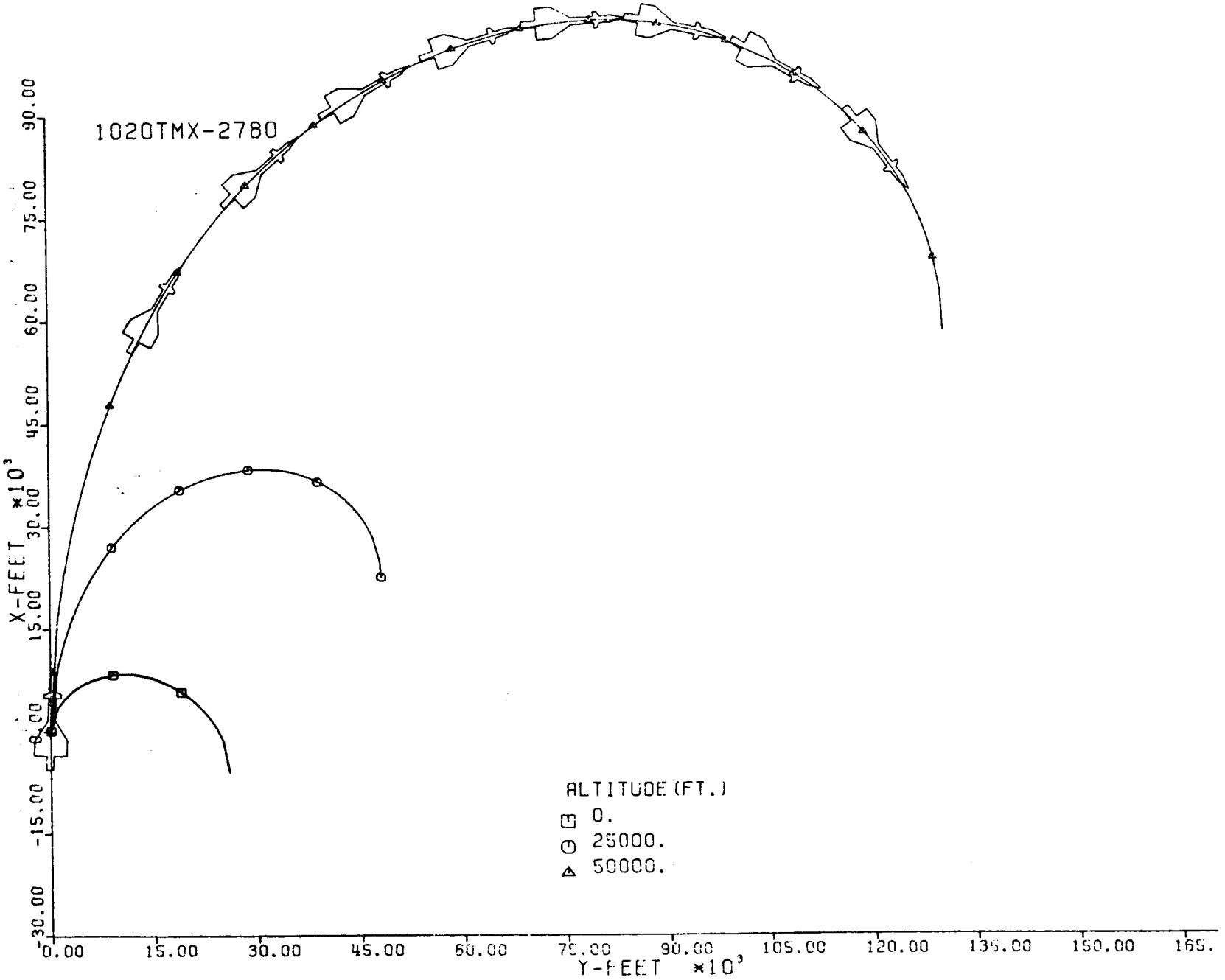
1020TMX-2780
X-FEET ×10³
90.00
75.00
60.00
45.00
30.00
15.00
0.00
-15.00
-30.00
0.00
15.00
30.00
45.00
60.00
75.00
90.00
105.00
120.00
135.00
150.00
165.
Y-FEET ×10³
ALTITUDE (FT.)
0.
25000.
50000.

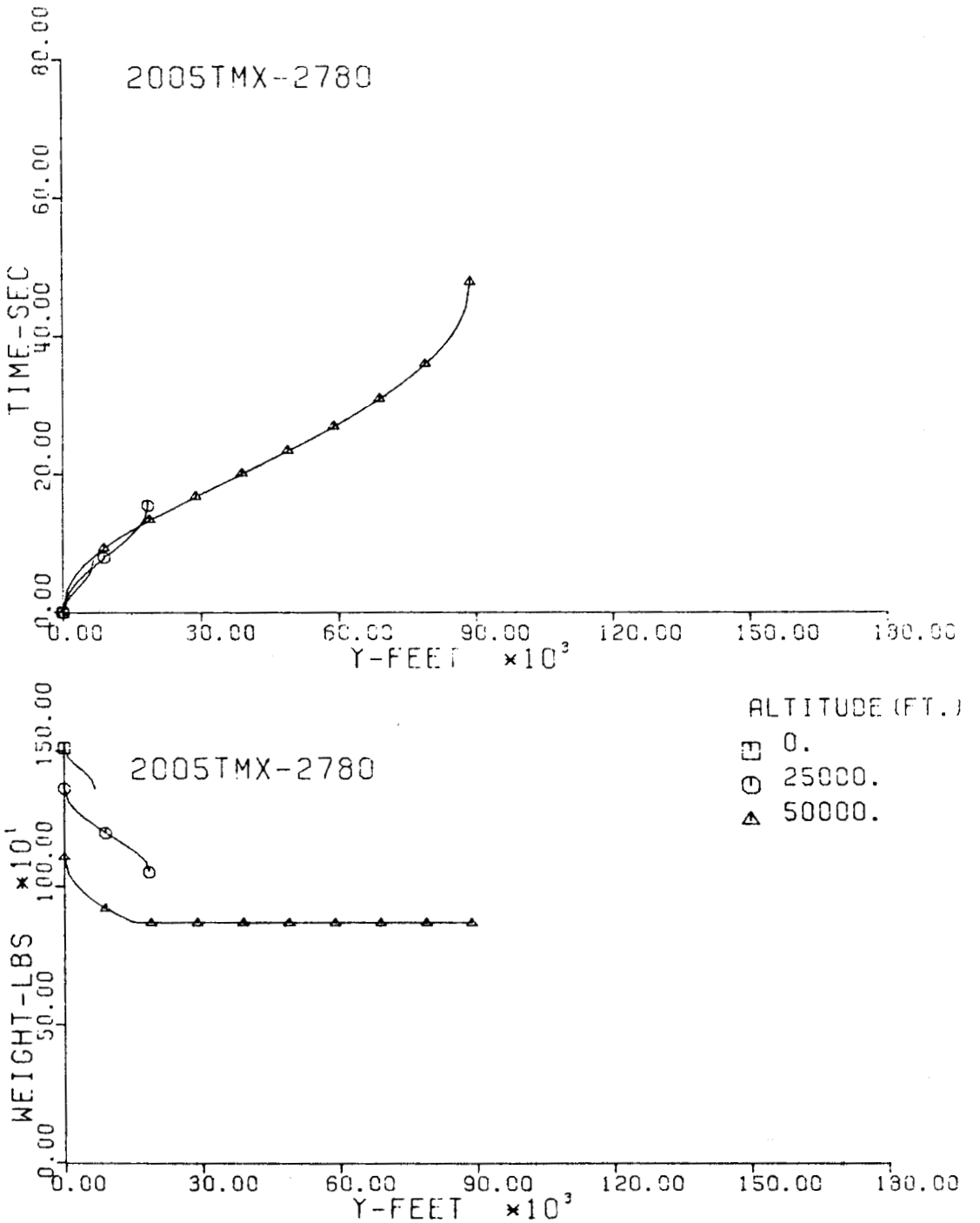

Fig. 198-III. Flight Time and Vehicle Weight vs. Downrange Distance, Y.

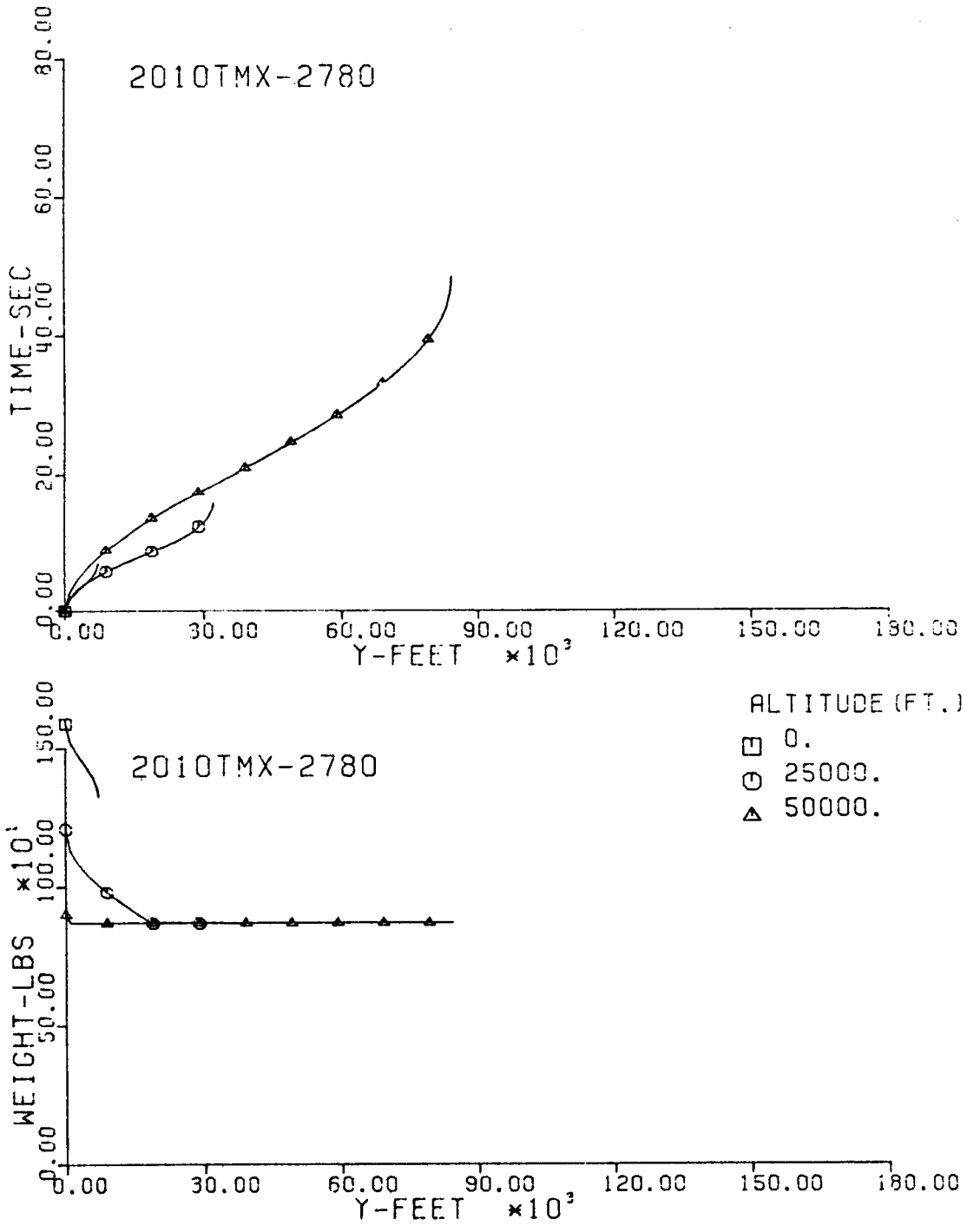

Fig. 199-III. Flight Time and Vehicle Weight vs. Downrange Distance, Y.

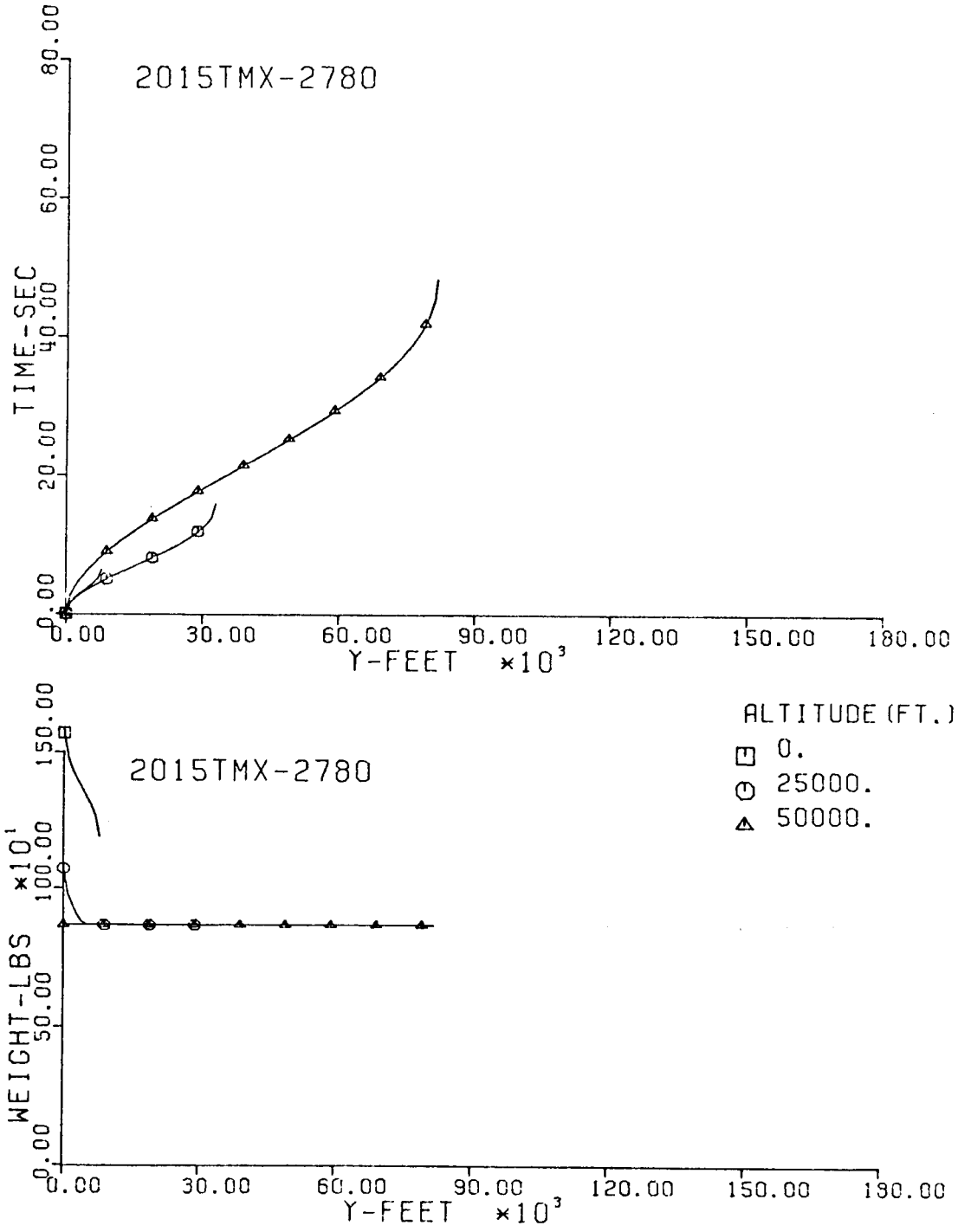

Fig. 200-III. Flight Time and Vehicle Weight vs. Downrange Distance, Y.

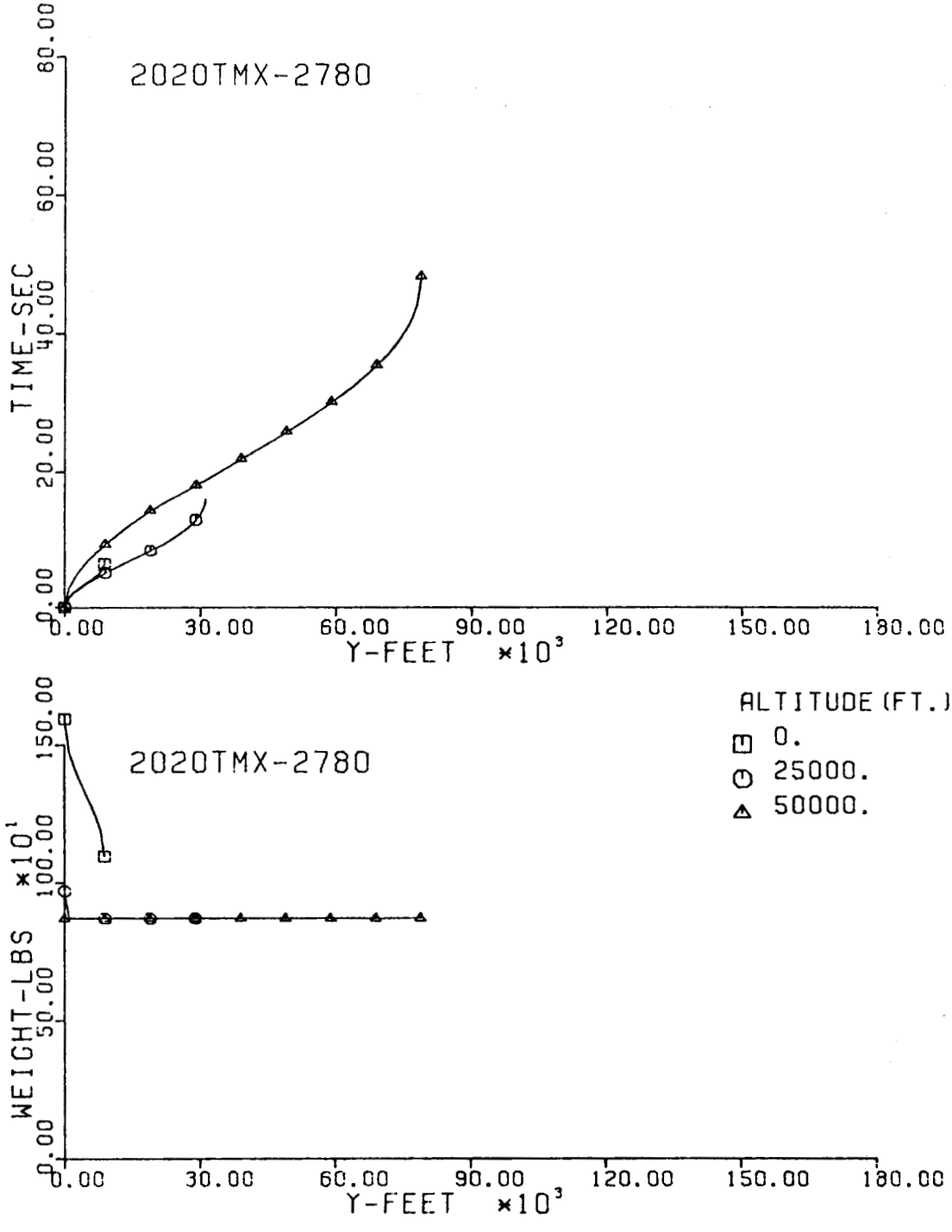

Fig. 201-III. Flight Time and Vehicle Weight vs. Downrange Distance, Y.

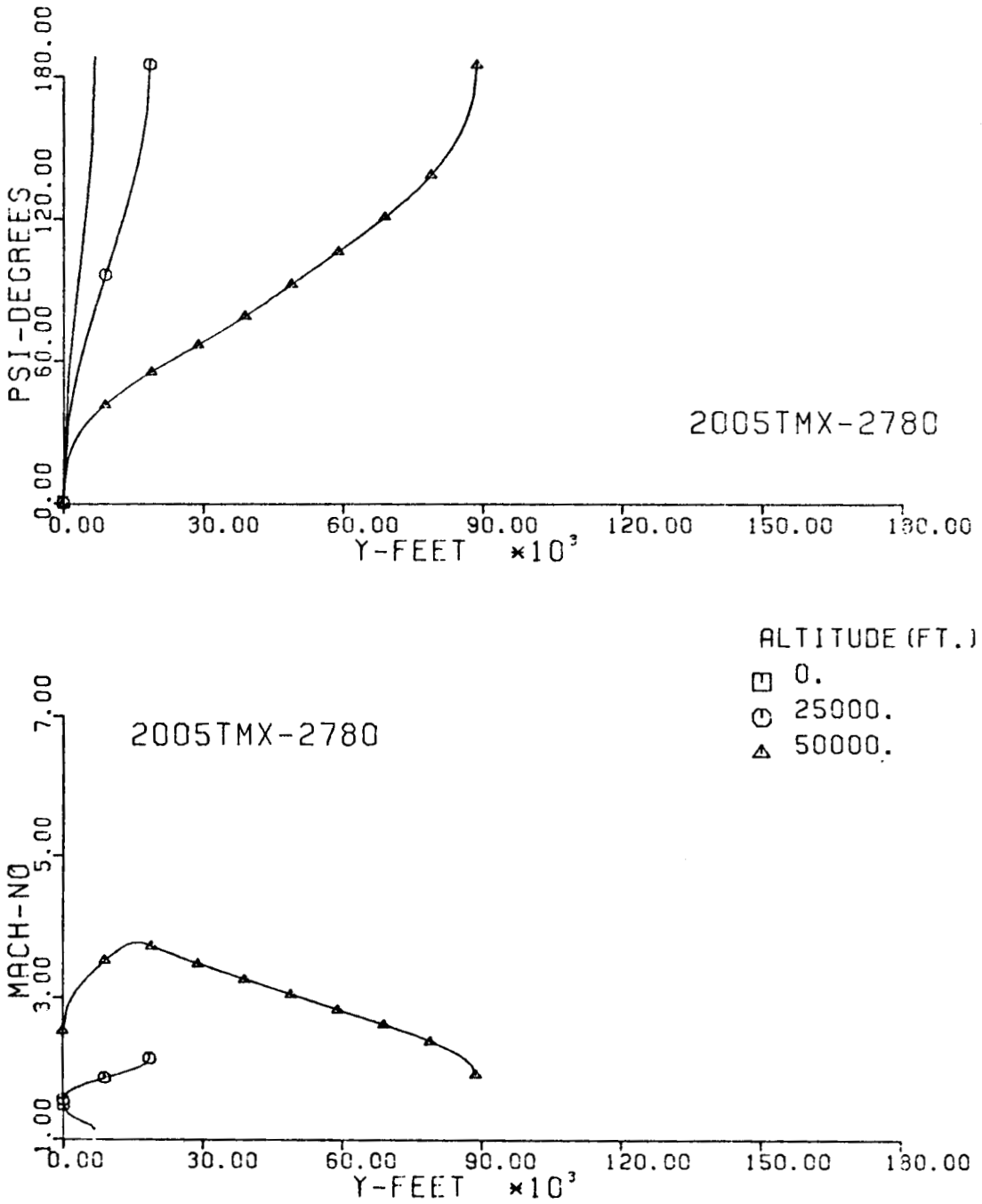

Fig. 202-III. Heading Angle and Mach No. vs. Downrange Distance, Y.

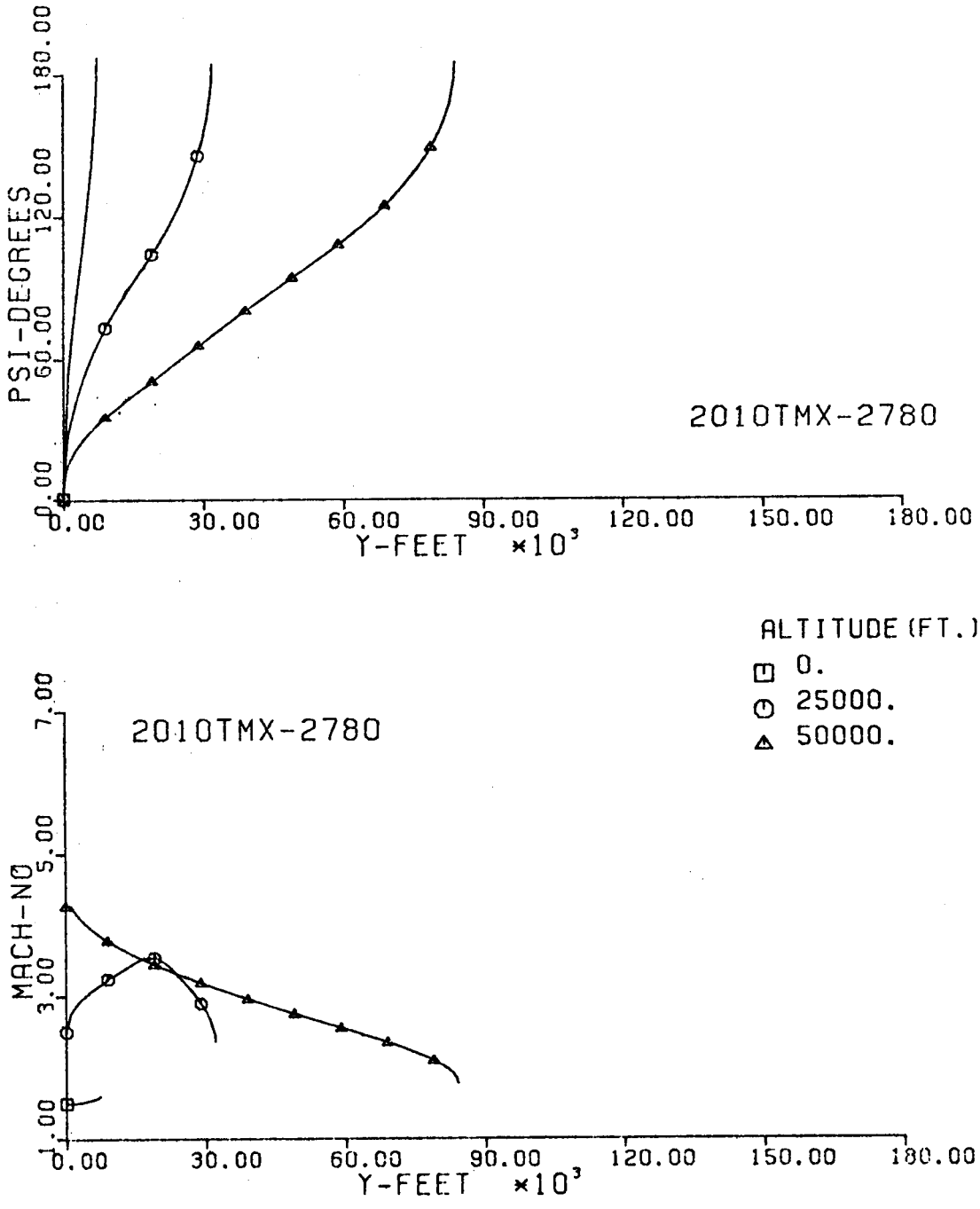

Fig. 203-III. Heading Angle and Mach No. vs. Downrange Distance, Y.

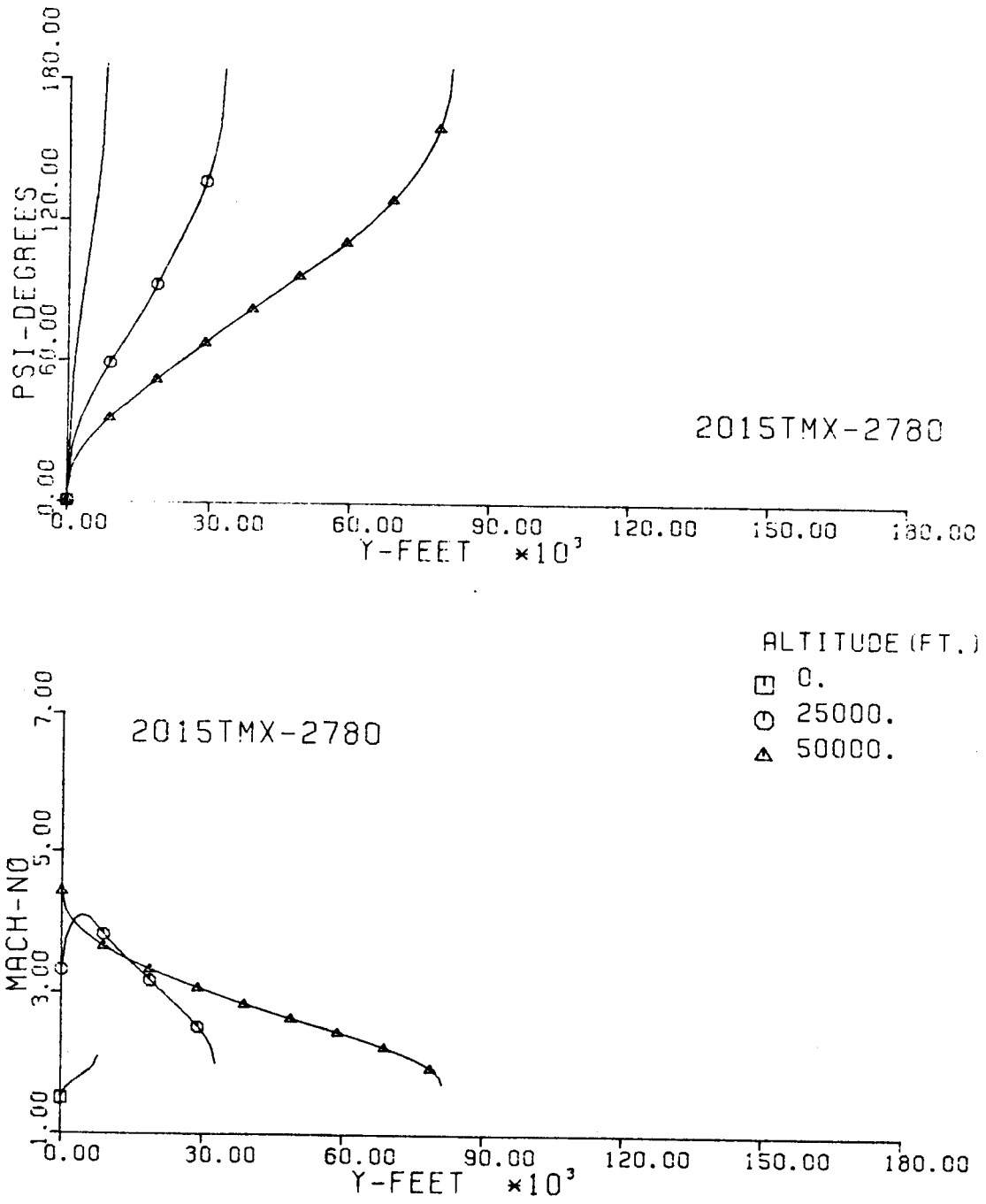

Fig. 204-III. Heading Angle and Mach No. vs. Downrange Distance, Y.

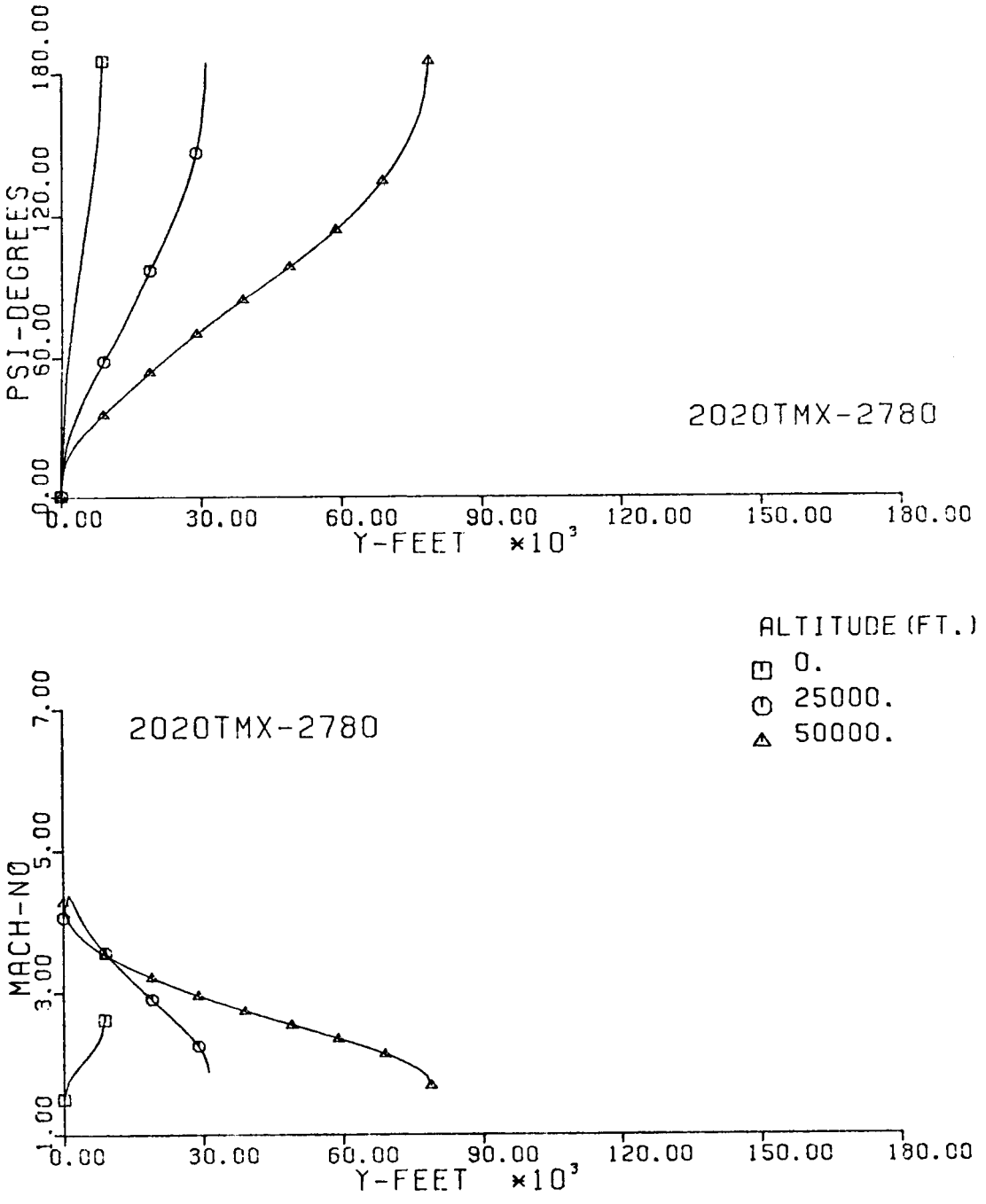

Fig. 205-III. Heading Angle and Mach No. vs. Downrange Distance, Y.

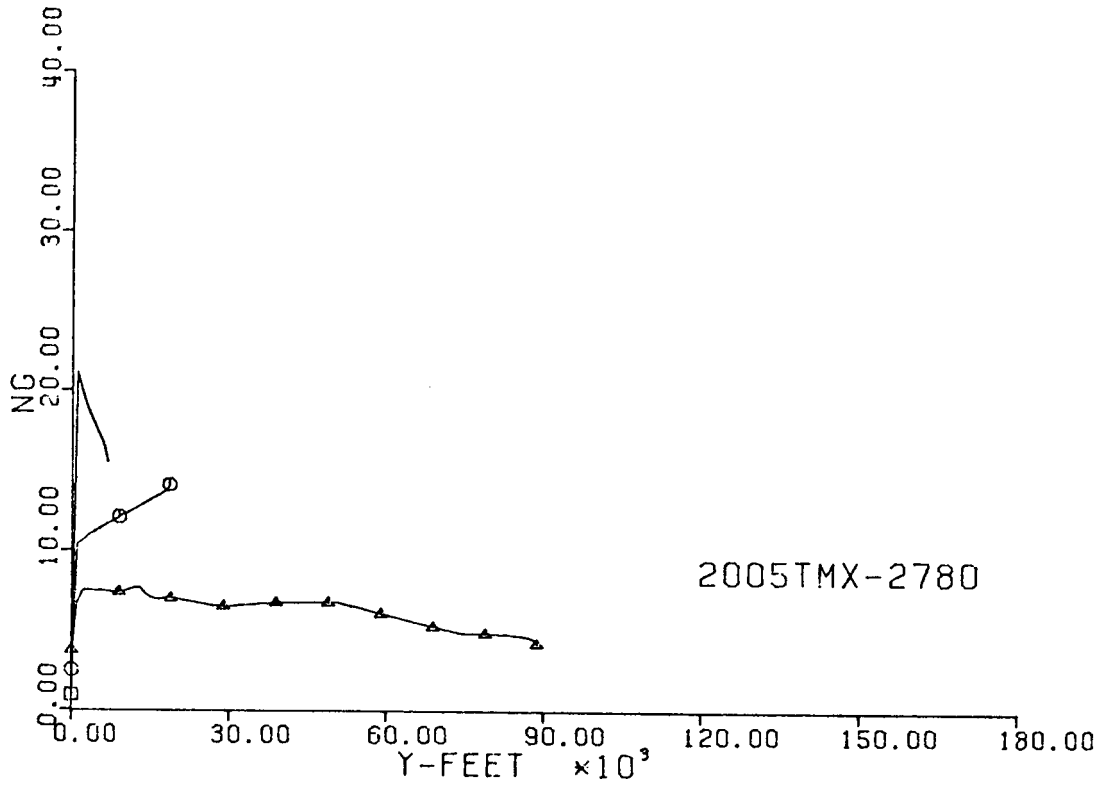

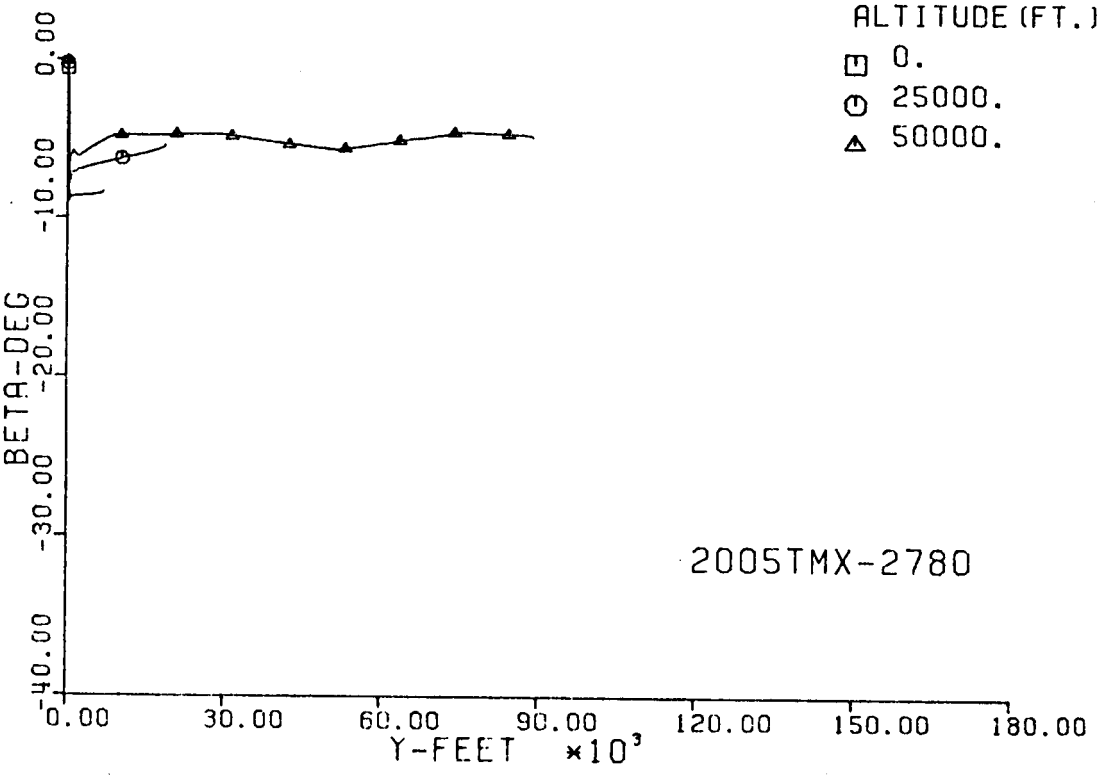

Fig. 206-III. Number of G's and Sideslip Angle vs. Downrange Distance, Y.

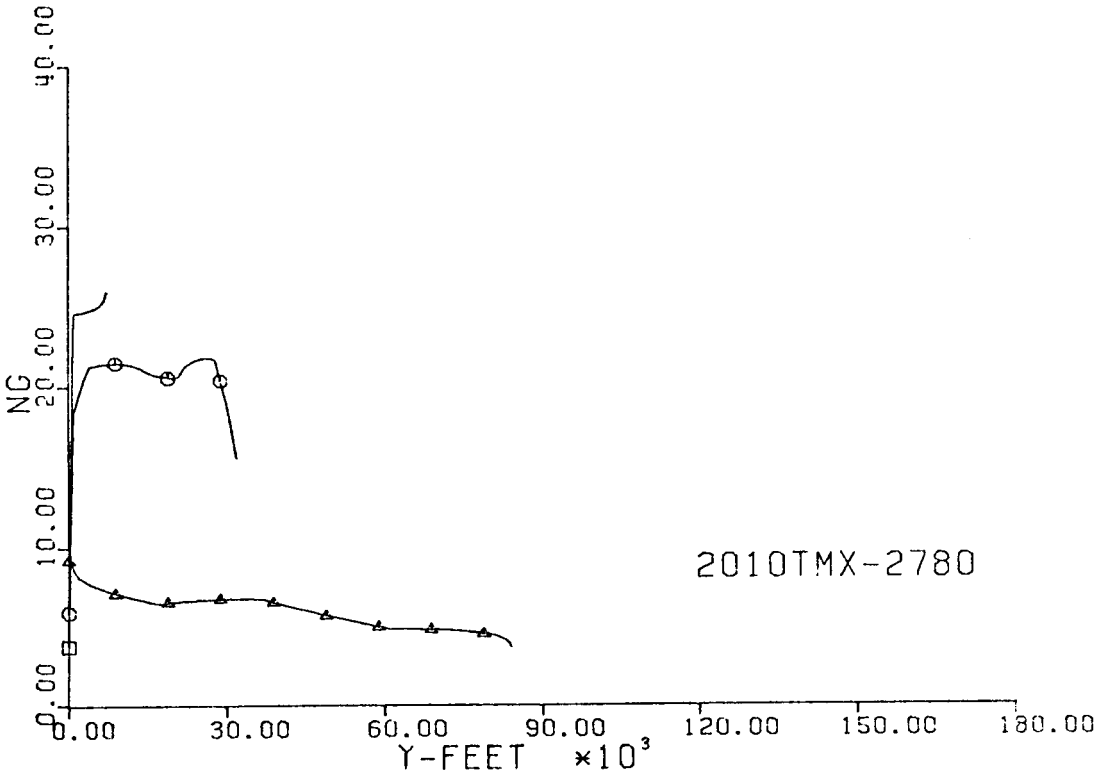

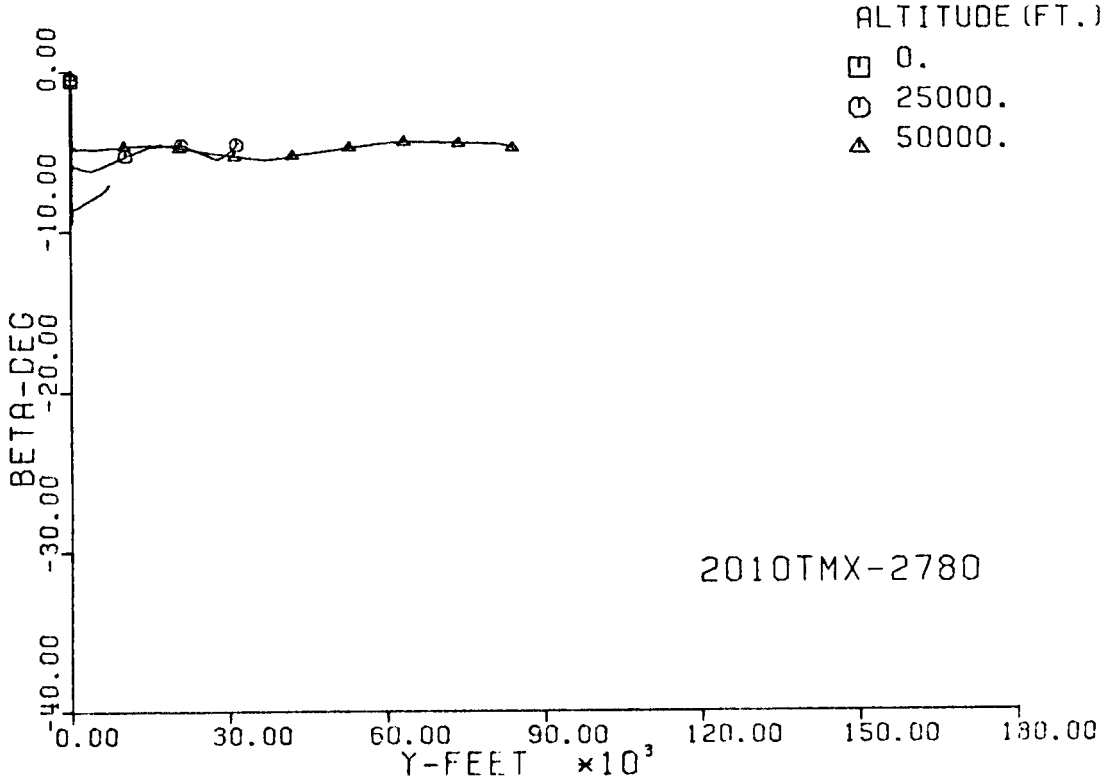

Fig. 207-III. Number of G's and Sideslip Angle vs. Downrange Distance, Y.

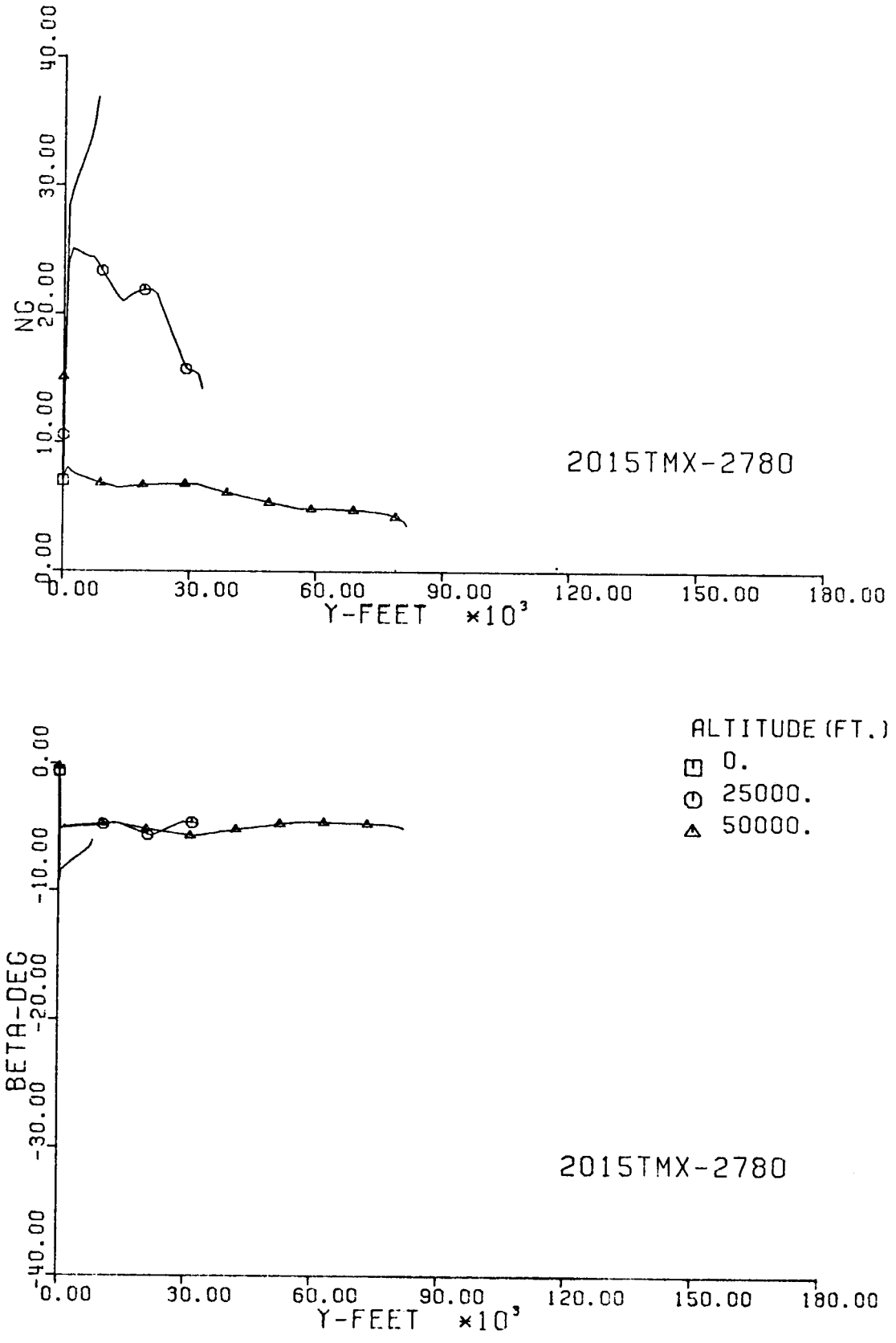

Fig. 208-III. Number of G's and Sideslip Angle vs. Downrange Distance, Y.

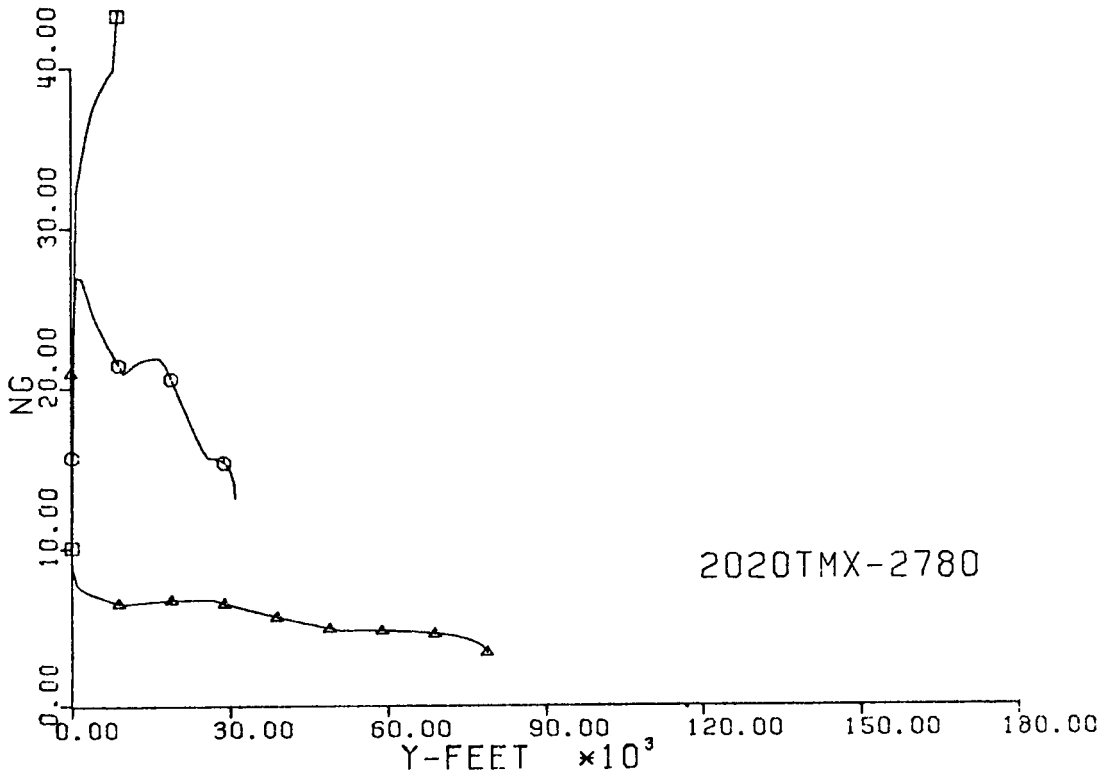

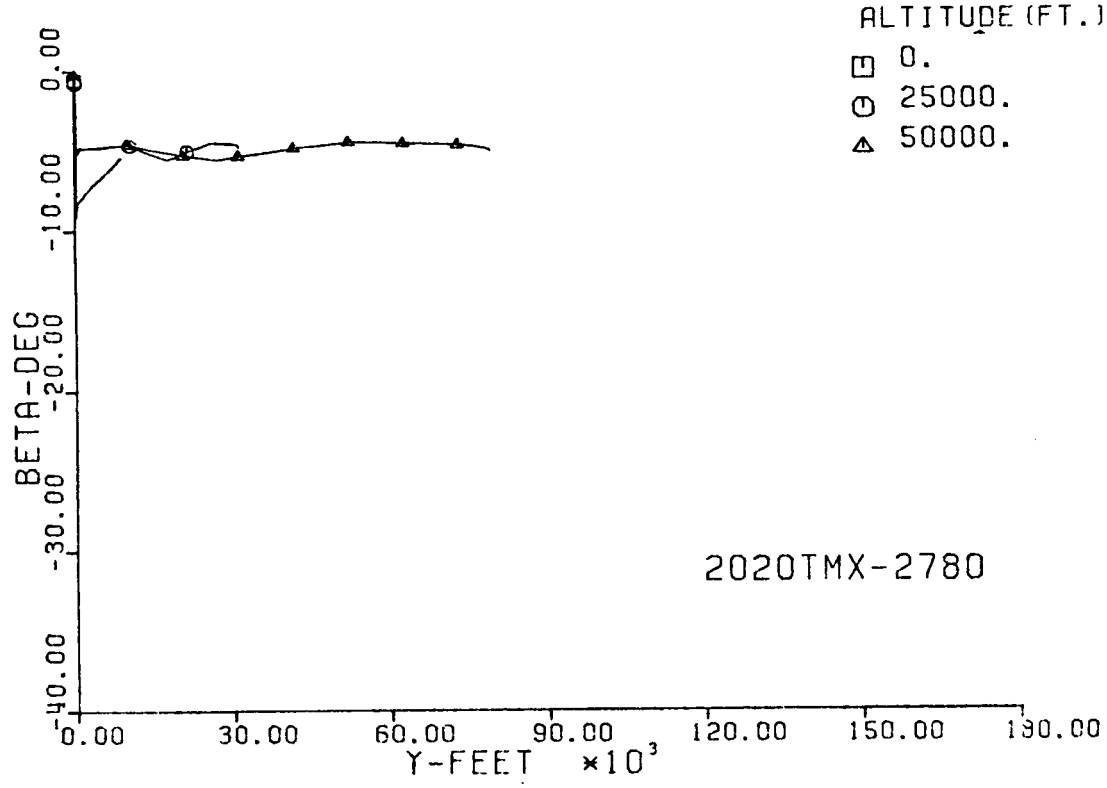

Fig. 209-III. Number of G's and Sideslip Angle vs. Downrange Distance, Y.

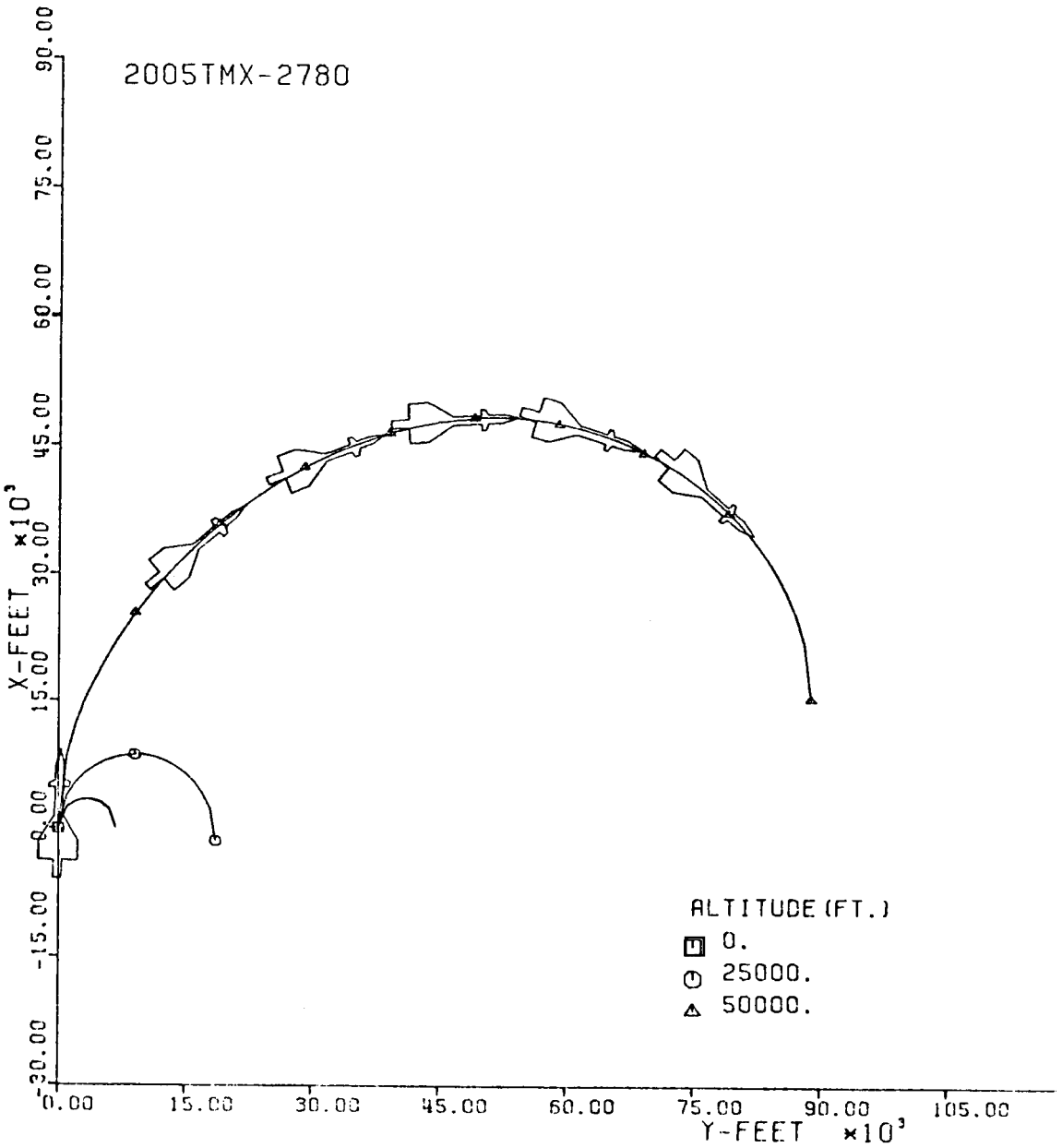

Fig. 210-III. Constant Altitude Flight Path, X vs. Y.

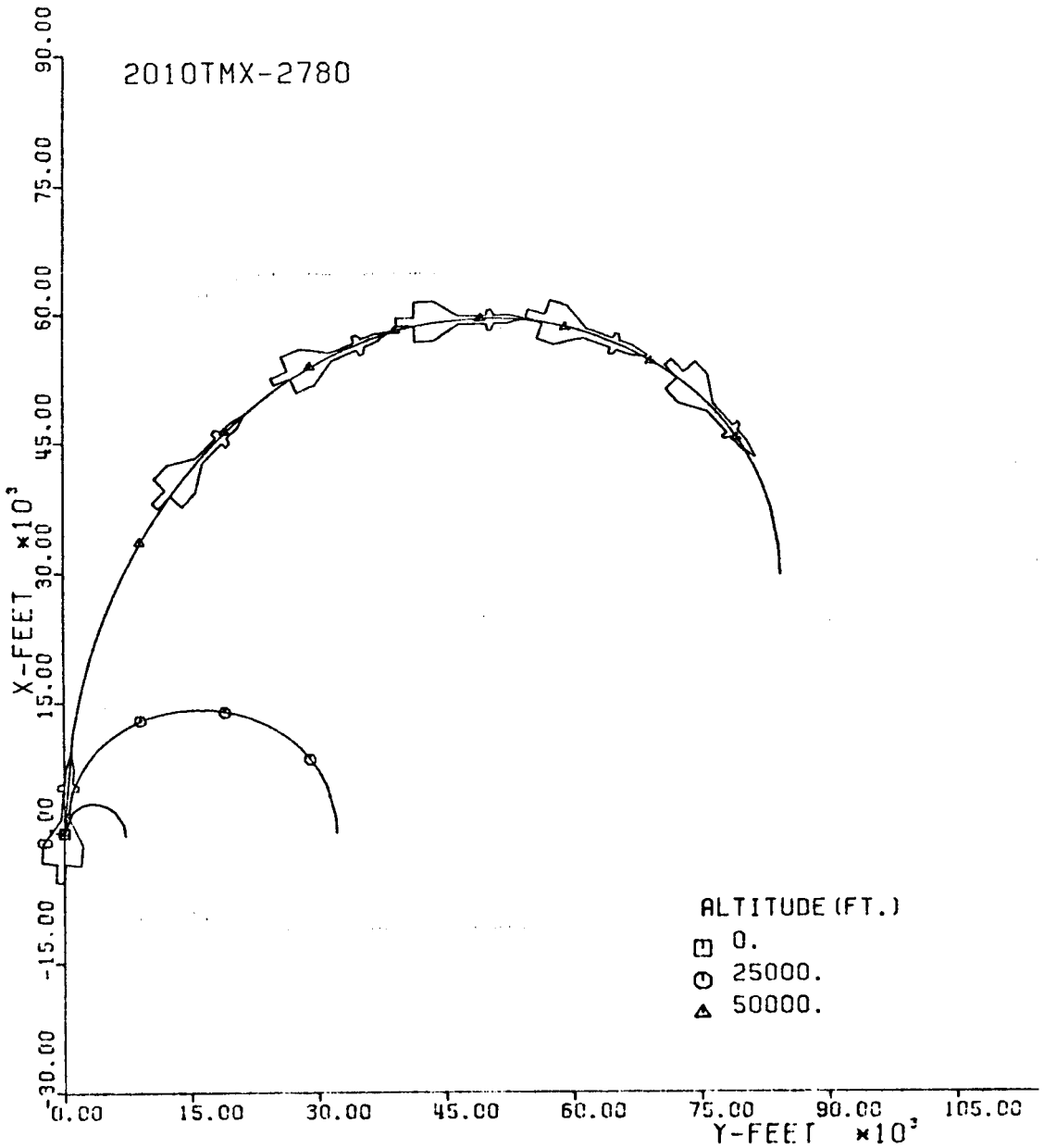

Fig. 211-III. Constant Altitude Flight Path, X vs. Y.

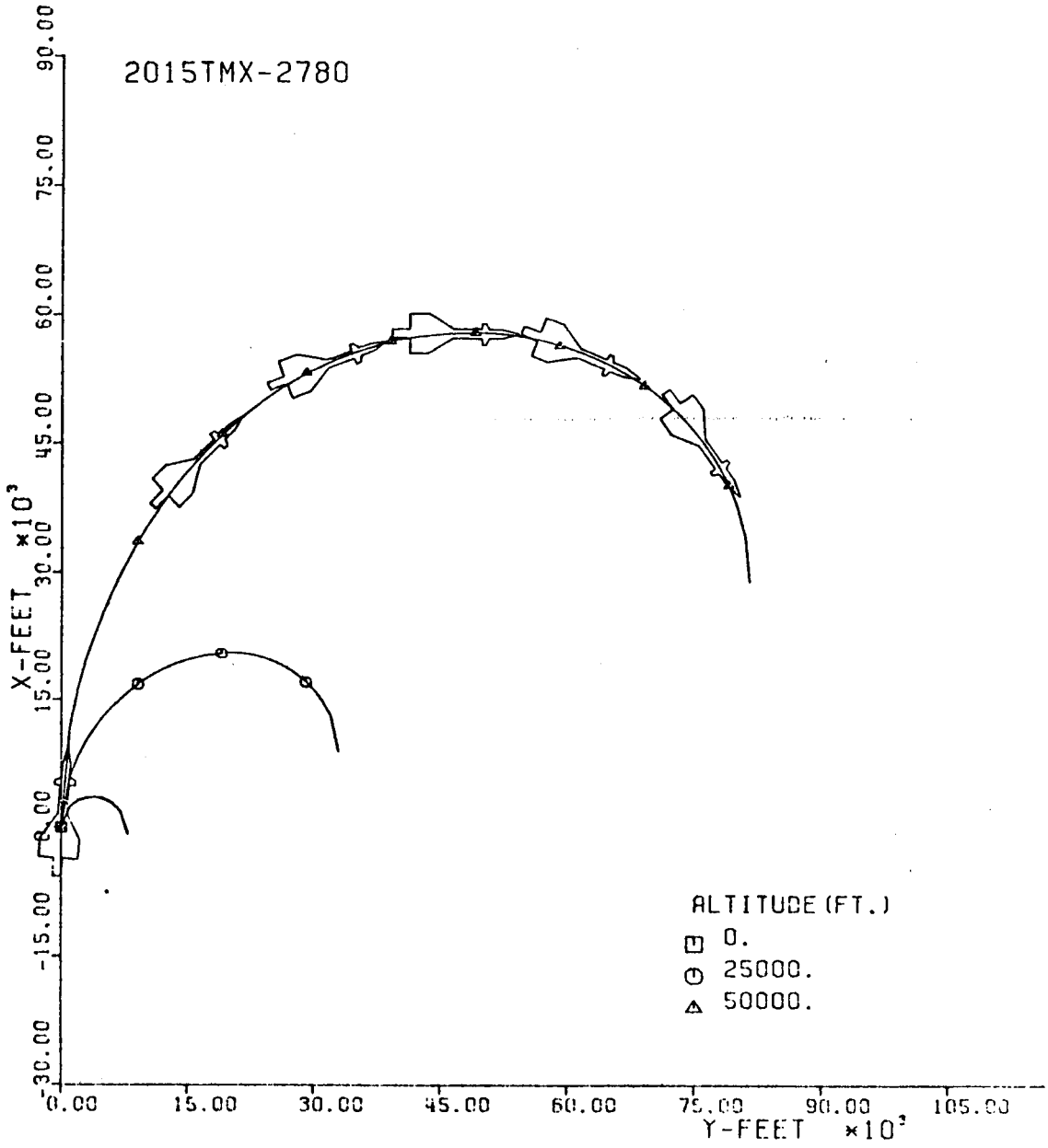

Fig. 212-III. Constant Altitude Flight Path, X vs. Y.

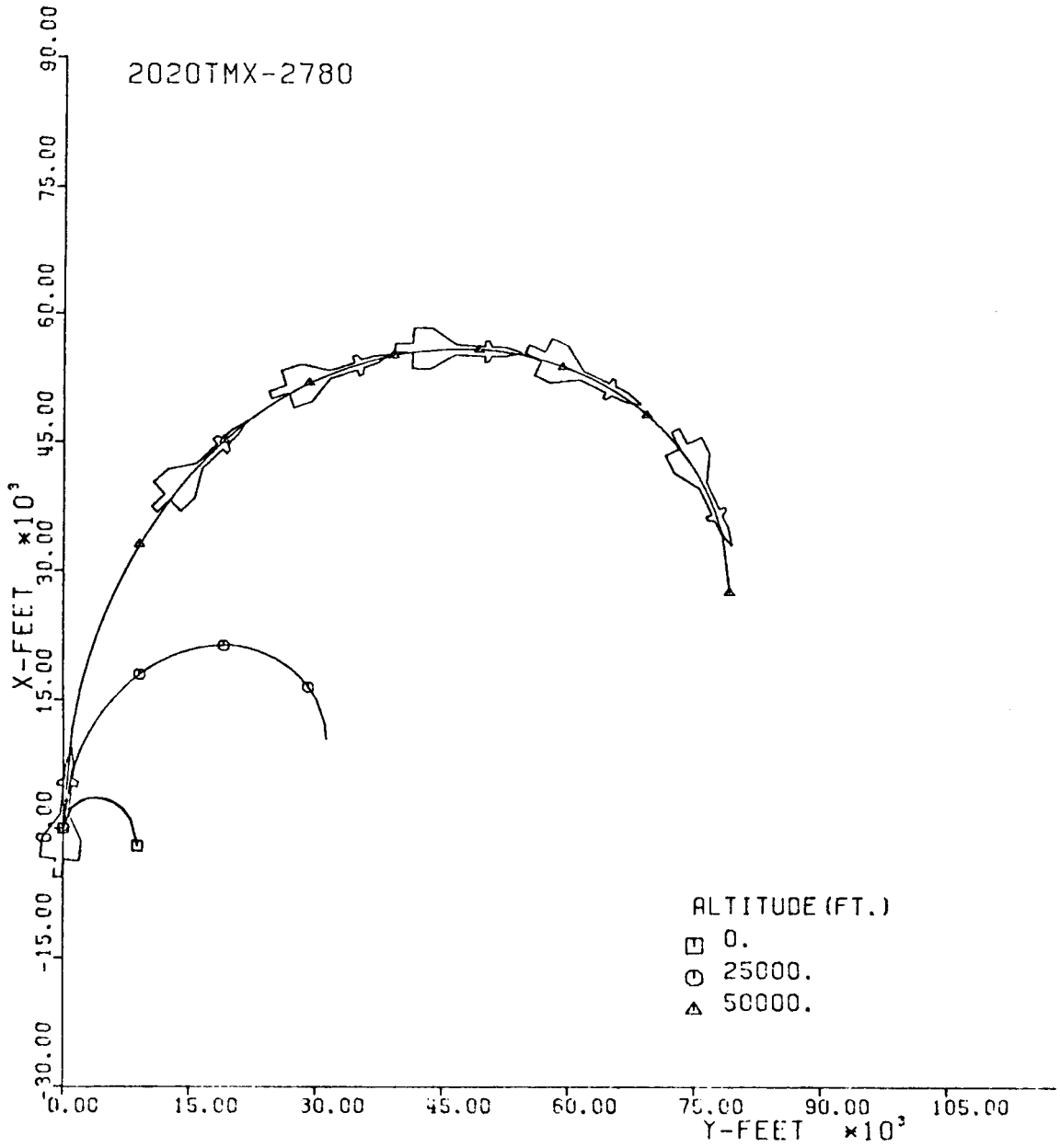

Fig. 213-III. Constant Altitude Flight Path, X vs. Y.

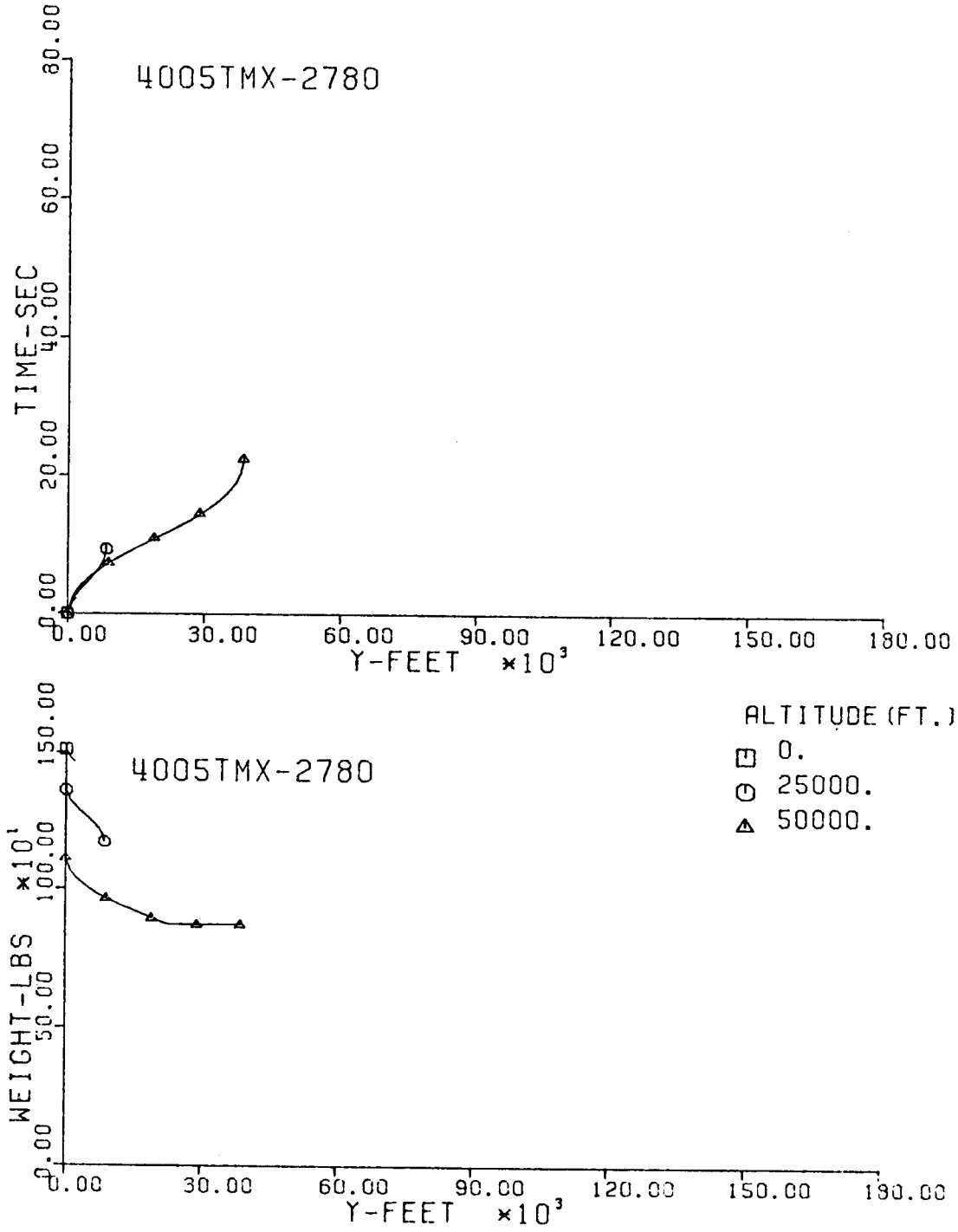

Fig. 214-III. Flight Time and Vehicle Weight vs. Downrange Distance, Y.

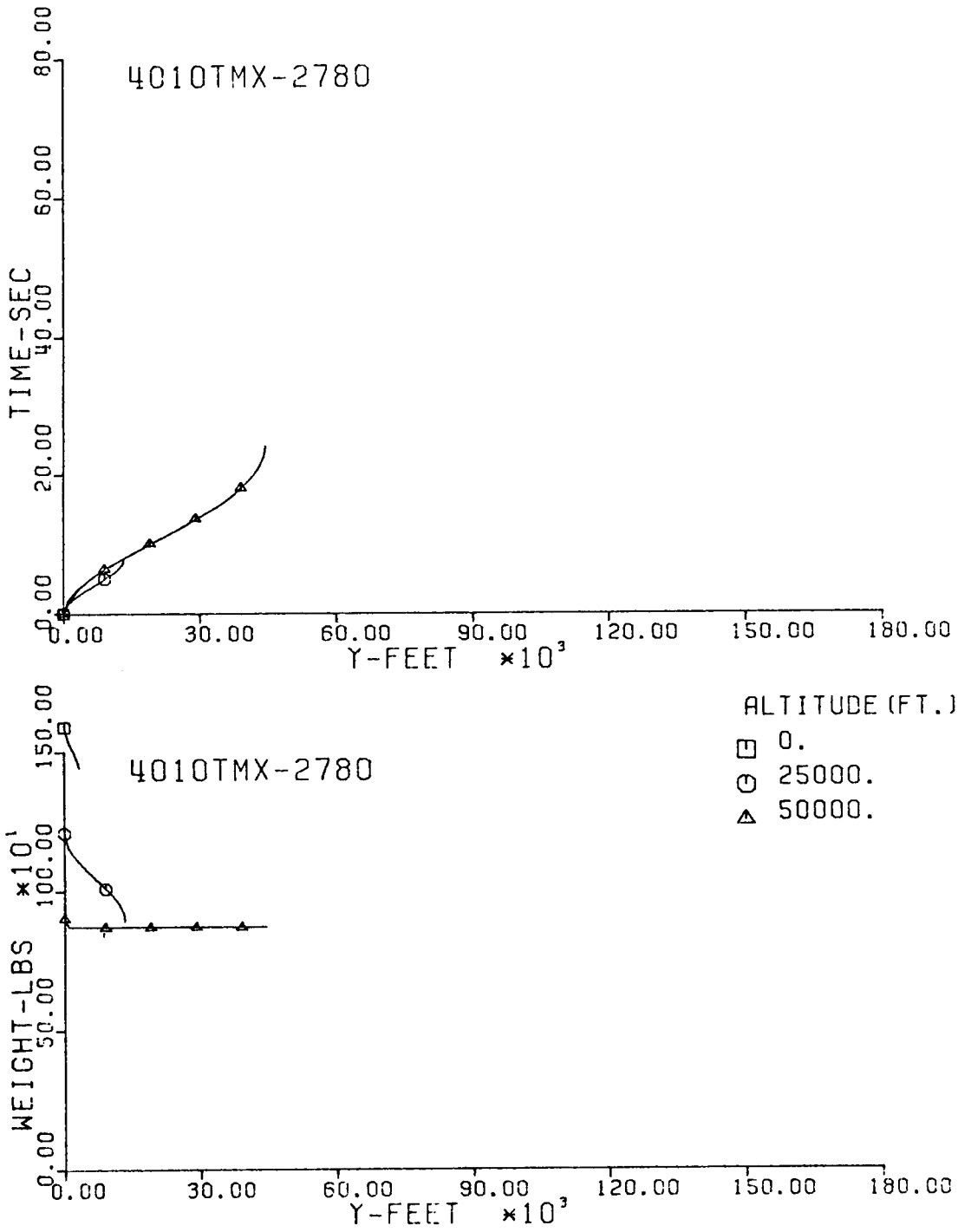

Fig. 215-III. Flight Time and Vehicle Weight vs. Downrange Distance, Y.

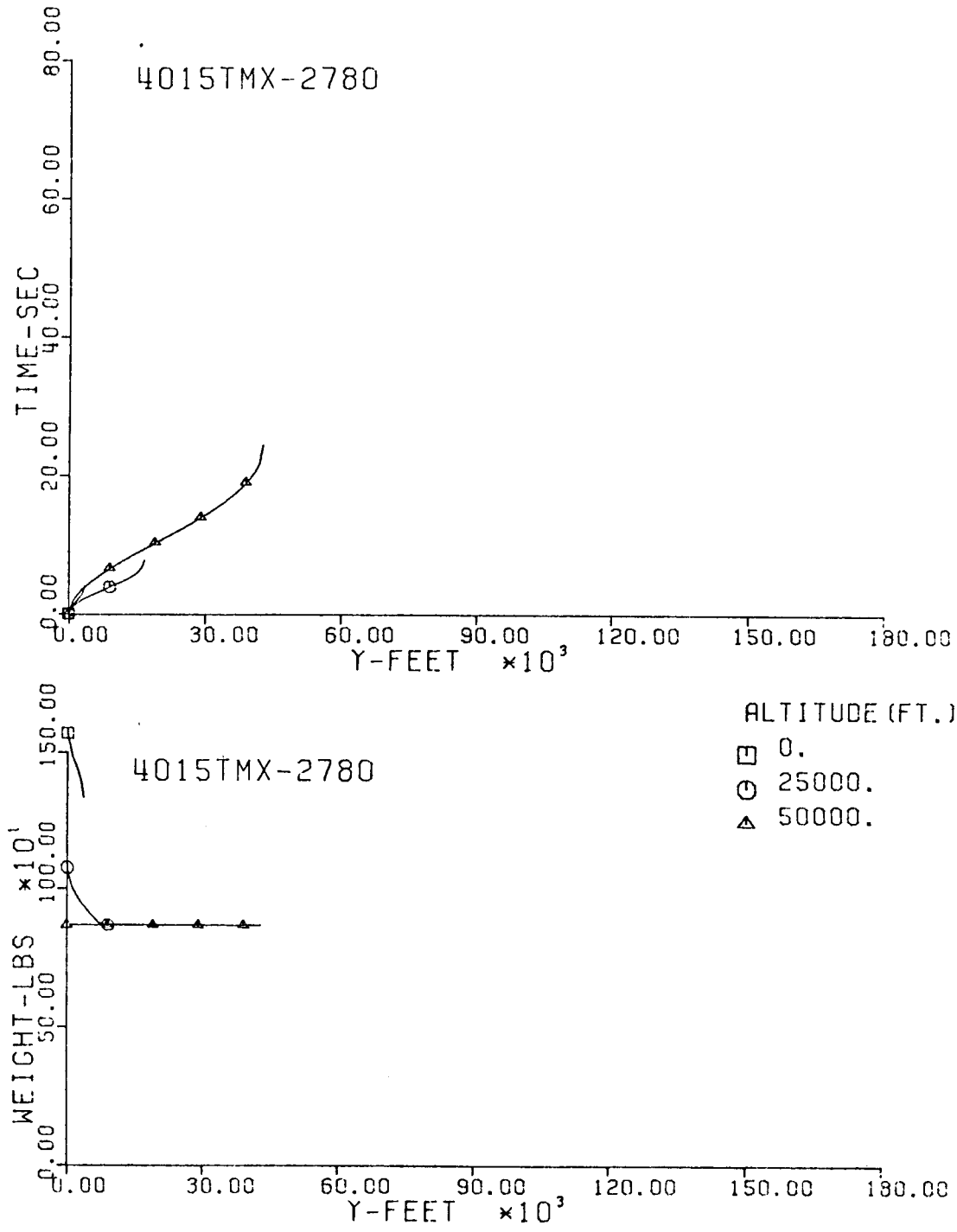

Fig. 216-III. Flight Time and Vehicle Weight vs. Downrange Distance, Y.

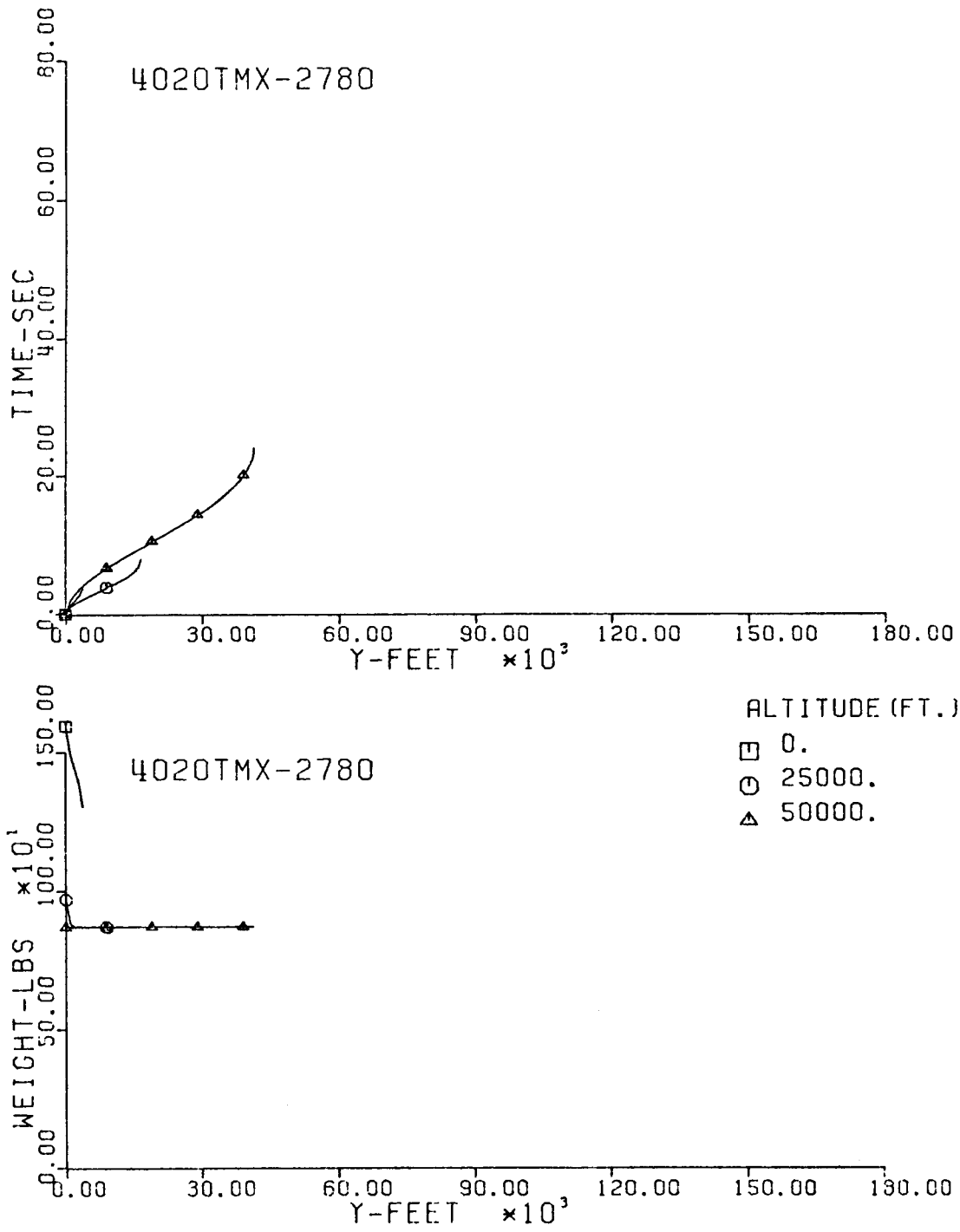

Fig. 217-III. Flight Time and Vehicle Weight vs. Downrange Distance, Y.

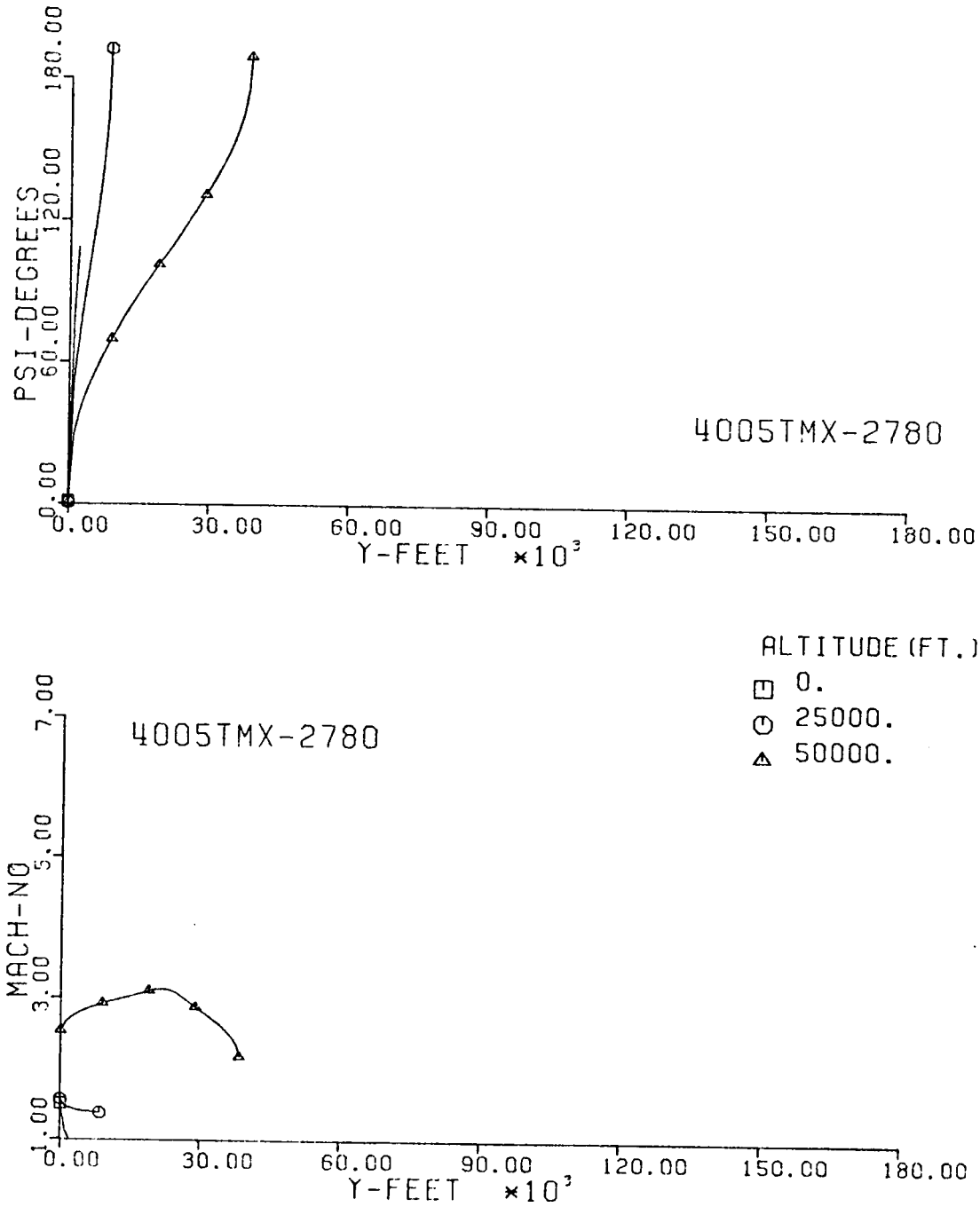

Fig. 218-III. Heading Angle and Mach No. vs. Downrange Distance, Y.

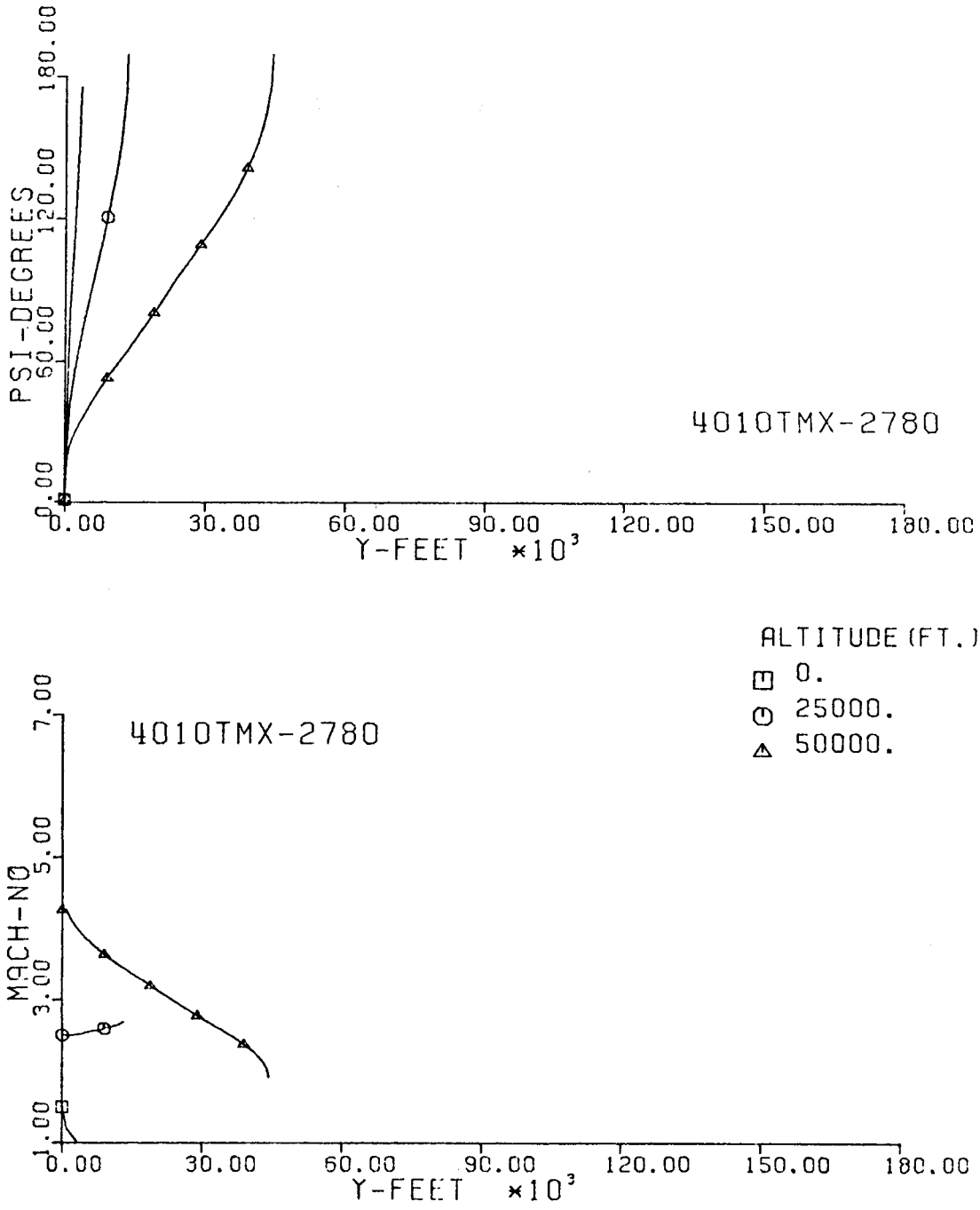

Fig. 219-III. Heading Angle and Mach No. vs. Downrange Distance, Y.

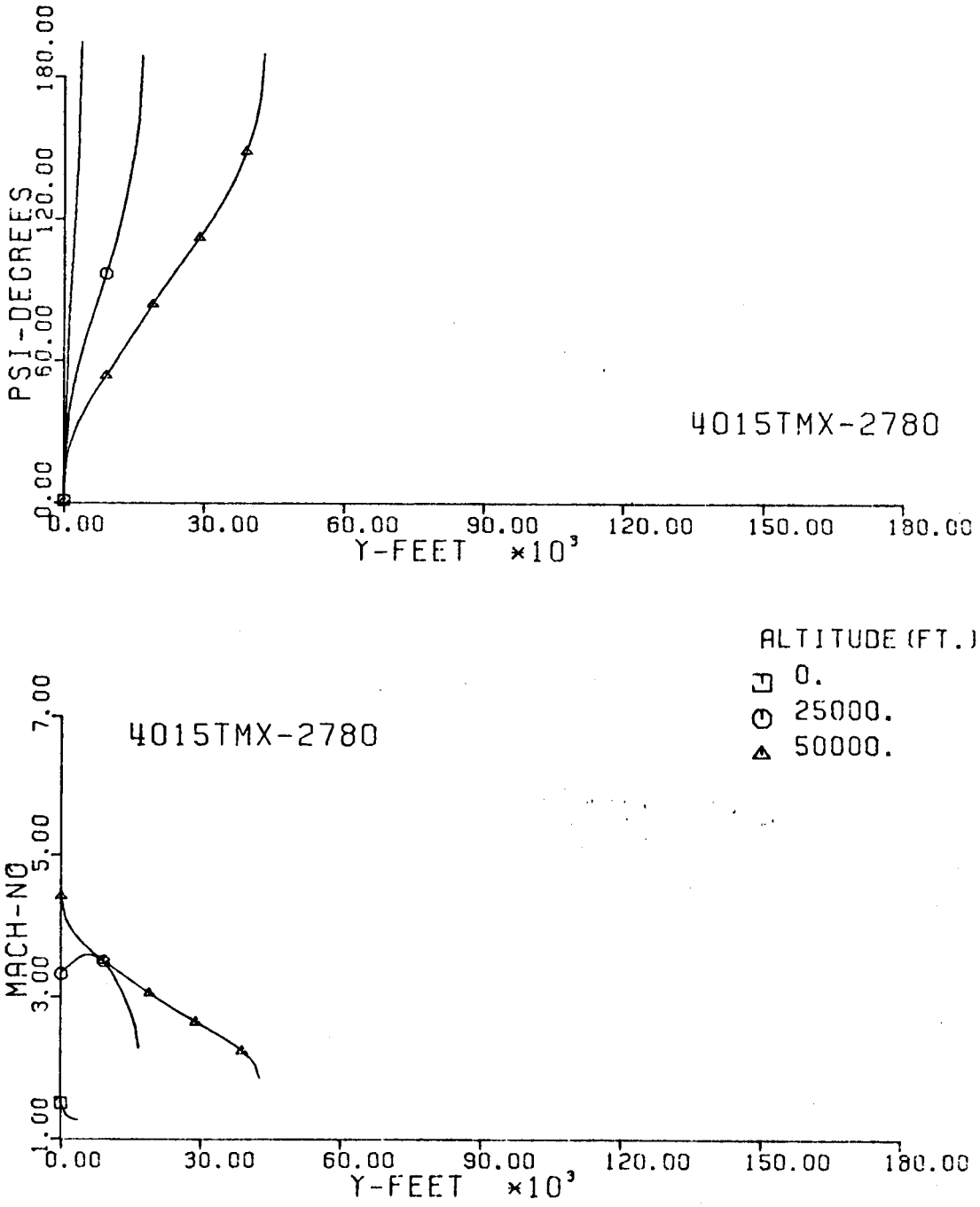

Fig. 220-III. Heading Angle and Mach No. vs. Downrange Distance, Y.

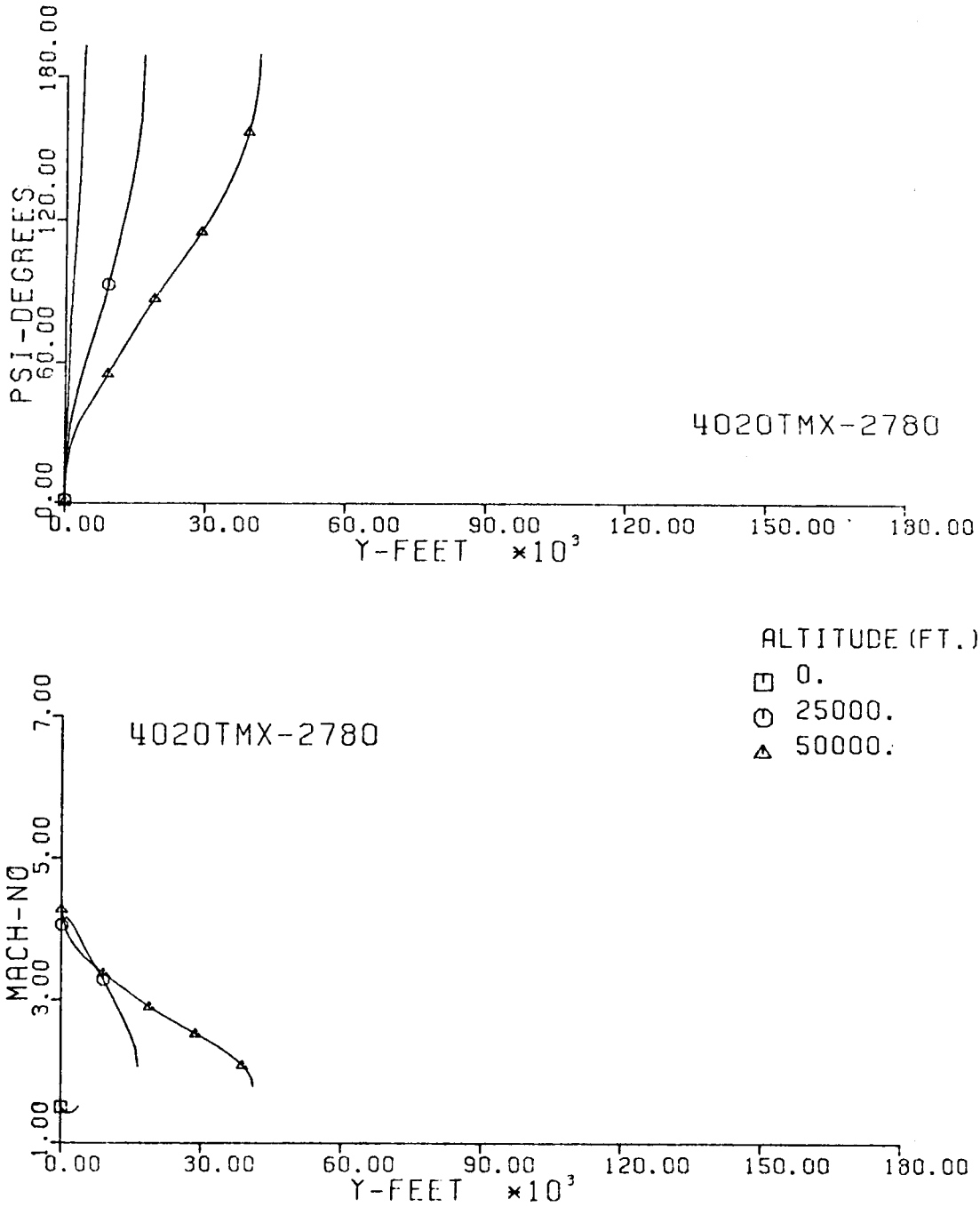

Fig. 221-III. Heading Angle and Mach No. vs. Downrange Distance, Y.

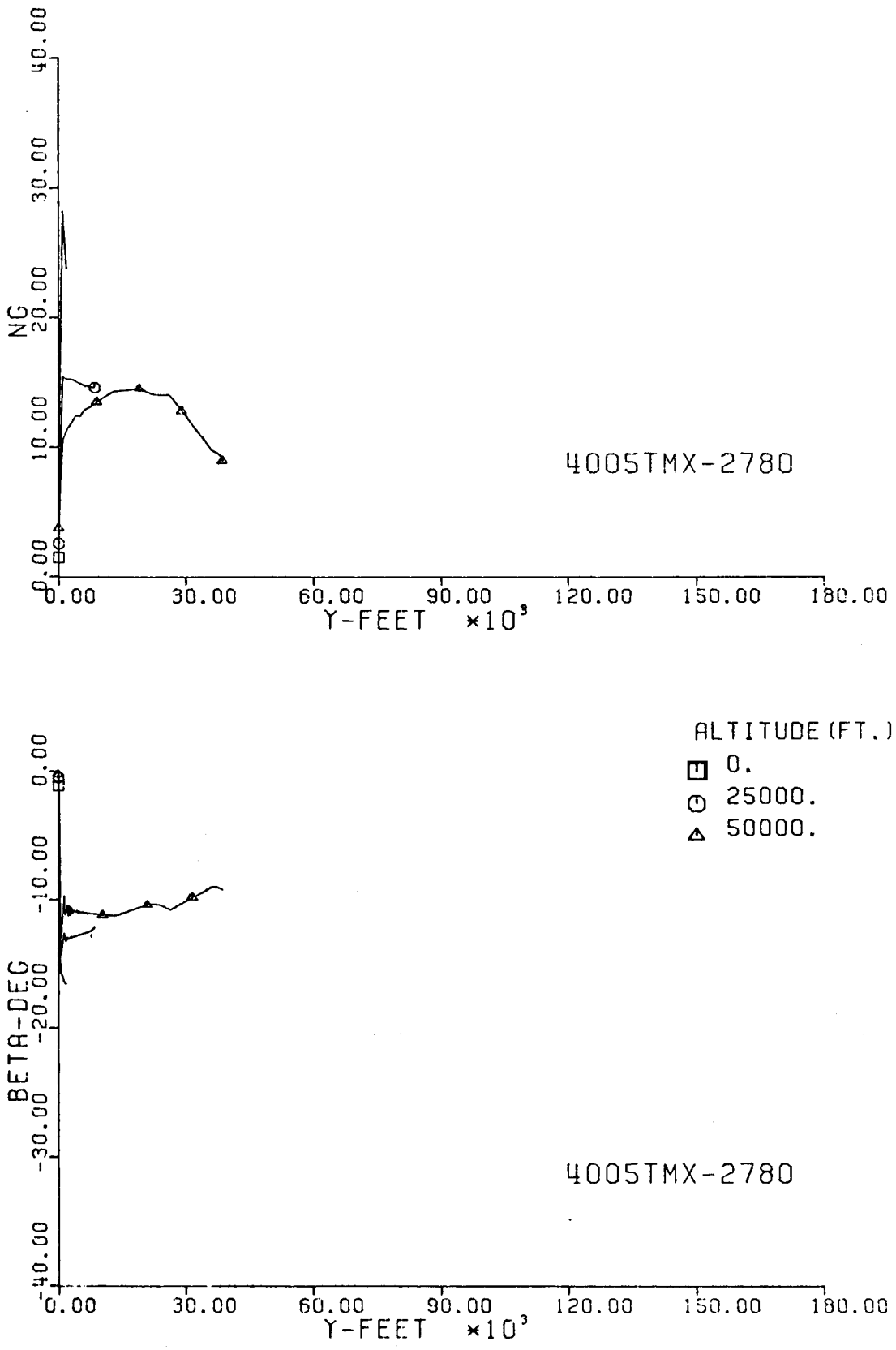

Fig. 222-III. Number of G's and Sideslip Angle vs. Downrange Distance, Y.

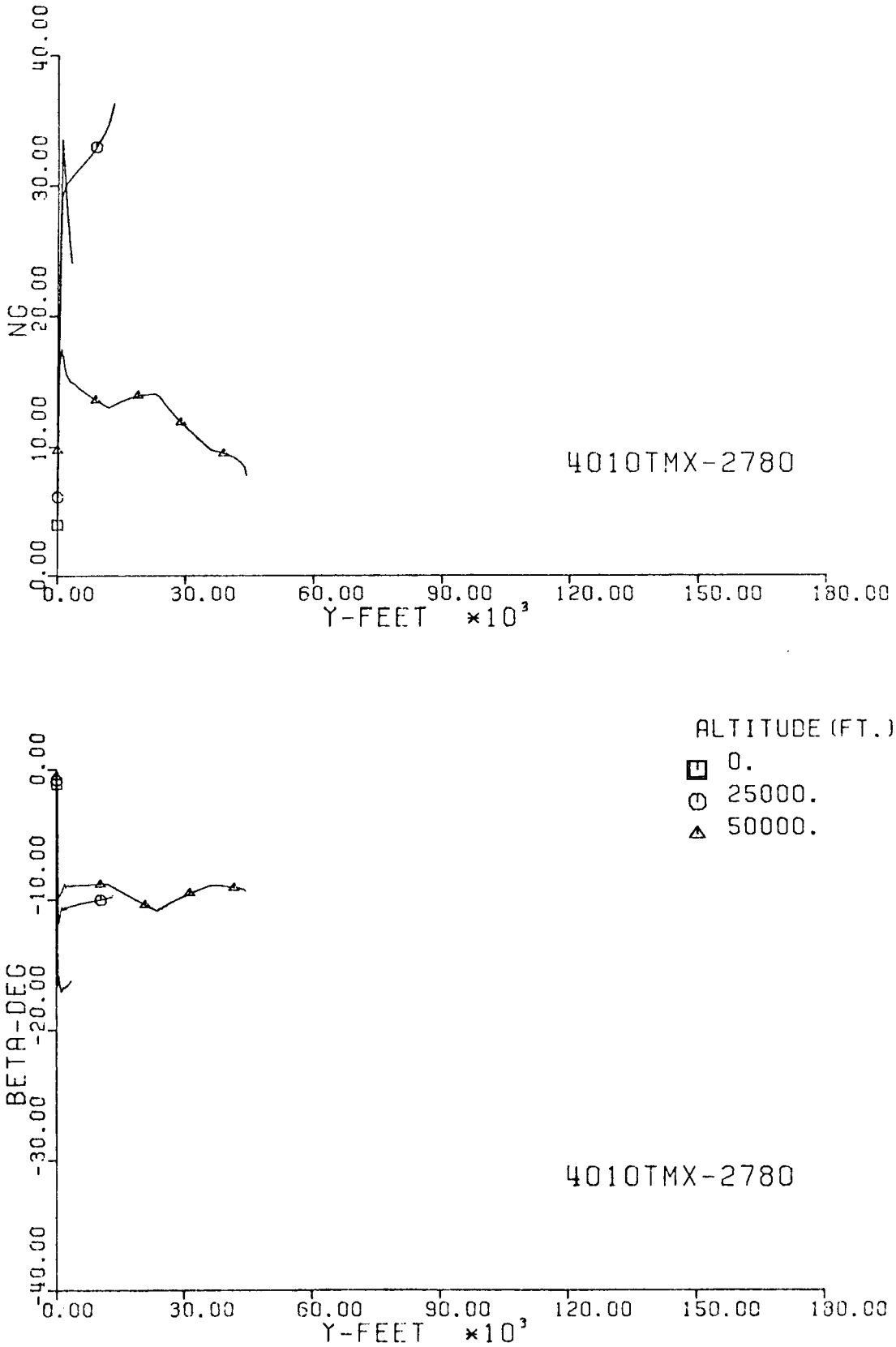

Fig. 223-III. Number of G's and Sideslip Angle vs. Downrange Distance, Y.

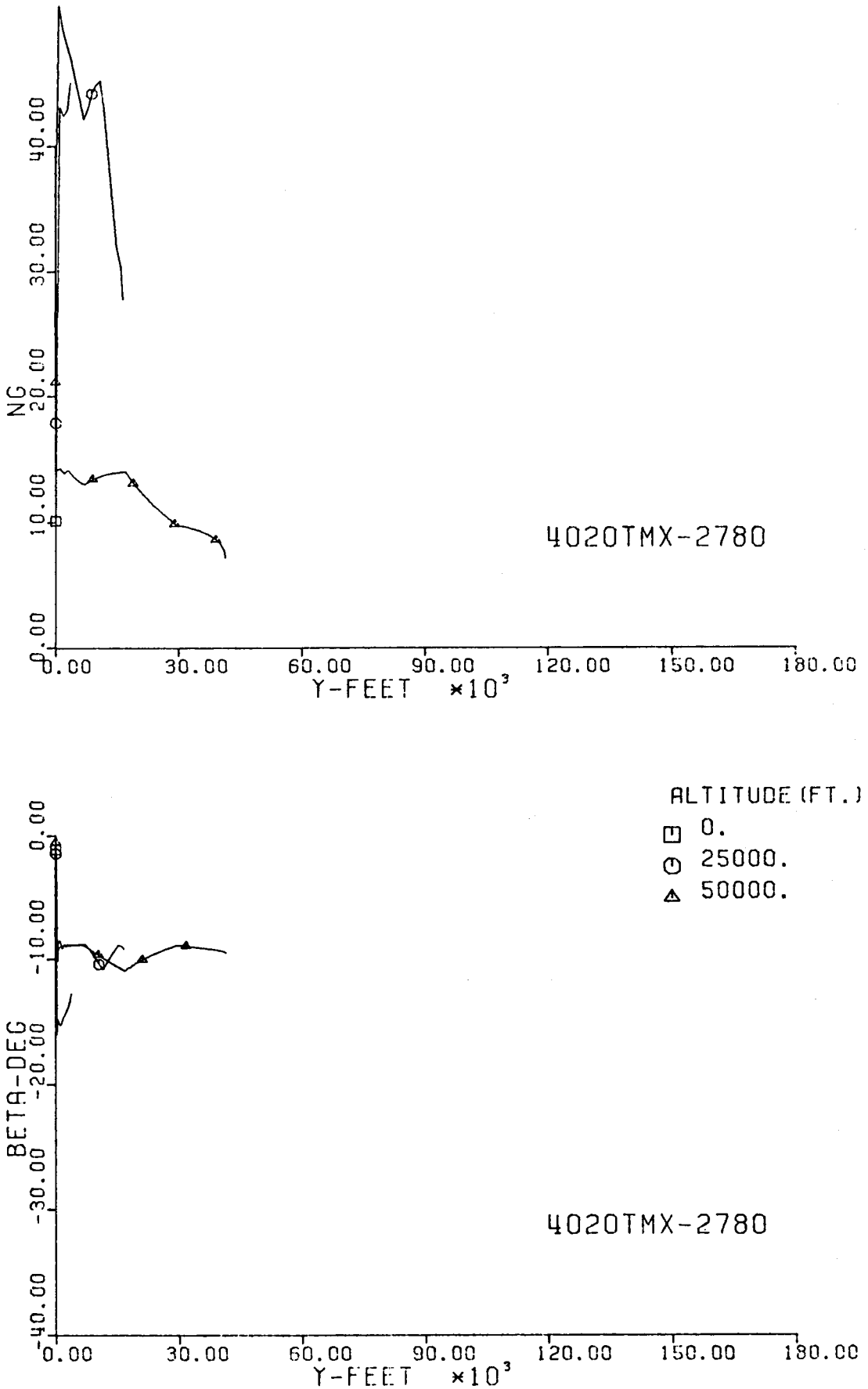

Fig. 224-III. Number of G's and Sideslip Angle vs. Downrange Distance, Y.

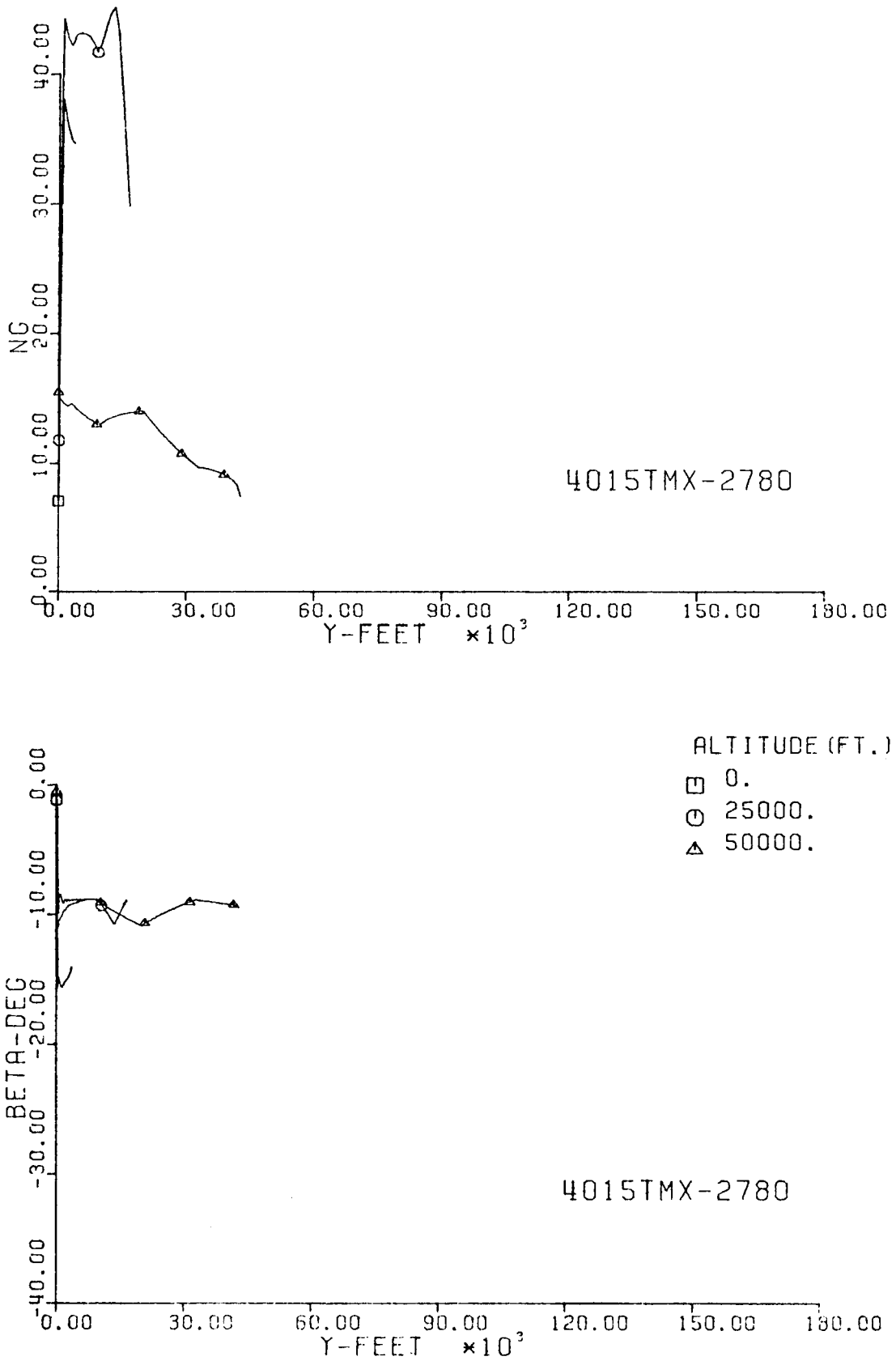

Fig. 225-III. Number of G's and Sideslip Angle vs. Downrange Distance, Y.

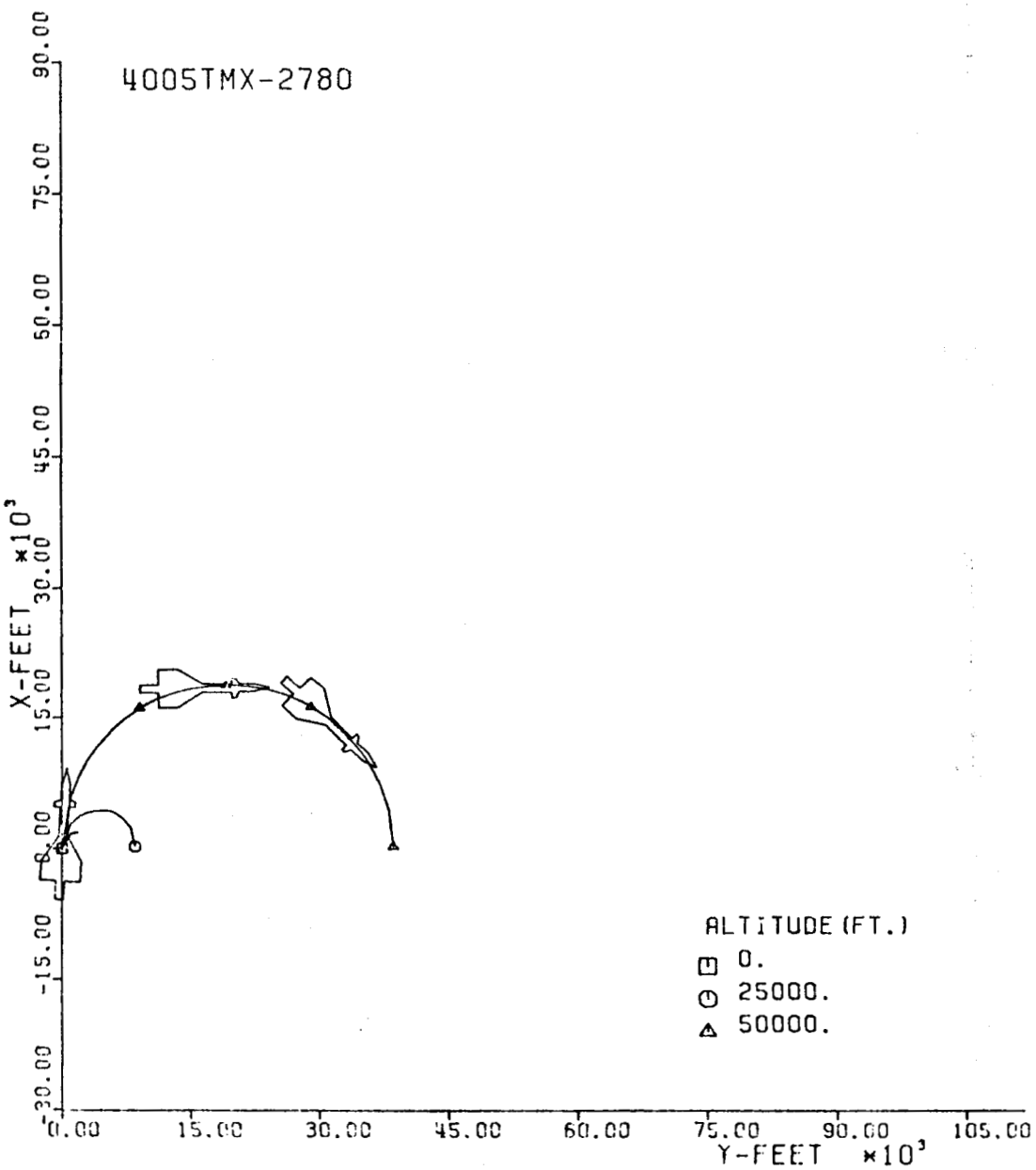

Fig. 226-III. Constant Altitude Flight Path, X vs. Y.

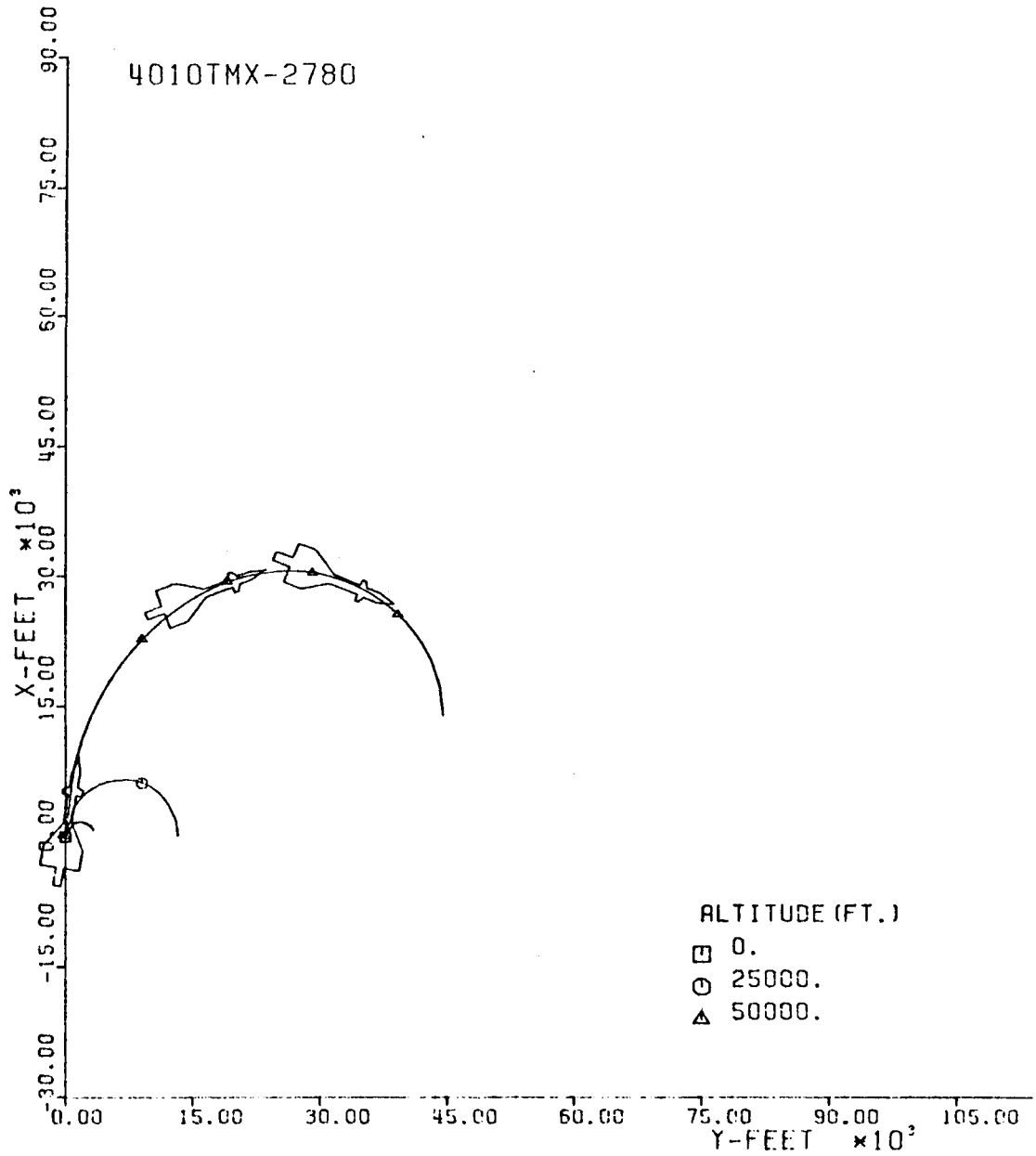

Fig. 227-III. Constant Altitude Flight Path, X vs. Y.

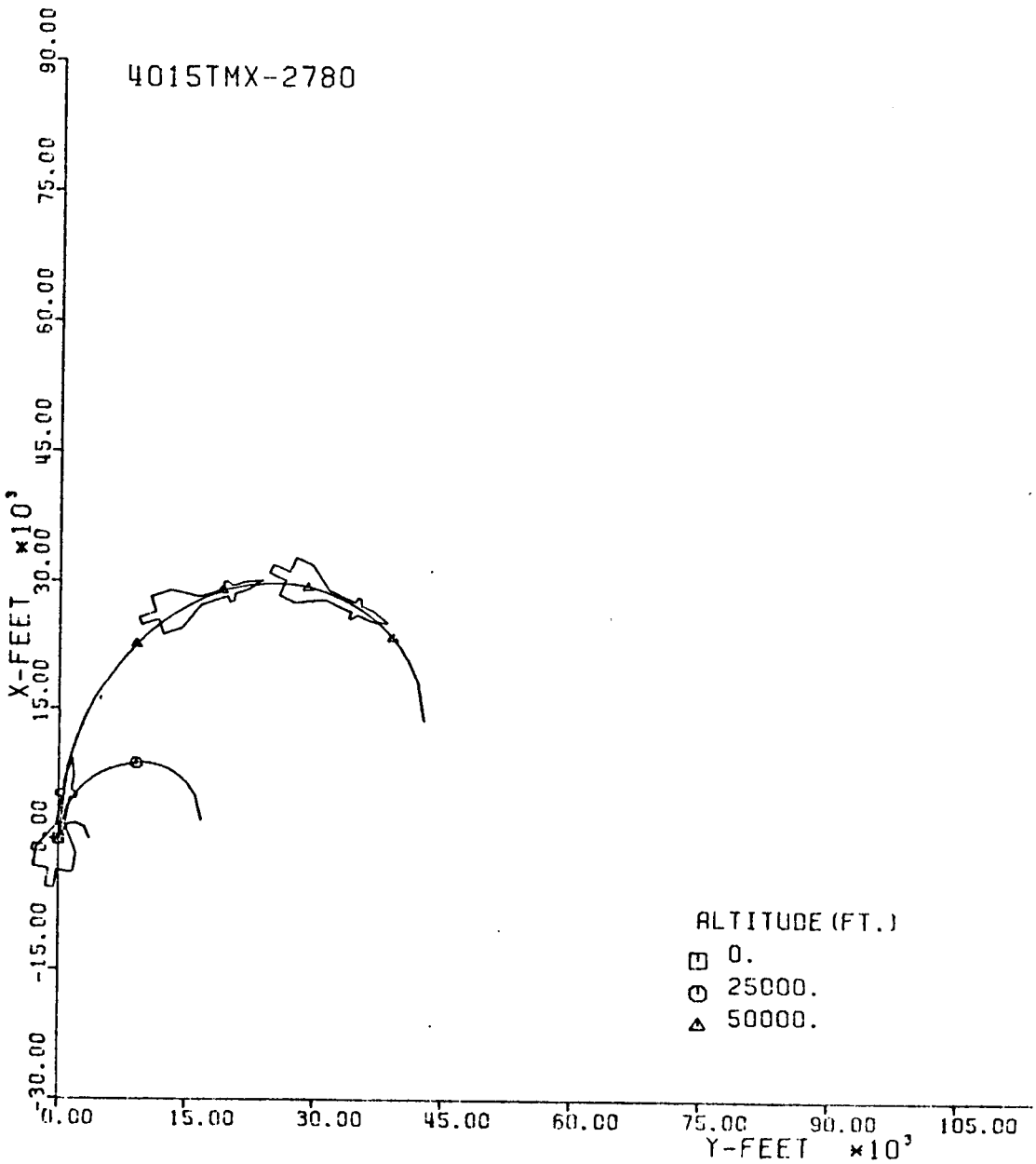

Fig. 228-III. Constant Altitude Flight Path, X vs. Y.

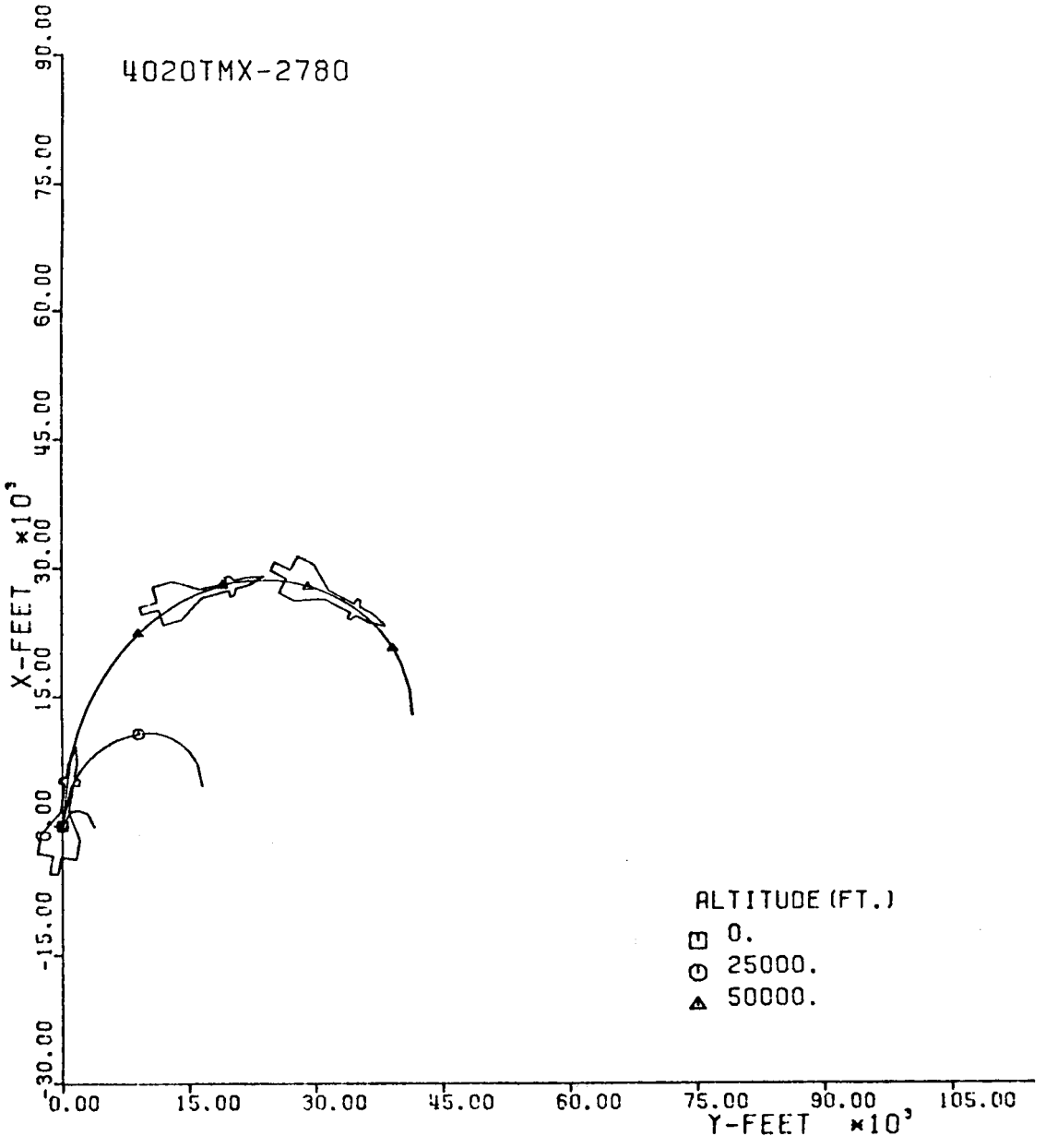

Fig. 229-III. Constant Altitude Flight Path, X vs. Y.

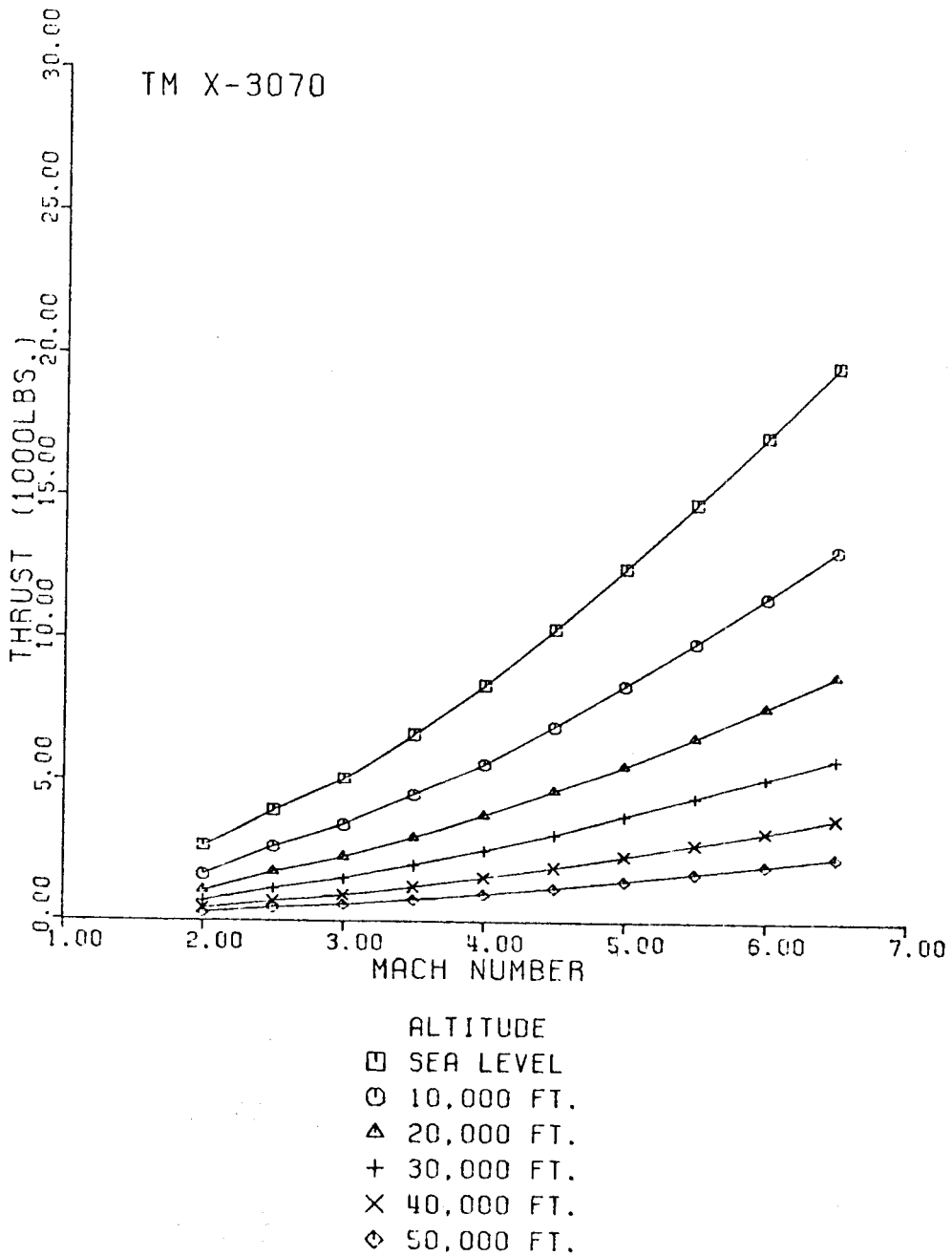

Fig. 230-I. Thrust vs. Terminal Mach No.

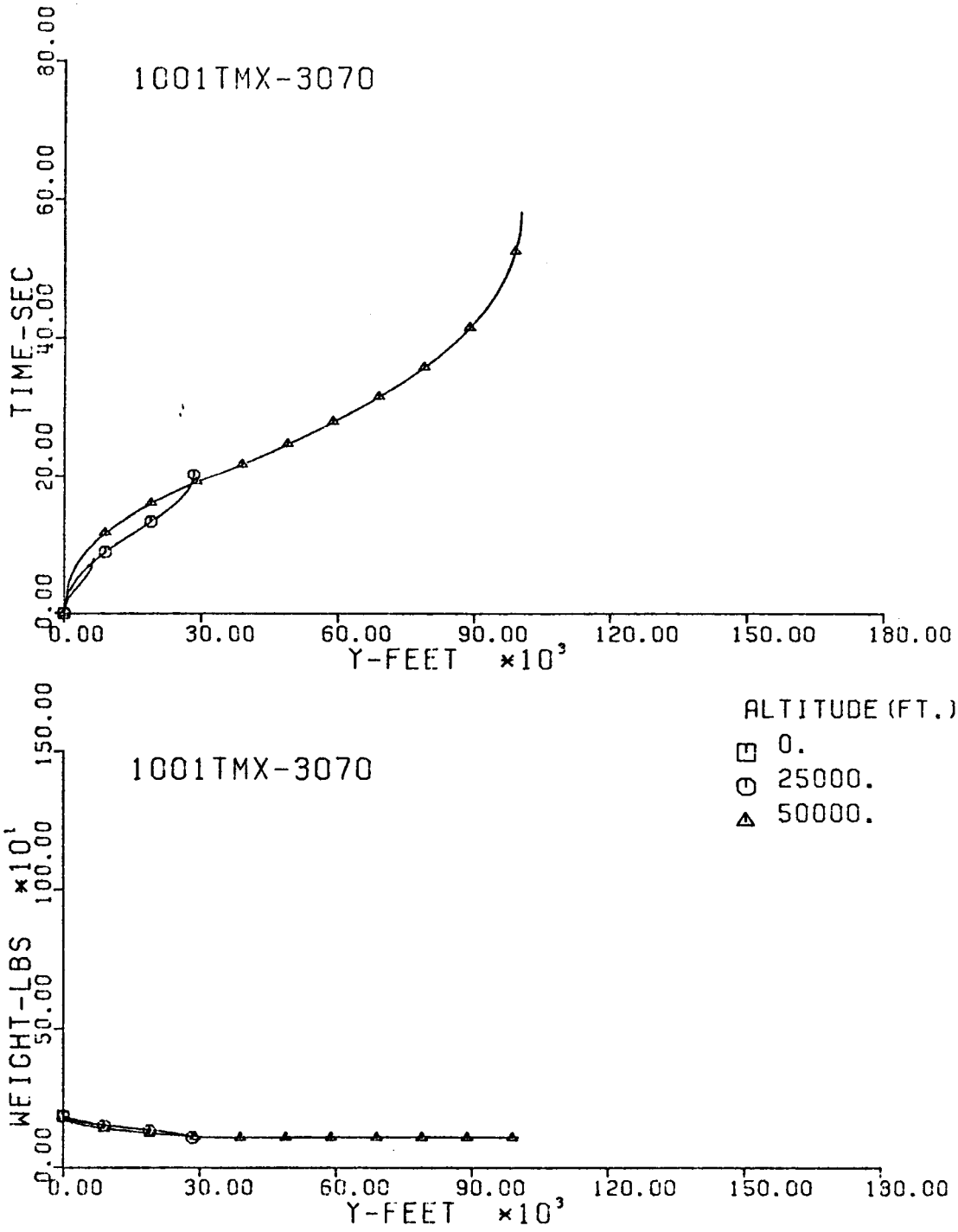

Fig. 231-III. Flight Time and Vehicle Weight vs. Downrange Distance, Y.

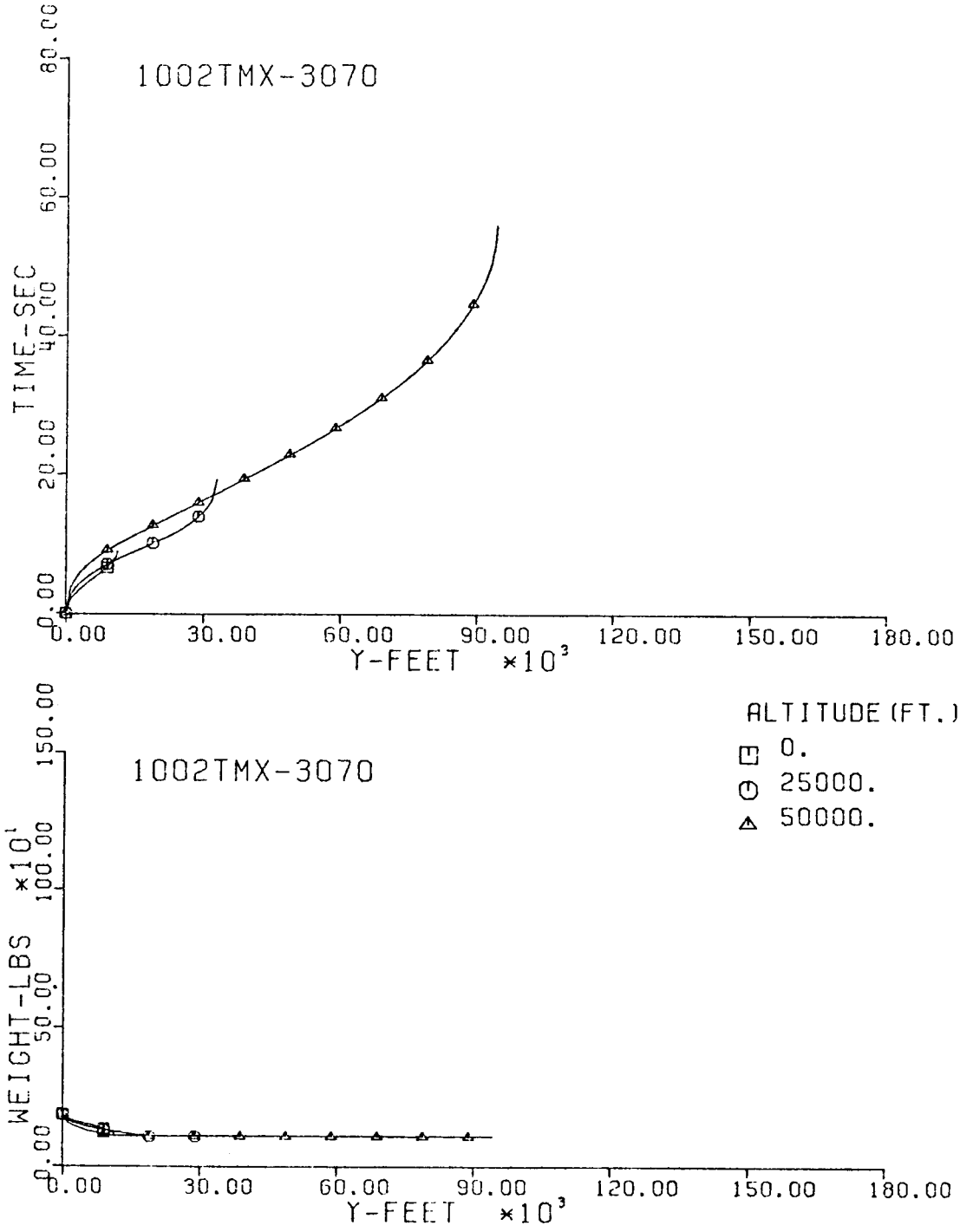

Fig. 232-III. Flight Time and Vehicle Weight vs. Downrange Distance, Y.

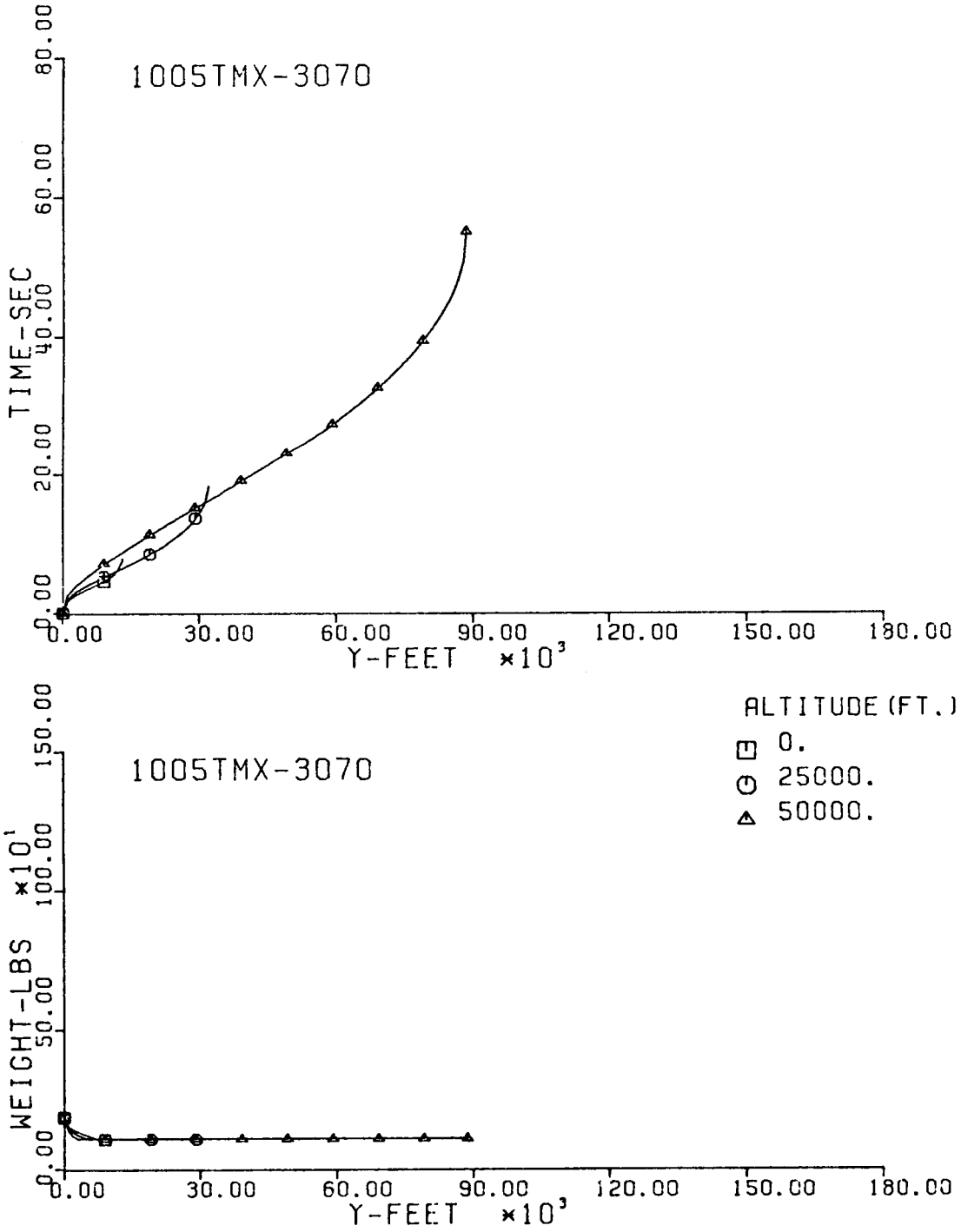

Fig. 233-III. Flight Time and Vehicle Weight vs. Downrange Distance, Y.

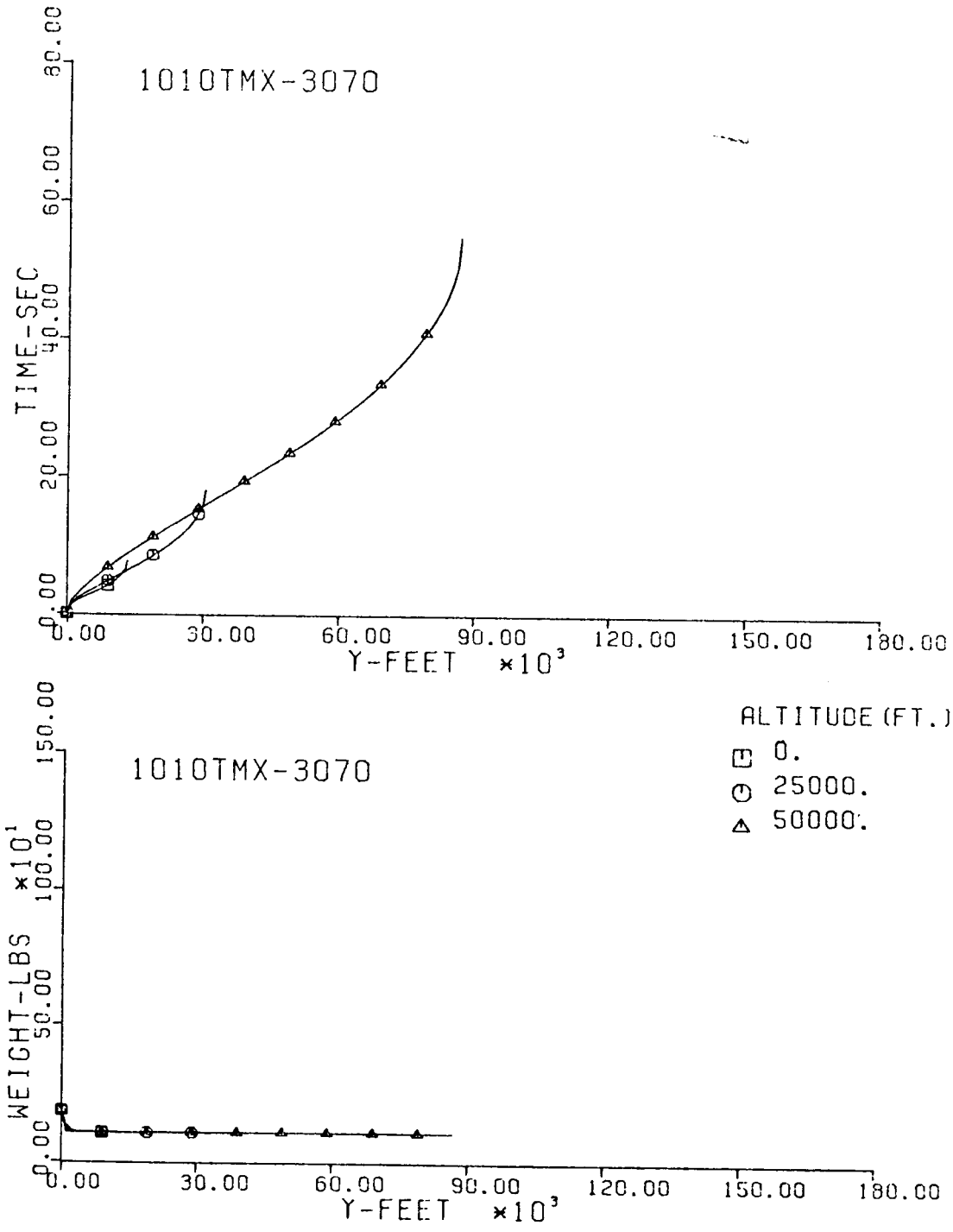

Fig. 234-III. Flight Time and Vehicle Weight vs. Downrange Distance, Y.

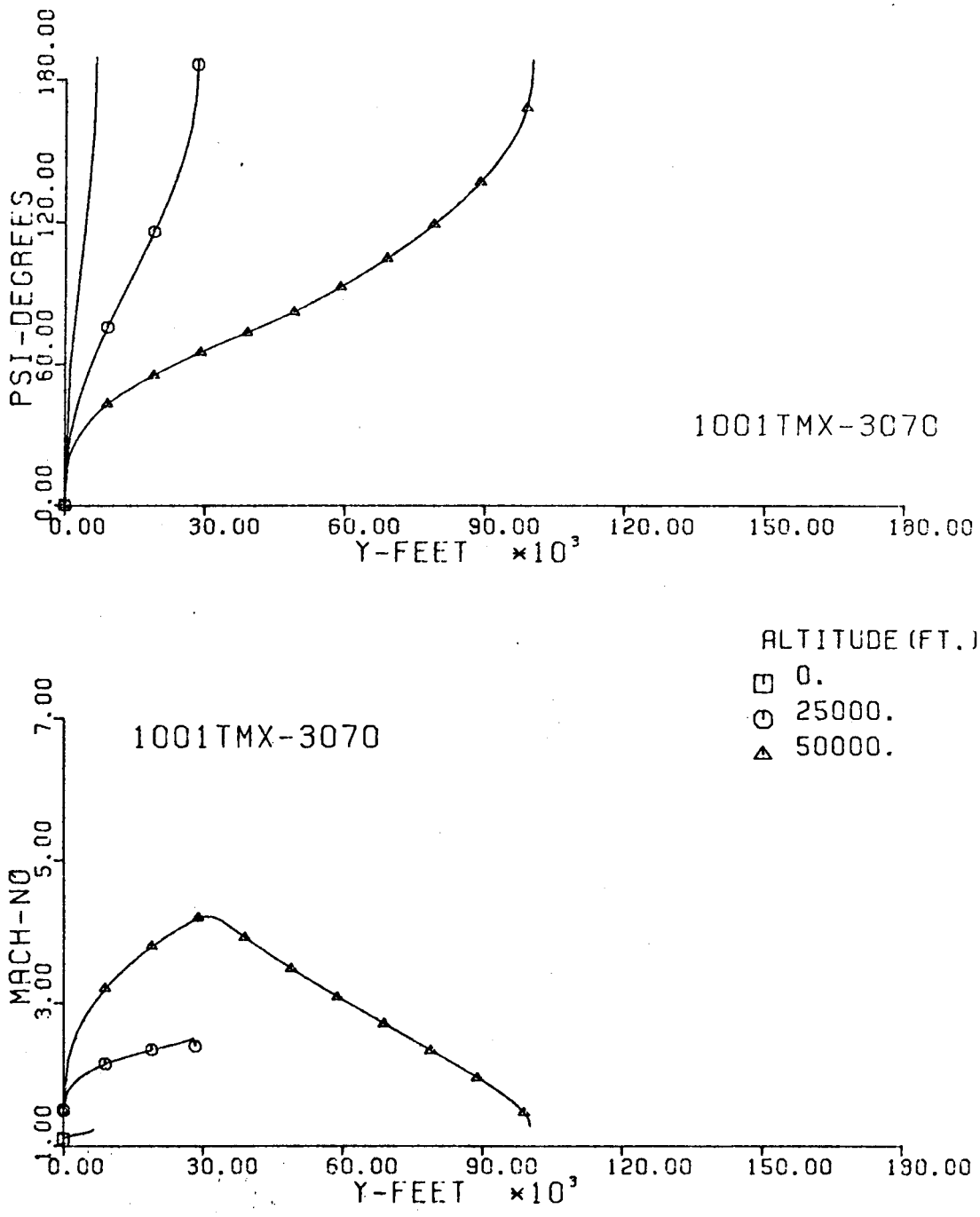

Fig. 235-III. Heading Angle and Mach No. vs. Downrange Distance, Y.

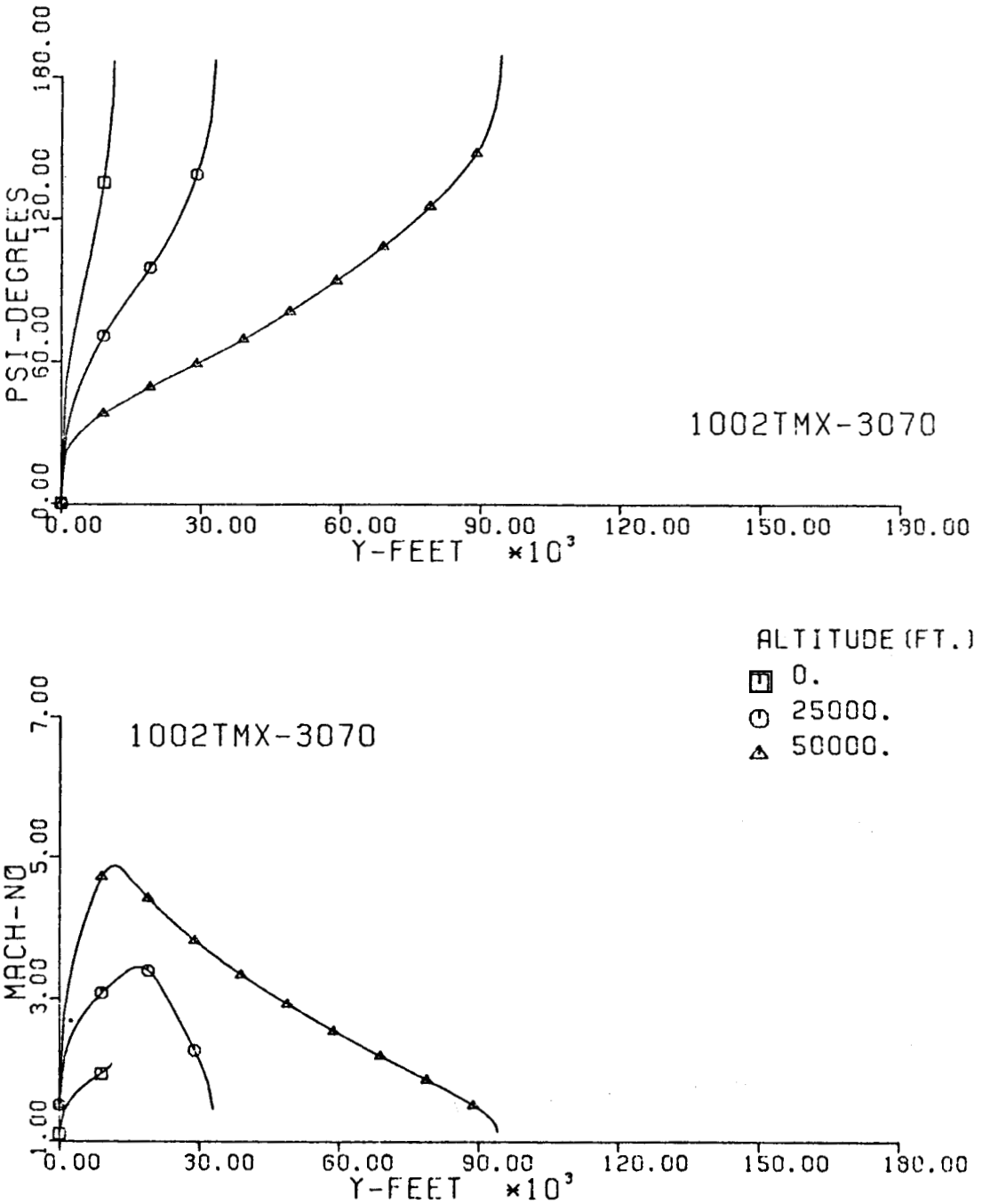

Fig. 236-III. Heading Angle and Mach No. vs. Downrange Distance, Y.

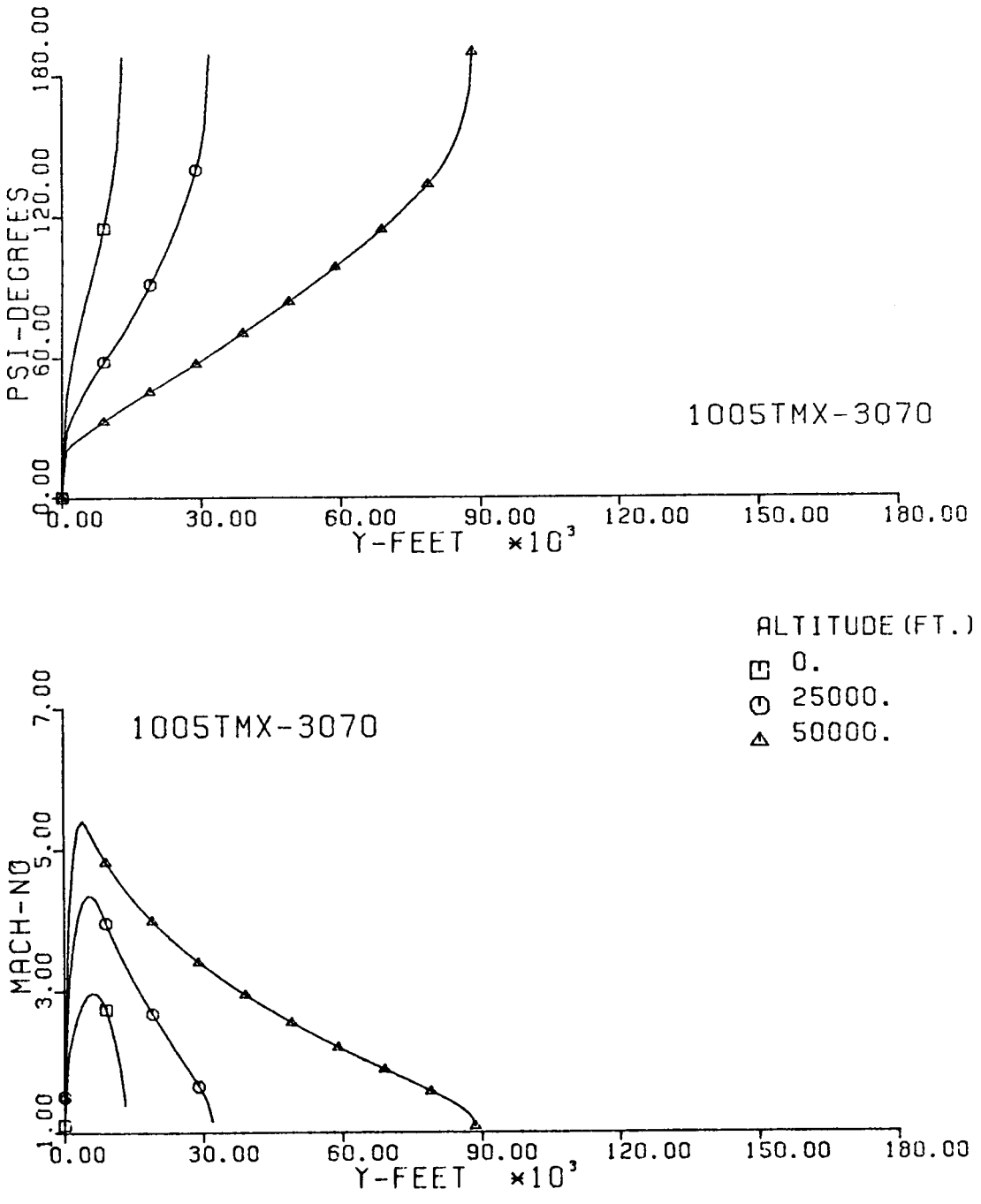

Fig. 237-III. Heading Angle and Mach No. vs. Downrange Distance, Y.

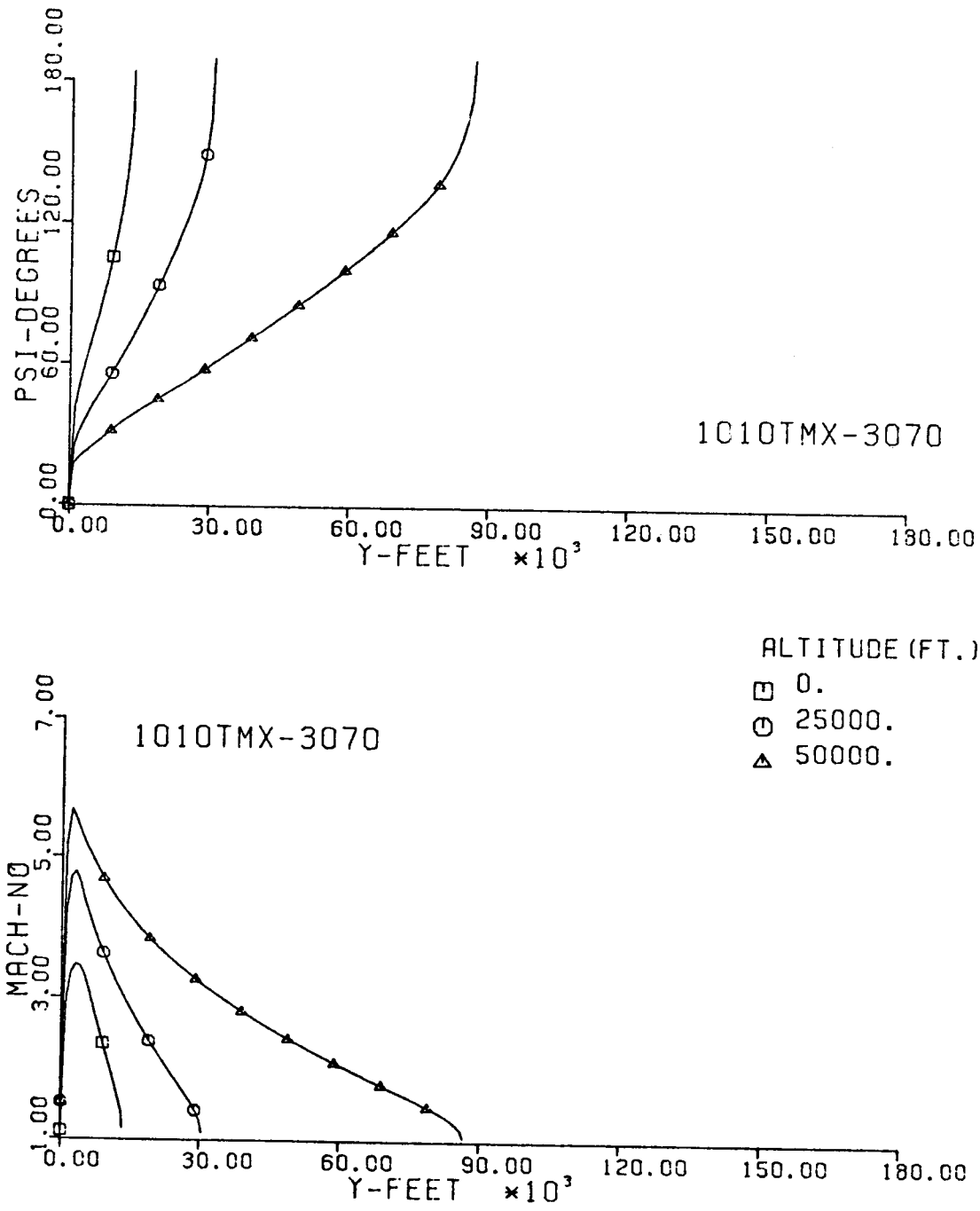

Fig. 238-III. Heading Angle and Mach No. vs. Downrange Distance, Y.

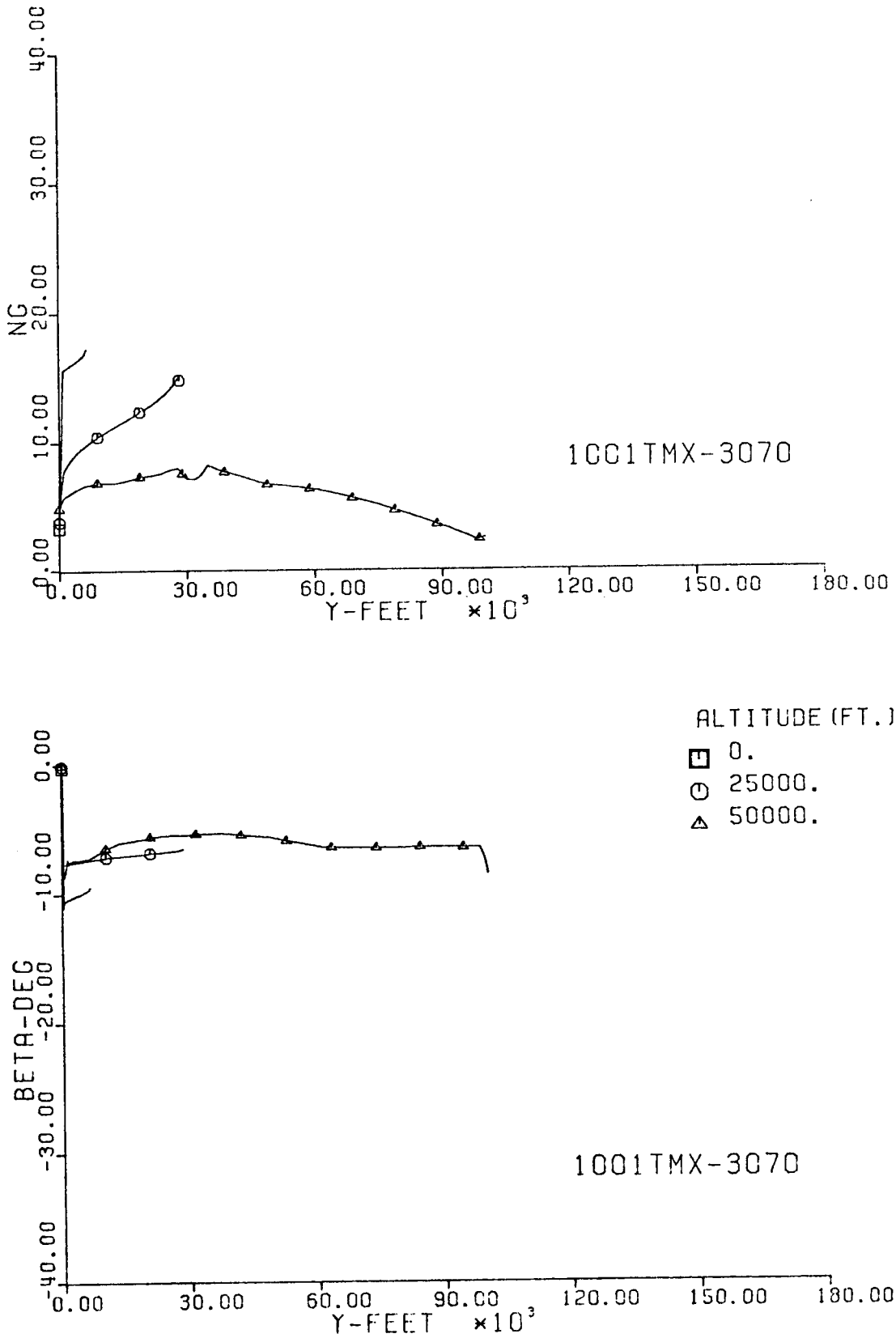

Fig. 239-III. Number of G's and Sideslip Angle vs. Downrange Distance, Y.

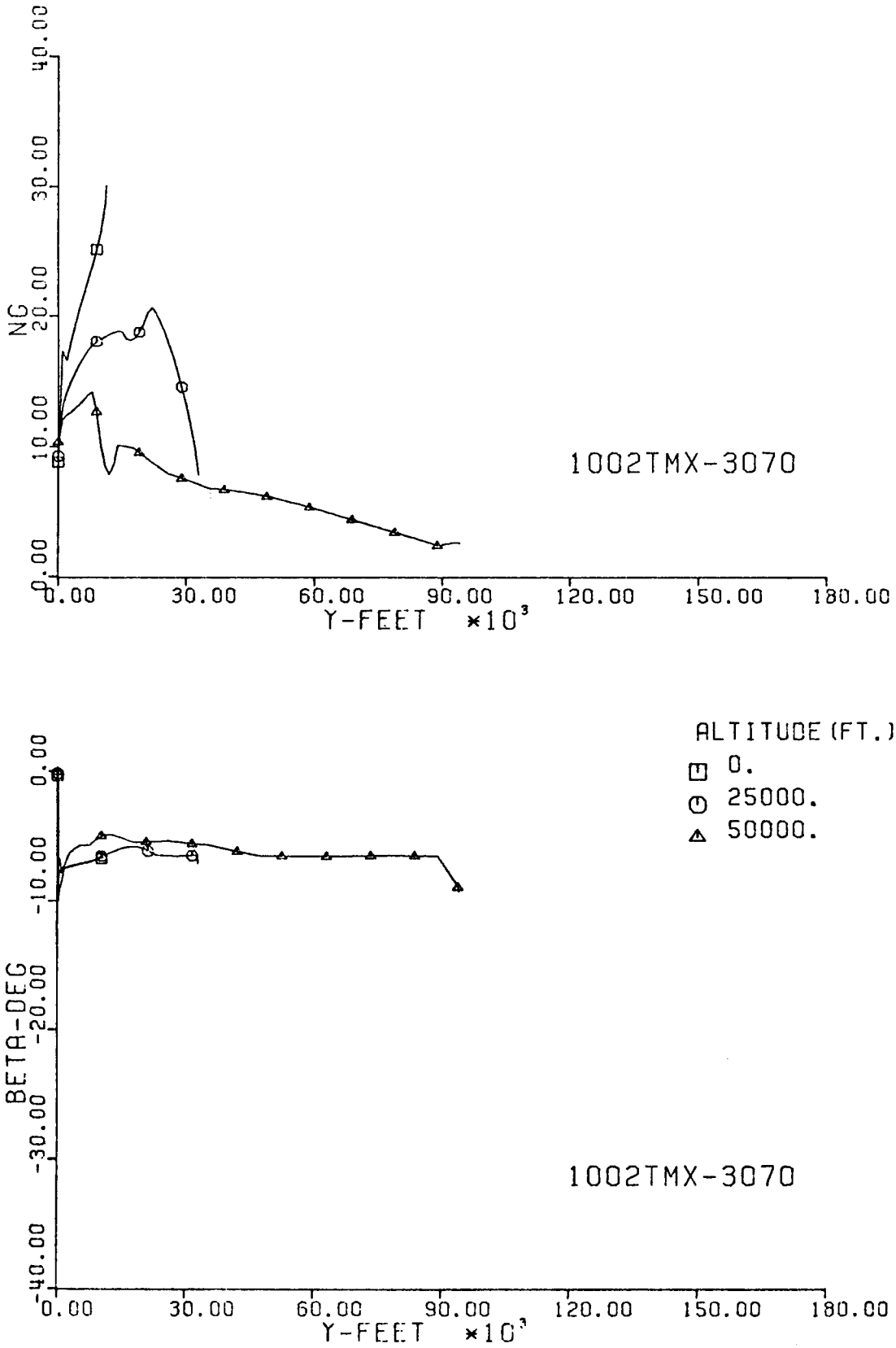

Fig. 240-III. Number of G's and Sideslip Angle vs. Downrange Distance, Y.

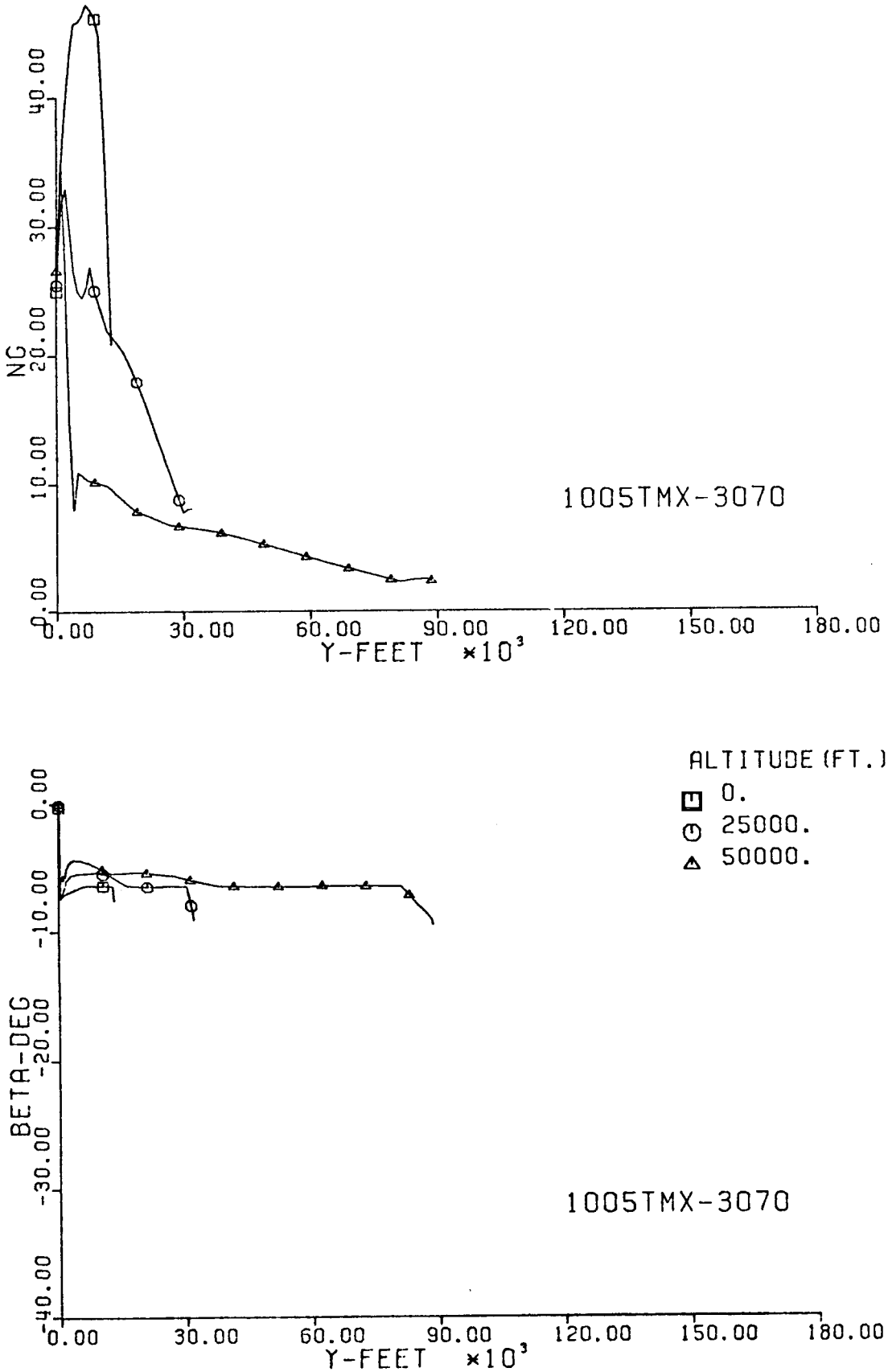

Fig. 241-III. Number of G's and Sideslip Angle vs. Downrange Distance, Y.

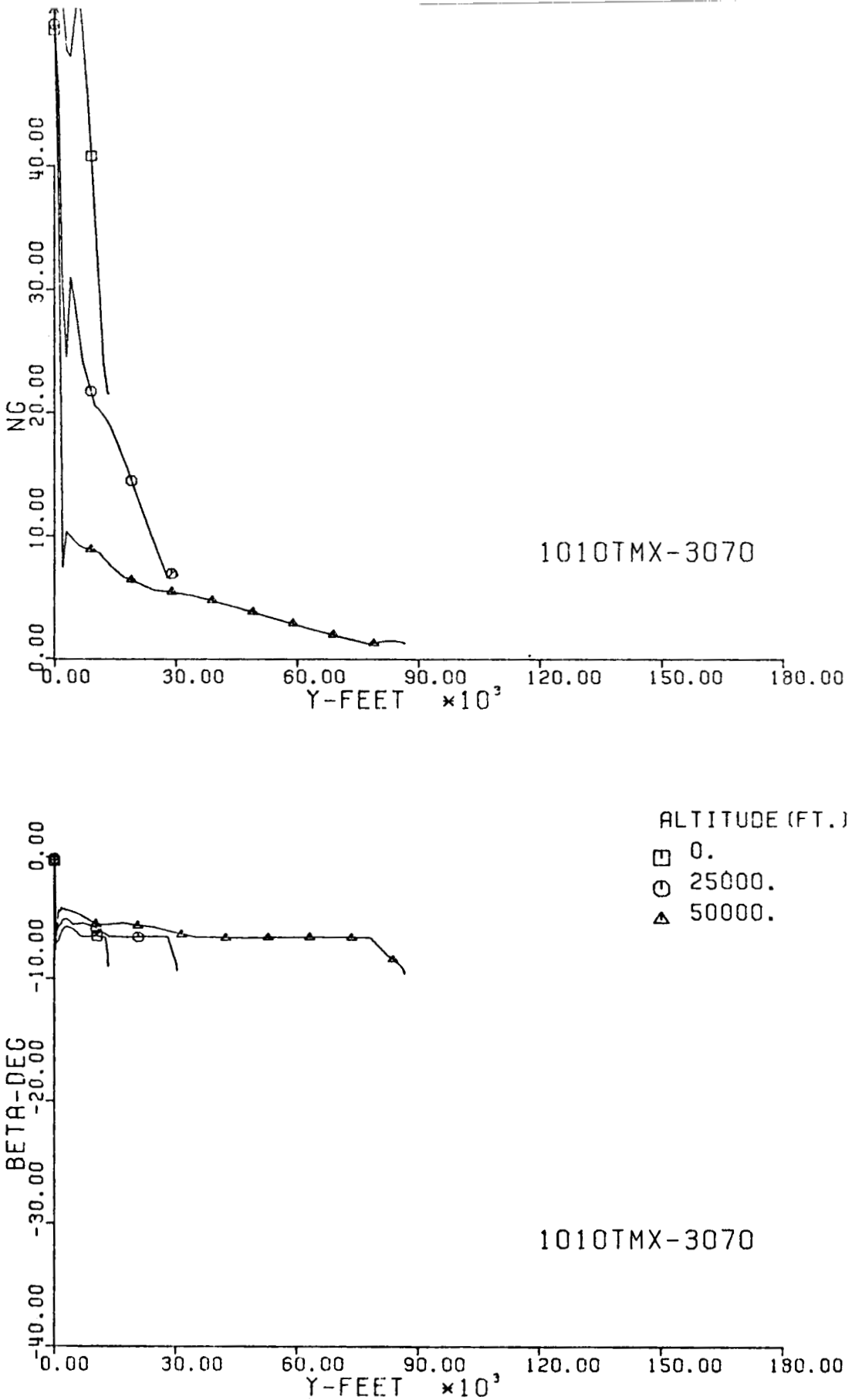

Fig. 242-III. Number of G's and Sideslip Angle vs. Downrange Distance, Y.

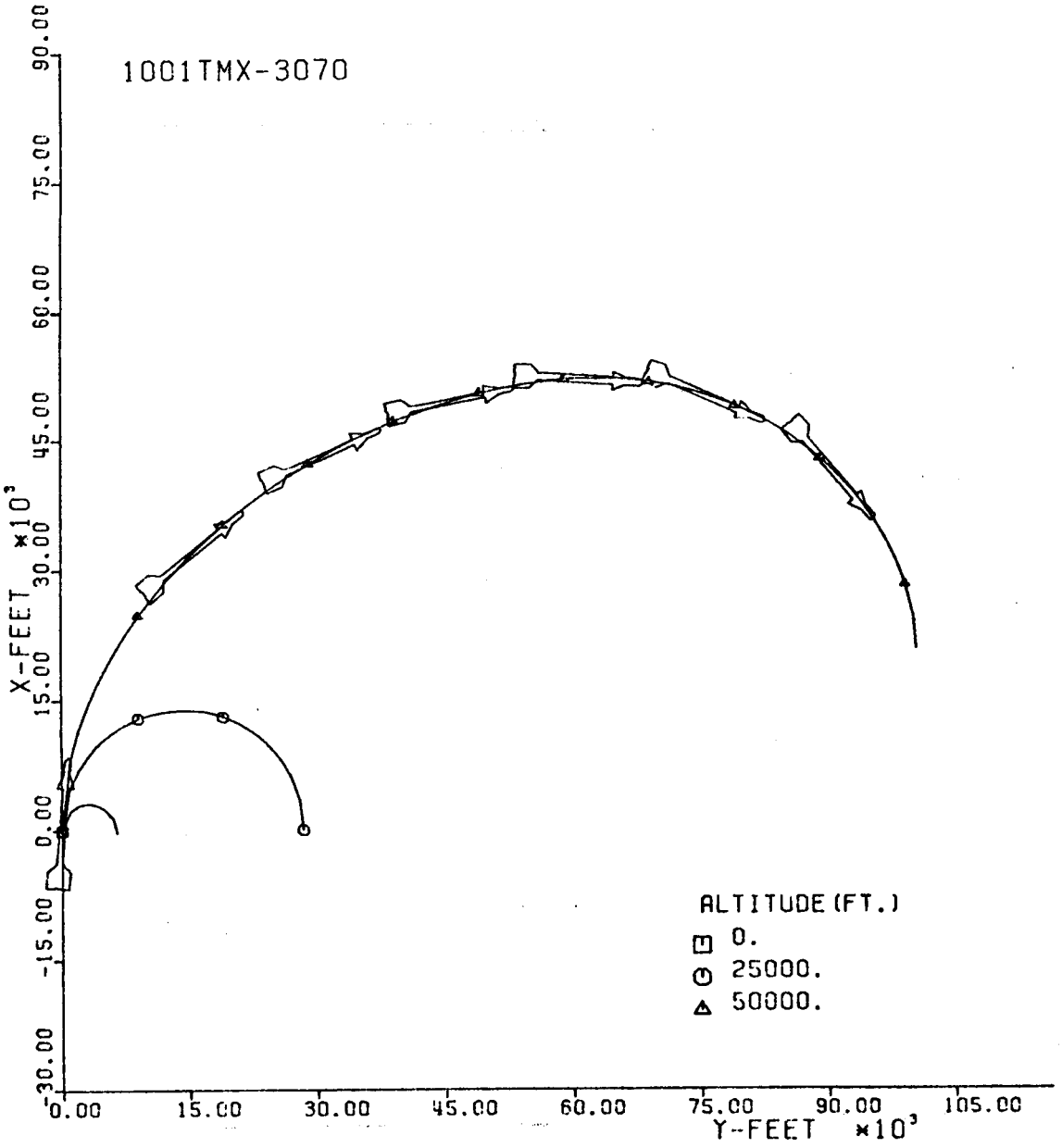

Fig. 243-III. Constant Altitude Flight Path, X vs. Y.

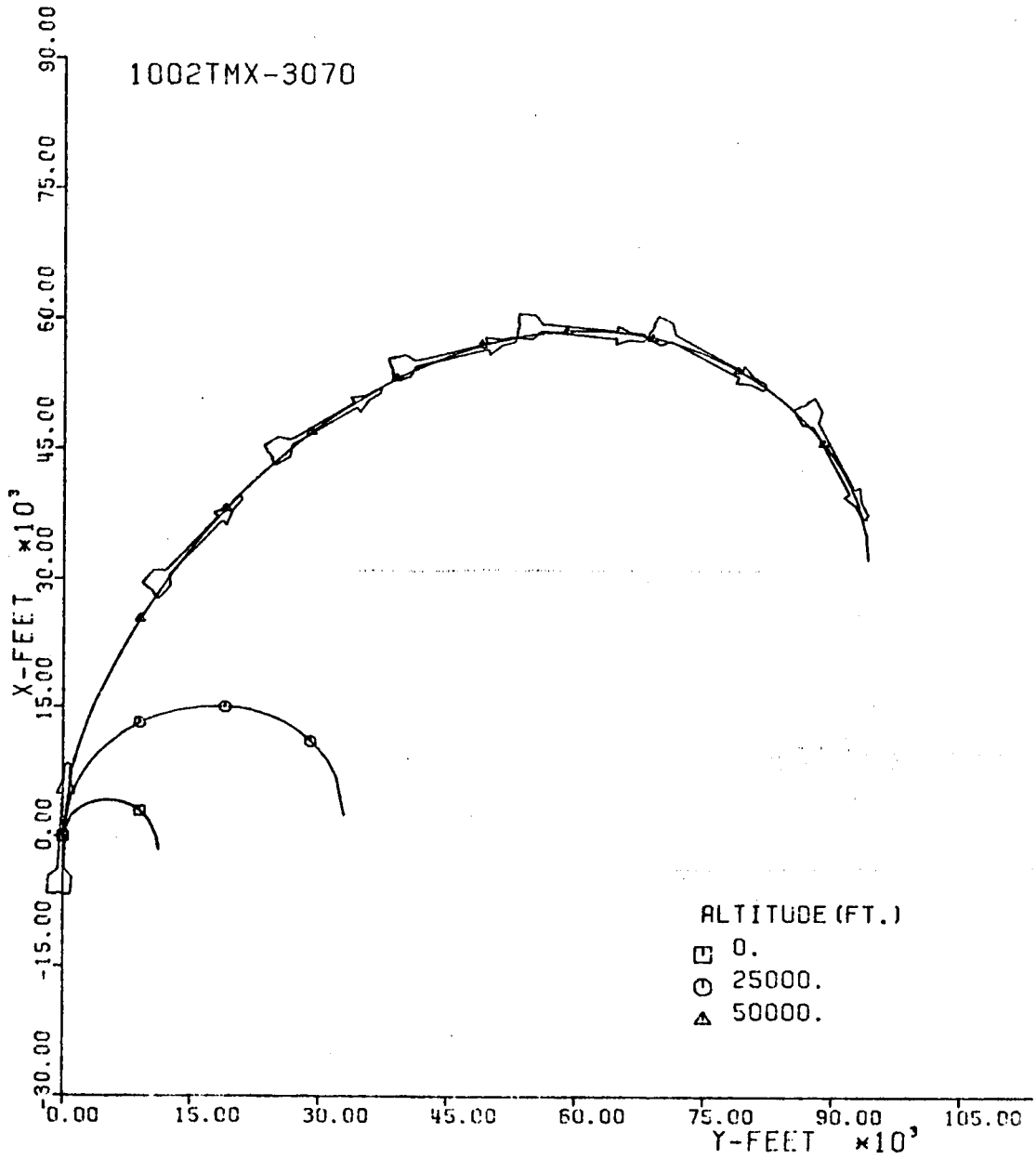

Fig. 244-III. Constant Altitude Flight Path, X vs. Y.

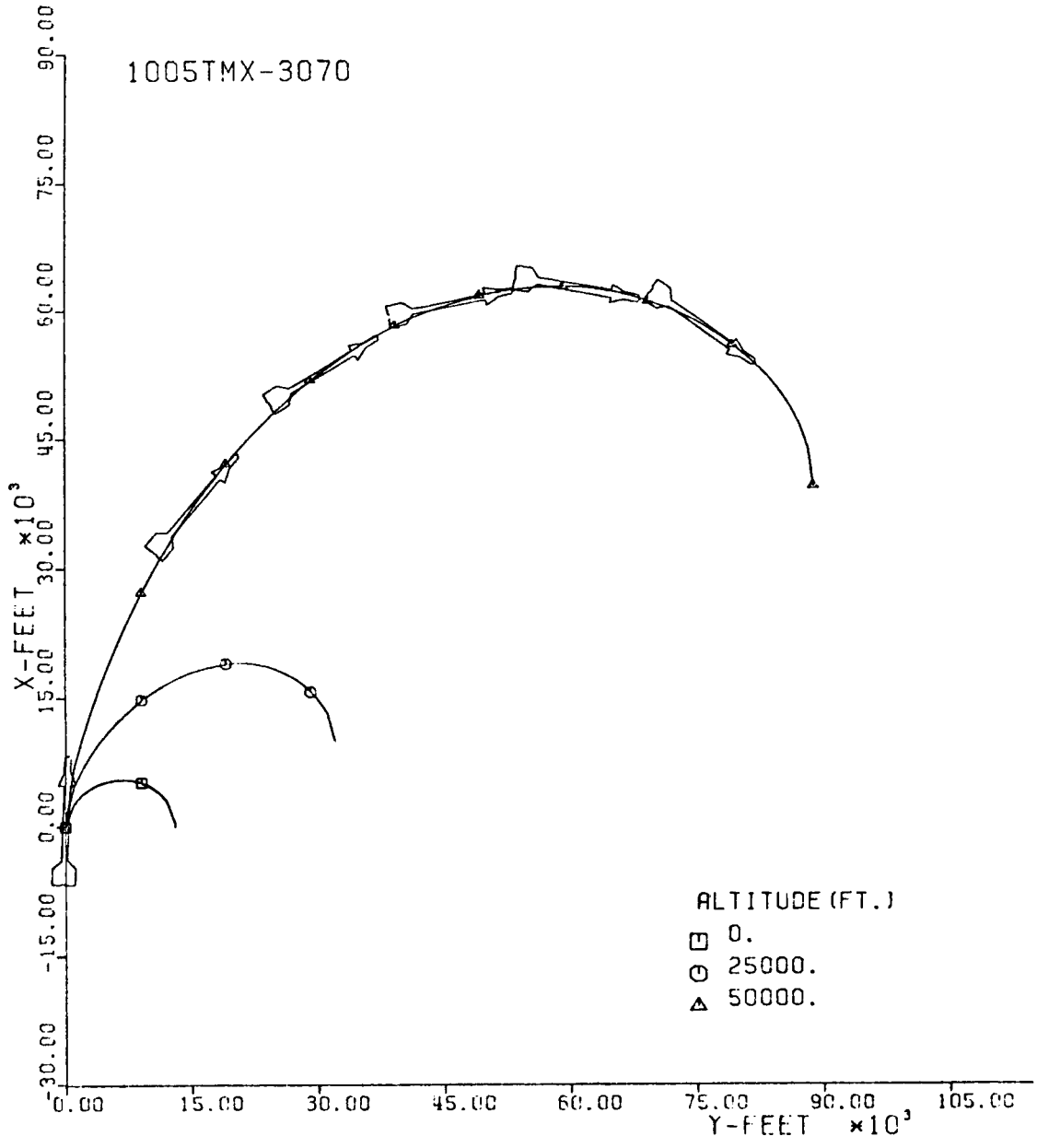

Fig. 245-III. Constant Altitude Flight Path, X vs. Y.

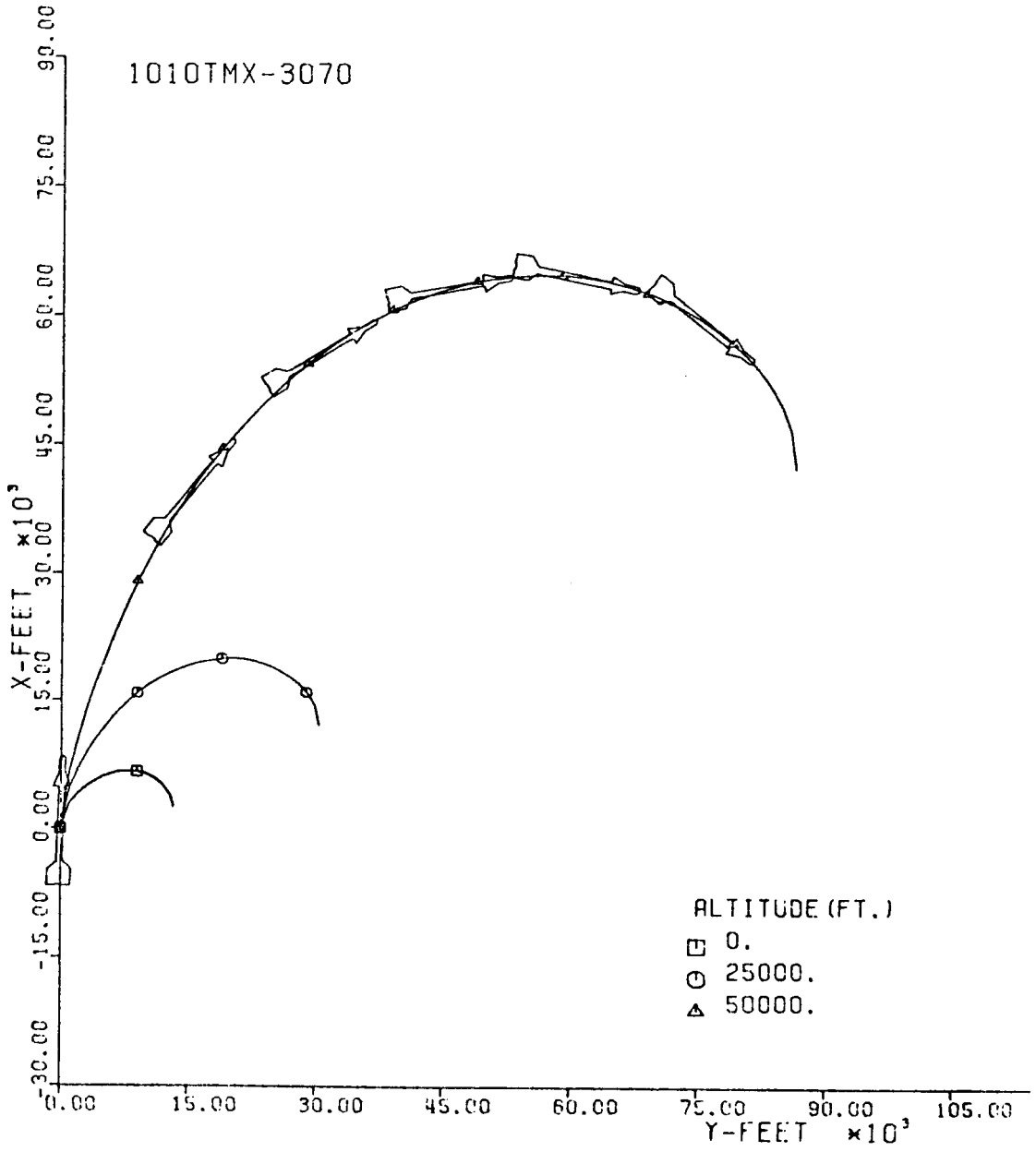

Fig. 246-III. Constant Altitude Flight Path, X vs. Y.

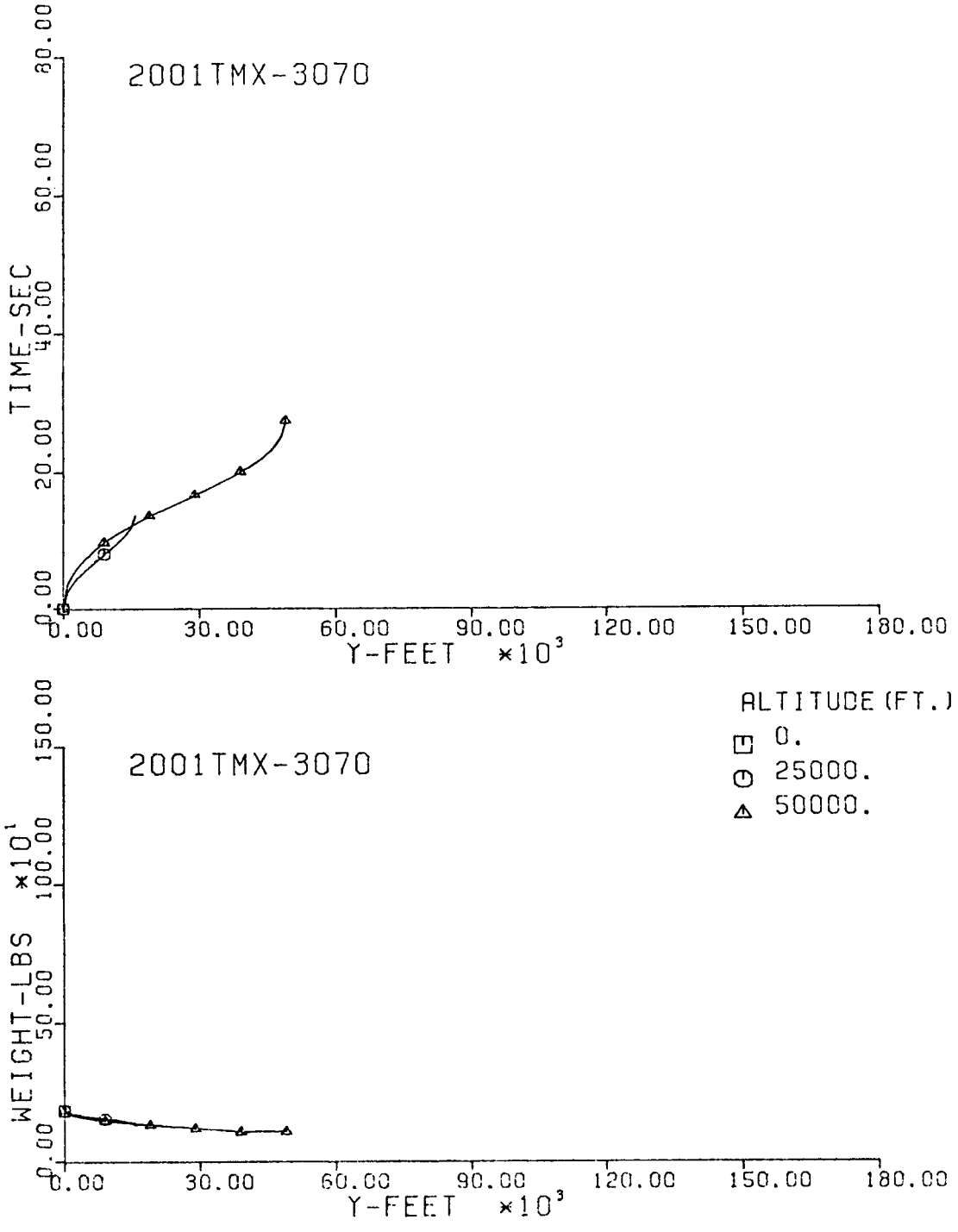

Fig. 247-III. Flight Time and Vehicle Weight vs. Downrange Distance, Y.

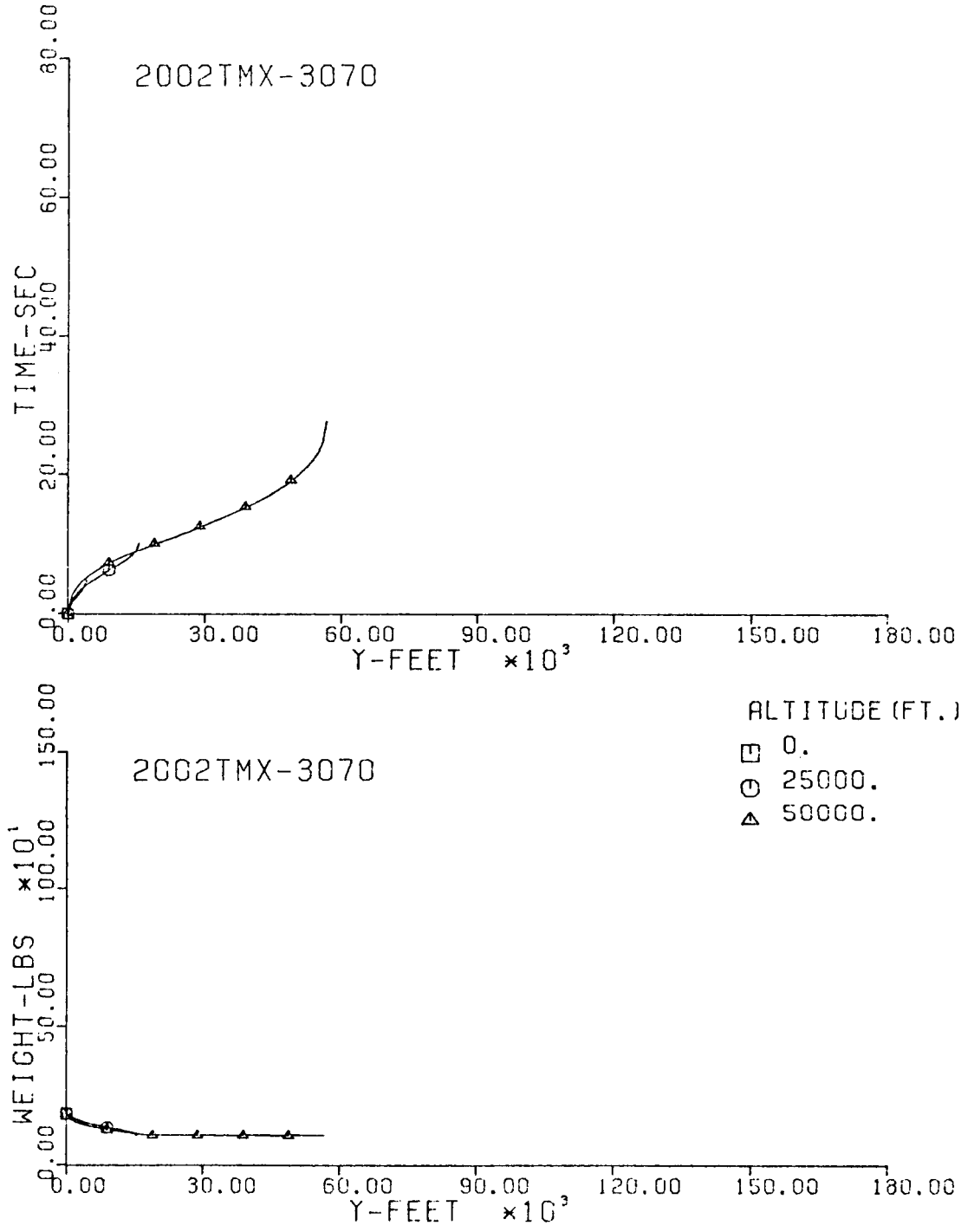

Fig. 248-III. Flight Time and Vehicle Weight vs. Downrange Distance, Y.

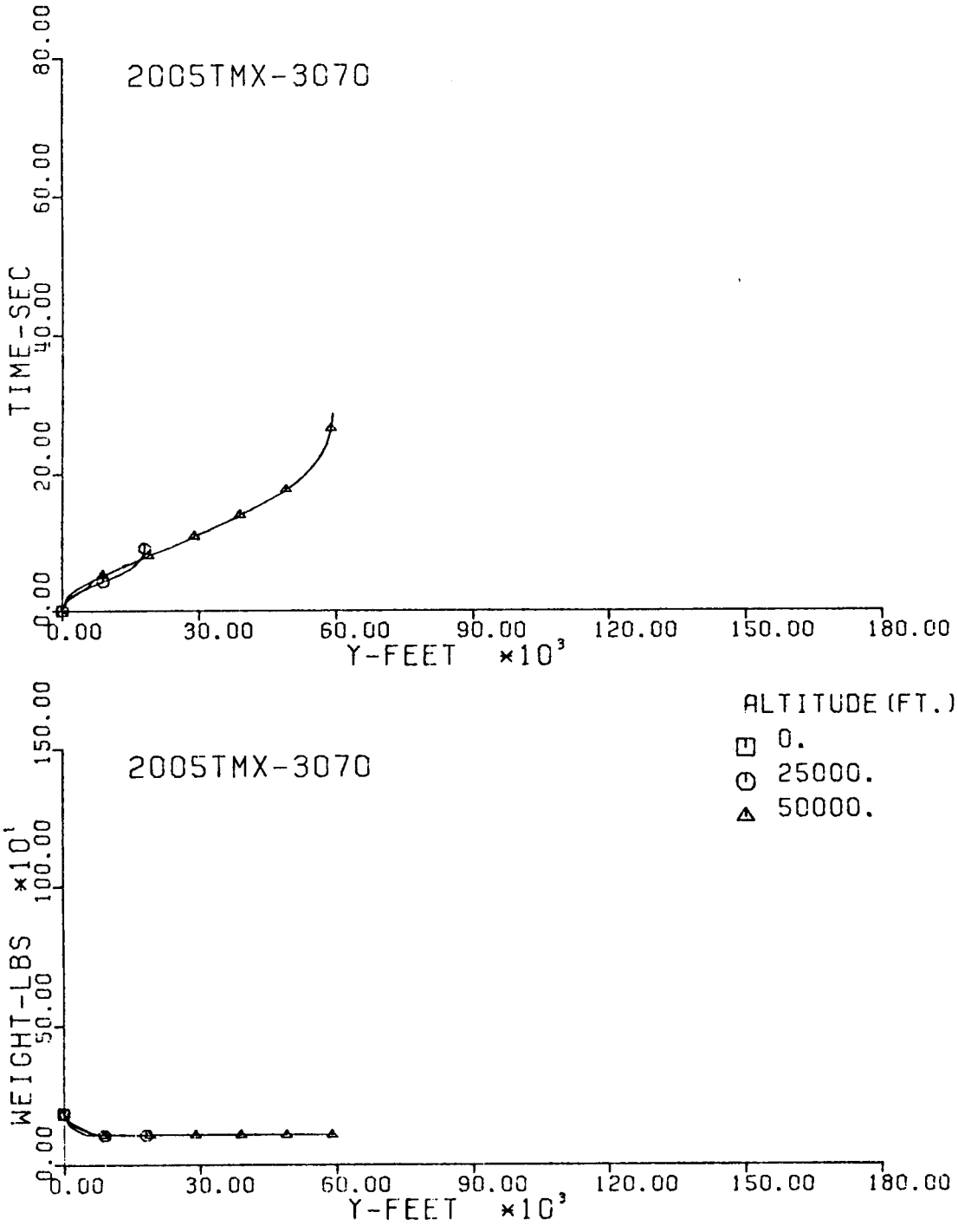

Fig. 249-III. Flight Time and Vehicle Weight vs. Downrange Distance, Y.

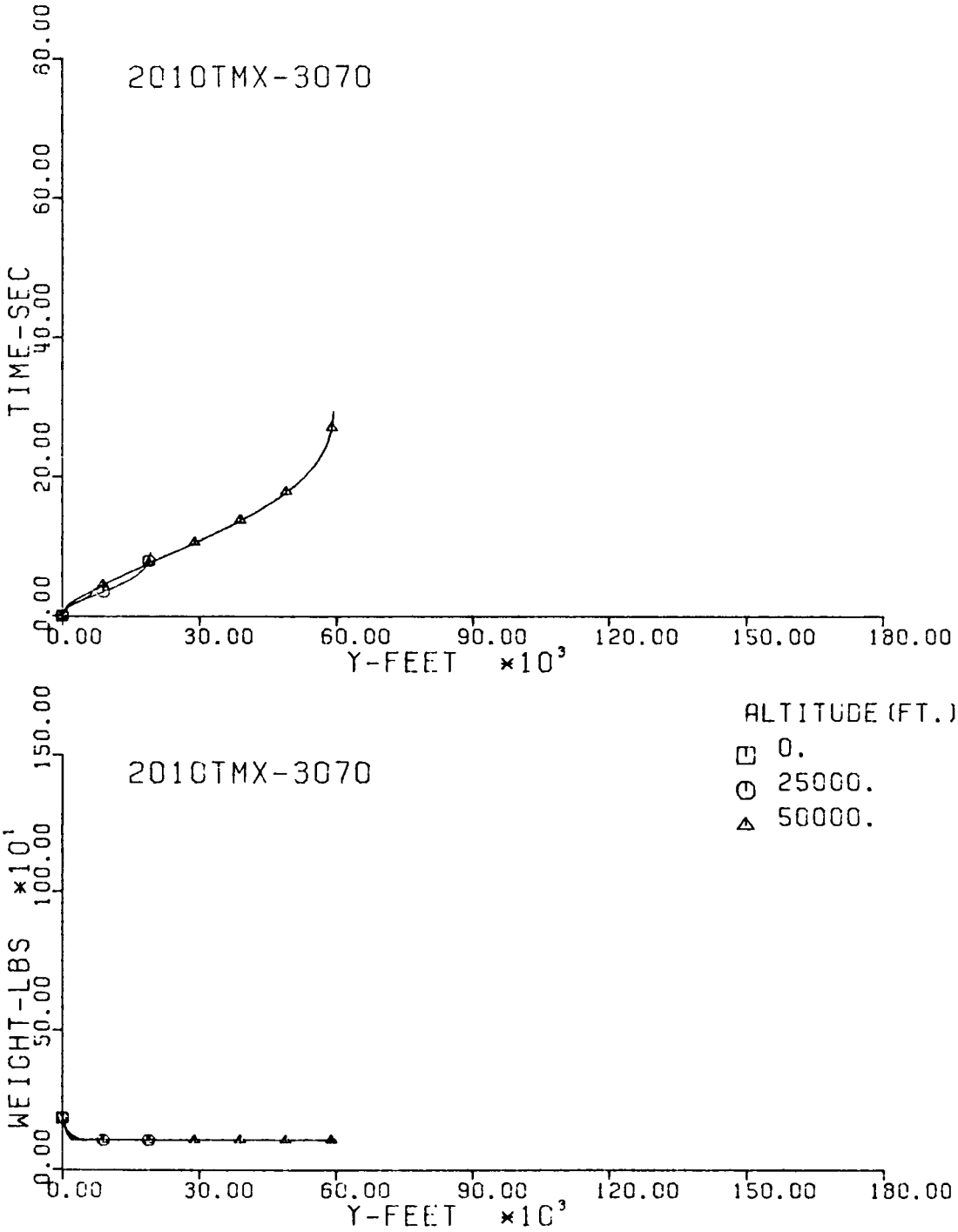

Fig. 250-III. Flight Time and Vehicle Weight vs. Downrange Distance, Y.

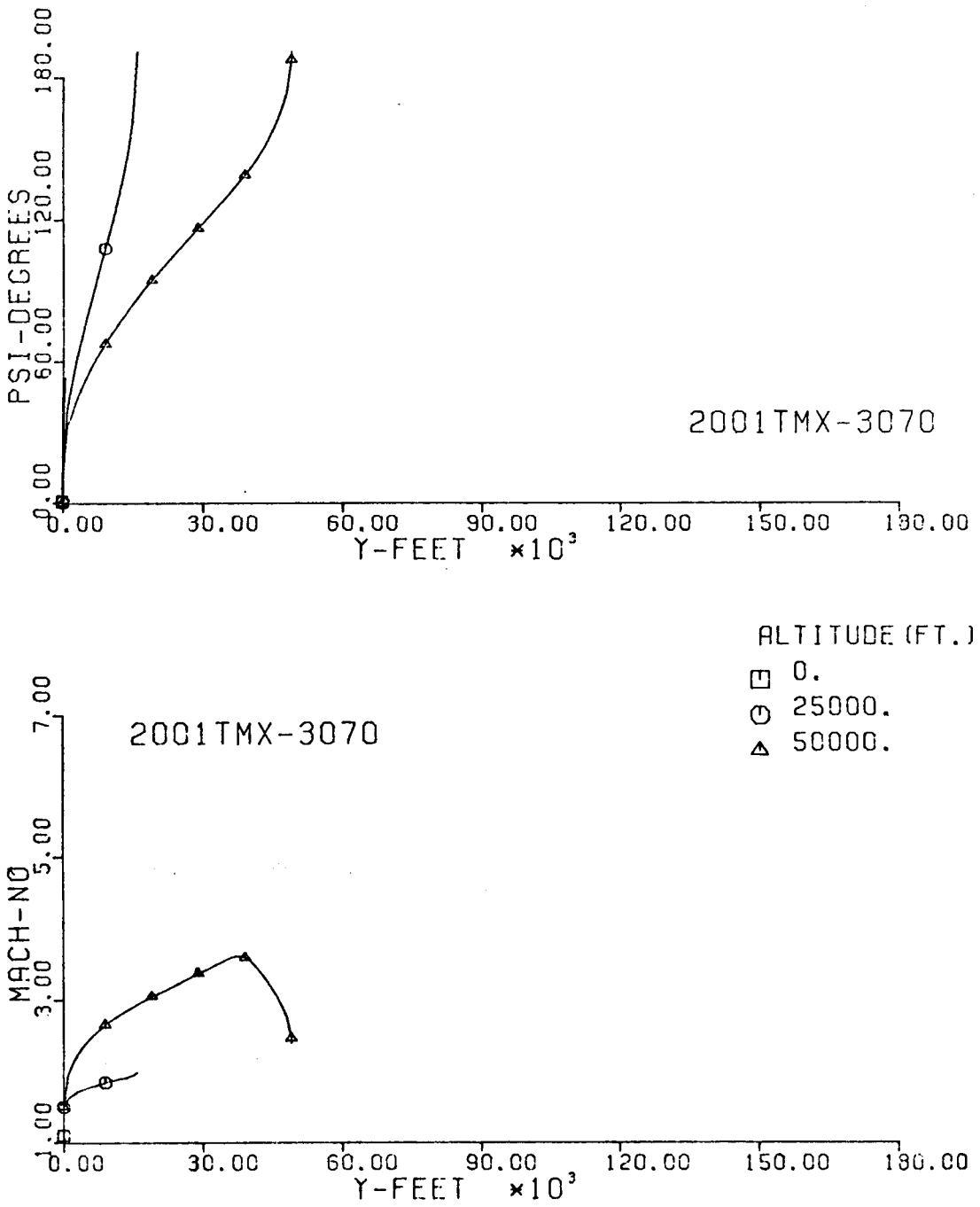

Fig. 251-III. Heading Angle and Mach No. vs. Downrange Distance, Y.

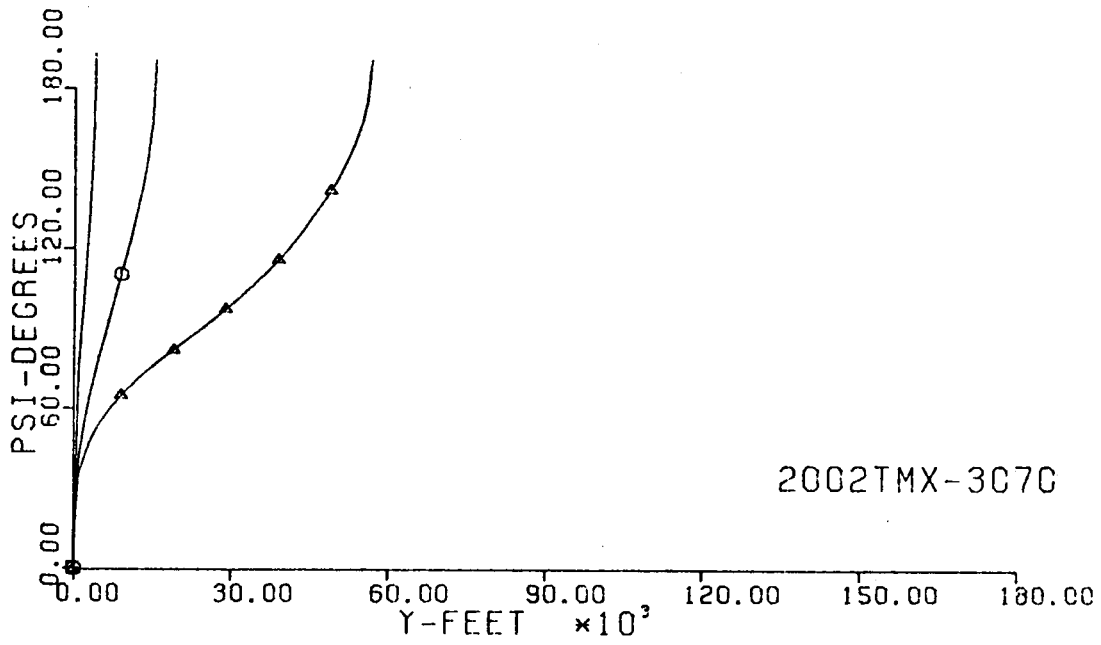

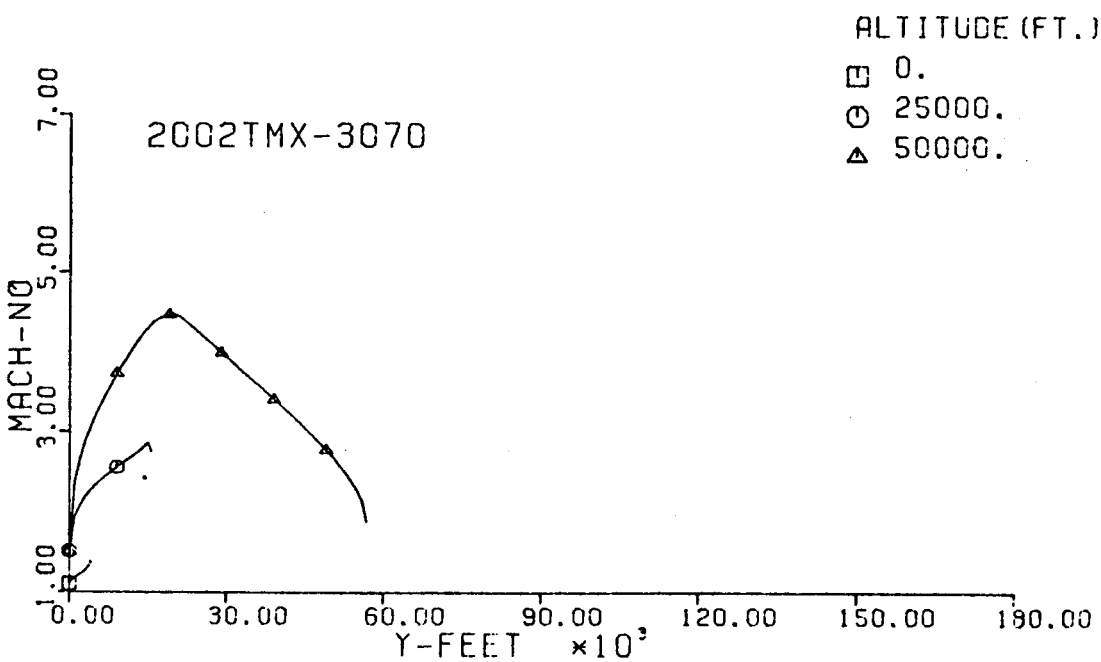

Fig. 252-III. Heading Angle and Mach No. vs. Downrange Distance, Y.

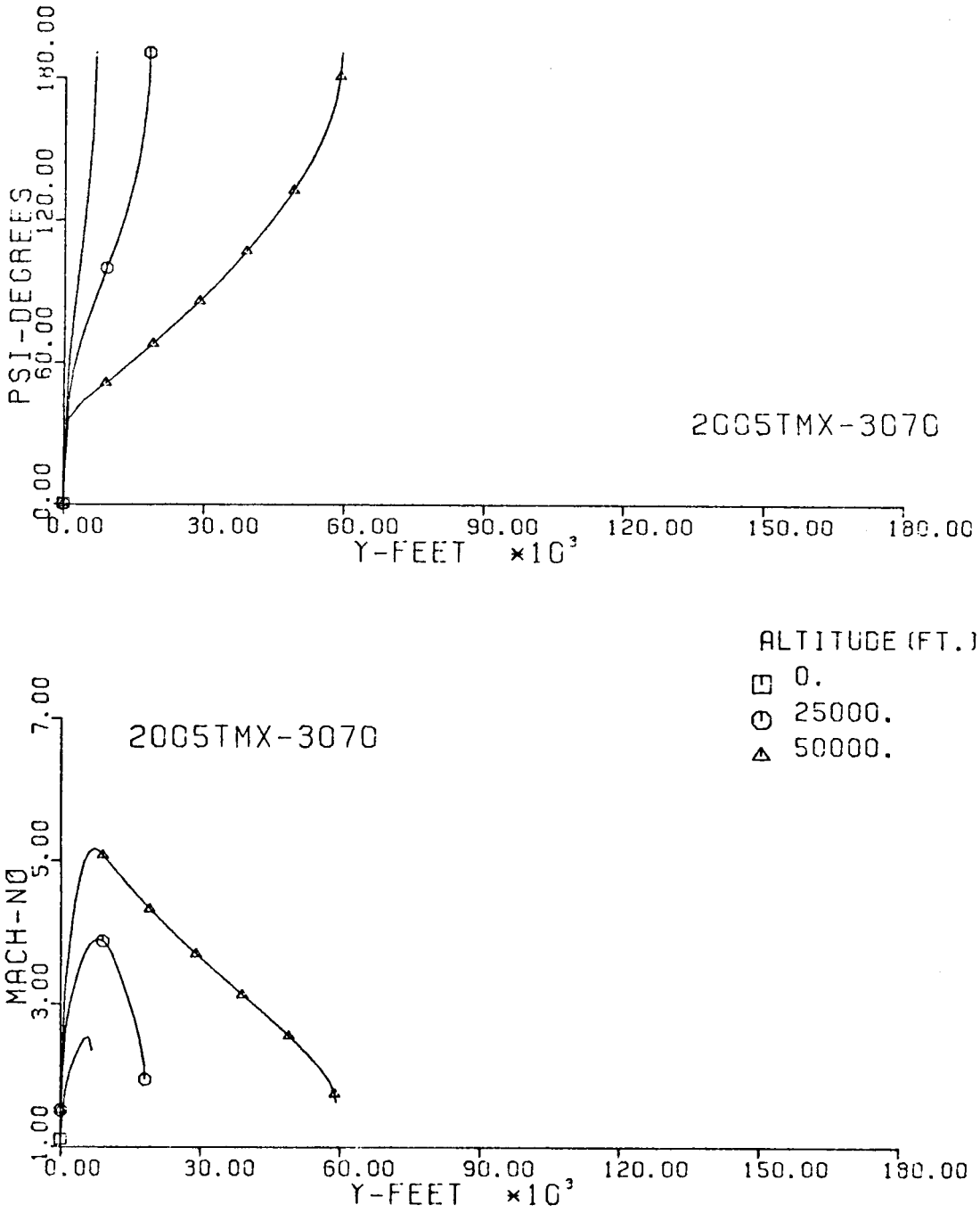

Fig. 253-III. Heading Angle and Mach No. vs. Downrange Distance, Y.

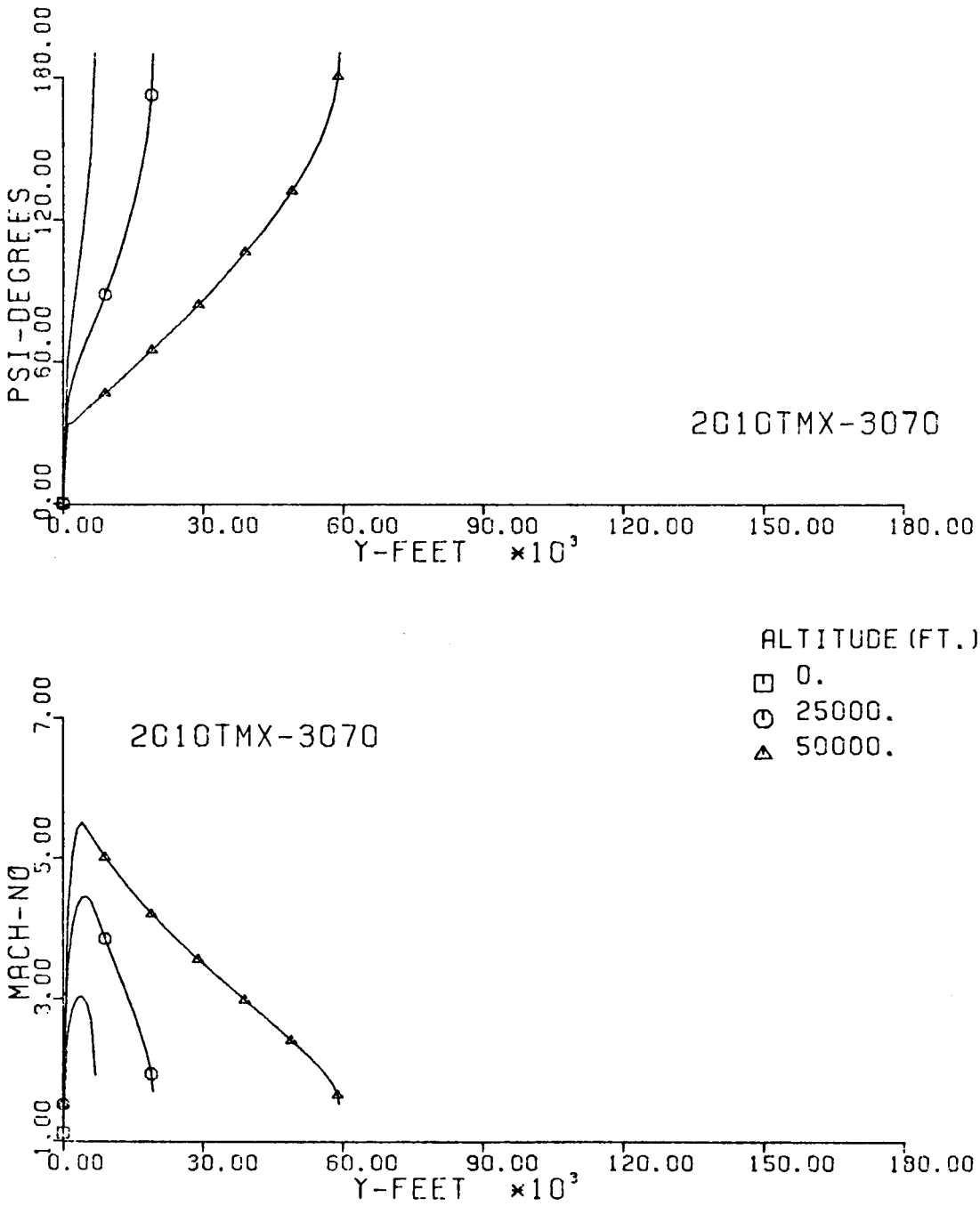

Fig. 254-III. Heading Angle and Mach No. vs. Downrange Distance, Y.

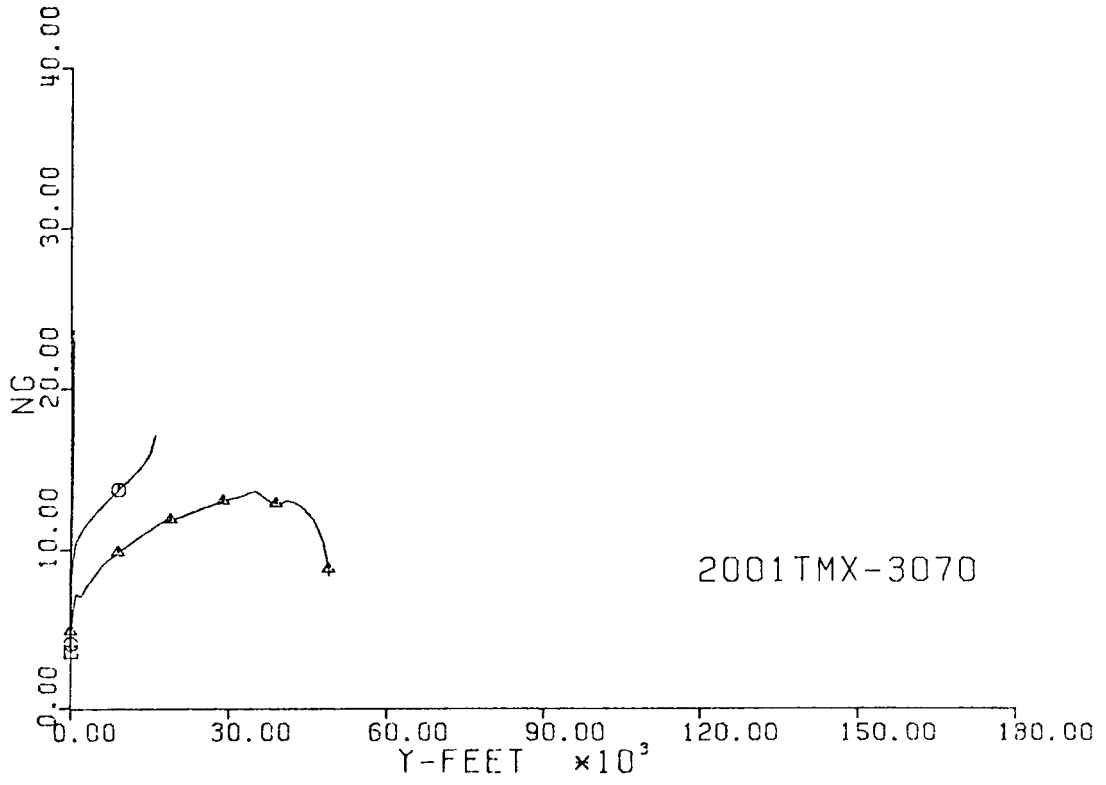

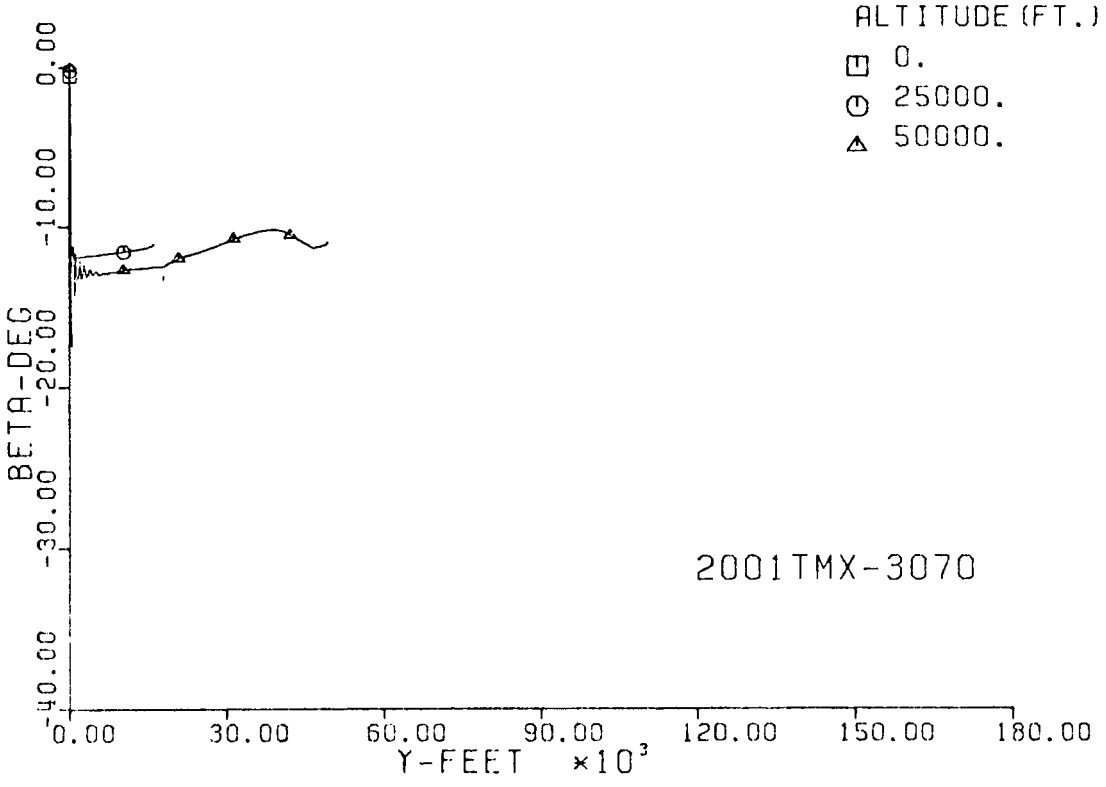

Fig. 255-III. Number of G's and Sideslip Angle vs. Downrange Distance, Y.

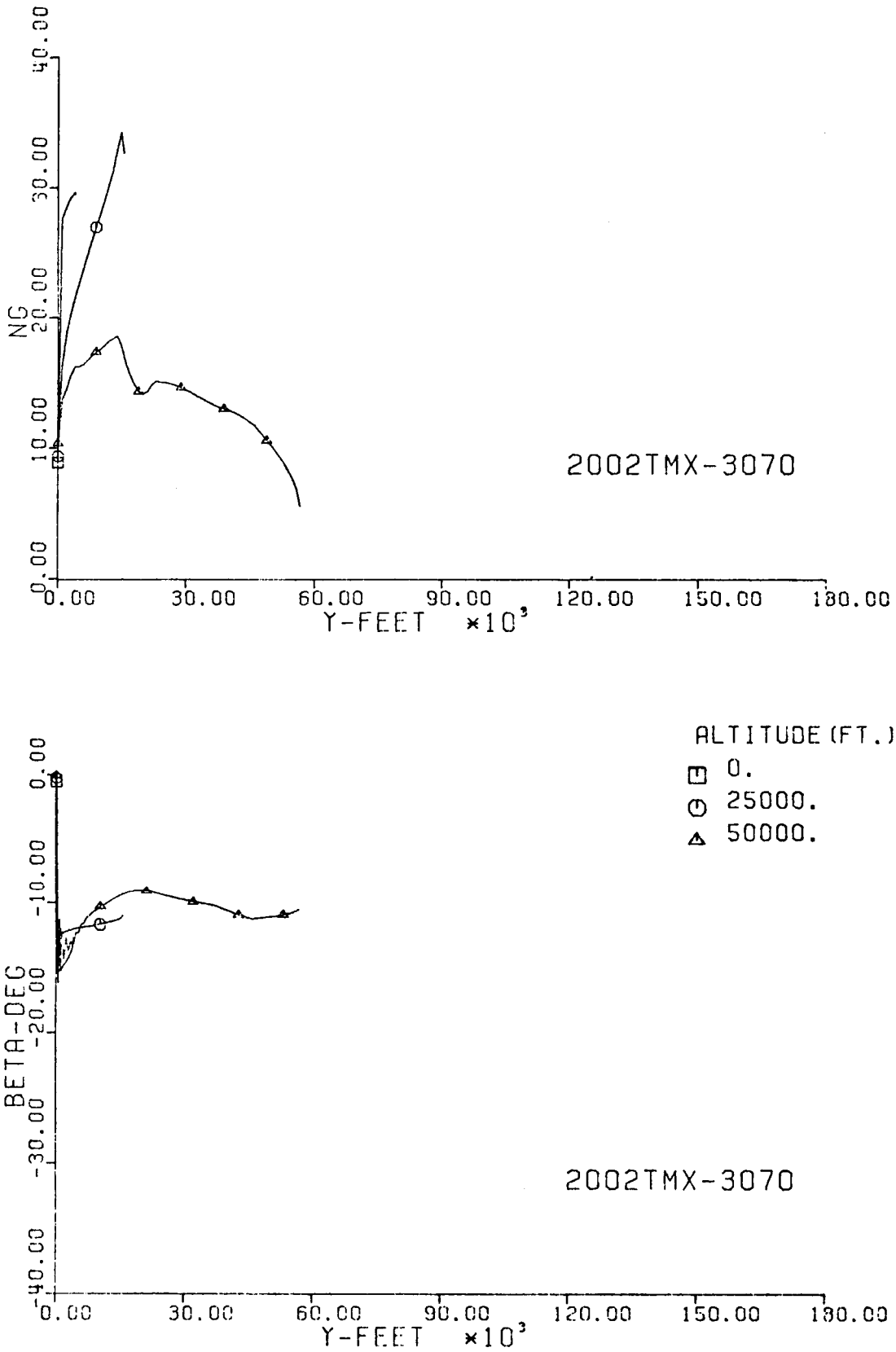

Fig. 256-III. Number of G's and Sideslip Angle vs. Downrange Distance, Y.

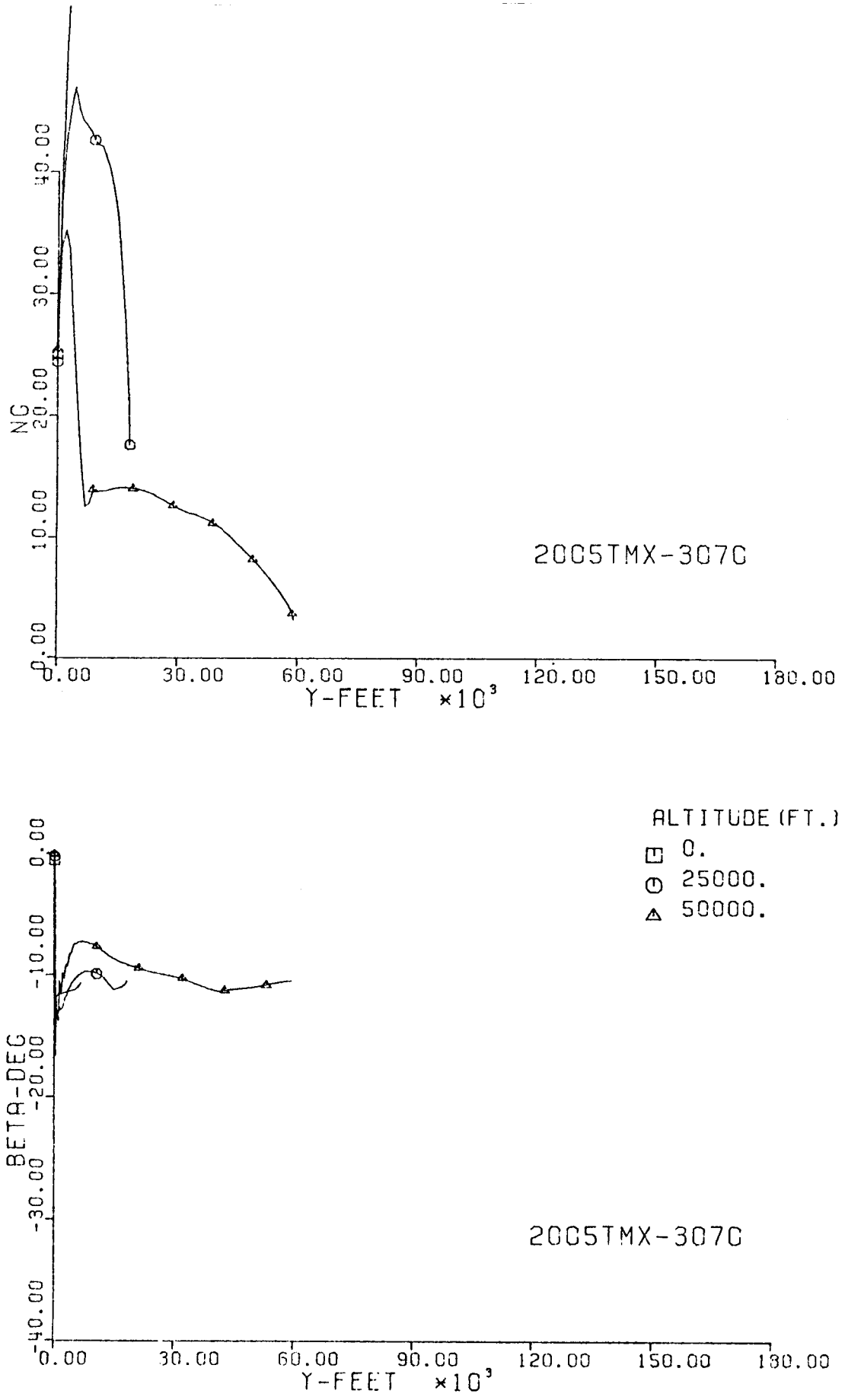

Fig. 257-III. Number of G's and Sideslip Angle vs. Downrange Distance, Y.

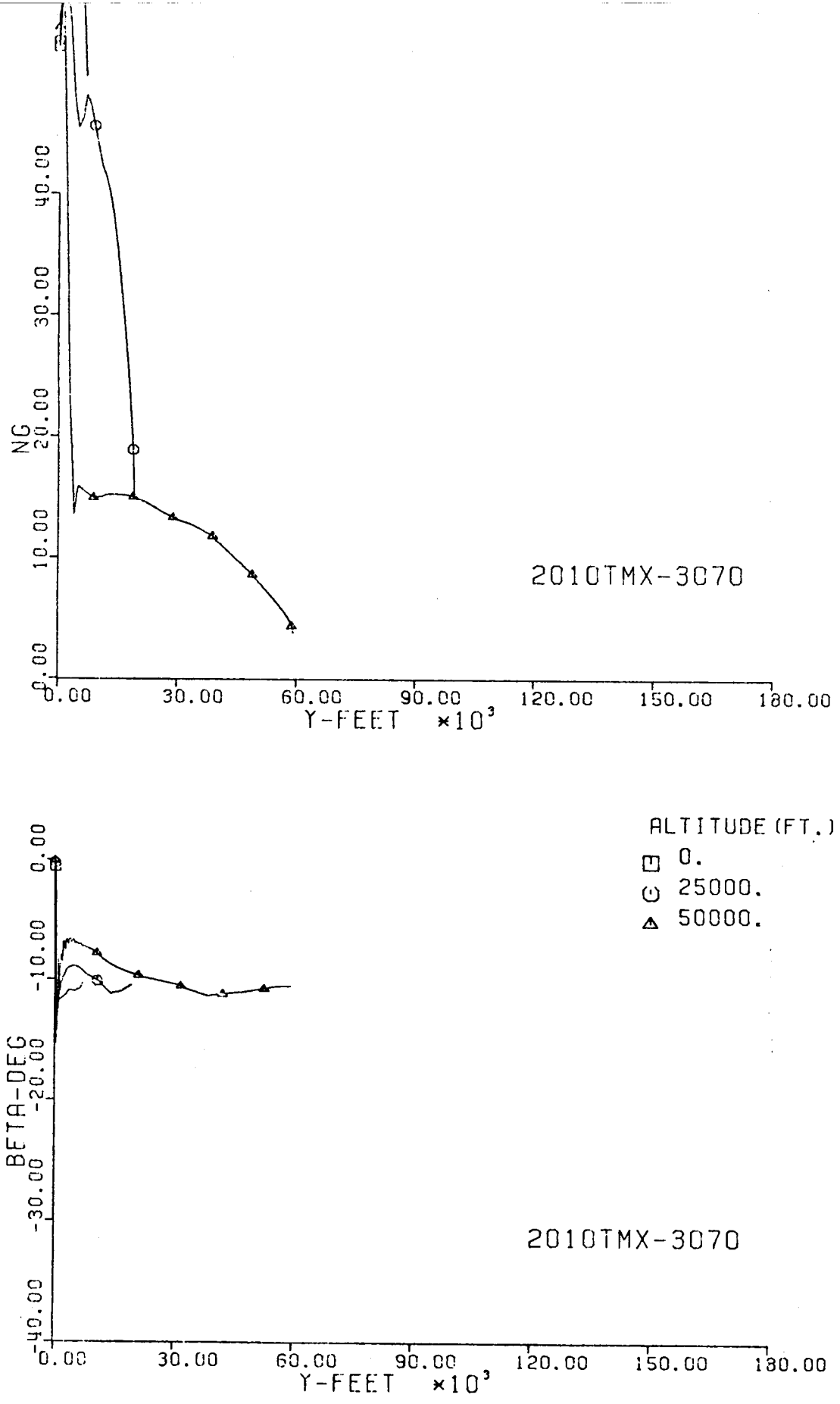

Fig. 258-III. Number of G's and Sideslip Angle vs. Downrange Distance, Y.

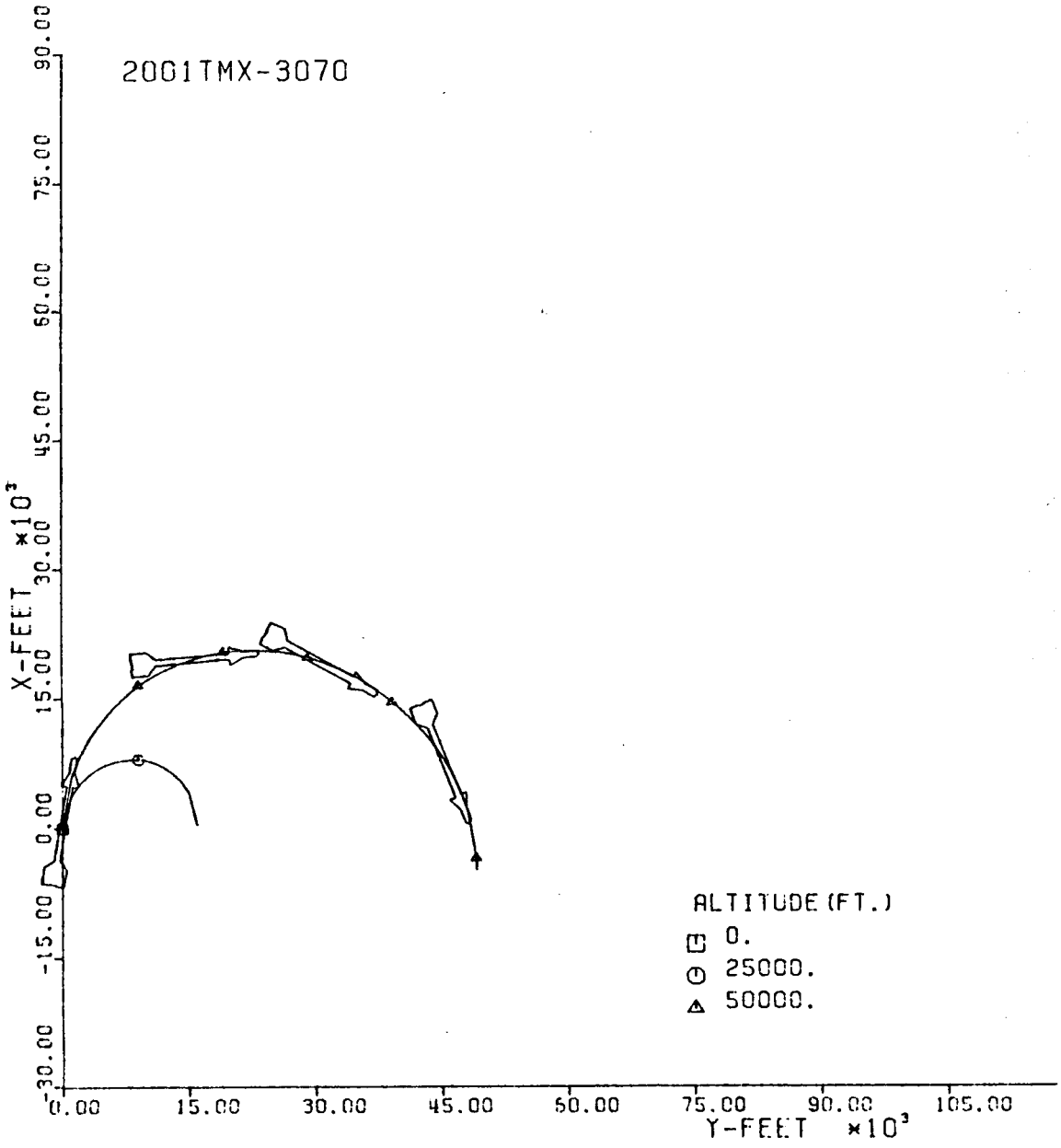

Fig. 259-III. Constant Altitude Flight Path, X vs. Y.

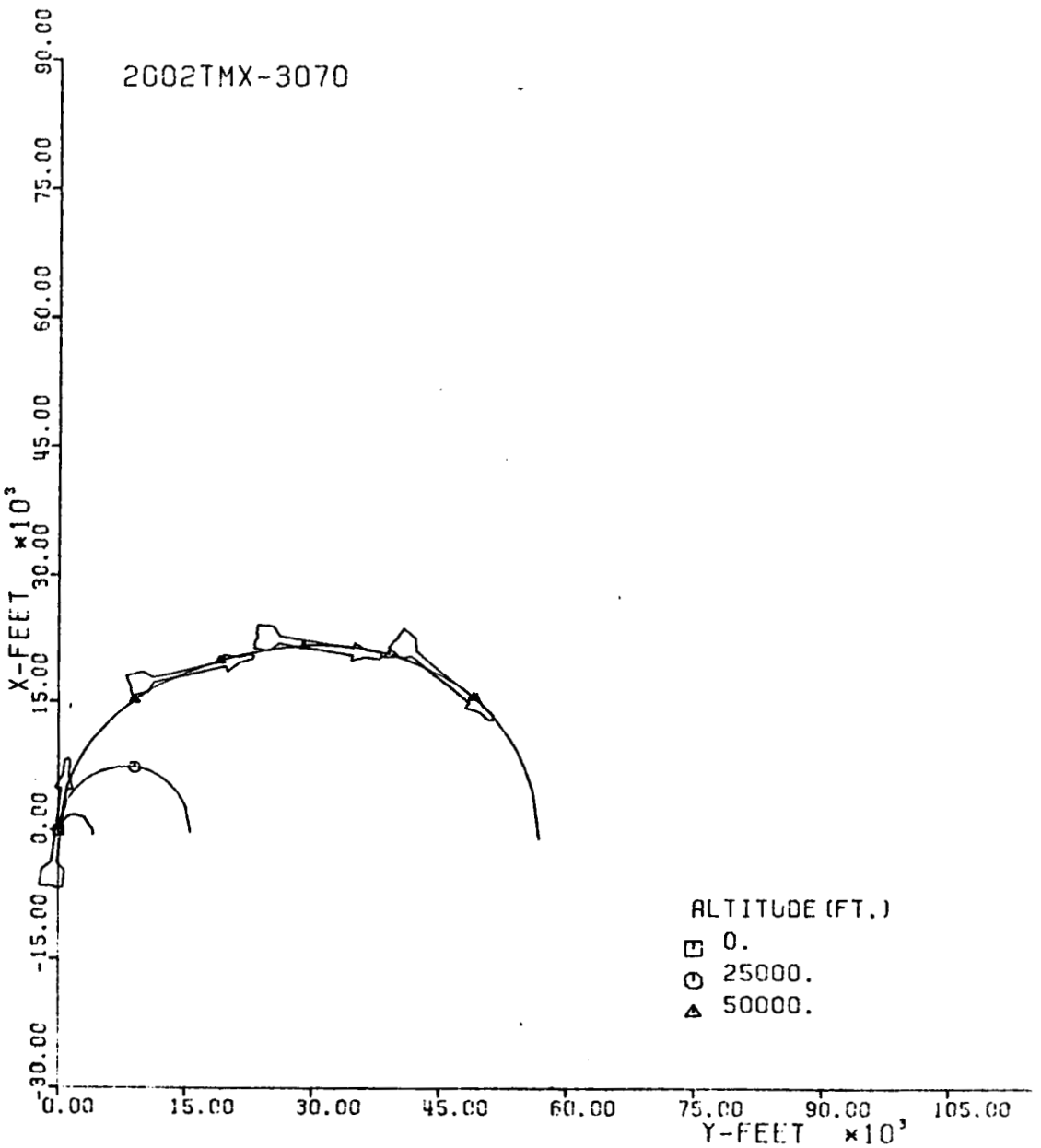

Fig. 260-III. Constant Altitude Flight Path, X vs. Y.

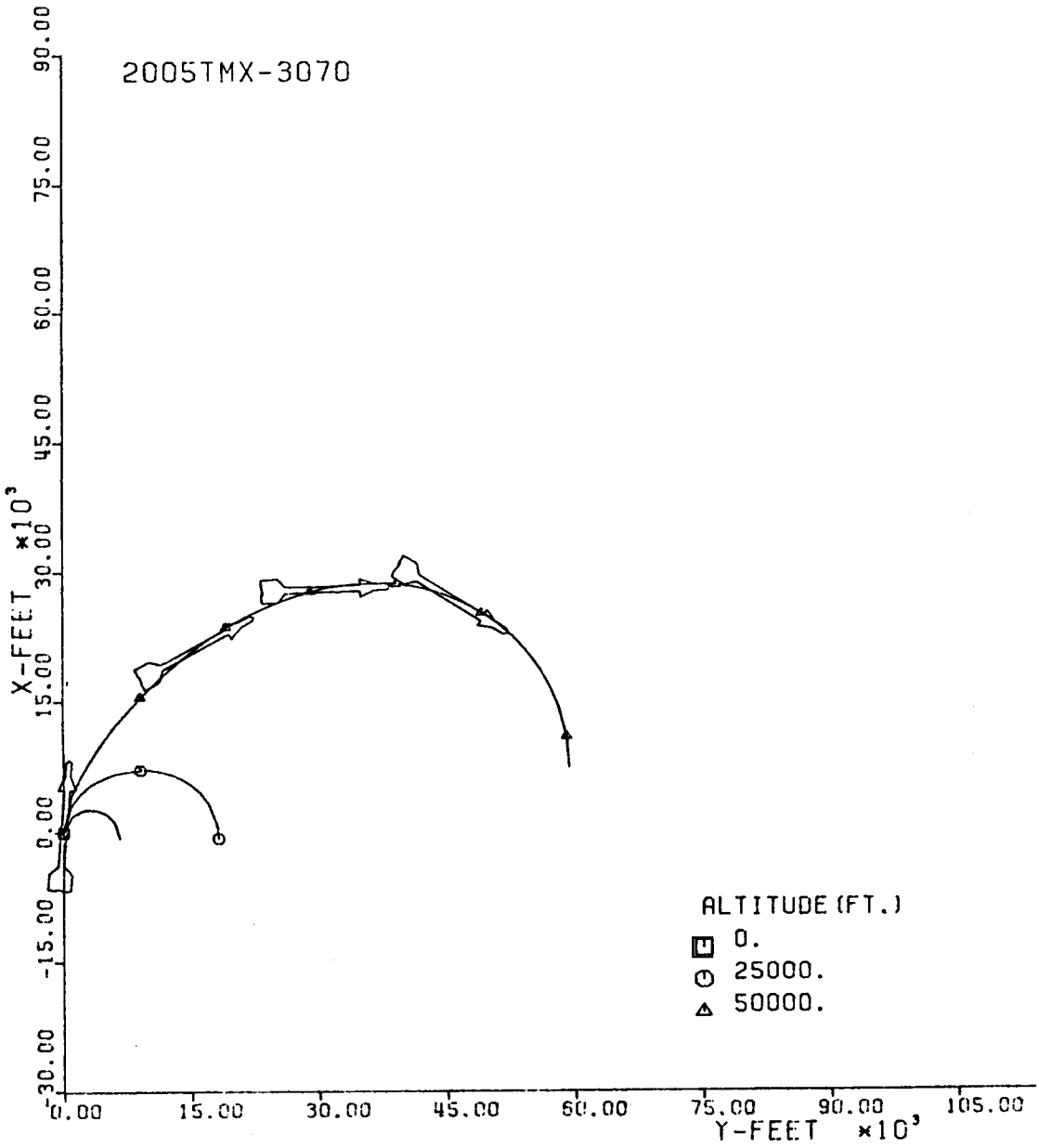

Fig. 261-III. Constant Altitude Flight Path, X vs. Y.

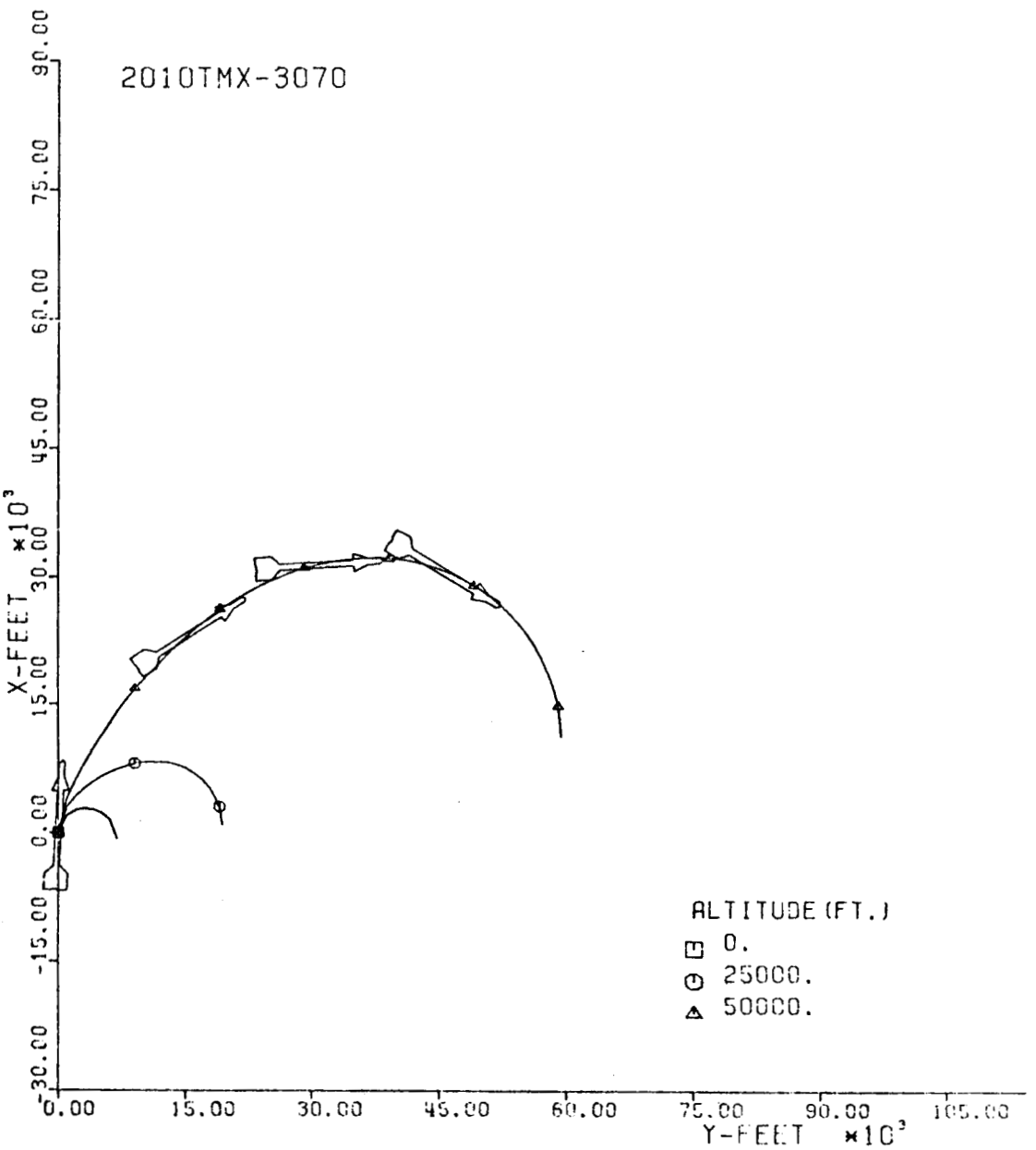

Fig. 262-III. Constant Altitude Flight Path, X vs. Y.

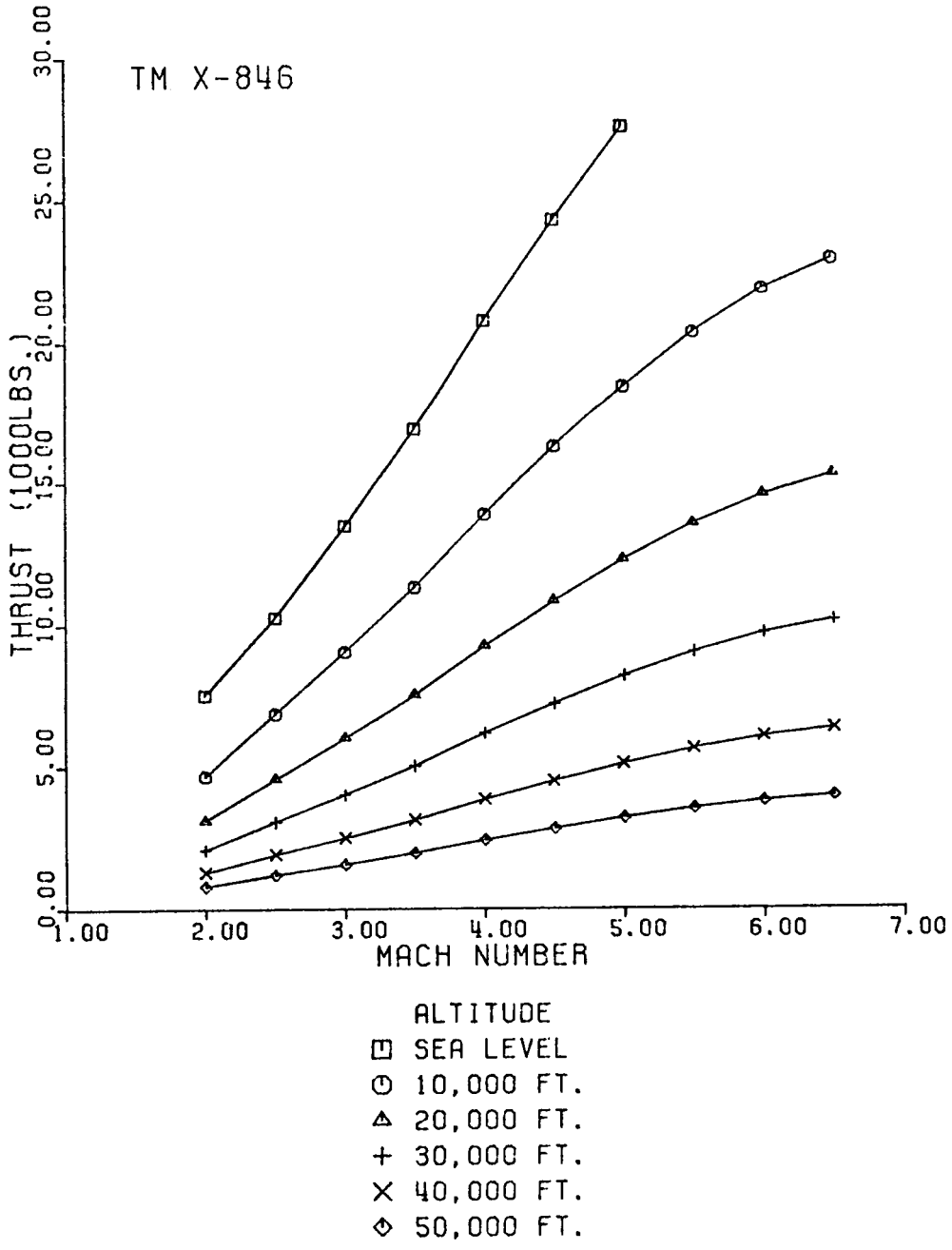

Fig. 263-I. Thrust vs. Terminal Mach No.

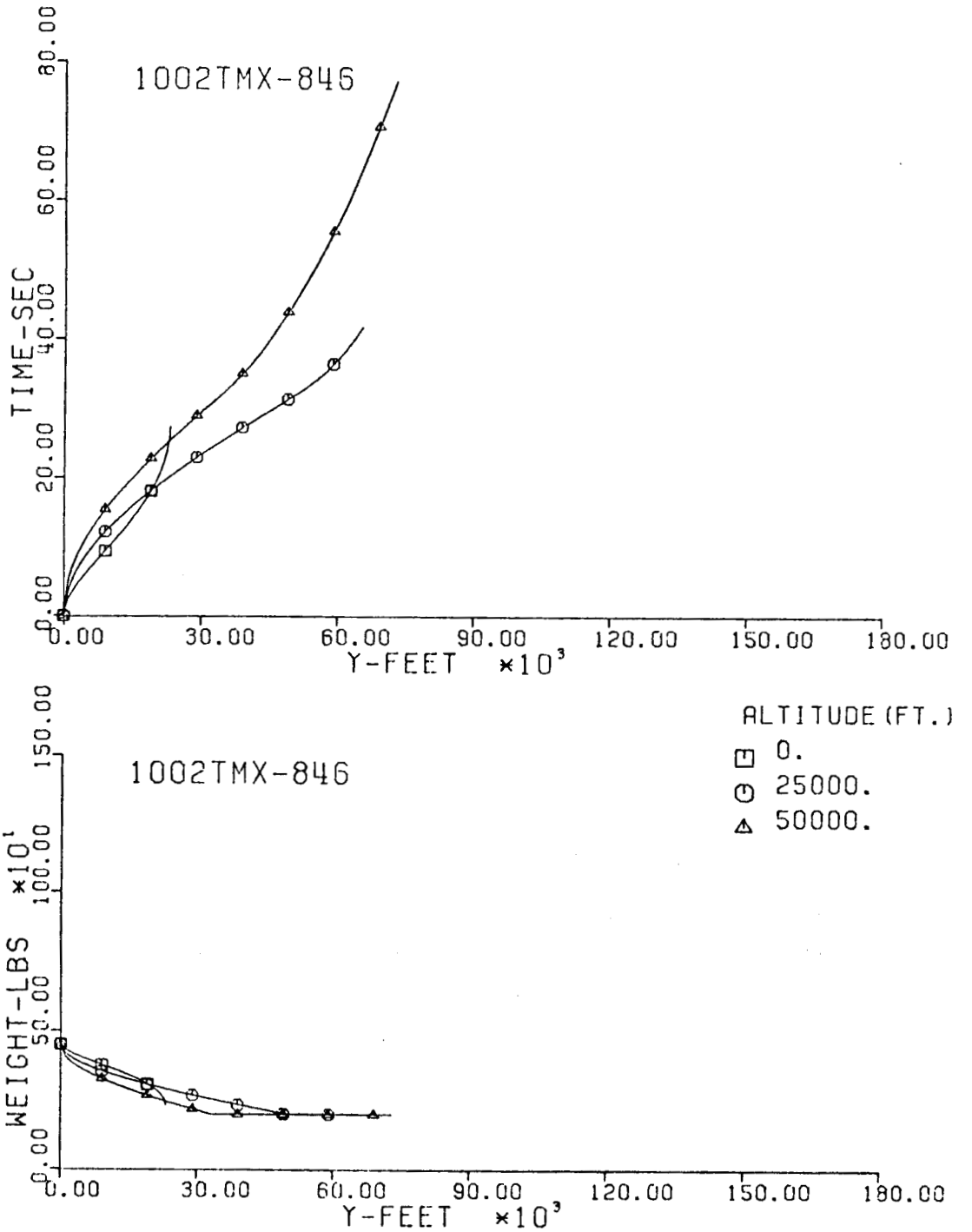

Fig. 264-III. Flight Time and Vehicle Weight vs. Downrange Distance, Y.

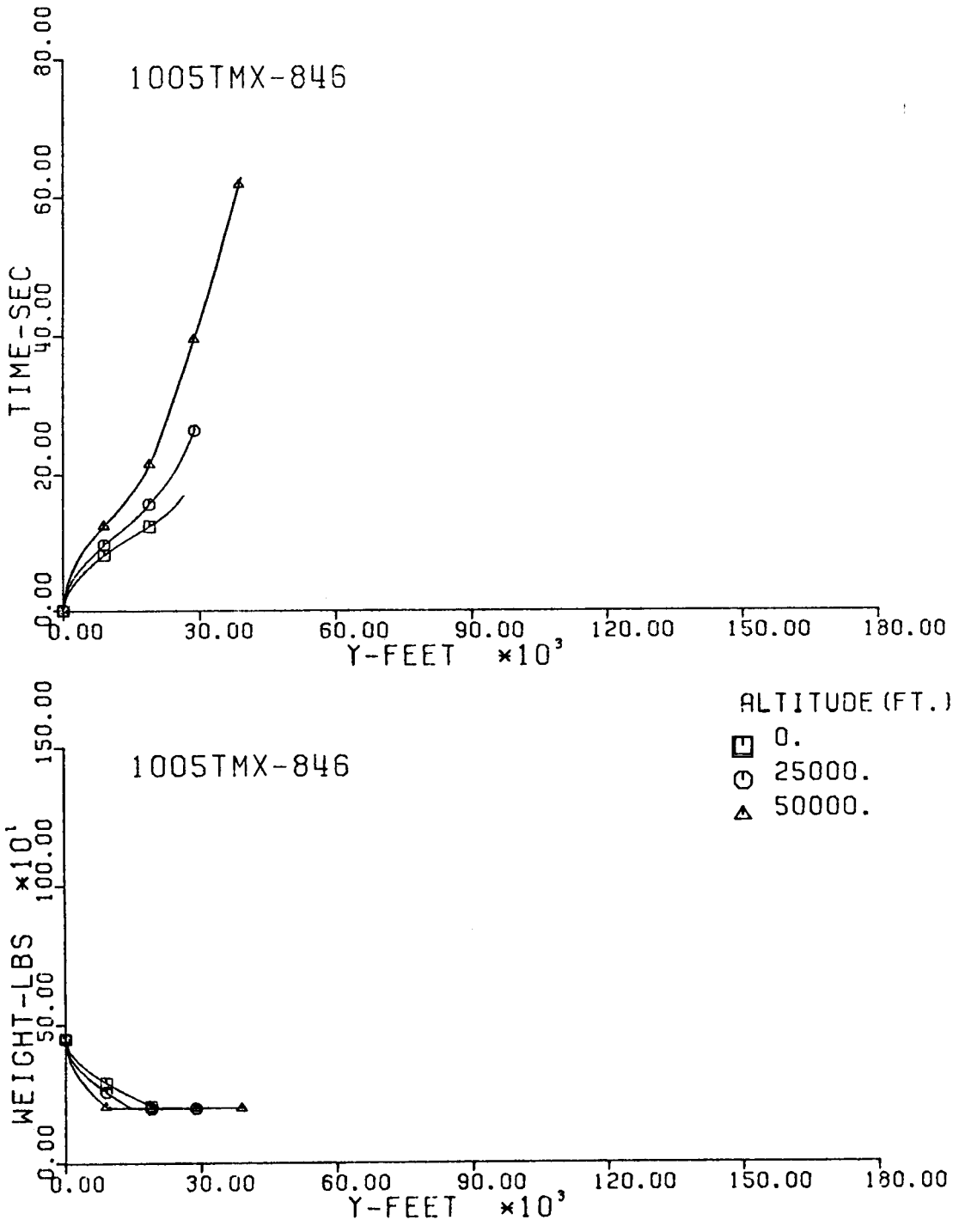

Fig. 265-III. Flight Time and Vehicle Weight vs. Downrange Distance, Y.

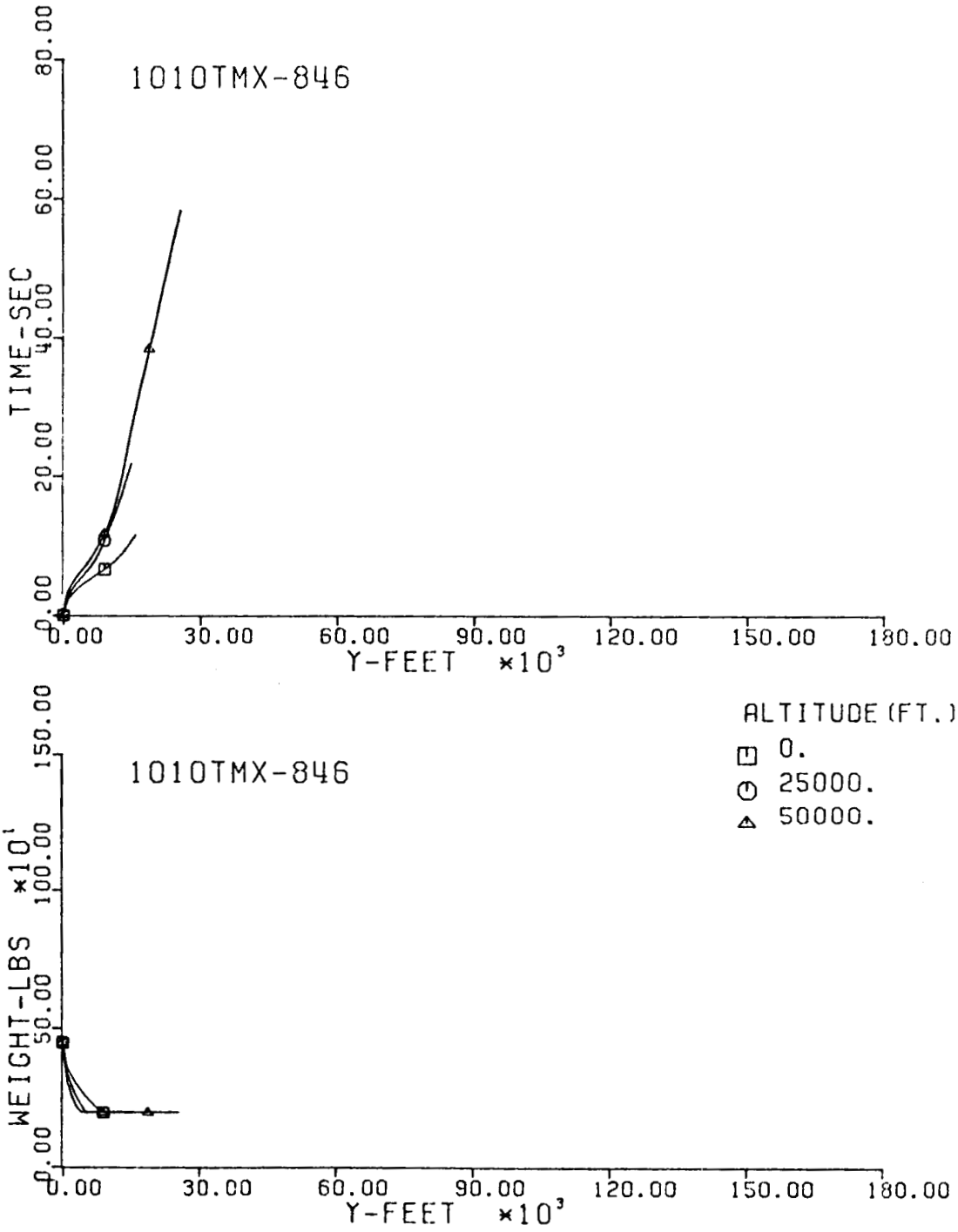

Fig. 266-III. Flight Time and Vehicle Weight vs. Downrange Distance, Y.

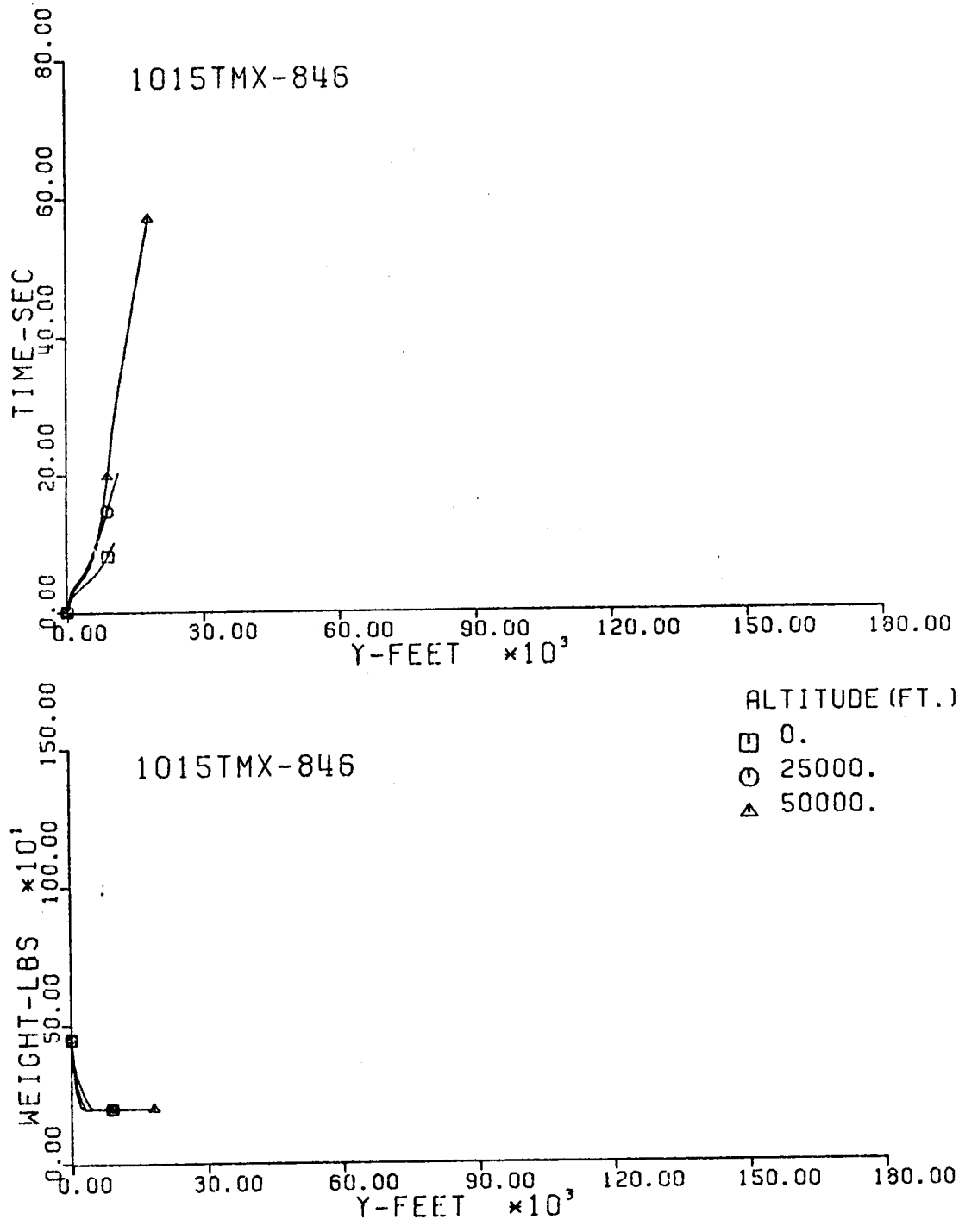

Fig. 267-III. Flight Time and Vehicle Weight vs. Downrange Distance, Y.

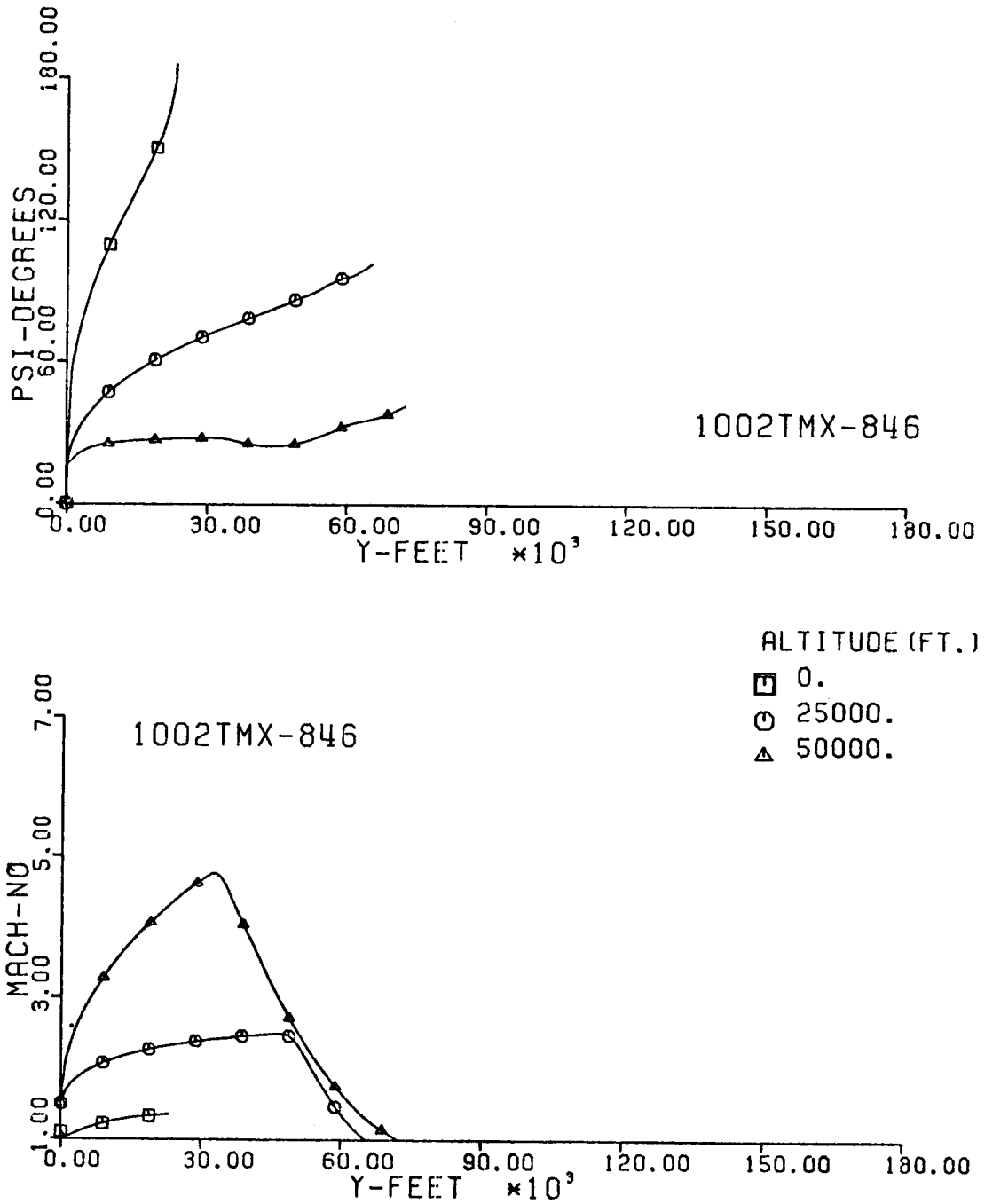

Fig. 268-III. Heading Angle and Mach No. vs. Downrange Distance, Y.

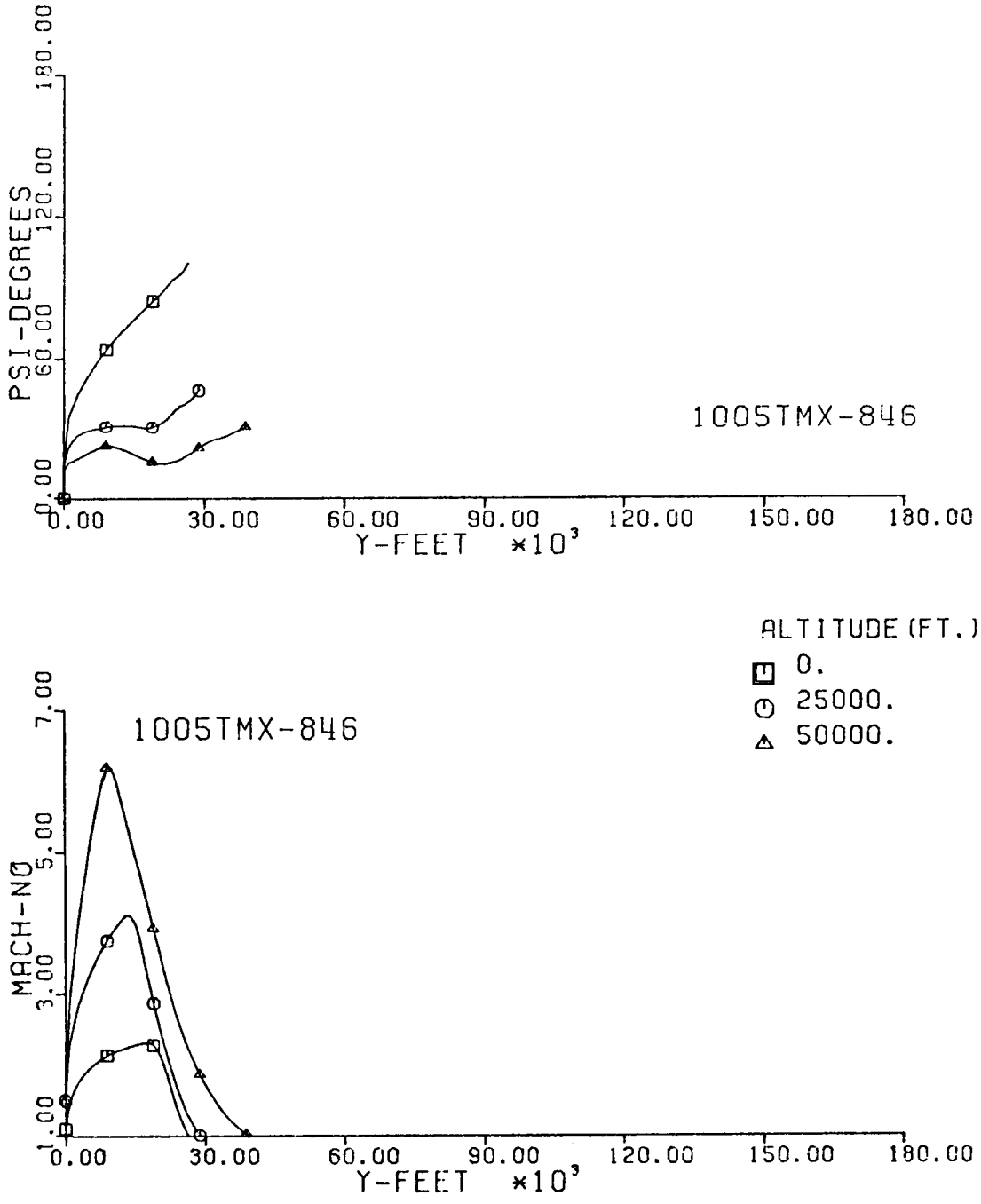

Fig. 269-III. Heading Angle and Mach No. vs. Downrange Distance, Y.

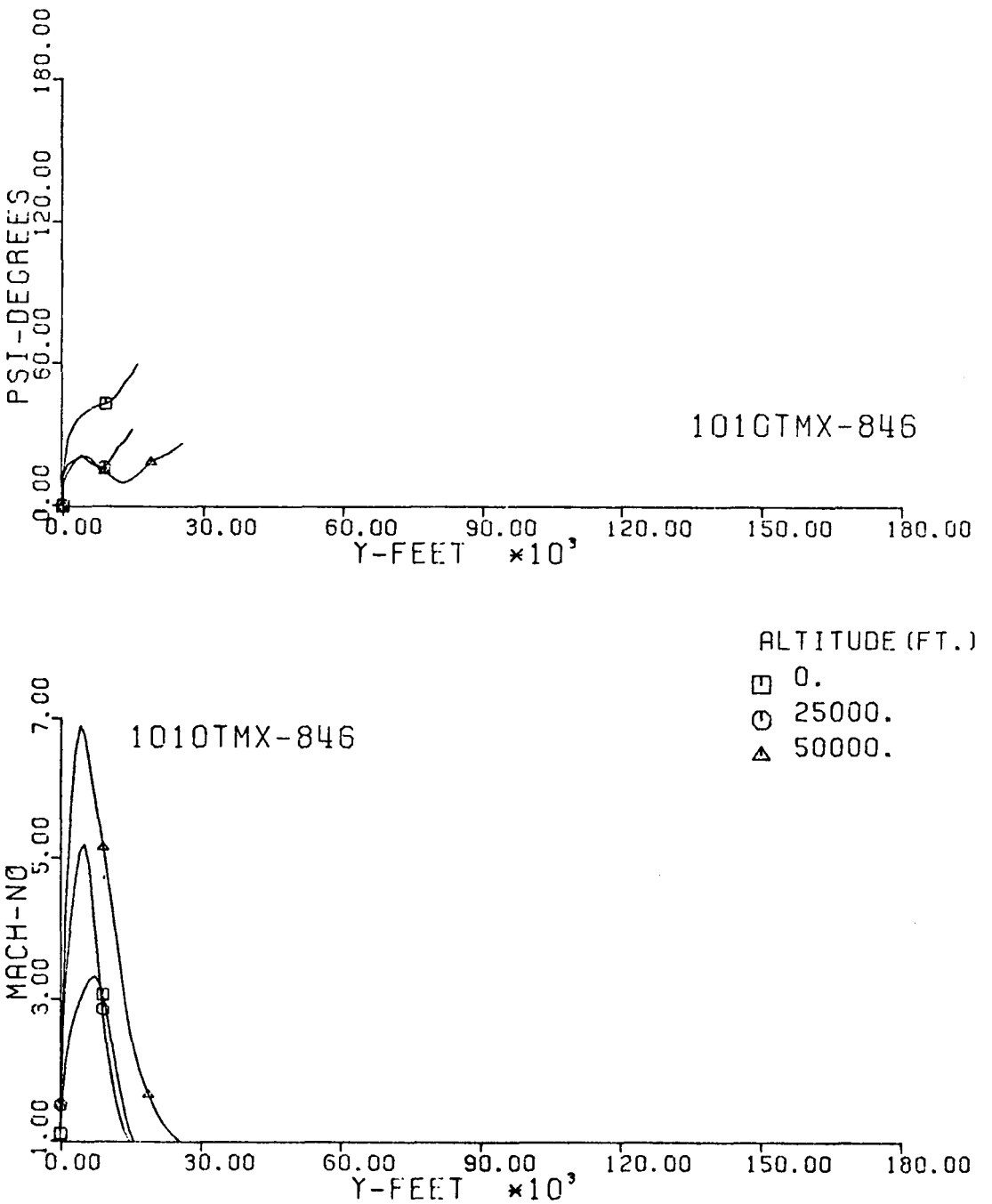

Fig. 270-III. Heading Angle and Mach No. vs. Downrange Distance, Y.

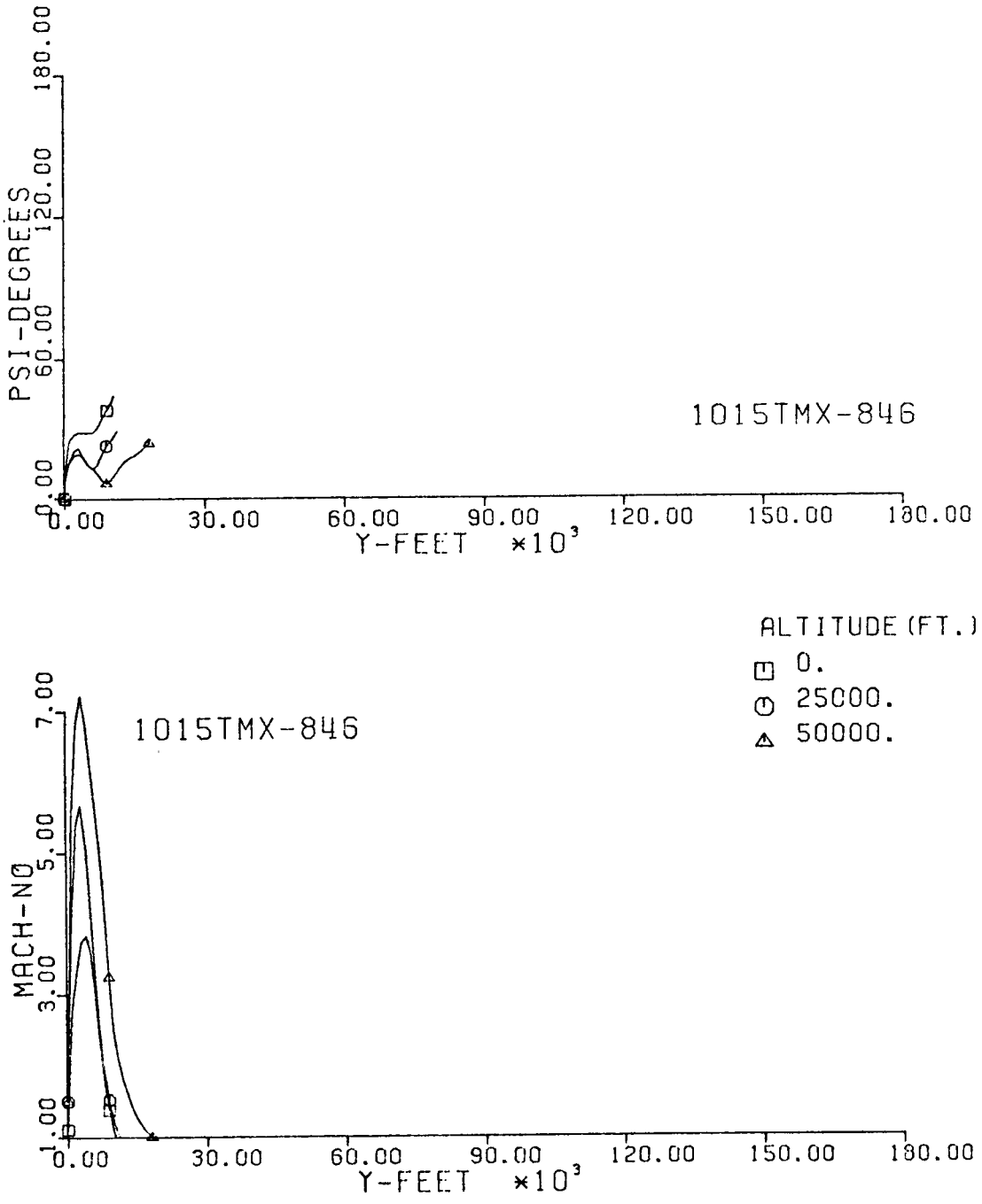

Fig. 271-III. Heading Angle and Mach No. vs. Downrange Distance, Y.

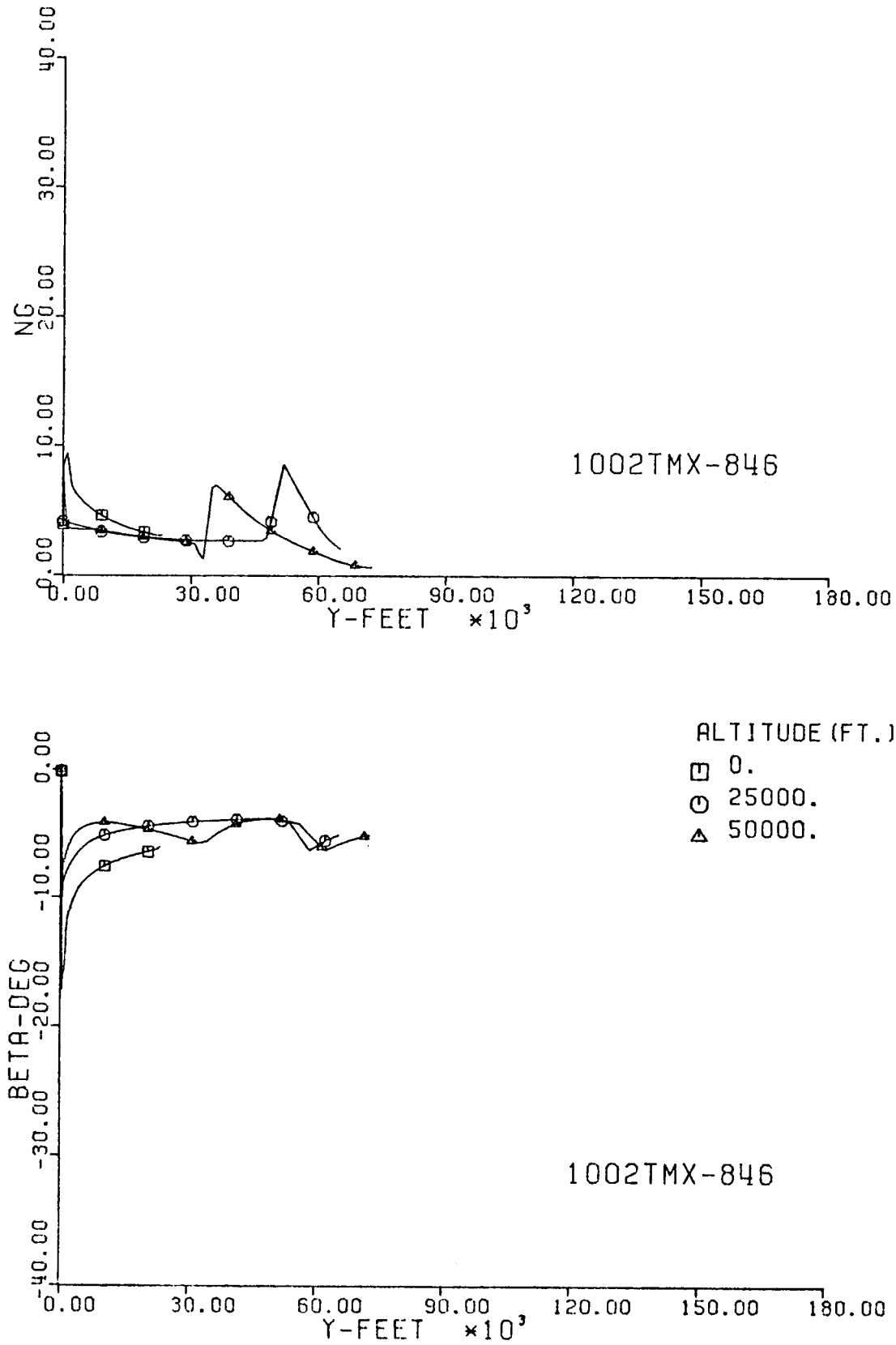

Fig. 272-III. Number of G's and Sideslip Angle vs. Downrange Distance, Y.

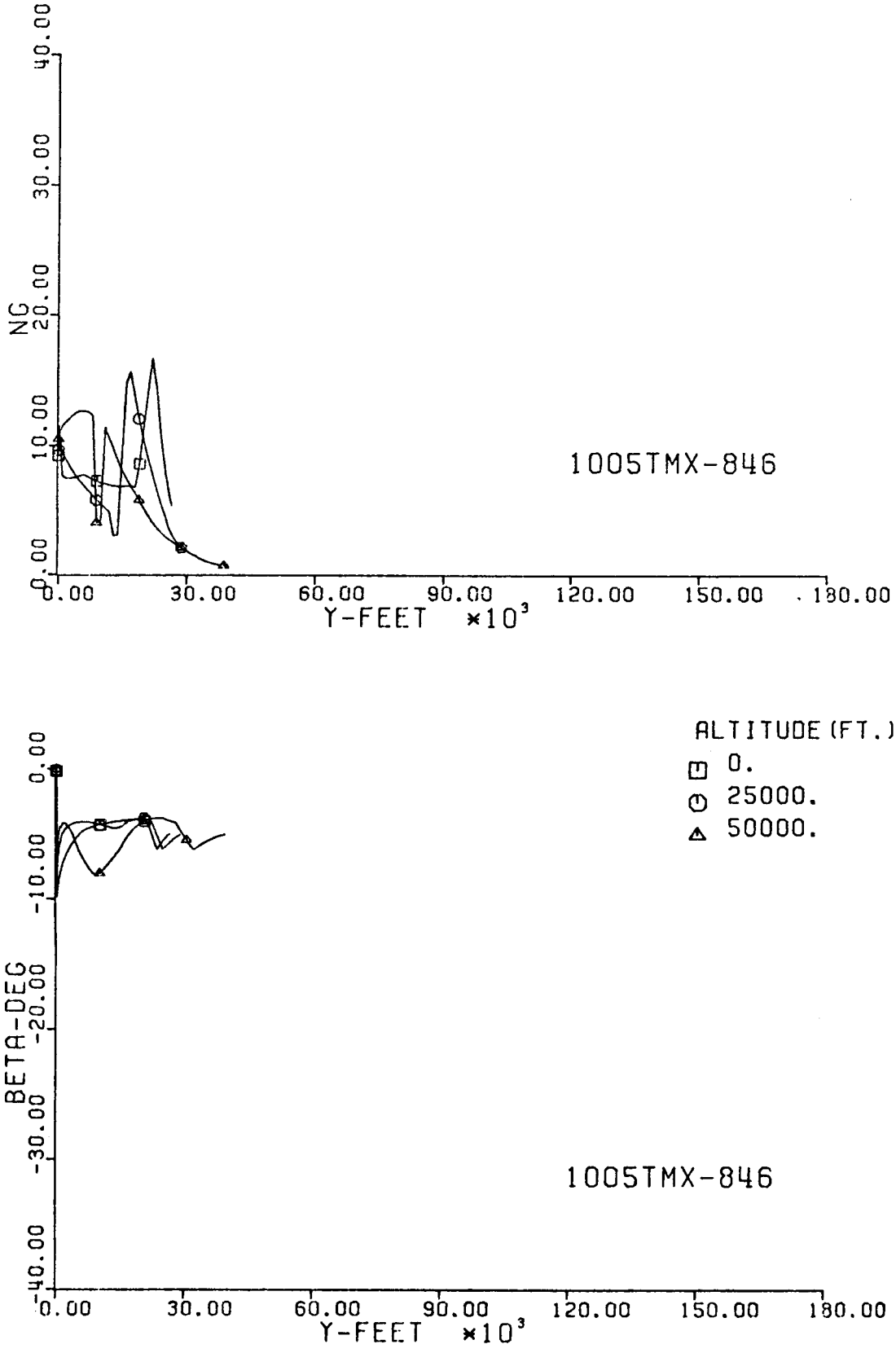

Fig. 273-III. Number of G's and Sideslip Angle vs. Downrange Distance, Y.

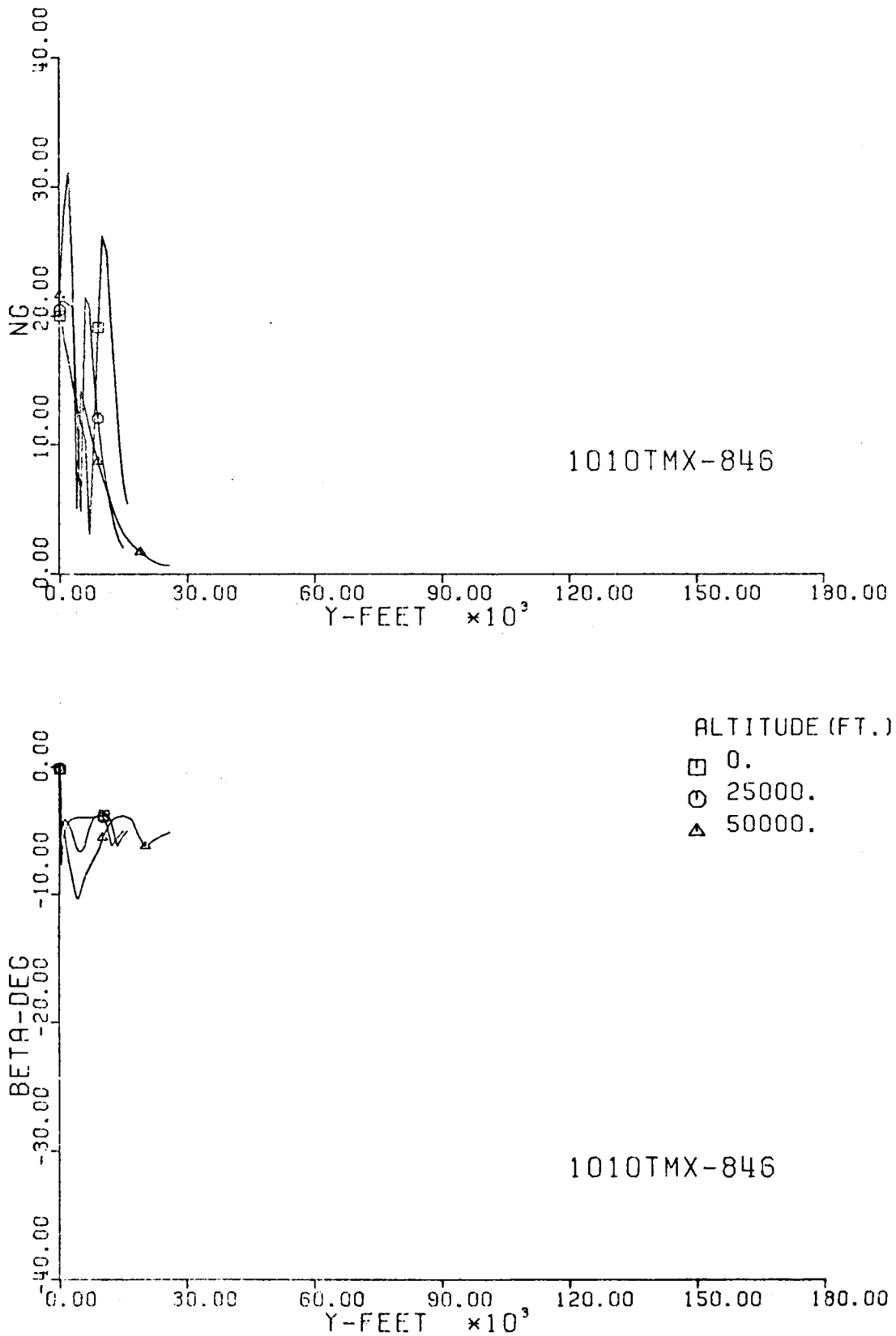

Fig. 274-III. Number of G's and Sideslip Angle vs. Downrange Distance, Y.

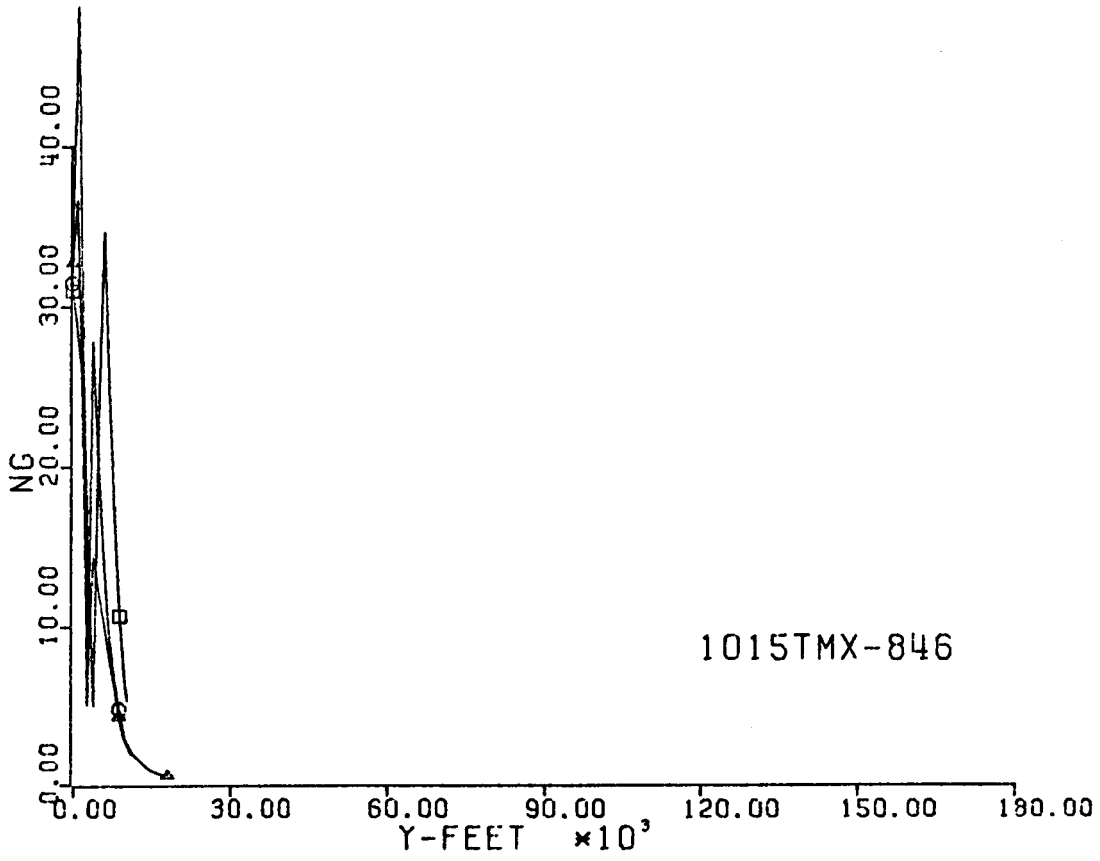

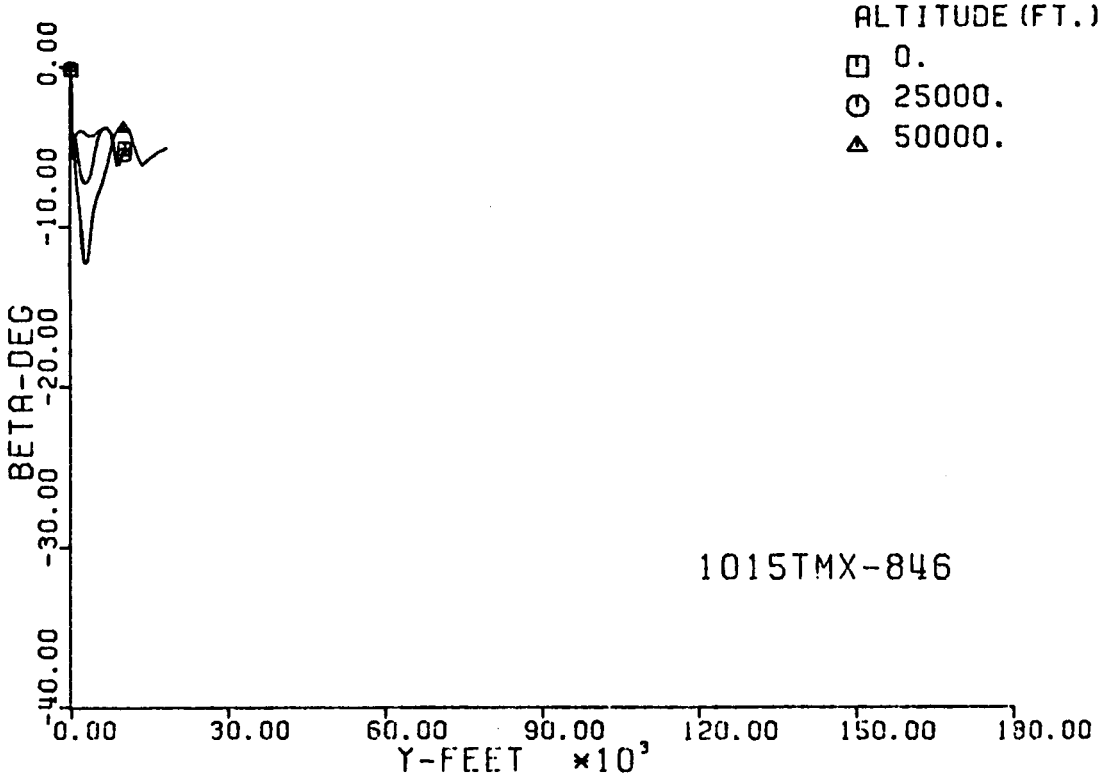

Fig. 275-III. Number of G's and Sideslip Angle vs. Downrange Distance, Y

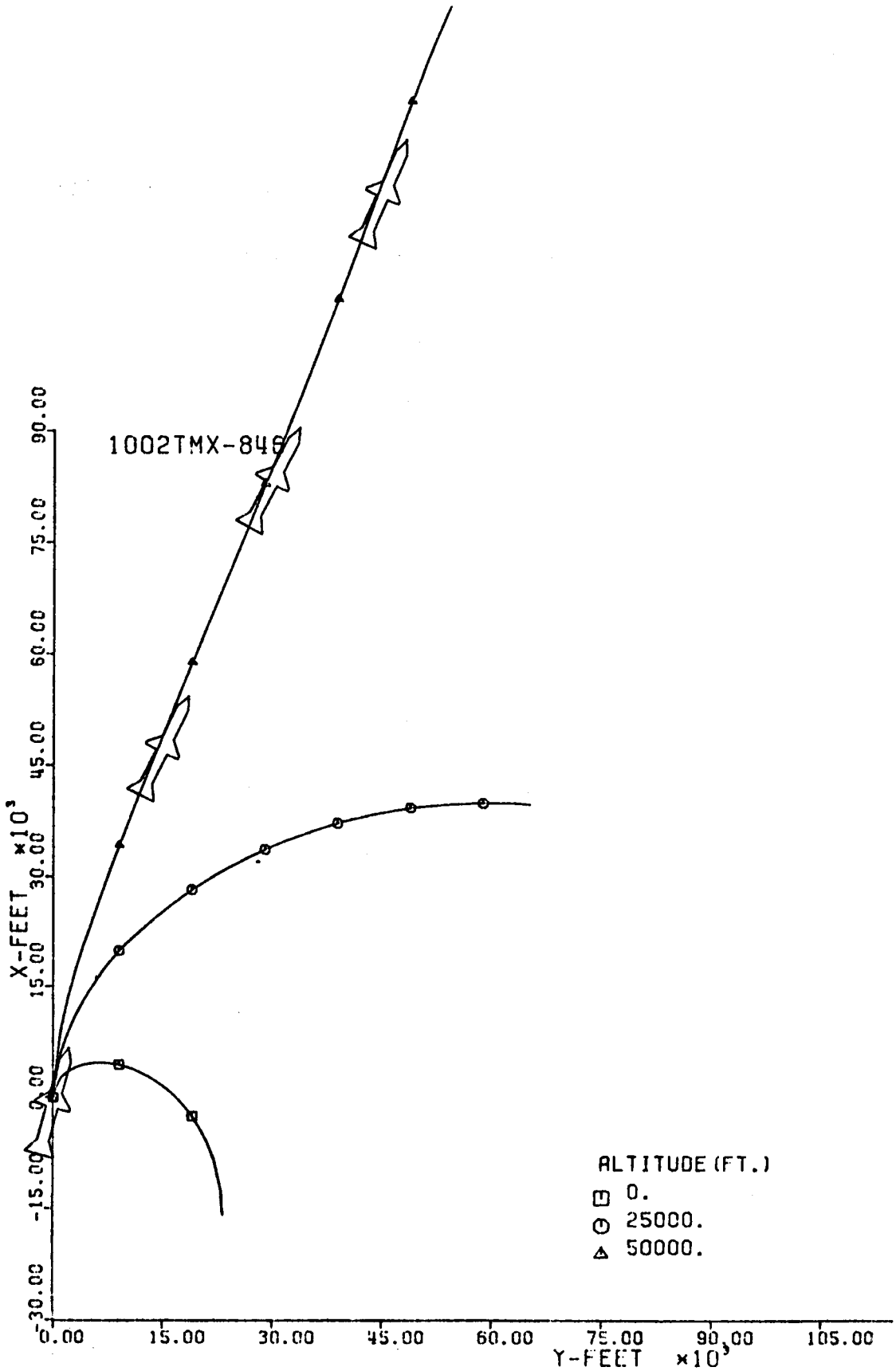

Fig. 276-III. Constant Altitude Flight Path, X vs. Y.

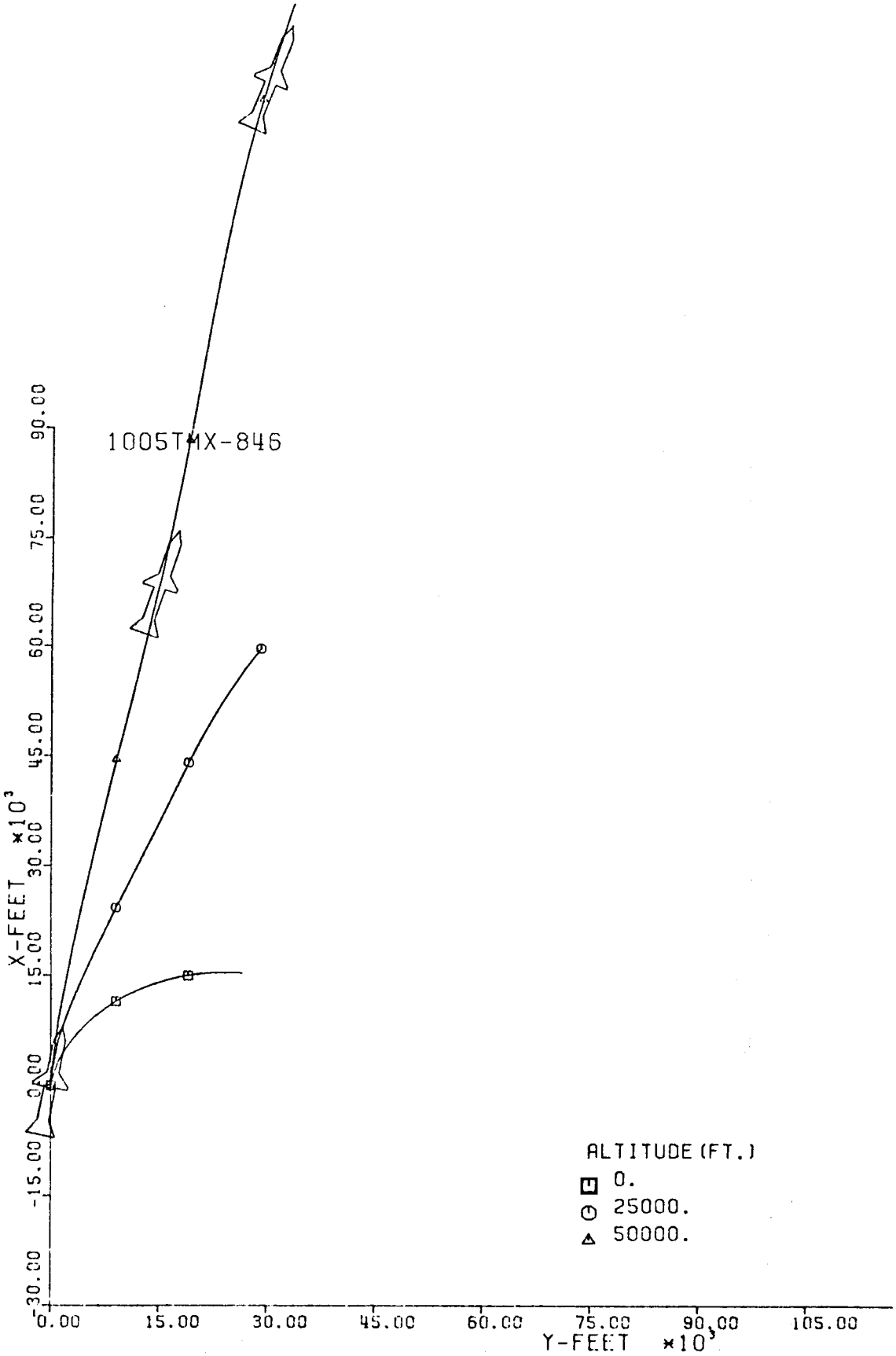

Fig. 277-III. Constant Altitude Flight Path, X vs. Y.

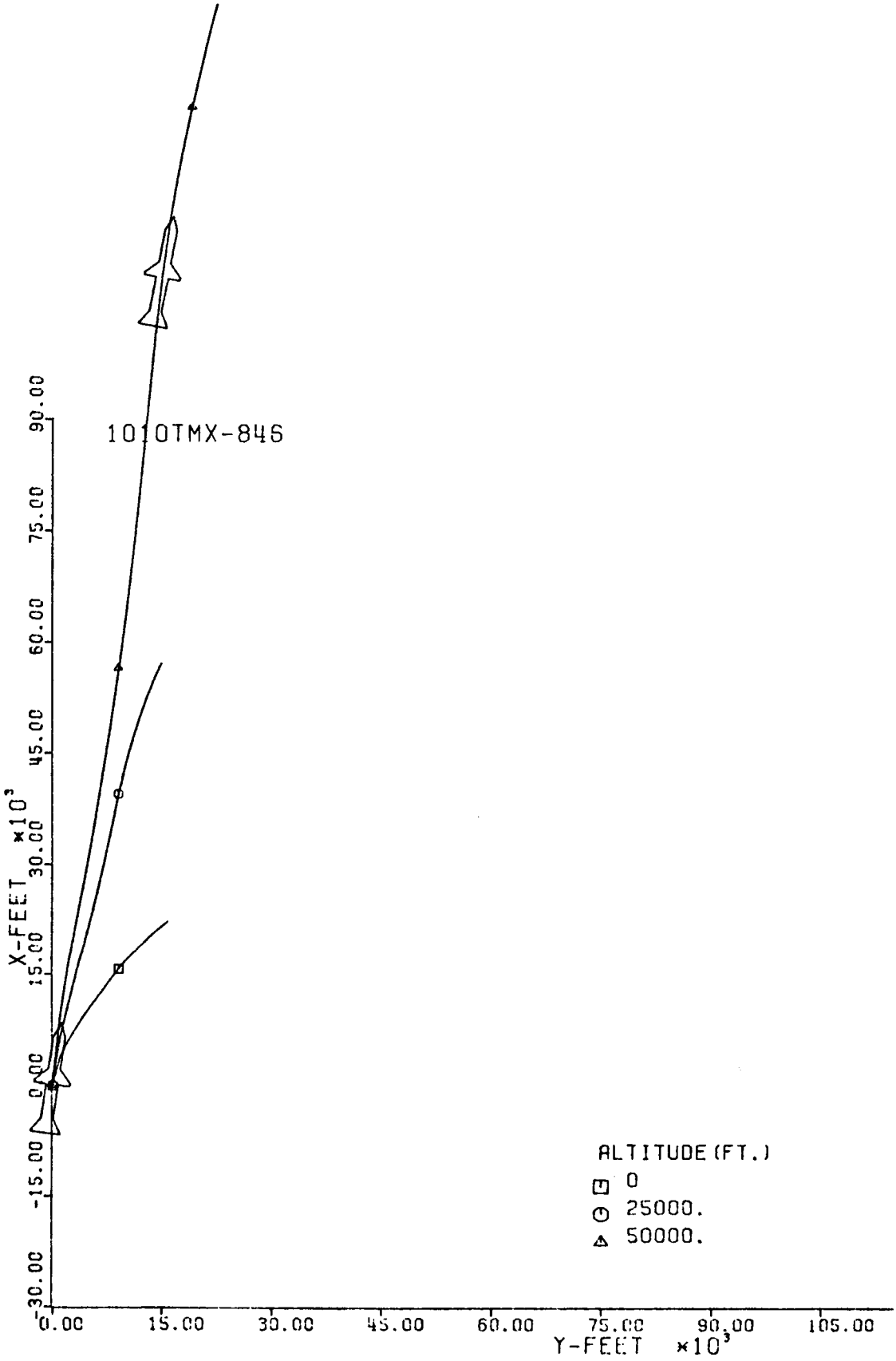

Fig. 278-III. Constant Altitude Flight Path, X vs. Y.

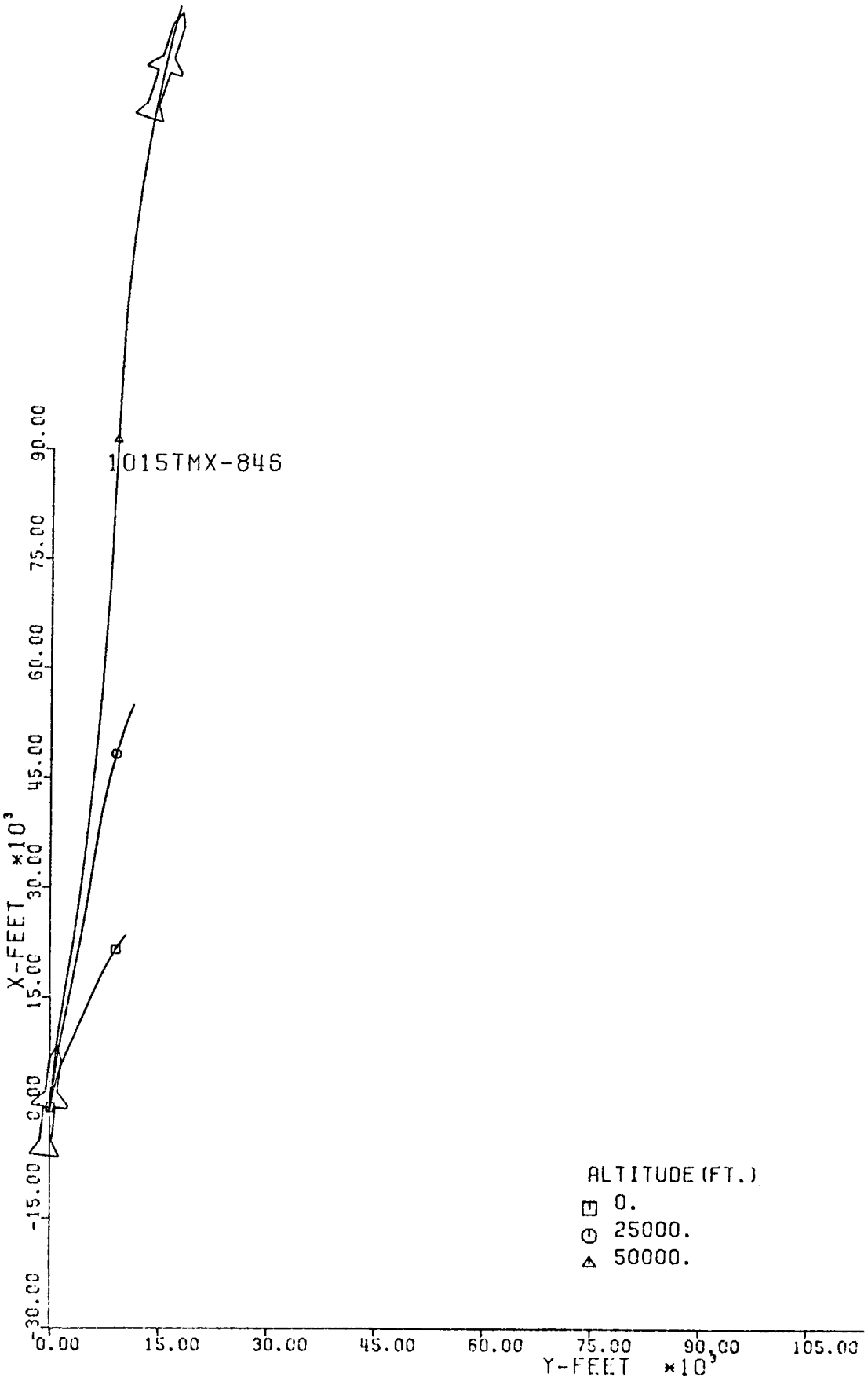

Fig. 279-III. Constant Altitude Flight Path, X vs. Y.

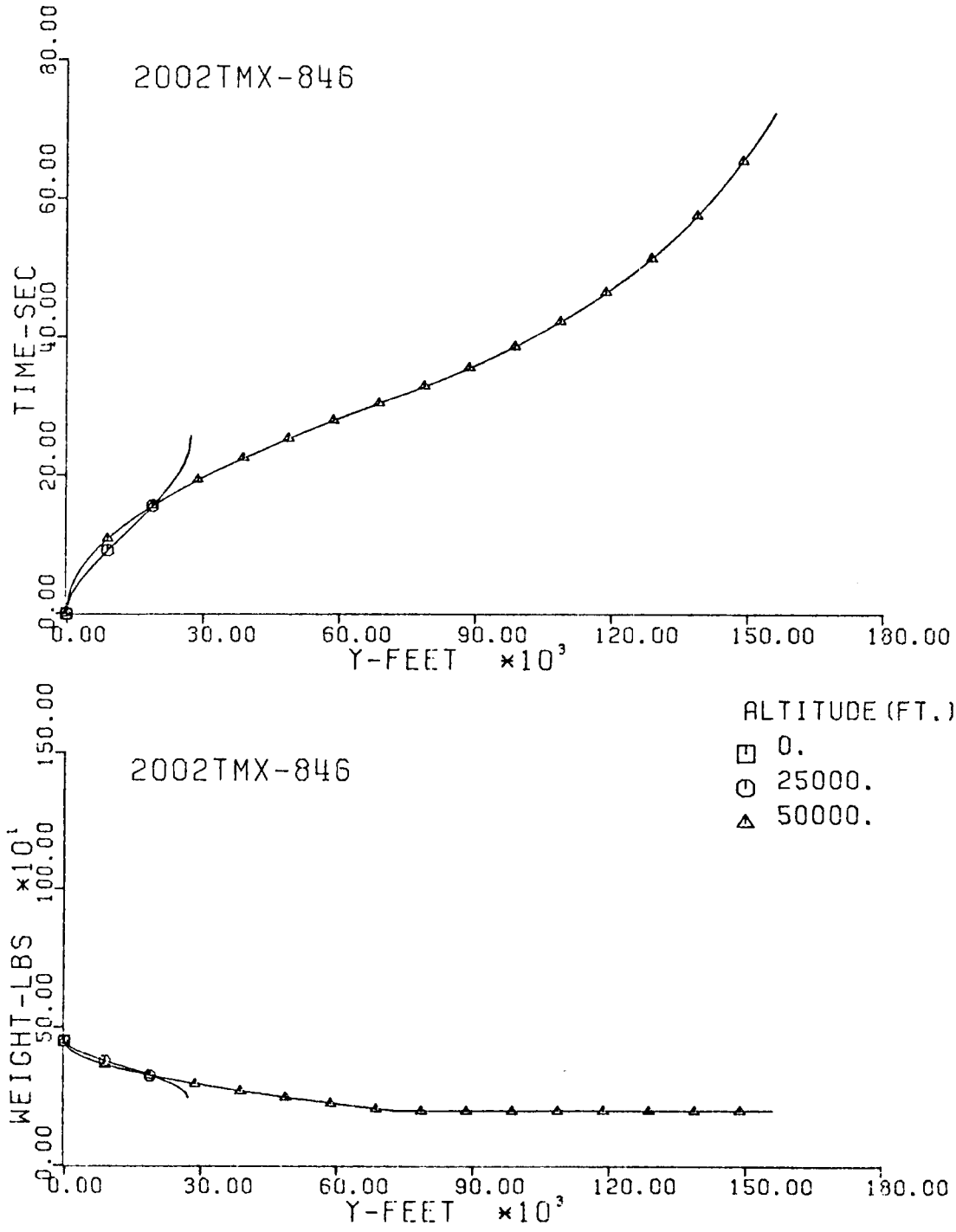

Fig. 280-III. Flight Time and Vehicle Weight vs. Downrange Distance, Y.

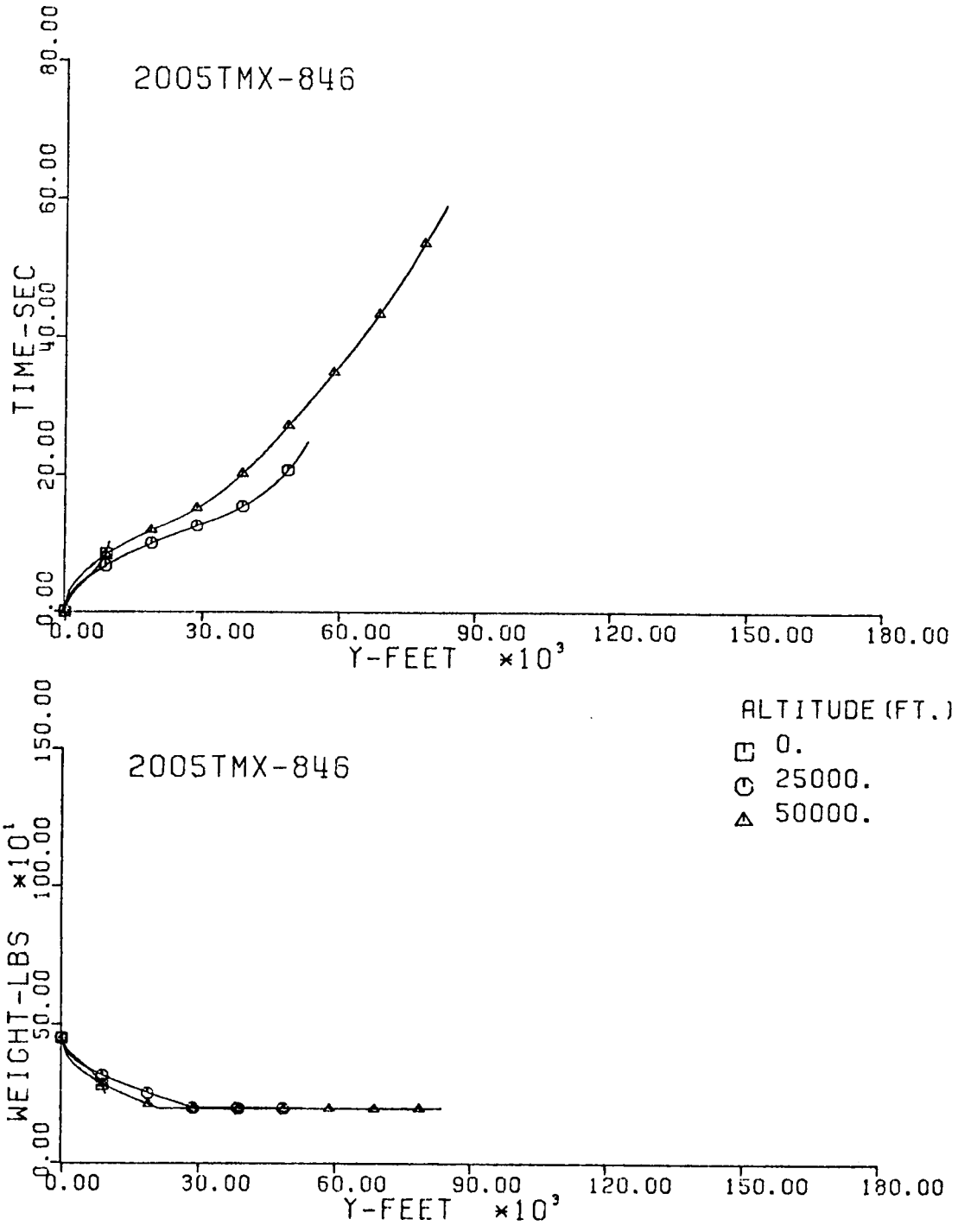

Fig. 281-III. Flight Time and Vehicle Weight vs. Downrange Distance, Y.

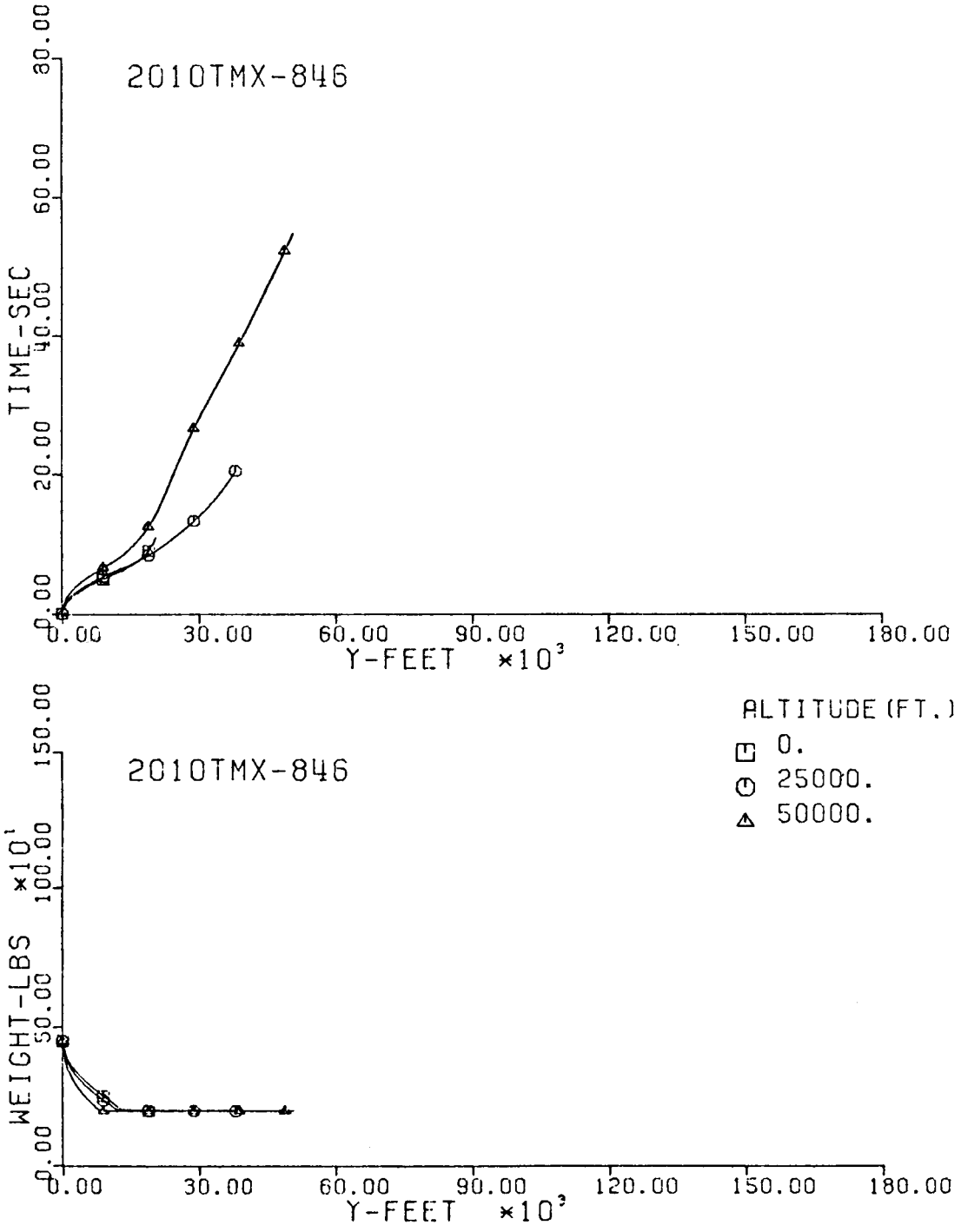

Fig. 282-III. Flight Time and Vehicle Weight vs. Downrange Distance, Y.

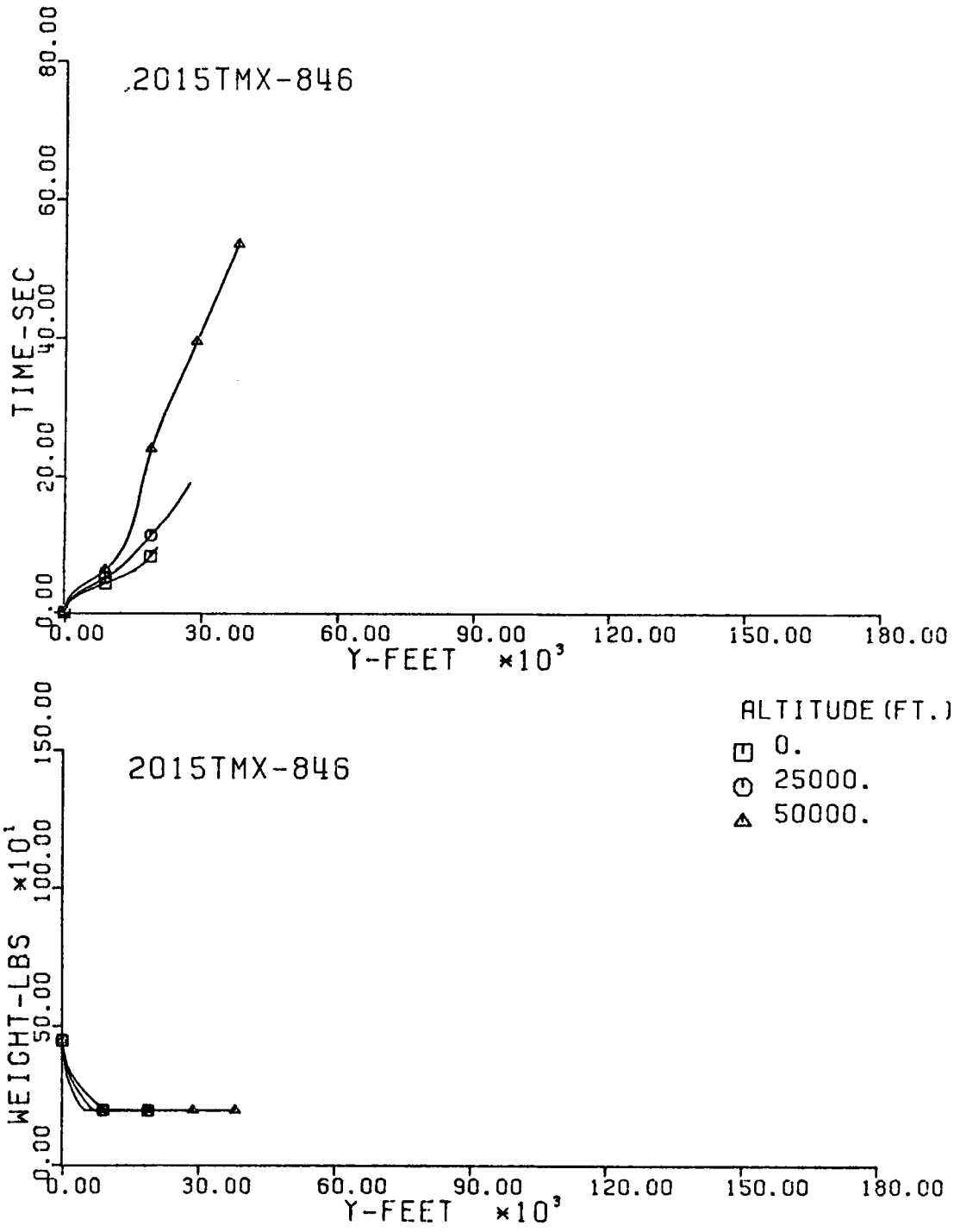

Fig. 283-III. Flight Time and Vehicle Weight vs. Downrange Distance, Y.

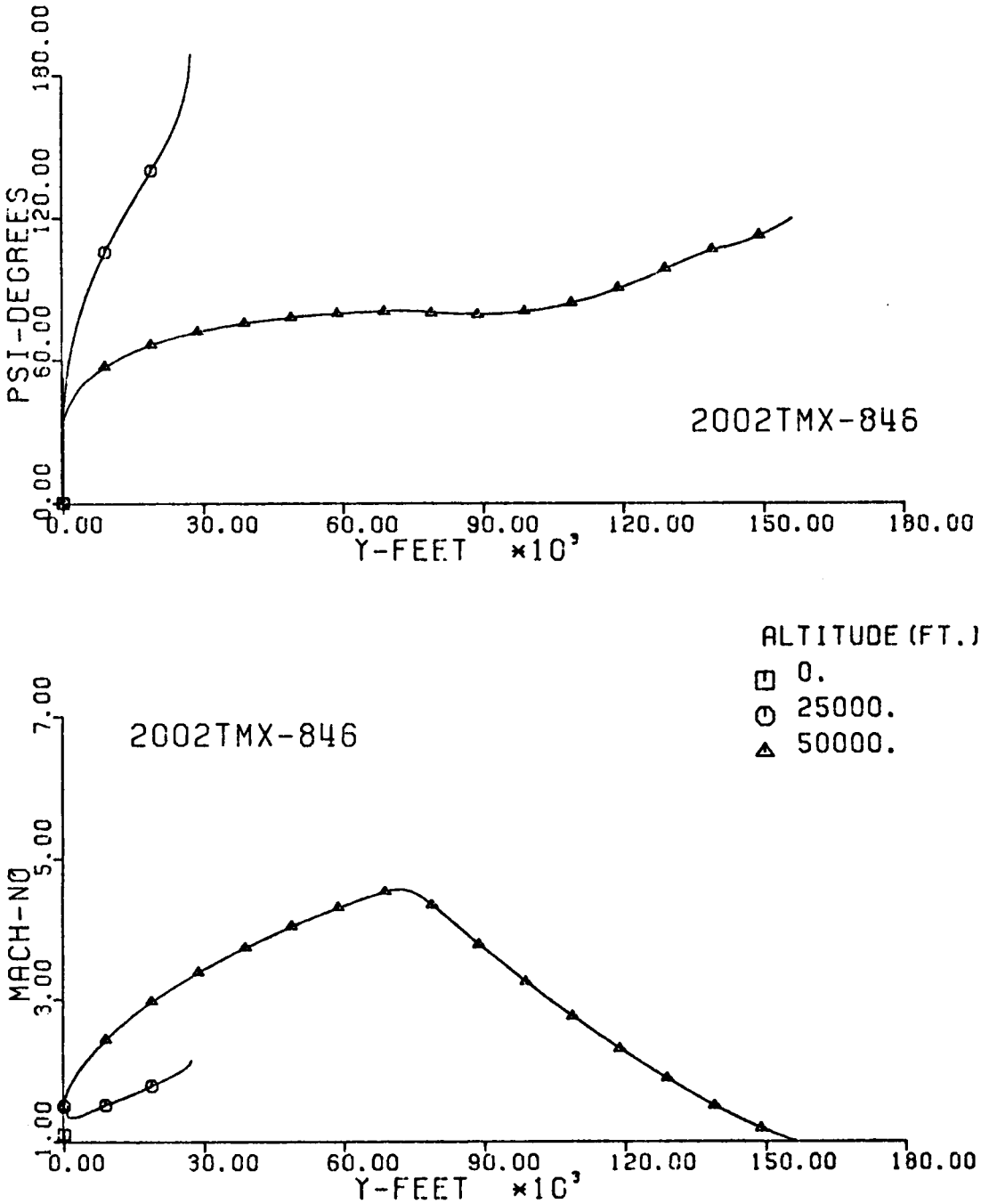

Fig. 284-III. Heading Angle and Mach No. vs. Downrange Distance, Y.

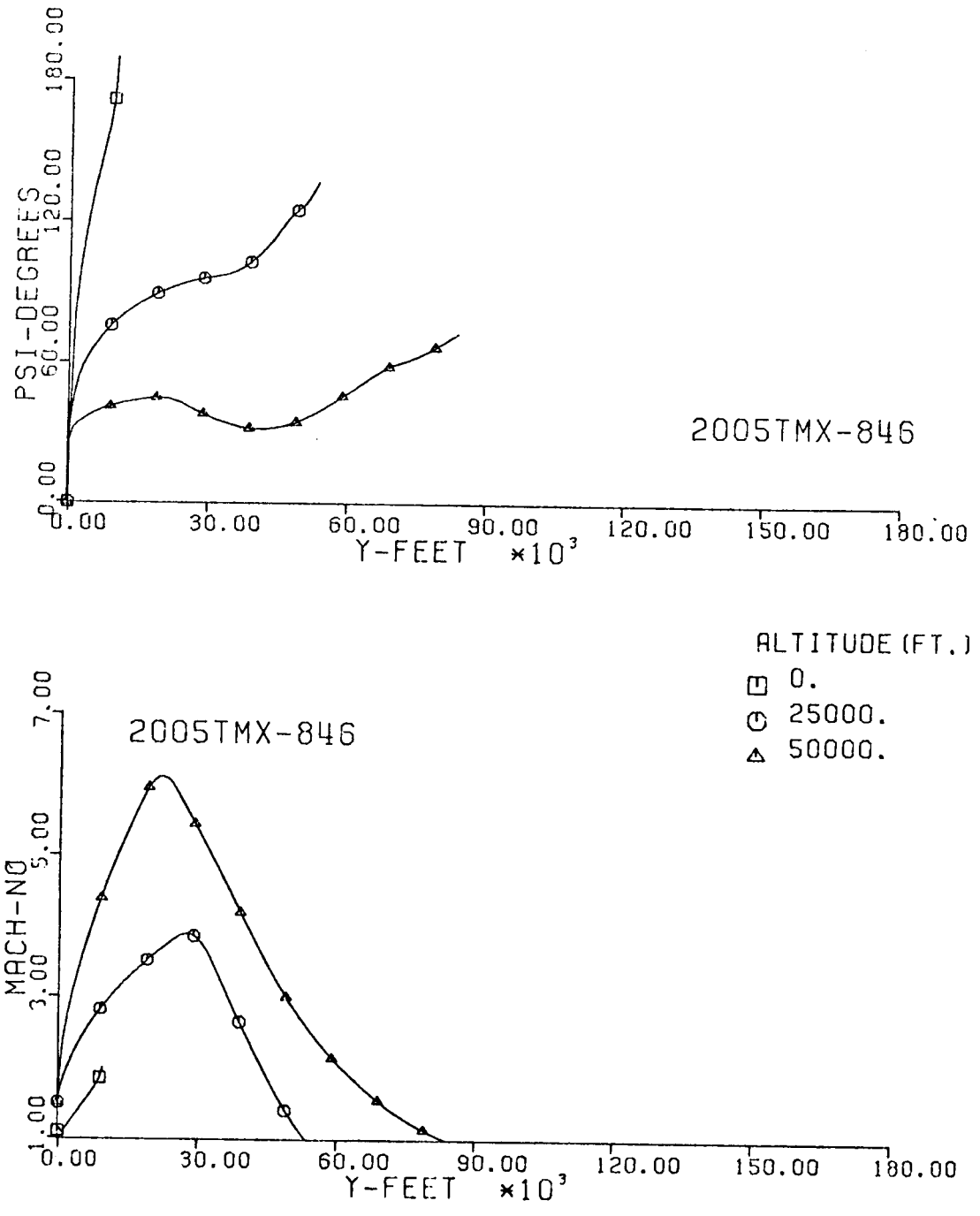

Fig. 285-III. Heading Angle and Mach No. vs. Downrange Distance, Y.

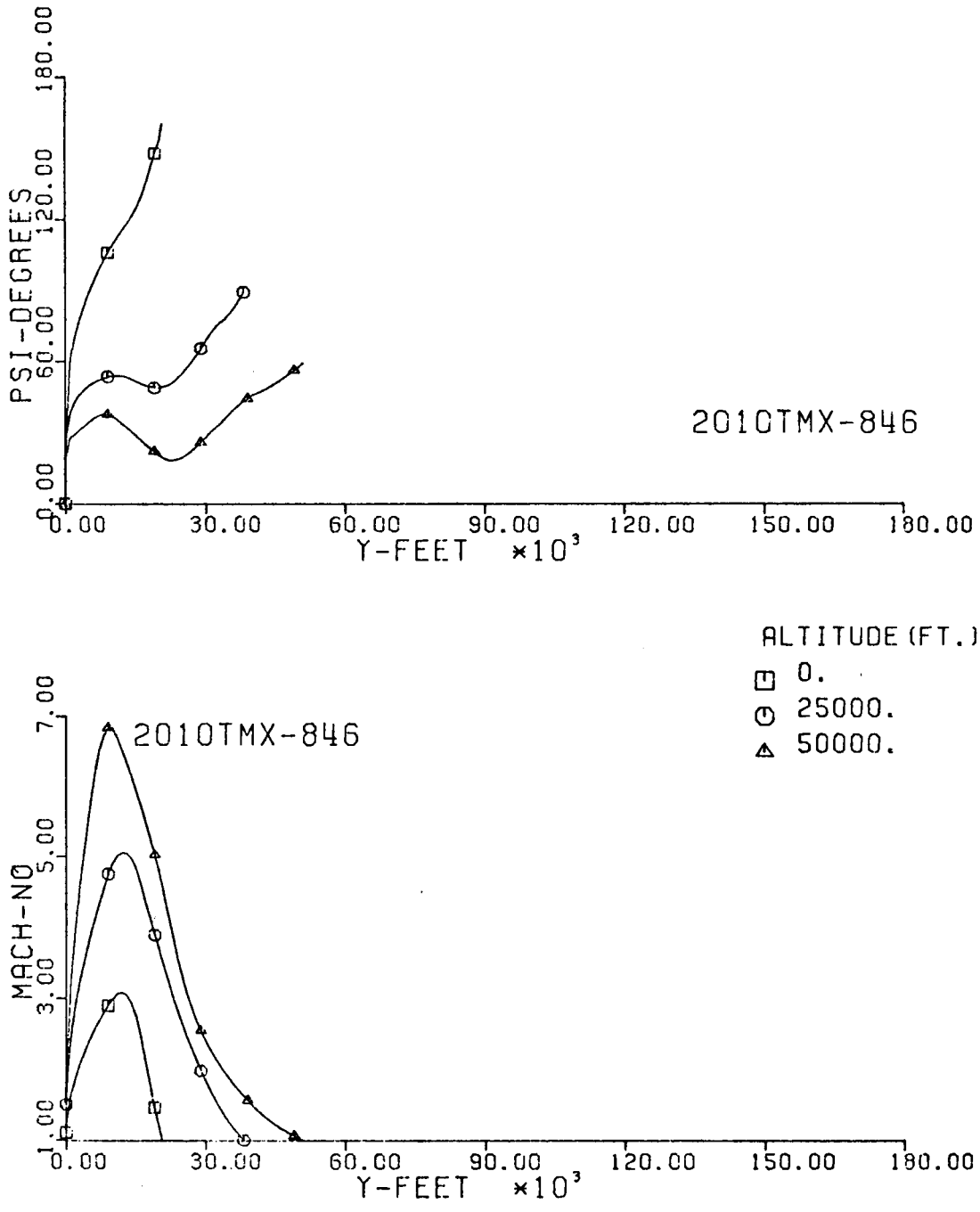

Fig. 286-III. Heading Angle and Mach No. vs. Downrange Distance, Y.

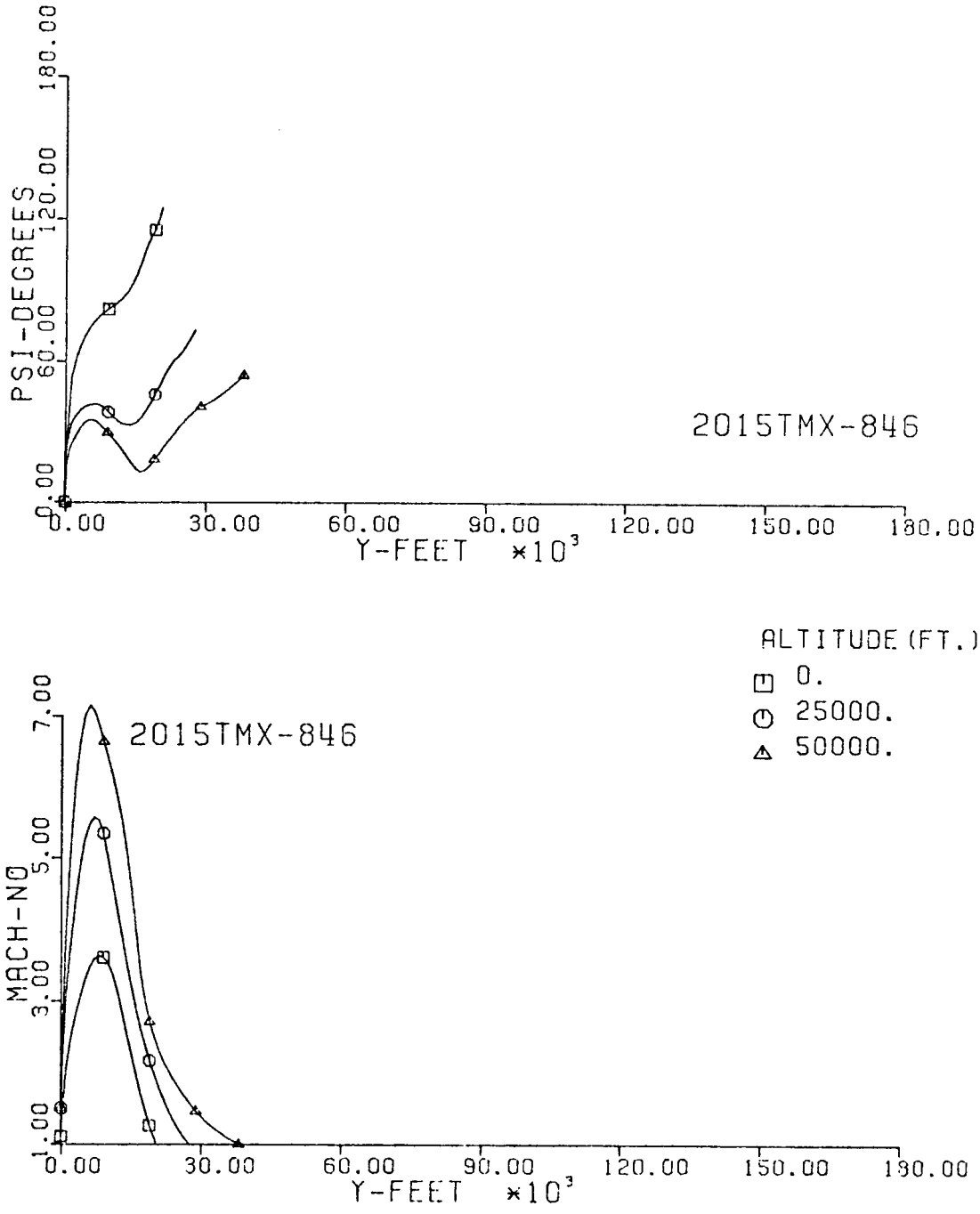

Fig. 287-III. Heading Angle and Mach No. vs. Downrange Distance, Y.

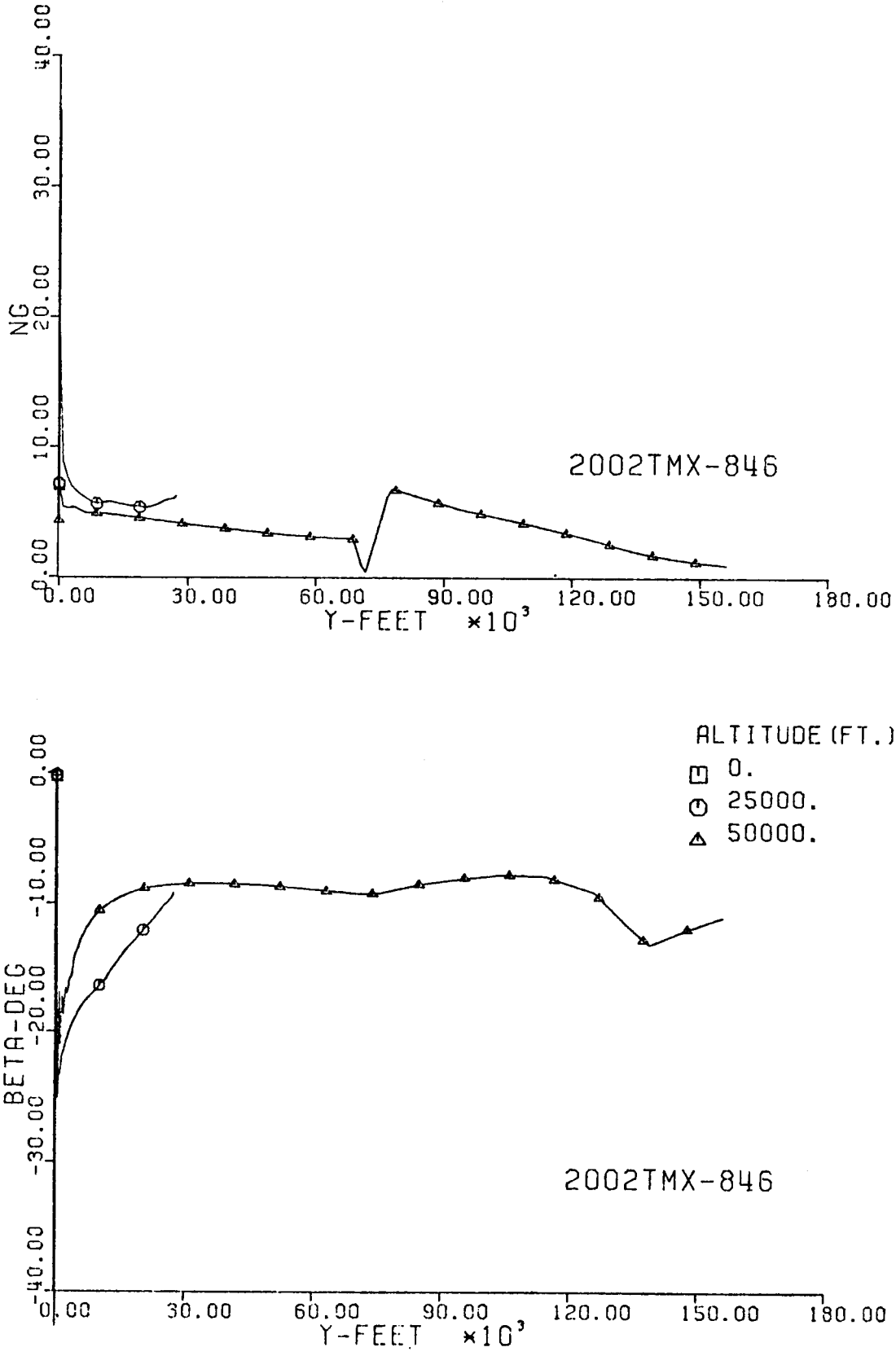

Fig. 288-III. Number of G's and Sideslip Angle vs. Downrange Distance, Y.

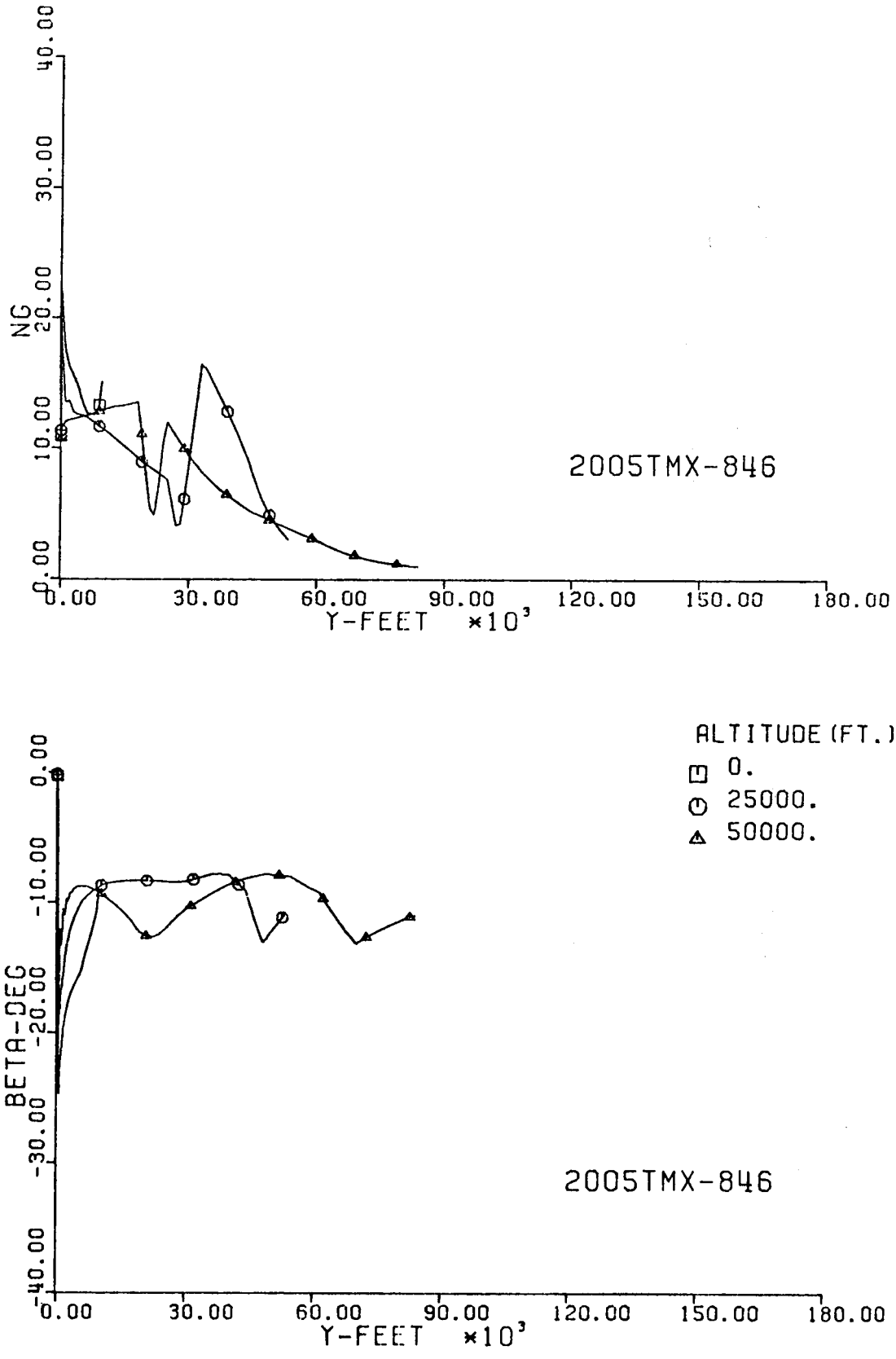

Fig. 289-III. Number of G's and Sideslip Angle vs. Downrange Distance, Y.

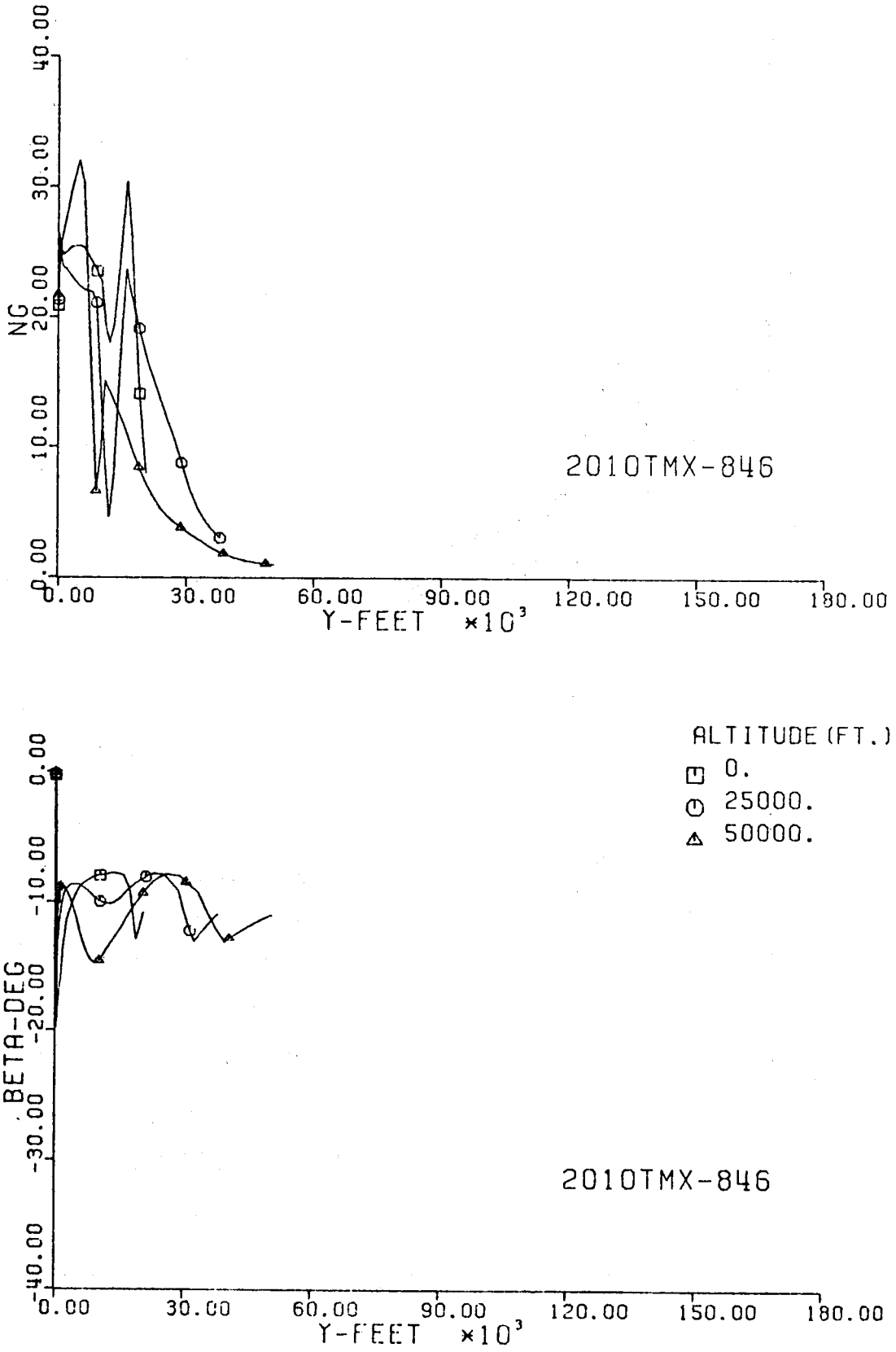

Fig. 290-III. Number of G's and Sideslip Angle vs. Downrange Distance, Y.

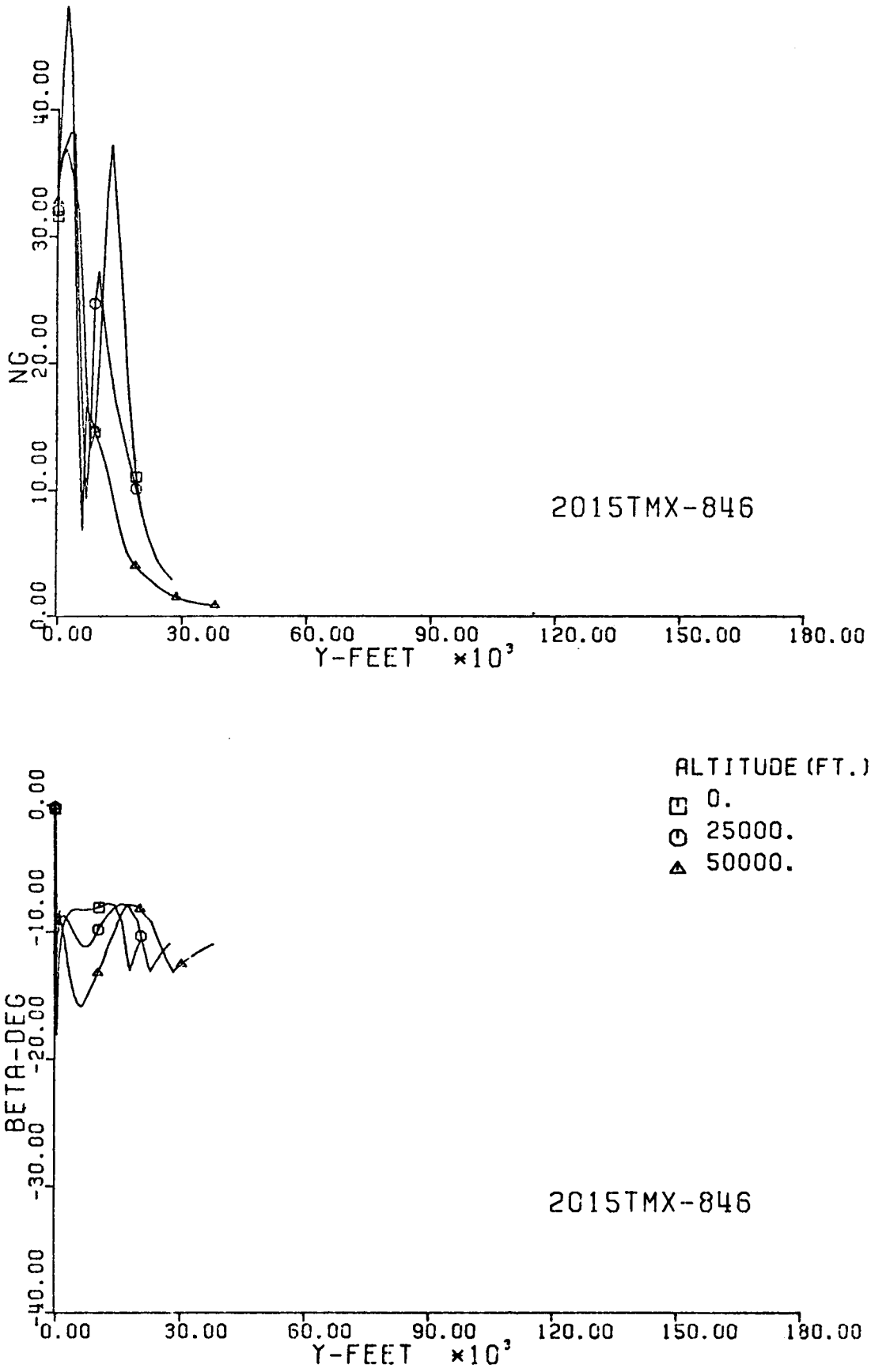

Fig. 291-III. Number of G's and Sideslip Angle vs. Downrange Distance, Y.

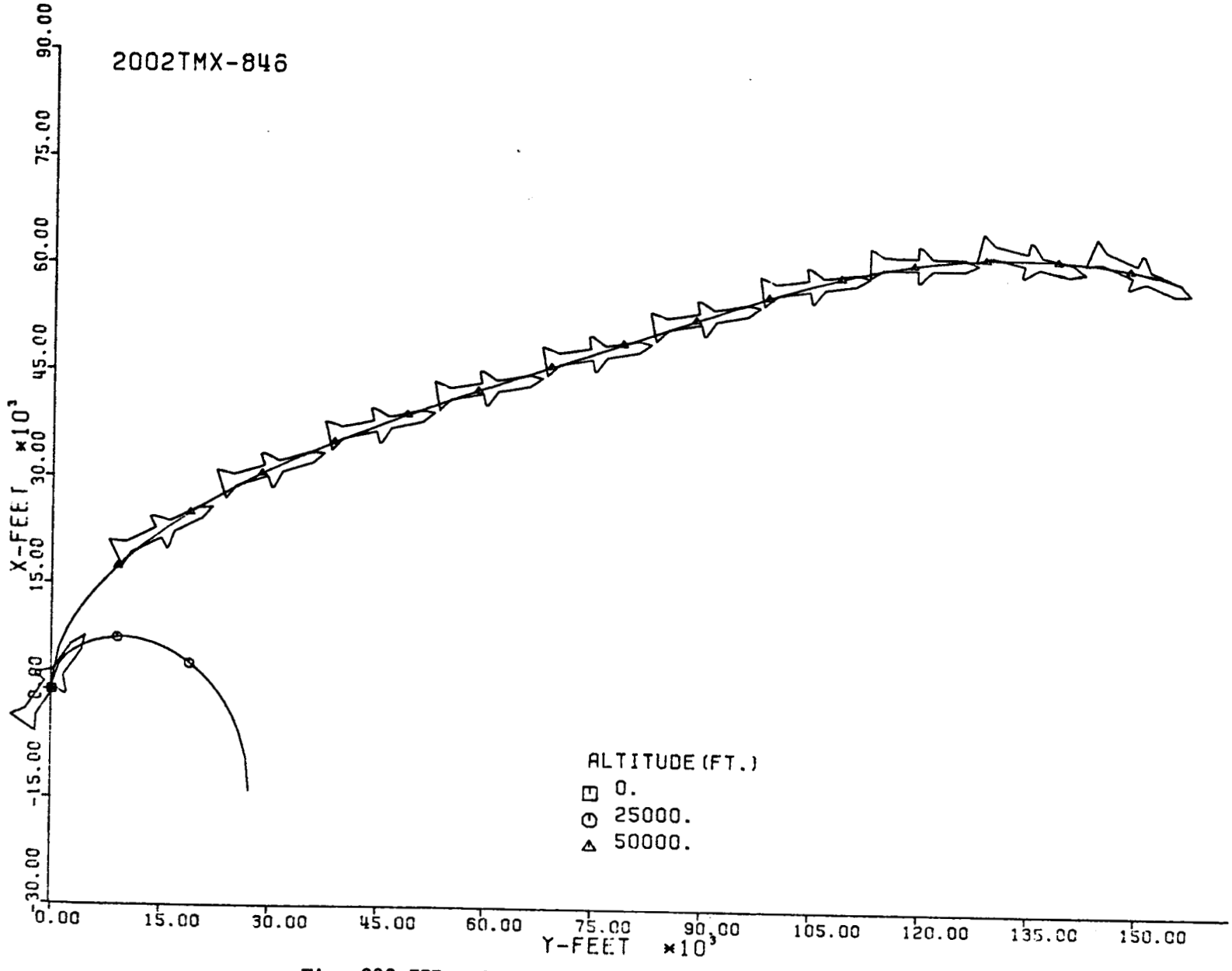

Fig. 292-III. Constant Altitude Flight Path, X vs. Y.

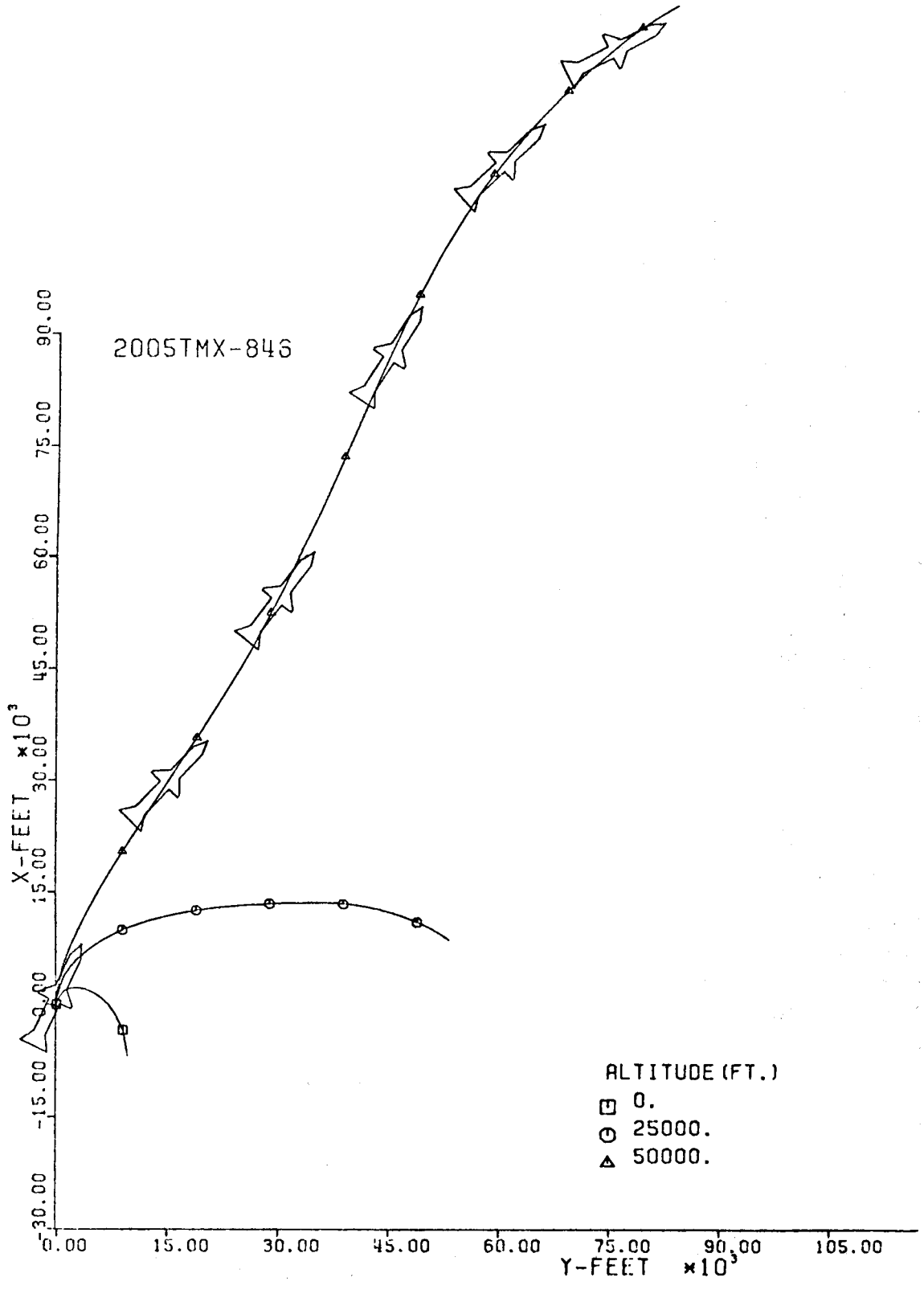

Fig. 293-III. Constant Altitude Flight Path, X vs. Y.

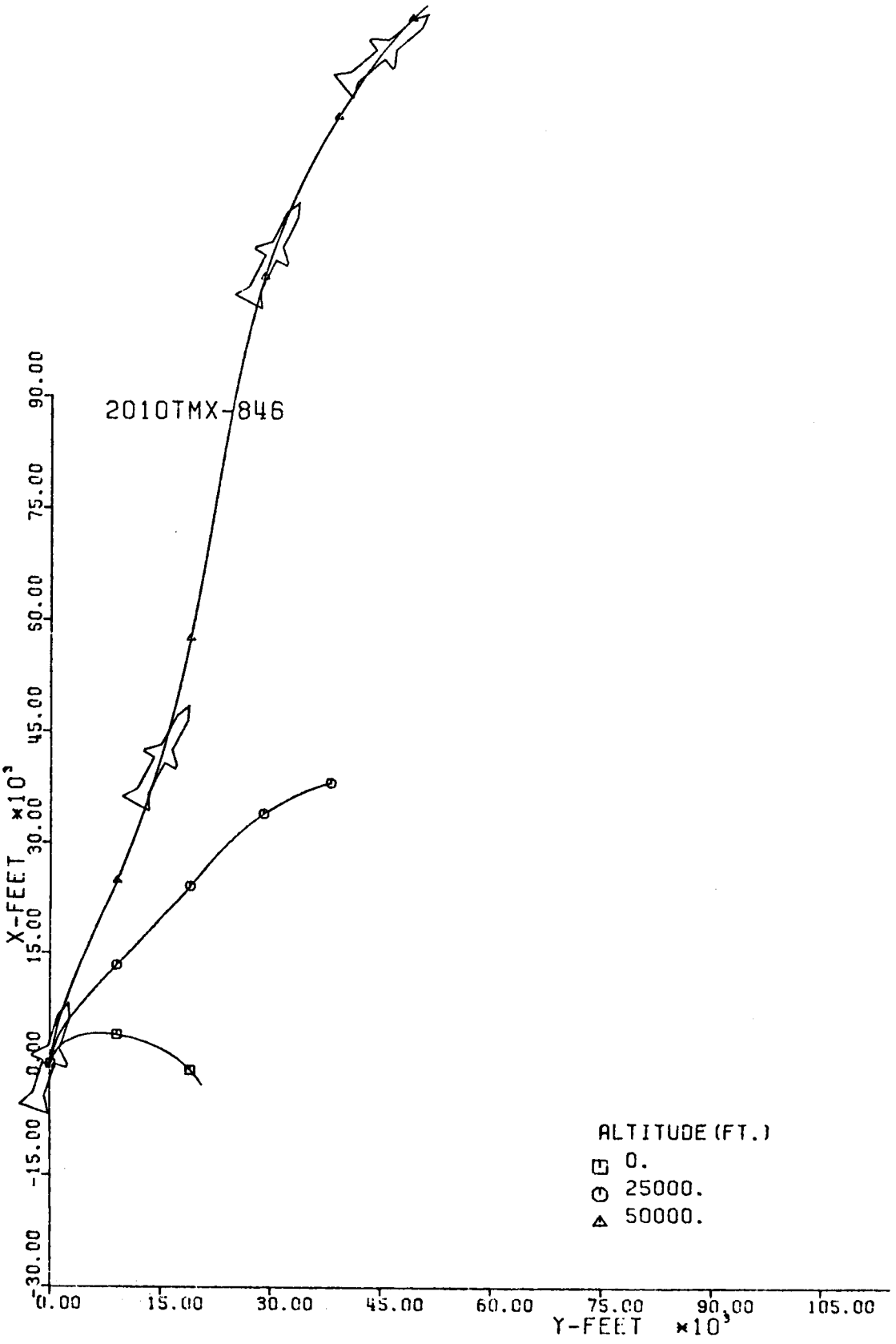

Fig. 294-III. Constant Altitude Flight Path, X vs. Y.

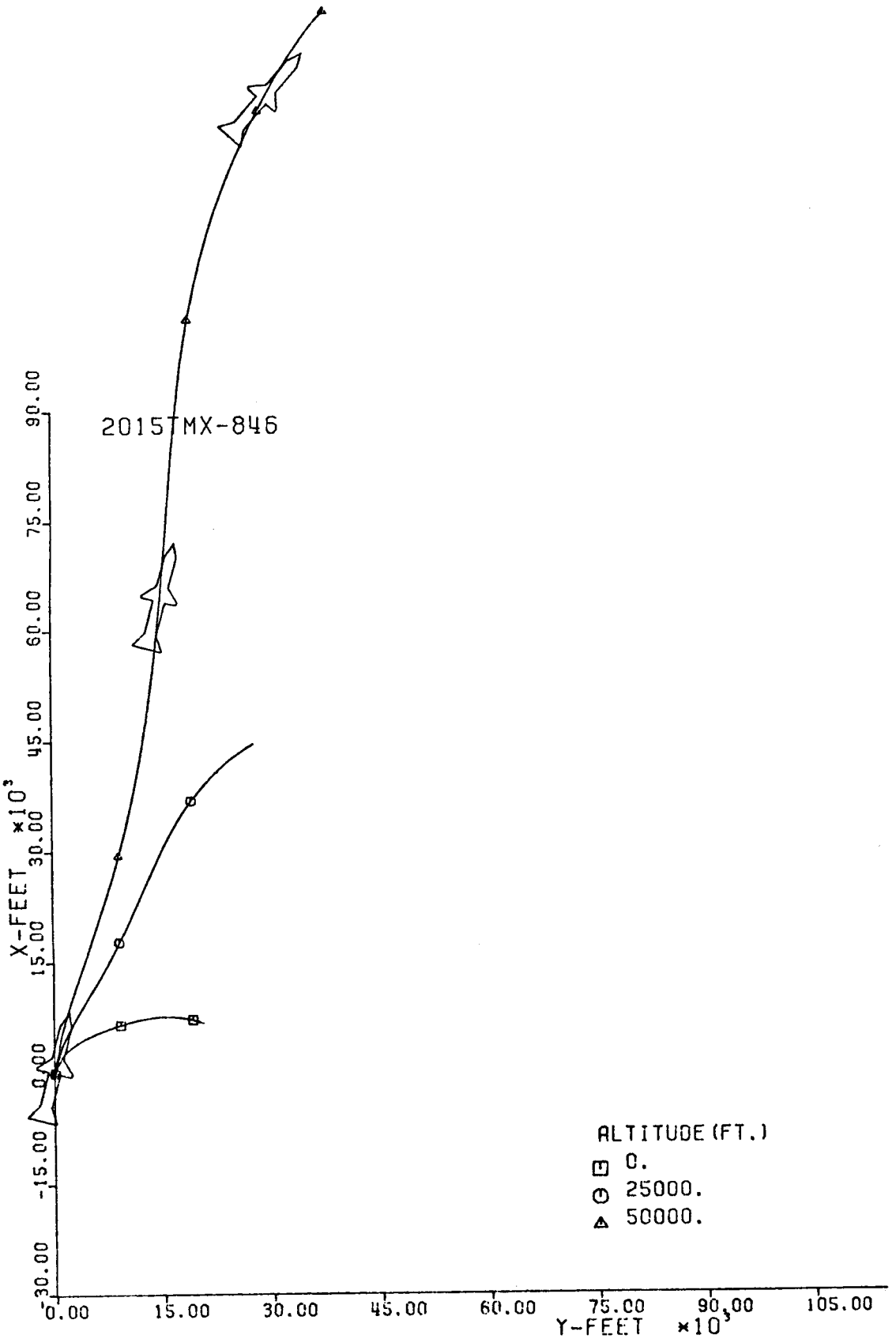

Fig. 295-III. Constant Altitude Flight Path, X vs. Y.

*U.S. GOVERNMENT PRINTING OFFICE: 1977 - 735-004/5